Ecole Doctorale SIMPPÉ (Sciences et Ingénierie des Molécules des Produits des Procédés et de l'Énergie)

Thèse

Présentée et soutenue publiquement pour l'obtention du titre de

DOCTEUR DE l'UNIVERSITE DE LORRAINE

Mention : Procédés Biotechnologiques

par **Thi Tuong LE**

Sous la direction de

Pr. Romain KAPEL et Pr. Jean-Pol FRIPPIAT

Purification et propriétés anti-inflammatoires et anti-oxydantes des fractions phénoliques issues de coproduits de production d'isolats protéiques d'oleoproteagineux

(Purification and anti-inflammatory and antioxidant properties of phenolic fractions from co-products of production of oleoproteaginous protein isolates)

15/12/2021

Membres du jury :

Directeur de thèse :	**M. Romain KAPEL**	**Professeur, LRGP, CNRS-UMR 7274, université de Lorraine, Nancy**
Co-directeur de thèse :	**M. Jean-Pol FRIPPIAT**	**Professeur, SIMPA UR7300, université de Lorraine, Nancy**
Rapporteurs :	**Mme. Loubna FIRDAOUS**	**Maître de conférences HDR, EA 7394 ICV, université de Lille, Lille**
	Mme. Hélène ROUX-DE BALMANN	**Directrice de recherches CNRS, LGC UMR CNRS 5503, université Toulouse 3, Toulouse**
Examinateurs :	**Mme. Christine GERARDIN (Président de jury)**	**Professeur, LERMAB EA 4370, université de Lorraine, Nancy**
	M. Eric MARCHIONI	**Professeur, IPHC UMR CNRS 7178, université de Strasbourg, Strasbourg**

ACKNOWLEDGEMENTS

I would like to thank my two supervisors, Professor Romain KAPEL and Professor Jean-Pol FRIPPIAT, for their great supervision and knowledge sharing. Especially from the bottom of my stomach, I would like to thank my main supervisor, Professor Romain KAPEL, for his guidance and encouragement and for keeping me on the right track.

I would like to thank Researcher-Lecturer Irina IOANNOU for her warm greeting to LRGP when I arrived in France in the very first day. I would also like to thank Professor Armelle ROPARS for her encouragement, guiding me during the days in SIMPA for biological tests, in scientific and non-scientific discussions. Without her support and advice, I cannot continue to write and accomplish my dreams in France. It was a pleasure working with her, and I hope there will be more collaboration in the future.

Moreover, I sincerely thank all the people who contributed to the achievements of this project:

- Research engineer Xavier FRAMBOISIER for his expertise in HPLC-HPLC/ESI/MS and assistance in the lab.
- Lab technician Arnaud AYMES at SVS took time packing column, working on AKTA with me for the purification process.
- Lab technicians Odile and Mélody for their expertise in using AKTA Flux for protein isolation and purification to produce permeate.
- My great and talented trainees, Mélanie and Armel, it has been fun and challenging to teach you about the adsorption and desorption of phenolic compounds on macroporous resins.

I would also like to thank all my BioProMo- and SIMPA-colleagues for your great help, support, and all the fun that we shared. Especially, I would like to thank Anastassia for her unconditional help.

Và người con muốn cảm ơn nhất là mẹ và gia đình lớn, nhỏ của con đã vì con mà hi sinh cả sức lực và giúp con hoàn thành quá trình gian nan nhưng đầy kỉ niệm này ở Pháp. Có lẽ con nói cảm ơn chưa bao giờ là đủ, và con yêu nhà nhiều <3

Cuối cùng, con tin là ba sẽ hạnh phúc và mỉm cười ở thế giới bên kia vì con đã làm được. Dù không còn ở thế giới này nữa nhưng con tin ba luôn ở đâu đó âm thầm ủng hộ và bảo vệ mẹ và các con và các cháu.

Nancy, 22/09/2020

Thi Tuong LE

Conference contributions

Conference contributions	
Oral presentations	
	Le, T.T., Aymes A., Framboisier X., Ioannou I., Kapel R.. Optimization of conditions for the purification of chlorogenic acid from a sunflower meal co-product by macroporous resins: static and dynamic study, European Congress of Chemical Engineering -12th, 5-19 September, 2019, Italy.
	Le, T.T., Ropars A., Aymes A., Frippiat J.-P.*, and Kapel R.* Multicriteria optimization of phenolic compounds capture from a sunflower protein isolate production process by-product by adsorption column and assessment of their antioxidant and anti-inflammatory effects, The 15th international symposium on Biochromatography and Separations, 17-20 May, 2021, Nancy, France
Posters	
	Le, T.T., Ropars A., Aymes A., Frippiat J-P., Kapel R. Optimization of purification chlorogenic acid from proteins side-product isolation from sunflower meal by macroporous resins: dynamic study and their bioactivity. Congress of American Oil Chemists' Society (AOCS), 5-9 May, 2019, USA
	Le, T.T., Ropars, A., Aymes, A., Frippiat, J.-P., & Kapel, R. Optimizing the purification of chlorogenic acid from protein by-product of sunflower meal and their bioactive functions. Congress of GreenFoodTech (GFT) 2020, May 5 and 6, 2020, Quebec City, Quebec, Canada.

List of publications

Publications	
Book chapter	**Le T.T.**, Ropars A., Sundaresan A., Crucian B., Choukér A., Frippiat J-P. Pharmacological Countermeasures to Spaceflight-Induced Alterations of the Immune System. In: Choukèr A. (eds) Stress Challenges and Immunity in Space. *Springer*. Cham., 2020. doi: 10.1007/978-3-030-16996-1_35
Paper 1	**Le T. T.**, Aymes A., Framboisier X., Ioannou I., Kapel R. Adsorption of phenolic compounds from an aqueous by-product of sunflower protein extraction/ purification by macroporous resins. J Chromatogr Sep Tech. 2020, 11:435. doi: 10.35248/2157-7064.20.11.435
Paper 2	**Le, T.T.**; Ropars, A.; Aymes, A.; Frippiat, J.-P.; Kapel, R. Multicriteria Optimization of Phenolic Compounds Capture from a Sunflower Protein Isolate Production Process by-Product by Adsorption Column and Assessment of Their Antioxidant and Anti-Inflammatory Effects. Foods 2021, 10, 760. doi: 10.3390/foods10040760
Paper 3	**Le, T.T.**; Framboisier, X.; Aymes, A.; Ropars, A.; Frippiat, J.-P.; Kapel, R. Identification and Capture of Phenolic Compounds from a Rapeseed Meal Protein Isolate Production Process By-Product by Macroporous Resin and Valorization Their Antioxidant Properties. Molecules 2021, 26, 5853. doi: 10.3390/molecules26195853

Abbreviations

A	Absorbance
ABTS	2,2'-azino-bis-(3-ethylbenzothiazoline-6-sulfonic
ACN	Acetonitrile
ANOVA	Analysis of variance
BBD	Box-Behnken design
BHA	Butylated Hydroxyanisole
BHT	Butylated Hydroxytoluene
BV	Bed volume
BV/h	Bed volume per hour
CA	Caffeic acid
cal	Calculated
CCD	Central composite design
CCF	Central composite face-centered
CGA	Chlorogenic acid
3-CQA	3-*O*-caffeoylquinic acid
4-CQA	4-*O*-caffeoylquinic acid
5-CQA	5-*O*-caffeoylquinic acid
3-diCQA	3-di-*O*-caffeoylquinic acid
4-diCQA	4-di-*O*-caffeoylquinic acid
5-diCQA	5-di-*O*-caffeoylquinic acid
COX	Cyclooxygenase
3D	Three-dimensional
DAD	Diode-array detector
DBC10	Dynamic binding capacity at 10%
DF	Diafiltration
DM	Dry matter
DMSO	Dimethyl sulfoxide
DoE	Design of experiment
DPPH	2,2-diphenyl-1-picrylhydrazyl
DV	Diavolume
DW	Dry weight
ELISA	Enzyme-linked immunosorbent assay
ESI-MS	Electrospray ionization- mass spectrometry
ESS	Error sum of square
exp	Experimental
FA	Formic acid
FAO	Food and Agriculture Organization
h	Hour
I-κB	Inhibitor of kappa B

IKK	I-κB kinase
IC	Inhibitory concentration
IL	Interleukin
IT	Ion trap
GAE	Gallic acid equivalent
HCl	Hydrochloric acid
H fraction	Hydrolyzed fraction
HPLC	High-performance liquid chromatography
LPS	Lipopolysaccharide
LRGP	Laboratoire Réaction et Génie des Procédés
MAR	Macroporous resin
mAU	milli-Absorbance Units
min	Minute
NF-κB	Nuclear factor-kappa B
N fraction	Non-hydrolyzed fraction
NO	Nitric oxide
NOE	Number of experiment
iNOS	Inducible nitric oxide synthase
NSAID	Non-steroidal anti-inflammatory drugs
OG	Octyl gallate
O.D.	Optical density
PBS	Phosphate buffer saline
PC	Phenolic compound
PFO	Pseudo-first-order
Ph.D.	Doctor of Philosophy
PKD	Protein kinase D
PG	propyl gallate
PGs	Prostaglandins
PGE_2	Prostaglandin E_2
PSO	Pseudo-second-order
PVDF	Polyvinylidene diflouride
QA	Quinic acid
RSM	Rapseed meal
SA	Sinapic acid
SAE	Sinapic acid equivalent
SAID	Steroidal anti-inflammatory drugs
SAR	Structural activity relationship
SDS-PAGE	Sodium dodecyl sulfate–polyacrylamide gel electrophoresis
SDVB	Styrene-divinylbenzene polymer
SIMPA	Laboratoire Stress, Immunité, Pathogènes

SE-HPLC	Size exclusion high-performance liquid chromatography
SF	Sunflower
SFA	Sunflower Albumin
SFM	Sunflower meal
SG	Sinapoyl glucose
SP	Sinapine
SS	Specific surface (m^2/ g)
TBHQ	tert-butylated hydroquinone
TCA	Trichloro acetic acid
TNF-α	Tumor necrosis factor-alpha
TPC	Total phenolic content
UF	Ultrafiltration
UHPLC	Ultra-high-performance liquid chromatography
W	Water
WHO	World Health Organization

Nomenclature

C	Constant associated with the thickness of the boundary layer (mg/g)
C/C_o	Ratio of the outlet to inlet concentration
C_d	Concentration of phenolic compounds in desorption solution
C_e	Equilibrium concentration of phenolic compound (mg/mL)
C_i	Initial concentration of phenolic compound (mg/mL)
EtOH	Ethanol
ΔG	Gibbs free energy change (kJ/ mol K)
ΔH	Enthalpy change (kJ/mol)
k_1	Rate constant of the PFO equation (1/min)
k_2	Rate constant of the PSO equation ($g/mg \times min$)
K_{eq}	Equilibrium distribution coefficient of adsorption isotherm
K_F	Freundlich constant $(\frac{mg}{g})/(\frac{mg}{L})^n$
k_i	Rate constant of the intra-particle diffusion model ($mg/g \times min^{1/2}$)
K_L	Langmuir constant (L/mg)
MeOH	Methanol
m/z	Mass to charge
n	Freundlich intensity parameter ($0 < n \leq 1$)
NaCl	Sodium chloride
NaOH	Sodium hydroxide
-OHs	Hydroxyl groups
Q_{max}	Maximum saturated monolayer adsorption capacity of polyphenol (mg/g)
q_t	Amount of adsorbate uptake per mass of adsorbent at any time t (min)
R	Ideal gas constant (8.314 J/ mol K)
R_L	Constant of separation factor
R^2	Coefficient of determination
q_e	Adsorption capacity (mg/g)
S	Surface adsorption capacity (mg/ m^2)
ΔS	Entropy change (kJ/mol K)
T	Temperature (K)
t_R	Retention time
V_d	Volume of desorption solution
Vitamin C	Ascorbic acid
v/v	Volume concentration
V_i	Volume of the initial sample solution (mL)
W	Weight of the tested dry resin (g)

Content

List of Tables

List of Figures

Chapter 1. Introduction

1.1. Contexte - problématique

En 2019, environ 56 millions de tonnes de graines de tournesol (*Helianthus annus* L.) et 70 millions de tonnes de graines de colza (*Brassica napus L.*) ont été produites annuellement dans le monde (FAO, 2019) (FAOSTAT, 2020a). En Europe, le tournesol et le colza sont les oléagineux les plus cultivés et sont les principales sources d'huile en France et en Europe. L'extraction industrielle de l'huile donne des coproduits solides, appelés "tourteaux", qui sont utilisés pour l'alimentation animale en raison de leur composition riche en protéines (jusqu'à 30 - 50 %) (Geneau-Sbartaï et al., 2008; Pickardt et al., 2011). Actuellement, ces tourteaux de tournesol (SFM) et de colza (RSM) sont considérées comme des sources prometteuses de protéines (González et al., 2011; Hudson, 1994) pour des applications en alimentation humaine sous forme d'isolats (pureté en protéine > 90%). La production d'isolats protéiques répond à une demande grandissante en protéines végétales de la part des pays industrialisée ainsi qu'à un enjeu majeur d'établi de nouvelles filières protéiques pour soutenir la croissance demographique mondiale.

La production d'isolats à partir de tourteaux d'oleoproteagineux peut être effectuée en deux étapes principales: une extraction aqueuse (modulée par T, pH et NaCl) et une purification des protéines par filtration tangentielle ou précipitation isoélectrique (Bongartz et al., 2016; Wildermuth et al., 2016). Ces procédés libèrent de grands volumes d'effluents liquides non valorisés à ce jour. Ils contiennent principalement des molécules hydrosolubles coextraites des protéines lors de l'étape d'extraction (Albe Slabi et al., 2019; Defaix et al., 2019). C'est à dire l'azote non protéique, des glucides hydrosolubles, des composés phénoliques, des minéraux et des sels. La valorisation de ces effluents constitue un enjeu crucial pour le développement de cette filière dans une optique d'économie circulaire. La capture des composés phénoliques de ces effluents liquides est une voie de valorisation interessante de ces effluents en raison de leur potentiel applicatif important dans des secteurs à haute valeur ajoutée (biomédical et / ou sécurité alimentaire).

Les produits agroalimentaires riches en lipides avec des acides gras polyinsaturés à longue chaîne sont facilement oxydés pendant la durée de stockage. Ce phénomène constitue le problème majeur de ces produits dans les domaines alimentaire, cosmétique et pharmaceutique. Lorsque les substances lipidiques sont dégradées en lipides, peroxyde d'hydrogène peut provoquer une perte de nutriments, toxique pour la santé humaine (Yagi, 1987). Les substances antioxydantes synthétiques sont généralement utilisées dans l'industrie alimentaire pour empêcher l'oxydation des produits riches en lipides, comme l'hydroxyanisole butylé (BHA), l'hydroxytoluène butylé (BHT) et la combinaison BHA/BHT pour surmonter ces problèmes. Néanmoins, l'utilisation de ces antioxydants synthétiques au cours de la vie peut entraîner une toxicité pour la santé humaine (Branen, 1975; Lindenschmidt et al., 1986). Il est donc important de remplacer ces antioxydants synthétiques par des antioxydants naturels dérivés de sources végétales (Halliwell, 1996).

L'inflammation est la défense immunologique contre les blessures ou les infections causées par diverses bactéries et virus. Cependant, une inflammation incontrôlée peut entraîner des maladies aiguës et chroniques telles que le cancer. La recherche de molécules permettant de moduler ces troubles inflammatoires a toujours suscité une grande attention de la part de la communauté scientifique. Les anti-inflammatoires stéroïdiens (SAID) et les anti-inflammatoires non stéroïdiens (NSAID) existent et sont bien documentés pour traiter les réponses inflammatoires par l'inhibition des isoenzymes de la cyclooxygénase (COX) (Flower & Vane, 1972). Bien que les SAIDs et les NSAIDs aient montré de nombreux effets bénéfiques dans le traitement de l'inflammation, ils ont tous deux des effets secondaires inévitables, tels que des effets secondaires gastro-intestinaux, rénaux et cardiovasculaires (Bjarnason et al., 1993; Harirforoosh & Jamali, 2009). De nos jours, les médicaments synthétiques en traitement long ne sont pas encouragés par l'OMS (organisation mondiale de la santé) à cause des effets secondaires. Par conséquent, la recherche de molécules alternatives non-toxique est un enjeu important.

Les composés phénoliques des tourteaux de tournesol et de colza ont montré des activités antioxydantes intéressantes (Salgado et al., 2012; Weisz et al., 2013; Žilić et al., 2010, Amarowicz et al., 2000; Matthäus, 2002; Vuorela et al., 2004; J. P. D. Wanasundara et al., 2016). Ainsi, des extraits éthanoliques de SFM riches en composés phénoliques présentent une activité antiradicalaire (Wanjari & Waghmare, 1994; Amarowicz et al., 2000; Matthäus, 2002; Vuorela et al., 2004; J. P. D. Wanasundara et al., 2016) superieures à l'hydroxytoluène butylé (BHT) utilisé industriellement. De manière interessante, la capacité antioxydante des polyphénols de RSM augmente notablement après hydrolyse (catalysée en conditions acides ou basiques) (Thiyam et al., 2006).

En outre, plusieurs articles rapportent que l'acide chlorogenique (CGA) qui est le composé phénolique principal du tournesol, présente une activité anti-inflammatoire. Ainsi, le CGA a montré une inhibition de la voie NF-κB et de l'expression des cytokines (Francisco et al., 2013; Shin et al., 2015; Z. Zhao et al., 2008). Le CGA a également atténué les cytokines pro-inflammatoires, notamment l'IL-1β et le TNF-α, de manière dose-dépendante sur les macrophages murins RAW 264.7 (Shan et al., 2009). De manière intéressante, Khadija Essafi-Benkhadir et al. (Essafi-Benkhadir et al., 2012) ont montré qu'un extrait de polyphénols d'écorce de coing contenant également du CGA pouvait inhiber la sécrétion du facteur de nécrose tumorale-alpha (TNF-α), un marqueur pro-inflammatoire, dans les macrophages THP-1. Cependant, à notre connaissance, il n'existe aucune référence concernant l'impact des extraits phénoliques de tournesol sur l'inflammation. L'activité antiinflammatoire des polyphénols de colza a été peu étudiée à ce jour et les résultats paraissent contradictoires (Vuorela et al., 2005, X. Huang et al., 2018; Yun et al., 2008).

La purification des composés phénoliques à partir d'extraits végétaux est largement abordée dans la litterature. Concernant les polyphénols de RSM et SFM, la plupart des articles traitent de purification à partir d'extrait utilisant des solvants organiques miscibles dans l'eau comme l'éthanol, l'acétone, le méthanol, ou des mélanges eau/éthanol (Canella & Sodini, 1977; Sripad & Rao, 1987). En effet, ce type d'extraction permet d'éliminer selectivement les composés polyphénoliques considérés

comme antinutritionnels dans les tourteaux pour les applications en alimentation animale (Weisz et al., 2009) (Naczk et al., 1992). Cependant, il existe peu de données sur l'identification et la capture des composés phénoliques de SFM et de RSM issus d'extraction aqueuse modulée par les sels et le pH (comme utilisée pour la production d'isolats de protéines).

Les composés phénoliques peuvent être purifiés par chromatographie (Ky et al., 1997), par des procédés membranaires (Conidi et al., 2017; Zagklis et al., 2015), ou par adsorption sur des résines macroporeuses (Jia & Lu, 2008). Ce dernier procédé s'est révélé particulièrement efficace pour la capture des composés phénoliques à partir de divers extraits de plantes (Jia & Lu, 2008; B. Liu et al., 2016; Q.-S. Liu et al., 2010). Les procédés de purification des composés phénoliques peuvent être facilement extrapolés, et certaines résines sont de qualité alimentaire (Weisz et al., 2013). Ainsi, ces procédés peuvent être facilement utilisés pour la purification industrielle des substances naturelles pour des applications en nutrition / santé.

La plupart des études menées sur la capture de composés phénoliques à partir d'extraits végétaux sont réalisés en batch. Elles caractérisent les cinétiques et isothermes d'adsorption ainsi que la composition des solvents la plus appropriée pour la désorption (C.-C. Liu et al., 2017). Ces études montrent que les résines macroporeuses les plus adaptées sont les résines faiblement à moyennement apolaires (SDVB et/ou acryliques, Moreno-González et al., 2020; Weisz et al., 2010, 2013). Les meilleurs solvents de desorption sont des mélanges ethanol / eau entre 30% et 70% v/v (Dong et al., 2015; B. Liu et al., 2016; Weisz et al., 2013). Cependant, le transport des molécules pendant les processus d'adsorption est rarement étudié, sauf dans une étude de capture des composés phénoliques de jus foliaires de luzerne (Firdaous et al., 2017). De plus, la caractérisation des fractions désorbées en termes de composition, et / ou bioactivité est rarement considérée.

D'autre part, la mise en œuvre industrielle la plus classique des procédés d'adsorption sur résine est la colonne d'adsorption (mise en œuvre « dynamique »). Cette mise en oeuvre est réalisée en plusieurs étapes : l'adsorption, le rinçage et la desorption. L'optimisation de ces systèmes est particulièrement complexe car chaque phase associe un jeu de conditions opératoires propres (débit, composition des phases mobiles, pH et force ionique de la charge d'alimentation, dimension des colonnes etc.) et de critères de performances (capacité d'adsorption dynamique, productivité, pureté et rendement) (Scordino et al., 2003; E. Silva et al., 2007). La plupart des études proposant une optimisation des colonnes d'adosorption proposent utilisent des méthodes d'optimisation type « un seul facteur à la fois » ou des plans d'expériences. Elles visent, dans la majorité des cas, à ne maximiser qu'un seul critère (le plus souvent la capacité de d'adsorption dynamique et / ou le rendement de récupération (C.-C. Liu et al., 2017; Moreno-González et al., 2020; Weisz et al., 2013). A notre connaissance, aucun article ne montre de méthodologie permettant une optimisation des procédés d'adsorption de composés phénolique integrant les trois critères de performances les plus importants (productivité, pureté des fractions et rendement).

1.2. Objectifs de la thèse

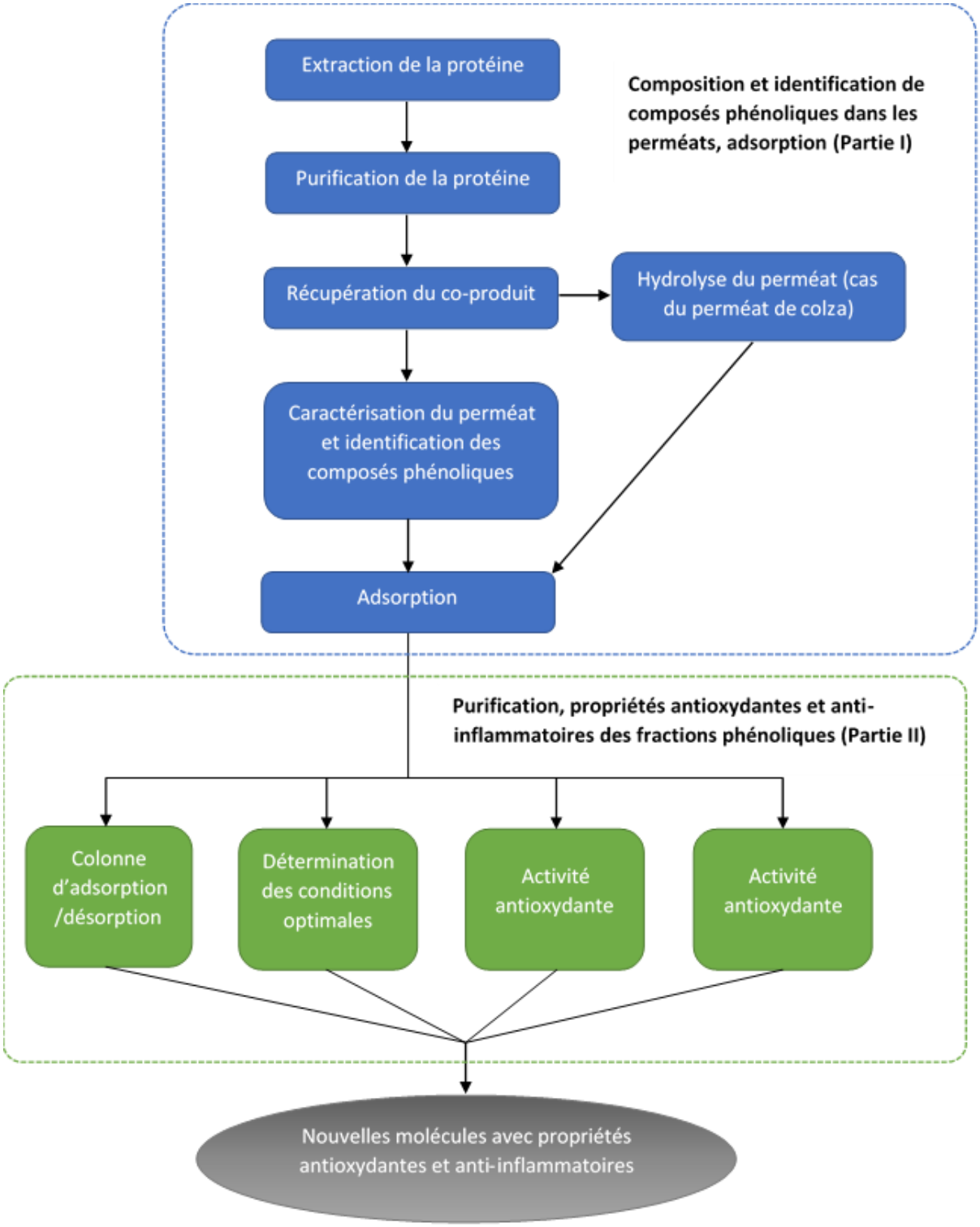

Figure 1.1. Schéma du projet complet de doctorat comprenant les deux parties (Partie I et Partie II)

Les principaux objectifs de ce travail étaient les suivants :

1) caractériser et identifier les composés phénoliques des effluents liquides issus de la production d'isolats de protéines à partir de la SFM et de la RSM ; 2) choisir les meilleures résines macroporeuses et étudier le mécanisme d'adsorption des composés phénoliques; 3) optimiser les

conditions dans la colonne d'adsorption des composés phénoliques; et 4) évaluer les activités biologiques des fractions phénoliques obtenues, notamment les propriétés antioxydantes et anti-inflammatoires. Les effluents utilisés dans le cadre de la thèse sont issus de travaux collaboratifs entre le groupe AVRIL (qui est le prinicpal acteur industriel français de la filière) et le LRGP qui ont ont été brevetés et fait l'objet de publications scientifques recemment (Albe Slabi et al., 2019; Defaix et al., 2019; Albe Slabi et al., 2020; Sara Slabi et al., 2021).

Afin d'atteindre ces objectifs, l'étude a été divisée en deux parties principales, comme le montre la Figure 1.1, à savoir "composition, identification des composés phénoliques et adsorption par lots (partie I)" et "adsorption dynamique (adsorption sur colonne) et valorisation biomédicale des fractions phénoliques, y compris les propriétés antioxydantes et anti-inflammatoires (partie II)".

Tout d'abord, l'identification des composés phénoliques dans les effluents des sous-produits des isolats de protéines SFM et RSM a été réalisée en utilisant la technique SE-HPLC et HPLC-MS. En particulier, les composés phénoliques dans le sous-produit aqueux de l'isolat de protéines RSM après et avant l'hydrolyse acide ont été identifiés par LC-MS. Ensuite, nous avons utilisé différentes résines macroporeuses, notamment XAD4, XAD7, XAD16, XAD1180 et HP20, pour choisir la résine appropriée pour capturer les composés phénoliques ciblés. Ces résines possèdent diverses propriétés en termes de polarité, de diamètre des pores et de surface spécifique. La meilleure résine a été sélectionnée sur la base de la capacité d'adsorption massique/surface et du rapport de désorption les plus élevés. Pour comprendre les mécanismes d'adsorption des composés phénoliques sur les résines, les données expérimentales ont été régressées avec différents modèles tels que le pseudo premier ordre (PFO), le pseudo second ordre (PSO), et les modèles de diffusion intra-particulaire. Les isothermes d'adsorption à différentes températures ont été utilisées pour élucider les comportements d'adsorption des composés phénoliques tels que les modèles de Langmuir ou de Freundlich. Les paramètres thermodynamiques ont également été calculés afin de comprendre le mécanisme physique et le processus exothermique de l'adsorption des composés phénoliques sur les résines. La désorption par différentes concentrations d'éthanol dans l'eau a également été étudiée. Le taux de désorption et la pureté de la fraction phénolique ont également été pris en compte pour choisir la résine la plus appropriée pour la capture phénolique de ces effluents.

Ensuite, les résines les plus appropriées ont été choisies dans l'adsorption par lots en utilisant une colonne de garnissage dans l'adsorption dynamique (adsorption en colonne). Comme nous l'avons mentionné dans la partie précédente, l'adsorption sur colonne est particulièrement complexe puisqu'elle dépend de plusieurs facteurs. C'est pourquoi, dans cette partie, nous avons évalué l'effet du débit et du pH sur la capacité de liaison dynamique (DBC), la productivité et la récupération en utilisant des plans d'expériences (DoE). Pour déterminer les conditions optimales de cette étape, une méthode d'optimisation multi-objectifs a été suivie sur la base des modèles DoE. En ce qui concerne l'étape de désorption, l'effet des concentrations d'éthanol sur la pureté et la récupération des fractions phénoliques a été étudié.

Enfin, l'activité antioxydante des fractions phénoliques obtenues après adsorption/désorption sur colonne a été comparée aux composés phénoliques authentiques tels que CGA, SP, et SA et à la vitamine C en utilisant les tests DPPH et ABTS. Cette étude a permis de révéler que les fractions phénoliques étaient considérées comme des agents antioxydants naturels dans les applications alimentaires. En outre, l'activité anti-inflammatoire a été évaluée en utilisant le modèle classique (Chanput, W. et al.,2014). Le niveau de production de la cytokine pro-inflammatoire TNF-α par les macrophages THP-1 traités au lipopolysaccharide (LPS) a été utilisé pour évaluer la propriété anti-inflammatoire de ces fractions phénoliques. Cette étude a permis de démontrer un effet protecteur de la fraction phénolique contre une future inflammation.

Chapter 2. Literature review

<u>Part I:</u> Oilseed meal production, composition, and phenolic fractions

2.1. Sunflower and rapeseed meals production

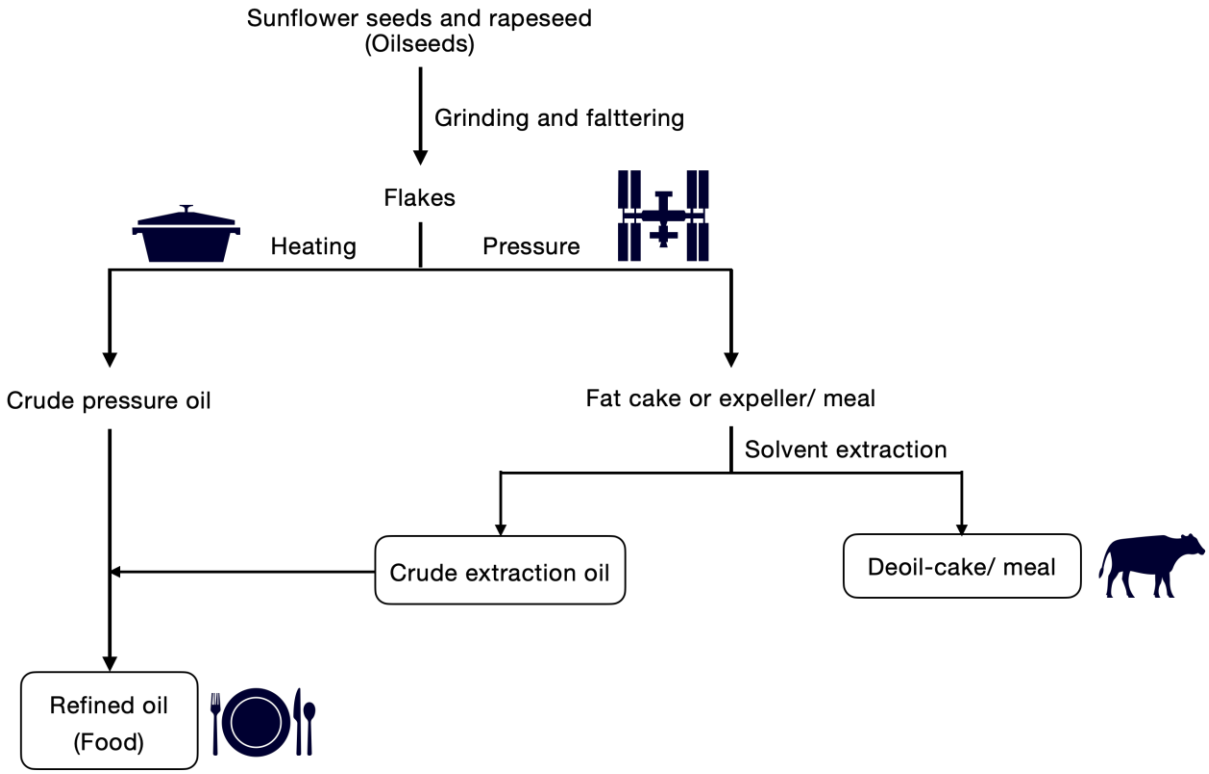

Figure 2.1. De-oiling sunflower seeds and rapeseed to produce sunflower and rapeseed meals. (adapted from Terres Univia, 2020, available online).

Figure 2.1. illustrates the process of oilseed de-oiling and oilseed meal production. Rapeseed and sunflower oils are the most consumed oils in the world (United Nations et al., 2019). Oilseeds with or without hulls used for oil production are ground and flattened. Usually, crude oil has undergone several mechanical processes, including heating continuously and pressing. Then, the edible oil is obtained by pressing, followed by solvent extraction using solvents such as food-grade hexane. Limiting using an organic solvent, directly cooking at high temperature with appropriate pressure has become more popular (Rodrigues et al., 2016). Although food grade standards are used for separating oil, further refinement of crude oil is necessary to eliminate undesirable compounds such as protein, phenolic compounds, and solvent traces. According to (FAOSTAT, 2020b), there were 600.47 million metric tons of oilseeds. Sunflower and rapeseed meals are co-products of oil processing. Hence, there are also enormous amounts of press meals of oil extraction. In particular, according to Terres Univia (Terres Univia, 2020), there are 560 tons of rapeseed meal and 540 tons of sunflower meal annually produced in France. Therefore, sunflower meal (SFM) and rapeseed meal (RSM) are promising alternative protein sources to meet the increasing demand for protein foods not only for animal feed but also for human consumption in the future (Arrutia et al., 2020). Indeed, sunflower meal (SFM) contains up to 40% protein when the sunflower seeds are subject to extraction by cooking, whereas in the oil extraction step

using an organic solvent, the percentage of protein is up to 55%. The proportion of protein varied greatly depending on if the seeds were de-hulled or not. With de-hulled seeds, the protein composition can range from 53 to 66%. Rapeseed meal (RSM) is also rich in protein, with a quantity of up to nearly 40%. In the following parts of this Ph.D. thesis, the components of SFM and RSM are described thoroughly.

2.2. Composition of sunflower meal and rapeseed meal

Rapeseed meal (RSM) and sunflower meal (SFM) are the by-products of the rapeseed de-oiling process. RSM and SFM are used for animal feed due to their richness in protein (40% for RSM and 66% for SFM) (Downey & Bell, 1990; Quinn et al., 2017). These oilseed meals also contain phenolic compounds (Quinn et al., 2017). Several authors have researched SFM and RSM's components for animal consumption purposes in the past decades due to their nutritional features such as protein, fibers, and minerals (Briones et al., 2012; González et al., 2011). These components can vary according to genotype, geography, degree of hull removal, and extraction methods (Wildermuth et al., 2016).

2.2.1. Sunflower meal (SFM)

In general, SFM contains protein (about 30% of dry matter on average), fiber (about 40%), and the minor composition of phenolic compounds, moisture, and ash. All the previous data of the composition of SFM presented in Table 2.1 on a range from minimal and maximal percentage.

Table 2.1. Composition of SFM on average according to bibliographic data

No.	Component	Composition range (%)	Bibliographic data* (%)
1	Crude proteins	29-55.5	55.5-29-34-32-31.7-36.33
2	Crude lipid	0.5-2.00	0.5-1.15-2.00-1-6
3	Crude fiber	29-50	37-29-50-33.6-43
4	Total phenolic content	2.4-4.7	3.4-2.4-4.7-2.7
5	Lignin	8.4-26.8	26.8-8.4
6	Moisture	6.5-10.4	6.5-8.0-9.0-10.4-9.92
7	Ash	4.3-11.202	8.5-6.0-4.3-6.6-7.1-11.202

Adapted from: * (Bautista et al., 1990; Boni et al., 1987; Dominguez et al., 1995; Geneau-Sbartaï et al., 2008; Lin et al., 1974; Parrado & Bautista, 1993; Ramachandran et al., 2007; Salgado et al., 2012; Wanjari & Waghmare, 2015)

According to Table 2.1, the composition of SFM after defatted oil is mostly proteins (29 to 55.5%) on a dry weight basis. This protein percentage dramatically increases up to 55.5% in de-hulled seeds used for protein extract. Besides, fiber increased from 29 up to 50%, the percentage of lipid is 0.5-2.00%, and lignin 8.4-26.8%, ash 4.3-11.202%, moisture 6.5-10.4% on a dry basis. Notably, total phenolic content ranges from 2.4 to 4.7% on the dry weight. It is noteworthy that the composition of SFM changes depending on the geographic zone. SFM originating from Italy contained mainly protein (29.0%) and non-nitrogen compounds (26.7%), and the crude fibers were proportioned at a high value of 28.9%. Meanwhile, saccharides and low molecular-weight oligosaccharides 6.0%. Notably, total phenolic compounds were 2.4%. It also contains moisture 8.0%, crude lipid 1.15%, and ash 6.1% (Boni et al., 1987). Hulls of sunflower contained 50% in polysaccharides, mainly xyloses (14-16%), glucose

(19-20%), protein 29%, and galacturonic acid (9-10%). In contrast, the ethanol-soluble carbohydrate was 25-30% (Thibault et al., 1989). Parrado and Batis (Parrado & Bautista, 1993) found that SFM contains amino acids such as leucine, valine, tyrosine, isoleucine, arginine, threonine, and histidine, and tryptophan. The major amino acids were arginine, leucine, valine, glycine, and phenylalanine (Ramachandran et al., 2007). The report of Dominguez et al. (Dominguez et al., 1995) indicated that the content of phenolic compounds in SFM ranged from 3 to 4% (w/w). The proportion of chlorogenic acid (CGA), an ester of caffeic acid and quinic acid, in these phenolic compounds was up to 70%. The other phenolic compounds presented in SFM were caffeic acid, p-hydroxybenzoic, p-coumaric, cinnamic, m-hydroxybenzoic, vanillic, syringic, trans-cinnamic, iso-ferulic, and sinapic acid. However, the composition of each compound was not investigated.

2.2.2. Rapeseed meal (RSM)

Rapeseed meal (RSM) is the by-product of rapeseed oil after oil extraction and is widely used for animal protein consumption (Downey & Bell, 1990). All the data regarding the composition of RSM in range values are synthesized in Table 2.2. In most cases, the crude proteins were 33.9-39.47%, crude fiber was 9.7-13.9%, total phenolic content ranged from 0.02 to 1.705g of sinapic acid equivalent (SAE)/ 100g of dry matter, and other components such as moisture 7.2-10.0%, crude lipids 1.7-3.8%, lignin 5.52-95%, and ash 6.3% (Lomascolo et al., 2012).

Table 2.2. Composition of RSM on average according to bibliographic data

No.	Component	Composition range (%)	Bibliographic data* (%)
1	Crude proteins	33.9-39.47	33.9-36.0-35.9-33.9-33.9-39.47
2	Crude lipids	1.7-3.8	2.6-1.7-3.8-1.7
3	Crude fiber	9.7-13.9	13.9-11.7-11.2-9.7-12.7
4	Total phenolic content	0.02-1.705	
5	Moisture	7.2-10.0	7.2-9.8-10.0-7.7-7.26
6	Ash	1.31-6.5	6.1-6.5-6.2-1.31
7	Lignin	5.52-95	95-5.52-32.39-7.9

Adapted from: * (Ballester et al., 1970; Bell, 1984; Bell & Jeffers, 1976; Blair & Scougall, 1975; Briones et al., 2012; Eriksson et al., 2009; Remón et al., 2018; Siddiqui & Wood, 1977; Theander et al., 1977; Vuorela et al., 2004; Zago et al., 2015).

Like the composition of SFM, the variance of RSM components derives from geography, genotypes, and the presence of hulls. In most cases, the crude fiber, protein, amino acids such as lysine, minerals such as calcium, phosphorus, and iron remained at a relatively high level (Ballester et al., 1970). Blair and Scougall performed the experiments of determining the RSM components source from European countries and Canada. They found that the lipid 1.7% found in *B. napus* was higher than in *B. canpestris*. The primary amino acids were found, including leucine, lysine, arginine, valine, threonine, phenylalanine, glycine, and isoleucine. RSM from Canada contained crude protein 35.9%, crude fiber 11.2%, lipid 3.8%, moisture 7.7%, and ash 6.5%. Regarding carbohydrates, RSM contained mainly pectins, pentosans, and cellulose (Bell, 1984; Siddiqui & Wood, 1977). Rapeseed meal has high nutraceutical values because it contains up to 40% protein and amino acids, is high in fiber, and rich in

mineral ingredients such as calcium, magnesium, zinc, and copper (Naczk et al., 1998). RSM also contains vitamins such as tocopherol, several B vitamins, and choline, making RSM of very high nutritional value (Naczk et al., 1998). RSM is also rich in phenolic compounds, and it contains the highest amounts of phenolic compounds among the oilseed plant, such as soybean, peanut, and cottonseed (Kozlowska et al., 1990a; Nowak et al., 1992). Among these phenolic compounds, sinapine, a choline ester of sinapic acid, is present up to 90% of total phenolic compounds (Kozlowska et al., 1990a; Vuorela et al., 2004). Sinapic acid in RSM exists as the ester forms of glucoside, glucopyranosyl sinapate (Amarowicz et al., 1994). A proportion of only less than 1.6% of sinapic acid exists in the RSM. Notably, the amount of SA derivates can vary from 6.390 to 18.370 mg/g upon to oilseed plant (Kozlowska et al., 1990b). RSM is also rich in mineral ingredients such as K and P 1.30%, S 0.91%, Ca 0.72%, Mg 0.54%, and Fe, Si, Al, and Na traces (Briones et al., 2012; Egües et al., 2010; Eriksson et al., 2009).

2.3. Phenolic compounds in sunflower and rapeseed meal

2.3.1. Phenolic compounds background

"Phenolics" can be defined as compounds that contain an aromatic ring linked directly with one hydroxyl group. Whereas the term "polyphenols" can be formed as compounds that possess one or more than one aromatic ring bearing several hydroxyl groups. In most literature, the two words "phenolics" and "polyphenols" were usually used frequently with the same meaning. Hence, in this Ph.D. work, those are used to indicate a similar meaning.

2.3.2. Classification of phenolic compounds

To give a better understanding, in this part of the Ph.D. project, we illustrated all general principle of chemical structures of these categories of phenolic compounds presented in plant sources, as shown in Figure 2.2. According to Bravo et al. (Bravo, 1998), based on their chemical structural characteristics; phenolic compounds can classify into two main groups, including flavonoids and non-flavonoids. Non-flavonoids are benzoic, and cinnamic acid (commonly known as phenolic acids) (Ambriz-Pérez et al., 2016), and several other phenolic acids are stilbenes, tannins, and lignins (Ambriz-Pérez et al., 2016). Non-flavonoids can be divided into two –subgroups of hydroxybenzoic, which in common have the C_6-C_1 structure, and hydroxycinnamic acids, which have three-carbon side chains attached directly with benzene ring commonly having the C_6-C_3 structure (Bravo, 1998). According to Hua Zhang and Rong Tsao (H. Zhang & Tsao, 2016), the non-flavonoids type can be represented in plants up to 30%. Typically, according to Kozlowska et al. (Kozlowska et al., 1983), the main phenolic compounds represented in oilseed plants, in general, are derivates of hydroxyl benzoic (C_6-C_1) and hydroxycinnamic acids (C_6-C_3) as well as coumarins (C_6-C_3), flavonoids, and lignins (C_6-C_3-C_6). Figure 2.3 represents several examples of compounds for hydroxybenzoic acids and hydroxycinnamic acids in natural sources.

On the other hand, flavonoid groups are the largest group of phenolics derived from plants (Dey & Harborne, 1997). Flavonoids possess two aromatic rings (ring A and ring B, Figure.2.2) linked through an oxygen heterocycle (ring C) to construct a typical C_6-C_3-C_6 skeleton structure (Figure.2.2). Depending on the degree of hydrogenation and oxygen heterocycle location, this group can be sub-classified as flavanones, flavonols, isoflavones, flavonols, and anthocyanidins. Notably, flavonoids are usually present in the plant as glycosides (Ambriz-Pérez et al., 2016).

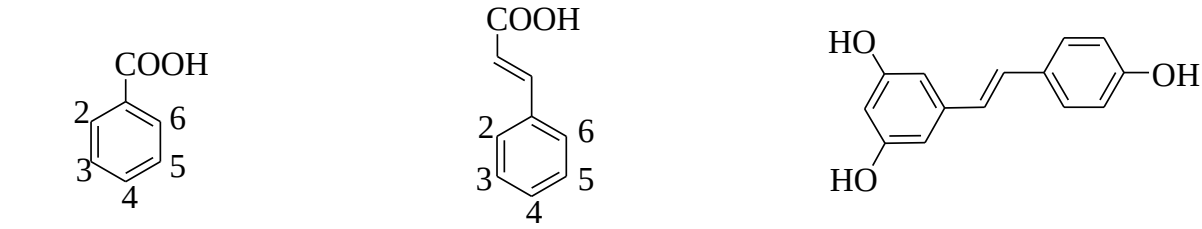

Benzoic acid (C_6-C_1) Cinnamic acid (C_6-C_3) Stilbenes (C_6-C_2-C_6)

General structure of the principal non-flavonoids compounds

Flavonoids (C_6-C_3-C_6)

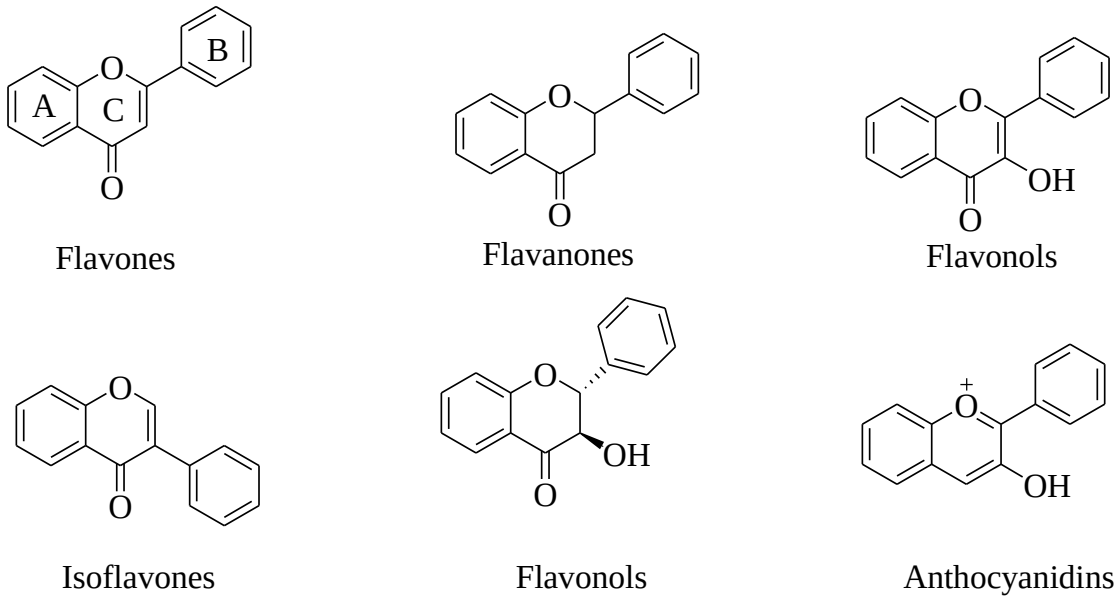

Flavones Flavanones Flavonols

Isoflavones Flavonols Anthocyanidins

General structure of the principal flavonoids compounds

Figure 2.2. General chemical structures of phenol and phenol derivatives (C6) in plant sources.

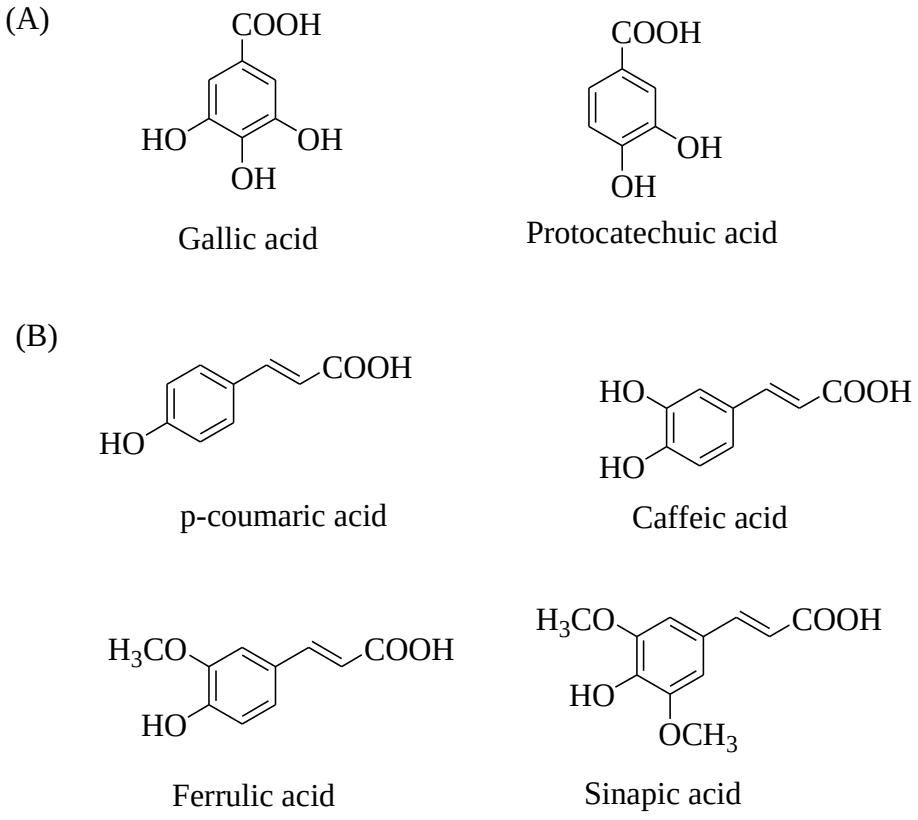

Figure 2.3. Examples of hydroxybenzoic (A) and hydroxycinnamic acids (B) commonly occur in plants (Adapted from N. Balasundram et al. (Balasundram et al., 2006)).

According to Porter (Porter, 1989), tannins, the high molecular weight molecules, also represent plants. Tannins consist of gallic acid esters (Figure 2.4) or the polymers of polyhydroxyflavan-3-ol monomers (also known as pro-anthocyanidins). Tannins can be subdivided into hydrolyzable and condensed tannins.

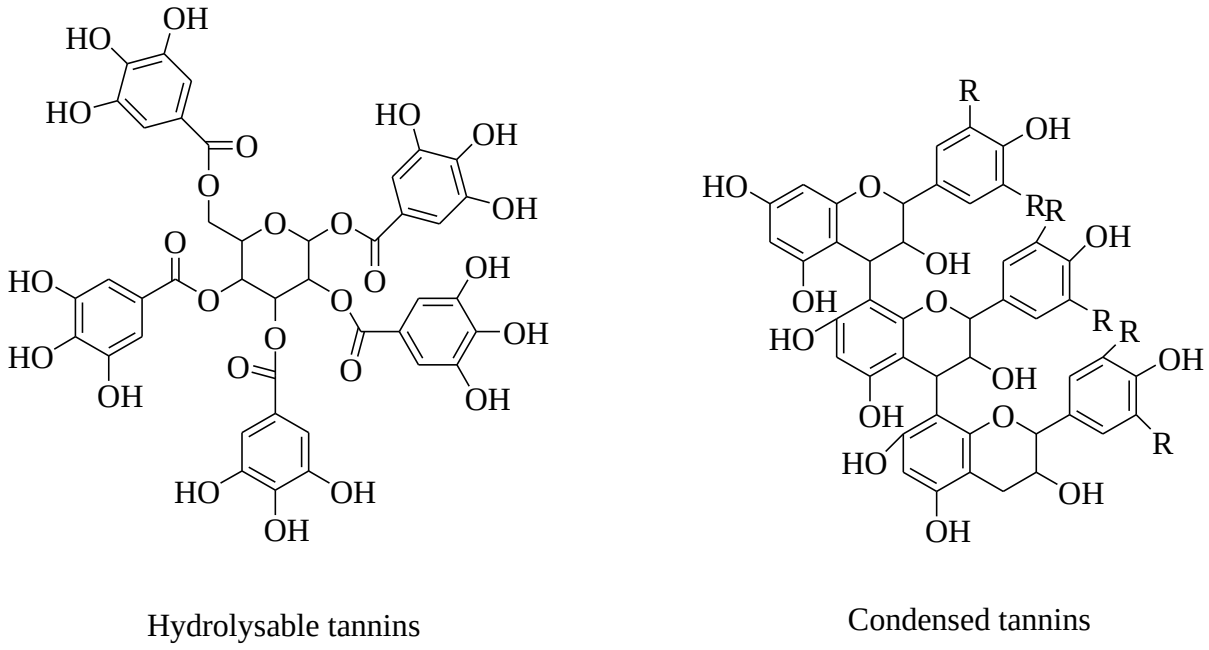

Figure 2.4. Chemical structure of tannins presented in plant sources.

Table 2.3 summarizes all the categories of these compounds in the literature through the chemical structures of various phenolic compounds found in plants.

Table 2.3. Phenolic compounds classification in plants.

(Adapted from Harborne, (Dey & Harborne, 1997))

Type of phenolic compound	Structure
Simple phenolics, benzoquinones	C_6
Hydroxybenzoic acids	C_6-C_1
Acetophenone, phenylacetic acids	C_6-C_2
Hydroxycinnamic acids, phenylpropanoids (coumarins, iso-coumarins, chromones, chromenes)	C_6-C_3
Napthoquinones	C_6-C_4
Xanthones	C_6-C_1-C_6
Stilbenes, anthraquinones	C_6-C_2-C_6
Flavonoids, iso-flavonoids	C_6-C_3-C_6
Lignans, neolignans	$(C_6$-$C_3)_2$
Biflavonoids	$(C_6$-C_3-$C_6)_2$
Lignins	$(C_6$-$C_3)_n$
Condensed tannins (proanthocyanidins)	$(C_6$-C_3-$C_6)_n$

2.3.3. Phenolic compounds in sunflower meal

In this Ph.D. project, we listed all the chemical structures of phenolic compounds reported from different authors' data for the general view of SFM and RSM phenolic compounds identification in Figure 2.5 and Figure 2.6 and Table 2.4. In general, SFM represents eight free phenolic acids, 12 esterified phenolic compounds, and five flavonoids derivates. SFM is composed mainly of CGA (from 1-2% of dry matter). There are free phenolic acids, insoluble-bound phenolic compounds, and esterified phenolic acids in RSM, major in sinapine and sinapic acid derivates. RSM presented sinapine, sinapic acid, and sinapoyl glucose as a primary compound (Thiyam et al., 2006). Besides, the complex phenolic compounds are as well known as condensed tannins also were found in RSM.

Table 2.4. Phenolic compounds identified in SFM and RSM in literature

No.	Phenolic compounds in SFM*	Phenolic compounds in RSM**
1	Ferulic acid	Ferulic acid
2	p-coumaric acid	p-coumaric acid
3	Caffeic acid (CA)	Caffeic acid
4	Quinic acid (QA)	Gallic acid
5	Sinapic acid (SA)	Sinapic acid (SA)
6	trans-cinnamic acid	Syringic acid
7	Vanillic acid	Vanillic acid
8	Syringic acid	Protocatechuic acid
9	3-*O*-Caffeoyl quinic acid (3-CQA)	p-hydroxybenzoic acid
10	4-*O*-Caffeoyl quinic acid (4-CQA)	Sinapine (majority) (SP)
11	5-*O*-Caffeoyl quinic acid (5-CQA) (majority)	Cyclic spermidine
12	3-*O*-p-Coumaroylquinic acid	Sinapoyl glucose (SG)
13	4-*O*-p-Coumaroylquinic acid	Sinapoyl glucopyranoside
14	5-*O*-p-Coumaroylquinic acid	1,2-di-*O*-sinapoylglucose
15	5-*O*-feruloylquinic acid	Disinapoyl glucopyranoside
16	3,4-di-*O*-caffeoylquinic acid (3,4-diCQA)	1,2-di-*O*-sinapoyl gentiobise
17	3,5-di-*O*-caffeoylquinic acid (3,5-di-CQA)	Trisinapoyl gentiobioside
18	4,5-di-*O*-caffeoylquinic acid (4,5-diCQA)	Sinapine (4-*O*-8')guaiacyl
19	Caffeoylferuloylquinic acid	Sinapine (4-*O*-8')guaiacyl-di-sinapoyl

20	Caffeoyl-di-methoxy cinnamoyl quinic acid	Feruloyl choline (5-8') guaoacyl
21	Ferulic acid dehydrotrimer	Feruloyl choline(5-8')guaiacyl
22	Quercetin derivative	Feruloyl choline(4-*O*-8')guaiacyl-di-sinapoyl
23	Quercetin glycoside	Kaempferol-3-*O*-β-sophoroside
24	Quercetin rutinoside	Kaempferol-3-*O*-sophoroside-7-*O*-β-glucopyranoside
25	Quercetin glucuronide	Sinapoyl-Kaempferol derivates
26	Flavanone	Kaempferol-di-hexoside-sinapoyl-hexoside
27	-	Kaempferol-sinapoyl-tri hexoside
28	-	Kaempferol-3-*O*-β-D-glucopyranosyl-(1→2)-β-D-glycopyranoside
29	-	Kaempferol-3-*O*-(2-*O*-sinapoyl)-β-D-glycopyranosyl-(1→2)-β-D-glucopyranoside-7-*O*-β-D-glucopyranoside
30	-	Tannin

Adapted from :* (Dabrowski & Sosulski, 1984; Karamać et al., 2012; Laguna et al., 2018; Romani et al., 2017; Sabir et al., 1974; Sastry & Rao, 1990; Sripad et al., 1982; Weisz et al., 2009). ** (Amarowicz et al., 1994, 2000; Dabrowski & Sosulski, 1984; Engels et al., 2012; Fang et al., 2012; Khattab, 2010; Koski et al., 2003; Krygier et al., 1982; Laguna et al., 2018; Naczk et al., 1998; Nowak et al., 1992; Quinn et al., 2017; Siger et al., 2013; Thiyam et al., 2006).

Table 2.5 gives the concentration of individual phenolic compounds and total phenolic content presented in sunflower meal (kernels and hulls) in the literature and their concentration ranges. The phenolic acid level in both meals depends on the genotypes, cultivated geography, and the degree of hull removal.

Table 2.5. The concentration of individual phenolic compounds and total phenolic content represent in sunflower kernels and hulls[a] available in bibliographic data (g/100g of dry matter)

Phenolic compounds	**Concentration range**	**Bibliographic data***
Ferulic acid	0.0058-0.17	0.0076-0.0105-0.0092-0.0058-0.17-0.16-0.14-0.009[a]
Caffeic acid (CA)	0.006-0.18	0.56-0.82-0.58[a]-0.17-0.02-0.9609-0.18-0.06-0.17-0.006[a]
Quinic acid (QA)	0.30-0.39	0.39-0.30-0.36[a]
trans-cinamic acid	0.006	0.006-0.06-0.07-0.05
Vanillic acid	0.0008	0.0008
Syringic acid	0.0022	0.0022
Sinapic acid	0.00-0.57	0.00-0.48-0.57-0.48
p-hydroxybenzoic acid	0.006-0.0014	0.006-0.0014
p-coumaric acid	0.0056-0.11	0.0056-0.09-0.11-0.10
3-*O*-Caffeoyl quinic acid (3-CQA)	0.0019-0.519	0.480-0.268-0.519-0.0019[a]
4-*O*-Caffeoyl quinic acid (4-CQA)	0.0018-0.118	0.058-0.118-0.091-0.0018[a]
5-*O*-Caffeoyl quinic acid (5-CQA /CGA)	0.02-3.0501	1.86-2-0.93[a]-2.00-0.0591-3.0501-0.0591-3.050-2.795-2.364-2.473-1.97-1.94-2.08-0.02[a]
Total chlorogenic acid (CGA) isomers	0.0253-70	0.44-55-70-3.358-2.773-3.104-0.17-0.13-0.12-0.0253[a]
5-*O*-p-Coumaroylquinic acid	0.0011-0.0113	0.0113-0.0102-0.0106-0.0011[a]
5-*O*-feruloylquinic acid	0.001-0.0173	0.0165-0.0173-0.0122-0.001[a]
3,4-di-*O*-caffeoylquinic acid (3,4-diCQA)	0.0011-0.0314	0.0149-0.0314-0.0299-0.0011[a]
3,5-di-*O*-caffeoylquinic acid (3,5-di-CQA)	0.0018-0.1171	0.0582-0.1171-0.0912-0.0018[a]
4,5-di-*O*-caffeoylquinic acid (4,5-diCQA)	0.0037-0.1338	0.0463-0.2275-0.1338-0.0037[a]
Total phenolic content (gCGA equivalent/100g of dry matter)	0.051-4.2	4.2-2.9388-4.1759-3.2919-3.611-2.530 -3.050-0.051[a]

Adapted from: * (Dabrowski & Sosulski, 1984; Laguna et al., 2018; Sabir et al., 1974; Sastry & Rao, 1990; Sripad et al., 1982; Weisz et al., 2009).

G. Sripad et al. (Sripad et al., 1982) found that in defatted sunflower seed flour extracted with aqueous methanol, ethanol, isopropanol, and acetone contained chlorogenic acid (CGA) up to 1.86g/100g SFM. Whereas, caffeic acid, and quinic acid were 0.56 and 0.39g/ 100g of SFM, respectively. Notably, the CGA in SFM was in the range of value from 1.42 to 4.00% on a dry basis (Dorrell, 1976; Shamanthaka Sastry & Subramanian, 1984). Notably, for SFM with hulls, these values were lower (0.93, 0.58, and 0.36%, corresponding to CGA, CA, and QA, respectively) (Sripad et al., 1982). CGA was the main phenolic compounds in SFM (Sripad et al., 1982). CGA, CGA isomer, and CA can constitute up to 70% of the total phenolic compounds (Sabir et al., 1974). In the kernel of sunflower (SF) seed, CGA and CA are the main phenolic compounds with amounts up to 700g/kg of total acids (Shamanthaka Sastry & Subramanian, 1984). There were four phenolic compounds present in the kernel, ranging from 94.6% to 99.3% of the whole seed's total phenolic contents, including CGA, CA, and two caffeoylquinic (CQA) derivates, including 1,4-di-CQA and 1,5-di-CQA (Pedrosa et al., 2000). The major phenolic compound was CQA ranging from 550 to 700g/kg depending on the genotype of SFM (Pedrosa et al., 2000). There were 11 individual compounds of non-oilseed and oilseed sunflower kernels and shells in different European countries such as Italy, France, and Germany (Weisz et al., 2009). The total phenolic content (TPC) ranged from 2938.8mg/100g to 4175.9mg/100g dry matter (DM) for the de-hulled kernels. Non-oilseed sunflower kernels had slightly differed in a range of 3291.9-3611.0 mg/100g DM. The lowest TPC was found in Italian SFM, and the highest was found in French samples (Weisz et al., 2009). 5-CQA (as called CGA) was predominant, 59.1/100g and 3050.5mg/100g DM in the kernels. Meanwhile, these other phenolics such as caffeic acid, ferulic acid, and quinic acid derivates only made up a minor proportion. Typically, these SFM contains non-esterified phenolic acids 0.8-3.6%, coumaric acid and ferulic acid derivates 0.4-5.9% (Salgado et al., 2012; Weisz et al., 2009). The new isomers of coumaroylquinic acid (probably 3-*O*-coumaroylquinic acid and 4-*O*-p-coumaroylquinic acid) and dicaffeoylquinic acid (probably 1,3-di-*O*-caffeoylquinic acid and 1,4-di-*O*-caffeoylquinic acid) were also found from sunflower meal (Albe Slabi et al., 2019; Karamać et al., 2012; Laguna et al., 2018; Romani et al., 2017). Total phenolic content in SFM was 25.3±0.4 mg CGA equivalent/ g dry matter (Laguna et al., 2018). All chemical structures of phenolic compounds present in SFM are illustrated in Figure 2.5.

2.3.4. Phenolic compounds in rapeseed meal

Table 2.6 expresses the concentration of the individual phenolic compound in RSM in bibliographic data. The quantification of each phenolic compounds also depends on genotypes, cultivated zone, and the degree of hulls. According to these data, it contains abundant phenolic compounds. Nowak et al. (Nowak et al., 1992), rapeseed possesses the highest phenolic contents among oilseeds investigated in his work. Phenolic compounds represented in rapeseed can be divided into three

sub-groups: free phenolic acids, esterified phenolic acids, and insoluble-bound phenolic compounds (Krygier et al., 1982; Naczk et al., 1998). Sinapic acid and its derivates are predominant in RSM (Siger et al., 2013). The crude extract's total phenolic content ranged from 1577 to 1705 mg/ 100g dry matter (Siger et al., 2013).

Table 2.6. The concentration of individual phenolic compounds represents total phenolic content in rapeseed and hulls[a] available in bibliographic data (g/100g of dry matter).

Phenolic compounds	**Concentration range**	**Bibliographic data***
Sinapic acid (SA)	0.017-0.639	0.024-0.059-0.0454-0.017-0.0454-0.639-1.837-0.0174-0.0364-0.033-1.110-0.09
Protocatechuic acid	Trace-0.0612	0.0028[a]-0.0612[a]-trace
Ferulic acid	0.0012-0.015	0.0012-0.015
p-coumaric acid	0.00-trace	0.00-trace
Caffeic acid	Trace-0.0008	0.0008-trace
Syringic acid	0.0011-0.0022	0.0022-0.0011
Vanillic acid	0.0007	0.0007
p-hydroxybenzoic acid	0.0009-0.0056	0.0009-0.0056
Sinapine (major) (SP)	0.0005-9.46	0.2861-0.307-0.0005-9.46-1.24
Sinapoyl glucose (SG)	2.37-4.01	2.37-4.01
Free phenolic acids content	6.0-26.2	24.4-26.2-24.8-9.8-8.4-6.0-7.2-11.9-14.4-6.2
Cyclic spermidine	0.039	0.039
Esterified phenolic acids content	57-152	120-147-146-98-120-57-70-118-152-121
Insoluble-bound phenolic acids content	0.5-10.5	9.6-10.5-10.1-0.5-0.5-3.9-6.9-5.1
Total phenolic content (gSAE/100 g of dry matter)	0.0203-1.705	1.577-1.705-0.783-0.881-1.379-0.0203-0.0407-0.64-1.28-1.66
Tannin	1.4-230[a]	1.4[a]-230[a]-151[a]-13[a]-12[a]-6[a]-9[a]-19[a]-59[a]

Adapted from: *(Fang et al., 2012; Kozlowska et al., 1983; Laguna et al., 2018; Q. Liu et al., 2012; Matthäus, 2002; Naczk et al., 1998; Nićiforović & Abramovič, 2014; Quinn et al., 2017; Siger et al., 2013).

Qin Liu et al. (Q. Liu et al., 2012) investigated the soluble and insoluble phenolic compounds from ten different varieties of RSM in China (*Brassica napus* L.). A total of seven soluble phenolic compounds and eight insoluble phenolic compounds have been identified. Seven soluble phenolic compounds found in RSM are sinapine (a major with an amount on average of 18.28 mg/ g dry matter), 2 and 3 sinapoyl glucoside isomers, cis- and trans-sinapic acid (0.18 mg/ g dry matter), disinapoyl gentiobise, and disinapoyl glucoside. Besides, eight insoluble phenolic compounds are protocatechuic acid, hydroxybenzoic acid, caffeic acid, syringic acid, coumaric acid isomer, p-coumaric acid, trans-ferulic acid, and trans-sinapic acid. The total phenolics on average is 24.54 mg/ g dry matter. Baumert et al. discovered the presence of phenolic compounds in RSM were 1,6-di-*O*-sinaopylglucose, glucose esters, two gentiobiose esters (1-*O*-caffeoylgentiobise and 1,2,6'-tri-*O*-sinapoylgentiobiose), and two kaempferol conjugates being 4'-(6-*O*-sinapoylglucoside)-3,7-di-*O*-glucoside and 3-*O*-sophoroside-7-*O*-(2-*O*-sinapoylglucoside). Wolfram et al. discovered the several minor compounds include 4-*O*-glycosides of syringate, caffeoyl alcohol, and its 7,8-dihydro derivates, sinapate, sinapine, sinapoylated kaempferol glycosides. Notably, the hexodise of cyclic spermidine alkaloid was also observed (average concentration of 1.94 µmol/g) (Fang et al., 2012). Several new phenolic compounds including

kaempferol-sinapoyl-trihexoside, sinapoyl-hexosiden disinapoyl-dihexoside, disinapoyl-hexoside, and sinapoyl conjugates, were observed (Engels et al., 2012). Oscar Laguna et al. (Laguna et al., 2018) found a total of nine phenolic compounds, with the main phenolic compound being sinapine with 12.4±0.2 mg/g dry matter (75% of all phenolics). The free sinapic acid accounts for 0.9±0.0mg/g dry matter. The other phenolic compounds were identified as sinapic acid ester forms comprising a sugar (glucose, gentiobise) or kaempferol moiety. The total phenolic content in RSM was 16.6±0.3 mg of sinapic acid equivalent (SAE)/ g dry matter.

Naczk et al. (Naczk et al., 1998) confirmed the presence of tannin in RSM with hulls. Tannin, a polyphenolic compound, can be divided into two small groups that are condensed and hydrolyzable tannins. Tannins are formed by polymerization of flavan-3-ol or flavan-3,4-diols is condensed tannins, and is present in RSM. The quantity of tannin can vary from 0.2 to 3% of dry matter (Naczk et al., 1998). Some of the RSM tannins exist in insoluble forms due to polymerization or complexes with the fiber (Naczk & Shahidi, 2004a).

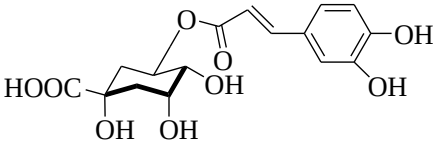

5-O-caffeoylquinic acid (5-CQA)

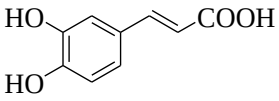

Caffeic acid

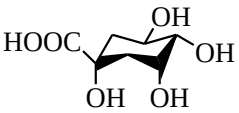

Quinic acid (QA)

The main phenolics in sunflower meal

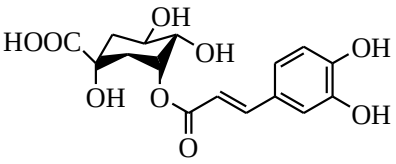

3-O-caffeoylquinic acid (3-CQA)

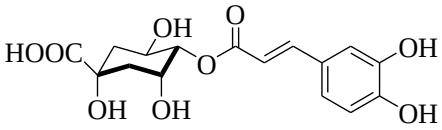

4-O-caffeoylquinic acid (4-CQA)

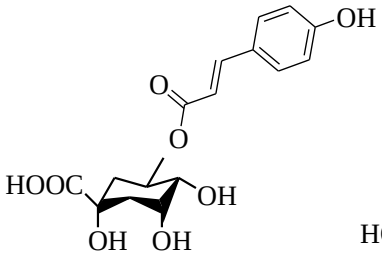

5-O-p-coumaroylquinic acid

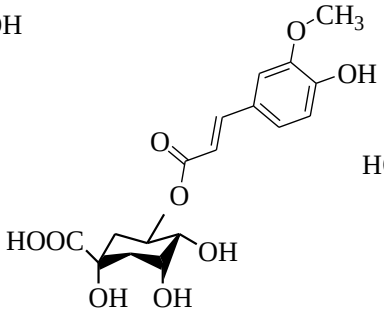

5-O-feruloylquinic acid

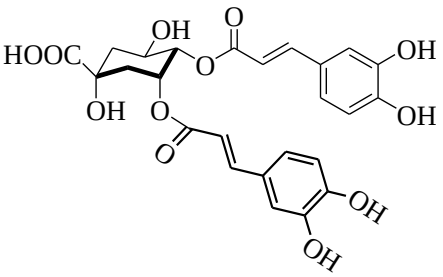

3,4-di-O-caffeoylquinic acid (3,4-diCQA)

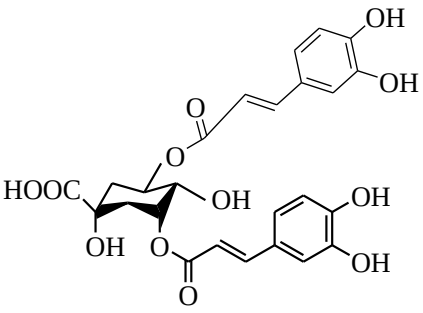

3,5-di-O-caffeoylquinic acid (3,5-diCQA)

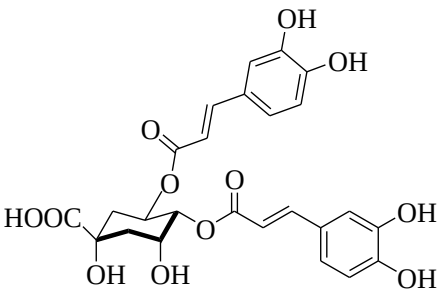

4,5-di-O-caffeoylquinic acid (4,5-diCQA)

The minor phenolics in sunflower meal

Figure 2.5. Phenolic compounds identified in rapeseed meal and their chemical structures.

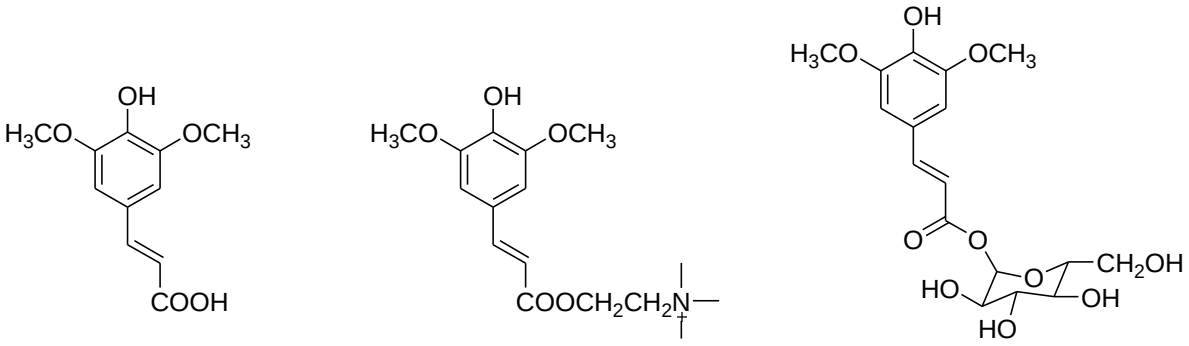

Sinapic acid Sinapine Sinapoyl glucose

The main phenolics in rapeseed meal

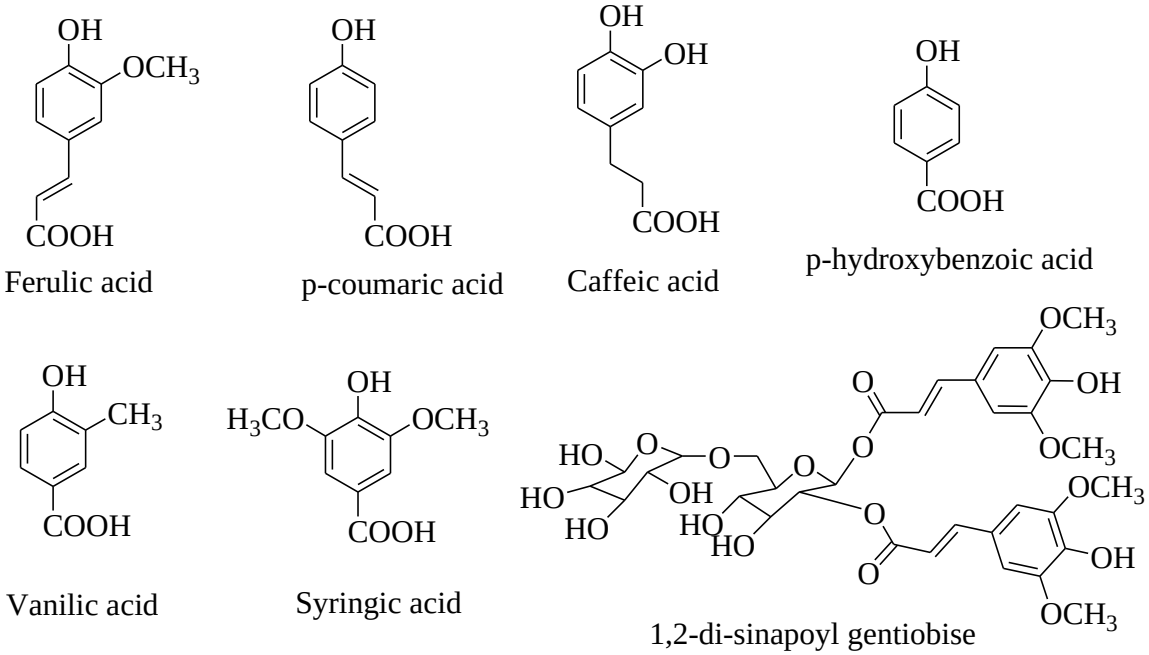

Ferulic acid p-coumaric acid Caffeic acid p-hydroxybenzoic acid

Vanilic acid Syringic acid 1,2-di-sinapoyl gentiobise

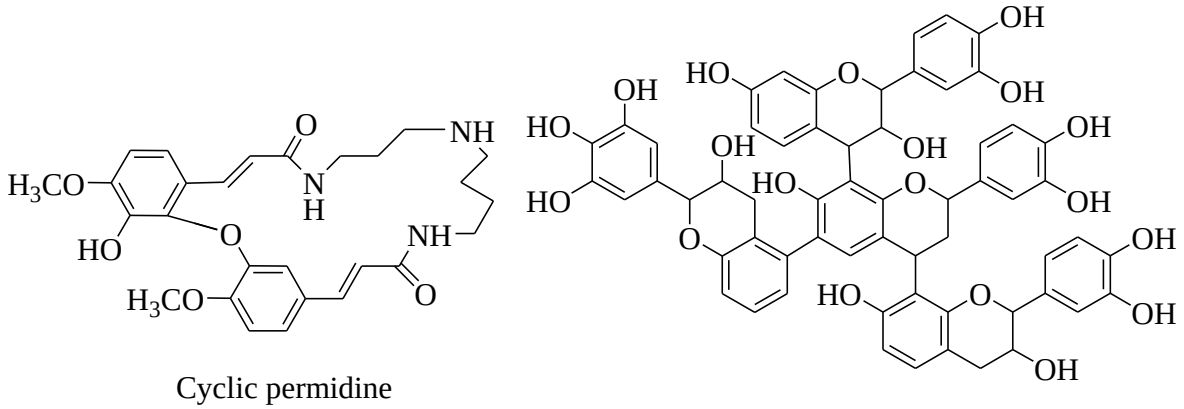

Cyclic permidine Condensed tannin

The minor phenolics in rapeseed meal

Figure 2.6. Phenolic compounds identified in rapeseed meal and their chemical structures.

Part II. Phenolic compounds extraction and purification process from sunflower and rapeseed meals

2.4. Extract of phenolic compounds from sunflower and rapeseed meals

The presence of phenolic compounds (PC) can interact with protein and acid amines presented in SFM and RSM (Weisz et al., 2010). As a consequence, these PC can lead to a reduced nutritional value (Shamanthaka Sastry & Subramanian, 1984). Therefore, many methods have been performed to remove the PC from SFM and RSM using aqueous, organic, and aqueous-organic solvents, as reviewed in this part of the Ph.D. project. However, organic solvents cause toxicity problems, environmental pollution, and safe status (Chemat et al., 2012). In particular, these phenolic compounds can be used in food and biomedical applications. Therefore, the novel extraction processes for recovering phenolic compounds from SFM have been carried out to date by using aqueous salt solution with different pH and different solid-liquid ratio to obtain the desired products (Albe Slabi et al., 2019; Geneau-Sbartaï et al., 2008; Shamanthaka Sastry & Subramanian, 1984; Sripad et al., 1982; Weisz et al., 2010). In the past decades, SFM and RSM were commonly extracted using an organic solvent such as methanol, ethanol, isopropanol, acetone, or a combination of these different methods described in Table 2.7 of recovery of phenolic compounds.

Table 2.7. Methods and solvents used for the extraction of sunflower and rapeseed phenolic compounds.

Extracted compounds	Extraction conditions	Main results	Reference
Sunflower meal SFM)			
Chlorogenic acid (CGA) from sunflower meal (SFM)	- water and salt solutions (NaCl, $CaCl_2$, and $MgCl_2$ solutions) - aqueous organic solvent (methanol, ethanol, isopropanol, and acetone, 0-80%, v/v) -pH 2-8	- pH 8 in water extract, CGA released up to 70% in a single extraction - NaCl did not affect -Maximum CGA extracted by organic solvent 20% (v/v) in water	(Sripad et al., 1982)
Chlorogenic acid (CGA) from SFM	- three extraction steps: (1) water-to-kernel ratio 12:1 (in 1% NaCl), (2) water-to-kernel ration 2:1, (3) water only	CGA was removal successfully after minimum two repeated extractions (up to 95% CGA removed	(Shamanthaka Sastry & Subramanian, 1984)
Caffeic acid, CGA, and their derivates in kernel and hull of sunflower seed	-Ethanol solution 80% (v/v) in water -Mechanical shaking for 30 min.	The extraction step was repeated four times to release phenolic compounds (PC) completely	(Pedrosa et al., 2000)
Phenolic compounds in kernel and hull of sunflower seeds	-Extracted twice in methanol solution in water (60%, v/v) -Room temperature -Stirring	-11 phenolic compounds were determined -CGA was found to be the predominant compound (up to 75% of the amount of total phenolic content)	(Weisz et al., 2009)
Phenolic compounds as co-extracted compounds in protein extracts from SFM	- NaCl 1.3M -at pH six during one h - Solid-to-solvent ranging from 0.05 to 0.13 g/mL	-CGA was achieved in a single extraction only, and repeated extractions were not necessary to perform -CGA was found to be the predominant compound (up to 75% of the amount of total phenolic content)	(Weisz et al., 2010)

Phenolic compounds in SFM as a co-extracted of protein extraction process from different SFMs	-Alkaline extraction (pH 12) - during 2 min at 50°C - solid: liquid ratio at 1:20	- Phenolic compounds was 4.7%/ total dry matter in averaged - CGA proportioned up to 2.8%/ total dry matter	(Geneau-Sbartaï et al., 2008)
Phenolic compounds from SFM	-80% (v/v) aqueous methanol -Shaking at 60°C -15 min in a water bath -extraction process was repeated in three times	5 sub-categories of phenolic compounds including non-esterified phenolic acids (0.935 mg/g of fraction), monoacylquinic acid (133.85 mg/g), diacyl quinic acids (32.78mg/g), ferulic acid dehydrotrimers (0.95mg/g), and flavonoids (4.26 mg/g)	(Karamać et al., 2012)
Phenolic compounds from SFM originated from India	-Extracted using absolute solvents include methanol, ethanol, acetone, isopropanol, ethylacetate - aqueous organic solvent in water include ethanol 50% and methanol 50% (v/v)	-The best conditions for PC extraction were 180 min, at solid: liquid = 5: 1 (v/w) and in any case of solvent systems. -the highest total phenolic content (TPC) belonged to ethanolic extract, whereas the lowest was observed for acetone extract.	(Wanjari & Waghmare, n.d.)
Phenolic compounds extracted from SFM originated from Italy	Ethanol 70% in water (v/v) extract	Five caffeoylquinic acids (CQA) were determined, including 3-CQA, 4-CQA, 5-CQA, 3,5-diCQA, and 4,5-diCQA	(Romani et al., 2017)
Phenolic compounds as a protein co-extracted of SFM derived from France	NaCl 0.5M solution with ratio of solid : liquid = 1 : 9 (v/w)	- 3 mono CQA isomers including 3-CQA, 4-CQA, and 5-CQA -Phenolic compounds, mainly in CGA (5-CQA), was relatively stable when extracted in a neutral and acidic range solution	(Albe Slabi et al., 2019)
Rapeseed meal (RSM)			
Free, esterified, and insoluble-bound phenolic acids extraction	- Several extractions needed (up to six times) - Methanol 70%: acetone 70% = 1:1 (v/v) in water - ratio of solid : liquid = 1 : 20 (v/w)	Total phenolic soluble and ester found after extraction was 9.8mg/100g of dry weight.	(Krygier et al., 1982)
Phenolic compounds, Sinapine	-Effect of the number of repetition (1-5 times) - Effect of duration (10-90 min)	-No statistical differences for the number of phenolic compounds extracted with the times and duration of extracts - A single extraction needed	(Thies, 1991; S. X. Wang et al., 1998)
Phenolic compounds	-Various concentration of methanol in water -Solvent to the meal: 100: 1	70% aqueous methanol would release PC greater than twice times when extracting with absolute methanol	(Naczk et al., 1992)
Phenolic compounds	-Various concentration of methanol in water -Solvent to meal: 6 : 1	No difference significantly when extract rapeseed phenolics with 100% methanol or with 70% (v/v) methanol at 75°C	(Cai & Arntfield, 2001; Thiyam et al., 2006; Vuorela et al., 2004)
Phenolic compounds	The organic solvent in water including 70% methanol, 70% isopropanol, or 70% ethanol	Methanol 70% (v/v) was the most effective solvent phenolic compounds extract compared to either 70% ethanol or 70% iso-propanol	(Khattab, 2010)

Tannins	Various acetone concentration	70% (v/v) aqueous acetone was most suitable used to extract rapeseed tannins	(Naczk et al., 2000)
Insoluble condensed tannins	-Different acetone concentrations -Mixture of various organic solvent	- Acetone 70% (v/v) is not an appropriate solvent for insoluble condensed tannins. -The mixed solvents include methanol, butanol, and hydrogen chloride is necessary to extract insoluble tannins in RSM.	(Q. Liu et al., 2012)

2.4.1. Extract of phenolic compounds from sunflower meal

Chlorogenic acid (CGA) can be extracted from SFM in water and salt solutions at different pH values (ranged 2-8) in aqueous organic solvents such as methanol, ethanol, isopropanol, and acetone (whose composition varied from 0-80%), and also in NaCl, $CaCl_2$, and $MgCl_2$ solutions. CGA released up to 70% in a single extraction at pH 8, while NaCl did not affect it. The maximum CGA is extracted by organic solvent 20% (v/v) in water (Sripad et al., 1982). However, another report confirms that CGA has been released up to 95% after three extraction steps were applied, including water-to-kernel ratio 12:1 (in 1% NaCl), then water-to-kernel ration 2:1, finally with water only (Shamanthaka Sastry & Subramanian, 1984). Following this method, Georg M. Weisz et al. (Weisz et al., 2010, 2013) used NaCl 1.3M at pH about 6 for 1 h to extract CGA from SFM. The ratio of solid-liquid was 0.05-0.13 g/mL. In this way, CGA was achieved up to 75% of the total phenolic content in a single extraction only, and repeated extractions were not necessary to perform. Phenolic compounds in SFM were also co-extracted with proteins by alkaline extraction (pH 12) for 2 min at 50°C for solid: liquid ratio at 1:20. Total phenolic compounds were estimated at 4.7% and 2.8% of CGA of the total dry matter (Geneau-Sbartaï et al., 2008). Three mono CQA isomers, including 3-CQA, 4-CQA, and 5-CQA in protein, co-extracted using NaCl 0.5M solution with a ratio of solid: liquid = 1: 9 (v/w) was also carried out. 5-CQA (known as CGA) was relatively stable when extracted in a neutral and acidic range solution (Albe Slabi et al., 2019). The extraction of phenolic compounds from SFM with aqueous salt solution with solid/ liquid ratio ranging from 1:2 to 1: 12 at pH 6-8 is the most common extraction method.

The extraction of phenolic compounds from SFM used not only aqueous salts solution but also organic solvent including ethanol (Pedrosa et al., 2000; Romani et al., 2017), methanol (Weisz et al., 2009), isopropanol, and ethyl acetate (Wanjari & Waghmare, n.d.) with different concentrations and with/ or without mechanical shaking (Pedrosa et al., 2000). Using ethanol solution concentration ranging 50-100% (v/v) in water to extract phenolic compounds from SFM has been well documented (Pedrosa et al., 2000; Romani et al., 2017; Wanjari & Waghmare, n.d.). The extraction step was repeated four times (Pedrosa et al., 2000). The highest total phenolic content (TPC) was 727.76 mg/g of gallic acid equivalent (GAE) on a dry basis belong to ethanolic extract (Wanjari & Waghmare, n.d.). In contrast, the lowest TPC (598 mg/g GAE) was observed for acetone extract (Naczk et al., 1992) with a solid : liquid ratio of 5:1 (v/w). Methanol concentration 50%-100% (v/v) has been used to extract

phenolic compounds in SFM at room temperature or at 60°C (Karamać et al., 2012; Wanjari & Waghmare, n.d.; Weisz et al., 2009).

2.4.2. Extract of phenolic compounds from rapeseed meal

Unlike the extraction of phenolic compounds from SFM, the extraction of those from RSM with aqueous methanol 70% (v/v) in water (Amarowicz et al., 1994; Cai & Arntfield, 2001; Khattab, 2010; Naczk et al., 1992; Thiyam et al., 2006) is the most common solvent used. Besides, the combination between methanol 70% and acetone 70% with ratio 1:1 and the ratio of solid: liquid = 1: 20 (v/w) also was used to yield a large amount of phenolic acid with total phenolic soluble and ester found after extraction was 9.8mg/100g of dry weight (Krygier et al., 1982). Surprisingly, Naczk et al. (Naczk et al., 1992) found that extract with 70% aqueous methanol would release greater than twice the PC than when extracting with pure methanol. However, in 2001, according to Cai and Arntfied (Cai & Arntfield, 2001), there was no difference significantly when extracting rapeseed phenolics with 100% methanol or with 70% (v/v) methanol at 75°C. One reason we can assume that this difference is due to the difference of solvent-to-meal ratio between two reports. This extraction method of Cai and Arntfied (Cai & Arntfield, 2001) was used again by Satu Vourela et al. (Vuorela et al., 2004) and Usha Thiyam et al. (Thiyam et al., 2009) in their work. The different solvents include 70% methanol, 70% isopropanol, or 70% ethanol on rapeseed phenolics extraction, were also investigated to find the most effective one in phenolic extraction (Khattab, 2010). The results showed that methanol 70% (v/v) was the best compared to 70% ethanol or 70% isopropanol.

Regarding the extraction duration process, the report of Thiers (Thies, 1991) demonstrated that the extraction time should not be more than 20 min. Nevertheless, there was no degradation of sinapine observed by Wang et al. (S. X. Wang et al., 1998). There were no statistical differences for the number of phenolic compounds extracted with the times and duration of extracts (Krygier et al., 1982). Hence, a single extraction with a short extraction time was suitable for phenolic compounds extraction from RSM.

Tannins in rapeseed meal were commonly extracted by 70% (v/v) aqueous acetone (Naczk et al., 2000). However, acetone 70% (v/v) is not an appropriate solvent for insoluble condensed tannins (Q. Liu et al., 2012). Mixed solvents including methanol, butanol, and hydrogen chloride are necessary to extract insoluble tannins in RSM (Naczk et al., 2000).

2.5. Hydrolysis phenolic compounds from rapeseed meal

To date, there is no data about hydrolysis of phenolic compounds from SFM. However, there are several reports regarding the hydrolysis of phenolic compounds from RSM. This issue might be the difference in chemical structures of phenolic compounds in RSM compared to in SFM. According to Thiyam-Holländer et al. (Thiyam et al., 2009), RSM's phenolic compounds comprise 61-70% sinapine, 14-27% sinapoylglucose, 7-10% sinapic acid, and 2-13% other phenolic compounds. Therefore, the hydrolysis sinapine or other conjugates of sinapic acid for analyzing sinapic acid and its derivates are two reasons. First, sinapine and sinapic acid derivates are not available as commercial standards. There

is only one company which can provide sinapine, but it is costly. Second, the separation process for sinapine carried out by Clandinin (Clandinin, 1961) is very time-consuming. Hydrolyzing phenolic compounds after extraction by sodium hydroxide to release free phenolic compounds from esters form has been done successfully in the past (Krygier et al., 1982; J. Li & El Rassi, 2002; Vuorela et al., 2003). Besides sinapic acid, a newly formed compound, probably the methyl ester of sinapic acid after hydrolysis, was observed (Siger et al., 2013). Alexander Thiel et al. (Thiel et al., 2015) used both methods including sodium hydroxide (NaOH) and hydrochloric acid (HCl), to yield sinapic acid. In this way, the amount of sinapic acid increased from 5.1 to 12.81 mg/g dry matter in the alkaline method. Meanwhile, the amount of sinapic acid after acidic hydrolysis was lower than in basic hydrolysis.

Besides chemical hydrolysis including acid and alkaline, enzymatic hydrolysis has been used to break down the ester bonds with sinapic acid. As a consequence, free SA can release. Satu Vuolera et al. (Vuorela et al., 2003) used ferulic acid esterase and Ultraflo L to hydrolyze sinapine as a main phenolic compound in RSM. There was up to 90% of sinapic acid derivates hydrolyzed to release SA. Besides, using enzymes for hydrolyzing sinapine to sinapic acid was more effective and less destructive to phenolic compounds compared with the basic hydrolysis method (Vuorela et al., 2003). Therefore, in this study, these authors recommended using enzymes for hydrolyzing.

On the contrary, according to Alexander Thiel et al. (Thiel et al., 2015), there was no significant difference between using alkaline hydrolysis and enzymatic hydrolysis in the yield of sinapic acid. Additionally, chemical hydrolysis has faster kinetics (Thiel et al., 2015). Hence, chemical hydrolysis should be preferred because it is less cost-effective, faster, and almost all sinapic acid esters were hydrolyzed (Thiel et al., 2015).

Overall, chemical (acid and alkaline) or enzymatic hydrolysis methods can break the linkages in RSM's phenolic compounds. However, it can also cause degradation of some phenolic compounds (using chemical hydrolysis) or lower recovery in the final extract due to high selectivity in certain phenolic compounds (using enzymes).

2.6. Capture phenolic compounds by adsorption

One of the techniques for separation of the selected phenolic compounds from dilute solution is adsorption. Adsorption shows several advantages compared to alternative technologies such as simple manipulation, operation, high capacity, ease of regeneration, scale-up, and low cost (Soto et al., 2011). That is why in this Ph.D. project, we used an adsorption/desorption process to obtain targeted phenolic compounds from SFM and RSM by-products from proteins extracts.

2.6.1. Background of adsorption

In general, the process of adsorbates adsorbing onto a solid surface of adsorbents is adsorption. It is based on the capability of pore filling of porous adsorbents along with several interactions, including hydrogen bonding, surface precipitation, and π-π interaction between adsorbents and adsorbates to capture the adsorbates. Figure 2.7 illustrates some basic terms of adsorption definitions. Adsorbents are the materials available to retain compounds on their solid surfaces, such as activated

carbons, zeolite, chitosan, and macroporous resins. Meanwhile, adsorbates are the targeted substances in the gas or liquid phase, such as phenolic compounds solute. These compounds can quickly accumulate on a solid surface of adsorbents. Nowadays, absorbate-adsorbent's adsorption process can be classified into two types, including physical and chemical adsorptions.

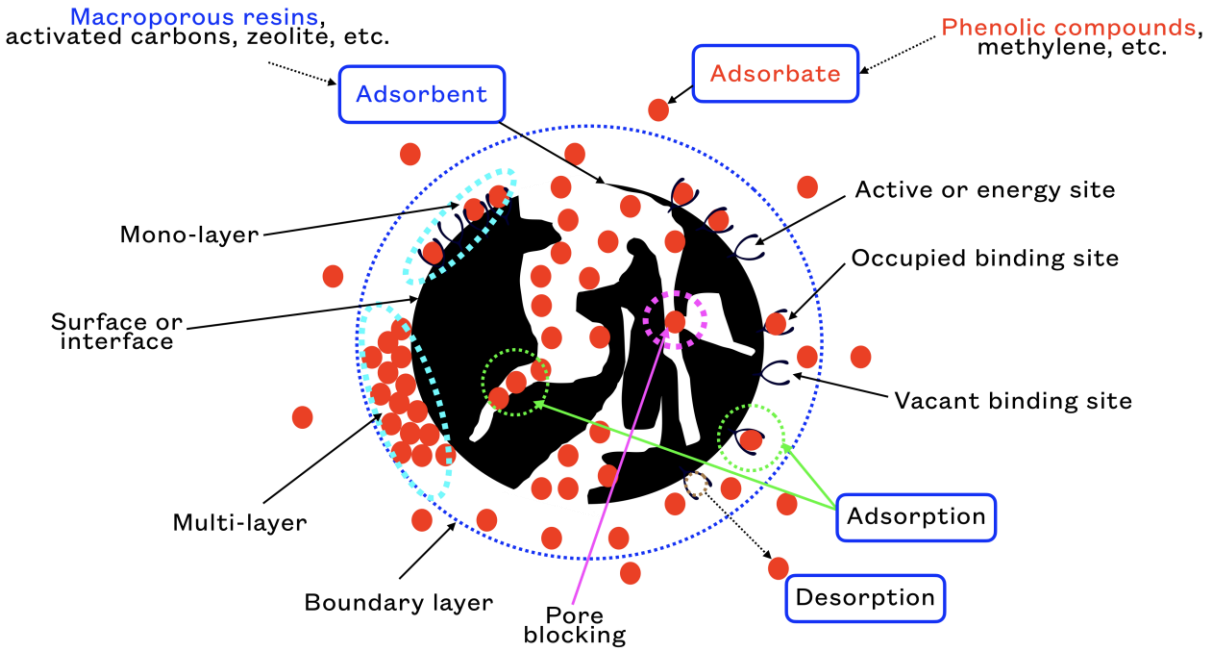

Figure 2.7. Basic terms using adsorption/ desorption science.

(Adapted with modification from H. N. Tran et al. (Tran et al., 2017)).

2.6.1.1. Physical adsorption (Physisorption)

Physical adsorption is based on the physical interaction between adsorbent-adsorbate. These interactions are Van de Waals forces, hydrogen bonding forces, π-π stacking interactions, and dipole interactions. Between adsorbates and adsorbed materials, there is no electrons exchange. Usually, this process is easy to occur and in a short time because of non-activation energy requirements. Besides, this process is non-specific and reversible. Therefore, after adsorption states reach the saturated point, eluted solvents can easily desorb the desired compounds.

2.6.1.2. Chemical adsorption (Chemisorption)

Unlike physical adsorption, chemical adsorption is achieved by the chemical interaction between adsorbents-adsorbates. Thus, this is specific, as well as irreversible. After the adsorption process, the electronic properties of adsorbents are also changed. The chemical adsorption process results in weak chemical adsorption (covalent bonds) or strong chemical adsorption (ionic bonds). Because of the required activation energy, the time needed to reach the equilibrium state in this type of adsorption can take time.

2.6.2. Adsorption mechanism

Figure 2.8 represents the mechanism of the adsorption process of the adsorbate molecules liquid-solid surface of the adsorbates/ adsorbents (Weber & Smith, 1987). There are four steps

associated with this adsorption process, which is proposed by Walter (Walters & Luthy, 1984). In the first stage, the adsorbates molecules transport from the bulk liquid phase to the external boundary layer. This step is known as bulk transport. It occurs quickly and can occur instantaneously; therefore, it can be negligible in most cases. In the second stage, it is film diffusion. This stage describes the mass transfer of adsorbates across from the external boundary layer into the solid particles through the hydrodynamic boundary layer or film. It occurs slowly. In the third stage, the adsorbate molecules travel from the particle surface into the adsorbents' pores and migrate along the pore-wall surfaces or both. This process is also known as intra-particle diffusion. It takes place slowly. The last stage involves the diffusion of adsorbate molecules from the pores into the active sites on the pore's interior surfaces. It may attach to the pore surface or adsorbents through surface diffusion. This process occurs quickly. Therefore, it is not significant for engineering design.

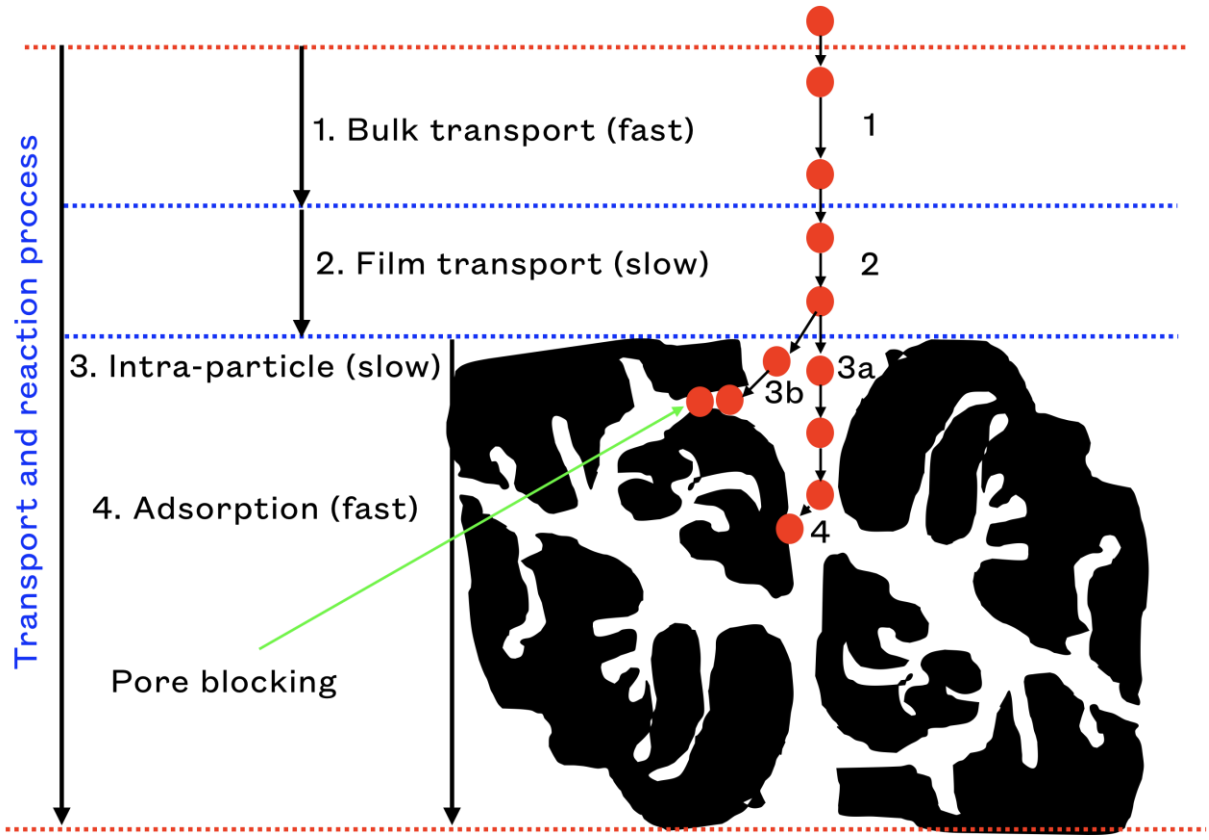

Figure 2.8. Particle diffusion mechanisms in adsorption by the porous adsorbent.
(Adapted with permission from Weber and Smith (Weber & Smith, 1987)).

2.6.3. Type of adsorbents to capture phenolic compounds

Nowadays, several types of adsorbents have been applied for adsorption-targeted compounds, such as phenolic compounds. These adsorbents can be classified as mineral adsorbents, activated carbons, and macroporous resins.

2.6.3.1. Mineral adsorbents

Several mineral adsorbents are siliceous materials, natural zeolite, and clay (J. Li & Chase, 2010). These materials also demonstrate ion exchangeability (X. S. Wang et al., 2008, p. 200). The

chemical modification of structure has also been proposed to increase minerals' affinity towards phenolic compounds' adsorption (Anirudhan & Ramachandran, 2006). The adsorption of phenolic compounds and lignin from olive mille wastewater has been investigated (Ugurlu & Hazirbulan, 2007).

2.6.3.2. Activated carbons

Activated carbons are self-assembled by free elementary carbon atoms to form many hydrophobic graphite layers. Usually, it constitutes about 3 to 4 parallel hexagonal carbon ring layers, as illustrated in Figure 2.9. The structure of activated carbons is constructed by randomly cross-linked and surrounded by numerous unpaired electrons. The geometric structure of activated carbons can form many porous. Therefore, activated carbon is also used for the adsorption of a wide range of molecules. The adsorption capacity of activated carbons material depends on their compositions, mechanical strength, and physicochemical properties (J. Li & Chase, 2010).

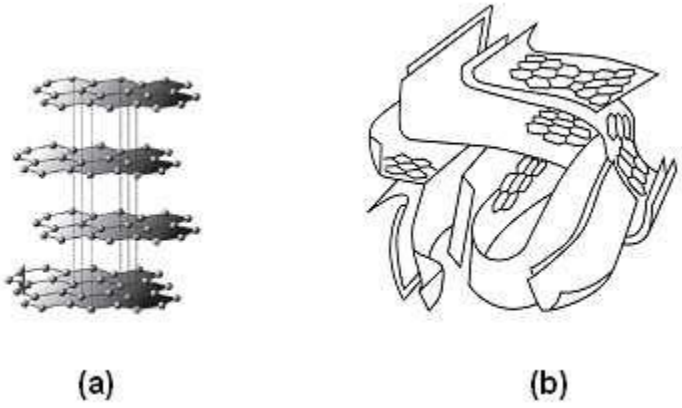

Figure 2.9. Structure of (a) carbon atoms in graphite crystal and (b) microstructure of the activated carbon.

(Reproduced with permission from the Internet).

2.6.3.3. Resins

These adsorbent materials are constructed by highly cross-linked and normally non-functionalized polymers and co-polymers. These characteristics of synthetic resins can provide a large amount of pore diameter (> 38 Å). For more detail regarding this information, consult Table. 2.8.

Table 2.8. Macroporous resins used in capture phenolic compounds in the literature

Resin	Pore diameter (Å)	Particle size (µm)	Surface area (m^2/g)	Matrix	Polarity	References
XAD-1	85-95	300-1250	800-1000 ≥ 1200	Styrene-divinylbenzene (SDVB)	Non-polar	(B. Fu et al., 2005; Jin et al., 2008)
XAD-2	90	250-840	330	Styrene-divinylbenzene (SDVB)	Non-polar	(J. Kim et al., 2014)
XAD-4	200-600 100	490-690	≥ 725-750	SDVB	Non-polar	(Dong et al., 2015a; J. Kim et al., 2014; Leyton et al., 2017; Moreno-González et al., 2020; Stanford et al., 2018; Q. Yang et al., 2016; Zagklis et al., 2015)
XAD-6	120-160	300-1250	450-500	SDVB	Polar	(Buran et al., 2014; Leyton et al., 2017; Zagklis et al., 2015)
XAD-7	90 80 450 200-600	250-840 560-710 300-1200	450 ≥ 380	Acrylic ester	Moderate-polar	(Buran et al., 2014; Idris et al., 2017; J. Kim et al., 2014; L. Lin et al., 2012; Moreno-González et al., 2020; Sandhu & Gu, 2013; Q. Yang et al., 2016; Zagklis et al., 2015)
XAD761	600	560-760	150-250	Phenol - formaldehyde	Polar	(Moreno-González et al., 2020; Sandhu & Gu, 2013)
XAD-16	210 150	250-840 560-710	630 ≥ 800	SDVB	Non-polar	(Buran et al., 2014; Dong et al., 2015a; Leyton et al., 2017; Moreno-González et al., 2020; Sandhu & Gu, 2013; Q. Yang et al., 2016; Zagklis et al., 2015)

XAD-1180	400	250-840	700	SDVB	Non-polar	(Buran et al., 2014; Moreno-González et al., 2020; Sandhu & Gu, 2013)
XAD-1600	150	250-840	800	SDVB	Non-polar	(Q. Yang et al., 2016)
HP-20	520 290	300-1250 250-850	600	SDVB	Non-polar	(Y. Chen et al., 2016; Firdaous et al., 2017; Idris et al., 2017; Leyton et al., 2017; Moreno-González et al., 2020; S. Wu et al., 2015a; Q. Yang et al., 2016)
HP-100	85-90	300-1250	650-700	SDVB	Non-polar	(Jia & Lu, 2008; Lv et al., 2008)
HP-200	85-90	300-1250	700-750	SDVB	Non-polar	(C. Ma et al., 2009)
HP-500	100-120	300-1250	500-550	SDVB	Polar	(Lv et al., 2008)
HP-600	100-120	300-1250	500-550	SDVB	Polar	(C. Ma et al., 2009)
HP-800	90-110	300-1250	700-750	SDVB	Moderate-polar	(M. Gao et al., 2007)
HP-850	85-95	300-1250	1100-1300	SDVB	Polar	(B. Zhang et al., 2008)
HP-2MGL	340	> 350	470	Methacrylate	Moderately-polar	(Y. Chen et al., 2016; Dong et al., 2015a; Guo, Guo, et al., 2018; L. Sun et al., 2013; Q. Yang et al., 2016)
NKA- II	145-155 140-160	300-1250	160-200	SDVB	Polar	(Chao et al., 2010; Y. Chen & Zhang, 2014; Guo, Guo, et al., 2018; L. Sun et al., 2013)
NKA-9	90-100 155-165	300-1250	500-550 250-290	170-250	Polar	(Dong et al., 2015a; Guo, Guo, et al., 2018; Ren et al., 2017)
AB-8	130-140	300-1250	480-520 450-530	SDVB	Weak-polar	(Y. Chen et al., 2016; Guo, Guo, et al., 2018; Ren et al., 2017; P.-C. Sun et al., 2015).
D101	90-150 100-110 130-140	300-1250	480-550 480-520	SDVB	Non-polar	(Ren et al., 2017; P.-C. Sun et al., 2015; S.

	200-300					Wu et al., 2015a; Q. Yang et al., 2016)
D4020	100-105	-	540-580	-	Non-polar	(L. Sun et al., 2013)
LS-305	150-250	-	400-500		Polar	
LS-46D	150-250	-	400-500		Polar	
ADS-2	105	250-600	650	-	Non-polar	(Firdaous et al., 2017)
ADS-5	250-300	300-1250	520-600	SDVB	Non-polar	(Ren et al., 2017)
ADS-7	250-300	-	≥ 100	-	Strong-Polar	(P.-C. Sun et al., 2015; S. Wu et al., 2015a)
ADS-17	90-150	300-1250	250-300	acrylic	Moderate-polar	(Ren et al., 2017; P.-C. Sun et al., 2015)
ADS-21	150-200	-	80-100	-	Polar	(P.-C. Sun et al., 2015)
ADS-F8	150-200	300-1250	100-120 170-250	-	Polar	(P.-C. Sun et al., 2015) (Ren et al., 2017)
ADS-8	120-160		450-500		Non-polar	
AL-2	150-250	300-1250	550-600	SDVB	Polar	(Y. Fu et al., 2006)
DM11	70-80	315-1250	≥500	SDVB	Non-polar	(Lv et al., 2008)
DM-301	140-170	300-1250	≥330	SDVB	Weak-polar	(Lv et al., 2008)
DM130	90-100	300-1250	500-550	SDVB	Weak-polar	(Y. Chen et al., 2016)
DS-401	120-140	300-1250	≥480	SDVB	Weak-polar	(X. S. Wang et al., 2008)
LSA-10	85-90	300-1250	500-540	methacrylic	Moderate-polar	(Y. Fu et al., 2006)
LSA-20	85-90	300-1250	420-500	methacrylic	Non-polar	(Y. Fu et al., 2006)
HPD-100	100-110	300-1250	500-550 480-520	-	Non-polar	(Guo, Guo, et al., 2018; Q. Yang et al., 2016)
HPD-400	85-90 75-80	300-1200	650-700 500-550	-	Middle polar	(Guo, Guo, et al., 2018; Q. Yang et al., 2016)
SP207	210	250	630	Brominated polystyrene/ divinylbenzene	Non-polar	(Dong et al., 2015a; Stanford et al., 2018; Q. Yang et al., 2016)
AER 1	-	425-1180	-	Trimethylamine	Strongly	(Firdaous et al., 2017)
AER 2	-	300-600	-	quaternary groups	basic anion-exchanger	
CER 1	-	200-240	-	Sulphonic acid	Strongly	
CER 2	-	225	-	groups	acid cation exchanger	
SP700	81	-	-	SDVB	Non-polar	(Conde et al., 2017)
SP-825	114	> 250	1050	Polystyrene	Weak polar	(Dong et al., 2015a; Q. Yang et al., 2016)
SP-850	38	300-800	930	SDVB	Non-polar	(Leyton et al., 2017)

X-5	290-300	290-300	500-600		Non-polar	(Y. Chen et al., 2016, 2016; L. Sun et al., 2013; P.-C. Sun et al., 2015; S. Wu et al., 2015a)
	250-290	300-1250	160-200		Polar	
FPX-66	200-250	600-750	≥ 700	SDVB	Non-polar	(Moreno-González et al., 2020; Sandhu & Gu, 2013)
HZ 816	60-70	300-1200	730-800		Non-polar	(Y.-J. Wang et al., 2012)
HZ 818	70-80	300-1000	880-920	-	Non-polar	
HZ 820	80-90	300-1200	680-800	-	Non-polar	
HZ 830	85-95	400-1000	780-820	-	Non-polar	
HZ 841	85-95	400-1200	500-600	-	Weak-polar	
HZ 806	60-70	300-1200	480-620	-	Medium-polar	
ENV+	800	90	1000	Hydroxylated polystyrene-divinylbenzene	Non-polar	(Bertin et al., 2011)
H-103	-	315-1250	1100	-	Non-polar	(Chao et al., 2010)
S-8	280-300	315-1250	100-120	-	Polar	(Y.-J. Wang et al., 2012)
Polyamid (30-60)	4500-10000	590-250	5-10	-	Hydrogen-bond	
Polyamid (60-100)	4500-10000	250-150	5-10	-	Hydrogen-bond	
EXA 90	105	250	630	SDVB	Non-polar	(Pompeu et al., 2010)
EXA 118	90	250	1200	SDVB	Non-polar	

SDVB: styrene–divinylbenzene

Besides activated carbons, mineral materials adsorbents, macroporous resin, and ion-exchange resins have been widely proposed to concentrate and purify phenolic compounds from natural sources (D. Kammerer et al., 2005; E. Silva et al., 2007; Soto et al., 2011). The first resins were synthesized by copolymerization of formaldehyde with phenolic compounds and aromatic amine derivates (Abrams & Millar, 1997). The ion-exchange resins also sufficiently synthesize to refine the sugar and deionization of water (J. Li & Chase, 2010). However, they showed a lack of several porous and stable skeletal structure for operation. Therefore, the better polymer structures were formed by using cross-linked polystyrenes to achieve the number of pores. The copolymerization of styrene (S) with up to 20% (w/w) amount of divinylbenzene (DVB) is used to synthesize styrene-divinylbenzene (SDVB) polymeric resins. The obtained degree of cross-linking of more than 10% is widely used to entrap non-polar or less polar organic compounds from aqueous solutions (J. Li & Chase, 2010). There are several synthetic polymeric resins that have been available (Soto et al., 2011). Although the adsorption capacity of macroporous resins is smaller than activated carbons ones, resins are durable, stable, can be re-used, high selectivity, easy to regenerate, scale-up, and enable applications in the food and pharmaceutical industry (S.-H. Lin & Juang, 2009).

Ion-exchange resins are manufactured by polymer matrix, including inorganic compounds (basic or acidic), polysaccharides, or modified synthetic resins with functional groups. The charge of the ion-active group defines the chemical properties of resins. The strong cation exchangers resins used

for removal of phenolic compounds compose sulfonic acid functional groups such as CER 1, 2 (Firdaous et al., 2017) (Table 2.8). The strong anion exchanger resins contain quaternary ammonium groups or trimethylamine quaternary groups such as AER1, 2 (Firdaous et al., 2017) or weak anion exchangers resins such as tertiary amine polymers.

2.6.4. Physical and chemical properties of the adsorbents

The most critical features of adsorbents, which determine usage, are the pore diameter, surface polarity, particle size, and the specific surface area.

2.6.4.1. Adsorbent pores

The total number of pores, shape, and particle size of macroporous resins are the critical factors influencing the adsorption capacity and the adsorbents' dynamic adsorption capacity. Therefore, the appropriate diameter pore size may result in the maximum capture of targeted compounds. Table 2.9 summarizes the range of pore sizes defined by the International Union of Pure and Applied Chemistry (IUPAC) (Rodriguez-Reinoso, 1989). The porous structure of the adsorbent is described in Figure 2.10. According to IUPAC, the macropores showed the largest pore size (the diameter is superior to 50 nm). This pore size is suitable for retaining phenolic compounds and is commonly used in literature. The pore diameter of dried resins usually ranges from 100 to 300 Å (J. Li & Chase, 2010). The lowest of this list are ultra-micropores (diameter is less than 0.7nm) and micropores (diameter is less than 0.2 nm). Whereas the super-micropores size is from 0.7 to 2nm and mesopore size ranges from 2 to 50 nm.

Table 2.9. IUPAC classification of pore sizes

Pores' types	Pore size (D, nm)
Ultra-micropores	D < 0.7
Super-micropores	0.7 < D <2
Micropores	D < 0.2
Mesopores	2-50
Macropores	D > 50

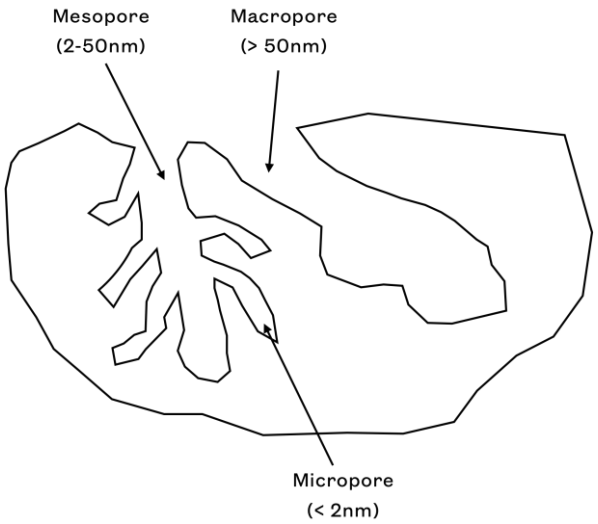

Figure 2.10. Illustration of different types of pores.

2.6.4.2. Adsorbent specific surface area

The specific surface area is one of the most crucial characteristics of adsorbents. Because it defines the adsorption capacity and range of usage of adsorbents surface, the total surface area of adsorbents can quantify the adsorption sites for adsorbates molecules attachment. The lower the specific surface area they possess, the larger amounts of molecules attached. Therefore, the micropores usually provide the largest proportion of the internal surface. As a result, most of the adsorption occurs in the micropores.

Meanwhile, the adsorbates are usually present on the external surface of mesopores, macropores adsorbents. Besides, to achieve the adsorbates molecules attach into the micropore, the adsorbates firstly have to also cross meso- and macropores. Figure 2.11 presents the external and internal adsorbent surface behavior of different pore sizes. Hence, meso- and macropores play an essential role in any adsorption case. Moreover, meso- and macropores adsorbents also may accumulate multilayer adsorption behavior. The dried macroporous resin's internal surface area contributes to the total specific surface area ranging from 80 up to more than 1200 m^2/g (Table 2.8). Meanwhile, activated carbon's specific surface area ranges from 500 to 2000 m^2/g (Suhas et al., 2007).

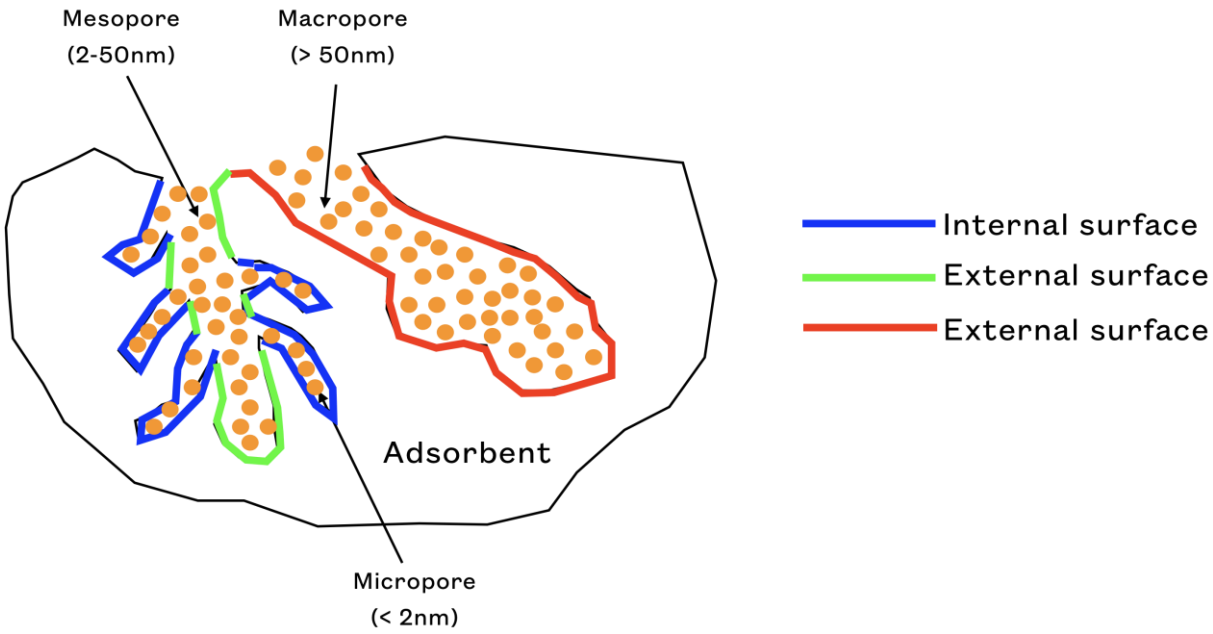

Figure 2.11. Illustration of external and internal different adsorbent surface.

2.6.4.3. Particle size of adsorbents

The particle size of macroporous resins is also a parameter that should be considered to choose the suitable resins for adsorption efficiency. As listed in Table 2.8, the particle size of macroporous resins for phenolic compounds adsorption ranges from 200 to 1250 µm. These mean values are considered as suitable ranges values for phenolic compounds adsorbed and desorbed easily. This parameter can be controlled during the process of synthetic resin.

2.6.4.4. Surface polarity of adsorbents

This Ph.D. project addresses the chemical properties and recently reported applications of adsorptive macroporous resins (MAR). Nowadays, the non-ionic macroporous resins are usually constructed from SDVB or acrylic-ester-based polymers. Chemical structures of different resins are described in Figure 2.12. Based on the monomer's composition for macroporous resin structures, the resins' polarity may vary, ranging from strongly polar (with the functional group) to non-polar (non-functionalize), as listed in Table 2.8. The adsorption capacity of macroporous resin depends not only on the degree of polarity but also on the geometric structures. The ion-exchange resins are the polymer matrix or synthetic resins with a modified functional group or conjugate with the functional group. Depending on the functional group of resin, these resins can act as strong or weak exchangers. Phenolic compounds were adsorbed onto the strong or weak anion, or cation exchange resins were also studied in the past (Ku et al., 2005; J. Li & Chase, 2010).

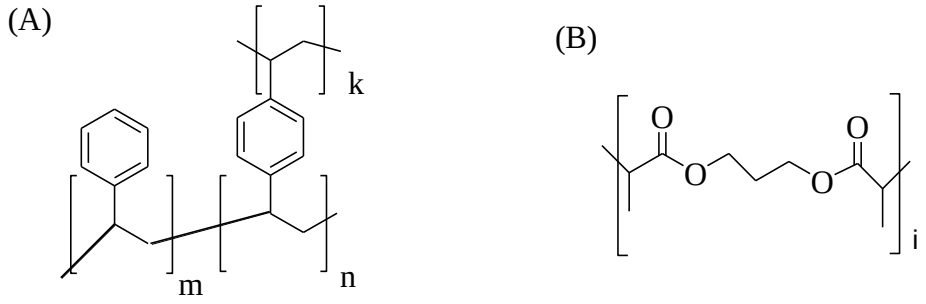

Figure 2.12. Chemical structures of SDVB (A) and acrylic resin (B)

2.6.5. Adsorption mechanisms and kinetics

Several factors can influence on adsorption capacity of resins, such as physical and chemical properties of resins and phenolic compounds, solutions, and interaction between adsorbents-adsorbates (Soto et al., 2011). Therefore, it is necessary to understand the adsorption mechanism to better predict the adsorption behavior onto macroporous resin of phenolic compounds. Before that, it is vital to determine the adsorption process's contact time to reach an equilibrium state (Tran et al., 2017). The duration of contact time can vary from 30 min to several days. The contact time needs to reach a real equilibrium state of the adsorption process. The difference in duration might come from the different adsorption mechanisms of these porous resins.

In most cases, macroporous resins' adsorption mechanism is the pore filling and interaction between adsorbents and adsorbates such as hydrogen bonding force or π-π interaction. Furthermore, desorption for the targeted compounds' recovery after reaching adsorption equilibrium is also well investigated (Weisz et al., 2013). Hence, to identify the required equilibrium time and optimal contact time for the adsorption process, adsorption kinetics should be conducted.

There are three kinds of kinetic reaction models that have been widely reported in the literature to describe the adsorption process of phenolic compounds onto different MAR including pseudo-first-order (PFO), pseudo-second-order (PSO), and intraparticle diffusion models as listed in Table 2.10.

Table 2.10. Adsorption kinetics mechanisms used to describe the adsorption of phenolic compounds from natural sources in the literature.

Diffusion controlled model	Resin	References
Intra-particle diffusion		
$q_t = k_i t^{\frac{1}{2}} + C$	AER 1 (Strongly basic anion-exchanger)	(Firdaous et al., 2017)
k_i: rate constant (mg/gmin$^{0.5}$)	HP-20 (Nonpolar absorber resin)	
C: constant associated with the thickness of the boundary layer (mg/g)	Hyper-cross-linked polymer	(X. Wang et al., 2004)
q_t: adsorption capacity (mg/g) at time t (min)	XAD7 and HP20 (Nonpolar, SDVB)	(L. Lin et al., 2012)
Pseudo-first-order		
$q_t = q_e (1\text{-}e^{-tk_1})$	XAD-7HP (Acrylic ester, weak-polar)	(Y. Chen et al., 2016)
$\ln(q_e - q_t) = \ln q_e - k_1 t$	FPX-66 (polystyrene- DVB, non-polar)	(Sandhu & Gu, 2013)
q_e and q_t: adsorption capacity (mg/g) at equilibrium and at time t (min)	XAD-16N (polystyrene-divinylbenzene (DVB)	(Sandhu & Gu, 2013)
	AB-8 (weak-polar)	(Y. Chen et al., 2016; Z. P. Gao et al., 2013)
k_1 is rate constant (1/min)	Polymeric resin	(D. Kammerer et al., 2005)
	NKA-II (polar resin)	(Y. Chen & Zhang, 2014)
	Non-polar resin (SDVB)	(Leyton et al., 2017)
Pseudo-second-order		
$\frac{1}{q_t} = \frac{1}{k_2 q_e^2} + \frac{t}{q_e}$	XAD7 (moderately polar) and HP20 (non-polar)	(Idris et al., 2017; L. Lin et al., 2012)
q_e and q_t: adsorption capacity (mg/g) at equilibrium and at time t (min)	XAD-1 (non-polar)	(X. Wang et al., 2004)
k_2: rate constant (g/mgmin)	XAD-1180 (polystyrene- DVB)	(Sandhu & Gu, 2013)
	NKA-II (polar)	(Stanford et al., 2018; L. Sun et al., 2013; Z. Wang et al., 2017a)
	SP207 (Brominated polystyrene/ divinylbenzene)	(Stanford et al., 2018)
	AER 1 (Strongly basic anion-exchanger)	(Firdaous et al., 2017)
	HP-20 (Nonpolar absorber resin)	(Firdaous et al., 2017; L. Lin et al., 2012)
	SP700 (Non-ionic polymer resin Sepabeads, PS-DVB copolymers)	(Conde et al., 2017)
	XAD-16 (polystyrene)	(Dong et al., 2015a; Q. Yang et al., 2016)
	SP-825 (polystyrene)	(Dong et al., 2015a)
	SP-207 (Brominated-polystyrene)	(Q. Yang et al., 2016)
	D101 (non-polar)	(S. Wu et al., 2015a)
	XAD-4 (Styrene-divinylbenzene)	(Bilgili, 2006)
	ADS-21 (polar)	(P.-C. Sun et al., 2015)
	H-103 (non-polar)	(Chao et al., 2010)

2.6.5.1. Intra-particle diffusion model

The intra-particle diffusion model is expressed (Table 2.10) according to Fick's second law (Soto et al., 2011). Intra particle diffusion model can provide useful information regarding adsorption mechanism, reaction pathways, and even predict the rate-controlling step. The adsorption of phenolic compounds from Alfalfa white proteins concentrate (Firdaous et al., 2017), phenolics, and rosmarinic

acid from *Rabdosia serra* (Maxim.) Hara leaf (L. Lin et al., 2012) followed by intra-particle diffusion model has been reported recently (Table 2.3).

2.6.5.2. Pseudo-first-order model

This model was originated from the work was done by Lagergren (Lagergren, 1898) when they studied the adsorption behavior of oxalic acid and malonic acid onto the charcoal. Pseudo-first-order (PFO) model is expressed in non-linear and linear forms, as presented in Table 2.10. In literature, the PFO model can modulate many different adsorption behaviors of adsorbates onto adsorbents, including (i) adsorption process near to equilibrium; (ii) adsorption process with time-dependent solute concentration; (iii) adsorption isotherm is linear equilibrium state; and (iv) a complex mixtures systems (Soto et al., 2011). Adsorption of phenolic compounds onto different resins fitted well with PFO model has been reported (Y. Chen et al., 2016; Z. P. Gao et al., 2013; Leyton et al., 2017; Sandhu & Gu, 2013).

2.6.5.3. pseudo-second-order model

Blanchard et al. (Blanchard et al., 1984) first presented Pseudo-second-order (PSO) model when they studied the adsorption of natural zeolites to remove heavy metals from water. The PSO equation is presented in Table 2.10. By comparing the calculated data with experimental data, the adsorption kinetics model can be determined. PSO can adequately describe the experimental kinetic data. PSO has been reported in most cases of adsorption of mixture phenolic compounds from natural sources as listed in Table 2.10. Several literature reports confirmed the phenolic compound's adsorption onto MAR followed by two or even three adsorption stages. Besides, most of the investigations presented in the literature indicated the phenol adsorption commonly describe by the PSO model. Some studies observed that phenolic compounds followed both PSO and intraparticle diffusion. In the past, adsorption of CGA and TPC from sunflower meal fitted well by PSO by XAD16 resin (Weisz et al., 2010). Besides, the adsorption kinetics of CGA from other plant sources also found that it followed by PSO. The adsorption of chlorogenic acid from the extract of *Eupatorium adenophorium* Spreng (B. Liu et al., 2016) onto NKA-II (polar) resin was also reported. The adsorption of other phenolic compounds or the mixture of phenolic compounds onto resins followed by PSO (Firdaous et al., 2017; Guo, Guo, et al., 2018; Idris et al., 2017; Y. Li et al., 2017; L. Lin et al., 2012, p. 20; Sandhu & Gu, 2013; Z. Wang et al., 2017a). Several resins' adsorption system can be well described by both models, including intra-particle diffusion and pseudo-second-order was addressed (Firdaous et al., 2017; L. Lin et al., 2012). However, there was no literature regarding the adsorption kinetic of phenolic compounds in RSM onto macroporous resins to date.

2.6.6. Batch adsorption

2.6.6.1. Adsorption isotherms

2.6.6.1.1. Adsorption isotherms definition

Adsorption isotherms are defined by adsorbents and adsorbates interaction, in which the maximal amount of adsorbate adsorbed onto one unit of adsorbents is quantified in constant of

temperature or solute concentration or pH (Foo & Hameed, 2010). In general, adsorption isotherms can describe the adsorption equilibrium behaviors based on the diffusion of adsorbates from porous materials. The adsorption capacity at the equilibrium of resins measured by the mass balance equation:

$$q_e = \frac{(C_o - C_e)V}{W} \quad (2.1)$$

where C_o and C_e is the concentration of initial and at equilibrium state of solute (mg/L), respectively; W is the mass of dried resin (g), and V is the isotherm solution volume (mL). q_e is adsorption capacity at the equilibrium state of resin (mg/g).

Hence, at a constant temperature, the relationship between the equilibrium concentration (C_e) of solute and adsorption capacity at equilibrium state (q_e) is determined by the adsorption isotherm.

2.6.6.1.2. Type of adsorption isotherms

According to IUPAC, there are five types of adsorption isotherms to describe the adsorption of adsorbates onto micro-and macro-porous adsorbents (Soto et al., 2011) as shown in Figure 2.13. A communication on the applications of the five types of isotherms has been reported elsewhere (Hamdaoui & Naffrechoux, 2007).

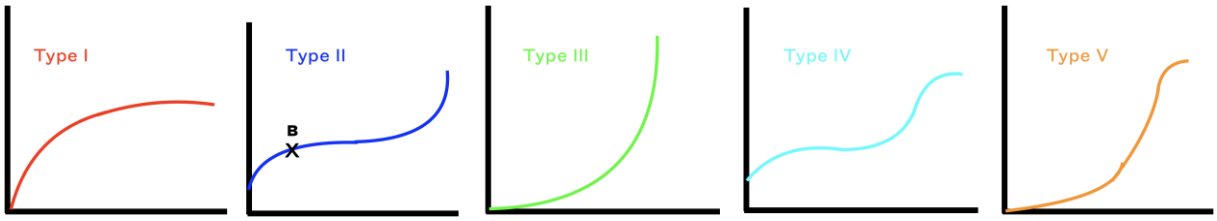

Figure 2.13. Different types of adsorption isotherms
(adapted from (L.-M. Sun & Meunier, 2003).

Type I isotherm: This model is used to describe the adsorption behavior contributed by microporous structure materials. This model is known as the Langmuir model. This isotherm is used to refer to homogeneous adsorption and monolayer adsorption, in which all sites of adsorbents have equal affinity for the adsorbates. Graphically, it is constructed by a plateau at the saturated status.

Type II isotherm: This model is used to characterize multilayer adsorption on macroporous structural materials. Point B in the graphic presents the monolayer adsorption status. Then, the multi-layer adsorption behavior starts to appear. Typically, the mixture of micro-and mesoporous material shows this type of graphic.

Type III and type IV isotherms: These models are typically used to describe the weak interaction between adsorbate-adsorbent and strong interaction between the molecules of adsorbates that form multi-layer adsorption behavior. Graphics show the convex shape at a high concentration of adsorbates solute. Micro- and meso-porous adsorbents present these isotherm models.

Type V isotherm: This model is used to describe the adsorption of mesoporous materials. The graphic shows the monolayer adsorption formation and the multilayer adsorption formation right after. The total pore volume controls the limit of adsorption.

2.6.6.1.3. Modelling techniques

Table 2.11 summarizes the equations, parameters involved, and a short description of several isotherms models used in the literature (Ayawei et al., 2017). The two-parameter isotherm models are widely used to fit phenolic compounds' adsorption data (Soto et al., 2011).

Table 2.11. Isotherm models commonly used in literature

Model	Equation	Parameter	Description
One-parameter isotherm			
Henrry's Isotherm	$q_e = K_{HE}\, C_e$	-q_e is the amount of the adsorbate at equilibrium (mg/g) -K_{HE} is Henrry's adsorption constant -C_e is the equilibrium concentration of the adsorbate on the adsorbent	-simplest adsorption -fit to the adsorption of adsorbate at relatively low concentration
Two-parameter isotherms			
Langmuir	$q_e = \frac{Q_{max} K_L C_e}{1 + K_L C_e}$	-K_L is Langmuir constant (mg/g) -Ce is the concentration of adsorbate at equilibrium (mg/g) -Qmax is the maximum saturated monolayer adsorption capacity of polyphenol (mg/g)	Describe the homogenous layer adsorption
Freundlich	$q_e = K_F C_e^n$	-n is Freundlich intensity parameter ($0 < n \leq 1$) -K_F is Freundlich constant $(\frac{mg}{g})/(\frac{mg}{L})^n$	Adsorption takes place on heterogonous surfaces
Temkin	$q_e = \frac{Rt}{b} lnK_T + \frac{RT}{b} lnC_e$	-b is Temkin constant ($Jmol^{-1}$) -K_T is Temkin isotherm constant (L/g)	Describe the interactions of the adsorbate-adsorbate
Hill	$q_e = \frac{q_{Sh} C_e^{n_H}}{K_D + C_e^{n_H}}$	q_{Sh}: Hill isotherm maximum uptake saturation K_D: Hill constant n_H: Hill coefficient	Describes the binding of different species onto homogeneous substrates
Three-parameter isotherms			
Redlich-Peterson	$q_e = \frac{Q_{max} K_{RP} C_e}{1 + K_{RP} C_e^{\alpha}}$	-K_{RP} is Redlich-Peterson constant (L/g) -α is Redlich-Peterson constant (mg/g)-g ($0 < \alpha \leq 1$)	A mix of the Langmuir and Freundlich models and does not follow ideal monolayer adsorption.
Toth	$q_e = \frac{Q_{max} C_e}{(K_T + C_e^n)^{1/n}}$	- n is Toth model exponent ($0 < \alpha \leq 1$) - K_T is Toth model constant	More useful in describing heterogeneous adsorption systems.

Sips	$q_e = \frac{K_S C_e^{\beta S}}{1 - \alpha_S C_e^{\beta S}}$	-K_S is Sips isotherm constant (L/g) -β_S is Sips isotherm exponent -α_S is Sips isotherm constant (L/g)	Suitable for predicting adsorption on a heterogeneous surface
Brunaeur-Emmett-Teller (BET)	$q_e = \frac{q_S C_{BET} C_e}{(C_S - C_e)\left[1 + (C_{BET} - 1)(\frac{C_e}{C_S})\right]}$	-C_S is adsorbate monolayer saturation concentration (mg/L) -C_{BET} is BET adsorption isotherm relating to the energy of surface interaction (L/mg)	-Describe the multi-layer adsorption -Applied in the gas-solid equilibrium systems

One-parameter model (Henrry's Isotherm):

Henrry model is the simplest model to describe the adsorption of gas onto the solid surface. This model is suitable to fit adsorbates' adsorption data in a low concentration range (Ruthven, 1984).

Two-parameter model:

Langmuir model was applied to describe gases' adsorption on a solid surface in the past (Langmuir, 1918). This model is also used frequently to estimate the adsorption mechanism and maximum adsorption capacity of macroporous resins in literature. These hypotheses construct the Langmuir model: i) adsorption is homogenous on MAR surface, ii) the affinity of solute in all the adsorption sites is equal, iii) no interaction between adsorbates and adsorbents site, iv) adsorption forms a monolayer on adsorbents surface. According to Bretage et al. (Bretag et al., 2009), the adsorption of these molecules in the liquid phase is not the same, and the model based on monolayer on the surface of adsorbents without interaction cannot be realistic. The equation of the Langmuir model is presented in Table 2.11. Q_{max} is the maximum adsorption capacity of adsorbents when the surface sites reach the saturated state. According to (Weber & Smith, 1986), a separation factor (R_L) can be illustrated as the equation:

$$R_L = \frac{1}{1+K_L C_o} \quad (2)$$

where K_L is the Langmuir constant, C_o is the initial concentration of the adsorbates (mg/L), and R_L is the dimensionless constant of the solid-liquid adsorption system. The R_L value can be used to predict the isotherm graphical shape. The various shape of the isotherm model is summarized in Table 2.12.

Table 2.12. Isotherm shapes and parameter value relationship
(adapted from (Worch, 2012).

Separation factor (R_L)	**Isotherm shapes**	**Describe**
R_L =0	Irreversible	Horizontal
R_L < 1	Favorable	Concave
R_L = 1	Linear	Linear
R_L > 1	Unfavorable	Convex

Unlike the Langmuir model, the Freundlich model is used to describe the heterogeneous surface with the equation presented in Table 2.11. Freundlich isotherm model does not illustrate the saturation behavior of macroporous resins (Tran et al., 2017). Besides, it does not imply a monolayer on the surface of adsorbents. Therefore, this model is suitable for modeling the non-ideal adsorption systems.

Freundlich model can give a reasonable interpretation of data over concentration range restriction (Dąbrowski et al., 2005).

Temkin model is a useful model to predict the gas phase equilibrium. However, the complex adsorption system, including the liquid phase, is not favorable (Temkin, M. J., and V. Pyzhe, 1940). In this isotherm model, the interaction between adsorbents and adsorbates is considered (Aharoni & Ungarish, 1977). Therefore, this model hypothesizes that all adsorbates' adsorption temperature in the layer can decrease linearly with coverage.

Hill model used to describe the homogeneous adsorption behavior of the adsorbates onto the substrates. This model hypothesizes that the adsorption process is a co-operative system with ligands' binding capability at one site on the adsorbents. This phenomenon may affect different binding sites at the same adsorbents.

Three-parameter model:

Redlich-Peterson model is a combination of Langmuir and Freundlich isotherm models. Therefore, this model can demonstrate either a homogeneous or heterogeneous adsorption system due to its versatility (Redlich & Peterson, 1959). The equation of this model is described in Table 2.11. There are three un-known parameters represented in this equation (Prasad et al., 2015). This model can describe the adsorption equilibrium over a wide concentration range (Hameed & El-Khaiary, 2008).

The Toth model is another equation developed from the Langmuir model (Toth, 1971) to reduce the error between experimental and predicted data, presented in Table 2.11. This model is an appropriate system to characterize the heterogeneous adsorption behavior that satisfied both the low and high-end boundary of solute concentration (Padmesh et al., 2006). The parameter n values can assume the adsorption characteristics of adsorbates onto adsorbents. If n = 1, the model is transformed into the Langmuir model. If the n value is far away from 1, the adsorption system is the heterogeneous system. Toth isotherm model has been applied to model the several multi-layer and non-homogeneous systems in the literature (Benzaoui et al., 2018; Koble & Corrigan, 1952).

Sips model (Sips, 1948) is another model that expresses both models, including Langmuir and Freundlich models. Therefore, this model is ideal to describe either a homogeneous or heterogeneous system. When the adsorbate concentration is relatively low, the model is favorable for the Freundlich model (hetero-layer adsorption). On the contrary, when the adsorbate concentration is high enough, this model is the Langmuir model (monolayer adsorption (Gunay, 2007). In particular, the Sips model parameters are controlled mainly by operational factors such as pH, temperature, and solute concentration (Pérez-Marín et al., 2007).

Brunaeur-Emmett-Teller (BET) model is mostly applied for physical adsorption of the gas-solid surface with equation presented in Table 2.11. This model is developed to describe the multilayer adsorption systems with pressure ranging from 0.05 to 0.30 (Foo & Hameed, 2010).

2.6.6.1.4. Applications

Langmuir, Freundlich, Redlich-Peterson, and Brunaeur-Emmett-Teller (BET) models are commonly used to describe phenolic compounds' adsorption behaviors in the previous studies and listed in Table 2.13. Among them, Langmuir and Freundlich's models are the most frequently used to assess different macroporous resins' adsorption process.

Table 2.13. Adsorption isotherms are commonly used to study the adsorption of phenolic compounds from natural sources.

Model	Resin	Reference
Langmuir	SP207 (Brominated polystyrene/ divinylbenzene)	(Stanford et al., 2018)
	XAD4 (polystyrene/ divinylbenzene)	
	Strongly basic anion-exchanger: AER 1	(Firdaous et al., 2017)
	XAD-7HP (weak-polar)	(Y. Chen et al., 2016; Firdaous et al., 2017; P.-C. Sun et al., 2015; S. Wu et al., 2015a, p. 10)
	AB-8 (weak-polar)	
	D101 (non-polar)	(S. Wu et al., 2015b)
	HP-20 (SDVB)	(Idris et al., 2017; J. Kim et al., 2014; L. Lin et al., 2012; Sandhu & Gu, 2013)
	XAD-7HP (acrylic ester)	
	FPX66 (Crosslinked aromatic polymer)	(Buran et al., 2014; Moreno-González et al., 2020; Sandhu & Gu, 2013)
	XAD761 (Crosslinked aromatic polymer)	
	H-103 (nonpolar)	(Chao et al., 2010)
	XAD-16 (styrene-divinylbenzene-SDVB)	(B. Liu et al., 2016; E. Silva et al., 2007; Weisz et al., 2010)
	NKA-II (polar)	(B. Liu et al., 2016)
	ADS-21 (polar)	(P.-C. Sun et al., 2015)
	X-5 (non-polar)	(L. Sun et al., 2013)
	H-103 (non-polar)	(Chao et al., 2010)
Freundlich	NKA-II (polar)	(Y. Chen & Zhang, 2014; Guo, Guo, et al., 2018; Z. Wang et al., 2017a)
	Non-ionic polymer resin Sepabeads SP700 (PS-DVB copolymers)	(Conde et al., 2017)
	XAD-16 (polystyrene), SP-207 (Brominated-polystyrene), SP-825 (polystyrene)	(Dong et al., 2015a; Q. Yang et al., 2016)
	D101 (non-polar)	(S. Wu et al., 2015b)
	AB-8 (weak-polar)	(L. Lin et al., 2012)
	HP-20 (polystyrene)	(Bertin et al., 2011; Idris et al., 2017; L. Lin et al., 2012)
	XAD-7HP (acrylate)	
	ENV+ (hydroxylated polystyrene-divinylbenzene)	(Bertin et al., 2011)
	XAD-4 (Polystyrene-non polar)	(A. Li et al., 2001)
	MX-4 (Acetyl group modified polystyrene-moderate polar)	
	SDVB and acrylic ester	(Leyton et al., 2017; Z. Wang et al., 2017a, p. 201)
	XAD-1	(Z. Wang et al., 2017a)
Redlich-Peterson	XAD-4 (Styrene-divinylbenzene)	(Bilgili, 2006)
	Hypercrosslinked polymer	(X. Wang et al., 2004)

Brunaeur-Emmett-Teller (BET)	Macroporous resin	(Juang & Shiau, 1999)

As listed in Table 2.13, the adsorption of phenolic compounds and natural compounds is mostly followed by the Langmuir model. In specific, the research of G. M. Weisz et al. (Weisz et al., 2013) observed that the adsorption of CGA and TPC in SFM was fitted with the Langmuir model. CGA and TPC's saturated adsorption capacity value onto XAD16HP resins was 42.7 and 181mg/g, respectively. Besides, in adsorption of sinapic acid in RSM onto XPF66 also fitted well by the Langmuir model with the adsorption capacity of sinapic acid being 63.53 mg/g resin (Moreno-González et al., 2020). The adsorption of phenolic compounds followed by the Langmuir model indicated that the physical adsorption was homogenous and reversible. Besides, the adsorption of phenolic compounds on HP20 (nonpolar, SDVB matrix) and H-103, X-5, D101, XAD4, and SP207 resins (Y. Chen et al., 2016; Firdaous et al., 2017; L. Lin et al., 2012; Xi et al., 2015) followed by Langmuir model has been reported. Moreover, the polar resins (NKA-II, AER1, and ADS-21) and weak-polar resin (XAD7 and AB-8) found to fit with the Langmuir model isotherm in describing the adsorption behavior of phenolic compounds (Y. Chen et al., 2016; Firdaous et al., 2017; L. Lin et al., 2012; B. Liu et al., 2016; P.-C. Sun et al., 2015; Xi et al., 2015).

The adsorption of phenolic compounds on the non-polar resins (XAD1, XAD16, SP700, SP-207, SP-825, D101, HP20, XAD4) (Dong et al., 2015a; Leyton et al., 2017; A. Li et al., 2001; L. Lin et al., 2012; Z. Wang et al., 2017a; S. Wu et al., 2015b; Q. Yang et al., 2016), on the moderate-polar resins (XAD7, AB-8, MX-4) (Idris et al., 2017; Leyton et al., 2017; A. Li et al., 2001; Z. Wang et al., 2017a), and on the polar resins (ENV+, MX-4, and NKA-II) (Bertin et al., 2011; A. Li et al., 2001) has been found. In particular, several resins, including XAD7, HP20, D101, XAD4, XAD16, and NKA-II, possess both Langmuir and Freundlich isotherm models in the literature.

Redlich-Peterson and BET isotherm models were found in the non-polar resins such as XAD4 (Juang & Shiau, 1999, p. 199; X. Wang et al., 2004). However, these models were not used to fit the experimental data of adsorption systems in most cases.

2.6.6.2. Adsorption capacity

The adsorption capacity of adsorbates onto one unit of mass of adsorbents is defined by equation one above. The adsorption capacity of resins depends on several factors (Soto et al., 2011). The maximum adsorption capacities of phenolic compounds from different natural sources onto macroporous resins have been well documented (Soto et al., 2011). The q_{max} values were recently reported for adsorption capacity for a mixture of phenolic compounds extracts. Also, the adsorption capacity of free phenolic compounds is summarized in Table 2.14.

Table 2.14. Adsorption capacities reported for phenolic compounds on different resins in litterature.

Extracted sources	Solution	Resins	Adsorption capacity (mg/g)	References
Apple juice	Phenolics	Non-polar	30.07	(D. R. Kammerer et al., 2007)
	5-CQA	Non-polar	2.38	
	4-CQA	Non-polar	0.19	
	4-Coumaroylquinic acid	Non-polar	0.59	
	Quercetin	Non-polar	0.09	
Canarium album	Phenolics	Non-polar resin	110.1-114.1	(He et al., 2008)
		Moderately polar	138.7	
		Polar	96.9-147.9	
Ginkgo biloba crude extracts	Flavonoids	Macroporous resins	43.0	(J. Li & Chase, 2009)
Green tea extract	Polyphenols	Macroporous copolymer	98	(W. Zhao et al., 2008)
Inga edulis leaves	Total phenolics	Macroporous resins	16-239	(E. Silva et al., 2007)
	Total flavonoids	Macroporous resins	4-64	
Orange juice	Limonin	Nonionic rein	2.56-3.18	(Ribeiro et al., 2002)
	Naringin	Nonionic rein	15.76-34.75	
Brown seaweed *Ecklonia cava*	Phlorotannins	SDVB nonpolar	PGE: phloroglucinol equivalents 20.1-57.8 mgPGE/ g	(J. Kim et al., 2014)
		Acrylic ester resin	54.7 mgPGE/g	
Canola/rapeseed meal extracts	Sinapic acid	SDVB nonpolar	102.6±11.7	(Moreno-González et al., 2020)
Kiwi fruit peel extracts	Polyphenols (Gallic acid, chlorogenic acid, catechin acid, 4-hydroxybenzoic acid, epicatechin, Rutin, Ferulic acid, Quercetin, Quercitrin)	Polar	6.15-21.28	(Guo, Guo, et al., 2018)
		Weak polar	8.01	
		Middle-polar	5.02	
		Nonpolar	6.11-18.92	
Vaccinium Bracteatum Thunb leaves	Flavones	Polar	9.55	(Y. Chen & Zhang, 2014)
Sweet potato (*Ipomoea batatas* L.) leaves	Phenolic compounds (three di-caffeoyl quinic acids)	Weak-polar	20.06 mg chlorogenic acid/ g	(Xi et al., 2015)
Extract of *Eupatorium adenophorium* Spreng	Chlorogenic acid	Polar	62.47	(B. Liu et al., 2016)
Helianthus tuberosus L. leaves extract		Polar	7.65-9.82	(P.-C. Sun et al., 2015)
Scutellariae barbatae herba extract	Total flavonoids	Weak-polar	60	(M. Gao et al., 2007)
Muscadine (*Vitis rotundifolia*) juice pomace	Anthocyanins	Non-polar	16.32-27.12	(Sandhu & Gu, 2013)

Glycyrrhiza glabra L. leaf	Flavonoids	Weak-polar	38.6	(Dong et al., 2015a)
Mulberry	Anthocyanins	Weak-polar	3.54	(Y. Chen et al., 2016)
Rabdosia serra (Maxim.) Hara leaf	Phenolics and rosmarinic acid	Nonpolar	15.95-17.338	(L. Lin et al., 2012)
Adlay bran	Free phenolics	Nonpolar Weak-polar	7.0-7.2 7.3	(Q. Yang et al., 2016)
Alfalfa white proteins concentrate	Polyphenols	Nonpolar Strongly basic anion exchanger	54.62 48.18	(Firdaous et al., 2017)
Thinned young apples	Total polyphenols, chlorogenic acid, phlorizin	Non-polar Polar	60.1-75.2 59.3-72.7	(L. Sun et al., 2013)
Platycladus orientalis (L.) Franco	Flavonoids	Semi-polar	35	(Ren et al., 2017)
Wastewater	Phenol	Non-polar	55.72-87.55	(Chao et al., 2010, p. 20)
Macrocystis Pyrifera (brown seaweed)	Phlorotannins	Non-polar Moderately-polar	156-190 79	(Leyton et al., 2017)
Olive waste	Phenolics	Non-polar Polar Weak-polar Hydrogen-bond	8.4687-10.8563 8.2203-11.0538 9.2827 5.9114-5.9253	(Z. Wang et al., 2017a)

In this table, the polarity of resins ranging from non-polar to strongly polar was considered to capture phenolic compounds in solute extractions. Notably, the adsorption capacity of sinapic acid onto non-polar resins is up to 102.6 mg/g in canola/ rapeseed meal extract (Moreno-González et al., 2020). Adsorption of chlorogenic acid (CGA) in mixture solutions being 2.38 mg/g onto non-polar resins has also been proposed by Kammerer et al. (D. R. Kammerer et al., 2007). Meanwhile, with polar resins, CGA adsorbed up to 62.47 mg/g in the research of Boyan Liu et al. (B. Liu et al., 2016).

2.6.6.3. Adsorption thermodynamics

Thermodynamic parameters determination helps us predict molecules' adsorption mechanism onto macroporous resins such as physical or chemical reactions. The thermodynamic parameters can be calculated using the following equation:

$$\Delta G = - RT \ln K_{eq} \qquad (2.2)$$

where ΔG (J/ mol) is the Gibbs energy change, $\ln K_{eq}$ is the natural logarithm of the constant of adsorption equilibrium (K_{eq}), R is the universal gas constant (8.3144 J/ (molK) and T is the Kelvin (K) temperature.

Enthalpy and entropy variations can be obtained from the slope and intercept of the linear plot $\ln K_{eq}$ *vs.* 1/T according to the linear form of Clausius-Clapeyron Eq. 2.3:

$$\ln K_{eq} = -\frac{\Delta H}{RT} + \frac{\Delta S}{R} \qquad (2.3)$$

where: ΔH is the enthalpy change (J/ mol), ΔS is entropy change (J/ mol).

The negative value of ΔG indicates that the adsorption process of phenolic compounds is feasible and spontaneous. Furthermore, the absolute value can evaluate the driving force of phenolic adsorption (Soto et al., 2011). Besides, a positive of ΔS value indicating the adsorption of adsorbates onto adsorbents interface is random. The phenolic compound's physical adsorption onto cross-linked styrene-divinylbenzene (SDVB) polymeric resins has been revealed elsewhere (B. Liu et al., 2016; P.-C. Sun et al., 2015). Positive ΔH value (calculated by Eq.2.3) suggests the adsorption process is endothermic. Endothermic adsorption was reported for natural molecules onto polymeric resins adsorption (Guo, Guo, et al., 2018). Some other endothermic adsorption processes are the compounds from apple extract onto macroporous resins (Gökmen & Serpen, 2002) and rutin compounds onto polymeric resins (Bretag et al., 2009). Whereas, negative ΔH value indicates exothermic adsorption. Almost all the adsorption of phenolic compounds onto macroporous resins in literature are exothermic processes (X. Wang et al., 2004). Exothermic adsorption was also observed for catechins (J.-L. Lu et al., 2010), puerarin, and other phenolic compounds (Y. Li et al., 2013) onto polymeric resins.

2.7. Desorption of adsorbents

2.7.1. Solvent regeneration

Several eluent solutions are used for the recovery of phenolic compounds from polymeric resins up to date. Table 2.15 represents several examples to obtain targeted phenolic compounds after adsorption onto different resins have been reported recently in the literature (Soto et al., 2011). The solvent regeneration methods show several advantages such as lower energy requirement, ease of implementation, and also enables recovery of adsorbents. Therefore, this method is used widely in the literature to recover phenolic compounds from macroporous resins after the adsorption process.

Table 2.15. The selective solvent for phenolic compounds recovery from natural extracted sources.

Extracted sources	Resins	Eluent	References
Citrus peel juice	XAD4, 7, and 16	Diluted NaOH	(Grohmann et al., 1999)
Olives	Ambertlite XAD	Ethanol	(Bertin et al., 2011)
Steam exploded hydrolyzates of olive by-products	Ion exchange and nonionic resin	Methanol:Water, 30% ethanol (v/v)	(Fernández-Bolaños et al., 2002)
Aqueous extract from citrus	Amberlite XAD16	96% ethanol, Ethylacetate	(Grohmann et al., 1999)
Acidic apple pomace extract	XAD16	Methanol	(Schieber et al., 2003)
Brassica oleraceae (anthocyanins)	XAD7	70% ethanol (v/v)	(Sandhu & Gu, 2013)
Orange peel	Sepabeads SP-70	Water, Acetone: water	(Manthey, 2004)
Grape pomace extracts (anthocyanins)	Nonpolar SDVB	Methanol, ethanol, 2-propanol	(D. Kammerer et al., 2005)
Olive mill wastewater (OMWW) (hydroxytyrosol and tyrosol)	XAD-7 and XAD-16	Ethanol : iso-propanol = 1:1	(Agalias et al., 2007)
Canarium album extracts	AB-8	70% ethanol (v/v)	(He et al., 2008)
Citrus peel water extracts	XAD-7	80% methanol (v/v)	(M.-R. Kim et al., 2007)
Mango peel acid extract	XAD16	Methanol	(Berardini et al., 2005)

Hawthron ethanolic extract	LSA-10	Ethanol:water=30-90:70-10	(Q.-S. Liu et al., 2010)
Brown seaweed *Ecklonia cava*	HP-20	Ethanol 40-95% (v/v)	(J. Kim et al., 2014)
By-product of sunflower protein extraction	XAD-16	60% isopropanol (v/v)	(Weisz et al., 2013)
Canola/rapeseed meal extracts	Amberlite FPX66	70% ethanol (v/v)	(Moreno-González et al., 2020)
Kiwi fruit peel extracts	NKA-II	80% ethanol (v/v)	(Guo, Guo, et al., 2018)
Vaccinium Bracteatum Thunb leaves		50% ethanol (v/v)	(Y. Chen & Zhang, 2014)
Extract of *Eupatorium adenophorium* Spreng		40% ethanol (v/v)	(B. Liu et al., 2016)
Sweet potato (*Ipomoea batatas* L.) leaves	AB-8	70% ethanol (v/v)	(Xi et al., 2015)
Heianthus tuberosus L. leaves extract	ADS-21	80% ethanol (v/v)	(P.-C. Sun et al., 2015)
Scutellariae barbatae herba extract	DM130	70% ethanol (v/v)	(M. Gao et al., 2007)
Muscadine (*Vitis rotundifolia*) juice pomace	FPX-66	70% ethanol (v/v)	(Sandhu & Gu, 2013)
Glycyrrhiza glabra L. leaf	SP825 XAD16	90% ethanol (v/v)	(Dong et al., 2015a)
Mulberry	XAD7, AB-8	40% ethanol (v/v)	(Y. Chen et al., 2016)
Rabdosia serra (Maxim.) Hara leaf	XAD7 and HP20	30% ethanol (v/v)	(L. Lin et al., 2012)
Adlay bran	XAD16, SP-207, and SP-825	50% ethanol (v/v)	(Q. Yang et al., 2016)
Olive mill wastewater	XAD4, XAD16, and XAD7	Ethanol	(Zagklis et al., 2015)
Thinned young apples	X-5	70% ethanol (v/v)	(L. Sun et al., 2013)
Platycladus orientalis (L.) Franco	AB-8	40% ethanol (v/v)	(Ren et al., 2017)
Wastewater	H-103	70% ethanol (v/v)	(Chao et al., 2010)
Macrocystis Pyrifera (brown seaweed)	Amberlite XAD4, XAD16	90% ethanol (v/v)	(Leyton et al., 2017)
Olive waste	XAD-1	40% and 60% ethanol (v/v)	(Z. Wang et al., 2017b)
Phanerochaete chyrosporium biomass extract	XAD-7 HP-20	50% ethanol (v/v) 30% ethanol (v/v)	(Idris et al., 2017)

One of the advantages of using macroporous resins for the adsorption/ recovery of phenolic compounds from plant extracts is desorption. This feature of MARs can lead to economic values. Almost all cases of phenolic adsorption onto crosslink polymeric resins followed physical adsorption. Physical adsorption is reversible because it implies the Van der Waals forces, hydrogen bonding force, and π-π stacking interaction between aromatic rings of phenolic compounds and polymeric resin backbone. In the past, polymeric resin's desorption of phenolic compounds using vapor pressure has been investigated (Hararah et al., 2010). The effect of ultra-sound on adsorption and desorption of phenolic compounds on polymeric resins has been also reported (Schueller & Yang, 2001). However, using organic solvents such as methanol, ethanol, and iso-propanol has been widely proposed for macroporous resins' regeneration regarding the microwave heating method. This is because it requires

lower energy, it is more easy to recover phenolic compounds with high purity, and macroporous resins can be re-used. Some examples of desorption of phenolic compounds using organic solvent for phenolic recovery are shown in Table 2.15.

One solvent regeneration that has been used to desorb is acetone (S.-H. Lin & Juang, 2009). Besides, iso-propanol was observed to be rapid, efficient, with high recovery rates elution in desorption of CGA and TPC in SFM extract (Weisz et al., 2013). However, these solvents, including acetone and iso-propanol, are less used nowadays for phenolic desorption due to their toxicity in humans.

Methanol also was used to elute grape phenolics (J. A. Cardona et al., 2009), sunflower phenolics (Weisz et al., 2013), and acidic apple pomace extract (Schieber et al., 2003). Moreover, methanol solutions (pure or in mixture with water) were also proposed to select the best one since they influence polarity, and then it can affect of desorption ratio of macroporous resins. In literature, the aqueous methanol concentration ranging from 50-80% (v/v) was a better desorption solution (Weisz et al., 2013). Nevertheless, methanol application as a desorbed eluent would require particular safety precautions due to toxicity for human health.

Thus, the most common solvent used in literature in the past decades for polyphenols desorption from macroporous resins is an ethanol solution (absolute or in water) due to its eco-friendly environmental properties and it being less toxic. Some examples of using methanol aqueous in desorption of tea phenolics (J. A. Cardona et al., 2009), sunflower polyphenols (Weisz et al., 2013), and rapeseed phenolics (Moreno-Castilla, 2004) from polymeric resins have been proposed (for more information and other sources, consults Table 2.15). Compared with methanolic desorption, ethanolic desorption concentration ranged 68-80% (v/v) showed a better phenolic recovery (Weisz et al., 2013). According to Monica Moreno-Gonzalez et al. (Moreno-González et al., 2020), the effective desorption of sinapic acid in RSM extract was observed with 70% (v/v) ethanol solution in water.

2.7.2. Other techniques for desorption

Other recovery techniques of phenolic compounds from adsorbent are thermal regeneration and microwave heating (Soto et al., 2011).

Thermal processing does not completely desorb all phenolic compounds adsorbed onto adsorbents such as activated carbons. Moreover, this technique can damage the pores of activated carbons. The thermal process is commonly adaptable for zeolites, proposed by several authors (A. Fungaro et al., 2013; Blanchard et al., 1984). However, the conventional thermal process requires high energy, long duration, and strict heating rate control.

Microwave application for polymeric resins' desorption of phenolic compounds has been reported elsewhere (Hararah et al., 2010). Because the microwave-based technique needs lower temperature, quick and easy temperature control, this method is more widely used to desorb molecules after adsorption. Ultrasound can enhance the mass-transfer. The effects of ultrasound on the adsorption/ desorption of phenolic compounds have been investigated (Breitbach et al., 2003; J. Li & El Rassi, 2002; Schueller & Yang, 2001).

Both methods for desorption have been investigated so far. However, it shows several drawbacks. Therefore, these methods are not widely used to recover targeted compounds in the literature.

2.8. Operational parameters influencing adsorption and desorption

Several factors can influence adsorption capacity, including physical features of adsorptive macroporous resins (pore diameters, particles size, and specific surface area), characteristics of phenolic compounds (functional group, polarity, solubility, ionic charge, molecular weight, size, and pK_a), conditions of solution (pH, temperature, solvent, ionic strength, concentration), and solid-liquid surface interactions (Soto et al., 2011).

2.8.1. Adsorption interaction types between phenolic compounds-macroporous resins

Adsorption of phenolic compounds onto macroporous resins is a physical adsorption process. This phenomenon is complex between multiple forces interactions, including π-π stacking interactions, hydrogen-bonding interactions, and hydrophobic-hydrophobic interactions. Understanding the interactions between phenolic compounds and macroporous resins is very important because it relates to macroporous resins' selectivity. As a result, we can use different techniques to improve the targeted compounds' separation and purification.

2.8.1.1. π-π dispersion interactions

The π-π stacking interaction is the predominant type of interaction of adsorbates-adsorbents. Phenolic compounds structure contains at least one aromatic ring, which is rich in electrons. Additionally, the styrene-divinylbenzene (SDVB) resin backbone also composes many electrons in benzene rings and delocalized π electrons in the resins' basal planes (Pompeu et al., 2010). This interaction is based on the dispersion forces that originated from electrons' mutual correlation. Figure 2.14A represents the π-π interaction type between phenolic compounds-macroporous resins.

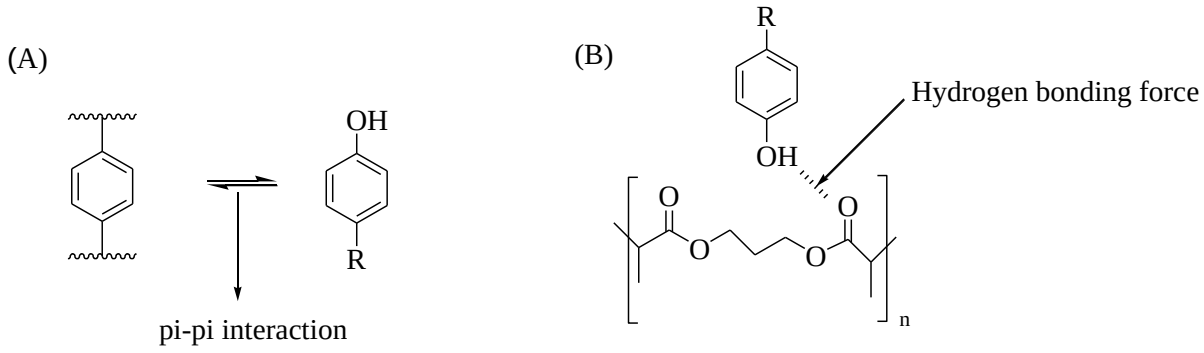

Figure 2.14. The schematic represents the proposed π-π interaction and hydrogen interaction between phenolic compounds onto SDVB (A) and acrylic resin (B).

The surface functional substituents of macroporous resins also play an essential role in characterizing phenolics' interaction and resins at the interface. Primary groups (such as in AER1 and AER2 resins) can increase the π electrons in resins' basal planes. Therefore, it might increase the adsorption capability of resins. Meanwhile, acidic functional groups (such as CER 1 and CER 2 resins) cause a decrease in

the π electrons in the basal planes. Consequently, the adsorption potential of resins is affected. This phenomenon was observed by the study of L. Firdaous et al. (Firdaous et al., 2017). Not only the Ambelite XAD resins showed π-π stacking interactions, but also the other resins such as EXA118 and EXA90 had a π-π interaction with caffeic acid, ferulic acid, catechin, and rutin (Pompeu et al., 2010).

2.8.1.2. Hydrogen bonding force interaction

The hydrogen-bonding force interaction between phenolic compounds and resins (acrylic resin) was illustrated in Figure 2.14B (Pompeu et al., 2010). Gallic acid possesses a hydrogen bonding interaction with the carbonyl group of acrylic resin (XAD7) has been found by Darly R. Pompeu et al. (Pompeu et al., 2010). In this case, the hydroxyl group of phenolic acid plays as a hydrogen-bonding acceptor. Meanwhile, the carbonyl groups from XAD7 resins are the hydrogen-bonding donor. Phenolic acid and water molecules in solution have a hydrogen-bonding interaction with macroporous resins that should be considered in adsorption studies. Water (H-OH) molecules can be adsorbed on adsorbents' surface in oxygen groups' presence by hydrogen bonding force interactions. Therefore, this phenomenon can make obstacles for phenolic compounds adsorption because some activated sites of adsorbents are occupied and can no longer adsorb phenolic compounds. Thereby, the adsorbed water molecules can block the entry of adsorbates molecules transport to pore wall or pore surface, which cause a decrease in the adsorption efficiency of adsorbents (Franz et al., 2000; B. Pan et al., 2008).

2.8.1.3. Hydrophobic-hydrophobic interaction

Hydrophobic-hydrophobic interaction between phenolic compounds and macroporous resins was also mentioned in the study of Darly R. Pompeu et al. (Pompeu et al., 2010). There is an interaction between the resin matrix's hydrophobic phenyl ring and the aromatic rings of phenolic compounds. Therefore, this interaction can also affect the adsorption capacity of resins.

2.8.2. Factors influencing adsorption and desorption

Several factors that affect the whole adsorption/ desorption process should be known to achieve a high recovery ratio and high purity of desirable compounds.

2.8.2.1. Influence of properties of the adsorbents

2.8.2.1.1. Pore size and specific surface area

Specific surface area and pore size are two key parameters influencing the adsorption/ desorption process (J. Li & Chase, 2009). In general, the smaller pore diameter values, the higher surface area observed. Both parameters strongly affect their adsorption capacity. In particular, pore size can play an essential role in retaining the targeted compounds due to adsorbates molecules being able to enter or leave the adsorbent particles during the adsorption system. The optimal ratio of pore diameter to the particle size was found ranging from 2 to 6 (Slejko, Frank L., ed., 1985) for the adsorption related in using macroporous resins. With small pore diameter, it can induce diffusional limitations by steric hindrance (Z. Xu et al., 1999; Q. Yang et al., 2016). Thereby, the adsorbates are challenging to transport from the bulk aqueous solution into the pores of particles. On the contrary, with a large pore diameter,

the adsorbed molecules can leave again because of the reversible adsorption process. Moreover, when the pore diameter is large, the surface area of the particle would be small. Therefore, there is no doubt that the pore size and surface area can influence the adsorption capacity of adsorbents.

2.8.2.1.2. Particle size

The particle size of adsorbents can greatly influence the adsorption rate in terms of intra-particle diffusion study (Ahmaruzzaman, 2008). Indeed, if the particle size of macroporous resins is small it would cause an increase in the surface area. Thanks to that, the adsorption of phenolic compounds onto the outer surface of macroporous resins would increase. Besides, particle diffusion from the external surface into the pores of resins is also possible. On the contrary, the if resins' particle size is too large, it will result in more excellent diffusional resistance to mass transfer. Due to this factor, most of the macroporous resins particle's internal part may be unutilized for adsorption. As a consequence, the adsorption efficiency might be low.

2.8.2.2. Influence of nature of the adsorbates

2.8.2.2.1. Substituent groups

Substituent groups in aromatic rings of the phenolic compound can define the electron donor-acceptor status. The effect of electron donor-acceptor substituents groups from phenolic compounds is an essential factor in adsorption capacity. Because it can contribute to π-π interaction between adsorbates and adsorbents. If the benzene ring attaches to the electron-withdrawing groups (such as -NO_2 and -Cl), the π-π interaction is accumulated by reducing π electrons' density. Wang et al. (J.-P. Wang et al., 2007) and Liu Q-S et al. (Q.-S. Liu et al., 2010) found that this effect plays a vital role in the adsorption of phenolic compounds on adsorbents.

2.8.2.2.2. Molecular weight and size

Molecular structures and size also have impacts on the adsorption. The adsorbates with the appropriate size would be adsorbed easier since they have more spaces on the surface, and they can diffuse into the pore of adsorbents. However, if the molecules' size is large, adsorbates' movement into the pores would be strenuous because of their steric. The effect of adsorbate molecules on the adsorption potential of D-101 and AB-8 resins were studied by Lisha Xi et al. (Xi et al., 2015) and Boyan Lin et al. (B. Liu et al., 2016), and Songhai Wu et al. (S. Wu et al., 2015b). The molecular diameter of flavonoid and glycoside in these studies can be determined around 2nm. The pore diameter of D-101 ranges from 9 to 30nm, and the pore diameter of AB-8 ranges from 13-14nm. The pore diameter of both resins is about 4.5 up to 7 times the flavonoid and glycosides diameter. Therefore, D-101 and AB-8 resins were used to purify flavonoids and glycosides, as in their reports.

2.8.2.2.3. Water solubility and polarity

The polarity and water solubility of phenolic compounds are essential factors involved in the adsorption process. There is no doubt that the more solubility in water, the lower the adsorption capacity. Typically, the solubility of adsorbates related to their polarity degree. The more polarized phenolic compounds, the higher solubility in a polar solution (water, for instance). The adsorption capacities of phenolic compounds depend on water solubility (Moreno-Castilla et al., 1995). In this report, the adsorption capacity of phenolic compounds increases with the decrease in their water solubility.

2.8.2.2.4. Hydrophobicity

Hydrophobic-hydrophobic interaction between aromatic rings of phenolic compounds with phenyl groups of macroporous resins was found to attribute phenols' adsorption capacity (Moreno-Castilla, 2004). The adsorbates with higher hydrophobicity possess a stronger tendency to be adsorbed onto non-polar macroporous resins surface. Therefore, the hydrophobic compounds are more captured comparing to the hydrophilic ones.

2.8.2.3. Influence of solution conditions

2.8.2.3.1. Ionic strength and pH solution

Ionic strength and pH aqueous solution are the key factors affecting the adsorption of phenolic compounds (Soto et al., 2011). Modification of pH values can lead to the transformation of chemical characteristics of adsorbates and adsorbents in case of ion exchange resins. If the solution is too acidic or alkali, adsorbates' chemical features are changed due to ion charged formation. These effects can cause significant alterations in the adsorption system (Garcia & Takashima, 2003). In the presence of functional groups, the adsorption capacity depends on the interaction with the water of adsorbates/ adsorbents (Contescu et al., 1998; B. Xia et al., 1999). The ionic of phenolate ion can be expressed as equation according to Banat et al. (Banat et al., 2000):

$$\Phi_{ion} = \frac{1}{1 + 10^{pK_a - pH}} \quad (2.4)$$

According to this equation, at pH < pK_a, the adsorbates are in the protonated form (positive charge), while adsorbates are in the deprotonated form (negative charge) at pH > pK_a. Therefore, the adsorption capacity is enhanced at the solution's acidic pH due to increasing phenolic compounds uptake (Dąbrowski et al., 2005). On the contrary, at alkaline pH value, the adsorption decreases owing to carboxyl groups and hydroxyl groups dissociation which has been reported recently (B. Fu et al., 2005). In particular, there is no pH influence in the acidic range of phenolic compounds adsorption on resins, which has also been published elsewhere (Scordino et al., 2003, 2004; E. Silva et al., 2007).

2.8.2.3.2. Temperature

The temperature of the given solution adsorption also can affect adsorption and desorption capacity. The solvent temperature can increase the circulation rate across from the external boundary layer to within the pores due to the decreased solution viscosity (Figure. 2.8). Temperature can

positively influence (Garcia & Takashima, 2003; Gökmen & Serpen, 2002) and negatively (Juang & Shiau, 1999; Ku & Lee, 2000) adsorption-desorption capacity for resins. Besides, the temperature of solvent affects the adsorption of water and affects the hydration degree of the phenolic compound molecules as reported by Dabrowski et al. (Dąbrowski et al., 2005). The negative effect of high temperatures on the adsorption of phenolic compounds on resins is expected because most cases of adsorption systems are physical adsorption and exothermic behavior (Catena & Bright, 1989). However, in some cases, higher temperatures were favorable for the adsorption process, but no influence was observed on acrylic resins (Scordino et al., 2003). The temperature did not significantly affect adsorption and desorption processes (D. Kammerer et al., 2005).

Besides, the solvent's temperature can change the adsorbents' capacity (Soto et al., 2011) because the adsorbents are strongly heterogeneous surfaces. This characteristic of adsorbents comes from geometrical and chemical properties. The differences in size and shape of pores can cause geometrical heterogeneity. Additionally, the difference of functional groups at a surface of particles and various surface contaminants can lead to chemical heterogeneity. Geometrical and chemical heterogeneity can define the adsorption/ desorption of adsorbents that have been reported by Pan et al. (B. Pan et al., 2008). The effect of chemical composition on phenolic compounds' adsorption decreases at high temperatures, and the geometrical property can determine phenolic compounds' adsorption capacity.

2.8.2.3.3. Addition of inorganic salts

Inorganic salts, such as sodium chloride (NaCl), influence the adsorption of phenolic compounds onto activated carbons as reported elsewhere (Halhouli et al., 1995). This study showed that the presence of salts had a slight effect on the phenolic compounds' absorbability. The presence of these ions (Na^+ and Cl^-) may block the active sites of adsorbents surface, hence, that can cause deactivation of the adsorbents towards the adsorbates molecules (Kamble et al., 2007). Yasuji Ihara (Ihara, 1988) studied inorganic salts' influences on the adsorption amount of sodium alkyl sulfates and fatty acid sodium salts onto ion exchange resins. They found that the amount of adsorption decreased with sodium chloride, compared to the absence of salts. The adsorption capacity of these compounds almost unchanged at high concentrations of NaCl. Therefore, inorganic salts in the adsorptive solution can harm the adsorption behavior of adsorbates-adsorbents.

On the other hand, Tang et al. (D. Tang et al., 2007) observed that phenolic compounds' equilibrium adsorption increased with increasing the sodium chloride in the solution. This observed phenomenon can be explained by the interactions between water molecules-ions and adsorbates-ions in a complex solution. A robust electrostatic environment attracted to water molecules formed around these ions. Therefore, it causes to strengthens the hydrophobicity level of adsorbates in the other direction (Arafat et al., 1999), which is favorable for the adsorption process. Overall, there is no clear general conclusion on inorganic salts effects found.

2.8.2.3.4. The presence of molecular oxygen

The adsorption of phenolic compounds presented surface oxygen-containing groups affected by the water molecules adsorption, dispersive and or repulsive interactions, hydrogen-bonding force, and donor-acceptor electrons interactions (Franz et al., 2000). However, the effect of oxygen atoms on phenolic compounds' adsorption onto resins has been moderately observed (Phenrat et al., 2008).

2.8.2.3.5. Competitive adsorption molecules

Understanding the competitive effects of various organic molecules in solute adsorption is vital to expect adsorbates/adsorbents' adsorption capacity. Because adsorption from the multi-component solution is a relatively complex system, especially in many individual components (D. R. Kammerer et al., 2007; E. Silva et al., 2007). Many factors affect the adsorption equilibria, including the chemical structures of adsorbates/ adsorbents, the energetic heterogeneity of adsorbents, and the differences in the physicochemical properties adsorbates been taken into consideration in adsorption studies (Q. Lu & Sorial, 2007). There are two mechanisms to describe the competitive adsorption system. Those are location competition and pore blockage (Y. Li et al., 2003). If the competitors possess a size comparable to that of the phenolic compounds, the adsorption capacity of targeted adsorbates molecules decreases due to site competition (W. Yang et al., 2011). Another side, the interactions between adsorbates may enhance the adsorption capacity of several adsorbates. However, the partial desorption process also coincides with high solute concentration (Garcia & Takashima, 2003).

2.9. Column study

Batch adsorption can give us the adsorption equilibrium data. The adsorbents should be packed into a column to make the adsorption process more efficient (Moreno-González et al., 2020; Weisz et al., 2013). These data are used to predict the dynamic adsorption capacity data, achieve high yields of targeted compounds and give useful information for scale-up. Studies on the adsorption/ desorption and dynamic adsorption of macroporous resins in the column have been investigated by many researchers (L. Lin et al., 2012; B. Liu et al., 2016; Weisz et al., 2013).

2.9.1. Dynamic behavior of fixed-bed reactor adsorption systems

According to Walter J. Weber and Jr. Edward H. Smith (Weber & Smith, 1987), the adsorption equilibrium and dynamics can be achieved by constructing breakthrough curves. The breakthrough curve also provides useful information to the design and operation of fixed-beds columns, enabling a desirable amount of targeted compounds after purification. Figure 2.15 represents the fixed-bed column's dynamic behavior, simulated in mass loading into columns (an active adsorption zone) and the saturation part of adsorbents. The continuous flow of adsorptive solution is applied from up to the bottom column. One parameter to design the length and diameter column is the amount of volume processed and operation time. From the length (L) and diameter of the packed column, the throughput (well known as bed volume (BV)) can be determined by the equation:

$$\text{Packed bed volume (BV, mL)} = \frac{\text{Column bed height (L, cm)}}{\pi\, r^2\ (cm^2)} \quad (2.5)$$

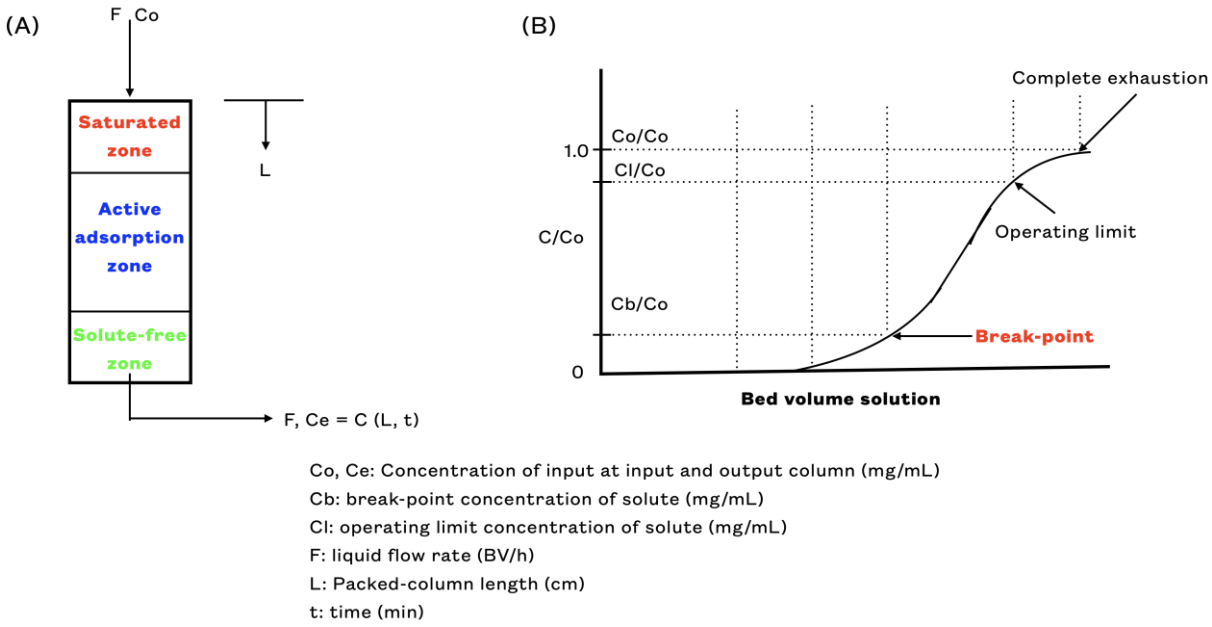

Figure 2.15. Illustration of packed column configuration (A) and breakthrough curve properties of a fixed-bed (B).

(Adapted with modification from Weber, W. J., Jr., Smith, E. H. (Weber & Smith, 1987).

The breakthrough curve of dynamic adsorption can be constructed by the solute outlet concentration ratio to the solute inlet concentration, represented in Figure 2.15B. Two parameters that can contribute to the breakthrough curve characteristic are the effluent concentration of solute and flow rate (Weber & Smith, 1987). The break-point, operating limit, and total exhaustion points can also be observed. Dynamic adsorption reaches an equilibrium state when C/C_o equal to 1. Several factors affect the dynamic adsorption, including the physical and chemical properties of adsorbates/ adsorbents, the bed's depth, and flow velocity (Weber & Smith, 1987). The break-point of phenolic compounds adsorption from natural sources onto resins can be defined by the ratio of C/C_o equal to 0.1, 0.01, or 0.05 (Abburi, 2003; B. Pan et al., 2008; Rodrigues et al., 2016; Zabkova et al., 2006). Phenolic compounds from food or by-products of protein extract also can be selectively separated using resins packed column (J.-L. Lu et al., 2010; Scordino et al., 2004; Weisz et al., 2010). A sequence of desorption-washing was conducted after dynamic adsorption of adsorbates reach a saturated point using an organic solvent (normally ethanol 30-90%, v/v with phenolic compounds) to obtain the fractionated elution of the targeted compounds (Aehle et al., 2004).

2.9.2. Mathematical modeling

The mathematical modeling is used to characterize the adsorption equilibrium dynamic behavior (Weber & Smith, 1987). This model can depict the equilibrium capacity or adsorption isotherm

of adsorbates/ adsorbents. The uptake of adsorbates within adsorbents is governed by resistance to mass transport rather than reaction velocity. The diffusion of adsorbates molecules into the pore walls of macroporous adsorbents is presented in Figure 2.8. The adsorption model is determined based on the thermodynamic principle of continuous mass. The continuous mass leads to the mass balance of individual components in liquid-solid phases and is defined by the equation (Weber & Smith, 1987):

$$Mass\ rate\ of\ component\ change = Mass\ flux\ of\ component\ input - Mass\ flux\ of\ component\ output \pm Mass\ rate\ of\ component\ adsorption \quad (2.6)$$

The flux of component input/ output can include bulk flow, dispersive flow, and molecular diffusion. Therefore, it is crucial to accurately determine the appropriate mathematical model to predict conditions to reach equilibrium adsorption states accurately.

2.10. Application in separation and phenolic purification compounds

2.10.1. Removal of phenolic compounds from industrial wastewaters

Food processing wastes contain the bioactive phenolic compounds that need to be removed due to their toxicity and anti-nutritional properties. It has been reported that adsorption onto macroporous resins is widely used to remove phenolic compounds from wastewater (Ahmed et al., 2000). Ion-exchange resins are also used to separate and recover phenolic compounds from olive mill wastewater (Al-Malah et al., 2000).

2.10.2. Purification of bioactive phenolic compounds

Macroporous resins are used widely in the separation, purification, and recovery of bioactive phenolic compounds from natural sources extracts based on the adsorption/ desorption principle. Synthetic resins have been applied to purify phenolic compounds from leaves (J. Li & Chase, 2009; E. Silva et al., 2007; L. Xu & Diosady, 2000), by-products of citrus (Doner et al., 1993), and cacao (K. H. Kim et al., 2004). Anthocyanins from grape pomace also have been purified by adsorption onto resins (D. Kammerer et al., 2005). Many phenolic compounds have been separated and recovered using macroporous resins from different natural sources listed in Table 2.7. Especially, Zhang et al. (B. Zhang et al., 2008) developed an efficient way to enrich chlorogenic acid (CGA) from crude honeysuckle extract using macroporous resins. Nine different MAR include HPD-300, HPC-450, HPD-700, HPD-750, HPD-850, X-5, AB-8, and NKA-II resins, were used for the screening test. Among them, HPD-850 was selected for further study due to their higher adsorption capacity and desorption ratio. The researchers found that pH lower than 3 had no impact on adsorption capacity and stability of CGA. When the pH value increased, the adsorption capacity decreased. After purification, the CGA obtained increased from 11.2 to 50% and recovery yield of 87.9%. Geogre M. Weisz et al. (Weisz et al., 2010) studied the adsorption of phenolic compounds in RSM during protein extraction to remove colored compounds. There were seven different MARs used in this study, including XAD16HP, XAD7HP, XAD1180N, FPX66, FPA90Cl, Dowex, and Lewatit resins. These authors found that the maximal binding rates belong to these ion exchange resin Dowex, Lewatit, and FPA90Cl with more than 94% (v/v) in any case, followed by XAD16HP and FPX66 which caused about 85.7 and 86.8 reductions of

total phenolic content (TPC) in SFM protein extract, respectively. XAD7HP and XAD1180N were not selected due to the lowest adsorption capacity, and potential interactions with the protein. Besides, color measurements were also carried out to find suitable resins in removing phenolic compounds and de-colorizing crude extract. They found that XAD16N was the best resins regarding adsorption capacity and de-colorization and its weak interaction with sunflower protein. A D-optimal experimental design was then applied to find maximal adsorptive phenolic compounds' operational conditions, including CGA and TPC. Finally, these authors conclude meal-solvent ratio was 0.05 g/mL, at temperature 20°C, and flow rate at three-bed volume (BV) per hour (h) were the best conditions for altogether removal of polyphenols. The simple and efficient method for separating CGA from the extract of *Helianthus tuberosus* leaves using macroporous resins was also studied by Peng-Cheng Sun et al. (P.-C. Sun et al., 2015). Ten different resins were used in this work: D101, D4020, AB-8, ADS-21, ADS-7, ADS-8, ADS-17, ADS-F8, X5, and NKA-9. They observed that ADS-21 was the best among tested resin for CGA adsorption. After packed column with ADS-21 for purification process, CGA increased from 12.0% to 65.2% with a recovery yield of 89.4%. These results also suggested this method was suitable for large-scale reparation of CGA. Boyan Liu et al. (B. Liu et al., 2016) also recommended a fast and straightforward CGA separation method from *Eupatorium adenophorium* Spreng extract. The adsorption capacity was evaluated using nine macroporous resins, including D101, HPD100, HP-20, AB-8, HPD-400A, XAD-7, NKA-II, and NKA-9. Among them, NKA-II was selected because it showed higher adsorption/desorption capacity at 25°C. After purification, CGA purity was 22.17%, and the recovery yield was 82.41%.

Regarding adsorption of phenolic compounds in RSM, Alexander Thiel et al. (Thiel et al., 2015) used zeolites for sinapic acid adsorption from hydrolysis solution. Zeolites are porous alum-inosilicates with abundant cavity structure (Ahmaruzzaman, 2008). They concluded the adsorption obtained the highest amount at 25°C for 1h adsorption and desorption with EtOH 70% (v/v). Sinapic acid can yield 96.3%, and the purity was up to 80% when using zeolites. Moreover, Monica Moreno-Gonzalez et al. (Moreno-González et al., 2020) studied the recovery of SA in RSM extract by adsorption. In this study, seven different food-grade MARs were used to screen the test, including the Amblite series (XAD4, XAD7, XAD16, XAD1180N, XAD761, and FPX66) and a Dianion (HP20). They discovered FPX66 showed the highest adsorption capacity (102.6±11.7 mg/g resin), followed by XAD16. Therefore, FPX66 was selected for the packing column for sinapic acid purification. Ethanol 70% (v/v) was the best eluent for the desorption process due to its high selectivity to sinapic acid over glucose, phytic acid, and glucosinolates. They also found that at pH higher than 6, significantly lower adsorption of sinapic acid on hydrophobic resins was observed.

2.11. Improve the purification of phenolic compounds using response surface methodology

Response surface methodology has been proposed to model and optimize wastewater treatment processes (Nair et al., 2014). The traditional approach to optimizing one process is based on the one-factor-at-time method. Consequently, the number of experiments required would be enormous

and would increase when increasing the sample size. Hence, this approach is very costly and time-consuming. The design of experiments regarding the interaction of all levels of factors has been studied to overcome these issues. The interaction between variables and responses can be considered. Response surface methodology is constructed by these interactions (Khuri & Mukhopadhyay, 2010). Response surface methodology involves mathematical and statistical techniques to propose the design of experiments (Khuri & Mukhopadhyay, 2010). Based on the experiment and experimental data design, the model can be built, and the optimal conditions can be obtained for a limited number of planned experiments. The first design of the experiment was proposed by Box and Wilson in 1951 (Box & Wilson, 1951). This approach has become a common tool for optimizing and analyzing the factors involved in responses in several domains, such as electronics and biotechnology (Nair et al., 2014; Weisz et al., 2013).

2.11.1. Definition of some terms

The experimental domain is the limitation of the minimum and maximum of the experimental variables studied.

Experimental design/ Design of experiments (DoE) is a specific set of experiments defined by a mathematical matrix through the different combination level of experimental variables. Thereby, the response values can be obtained by doing experiments based on the conditions of these variables.

Factors and independent variables are the experimental conditions that can be changed independently. In the adsorption process, the independent variables can be defined, such as pH, flow rate, temperature.

Responses or dependent variables are the values observed by doing the experiments. Typical dependent variables in the adsorption and purification process are recovery ratio (%), purity (%), and productivity of the whole process.

Residual is the difference in values between calculated data from the mathematical model and experimental data from doing the experiments. Therefore, a good model must achieve a low residual value.

2.11.2. Response surface methodology procedure

Several steps for response surface methodology application are i) selecting the independent factors and their response in a specific range, ii) preselecting the experimental design, iii) performing the experiments, iv) production of the mathematical equation based on the experimental data, v) validation of the model, and vi) achieving the optimal conditions.

2.11.3. Types of experimental design

Some examples of experimental designs are frequently used in literature, including full factorial design (FFD), Box-Behnken design (BBD), D-optimal design, and central composite design (CCD) ((Bezerra et al., 2008). These designs of experiments (DoE) are presented in Figure 2.16.

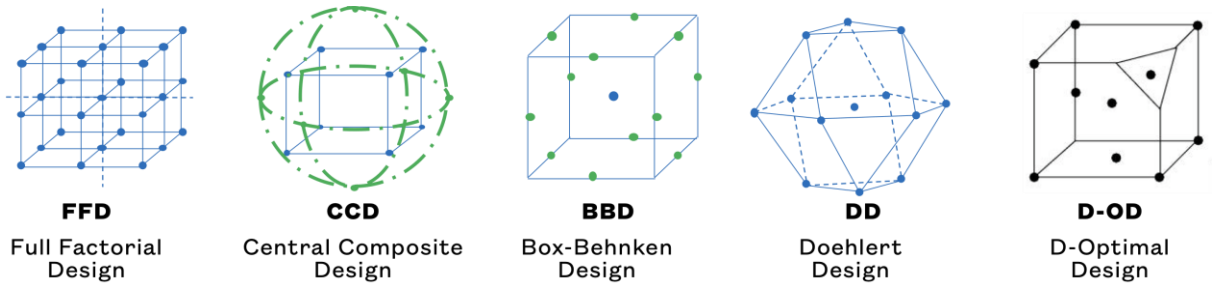

Figure 2.16. The different experimental designs (Adapted with modification from S. Karimifard and M. R. Alavi Moghaddam.

(Karimifard & Alavi Moghaddam, 2018)).

2.11.3.1. Full factorial design (FFD)

Full factorial design (FFD) is an experimental design for two or three levels of variables. The factor Number of experiments of this design are 2^k designs where k is the number of factors. Besides, the more common design used to research is the full three-level factorial design (3-FFD). The factors can be defined as three levels: low, center, and high. Therefore, the number of experiments is 3^k. A full three-level factorial design is ideal for the application of two factors. For more than two factors investigated, this model will give a large number of experiments. Therefore, other designs of experiments are recommended.

2.11.3.2. Central composite design (CCD)

Central composite design (CCD) is an alternative of full three-level factorial design and is also known as central composite face-centered (CCF) design, which was first proposed by Box and Wilson (Box & Wilson, 1951). This CCF design can be relatively efficient and simple when the factors are up to five or six (Nair et al., 2014). Therefore, CCF design can be applied for optimization and is widely used for building the second-order response surface model in environmental processes (Karimifard & Alavi Moghaddam, 2018). CCD can give equal information as the FFD model, but fewer experimental runs are required. Besides, CCD can provide useful information for linear and quadratic interaction effects of factors influencing the response values. This model needs three types of points, including center, axial, and cube points (illustrated in Figure 2.16). The total number of experiments can be expressed in the equation:

$$Total\ number\ of\ experiments = 2^k + 2k + C_0 (2.7)$$

Where k is the number of factors, 2k is the cubic runs, 2k is the axial runs, and Co is the center point runs.

2.11.3.3. Box-Behnken design (BBD)

Unlike full three-level factorial design, Box-Behnken design (BBD) (Box & Behnken, 1960) is generally used in industrial research due to reduced experiments compared with full factorial design. The total number of experiments is determined from the equation:

$$Total\ number\ of\ experiments = 2k(k-1) + C_o (2.8)$$

Where k is the number of factors, C_o is the number of center points.

Based on this equation, this design of the experiment needs the number of factor ≥ 3. One of the drawbacks of this model is that it is not suitable for the experimental works to consider extreme conditions.

2.11.3.4. Doehlert design (DD)

Doehlert design (DD) is a flexible design with a k-dimensional and one point in the center, where k is the number of factors. This DoE needs a small number of running experiments. Many factors can be added to the matrix of design easily. This model also allows the researcher to study more significant factors affecting the value of responses. The total number of experiments can be calculated as follow:

$$Total\ number\ of\ experiments = k^2 + k + C_o (2.9)$$

Where k is the factors and C_o is the number of center points.

2.11.3.5. D-optimal design

Unlike CCF design, D-optimal design is mentioned in the literature, but this design is rarely used in wastewater treatment (Nair et al., 2014; Weisz et al., 2010).

Table 2.16 summarizes all the characteristics of response surface methods used to optimize in literature.

Table 2.16. Characteristics of design of experiments commonly used in literature.
(adapted with modification from L. Vera Candioti et al. (Vera Candioti et al., 2014)).

Design	Type of factors	Factor levels	Number of experiments
Central composite (CCD)	Numerical Categorical	5	2^k+2k+C_o
Box-Behnken (BBD)	Numerical Categorical	3	$2k(k-1)+C_o$
Full factorial design at three levels (3-FFD)	Numerical Categorical	3	3^k
Doehlert design (DD)	Numerical Categorical	Different for each factor	2^k+k+C_o
D-Optimal	Numerical Categorical	Different for each model. Irregular experimental domains.	The selected subset of all possible combinations.

Note: k: number of factors, C_o: number of center points

2.11.4. Modeling procedure

The equation describes the interaction between factors, and responses must be determined to determine the critical point. The most widely used method to build a highly accurate relationship between these parameters is based on the polynomials model.

2.11.4.1. Model building for response surface methodology

Since the linear equation cannot describe the effects between different parameters, the second-order mathematical model is usually used in literature. In response surface methodology, the interactions between different parameters can express in the full quadratic second-order equation (Nair et al., 2014):

$$Y = f(X_1, X_2) = \beta_0 + \beta_1 X_1 + \beta_2 X_2 + \beta_{11} X_1^2 + \beta_{22} X_2^2 + \beta_{12} X_1 X_2 \quad (2.10)$$

Where: Y is the dependent variable; β_0 is constant&; β_1, β_2 are the linear coefficients; β_{11} and β_{12} are the quadratic coefficients, and β_{12} is the interaction coefficient between variables 1 and 2, X_1 and X_2 are codes of independents variables.

2.11.4.2. Evaluation of the model

The predictive equation of the model should be validated before using for prediction data. The different indexes used for this validation step are the coefficient of determination (R^2), adjusted R^2, and the lack of fit. R^2 can be calculated from the regression sum of squares divided by to total sum of the square. R^2 value should be close to 1 for a good prediction model. However, R^2 can increase if the number of terms in the model is increased. Therefore, to validate the model, R^2 should not be assessed alone instead of being compared with R^2 adjusted value (Khuri & Mukhopadhyay, 2010; Nair et al., 2014). R^2 and R^2 adjusted values need to be close to 1, and the difference between R^2 and R^2 adjusted no more than 0.2 to be considered a good model (Khuri & Mukhopadhyay, 2010; Nair et al., 2014). Another statistic value that needs to be investigated is the error sum of squares (PRESS). This value reflects how well the model fitted with the experimental data. On an excellent prediction mathematical model, the PRESS value should be small (Khuri & Mukhopadhyay, 2010; Myers et al., 2016; Nair et al., 2014). Moreover, the model can also be verified by the lack of fit test. The lack of fit of the model should be lower than the F value for a good model (Nair et al., 2014) (*p*-value > 0.05). Table 2.17 summarizes all the variances and shows the squares and media of squares for these various sources.

Table 2.17. Analysis of variance (ANOVA) for a fitted mathematical model to an experimental data set using multiple regression.

(adapted from M. A. Bezerra et al. (Bezerra et al., 2008)).

Variation source	Sum of the square (SS)	Degree of freedom	Media of the square (MS)
Regression	$SS_{reg} = \sum_i^m \sum_j^{n_i} (\hat{y}_i - \bar{y})^2$	p-1	$MS_{reg} = \frac{SS_{reg}}{p-1}$
Residuals	$SS_{res} = \sum_i^m \sum_j^{n_i} (y_{ij} - \hat{y}_i)^2$	n-p	$MS_{res} = \frac{SS_{res}}{n-p}$
Lack of fit	$SS_{lof} = \sum_i^m \sum_j^{n_i} (\hat{y}_i - \bar{y}_i)^2$	m-p	$MS_{lof} = \frac{SQ_{lof}}{m-p}$
Pure error	$SS_{pe} = \sum_i^m \sum_j^{n_i} (y_{ij} - \bar{y}_i)^2$	n-m	$MS_{pe} = \frac{SS_{pe}}{n-m}$
Total	$SS_{tot} = \sum_i^m \sum_j^{n_i} (y_{ij} - \bar{y})^2$	n-1	

n_i, number of observations;
m, the total number of level in the design
p, number of parameter of the model
$\hat{y}_i$, estimated value by the model for the level i
$\bar{y}$, overall media
y_{ij}, replicates performed in each level
$\bar{y}_i$, media of replicates performed in the same set of experimental conditions.

2.11.4.3. Response surface optimization

Response surface can be analyzed to achieve the maximum or minimum-targeted or saddle values and the optimal conditions. With multiple responses, the obtained conditions have to meet all criteria (Nair et al., 2014). With the quadratic equation, the maximal or minimal points can easily be calculated by setting the first derivate of the mathematical function equal to 0 (Bezerra et al., 2008). The predict model equations also can be visualized by the surface response plot. Through the plot of surface response, the critical point and optimal conditions also can be predicted.

2.11.5. Applications

2.11.5.1. Purification phenolic compounds from adsorption

Several objectives should be considered: productivity, recovery, scalability, and cost-effectiveness to conduct the purification process for phenolic compounds. For these purposes, the multi-stages or combination of adsorption and chromatography technique has been investigated to recover phenolic compounds from macroporous resins (Weisz et al., 2013). The efficiency of this purification process involved several factors. Therefore, it is necessary to optimize this process to obtain the maximal yield of phenolic recovery and purity. Notably, Georg M. Weisz et al. (Weisz et al., 2013) used D-optimal experimental design for determining the optimal conditions for phenolic compounds in SFM desorption from macroporous resins (Weisz et al., 2013). G. M. Weisz et al. (Weisz et al., 2010) used response surface methodology with a D-optimal design to investigate the recovery targeted compounds. The factors compromised in this study were column temperature (20-60°C), solvent concentration (40-100%), and flow rate (2-6 BV/h). They found that the maximum removal of 99% CGA and TPC was obtained with a solvent concentration of 70%, flow rate 5.5BV/h, and under moderate temperatures of 40-50°C.

2.11.5.2. Adsorption

Response surface methodology was also used in the adsorption process to remove heavy metals and toxic organics from water (Nair et al., 2014). The critical factors, in this case, were pH, ionic strength, adsorbent/adsorbate ratio (Hameed & El-Khaiary, 2008). Tripathi et al. (Tripathi et al., 2009) used Box-Behnken Design to study methyl orange removal using activated carbons. The adsorbent dose, contact time, temperature, and pH were the investigated factors in this study. The optimal conditions were also observed for an adsorbent dose at 15.7 mg/L, 4h of contact time, the temperature at 40°C, and pH 2. Therefore, the maximal removal can obtain up to 99.11%. Other studies on the removal of methylene, recovery of the dye, and optimization of biosorption of heavy metal using response surface methodology have been reported (Sarabia & Ortiz, 2009; Sarkar & Majumdar, 2011).

2.11.5.3. Other applications

Response surface methodology was also widely used to determine the optimal conditions in other sectors, such as food processing, antioxidant, and extraction.

Part III: Biological properties of phenolic compounds in sunflower and rapeseed meals

2.12. Antioxidants

2.12.1. Antioxidants background

Antioxidants have been defined in several ways in the literature (Hamid et al., 2010; MacDonald-Wicks et al., 2006). Inflammatory and degenerative diseases derive from oxidative stress, including reactive oxygen species (ROS) and reactive nitrogen species (RNS). Therefore, in these cases, the role of antioxidants is vital. Antioxidants can interact and stabilize the free radicals that cause chronic diseases, including cancer (Hamid et al., 2010). Nowadays, there is widespread interest in antioxidant activity efficacy not only in foods but also in human biological systems. Several antioxidants such as vitamin C, E, beta-carotene, lycopene, and other compounds (Sies, 1997).

From a food processing point of view, antioxidants have been defined as a small number of substances that can prevent or protect the macromolecules such as fats from oxidation (MacDonald-Wicks et al., 2006). Thus, the oxidation in foods is a chemical reaction involved in chain-breaking inhibitors of lipid peroxidations. Indeed, the free radicals can be produced by the oxidation reactions process at the beginning of chain reactions. Then, these free radicals can be removed or inhibited by the antioxidants (Sies, 1997).

From the biological systems point of view, the antioxidants are defined as the substances present at low concentrations compared to those of oxidizable substrates, but significantly inhibit or prevent the oxidation of substrates (MacDonald-Wicks et al., 2006). Low levels of antioxidants can cause oxidative stress and might kill cells. Oxidative stress can cause chronic degenerative diseases and the degenerative process involved in aging (Berk et al., 2011). Therefore, the antioxidants are widely studied in the treatments for stroke and neurodegenerative diseases (MacDonald-Wicks et al., 2006).

2.12.2. Sources and origin of antioxidants

2.12.2.1. Antioxidants in natural sources

Many antioxidants present in the fruits, vegetables, and plants such as nuts, grains, or in some animals such as meats, poultry, and fish (MacDonald-Wicks et al., 2006). The common antioxidants are beta-carotenes. Beta-carotenes were found in sweet potatoes, carrots, pumpkin, and mangoes (Borek, 1991). Besides, lutein and lycopene are also known as antioxidants that come from natural plants. In particular, lycopene was found in tomatoes, watermelon, guava, papaya, and other foods (Matioli & Rodriguez-Amaya, 2003; Xianquan et al., 2005). Selenium is a mineral and component of antioxidant enzymes (MacDonald-Wicks et al., 2006). The primary dietary sources of selenium are rice and wheat. Vitamin A is an antioxidant found in liver, sweet potatoes, carrots, milk, egg yolks, and cheese (Baublis et al., 2000). There are three main chemical structures of vitamin A which include retinol (vitamin A1), 3, 4-didehydroretinol (vitamin A2), and 3-hydroxyretinol (vitamin A3). A high abundance of vitamin C (as called ascorbic acid, Figure 2.18) was found in many fruits and vegetables such as guava and cereals. This vitamin also is found in beef, poultry, and fish (Wolfe & Liu, 2007). Vitamin E (α-tocopherol, Figure 2.18) is an antioxidant, also is found in fruits and vegetables such as almonds, soybean oil, broccoli, and other foods (Herrera & Barbas, 2001). Other phenolic compounds originate

from plants, fruits, seeds, or synthetic chemical processes which also show an excellent antioxidant activity reported elsewhere (Hajimahmoodi et al., 2014).

2.12.2.2. Antioxidant present in typical extracted oilseed meals

Table 2.17 summarizes the phenolic compounds represented in typical oilseed meals. In general, extracted oilseed meals do not contain the liposoluble antioxidants except for rapeseed meal such as α-tocopherol. However, oilseed meals contain many phenolic acids, either free or esterified or condensed in an insoluble form. As presented in Table 2.18, some phenolic compounds showed antioxidant capacity, such as caffeic acid, ferulic acid, and sinapic acids, reported in these oilseed meal extracts (Nenadis et al., 2003). Among them, rapeseed meal is the richest in phenolic compounds (77-81 mg/ kg of dry weight), mainly in sinapic acid derivates (Figure 2.6) (Amarowicz et al., 2001). However, sinapine (Figure 2.6), the ester of sinapic acid and choline, did not show any antioxidant activity (Krygier et al., 1982; L. Xu & Diosady, 1997). Besides, the mustard seed meal also contains the antioxidant compounds as in rapeseed meal. Besides, flavonoids, the potent antioxidant agents, are also detected in nearly all oilseed meals. Whereas lignans are present in a minor amount in oilseed meals in general.

Table 2.18. Phenolic compounds antioxidants identified in several typical oilseed-extracted meals**.** (Adapted with permission from Stefan Schmidt and Jan Pokorny (Schmidt & Pokorný, 2011).

Oilseed	Substances with antioxidant activities	References
Rapeseed, canola	Sinapine, benzoic acid and cinnamic acid derivates, phenolic acid esters, and glycosides	(Amarowicz et al., 2001; Kozlowska et al., 1983; Krygier et al., 1982)
Mustard seed	Sinapine, esters of phenolic acids	(Dabrowski & Sosulski, 1984; Krygier et al., 1982)
Soybeans	Syringic, vanillic, ferulic, salicylic, p-coumaric acids and esters, chlorogenic, caffeic, sinapic acids, isoflavones, and their glucosides	(Amarowicz et al., 1996; Hoppe et al., 1997; Murakami et al., 1984; Walter, 1941)
Peanuts	Phenolic acids and esters, such as p-hydroxybenzoic, p-coumaric, syringic, gallic, vanillic acids, epicatechin, catechin	(Walker et al., 1982)
Sunflower seed	Chlorogenic, caffeic, cinnamic, m- and p-hydroxybenzoic, vanillic, syringic, gallic, and vanillic acids, epicatechin, catechin	(Sabir et al., 1974)
Evening primrose seed	Proanthocyanidins and their gallates, isoflavones	(Amarowicz et al., 1996)
Linseed	Sinapic, p-hydroxybenzoic, coumaric, ferulic acids, lignans	(Amarowicz et al., 1996; Walker et al., 1982)
Cottonseed	Sinapic acid, ferulic, p-hydroxybenzoic acids, quercetin, rutin	(Amarowicz et al., 1996; Walker et al., 1982)
Sesame seed	Lignans, coumaric, ferulic, vanillic, sinapic acids	(Amarowicz et al., 1996; Walker et al., 1982)
Olive fruits, cakes	Hydroxytyrosol, secoiridoids, flavonoids, lignans	(Gennaro et al., 1998)
Grapeseed	Catechin, epicatechin, procyanidin	(Jayaprakasha et al., 2001)

Soybean flour has been used as antioxidants because of isoflavones and cinnamic acid derivates (Arai et al., 1966). These results consisted of the finding from Murakami et al. (Murakami et al., 1984). In this report, they observed that soybean hydrolysates' antioxidant activity is mostly due to isoflavone aglycones. The antioxidant properties of peanuts is mainly contributed by phenolic acids and esters such as p-hydroxybenzoic, *p*-coumaric, and vanillic acids. Besides, sunflower meal (SFM) contained up to 3.0-3.5 g/kg of phenolic compounds' dry weight. Among them, chlorogenic acid (Figure 2.5) and caffeic acid (Figure 2.5) composed up to 70% of phenolic antioxidants (Sabir et al., 1974). Evening primrose seed extract showed antioxidant activity because it is rich in phenolic compounds such as proanthocyanidins and their gallates isoflavones (Amarowicz et al., 1996). Defatted grapeseed meal also contains catechin, epicatechin, and procyanidin, as shown in Figure 2.25, responsible for antioxidant properties (Saito et al., 1998). The main antioxidant property of olive fruits and cakes is the contribution of phenolic antioxidants. Indeed, olive fruits contain simple phenolic compounds such as hydroxytyrosol, secoiridoids, flavonoids, and lignans (Gennaro et al., 1998). Similarly, lignans are found in linseed defatted meal beside the other phenolic compounds such as sinapic, p-hydroxybenzoic, coumaric, and ferulic acids (Amarowicz et al., 1994, 1996; Walker et al., 1982). Moreover, lignans were observed in sesame seed meal. According to Kozlowska et al. (Kozlowska et al., 1983), sesame seed-defatted meals also contain 41mg/kg free phenolic acids, 325 mg/kg esterified acids, and 14 mg/kg insoluble phenolic acids. This composition of phenolic compounds can explain the antioxidant activity of sesame seed meal. Cottonseed meal exhibited antioxidant activity due to several phenolic compounds such as sinapic acid, ferulic, p-hydroxybenzoic acids, quercetin, and rutin were reported (Amarowicz et al., 1994, 1996; Walker et al., 1982).

2.12.2.3. Antioxidant present in extracted sunflower and rapeseed meals

Some reports regarding the anti-oxidant properties of sunflower meal (SFM) phenolics have been investigated elsewhere. Two methods are frequently used to estimate phenolics' antioxidant activity: radical scavenging activities such as DPPH and ABTS assays due to them being simple, fast, and highly efficient, especially when the sample size is large. According to Žilić, S. et al. (Žilić et al., 2010), phenolic compounds in SFM had potential in anti-oxidant actions. Typically, phenolic compounds in sunflower kernels had a higher DPPH scavenging activity than a sunflower seed. Another report from Pablo R. Salgado et al. (Salgado et al., 2012) confirmed that phenolics in SFM strongly exhibited anti-oxidant properties by using ABTS scavenging assay. Georg M. Weisz et al. (Weisz et al., 2013) found that CGA and TPC from SFM after desorption with organic solvent showed an excellent antioxidant capacity using ferric ion reducing antioxidant power (FRAP) assay. Besides, Nikita Wanjari et al. (Wanjari & Waghmare, n.d.) also revealed that phenolic extract from SFM by ethanol solution exhibited the highest antiradical activity than other organic solvent extracts. These authors also highlight that the effectiveness in DPPH radical scavenging activity of phenolic extracts was found even better than butylated hydroxytoluene (BHT) (Vuorela et al., 2004).

Anti-oxidant properties of phenolic compounds in rapeseed meal (RSM) also have been reported in the literature. The effect of rapeseed phenolics on scavenging the radicals has been investigated in the report of Amarowicz et al. (Amarowicz et al., 2001) and Matthäus (Matthäus, 2002). They found that effective radical scavenging activity relied on the phenolic solvent extract fraction. Amarowicz et al. (Amarowicz et al., 2001) observed that phenolic rapeseed extract with 70% acetone showed the highest radical capacity. They also discovered that there was no correlation between the TPC and the antioxidant activity. However, in an earlier study of Wanasundara et al. (U. N. Wanasundara et al., 1995), the crude ethanolic extract's antioxidant activity was higher than the purified phenolic fraction one. This phenomenon is due to the phenolic fraction containing several phenolic compounds. Therefore, the antioxidant increased because of the synergistic effect. Later, Satu Vourela et al. (Vuorela et al., 2004) investigated the impact of isolation of phenolic compounds from RSM with aqueous methanol, aqueous ethanol, hot water, and enzymes (ferulic acid esterase) on the antioxidant activity. They observed that all isolate fractions showed a radical scavenging rate of more than 60%. However, they recommended using either water or enzyme to isolate rapeseed phenolics due to their suitable method to avoid using an organic solvent. Usha Thiyam et al. (Thiyam et al., 2006) also indicated that sinapine had a significantly lower free radical scavenging capacity than sinapic acid in RSM.

Meanwhile, the previous studies of Krygier et al., Xu and Diosady (Krygier et al., 1982; L. Xu & Diosady, 1997) addressed that sinapine did not exhibit any antioxidant activity. Other researchers showed a correlation between total phenolic content in rapeseeds with an antioxidant capacity (Szydłowska-Czerniak et al., 2010). The antioxidant capacity of basic and acidic hydrolysis rapeseed phenolic extract was also conducted by Aleksander Siger et al. (Siger et al., 2017). These authors confirmed that after hydrolysis, the antioxidant capacity increased. That might be due to the release of free phenolic compounds sinapic acid from their conjugates such as esters or glycosides.

2.12.3. Types of antioxidants

Figure 2.17 represents all the chemical structures of antioxidants commonly used in the food and biological system reported in the literature (Hamid et al., 2010). Thereby, antioxidants have been classified into two main groups, including natural antioxidants and synthetic antioxidants.

2.12.3.1. Natural antioxidants

Natural antioxidants are known as chain-breaking antioxidants. These molecules can react with lipid radicals and convert them into more stable products. According to Hurrel (Hurrell, 2003), this group is composed mainly of phenolic compounds. Besides, it contains also:

Antioxidants minerals are known as the co-factors of antioxidants enzymes (Hamid et al., 2010). They are selenium, copper, iron, zinc, and manganese. Without these compounds, abundant macromolecules such as carbohydrates would be affected in their metabolism.

The vitamins antioxidants are also included in this group. They are composed of vitamin C, vitamin E, and vitamin B. These vitamins are necessary for body metabolism.

Phenolic compounds from the vegetables, fruits, grains, seeds, and flowers are natural antioxidants (U. N. Wanasundara et al., 1995). Phenolic compounds have potent antioxidants and free radical scavengers, widely studied in the literature (Tung et al., 2007).

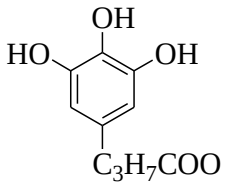

Progylgallate (PG)

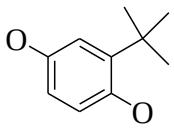

t-butylhydroquinone (TBHQ)

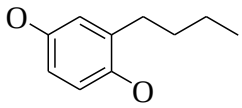

butylhydroquinone (BHQ)

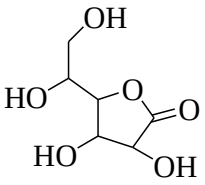

Ascobic acid (Vitamin C)

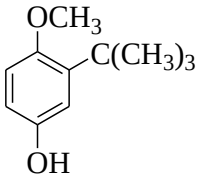

Butylate hydroxyanisole (BHA)

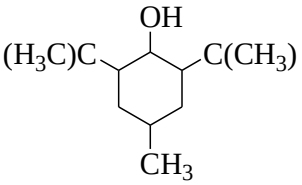

Butylated hydroxytoluene (BHT)

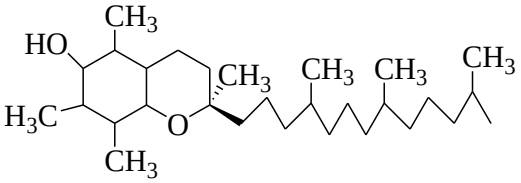

alpha-tocopherol (Vitamin E)

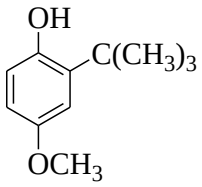

Phenolic acid

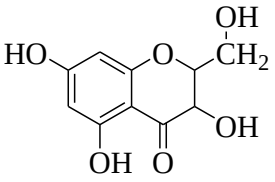

Flavonoids

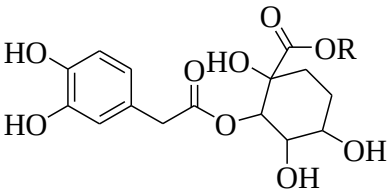

Phenolic acid and ester

(R = alkyl, phenolic ester)

Figure 2.17. Chemical structures of several antioxidants commonly used.
(adapted with modification from A. A. Hamid et al. (Hamid et al., 2010)).

Figure 2.18 shows the classification of phenolic antioxidants. In natural sources, phenolic compounds can be present in various types include phenolic acids, flavonoids, stilbenes, coumarins, lignans, and tannins (Shahidi, 2015).

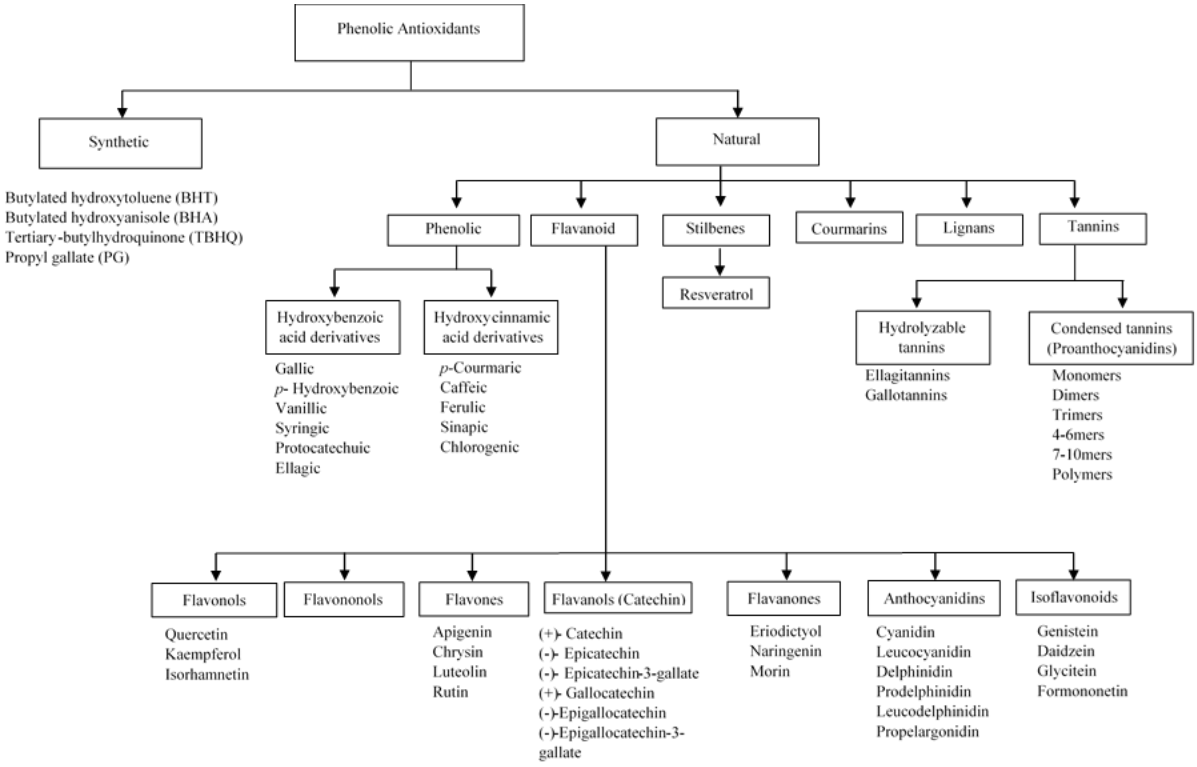

Figure 2.18. The types of antioxidants from phenolic compounds.
(Adapted from Fereidoon Shahidi (Shahidi, 2015)).

The predominant phenolic acids in plants are in hydroxybenzoic and hydroxycinnamic acids derivates. The most common hydroxybenzoic acid derivates potent in anti-oxidant capacity is gallic, p-hydroxybenzoic, vanillic, syringic, protocatechuic ellagic acid. The most well-known hydroxycinnamic acid derivates are *p*-coumaric, caffeic, ferulic, sinapic, and chlorogenic acids. Among them, caffeic acid is responsible for selectively blocking the biosynthesis of leukotrienes, which is involved in immunoregulation diseases (Yasuko et al., 1984). Some studies have also demonstrated that caffeic acid might act as an anti-tumor treatment such as colon cancer (Robbins, 2003).

Natural antioxidants phenolic compounds exist in flavonoids, stilbenes, coumarins, lignans, and tannins forms. The family of flavonoids can be divided into several sub-groups, including flavones, flavonols, isoflavonoids, flavanones, flavanones, flavanols, and anthocyanidin. The general chemical structures of flavonoid derivatives are also mentioned in section 2.3.2 in this Ph.D. thesis. Based on the different chemical structures of flavonoids, these compounds' potent antioxidant capacity is different (Han et al., 2012). Flavones and flavonols were found in moringa (*Moringa oleifera*), strawberry, peepal, and spinach (Burns et al., 2002). Besides, flavanones were observed in celery, parsley, and artichoke (D. Chen et al., 2005). Flavan-3-ols are presented in some fruits such as sour cherries, grapes, and blackberries. Meanwhile, flavanones are provided from citrus fruits in their glycosidic forms (D. Chen et al., 2005). Whereas anthocyanins present in fruits such as blackberry, elderberry, and cranberry (D. Chen et al., 2005). Isoflavones are found mostly in soybeans, and isoflavones occur in black beans and green beas. Some flavanols such as catechin, epicatechin, epicatechin-3-gallate, gallocatechin,

epigallocatechin, and epigallocatechin-3-gallate have been found in green tea polyphenols acting as radical scavengers (Salah et al., 1995; Yao et al., 2004). Besides, the synergistic effect of (−)-epicatechin and quercetin with α-tocopherol in egg yolk. The regular drinking of red wine, which contains approximately 200mg of flavonoids per glass and resveratrol about 0.1-15 mg/ L, can prevent coronary heart disease in some France regions, as well-known as the "French paradox" (Padmesh et al., 2006).

Stilbenes, in particular resveratrol, and its glucoside were found to be potent in antioxidative and anti-tumor activities (Burns et al., 2002; Torres et al., 2010). In the natural, resveratrol occurs mainly from red wine and peanuts (Burns et al., 2002). Resveratrol possesses potent antioxidants in various in vitro assay such as DPPH, ABTS, hydrogen peroxide scavenging, and metal chelating activities, when compared to standard antioxidant agents such as butylated hydroxyanisole (BHA), butylated hydroxytoluene (BHT), and α-tocopherol, have been reported (Gülçin et al., 2010). In the pharmaceutical sector, resveratrol was also used in preventing lipid oxidation of medical products or retarding the toxic oxidation formation (Shahidi, 2015).

Tannins are polymers of phenolic acids, as proanthocyadinins with chemical structure, as shown in Figure 2.4. The condensed tannins have been found in several fruits such as rapeseed, berries, cocoa, or in some beverages such as beer and tea (Ferreira & Li, 2000). Besides, the hydrolyzable tannins occur in some berries, leaves of vegetables (Serrano et al., 2009). The inhibition of lipid peroxidation, lipoxygenases in vitro, the ability to scavenge radicals such as hydroxyl and superoxide of tannins have been reported (Gyamfi & Aniya, 2002).

2.12.3.2. Synthetic antioxidants

In the food sector, the synthetic phenolic compounds commonly used as antioxidants agents are butylated hydroxyanisole (BHA), butylated hydroxytoluene (BHT), propyl gallate (PG), and tertiary-butylhydroquinone (TBHQ), as shown in Figure 2.17. Besides, octyl gallate (OG) and dodecyl gallate (DG) was also used as a synthetic antioxidant (Makahleh et al., 2015). These synthetic phenolic antioxidants were added to food products to prevent or retard lipid oxidation (Saad et al., 2007). These antioxidants were also used in fats, oils, and lipid-containing foods stored (Saad et al., 2007). However, antioxidants' efficiency of synthetic antioxidants might not be high in preventing oxidative deterioration of fats and oils originated from vegetables (Verhagen et al., 1991). Moreover, the use of synthetic antioxidants in foodstuffs is also regulated by administrative governments due to their potential toxicity for humans or even causing some disease such as liver and carcinogenesis (Biparva et al., 2012). Therefore, it rises to high demand for searching natural antioxidants (Berdahl et al., 2010).

Butylated hydroxyanisole (BHA) is a mono-phenolic antioxidant (Figure 2.17), which occurs as white waxy flakes. BHA is soluble in fats and oils. Therefore, it showed strong antioxidant effects in essential oils (Hettiarachchy et al., 1996). Butylated hydroxytoluene (BHT) is also a mono-phenolic antioxidant as known as a white crystalline compound. Nevertheless, BHT is not as effective as BHA

in terms of radical scavenging activity due to two tert-butyl groups, which cause more significant steric hindrance than BHA to the molecule (Nanditha & Prabhasankar, 2008). Like BHA, BHT is soluble in fats and oils. Besides, BHT shows significant effectiveness in inhibiting the oxidation of animal fats than vegetable oils in the report of Dziezak (Dziezak, 1986). Besides, tertiary-butylhydroquinone (TBHQ) is an antioxidant agent for preserving unsaturated vegetable oils, animal fats, and meat products by increasing oxidative stability (Dziezak, 1986). TBHQ is also known as a food additive (Okubo et al., 2003). TBHQ is a more potent synthetic antioxidant than BHA and BHT (M. A. Khan & Shahidi, 2001). Propyl gallate (PG) is an antioxidant used for stabilization of cosmetic, food-packaging materials, foods containing fats, oils, mayonnaise, and using as an additive in edible fats (Zurita et al., 2007). Propyl gallate is the ester of gallic acid with propyl alcohol. Thereby, PG is soluble in ethanol but insoluble in water solution (Naczk & Shahidi, 2004a). The synergistic interaction of antioxidant efficiency between PG and BHA and BHT was reported (Shahidi et al., 1992). However, the combination of PG and TBHQ is not accepted (Shahidi et al., 1992). Additionally, PG can cause liver toxicity and stimulate carcinogenesis (Eler et al., 2009; Okubo et al., 2003). Several studies showed that the antioxidant and cell protection of PG might lead to pro-oxidative, cytotoxic, and genotoxic in the presence of Cu(II) (Jacobi, 1998; Jacobi et al., 1999).

2.12.4. Antioxidant mechanisms of phenolic compounds

There are two principal mechanisms of the antioxidant process for antioxidant compounds proposed in the literature (Hamid et al., 2010), including (1) chain-breaking mechanism and (2) removal of reactive oxygen species (ROS) and reactive nitrogen species (RNS) initiator by quenching chain catalyst mechanism.

2.12.4.1. Chain-breaking mechanism

Firstly, the antioxidants donate electrons for the free radicals. The chain-breaking mechanism follows this process. Figure 2.19 shows the example of lipid-free radical during the auto-oxidation of lipids.

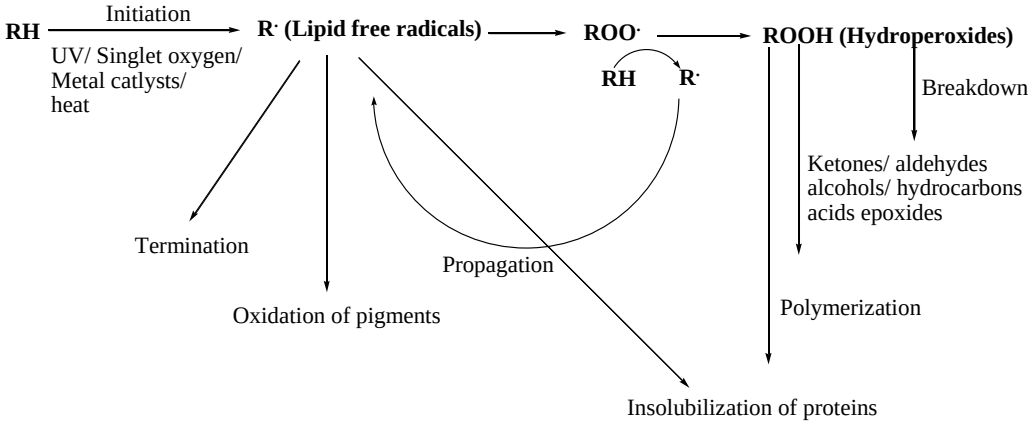

Figure 2.19. Polyunsaturated fatty acids (RH) auto-oxidation process.
(Adapted from Fereidoon Shahidi (Shahidi, 2015)).

The pathway for lipid degradation is the auto-oxidation process. This process involves a free radical chain reaction, which is stimulated by the exposure of lipids to UV, heat, and metal ions catalysts (Figure 2.19) and form the lipid-free radicals. According to Borek (Borek, 1991), the conventional way to form the auto-oxidation process include initiation (rise the free radicals), propagation (hydro-peroxides in oxidation reaction), and termination (obtain a non-radical product) stages (Shahidi et al., 1992). These chain reactions of free radicals are represented in Figure 2.20.

Initiation stage

(1) $RH \longrightarrow R^{\cdot} + H^{\cdot}$

(2) $R^{\cdot} \longrightarrow R^{\cdot} + O_2 \longrightarrow ROO^{\cdot}$

(3) $2ROOH \longrightarrow ROO^{\cdot} + RO^{\cdot} + H_2O$

Propagation stage

(1) $R^{\cdot} + O_2 \longrightarrow ROO^{\cdot}$

(2) $ROO^{\cdot} + RH \longrightarrow ROOH + R^{\cdot}$

(3) $RO^{\cdot} + RH \longrightarrow ROH + R^{\cdot}$

Termination stage

(1) $R^{\cdot} + R^{\cdot} \longrightarrow R\text{-}R$

(2) $R^{\cdot} + ROO^{\cdot} \longrightarrow ROOR$

(3) $ROO^{\cdot} + ROO^{\cdot} \longrightarrow ROOR + O_2$

(4) Antioxidants + O_2 $\longrightarrow$ oxidized antioxidants

11

$LOO^{\cdot} + FL{-}OH \longrightarrow LOOH + FL{-}O^{\cdot}$ (i)

Flavonoid $\longrightarrow$ Phenonyl radical (ii)

$LOO^{\cdot}/\ L^{\cdot}/\ LO^{\cdot} + FL{-}OH \longrightarrow LOOH/\ LH/\ LOH = FL{-}O^{\cdot}$ (iii)

Figure 2.20. Schematic representation of the flavonoids antioxidants reaction mechanisms.
(adapted from A.A.Hamid et al. (Hamid et al., 2010))

In this process, the termination of lipid radical ($L^{\cdot}$), lipid peroxy radical ($LOO^{\cdot}$), and alkoxyl radical ($RO^{\cdot}$) produced the re-initiation of lipid peroxidation, as shown in stage (iii).

2.12.4.2. Quenching chain initiator catalyst mechanism

Reactive oxygen species (ROS) and reactive nitrogen species (RNS) over regeneration may lead to inflammation (Willcox et al., 2004). Phenolic compounds can scavenge radicals and form metal

ion chelation (Heim et al., 2002). Therefore, it can block the ROS formation (Mishra et al., 2013). Besides, phenolic compounds can inhibit the catalytic activity of enzymes, which participate in ROS generation. The ion chelating and iron-stabilizing quercetin properties have been reported (Mishra et al., 2013). The hydrogen atom (H+) donation from flavonoid to suppress lipid-peroxyl radicals to protect the membrane phospholipids was also found in the literature (Hamid et al., 2010).

2.12.5. Antioxidant capacity methods

2.12.5.1. Mechanism of antioxidants capacity methods

According to Ayse Karadag et al. (Karadag et al., 2009), the mechanism of antioxidants capacity methods can be divided into (i) hydrogen atom transfer (HAT) and (ii) electron transfer (ET). However, it is difficult to distinguish these mechanism methods (Prior et al., 2005). In most cases, HAT-base mechanism methods are dominant.

2.12.5.1.1. Hydrogen atom transfer-based method

The hydrogen atom transfer (HAT) based method can determine antioxidant substances' ability to scavenge free radicals by hydrogen donation behavior to produce stable compounds (Prior et al., 2005). HAT-based mechanism method is involved in radical chain-breaking antioxidant capacity (Karadag et al., 2009) as illustrated in reaction (i).

$$\text{(i)}\quad AH + X^{\cdot} \longrightarrow XH + A^{\cdot}$$

There are two factors in HAT-based methods in antioxidant activity measurement, including the bond dissociation energy of the H-donating group and ionization potential of antioxidant agents. HAT reactions depend on the solvent and pH value. This method of reaction usually is relatively rapid, which can complete in seconds to minutes. The majority of HAT-based methods are governed by competitive reaction kinetics. Based on the kinetic curve, the quantitation of antioxidant ability is calculated. Besides, HAT-based methods are usually conducted in the presence of a synthetic-free radical generator such as AAPH, ABAP, ABTS, DPPH (Valkonen & Kuusi, 1997; Wolfe & Liu, 2007), fluorescein such as FL (Parry et al., 2006), and a tested antioxidant.

In particular, the HAT-based methods using fluorescent probes have a similar mechanism to lipid peroxidation (Karadag et al., 2009). In this assay condition, the substrate (probe) concentration is smaller than the antioxidant agent concentration. However, the antioxidant concentration is much smaller than the substrate (for instance, lipid) concentration in the whole food system. Therefore, it is questionable whether antioxidant capacity, which is determined using a molecular probe, can exhibit antioxidant activity in a real solution (D. Huang et al., 2005).

2.12.5.1.2. Electron transfer-based method

Electron transfer (ET) based methods measure antioxidant ability in transferring one electron to reduce any compounds, including metals, carbonyls, and radicals. ET-based method mechanisms can be expressed as in reaction (ii).

$$\text{(ii)}\quad M(III) + AH \longrightarrow AH^{\cdot} + M(II)$$

ET-based methods are based on the deprotonation and ionization of the reactive functional groups. Therefore, the pH of the reaction solution is a critical factor of ET-based methods. In general, when pH values increase, the ionization values decrease, reflecting the increasing electron-donating capacity with deprotonation (Prior et al., 2005). According to Huang et al. (D. Huang et al., 2005), there is protonation of antioxidant compounds in acidic conditions. Therefore, the reducing capacity of antioxidants can be inhibited. However, in basic conditions, in the case of phenolic compounds, the proton dissociation would induce the sample's reducing capacity. Unlike HAT-based methods, ET-based methods take time to reach completion. These methods are determined based on the percent decrease in substrate rather than kinetics or total antioxidant capacity (Ozgen et al., 2016). ET-based method mechanism also depends on the solvent due to the stabilization of charged compounds (Ou et al., 2002).

There are two components involved in ET-based methods, including antioxidant and oxidant (probe). The reaction occurs between the probe and an electron from the antioxidant agent, leading to a change in the probe's color. The level of color-changing is correlated to the antioxidant concentration. Therefore, to make the correlation equation, the antioxidant capacity is equal to reducing capacity.

2.12.5.2. *In vitro* antioxidant capacity methods commonly used in literature

The antioxidant activity of phenolic compounds is based on their capability in donating hydrogen or electron as well their ability to delocalise the unpaired electron within an aromatic ring (Fernandez-Panchon et al., 2008a). From a biological point of view, the antioxidant capacity of phenolic compounds lays in their ability in protecting molecules from oxidative stress. Table 2.19 summarizes the frequently used in vitro methods that have been used to evaluate the antioxidants properties of phenolic compounds.

Table 2.19. Description of antioxidant activity methods.

(Adapted with modifications from M. S. Fernandez-Panchon et al. (Fernandez-Panchon et al., 2008a)).

Method	Radical	Measurement and method	Result expression	Samples	References
DPPH	$DPPH^{\cdot}$	- Decrease of $DPPH^{\cdot}$ - Spectrophotometry	EC50 (sample amount reduce $DPPH^{\cdot}$ to 50%)	Phenols, foods	(Brand-Williams et al., 1995; Sánchez-Moreno et al., 1998)
ABTS	$ABTS^{\cdot+}$	- Decrease of $ABTS^{\cdot+}$	Equivalents of TROLOX	Phenols, foods, biological samples	(Alonso et al., 2002; Cano et al., 1998)
ORAC	AAPH/H_2O_2-Cu^{2+}/ $CuSO_4$	- Inhibition of fluorescence decrease of PE or FL	Equivalents of TROLOX	Phenols, foods, biological samples	(Cao & Prior, 1999)
Luminol-photo-chemiluminescence (PCL) Assay	$Luminol^{\cdot}$	- Inhibition of quimioluminiscence - Quimioluminiscence	Equivalents of TROLOX	Biological samples	(Alho & Leinonen, 1999)
β-carotene linoleic acid bleaching Assay (or Crocin-Bleaching Assay)	ABAP	- Inhibition of crocin oxidation - Spectrophotometry	Equivalents of TROLOX	Biological samples	(Lussignoli et al., 1999)
FRAP		- Spectrophotometry - Reduction (TPTZ-Fe^{3+} to TPTZ-Fe^{2+}) - Spectrophotometry	µmol Fe^{2+}/ L	Foods, biological samples	(Benzie & Strain, 1996)
TRAP	ABAP	- Consumed oxygen - Oxygen electrode	Equivalents of TROLOX	Foods, biological samples	(Wayner et al., 1985)

Note : TRAP: Total radical-trapping antioxidant potential, ORAC: Oxygen radical absorbance capacity, DPPH: 2,2-diphenyl-1-picrylhydrazyl, ABTS : 2,2'-azinobis(3-ethylbenzothiazoline-6-sulfonic acid), FRAP : Ferric reducing ability of plasma, AAPH : 2,2'-diazobis (2-amidinepropane) dihydrochloride, ABAP : 2,2'-azobis (2-amidinopropane) dihydrochloride, PE : phycoerythrin, FL :fluorescein, TPTZ : 2,3,5-triphenyl-1,3,4-triaza-2-azoniacyclopenta-1,4-diene chloride, TROLOX : 6-hydroxy-2,5,7,8-tetramethyl-chroman-2-carboxylic acid.

2.12.5.2.1. DPPH method

The 2,2-diphenyl-1-picrylhydrazine (DPPH) radical scavenging assay was proposed by Blois (Blois, 1958) and was slightly modified by several researchers. DPPH method is the most widely used for antioxidant evaluation for plant samples (Krishnaiah et al., 2011).

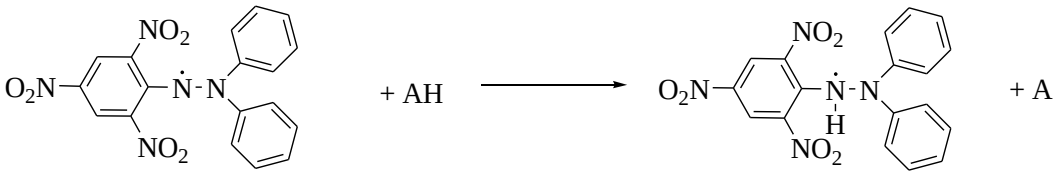

Diphenylpicrylhydrazyl (free radical) Diphenylpicrylhydrazine (non-radical)

Figure 2.21. Mechanism of DPPH assay.

Figure 2.21 shows the mechanism of DPPH acting as an antioxidant in solution. Herein, DPPH is a stable radical free radical that can donate a hydrogen atom when interacting with phenolic compounds. The DPPH method aims to scavenge DPPH radicals via antioxidant agents, decolorizing the DPPH stock solution. The antioxidant activity is measured by changing the absorption solution at wavelength 515-517nm for 30 min. The high decrease in the mixture solution's absorbance demonstrates the significant free radical scavenging capacity of tested samples.

2.12.5.2.2. ABTS method

Along with the DPPH assay, the ABTS radical scavenging assay is the second most used for antioxidant capacity evaluation from plant extracts. The oxidation reaction of ABTS with potassium persulfate produces the ABTS radical cation. The inhibition of ABTS radical cation in the presence of hydrogen-donating antioxidants is determined by spectrophotometry technique at a wavelength of 734nm. This method can assess both lipophilic and hydrophilic compounds. Antioxidant activity can be expressed in Trolox-equivalent antioxidant capacity (TEAC) concentration (TEAC/mg).

2.12.5.2.3. ORAC assay

The oxygen radical absorbance capacity (ORAC) method can measure the antioxidant capacity of foods and other chemical substances such as phenolic compounds. 2,2'-azobis (2-amidinopropane)dihydrochloride (AAPH) is a peroxyl radical generator, and Cu^{2+}-H_2O_2/ $CuSO_4$ is a hydroxyl radical generator of ORAC assay. This method is evaluated based on the area under the curve (AUC) technique and measures the kinetic of free radicals reaction. ORAC assay has been used by many researchers to assess the antioxidant from plants in recent years.

2.12.5.2.4. PCL assay

Luminol-photo-chemiluminescence (PCL) assay is used to determine superoxide radical inhibition of a pure compound or mixture compounds from various sources such as vegetables, fruits, and synthetic. This assay can be used to measure the antioxidant capacity of both hydrophilic and lipophilic substances in lipid and aqueous phases. Because of photosensitizer presence, this method is based on a 1000-fold enhancement of the oxidative reaction compared to normal conditions. PCL method is a rapid and sensitive technique.

2.12.5.2.5. β-carotene linoleic acid bleaching Assay (or Crocin-Bleaching Assay)

The β-carotene linoleic acid bleaching Assay (or Crocin-Bleaching assay) is one of the techniques, which is suitable for natural antioxidants (H. E. Miller, 1971). In this assay, quercetin, BHT, and α-tocopherol are used as standards. This method allows quantifying the inhibition of volatile organic compounds and conjugated diene hydroperoxides obtaining from linoleic acid oxidation of antioxidant agents. As a result, β-carotene is discolored.

2.12.5.2.6. FRAP assay

Ferric reducing-antioxidant power (FRAP) assay evaluates the ability to reduce ferric iron of antioxidants. The principle of this method is to inhibit the complex between ferric iron and 2,3,5-triphenyl-1,3,4-triaza-2-azoniacyclopenta-1,4-diene chloride (TPTZ) to produce the ferrous form at low pH. Antioxidants' inhibition capacity can measure the changing of absorbance value at 593nm wavelength using a diode-array spectrophotometer. FRAP values can be determined by changing the absorbance value of TPTZ-Fe^{3+} to TPTZ-Fe^{2+} of tested samples (Benzie & Strain, 1996).

2.12.5.2.7. TRAP assay

The total radical-trapping antioxidant parameter (TRAP) method is based on the retarding of antioxidants on R-phycoerythrin's fluorescence decay (R-PE) peroxidation reaction. 2,2'-azobis (2-amidinopropane) dihydrochloride (ABAP) is a radical generator in this method, which can suppress R-PE's fluorescence. This inhibition reaction is determined in the presence of antioxidant substances. Therefore, through quantification of the decay in decoloration of samples, the antioxidant capacity is evaluated. TRAP values are obtained from the length of the lag-phase and compared to standards.

2.12.5.3. Measurement of reactive oxygen/ nitrogen species method

2.12.5.3.1. Hydrogen peroxide scavenging (H_2O_2) assay

Nowadays, human beings are indirectly exposed from the environment to about 0.28mg/kg/day of hydrogen peroxide (H_2O_2) through respiration, eye, or skin contact. In the body, H_2O_2 can quickly decompose into oxygen and water, which may produce the hydroxyl radical ($OH^{\cdot}$). Hydroxyl radical ($OH^{\cdot}$) in the body can cause DNA damage. Therefore, it is vital to protect the body from hydrogen peroxide by using antioxidant agents. The antioxidant capacity is determined by the ability to scavenge hydrogen peroxide, according to Ruch et al. (Ruch et al., 1989) method. This method is based on determining the changing absorbance at 230nm of hydrogen peroxide before adding the antioxidant substances using a spectrophotometer.

2.12.5.3.2. Nitric oxide scavenging activity

In biological tissues, nitric oxide ($NO^{\cdot}$) radical is produced by specific nitric oxide synthases (Ghafourifar & Cadenas, 2005). This method is based on decomposing in an aqueous solution to sodium nitroprusside's physiological conditions to produce nitric oxide ($NO^{\cdot}$). The sample's antioxidant capacity can be measured by changing the absorbance at 546nm of tested samples and the Griess agent's presence (Marcocci et al., 1994).

2.12.5.3.3. Peroxynitrite radical scavenging activity

Peroxynitrite ($ONOO^{\cdot}$) radical is a cytotoxic substance, which can cause cell death, lipid peroxidation, carcinogenesis, and aging. Peroxynitrite ($ONOO^{\cdot}$) is produced *in vivo* by several cell types such as endothelial, Kupffer, neutrophils, and macrophage cells. The method is reported by Kooy et al. (Kooy et al., 1994) using the dihydroxyrhodamine 123 (DHR 123) as a radical scavenger.

Scavenging activity for peroxynitrite of studied solution can be measured on a microplate fluorescence spectrophotometer at a wavelength of 485-530nm.

2.12.5.4. *In vivo* methods

The antioxidants capacity of phenolic compounds is also measured by in vivo methods. In this step, samples have to be tested using animal models such as mice and rats in a dose-dependent manner. After the determined time, the animal's blood and tissues have to be treated for the assays. Several assays were used for this test, and the most common method are the ferric reducing ability of plasma, reduce glutathione (GSH) estimation, lipid peroxidation, and LDL assays (Alam et al., 2013). However, in this Ph.D. part, we focus on the *in vitro* antioxidant capacity methods.

2.12.6. Chemical structures of phenolic compounds and antioxidants activity relationship

Phenolic compounds have the phenyl moiety (hydroxyls substituents on the benzene rings) responsible for antioxidant activity. The antioxidants mechanism for phenolic compounds can be defined by radical scavenging via hydrogen atom donation (H^+/ $H^\cdot$). Other antioxidants are defined as a radical suppression mechanism by electron donation and singlet oxygen inhibition (Shahidi, 2015). Therefore, the antioxidant property of phenolic compounds is estimated based on the ability to scavenge free radicals, hydrogen atoms donation, electrons donation, and chelate metal cations interaction (Amarowicz et al., 2004). The chemical structure of phenolic compounds is a significant factor in defining their radical scavenging and metal chelating activity. Thus, understanding the structure-activity relationship (SAR) in phenolic compounds' antioxidants activity is vitally important.

2.12.6.1. Phenolic acids (C6)

Figure 2.2 represents the general structure of phenolic compounds and sub-classified flavonoids from plants. The classification of natural phenolic compounds is also mentioned in 2.3.2 of this chapter. Structures-antioxidants activity relationship of phenolic compounds has been addressed in the literature (Balasundram et al., 2006).

For phenolic acids, the relationship between antioxidant capacity with the numbers and position of hydroxyl groups to the carboxyl functional groups has been reported (Rice-Evans et al., 1996). Interestingly, the –OH moiety at the ortho- or para-position to the –COOH showed no antioxidant effect with monohydroxybenzoic. However, it showed antioxidant activity in the case of m-hydroxybenzoic acid (Rice-Evans et al., 1996). Moreover, phenolic compounds' antioxidant capacity increases when increasing the level of hydroxylation, such as trihydroxylated gallic acid, which shows a high antioxidant activity (Balasundram et al., 2006). The higher degree of –OH groups in the aromatic ring of phenolic compounds, the higher Trolox equivalent antioxidant capacity (TEAC) values were also observed by ABTS and DPPH methods (Sevillano et al., 2013). Nevertheless, the substitution of –

OH groups at the 3- and 5-position in benzene ring such as syringic acid (Figure 2.23A) reduces the antioxidant capacity as found by Rice-Evans et al. (Rice-Evans et al., 1996).

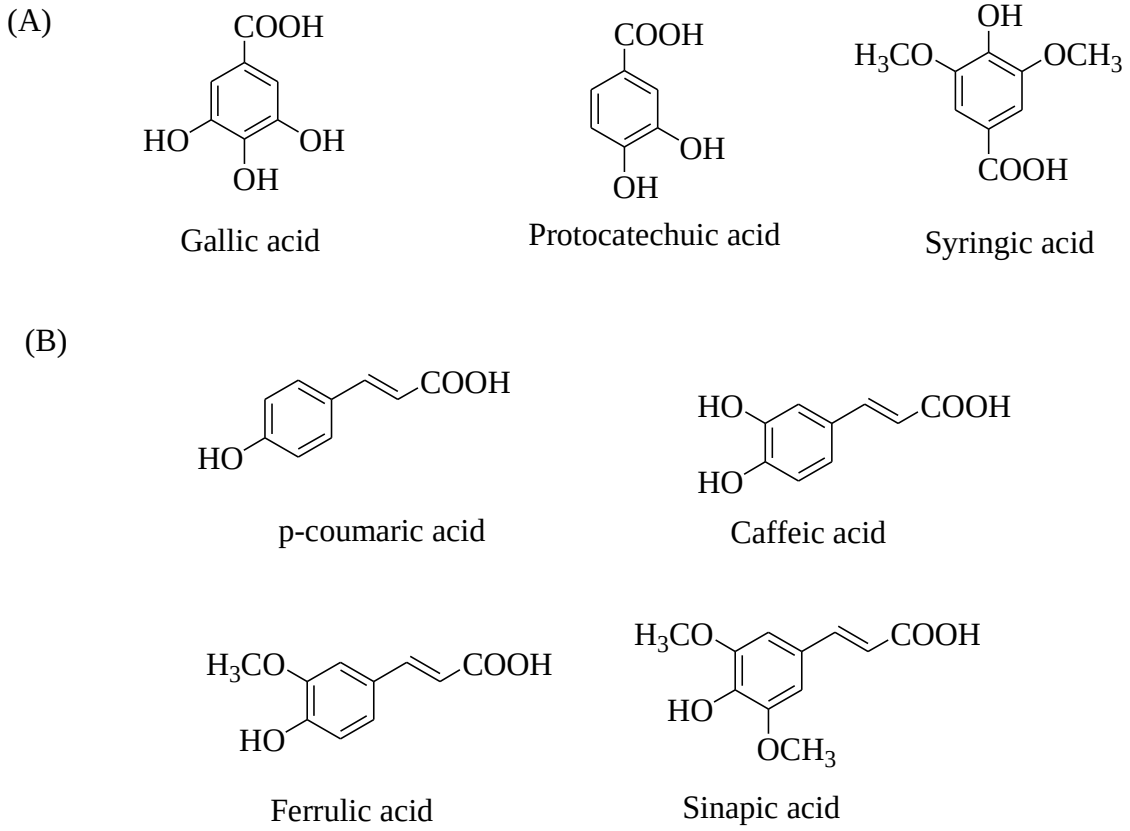

Figure 2.22. Examples of phenolic antioxidants in hydroxybenzoic (A) and hydroxycinnamic acids forms (B).

2.12.6.2. Hydroxybenzoic (C6-C1) and hydroxycinnamic acids (C6-C3)

Hydroxycinnamic acids (Figure 2.22B) possess a higher antioxidant capacity compared to hydroxybenzoic acids (Figure 2.23A) (Andreasen et al., 2001). This difference might come from the –CH=CH-COOH group of hydroxycinnamic acids type because this group may give more remarkable H-donating ability and radical stabilization than the –COOH functional group case hydroxybenzoic acids (Rice-Evans et al., 1996). The presence of ortho-dihydroxy substitution in the aromatic ring also plays a vital role in the antioxidant activity (H. Wang et al., 2008). In the report of Fernandez-Panchon et al. (Fernandez-Panchon et al., 2008b), the higher ORAC values of protocatechuic and caffeic acid compared to tested phenolic compounds were found.

The ester form of gallic acid and catechin showed higher antioxidant activity has been observed (Fernandez-Panchon et al., 2008b). They found that the enhancement of radicals scavenging of catechin-gallate esters by ABTS assay to catechins and gallic acid might be thanks to the contribution of the trihydroxybenzoate form.

2.12.6.3. Flavonoids (C6-C3-C6)

Figure 2.23 shows the generic chemical structures of several flavonoids types present in plants. Unlike the relationship between hydroxybenzoic and hydroxycinnamic acids with the antioxidant activity, the SAR of flavonoids is more complicated due to the relative complexity of flavonoid molecules (Balasundram et al., 2006). The substitutions' chemical structure properties on ring B and C (Figure 2.23) can determine flavonoids' antioxidant activity. The difference between the degree and positions of substitutions cause the difference in these phenolic compounds' antioxidant capacity.

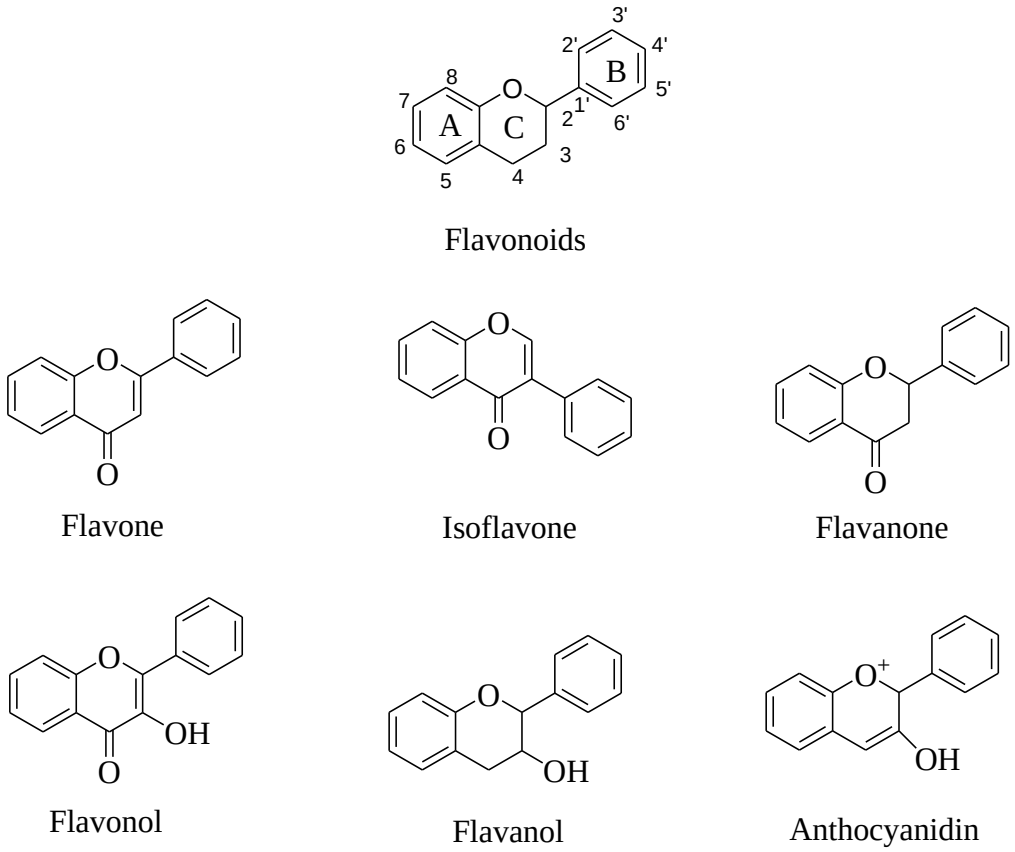

Figure 2.23. General chemical structure of flavonoid molecules and significant classes of flavonoids.

The level and position of hydroxyl groups in the B ring, particularly an ortho-dihydroxyl structure of ring B (catechol group), may lead to higher antioxidant activity. The higher stability may explain this characteristic for the aroxyl radical by electron delocalization (Van Acker et al., 1996). Moreover, according to Pietta (Pellegrini et al., 2000), ring B's ortho-dihydroxyl structure can also act as the preferred binding site for trace metals. (+)-catechin, (-)-epicatechin, and quercetin (Figure 2.24) possess ortho-dihydroxyl structure showed higher antioxidant capacity in ORAC values (Fernandez-Panchon et al., 2008b).

The presence of –OH groups at the 3', 4', and 5'-position of ring B (pyrogallol group) showed a higher antioxidant capacity than those that have only one –OH group, according to Van Acker et al. (Van Acker et al., 1996). However, these compounds can work as pro-oxidants under some conditions.

Hence, it can counteract the antioxidant effects (Van Acker et al., 1996). This observation was also consistent with the finding of Seeram and Nair (Seeram & Nair, 2002). They found that anthocyanidin's antioxidant capacity increases in 3', 4', and 5'-hydroxyl group in B ring compared to 3', 4'-OHs decreasing the antioxidant capacity for the case of catechins.

The antioxidant capacity of flavonoids enhances double bonds between C-2 and C-3, and conjugated with the 4-oxo group in ring C has been reported by Pietta (Pellegrini et al., 2000). The participation in electron delocalization from the B ring contributes to this effect (N. J. Miller & Rice-Evans, 1997). Therefore, quercetin (Figure 2.24) exhibited a higher TEAC value than catechin (Salah et al., 1995). With the same hydroxylation patterns in the structure, flavones showed higher antioxidant capacity than anthocyanidins tested (H. Wang et al., 1997). Whereas, in the report of Lien et al. (Lien et al., 1999), there was no significant difference in antioxidant activity in the presence or absence of the C2 and C3 double bond. Besides, the number of –OH groups in the C ring in flavones and isoflavones is responsible for ORAC values (Rice-Evans et al., 1996).

The radical scavenging ability of flavonoids is also enhanced by the double bond between C-2 and C-3, combined with a hydroxyl group at C-3 in ring C as observed in kaempferol (Van Acker et al., 1996). However, in Seeram and Nair's (Seeram & Nair, 2002) study, the substitution of the 3-OH caused the reduced antioxidant activity of flavonoids. This phenomenon can be explained by the increasing torsion angle and loss of coplanarity in the presence of 3-OH in ring C. The most significant ABTS values were found in the case of flavan-3-ols with several hydroxyl groups, according to Salah et al. (Salah et al., 1995). Meanwhile, the study about the antioxidant capacity for anthocyanidins by ORAC assay (H. Wang et al., 1997) and flavan-3-ols (Fernandez-Panchon et al., 2008b) against previous results. Besides, the relationship between peroxyl radical adsorbing activity and the number of –OH groups in flavonoids is linear in the case of flavones, but curvilinear for flavanones as observed in the report Cao et al. (Cao et al., 1997).

The radical scavenging capacity of flavonoids also can be affected by the presence of methoxyl groups in ring B instead of hydroxyl groups as has been reported by several researchers (Seeram & Nair, 2002). Indeed, the contribution of the 3-OH group in flavonoids is vitally essential in terms of antioxidant activity reported elsewhere (Heijnen et al., 2001). The inhibition of antioxidant activity for rutin (Figure 2.24) when blocking the 3-OH group in the B ring has been published (Salah et al., 1995).

Additionally, Rice-Evans et al. (Rice-Evans et al., 1996, p. 1) found that 3- and 5-OH groups with the 4-oxo function in A and C rings were necessary for the effectiveness of free radical scavenging activity.

All flavonoids molecules structure with the antioxidant relationship are mentioned above are illustrated in Figure 2.24.

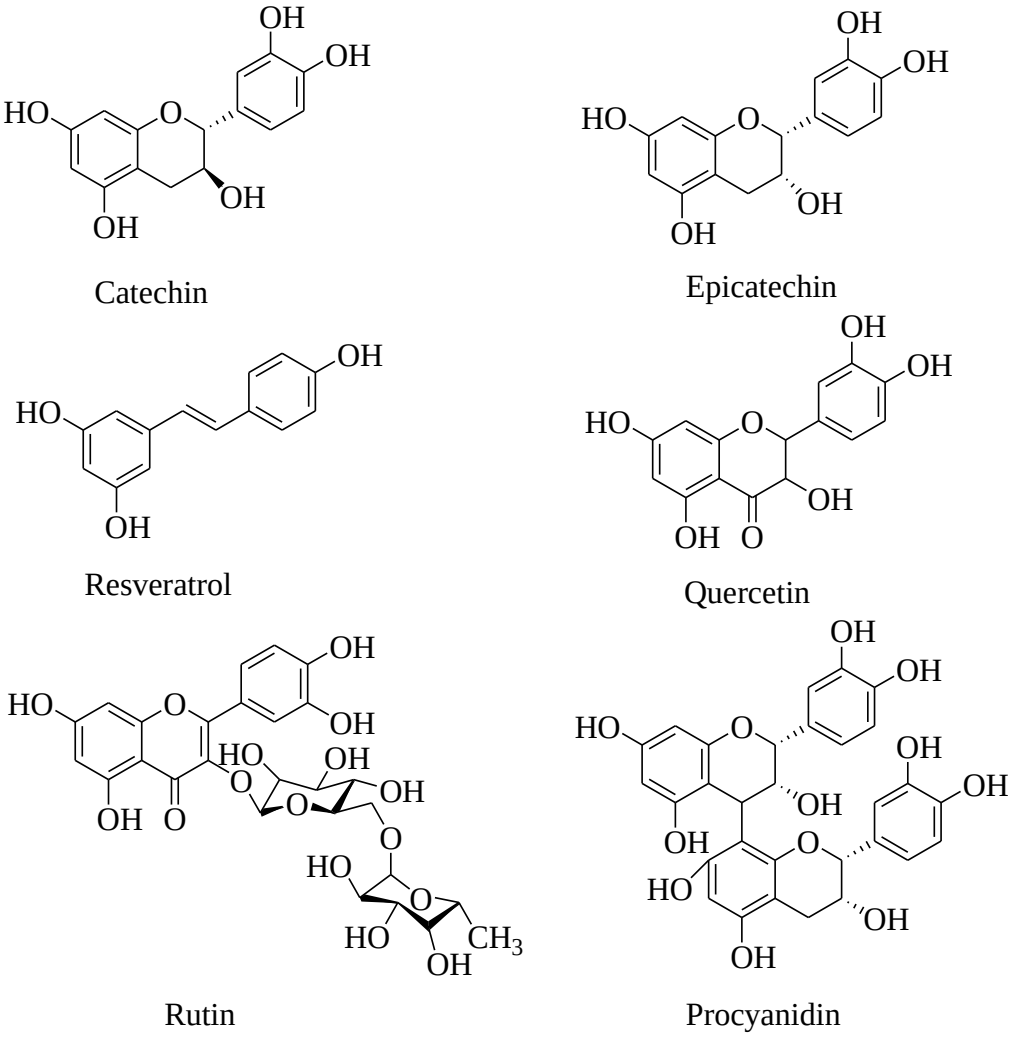

Figure 2.24. Example structures of antioxidants flavonoids.

2.12.7. Phenolic compounds and antioxidants applications

The antioxidant phenolic compounds from synthetic and natural sources have been applied in the food processing system and the body's health system. However, the concerning safety of phenolic synthetic antioxidants compounds such as BHA, BHT, TBHQ, and PG led to an interest in natural antioxidants compounds (U. N. Wanasundara & Shahidi, 1998). Indeed, phenolic compounds from plant sources are considered natural antioxidants in numerous edible oils such as corn, cottonseed, fish, olive, rapeseed, sunflower, and soybean oils (Yanishlieva & Marinova, 2001).

2.12.7.1. Phenolic compounds as food antioxidants

The possible application of antioxidant phenolic compounds is based on the type of food products. The direct application of ground oilseed has been considered in meat products (Schmidt & Pokorný, 2011). In particular, the application of oilseed meals antioxidants to several products such as bakery, meat, or potato products has been found (Schmidt & Pokorný, 2011). Rosemary extracts containing carnosol, and carnosic acid has exhibited useful antioxidant properties in corn, soybean,

peanut, and fish oil tested in the bulk system (Frankel, 1996). Moreover, synthetic antioxidant BHT, combined with rosemary extract, can increase the antioxidant activity in the suppression oxidation of soybean oil (Basaga et al., 1997). Antioxidant phenolic compounds from green tea extract can be used in marine oils (U. N. Wanasundara & Shahidi, 1998). Tea catechins were also reported by Tang et al. (S. Tang et al., 2001) to be more effective than α-tocopherol in suppressing the lipid oxidation in fresh meats, poultry, and fish. Pistachio hull phenolic extract at 0.06% (w/w) can be as effective as BHA and BHT at 0.02% antioxidant in inhibiting the oxidation of soybean oil (Goli et al., 2005).

2.12.7.2. Phenolic antioxidants in health effects

The intake of phenolic compounds daily from plant sources such as fruits, leaves, and seeds can significantly affect individual health status (Naczk & Shahidi, 2004b). Phenolic compounds such as hydroxycinnamic acid conjugates and flavonoids possess high antioxidant activities *in vitro* against cardiovascular disease and cancer (Boudet, 2007; N. J. Miller & Rice-Evans, 1997). Neoplasia, atherosclerosis, and neurodegenerative diseases are involved in the oxidative stress process, which is implied by reactive oxygen species (ROS). Therefore, the phenolic compounds, including flavonoids, were considered the efficacies of antioxidants due to their direct scavenging of free radicals (Heim et al., 2002). Thereby, the ROS levels can be decreased in the body (M. J. Park et al., 2006). Low risk of cancer was supplemented with multiple antioxidant products (M. J. Park et al., 2006). The additive and synergistic effects of phenolic antioxidants are likely to lead to cancer (L. Liu et al., 2004) reported that the combination of antioxidant compounds in fruits such as orange, apple, grape, and blueberry could gain a synergistic effect on antioxidant activity *in vitro*. The half-maximal effective concentration (EC50) of this combination was up to five time higher than individual antioxidants (Lien et al., 1999). Hydrocinnamic acid derivates and flavonoids can exhibit antioxidant and other biological activities *in vivo* (Olthof et al., 2001). These phenolic compounds can act as anti-allergenic, anti-atherogenic, anti-inflammatory, antimicrobial, antioxidant, anti-thrombotic, cardioprotective vasodilatory agents (Manach et al., 2005; Middleton et al., 2000). Tea polyphenols including epigallocatechin-3-gallate (EGCG), the primary catechin in green tea, can be used as cancer chemopreventive agents such as in lungs, liver, gastrointestinal tract, skin, and prostate cancer (N. Khan & Mukhtar, 2010; Klaus et al., 2005). The antioxidant activity and colon cancer treatment of EGCG enhanced upon conjugation with docosahexaenoic acid (DHA) (Zhong & Shahidi, 2012). Orange peel extract containing poly-methoxy flavones showed anti-inflammatory, anti-carcinogenic, anti-viral, antioxidant, anti-thrombogenic anti-atherogenic properties (Manach et al., 2005; Middleton et al., 2000).

Phenolic compounds antioxidants were found as anti-obesity agents. Huang Liu et al. (X. Huang et al., 2009) found that antioxidant phenolic compounds in orange peel, black tea extract, caffeine could suppress the body weight gain and adipose tissue formation. In particular, caffeine could lose weight by suppressing food intake and reducing adipose tissue mass (Kobayashi-Hattori et al., 2005; Tremblay et al., 1988). Resveratrol, a robust antioxidant product mainly found in red wine, was

reported to be one of the most effective in obesity treatment (Rayalam et al., 2008). Resveratrol could inhibit adipogenesis and induce adipocytes apoptosis by effecting the expression of genes that can modulate mitochondrial function. EGCG was an anti-obesity active compound (N. Khan & Mukhtar, 2010; Klaus et al., 2005).

Hydroxytyrosol, a primary phenolic compound composes in olive oil, was found to reduce the risk of coronary heart disease (Tuck & Hayball, 2002). Resveratrol is a phenolic compound that exhibited high antioxidant activity for anti-aging-related diseases such as cancer, type 2 diabetes, and cardiovascular (Marques et al., 2009). Resveratrol is found in plant sources such as grapes, pistachio, peanuts, berry fruit, or in the beverage such as red wine (J. Wu et al., 2001). EGCG, an antioxidant phenolic, also can be used as a cardiovascular protective compound (N. Khan & Mukhtar, 2010; Klaus et al., 2005).

2.13. Inflammation

2.13.1. Background

2.13.1.1. Definition

Inflammation is a protective response to tissue injury, bacteria, viruses, pathogens, or harmful external stimuli such as allergens and irritants (Costa et al., 2012; Joseph et al., 2016). During inflammation, proteins and leukocytes from blood travel up to the extra-vascular tissue causing clinical characteristics of inflammation, swelling, warmth, redness, and pain (Yoon & Baek, 2005). The objective is to suppress the injurious stimuli and onset tissue healing (Rathee et al., 2009). Inflammation is modulated to avoid immune system's over-activation and unwanted immune response (Rathee et al., 2009). Many immune cell types participate in this action, including T cells, B cells, natural killer (NK) cells, mast cells, and neutrophils (Rathee et al., 2009).

2.13.1.2. Inflammatory response

Inflammatory response is important to suppress infection and repair damaged tissues (Joseph et al., 2016). There are two types of inflammation; acute and chronic inflammation (Costa et al., 2012). Acute inflammation is regulated by the responses of immune cells, is rapid, effective, and self-limiting. Unlike acute inflammation, chronic inflammation happens when inflammation persists for an extended period due to inefficient regulation. Inflammatory responses are associated to the production of pro-inflammatory molecules and cytokines, whose expression is regulated by several signaling pathways. There is a myriad of inflammatory mediators produced by immune cells, such as nitric oxide (NO); reactive oxygen species (ROS); adhesion molecules including intercellular adhesion molecule (ICAM)-1, vascular cell adhesion molecule (VCAM)-1, and E-selectin; lipid-derived eicosanoids such as prostaglandin (PG) E2, PGI2, leukotriene (LT) B4, and LTC4; cytokines such as tumor necrosis factor (TNF)-α, interleukin (IL)-1β, IL-6, and IL-10; and chemokines such as chemokine ligands CXCL8, CCL2 and CCL3. The production of these mediators is controlled by transcription factors such as

nuclear factor kappa-light-chain-enhancer of activated B cells (NF-κB), activator protein (AP)-1, and nuclear factor erythroid 2-related factor 2 (Nrf-2). Their DNA-binding capacity is regulated by several signaling pathways such as mitogen-activated protein kinases (MAPKs), phosphatidylinositol 3-kinase (PI3K)/RAC-α serine/threonine-protein kinase (Akt), and the ubiquitin-proteasome system (Costa et al., 2012). The overexpression of inflammatory mediators during chronic inflammation is associated to chronic diseases such as Alzheimer's disease, diabetes, atherosclerosis, and cancer. Slowing down or suppressing inflammatory activity is a way to treat or prevent these diseases. This is why anti-inflammatory drugs are widely used. However, these synthetic drugs have side effects, including gastrointestinal disorders, renal failure, water retention, and hypersensitivity (Hawkey, 2003; Tamblyn, 1997). Furthermore, there are growing resistance to anti-inflammatory drugs. It has thus become necessary to discover new classes of this type of treatment. Searching new and safe natural anti-inflammatory drugs from plants, seeds, flowers, and fruits is a promising strategy. Among natural compounds, phenolic compounds have attracted scientific community's attention in recent years due to their anti-inflammatory properties (Ambriz-Pérez et al., 2016).

2.13.2. Signaling pathways involved in inflammation

2.13.2.1. Transcription factors

2.13.2.1.1. The NF-κB signaling pathway

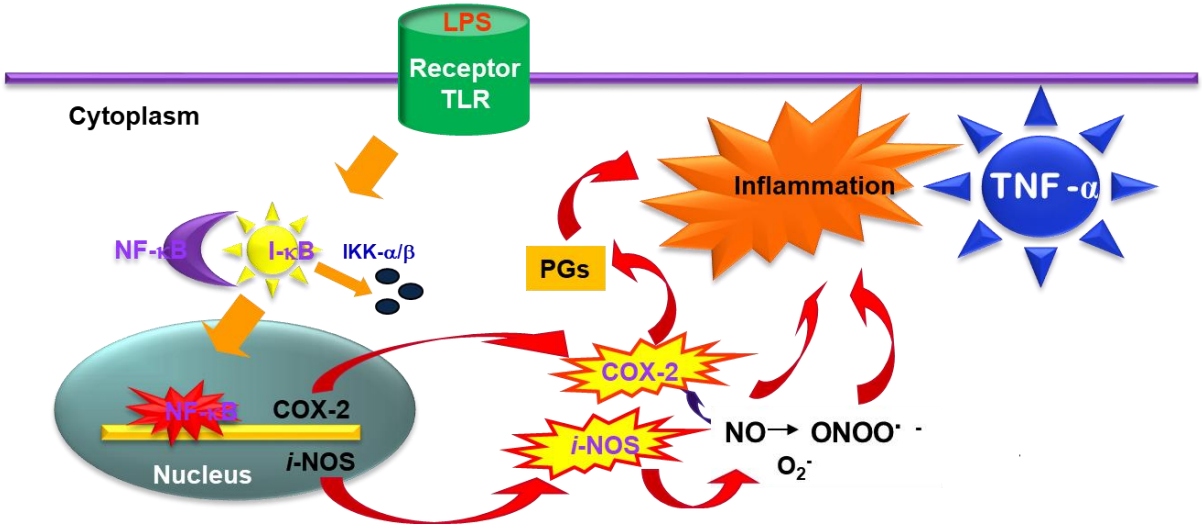

Figure 2.25. NF-κB signaling pathway and inflammation.
NF-κB: Nuclear factor-kappa B; I-κB: Inhibitor of κB; IKK: IκBα kinase; COX-2: cyclooxygenase 2; i-NOS: inducible nitric oxide synthase; PGs: prostaglandins; TNF-α: tumor necrosis factor-α; NOS: nitric oxide synthase; LPS: Lipopolysaccharide; TLR: toll-like receptor.

The NF-κB signaling pathway has a crucial role in DNA transcription leading to the production of several cytokines, chemokines, immunoreceptors and cell adhesion molecules. The activation of the NF-κB pathway allows the expression of genes involved in inflammatory progression as illustrated in

Figure 2.25. Under normal conditions, NF-κB is in the cytoplasm in an inactive form because it is combined with the inhibitor proteins I-κB (I-κBα, I-κBβ, I-κBε). When there is an inflammatory stimulus, like lipopolysaccharide (LPS), this transcription factor is transformed into an active form through the phosphorylation of I-κB by I-κB kinases (IKKα, IKKβ, IKKε). Therefore, the complex between NF-κB and I-κB is broken to release NF-κB and I-κB. Then, I-κB is degraded and NF-κB translocates into the nucleus. This process allows NF-κB to induce the transcription of genes related to inflammation, such as inducible nitric oxide synthase (iNOS) and cyclooxygenase 2 (COX-2), as well as several inflammatory mediators such as TNF-α, IL-6, and CXCL8. Therefore, new anti-inflammatory agents should act on the NF-κB signaling pathway to reduce inflammation (Manna et al., 2000).

2.13.2.1.2. Activator protein-1

Activator protein 1 (AP-1) is a transcription factor produced in response to infection and cytokines. AP-1 is a complex between the Jun protein family, Fos, and the activating transcription factor (ATF). AP-1 binding to DNA modulates the expression of genes involved in inflammation (Schonthaler et al., 2011). Several reports demonstrated that AP-1 activity is governed by mitogen-activated protein kinases (MAPK), especially by c-Jun N-terminal kinase (JNK) via cJun phosphorylation (Erdèlyi et al., 2005). Besides, a positive synergetic interaction between NF-κB and AP-1 activities was observed (Stein et al., 1993). Therefore, reducing AP-1 activity could limit the inflammation process.

2.13.2.1.3. Nuclear factor erythroid 2-related factor 2

Leukocytes locates in damaged tissue during inflammation. Consequently, there is a respiratory burst phenomenon due to the increase in the damaged site's oxygen level. Along with that, damaged tissue significantly increases reactive species (ROS) production. Besides, inflammatory cells release soluble mediators like cytokines and chemokines. The nuclear factor erythroid 2-related factor 2 (Nrf-2) is an emerging regulator of cellular resistance to oxidants. Nrf-2 controls the basal and induced expression of an array of antioxidant response element-dependent genes to regulate the physiological and pathophysiological outcomes of oxidant exposure (Q. Ma, 2013). Therefore, acting on the Nrf-2 signaling pathway could be another way to prevent tissue from inflammation.

2.13.2.2. Protein tyrosine kinase

Protein tyrosine kinase (PTK) is a catalyst for the tyrosine phosphorylation of proteins related to the Toll-like receptor (TLR) signaling pathway. Hence, PTK is a critical factor for cytokine production. Besides, PTK is involved in the intracellular response to abundant cytokines such as TNF-α, IL-6, and IL-10 (Page et al., 2009). Therefore, regulation of PTK activity can be a way to regulate the inflammatory response.

2.13.2.3. Mitogen-activated protein kinases signaling pathway

The mitogen-activated protein kinases (MAPK) signaling pathway is activated by pro-inflammatory stimuli such as TNF-α and IL-1β. There are three main sub-groups of MAPK (ERK1/2, JNK, and p38 MAPK) which can differently control the expression of target genes. The ERK1/2 signaling pathway is commonly referred to as cell differentiation and survival. Meanwhile, JNK and p38 MAPK are activated by pro-inflammatory cytokines and oxidants responsible for modulating pro-inflammatory mediators' level. MAPK activation can modulate several transcription factors such as NF-κB, AP-1, and Nrf2. This process increases the expression of target genes and inflammatory mediators' production (Broom et al., 2009). Hence, the inhibition of MAPK signaling could also contribute to limit inflammation.

2.13.2.4. Phosphatidylinositol 3-kinase (PI3K)/Rac-alpha serine/threonine-protein kinase (Akt)

The PI3K pathway is activated by numerous inflammatory mediators, growth factors, and hormones. The activation of PI3K induces the production of phosphatidylinositol (3,4,5)-triphosphate (PIP3) which activates Akt. Akt is a protein responsible for cell growth, proliferation, survival, and inflammatory response. Therefore, regulating PI3K signaling pathway can inhibit inflammation.

2.13.3. Mediators of inflammation

During the inflammatory process, cell activation induces the production of different mediators. Table 2.20 presents some of them.

Table 2.20. Examples of cell-derivated mediators.
(Reproduced with modifications from Internet, en.wikipedia.org/Inflammation retrieved).

Mediator	Classification	Origin	Main functions and characteristics
Lysosome granules	Enzymes	Granulocytes	Contain abundant enzymes acting as inflammatory mediators.
Histamine	Vasoactive amine	Mast cells, basophils, platelets	Histamine is liberated in the inflammatory response and stored in granules.
IFN-γ	Cytokine	T-cells, NK cells	- Antiviral, immune-regulatory, and anti-tumor properties. - A vital role in the maintenance of chronic inflammation.
IL-8	Chemokine	Macrophages	-Activation and chemo-attraction of neutrophils. -Slightly affect monocytes and eosinophils.
Leukotriene B4	Eicosanoid	Leukocytes	- Mediates leukocyte adhesion and activation. - A chemoattractant in neutrophils. - Induces the production of reactive oxygen species and of lysosomes.
Nitric oxide	Soluble gas	Macrophages, endothelial cells, some neurons	- A potent vasodilator. - Relaxes smooth muscle, reduces platelet aggregation. - Support for leukocyte recruitment. - Antimicrobial capacity in high concentrations.

Prostaglandins	Eicosanoid	Mast cells	- A family of lipids. - Cause vasodilation, fever, and pain.
TNF-α and IL-1	Cytokines	Macrophages	Affect numerous cells to trigger inflammatory reactions like fever, production of cytokines, endothelial gene regulation, chemotaxis, leukocyte adherence, activation of fibroblasts.

2.13.3.1. Nitric oxide

Nitric oxide (NO) is produced from L-arginine by nitric oxide synthase (NOS). Inflammatory factors induce iNOS (inducible NOS) production in macrophages (Geller & Billiar, 1998). Overproduction of NO from iNOS (Figure 2.25) for a long duration is responsible for the pathogenesis of inflammatory disease (Broom et al., 2009). Thus, the inhibition of NO production and iNOS expression activity is crucial for developing new drugs for inflammatory treatment.

2.13.3.2. Arachidonic acid signaling pathway

The arachidonic acid (AA) signaling pathway also generates inflammatory mediators. AA is an unsaturated fatty acid that is a normal constituent of membrane phospholipids. It is released from the phospholipids by the actions of phospholipase A2. Then, cyclooxygenase (COX) and lipoxygenase (LOX) metabolize it. COX-1 generates thromboxane A2 (TXA2), and COX-2 produces prostaglandin (PG) E2. LPS and pro-inflammatory cytokines activate COX-2 expression (Figueirinha et al., 2010). Meanwhile, LOX is responsible for generating 5-hydroxyeicosatetraenoic acid (5HETE) and leukotrienes (LT). Thus, the inhibition of COX-2 and LOX can reduce the production of critical mediators of inflammation.

2.13.3.3. Cytokines and chemokines

Cytokines and chemokines are important for the modulation of vascular changes, the arrival of immune cells at the inflammatory foci, and intercellular communication. Indeed, cytokines are involved in various inflammatory diseases. Besides, chemokines are a family of small chemotactic cytokines that can modulate leukocyte migration. A good example is CXCL8, a chemokine generated by macrophages and epithelial cells. These molecules are inflammatory mediators and their inhibition is a new journey in discovering anti-inflammatory drugs.

2.13.3.4. Cell adhesion molecules

The function of vascular endothelial cells is to regulate the interactions between blood and vessels. Vascular endothelial cells exhibit a vital role in physiological and pathological systems. In inflammation and atherosclerosis, the adhesion of circulating monocytes to vascular endothelial cells is an important activity. Furthermore, endothelial cells respond to pro-inflammatory stimuli such as TNF-α, IL-β, and LPS. Besides, the expression of adhesion molecules, such as vascular cell adhesion

molecules (VCAM-1) and intercellular adhesion molecules (ICAM-1), can allow the migration of leukocytes. For this reason, the modulation of cell adhesion molecules expression can be useful in the context of drug development.

2.13.4. Inflammation treatment

There are two avenues for inflammatory treatment, namely conventional and alternative treatments. Conventional treatments involve synthetic drugs like NSAID (Nonsteroidal anti-inflammatory drugs). Alternative treatments refer to natural products such as phenolic compounds to prevent or suppress inflammation. In this section, I will present the anti-inflammatory effects of NSAID and phenolic compounds.

2.13.4.1. Conventional Treatment: NSAIDs

Nowadays, NSAIDs are the most widely used drugs for treating various diseases that involve inflammation (Tamblyn, 1997). According to a report about medication use in the US, more than 37% of adults consumed NSAID at least once per week. There are about 70 million prescriptions of NSAID yearly in the USA. The activity of NSAIDs is based on several mechanisms like inhibition of enzymes, cytokines production, and kinases. However, NSAIDs are not selective. For instance, some drugs can act as inhibitors of prostaglandin synthase enzymes like COX-1 and COX-2. The mechanism is to modify these enzymes covalently and combat with the substrates at the active location (Williams et al., 1999). Due to their non-selective action on COX family, using NSAIDs in the long-term cause numerous adverse side effects. These side effects occur because of reducing COX-1 production. The main side effects are gastrointestinal disorders. Using NSAIDs for an extended period can lead to salt and water retention, renal function deficiency, and hypertension (Hawkey, 2003). Up to 7600 deaths and 76000 hospitalizations are related to NSAID use in the US (Tamblyn, 1997). Nowadays, coxibs are the number one COX-2 selective drug inhibitors due to their fewer gastrointestinal side effects and their similar anti-inflammatory effect compared to non-selective drugs (Bombardier et al. 2000; Vane 2000). However, one of the severe side effects of coxibs is to enhance renal sodium reabsorption. Consequently, patients using coxibs can suffer of unwanted hypertension (Hawkey, 2003).

2.13.4.2. Alternative Treatment: phenolic compounds

Since using NSAIDs cause severe side effects, searching for new natural drugs is a promising way to inhibit inflammatory development and progression. Phenolic compounds are abundant small molecules present in plants, fruits, leaves, and seeds. They are very attractive to researchers because of their anti-inflammatory properties. I will therefore present the anti-inflammatory activities of phenolic compounds from natural resources.

2.13.4.2.1. Effects of phenolic compounds on transcription factors

The inflammatory response is associated with a series of intracellular signaling pathways that be modulated by phenolic compounds (Figure 2.26). These compounds can regulate the NF-κB pathway from the early stage, like IKK phosphorylation, up to the later stage, like the binding of NF-κB to DNA which induces the expression of target genes involved in the inflammatory response.

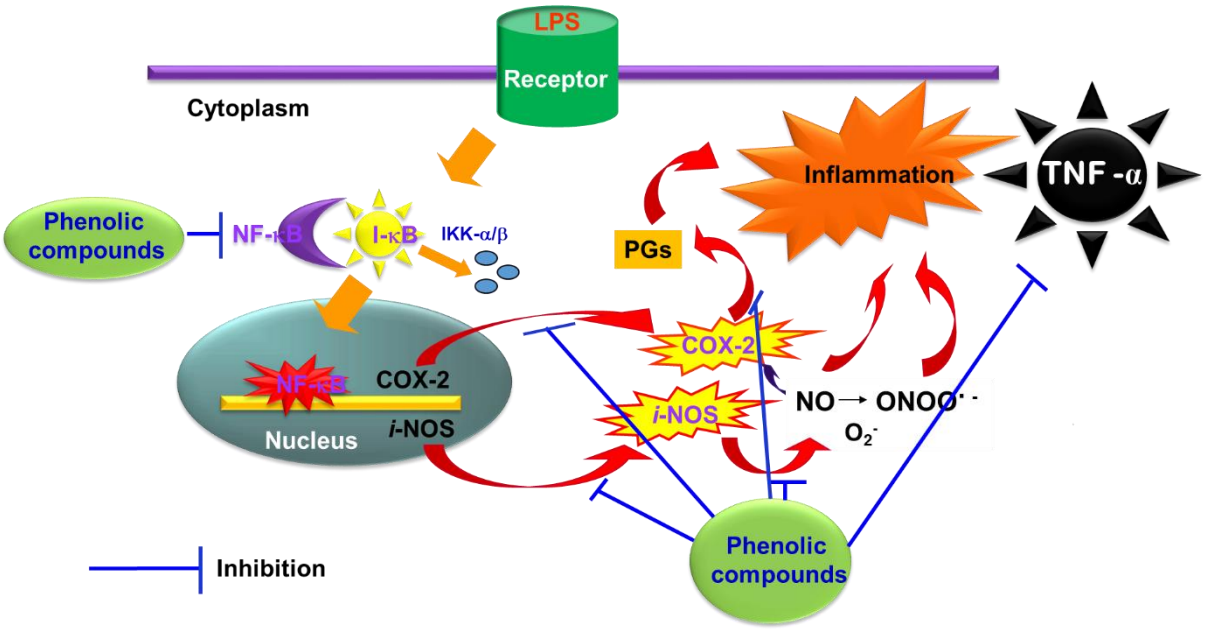

Figure 2.26. Schematic representation of the action of phenolic compounds.
Phenolic compounds can inhibit the NF-κB signaling pathway by acting on IKK, I-κB, p65, translocation to the nucleus, and DNA binding. NF-κB: Nuclear factor-kappa B; I-κB: Inhibitor of κB; IKK: IκBα kinase; COX-2: cyclooxygenase 2; i-NOS: inducible nitric oxide synthase; NO: nitric oxide; PGs: prostaglandins; TNF-α: tumor necrosis factor-α; NOS: nitric oxide synthase; LPS: Lipopolysaccharide; TLR: toll-like receptor.

At the early stage, the phosphorylation of IKK triggers the activation of the NF-κB signaling pathway. Therefore, all phenolic compounds that can inhibit NF-κB activation through IKK are promising anti-inflammation agents. For example, it was reported that IKK phosphorylation and activity are inhibited by apigenin (Figure 2.26) (C.-C. Chen et al., 2004; Liang et al., 1999a), luteolin (C.-C. Chen et al., 2004), chrysin (C.-C. Chen et al., 2004), quercetin (Chen J. C. et al. 2005), kaempferol (C.-C. Chen et al., 2004), morin (Manna et al., 2007), and epigallocatechin gallate (EGCG) (Aneja et al., 2004). Besides, it was shown that morin (Manna et al., 2007), EGCG (Kundu & SURH, 2007), catechin and epicatechin (Mackenzie et al., 2004) can inhibit I-κB phosphorylation. These compounds were also found as I-κB degradation inhibitors. Caffeic acid (Moon et al., 2009), apigenin (C.-C. Chen et al., 2004; Liang et al., 1999a), luteolin (C.-C. Chen et al., 2004), and kaempferol (C.-C. Chen et al., 2004) also inhibit I-κB degradation. The phosphorylation of p65 is another way to activate the NF-κB signaling pathway. Thus, phenolic compounds such as EGCG (Kundu & SURH, 2007), caffeic acid (Moon et al., 2009), resveratrol (Manna et al., 2000) and morin (Manna et al., 2007) that inhibit p65 phosphorylation

are also promising anti-inflammatory agents. Additionally, it was shown that catechin and epicatechin (Mackenzie et al., 2004), curcumin (G. Kang et al., 2004), resveratrol (Manna et al., 2007), quercetin (C.-C. Chen et al., 2004), and morin (Manna et al., 2007) can inhibit the binding of NF-κB to DNA. Several compounds such as resveratrol, quercetin, EGCG, catechin, epicatechin, and morin are inhibitors of the NF-κB signaling pathway in different ways and by targeting various molecules. Thus, one phenolic compound can regulate the signaling cascade at several levels and affect all subsequent processes as illustrated in Figure 2.26.

AP-1 activation is controlled by reactive oxygen species (ROS) and is modulated by several inflammatory mediators. This pathway is deactivated by antioxidants such as phenolic compounds. Indeed, luteolin (Hirano et al., 2006), chrysin (C.-C. Chen et al., 2004), EGCG (Aneja et al., 2004) can inhibit cJun phosphorylation. Luteolin (Hirano et al., 2006), apigenin (C.-C. Chen et al., 2004) and kaempferol (C.-C. Chen et al., 2004) have negative effects on the mRNA levels of cJun and cFos. Furthermore, DNA binding is reduced by the presence of curcumin (G. Kang et al., 2004), resveratrol (Manna et al., 2000), apigenin (C.-C. Chen et al., 2004), luteolin (C.-C. Chen et al., 2004), quercetin (Wadsworth T. L. et al. 2001), EGCG (Aneja et al., 2004), and kaempferol (C.-C. Chen et al., 2004). Besides, it was reported that these compounds inhibit the transcriptional activity of AP-1. Thus, these phenolic compounds extracted from plants can be candidates for inflammatory treatment.

2.13.4.2.2. Effects of phenolic compounds on protein tyrosine kinases

As indicated above, the regulation of PTK activity can be an efficient strategy to treat inflammatory processes. Phenolic compounds are modulators of PTK activity. Indeed, the upstream regulator of MAPK can be inhibited by luteolin (Byun et al., 2010) and kaempferol (S.-J. Kim et al., 2010). Furthermore, curcumin can down-regulate the spleen tyrosine kinase (Syk) through binding on the activated site (Gururajan et al., 2007). Syk kinase activity is also inhibited by apigenin, quercetin, myricetin, and morin in a concentration-dependent manner. The inhibition of Janus tyrosine kinase (JAK) is another strategy for regulating pro-inflammatory responses induced by cytokines. The inhibition of JAK can inhibit signal transducer and activator of transcription (STAT) and consequently the inflammation process. In that context, myricetin and piceatannol are considered as strong candidates to inhibit STAT3 activity.

2.13.4.2.3. Effects of phenolic compounds on mitogen-activated protein kinase

The inhibition of MAPK signaling can lead to anti-inflammatory effects. Phenolic compounds are interesting in that context because the activation of p38 MAPK can be blocked by curcumin (Camacho-Barquero et al., 2007), apigenin (C.-C. Chen et al., 2004), luteolin (C.-C. Chen et al., 2004), quercetin (Min et al., 2007), icariin (Figure 2.29) (S.-R. Chen et al., 2010), EGCG (Ichikawa et al., 2004), and gallotanin (Erdelyi et al., 2005). The inhibition of ERK activation was observed with all these phenolic compounds, except icariin. Besides, it was shown that luteolin (C.-C. Chen et al., 2004),

quercetin (Wadsworth et al., 2001), chrysin (C.-C. Chen et al., 2004), and kaempferol (C.-C. Chen et al., 2004) can inhibit JNK activation.

2.13.4.2.4. Effects of phenolic compounds on phosphatidylinositol 3-kinase/Rac-alpha serine/threonine-protein kinase (PI3K/Akt)

Activation of the PI3K/Akt signaling pathway is involved in the regulation of inflammation (Fougerat et al., 2009). Interestingly, this activation is inhibited by quercetin (M. K. Hwang et al., 2009) and morin (Manna et al., 2007). Icariin can induce Akt phosphorylation through PI3K signaling thereby regulating the downstream NF-κB signaling pathway (C.-Q. Xu et al., 2010). Thanks to this regulation, icariin exhibits anti-inflammatory effects on LPS-activated macrophages.

2.13.4.2.5. Effects of phenolic compounds on inflammatory mediators

2.13.4.2.5.1. Effects of phenolic compounds on nitric oxide

The inhibition of NO production and iNOS expression in LPS-stimulated macrophages (Francisco et al., 2011) and dendritic cells (Figueirinha et al., 2010) by plant phenolic fractions has been reported. Curcumin (Chan et al., 1998), resveratrol (Donnelly et al., 2004), apigenin (Liang et al., 1999b), wogonin (M.-H. Pan et al., 2006), quercetin (J.-C. Chen et al., 2005), and tyrosol could reduce iNOS mRNA and protein levels as well as NO production. Furthermore, apigenin (Liang et al., 1999b) and quercetin (J.-C. Chen et al., 2005) were shown to block iNOS transcriptional activity.

2.13.4.2.5.2. Effects of phenolic compounds on the arachidonic acid signaling pathway

The modulation of eicosanoid production is also promising to fight inflammation. In this context, it was shown that phenolic compounds of the anthocyanidin family such as malvidin, peonidin, and petunidin can inhibit PLA2 activity (Dreiseitel et al., 2009). The expression of 5-LOX can be inhibited by curcumin. Other reports showed indirectly the inhibition of 5-LOX activity by studying LT production level. The level of LTB4 was reduced by some phenolic compounds such as tyrosol (de la Puerta et al., 1999), and caffeic acid (de la Puerta et al., 1999).

The expression COX-2 is involved in LPS-induced inflammation. Therefore, COX-2 inhibition by phenolic compounds has raised researchers' attention to obtain safer anti-inflammatory drugs. Wogonin (M.-H. Pan et al., 2006), quercetin, and isoquercetin (Morikawa et al., 2003) can inhibit COX-2 mRNA expression. COX-2 protein expression is blocked by quercetin (S.-C. Shen et al., 2002), kaempferol (Liang et al., 1999b), rutin (Y.-C. Chen et al., 2001), and anthraquinone chrysophanol (S.-J. Kim et al., 2010). EGCG (Liang et al., 1999b), epigallocatechin (EGC), catechin gallate (CG), catechin, apigenin (Liang et al., 1999b) and epicatechin (Seeram et al., 2003) inhibit COX-2 expression and activity. Additionally, PGE2, a product of COX-2 metabolism, could be suppressed by wogonin (M.-H. Pan et al., 2006), isoquercetin (Morikawa et al., 2003), rutin (Y.-C. Chen et al., 2001), and kaempferol (Liang et al., 1999b).

2.13.4.2.5.3. Effects of phenolic compounds on cytokines and chemokines

Phenolic compounds have been shown to regulate the expression of pro-inflammatory cytokines and chemokines. Quercetin can decrease the mRNA and protein levels of TNF-α (Morikawa et al., 2003) and reduce interleukin-1β production (Min et al., 2007). Caffeic acid (Moon et al., 2009), luteolin (Xagorari et al., 2002), and EGCG (Ichikawa et al., 2004) can inhibit the expression of IL-1, IL-8, IL-12, and TNF-α at the protein level. Studies have documented that IL-1α production, associated with inflammation, can be inhibited by apigenin (Gerritsen et al., 1995) and quercetin (Min et al., 2007). Regarding chemokines, caffeic acid (Moon et al., 2009), resveratrol (Donnelly et al., 2004), apigenin (Gerritsen et al., 1995), quercetin (Min et al., 2007), and anthocyanins (Youdim et al., 2002) can inhibit CXCL8 expression.

2.13.4.2.5.4. Effects of phenolic compounds on cell adhesion molecules

Phenolic compounds possess an anti-inflammatory activity through monocyte adhesion molecules modulation. Caffeic acid (Moon et al., 2009), hydroxytyrosol (Carluccio et al., 2003), resveratrol (Carluccio et al., 2003), apigenin (J.-S. Choi et al., 2004), luteolin (Gerritsen et al., 1995), and quercetin (Gerritsen et al., 1995) inhibit VCAM-1 expression. ICAM-1 is vital for transendothelial migration of leukocytes and T cells activation. Therefore, inhibition of ICAM-1 could be a new strategy for drug development. In that context, several reports showed that ICAM-1 levels can be suppressed by hydroxytyrosol (Carluccio et al., 2003), caffeic acid (Moon et al., 2009), curcumin (H. Y. Kim et al., 2003), resveratrol (Carluccio et al., 2003), apigenin (Gerritsen et al., 1995), luteolin (C.-C. Chen et al., 2004), and quercetin (C.-C. Chen et al., 2004).

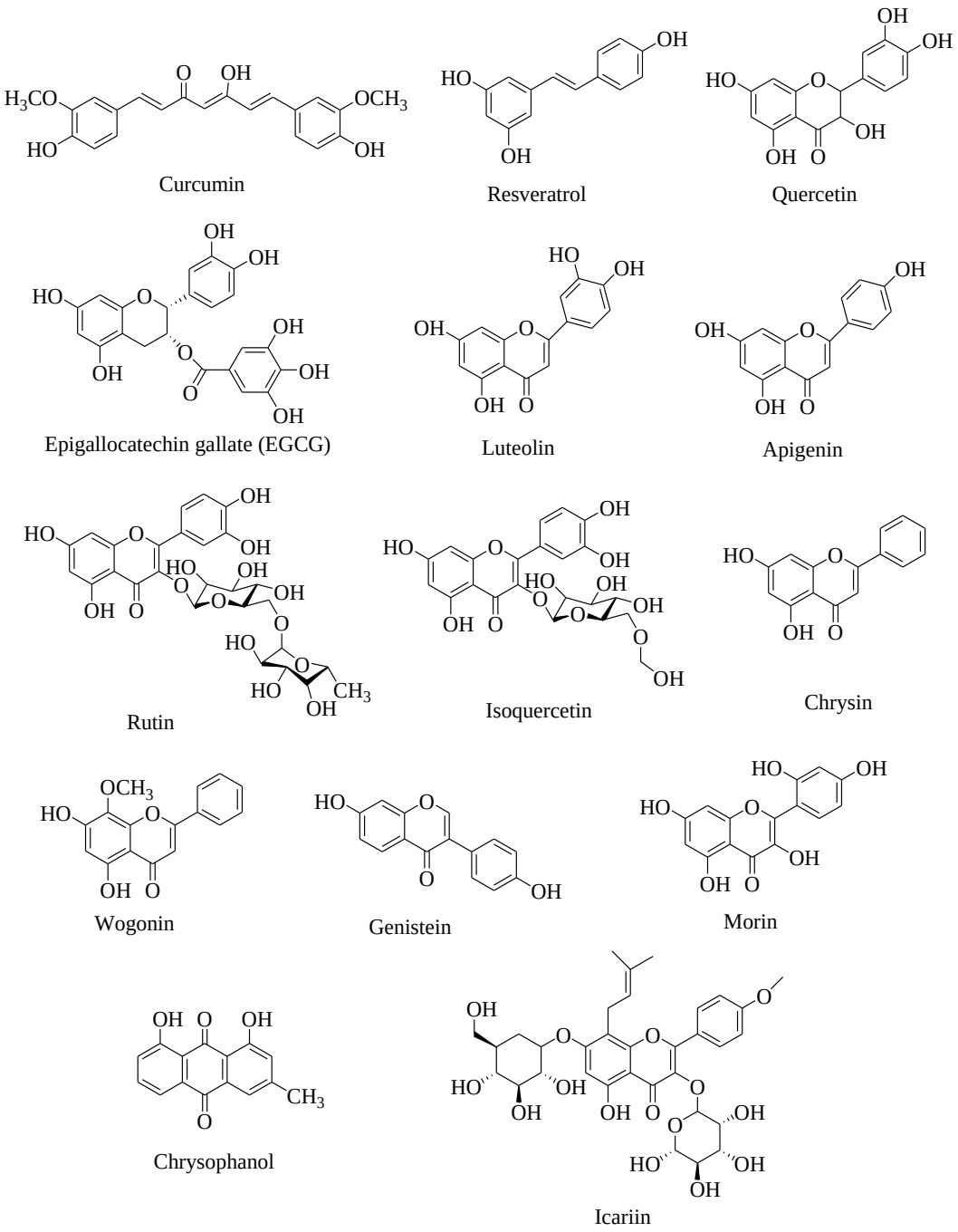

Figure 2.27. Chemical structures of phenolic compounds from plants having *in vitro* and *in vivo* anti-inflammatory activities.

Figure 2.27 presents the chemical structures of phenolic compounds from plants which have anti-inflammatory activities via their action on three main signaling pathways involved in the inflammatory response. As shown in Figure 2.28, phenolic compounds can regulate NF-κB pathway activation via different events such as affecting IKK phosphorylation, nuclear translocation of p50 and p65, NF-κB binding to DNA and inhibiting transcription factors actions, resulting in anti-inflammatory effects. Moreover, phenolic compounds can inhibit the MAPK activation cascade by inhibiting JNK, ERK, and p38 expression. In the arachidonic acid signaling pathway, phenolic compounds reduce the

liberation of critical factors such as arachidonic acid, PG, and LT. It is noteworthy that compounds presented in Figure 2.28 exhibit anti-inflammatory effects not only in *in vitro* conditions but also in *in vivo* models. The mechanism of action of phenolic compounds which are the most cited in the literature are summarized in Table 2.21.

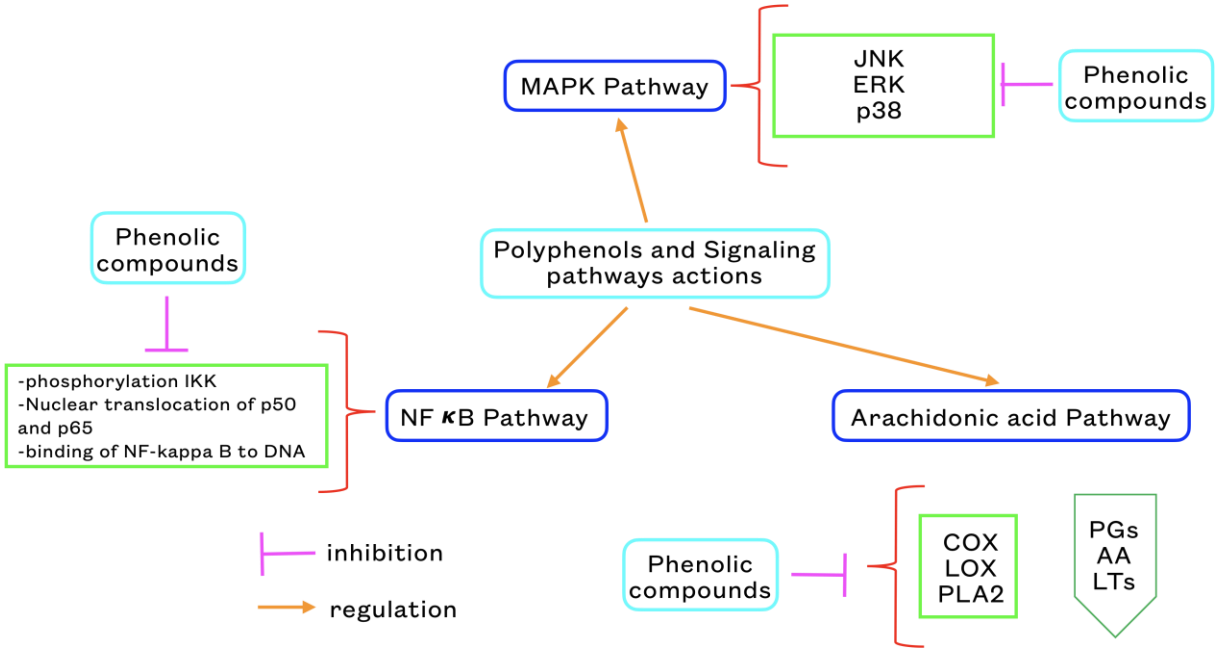

Figure 2.28. Action of phenolic compounds on the three main signaling pathways involved in the inflammatory response.

(Adapted with modifications from Yahfoufi N. et al. (Yahfoufi et al., 2018). Phenolic compounds can regulate several signaling pathways to reduce inflammation. NF-κB: nuclear factor kappa-light-chain-enhancer of activated B cells; IKK: I-κB kinase; ERK: extracellular signal-related kinase; JNK: cJun amino-terminal kinase; p38 MAPK: p38 mitogen-activated protein kinase; COX: cyclooxygenase; LOX: lipoxygenase; AA: arachidonic acid; PLA2: phospholipase A2; PGs: prostaglandins; LTs: leukotrienes; DNA: deoxyribonucleic acid.

Table 2.21. Phenolic compounds act as natural anti-inflammatory agents *in vitro* and *in vivo*.

(Adapted with modifications from Costa G. et al. (Costa et al., 2012) and updated with recent literature).

Phenolic compounds	**Mechanism action**	**Experimental condition**	**References**
Phenolic derivates			
Tyrosol	Inhibition of: -NF-κB binding to DNA, iNOS, and NO production. -COX-2 levels and PGE2 production.	IFN-γ stimulated RAW 264.7 macrophages.	(De Stefano et al., 2007)
	-LTB4 production.	Rat peritoneal leukocytes stimulated with calcium ionophore A23187	(de la Puerta et al., 1999)

	Inhibition of IL-1β production.	LPS-stimulated human whole blood.	(Miles et al., 2005)
	Inhibition of oxidative stress & of TNF-α expression	Human umbilical vein endothelial cells (hECs)	(Muriana et al., 2017)
	Reduction of pro-inflammatory cytokines (TNF-α, IL-1β, IL-6). Suppression of iNOS activation, COX-2, and phosphorylated-IκBα	BALB/c mice	(S.-J. Kim et al., 2010)
Hydroxytyrosol	Inhibition of LTB4 production.	Human leukocytes stimulated with calcium ionophore A23187	(Petroni et al., 1997)
	Inhibition of VCAM-1 mRNA and protein levels through NF-κB and AP-1 binding to DNA and transcriptional activity. Inhibition of ICAM and E-selectin cell-surface protein expression.	TNF-α–stimulated HUVECs.	(Carluccio et al., 2003)
	Decreased production of nitric oxide and prostaglandin E2 production.	RAW264.7 macrophages cells.	(Plastina et al., 2019)
	Reduced production of COX2 and TNF-α	Balb/c mice	(Fuccelli et al., 2018)
Hydroxycinnamic acid			
Caffeic acid	Inhibition of NF-κB through I-κB degradation, p65 translocation to the nucleus, and DNA binding. Chemokines production: CXCL8 and CCL2. Inhibition of VCAM-1, ICAM-1, and E-selectin levels.	TNF-α–stimulated HUVECs.	(Moon et al., 2009)
	Inhibition of AP-1 transcriptional activity	Phorbol 12-myristate 13-acetate (PMA)-induced luciferase expression in transfected MCF-7 cells.	(Maggi-Capeyron et al., 2001, p.)
	5-LOX activity and LTB4 production.	Rat peritoneal leukocytes stimulated with calcium ionophore A23187	(de la Puerta et al., 1999)
	Inhibition of cytokines production: TNF-α, IL-6, IL-1β	TNF-α–stimulated HUVECs. Human whole blood cells in culture.	(Moon et al., 2009)
	Inhibition of the production of inflammatory cytokines, such as IL-1β. Decreased phosphorylation of c-Jun N-terminal kinase. Suppression of IκBα phosphorylation	HMC-1 human mast cells	(J.-S. Choi et al., 2004)
	Decrease TNF-α, COX-2, & iNOS mRNA levels	RAW264.7 macrophages	(W. S. Yang et al., 2013)

	Inhibition of the nuclear translocation of AP-1		
	Inhibition of the production of NO, COX-2, iNOS	RAW264.7 macrophages	(H. G. Choi et al., 2018)
Hydroxybenzoic acid			
Gallic acid	Inhibition of AP-1 transcriptional activity.	PMA-induced luciferase expression in transfected MCF-7 cells.	(Maggi-Capeyron et al., 2001, p.)
	Inhibition of NO, PGE-2, IL-6, and COX-2 production	RAW264.7 macrophages	(BenSaad et al., 2017)
Phenolic acids derivates			
Curcumin	Inhibition of NF-κB activation through DNA binding transcriptional activity.	LPS-stimulated human monocytic macrophages, LPS-stimulated BV-2 microglial cells, PMA-stimulated human monocytes U937.	(Lim & Kwon, 2010)
	Inhibition of AP-1 activation through DNA binding transcriptional activity.	LPS-stimulated BV-2 microglial cells, PMA-stimulated human monocytes U937.	(Lim & Kwon, 2010)
	Inhibition of Syk activity.	B lymphoma cells.	(Gururajan et al., 2007)
	Inhibition of iNOS and NO production.	LPS- or IFN-γ-stimulated murine BV-2 or rat primary microglia.	(H. Y. Kim et al., 2003)
	Inhibition of COX-2 levels.	LPS-stimulated murine BV-2 or IFN-γ-stimulated rat primary microglia.	(H. Y. Kim et al., 2003)
	Inhibition of cytokines production (TNF-α, IL-10, IL-1β)	LPS-stimulated human monocytic macrophages.	(Chan, 1995)
	Inhibition of CCL2 production.	IFN-γ-stimulated rat primary microglia.	(H. Y. Kim et al., 2003)
	Inhibition of CCL2 expression through the ERK pathway.	PMA-stimulated human monocytes U937.	(Lim & Kwon, 2010)
	Inhibition of ICAM protein expression	IFN-γ-stimulated rat primary microglia.	(H. Y. Kim et al., 2003)
	Inhibition of the NF-κB and MAPKs pathways	RAW264.7 macrophages	(Xie et al., 2020)
	Inhibition of JAK2 and STAT3 phosphorylation	Murine BV-2 microglial cells	(Porro et al., 2019)
	Inhibition of COX-2 expression, NF-κB activation, NO production	Chronic myeloid leukemia cells	(Güran et al., 2019)
Stilbenes			
Resveratrol	Inhibition of NF-κB activation through I-κB phosphorylation and degradation, p65 phosphorylation, and translocation to the nucleus, DNA binding transcriptional activity.	TNF-stimulated U937, IL-1β-stimulated A549 epithelial cells	(Manna et al., 2000)

	Inhibition of AP-1 activation through DNA binding transcriptional activity.		
	Inhibition of iNOS & COX-2 mRNA levels, CXCL8 release.	IL-1β-stimulated A549 epithelial cells.	(Donnelly et al., 2004)
	VCAM-1 mRNA and protein levels through NF-κB and AP-1 binding to DNA and transcriptional activity. ICAM and E-selectin cell-surface protein expression.	TNF-α–stimulated HUVECs.	(Carluccio et al., 2003)
	Inhibition of TNF-α and IL-6 production, COX-2 levels, ROS production, and caspase-3/9 activity.	Rabbit model of acute pharyngitis	(Zhou et al., 2017)
	Inhibition of TNF-α-induced ICAM-1 expression, p38 phosphorylation, IκB phosphorylation and translocation of NF-κB p65	TNF-α–stimulated HUVECs.	(C.-C. Liu et al., 2017)
Flavonoids			
Apigenin	Inhibition of NF-κB activation through IKK activity, I-κB degradation, p65 translocation to the nucleus, DNA binding transcriptional activity.	LPS-stimulated RAW 264.7 macrophages, TNF-α–stimulated HUVECs, TNF-α–stimulated A549 epithelial cells.	(C.-C. Chen et al., 2004)
	Inhibition of AP-1 activation through cJun and cFos mRNA levels, DNA binding transcriptional activity.	TNF-α–stimulated A549 epithelial cells.	(C.-C. Chen et al., 2004)
	Syk activity.	IgE-stimulated human cultured mast cells (HCMC).	(Shichijo et al., 2003)
	Inhibition of MAPKs activation, namely p38 MAPK, ERK, and JNK enzyme activity.	TNF-α–stimulated A549 epithelial cells.	(C.-C. Chen et al., 2004)
	Inhibition of iNOS levels and transcriptional activity, NO production.	LPS-stimulated RAW 264.7 macrophages, LPS-stimulated NR8383 macrophages.	(Liang et al., 1999b)
	Inhibition of COX-2 levels transcriptional activity, PGE2 production.	LPS-stimulated RAW 264.7 macrophages, TNF-α–stimulated HUVECs.	(Gerritsen et al., 1995)
	Inhibition of IL-6 production.	TNF-α–stimulated HUVECs.	(Gerritsen et al., 1995)
	Inhibition of CXCL8 production.	TNF-α–stimulated HUVECs.	(Gerritsen et al., 1995)
	Inhibition of VCAM-1, ICAM-1, and E-selectin expression.	TNF-α–stimulated HUVECs, TNF-α-stimulated A549 epithelial cells.	(C.-C. Chen et al., 2004)
	Inhibition of ICAM-1 expression and transcriptional activity mediated by AP-1.	LPS-stimulated RAW 264.7 macrophages.	(Liang et al., 1999b)

	Inhibition of ox-LDL induced COX-2 expression	Human PBMCs	(Kumar et al., 2018)
	Inhibition of the TLR-NF-κB signaling pathway Inhibition of NO, TNF-α, and IL-6 production	RAW 264.7 macrophages.	(Y. Chen et al., 2019)
Luteolin	Inhibition of NF-κB activation through IKK activity, I-κB degradation, p65 translocation to the nucleus, DNA binding transcriptional activity.	TNF-α–stimulated HUVECs and A549 epithelial cells.	(C.-C. Chen et al., 2004)
	Inhibition of AP-1 activation through cJun phosphorylation, cJun, and cFos mRNA levels, DNA binding transcriptional activity.	TNF-α-stimulated A549 epithelial cells, LPS-stimulated RAW 264.7 macrophages.	(C.-C. Chen et al., 2004)
	Inhibition of Src activity.	UVB-induced JB6 P+ mouse epidermal cell line.	(Byun et al., 2010)
	Inhibition of Syk activity.	IgE-stimulated human cultured mast cells (HCMC).	(Shichijo et al., 2003)
	Inhibition of MAPKs activation, namely p38 MAPK, ERK, and JNK enzyme activity.	TNF-α-stimulated A549 epithelial cells, LPS-stimulated RAW 264.7 macrophages.	(C.-C. Chen et al., 2004)
	Inhibition of iNOS protein level and transcriptional activity, NO production.	TNF-α-stimulated A549 epithelial cells, LPS-stimulated RAW 264.7 macrophages.	(van Meeteren et al., 2004)
	Inhibition of TNF-α production & release through p38 MAPK, and ERK pathway.	LPS-stimulated mouse peritoneal macrophages, LPS-stimulated RAW 264.7 macrophages.	(Xagorari et al., 2002)
	Inhibition of VCAM-1, ICAM-1, and E-selectin expression.	TNF-α-stimulated A549 epithelial cells, TNF-α–stimulated HUVECs.	(C.-C. Chen et al., 2004)
	Inhibition of TNFα, IL-6, IL-10, inhibition of COX-2 production, phosphorylated STAT1, and phosphorylated STAT3 expression levels. Inhibition of TNF-α production	Male mice RAW 264.7 macrophages	(N. Xia et al., 2016; J. Xiong et al., 2017)
Chrysin	Inhibition of NF-κB activation through IKK activity, I-κB degradation, p65 translocation to the nucleus, DNA binding transcriptional activity.	TNF-α-stimulated A549 epithelial cells.	(C.-C. Chen et al., 2004)
	Inhibition of AP-1 activation through cJun mRNA levels, DNA binding transcriptional activity.		
	Inhibition of MAPK activation, namely JNK enzyme activity.		

	Inhibition of ICAM-1 protein expression		
	Inhibition of the production of NO and PGE2, COX-2	Human osteoarthritis chondrocytes	(Zheng et al., 2017)
	Inhibition of the activation of NF-κB		
	Inhibition of the production of IL-1β, IL-6, and TNF-α	Male Wistar rats	(Farkhondeh et al., 2019)
Wogonin	Inhibition of NF-κB activation through inhibition of transcriptional activity.	LPS-stimulated RAW 264.7 macrophages.	(M.-H. Pan et al., 2006)
	Inhibition of iNOS levels and NO production.	LPS-stimulated RAW 264.7 macrophages and peritoneal macrophages.	(M.-H. Pan et al., 2006)
	Inhibition of COX-2 levels and PGE2 production.		
	Inhibition of the expression of IL-6 and TNF-α	Mice with alcoholic liver disease.	(Y. Li et al., 2017)
	Inactivation of NF-κB-P65 and NF-κB-p-P65 expression through PPAR-γ activation	EtOH-induced RAW264.7 cells	
	Inhibition of STAT3 and ERK pathways activation	LPS-activated B cells	(Yu et al., 2020)
Genistein	Inhibition of iNOS protein level and NO production.	LPS-stimulated RAW 264.7 macrophages.	(Liang et al., 1999b)
	Inhibition of COX-2 protein level and PGE2 production.	Aβ-stimulated astrocytes.	
	Inhibition of IL-1β.	Human osteoarthritis chondrocytes	(F.-C. Liu et al., 2019)
	Inhibition of COX-2 production		
	Inhibition of the expression of IL-1β, IL-6, and TNF-α	Human keratinocyte HaCaT cells.	(A. Wang et al., 2019)
Quercetin	Inhibition of NF-κB activation through IKK activity, I-κB degradation, p65 translocation to the nucleus, and DNA binding transcriptional activity.	TNF-α–stimulated HUVECs, PMA-plus A23187-stimulated human mast cell (HMC-1), LPS- or IFN-γ-stimulated BV-2 microglial cells, LPS-stimulated RAW 264.7 macrophages, RAW 264.7 macrophages stimulated with IFN-γ plus gliadin. TNF-α-induced JB6 P+ epidermal cells.	(J.-S. Choi et al., 2004)
	Inhibition of AP-1 activation through cJun phosphorylation, DNA binding transcriptional activity.	LPS- or IFN-γ-stimulated BV-2 microglial cells, LPS-stimulated RAW 264.7 macrophages, TNF-α-induced JB6 P+ epidermal cells.	(M. K. Hwang et al., 2009)
	Syk activity.	IgE-stimulated human cultured mast cells (HCMC).	(Shichijo et al., 2003)

	Inhibition of MAPKs activation, namely ERK, JNK, and p38 MAPK phosphorylation activity.	PMA-plus A23187-stimulated HMC-1, LPS-stimulated RAW 264.7 macrophages, IL-1-stimulated HMC-1.	(Marone et al., 2008)
	Inhibition of PI3K activity and Akt phosphorylation.	TNF-α-induced JB6 P+ epidermal cells,	(M. K. Hwang et al., 2009)
	Inhibition of iNOS levels and transcriptional activity, NO production.	LPS-stimulated NR8383 macrophages, LPS- or IFN-γ-stimulated BV-2 microglial cells, LPS-stimulated RAW 264.7 macrophages. RAW 264.7 macrophages stimulated with IFN-γ plus gliadin.	(de la Puerta et al., 1999)
	Inhibition of COX-2 levels and PGE2 production.	LPS-stimulated RAW 264.7 macrophages, RAW 264.7 macrophages stimulated with IFN-γ plus gliadin.	(de la Puerta et al., 1999)
	Inhibition of TNF- α, IL-1β, IL-6 production.	LPS-stimulated mouse peritoneal macrophages, PMS-plus A23187-stimulated HMC-1, LPS-stimulated RAW 264.7 macrophages, IL-1-stimulated HMC-1.	(Cho et al., 2003)
	VCAM-1, ICAM-1, and E-selectin expression.	TNF-α-stimulated HUVECs.	(J.-S. Choi et al., 2004)
	Inhibition of COX-2 expression, NF-κB activation, NO production	Chronic myeloid leukemia cells	(Güran et al., 2019)
	Suppression of ICAM-1 and MMP-9 expression	Human retinal pigment epithelial cells and THP-1 cells	(Cheng et al., 2019)
	Inhibition of TNF-α-activated MEK1/2–ERK1/2–c-Jun pathway.		
	Inhibition of NF-□B through PKCδ– JNK1/2 pathway.		
	Inhibition of the production of TNF-α, IL-1β, and IL-6	LPS-Induced RAW264.7 cells	(J. Tang et al., 2019)
Kaempferol	Inhibition of NF-κB activation through IKK activity, I-κB degradation, and DNA binding transcriptional activity.	TNF-α-stimulated A549 epithelial cells.	(C.-C. Chen et al., 2004)
	Inhibition of MAPK activation, namely JNK activity.		
	Inhibition of ICAM-1 protein expression.		
	Inhibition of AP-1 activation through cJun and cFos mRNA	TNF-α-stimulated A549 epithelial cells, LPS-	(C.-C. Chen et al., 2004)

	levels and DNA binding transcriptional activity.	stimulated RAW 264.7 macrophages.	
	Inhibition of TNF-α, IL-1β, and IL-8 production	*Helicobacter pylori*-induced inflammation	(Yeon et al., 2019)
	Inhibition of IL-1β-activated NF-κB signaling	Acute lung injury in mice	(Qian et al., 2019)
	Inhibition of the overproduction of TNF-α, IL-1β, IL-6, ICAM-1, and VCAM-1	LPS-stimulated rat intestinal microvascular endothelial cells	(Bian et al., 2018)
Rutin	Inhibition of iNOS expression and NO production.	LPS-stimulated RAW 264.7 macrophages.	(Y.-C. Chen et al., 2001)
	Inhibition of COX-2 protein levels and PGE2 production.		
	Inhibition of IL−1β, IL-6, and TNF−α mRNA expression	Adipocyte 3T3-L1 and Colon Cancer SW-480 cells	(Lee & Seo, 2019)
	Inhibition of COX-2 and iNOS mRNA levels		
	Inhibition of NO, TNF-α, IL-1β, and IL-6 production	LPS-induced RAW 264.7 cells	(tian et al., 2019)
Morin	Inhibition of NF-κB activation through IKK activity, I-κB degradation, p65 translocation to the nucleus, and DNA binding transcriptional activity.	TNF-α-stimulated KBM-5 cells.	(Manna et al., 2007)
	Inhibition of PI3K/Akt activation through inhibition of Akt phosphorylation.		
	Inhibition of COX-2 protein levels and transcriptional activity.		
	Inhibition of the expression of TNF-α, IL-6, NFκB, IKKβ	Male albino Wistar rats	(Verma et al., 2019)
	Inhibition the JNK & c-Fos expression	Male rats	(Çelik et al., 2020)
	Inhibition NF-κB activation, TNF-α, and NOS production.		
Icariin	Inhibition of NF-κB activation through IKK activity, I-κB degradation, p65 translocation to the nucleus, and DNA binding transcriptional activity.	LPS-induced acute lung inflammation, LPS-stimulated RAW 264.7 macrophages.	(S.-R. Chen et al., 2010)
	Inhibition of iNOS levels and NO production.		
	Inhibition of COX-2 levels and PGE2 production.		
	Inhibition of MAPK activation, namely p38 MAPK phosphorylation.	LPS-stimulated RAW 264.7 macrophages.	(S.-R. Chen et al., 2010)
	Inhibition of IL-1β, IL-6, IL-8, and TNF-α production	Caco-2 cells	(W. Xiong et al., 2019)
	Enhancement of the HO-1 mRNA expression through modulation of the Nrf-2 pathway	Rats	(El-Shitany & Eid, 2019)
	Inhibition of the NF-κB activation		
	Inhibition COX-2 expression		

Epigallocatechin gallate (EGCG)	Inhibition of NF-κB activation through IKK activity, I-κB degradation, p65 translocation to the nucleus, and DNA binding transcriptional activity.	LPS-stimulated J774 macrophages, TPA-induced mouse skin.	(Kundu & Surh, 2007)
	Inhibition of NF-κB pathway activation	Human coronary artery endothelial cells	(Reddy et al., 2020)
	Inhibition of TNF-α and IL-1β gene expression	LPS induced otitis in rats	(Kaya et al., 2019)
	Inhibition of NF-κB-p65 transcriptional activity	Human bronchial epithelial cells	(Lakshmi et al., 2020)
Epicatechin gallate (ECG)	Inhibition of COX activity.	COX-enzyme inhibitory assay.	(Seeram et al., 2003)
	Inhibition of the PGE2, TNF-α, IL-1β, and IL-6 production	Carrageenan-induced paw edema model	(Al-Sayed & Abdel-Daim, 2018)
	Inhibition of IL-6, IL-8, and MMP-2 production Inhibition of the COX-2 expression.	Primary human rheumatoid arthritis synovial fibroblasts	(Fechtner et al., 2017)
Catechin	Inhibition of IL-6, IL-8, and MMP-2 production Inhibition of the COX-2 expression.	Primary human rheumatoid arthritis synovial fibroblasts	(Fechtner et al., 2017)
	Inhibition of the NF-κB pathway	Nasal mucosa of allergic rhinitis mice.	(Z. Pan et al., 2018)
Epicatechin	Inhibition of IL-6, IL-8, and MMP-2 production Inhibition of COX-2 expression.	Primary human rheumatoid arthritis synovial fibroblasts	(Fechtner et al., 2017)
	Inhibition of LPS-induced NF-κB activation and TLR4 expression. Inhibition of LPS-induced NOX expression and activation	Male Sprague Dawley rats	(Prince et al., 2017)
Anthocyanins	Inhibition LOX and COX-2 activity	Human leukemia cell lines: J45 and HL60	(Szymanowska et al., 2018)
	Inhibition of IκBα phosphorylation and of the NFκB signaling pathway	Primary Dermal Fibroblasts	(Palungwachira et al., 2019)
Anthraquinones			
Chrysophanol	Inhibition of NF-κB through I-κB degradation, p65 translocation to the nucleus. Inhibition of COX-2 protein expression and PGE2 production. Inhibition of TNF-α and IL-6 production.	LPS-stimulated murine peritoneal macrophages.	(S.-J. Kim et al., 2010)
	Inhibition of the nuclear translocation and activity of NF-κB p65. Reduction of the level of IL-4, IL-5, IL-13, TNF-α, and iNOS. Inhibition of the activation of the NF-kB signaling pathway.	BALB/c mice. TNF-α-treated BEAS-2B cells.	(Song et al., 2019)

2.13.5. Phenolic compounds and reactive oxygen species

The production of reactive oxygen species (ROS) can cause tissue injury and trigger the inflammatory process (Naik & Dixit, 2011). Phenolic compounds through their capacities to scavenge free radicals and chelate metal ions (Heim et al., 2002) can block ROS-induced inflammation as illustrated in Figure 2.29. Phenolic compounds can also inhibit several enzymes responsible for ROS generation (Mishra et al., 2013). Thus, phenolic compounds are promising anti-inflammatory candidates.

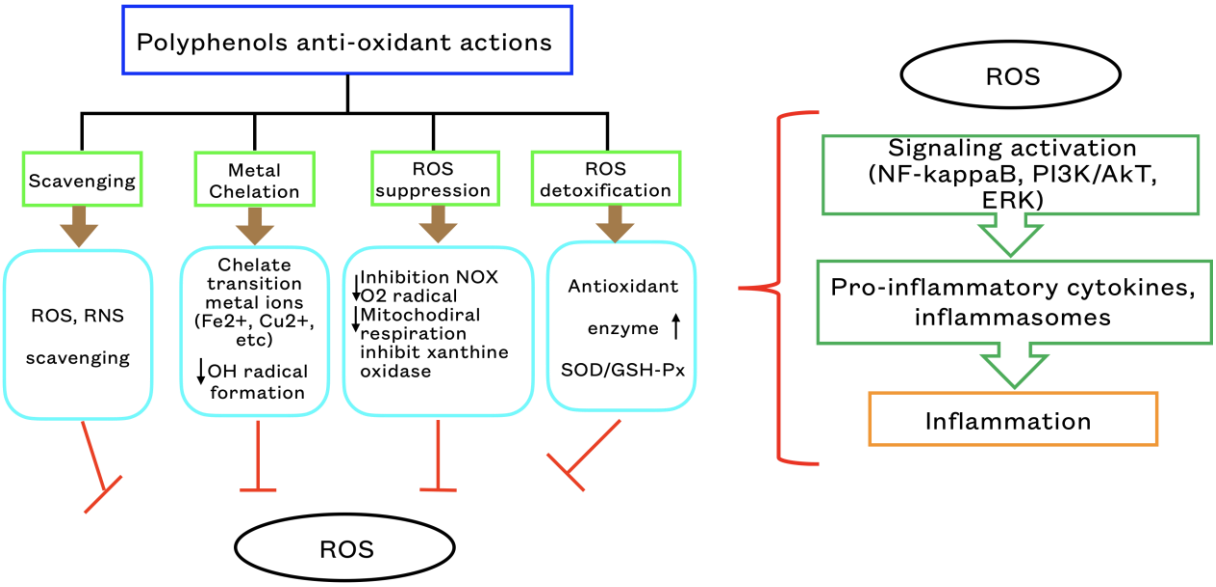

Figure 2.29. Links between antioxidant properties of phenolic compounds and their anti-inflammatory effects

(Adapted with permission from (Yahfoufi et al., 2018). Phenolic compounds can scavenge free radicals, chelate metal ions, inhibit ROS production, and induce ROS detoxification. ROS can stimulate inflammation by regulating several signaling pathways and pro-inflammatory cytokines. ROS: reactive oxygen species; RNS: reactive nitrogen species; NOX: NADPH oxidase; SOD: superoxide dismutase; GSH-Px: glutathione peroxidase; ERK: extracellular signal-regulated kinase; PI3K/Akt: phosphatidylinositide 3-kinase/ protein kinase B.

H_2O_2 can react with transition metal ions, like Fe^{2+} and Cu^{2+}, to produce free $OH^{\cdot}$ radicals (Prousek, 2007). Phenolic compounds can compete with this process and reduce inflammation. For example, curcumin can chelate Fe^{2+} and Cu^{2+} ions. EGCG and quercetin can also chelate iron ions (Heim et al., 2002). The reduction of $O_2^{\cdot}$ liberation by curcumin and resveratrol can block NOX (NADPH oxidase) (Youdim et al., 2002). Besides, by inhibiting the mitochondrial respiratory chain and ATPase, phenolic compounds can reduce mitochondrial ATP synthesis. As a consequence, ROS production is decreased. Some reports have shown that curcumin (L. Shen & Ji, 2009), EGCG, quercetins, and anthocyanins (Hajimahmoodi et al., 2014) can inhibit xanthine oxidase. Therefore, these phenolic compounds can attenuate ROS formation. In particular, curcumin and EGCG can trigger antioxidant enzymes such as superoxide dismutase (SOD), catalase, and glutathione (GSH) peroxidase

(Px). Thereby, ROS production can be diminished *in vivo* (Sporn & Liby, 2012). Hence, antioxidant phenolic compounds can exhibit anti-inflammatory action via different mechanisms, as illustrated in Figure 2.29.

2.13.6. Plant phenolic fractions

Several studies showed that plant phenolic fractions can be beneficial because of their antioxidant and anti-inflammatory properties.

Table 2.22. Examples of *in vitro* anti-inflammatory effects of plant phenolic fractions.
(Adapted with modifications from Zhu F.., Bin D., and Baojun X. (F. Zhu et al., 2018) and updated with recent literature).

Sources	Mechanism of actions	Experimental model	References
Polyphenols from the blueberry extract	Inhibit the production of NO, IL-1β, and TNF-α	LPS-activated BV2 microglial cells	(Lau et al., 2007)
Zerumbone and 3-O-methyl kaempferol from ginger	Inhibit NO and PGE2 production, iNOS expression	RAW 264.7 macrophages	(Chien et al., 2008)
Flavonoids and hydrolyzable tannins from pomegranate peels extracts	A potent inhibitor of the pro-inflammatory cytokine, reduces the production of NO and PGE2	RAW 264.7 macrophages	(Romier et al., 2008)
Flavones from Acai fruit	Anti-inflammatory capacity	RAW 264.7 macrophages	(J. Kang et al., 2011)
Phenolic compounds from *Cymbogng citratus* leaves extract	Inhibition of proteasome, NF-□B pathway, and cytokine expression	RAW 264.7 macrophages	(Francisco et al., 2013)
Quince peel polyphenols extract	Inhibition of TNF-α secretion	THP-1 macrophages	(Essafi-Benkhadir et al., 2012)
Procyanidin extract from grape seeds	Inhibition of NO production, PGE2 synthesis	RAW 264.7 macrophages	(Terra et al., 2007)
Sida rhombifolia Linn. (Malvaceae) extract	Inhibition of NO production	RAW 264.7 macrophages	(Mah et al., 2017)
Sonchus oleraceus L. (Asteraceae)	Suppress the expression of TLR-4, COX-2, NF-κB, and pSTAT	RAW 264.7 macrophages	(Y. Li et al., 2017)
Thymus zygis subsp. *zygis* an Endemic Portuguese Plant	Reduce NO release	RAW 264.7 macrophages	(A. M. Silva et al., 2020)

Mulberry Leaf (*Morus alba* L.) neochlorogenic acid extract	Reduce the production of TNF-α, IL-6, NO, iNOS, COX2 and PEG2	A549 cells	(Yu et al., 2020)
Sixteen Table Grape (*Vitis vinifera* L.) varieties phenolic compounds extract	InhibitIL-8 production	AGS cells	(Colombo et al., 2019)
Phenolic compounds in green tea extract	Activate the Nrf2 pathway and increase the level of anti-oxidant protein HO-1.	Human gingival epithelial keratinocytes	(Hagiu et al., 2020)
Smilax campestris Griseb (Smilacaceae) flavonoids extract	Inhibit the production of TNF-α, IL-1β, IL-6, and IL-8. Suppression the expression of NF-κB p65 subunit	THP-1 human macrophages	(Salaverry et al., 2020)

As shown in Table 2.22, phenolic compounds from blueberry can attenuate the LPS-induced inflammatory response of the BV2 microglia cell line (Lau et al., 2007). Polyphenols from blueberry extract inhibited the production of NO, IL-1β, and TNF-α, thereby leading to anti-inflammation. Another report showed that phenolic compounds from ginger, such as zerumbone and 3-O-methyl kaempferol, inhibit NO production through suppression of iNOS expression in LPS-activated RAW 264.7 macrophages (Chien et al., 2008). Zerumbone showed a greater anti-inflammatory capacity than 3-O-methyl kaempferol. The extract from pomegranate peels, which is rich in phenolic compounds such as flavonoids (like anthocyanins and catechin) and hydrolysable tannins (like punicalin and pedunculagin) (Ismail et al., 2012), has an anti-inflammatory action by inhibiting NO and PGE2 production (Romier et al., 2008). Another study showed that narirutin fraction from citrus peels extract reduces the generation of NO and PGE2 by attenuating iNOS and COX-2 expression, respectively, in LPS-stimulated macrophages (Ha et al., 2012). This fraction also reduced IL-1β and TNF-α production (Ha et al., 2012). Thus, narirutin phenolic fraction can be considered as an effective anti-inflammatory agent. Kang et al. (Kang et al., 2011) reported that the acai fruit extract, rich in phenolic components, notably flavones, has significant anti-inflammatory effects on RAW 264.7 macrophages. Phenolic compounds from *Cymbogng citratus* leaves extract can inhibit the NF-κB pathway and cytokine expression in RAW 264.7 macrophages (Francisco et al., 2013). Besides, quince peel polyphenols extract reduces TNF-α secretion by THP-1 macrophages (Essafi-Benkhadir et al., 2012). Terra et al. (Terra et al., 2007) reported that procyanidin extract from grape seeds can inhibit the ability of RAW 264.7 macrophages to produce NO and PGE2. The phenolic extract from *Sida rhombifolia* showed anti-inflammatory properties by inhibiting NO production in RAW 264.7 macrophages (Mah et al., 2017). NO production was also reduced by *Thymus zygis* subsp. *zygis* plant phenolic compounds extract in murine macrophages (Silva et al., 2020). The NF-κB signaling pathway was inhibited by *Sonchus oleraceus* L. (Asteraceae) phenolic compounds extract (Li et al., 2017). Moreover, this extract suppressed the expression of TLR-4 and COX-2. The expression of TNF-α, IL-6, NO, COX-2, and

PGE2 were inhibited by neochlorogenic acid extract from Mulberry Leaf (*Morus alba* L.) in A549 cells (X.-H. Gao et al., 2020). Phenolic compounds from *Vitis vinifera* L. extract inhibited the production of IL-8 by gastric epithelial cells (Colombo et al., 2019). Besides, phenolic compounds from green tea extract exhibit anti-inflammatory properties through activation of the Nrf-2 pathway and the increase of HO-1 production in human gingival epithelial keratinocytes, as reported by Hagiu A. et al. (Hagiu et al., 2020). Finally, Salaverry L. S. et al. (Salaverry et al., 2020) observed that flavonoids extract from *Smilax campestris* Griseb (Smilacaceae) can reduce the production of TNF- α, IL-1β, IL-6, and IL-8. This extract can also suppress the expression of the NF-κB p65 subunit in THP-1 human macrophages.

2.13.7. Phenolic compounds in oilseed meals as sources of anti-inflammatory agents

Sunflower (SFM) and rapeseed (RSM) meals are two abundant products containing phenolic compounds that could be valorized in the biomedical field. Among phenolic compounds present in SFM, chlorogenic acid (CGA) is the most abundant one; it represents 1-2% of the dry matter. Besides, sinapine (SP) and sinapic acid derivates are the major phenolic compounds found in RSM. An overview of the anti-inflammatory properties of pure chlorogenic acid (CGA) and sinapic acid (SA) is presented in Figure 2.30.

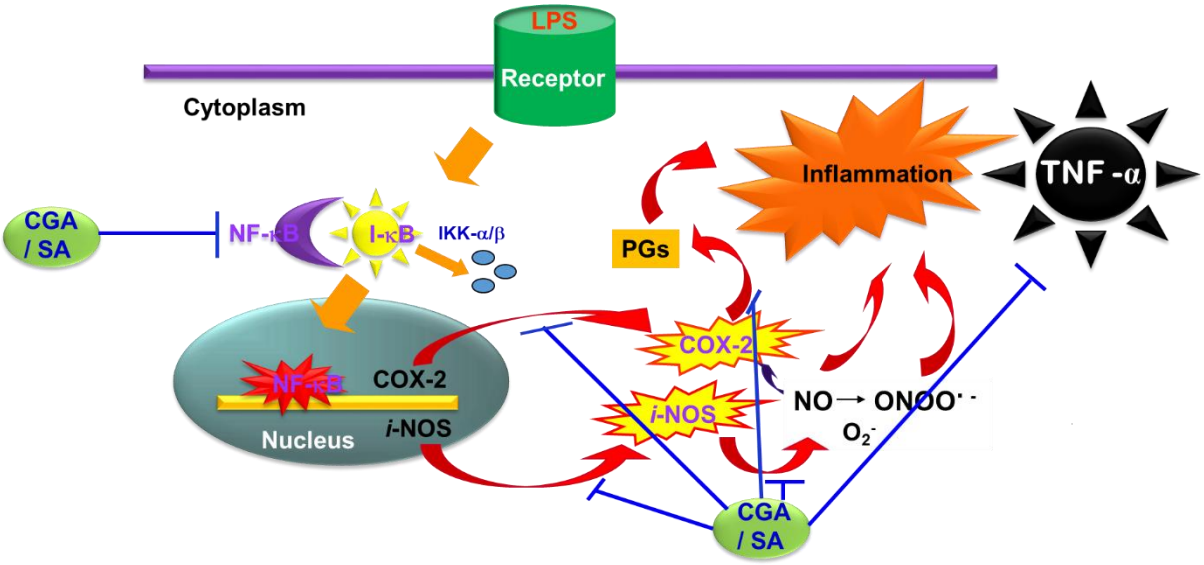

Figure 2.30. Anti-inflammatory activities of chlorogenic acid (CGA) and sinapic acid (SA).
CGA and SA can inhibit NF-κB activation and transcriptional activity, COX-2 and iNOS expression, as well as TNF-α production. NF-κB: Nuclear factor-kappa B; I-κB: Inhibitor of κB; IKK: IκBα kinase; COX-2: cyclooxygenase 2; i-NOS: inducible nitric oxide synthase; NO: nitric oxide; PGs: prostaglandins; TNF-α: tumor necrosis factor-α; NOS: nitric oxide synthase; LPS: Lipopolysaccharide; TLR: toll-like receptor; CGA: chlorogenic acid; SA: sinapic acid.

Several publications showed that pure CGA can inhibit oxidative stress-induced IL-8 production at the protein and mRNA levels in Caco-2 cells (Shin et al., 2015). Furthermore, as indicated above, it was shown that *Cymbogng citratus* leaves extract, which contains CGA, has anti-inflammatory effects through the inhibition of the NF-κB pathway, and cytokine expression (Francisco et al., 2013).

Hwang S. J. et al. (S. J. Hwang et al., 2014) showed that the expression of COX-2 and iNOS are significantly inhibited in the presence of pure CGA. This product did also attenuate IL-1β and TNF-α production in a dose-dependent manner in RAW 264.7 murine macrophages. Finally, Shan J. et al. (Shan et al., 2009) showed that CGA can suppress LPS-induced COX-2 expression through an inactivate NF-κB signaling pathway.

Regarding pure sinapic acid, Yun K.-J. et al. (Yun et al., 2008) showed that this product can inhibit LPS-induced NO, PGE2, TNF-α, and IL-1β production in RAW 264.7 macrophages. Sinapic acid also suppressed LPS-induced activation of the NF-κB signaling pathway in these cells. Consistent with these findings, Huang X. et al. (X. Huang et al., 2018) showed that pure sinapic acid can suppress iNOS, COX-2, and PGE2.

Taken together, these data show that oilseed meals are sources of interesting products to fight inflammation.

2.13.8. Relationships between chemical structures and anti-inflammatory activities of phenolic compounds

Structure-activity relationships (SAR) provide useful information to develop and discover new anti-inflammatory drugs from natural sources (Costa et al., 2012). Flavonoids have been studied in recent years because of the strong correlation between their anti-inflammatory effects and the presence of functional groups in the C6-C3-C6 skeleton (Gautam & Jachak, 2009).

Table 2.23. Chemical structures of flavonoids and activity relationships.
(adapted with modifications from Costa G. et al. (Costa et al., 2012)).

Principle functional groups	Generic structure	Anti-inflammatory activity	References
Generic structure of flavonoids (C6-C3-C6 skeleton)	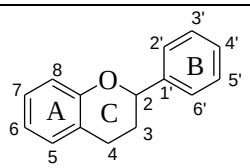		
C2 = C3 double bond (Unsaturation in C ring)	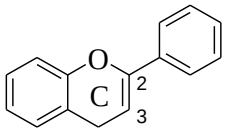	-Inhibition of NO production, - PLA_2 activity, 5-and 12-LOXs activity, - ICAM-1 expression	(Bonfili et al., 2008)
5,7-dihydroxyls (in A ring)	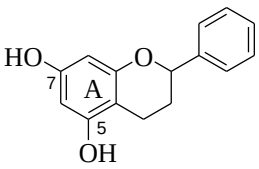	-Inhibition of NO, TNF-α production, - ICAM-1 expression	(Benavente-García & Castillo, 2008; Bonfili et al., 2008; K. H. Kim et al., 2004; Shie et al., 2010)
3',4'-dihydroxyl in B ring (catechol group)	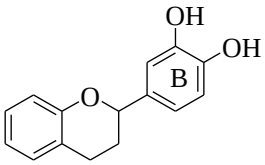	- Inhibition of proteasome activity, - Granulomatic inflammation, - TNF-α production, - ICAM-1 expression	(Benavente-García & Castillo, 2008; Bonfili et al., 2008; K. H. Kim et al., 2004; Shie et al., 2010)
4-ketonic carbonyl (in C ring)	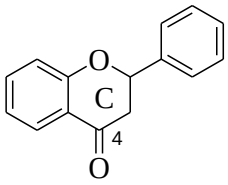	-Inhibition of proteasome activity, - ICAM-1 expression	(Benavente-García & Castillo, 2008)

Flavonoids exhibit anti-inflammatory activities due to the planar ring system A-C-B (Table 2.23) (Ambriz-Pérez et al., 2016). Inhibition of NO production depends on the C2-C3 double bond in the C-ring. The activities of PLA2, 5-LOX, and 12-LOX enzymes, involved in the production of PGs and LTs, depend on the C2-C3 double bond (Bonfili et al., 2008). Furthermore, the study of Benavente-Garcia O. et al. (Benavente-García & Castillo, 2008) demonstrated that the presence of the C2-C3 double bond in C ring decreases TNF-α-induced ICAM-1 expression by luteolin.

The biomedical properties of flavonoids are strongly correlated with their chemical structures. Indeed, according to Bonfili L. et al. (Bonfili et al., 2008), the presence of hydroxyl groups in A ring can influence the affinity of flavonoids for cellular membranes, permeability, and intestinal absorption. Hydroxyl groups, especially in positions 5 and 7, affect flavonoids' antioxidant activity (Bonfili et al., 2008), NO production (Kim et al., 2004), and cell adhesion molecule expression, for instance ICAM-1 (Chen C. C. et al., 2004; Gerritsen M. E. et al., 1995). Hydroxyl group's presence at the C3 position of

the C ring of flavonoids can slightly increase ICAM-1 expression (Chen C. C. et al. 2004) while methoxyl group's presence at the C8 position in A ring inhibits NO production (Kim et al., 2004).

Kim H. P. et al. (Kim et al., 2004) studied catechol type with 3',4'-dihydroxyl groups or 3',4'-dimethoxy groups (guaiacol type) in B ring and showed that these groups play an essential role in the inhibition of granulomatic inflammation. According to Ueda et al. (Ueda et al., 2004), the inhibition of TNF-α production depends on the presence of these hydroxyl groups in B ring. Conversely, the level of TNF-α increases when these groups are absent. 4'-OH substitution in B ring increased the anti-inflammatory activities of flavonoids through the inhibition of LPS-induced NO production and ICAM-1 expression (Benavente-García & Castillo, 2008).

According to Benavente-Garcia O. et al. (Benavente-García & Castillo, 2008), luteolin with a carbonyl functional group at the C4 position in C ring has potent anti-inflammatory effects. Moreover, the C ring's 4-oxo functional group can be considered as an essential factor in inhibiting prostaglandin production.

Additionally, flavonoids aglycones present higher potent in anti-inflammation compared to glycosides in the case of diosmetin and diosmin (Figure 2.31) (Benavente-García & Castillo, 2008). The hydrophilicity of flavonoid glycosides can explain this observation. Moreover, large glycosyl groups can cause steric obstacles (Kim et al., 2004). Nevertheless, the role of glycosides is still controversial because, in some cases, this type of compound decreased the anti-inflammatory activity (Kim et al., 2004).

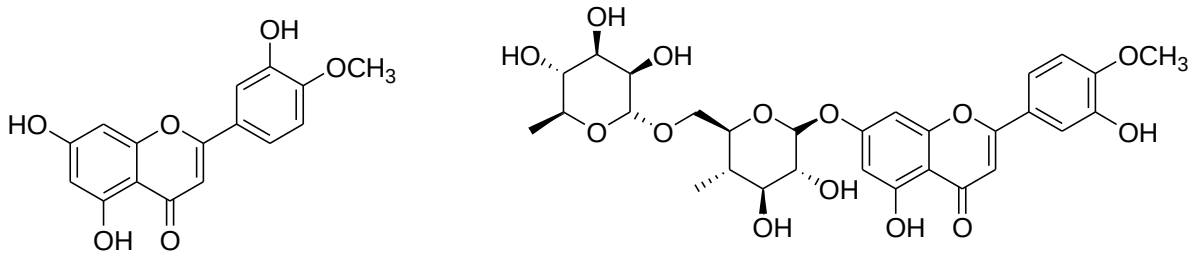

Figure 2.31. Chemical structures of diosmetin and diosmin.

Thus, it appears that chemical features of phenolic compounds can affect their anti-inflammatory properties and that such features have to be considered when searching for new candidates for anti-inflammation.

2.14. Conclusion for chapter 2

Rapeseed meal (RSM) and sunflower meal (SFM) are the by-products of the deoiling process and rich in proteins. Besides, it contains phenolic compounds with the main phenolic compounds was CGA in SFM and sinapine in RSM (Weisz et al., 2010, Siger et al., 2013). Besides, sinapic acid and its

derivates were predominant in RSM. Several studies used the organic solvent for extraction and purification phenolic compounds from SFM and RSM such as methanol, ethanol, and iso-propanol in water. Then, these extraction solutions were applied into the macroporous resin column (non-polar, slightly polar, and polar resins) to obtain the phenolic fraction and/ or to remove the phenolic compounds from SFM and RSM. There were report of Weisz et al. (Weisz et al., 2010) which used the design of experiment for eliminating the CGA in proteins isolation/ purification. There were several reports regarding the hydrolysis of phenolic compounds in RSM using acid, base, and enzyme to convert the sinapic acid derivates into free sinapic acid.

The adsorption mechanisms of phenolic compounds in SFM and RSM were investigated. These data showed that the adsorption mechanism of phenolic compounds in SFM and RSM, in general, followed by pseudo-second-order and Langmuir models. These results demonstrated that the adsorption of PCs were homogenous layer behavior and physical adsorption.

The biological activities such as anti-oxidant and anti-inflammation of PCs in SFM and RSM were tested in *in vitro.* The results from literature showed that the anti-oxidant activity of PCs in both meals were promising. The anti-oxidant capacity of sinapic acid were more powerful than sinapine or sinapic esterifed forms in RSM. Several reports showed that the pure CGA can exhibit the anti-inflammatiory activity in different cell line. However, there was little reports that reported the activity of sinapic acid in anti-inflammatory effects. Taken together, these data showed that oilseed meals were the source of interesting products to fight inflammation.

Chapter 3. General scientific approaches

This chapter presents the general scientific approaches to fulfill this Ph.D. project. This work was divided into two main parts (Part I: extraction, characterization, and batch adsorption and Part II: Dynamic adsorption and bioactive functions of the phenolic fractions), to conduct the objectives of this project as mentioned in chapter 1. Figure 3.1 illustrates the experimental design and general scientific approaches of this project.

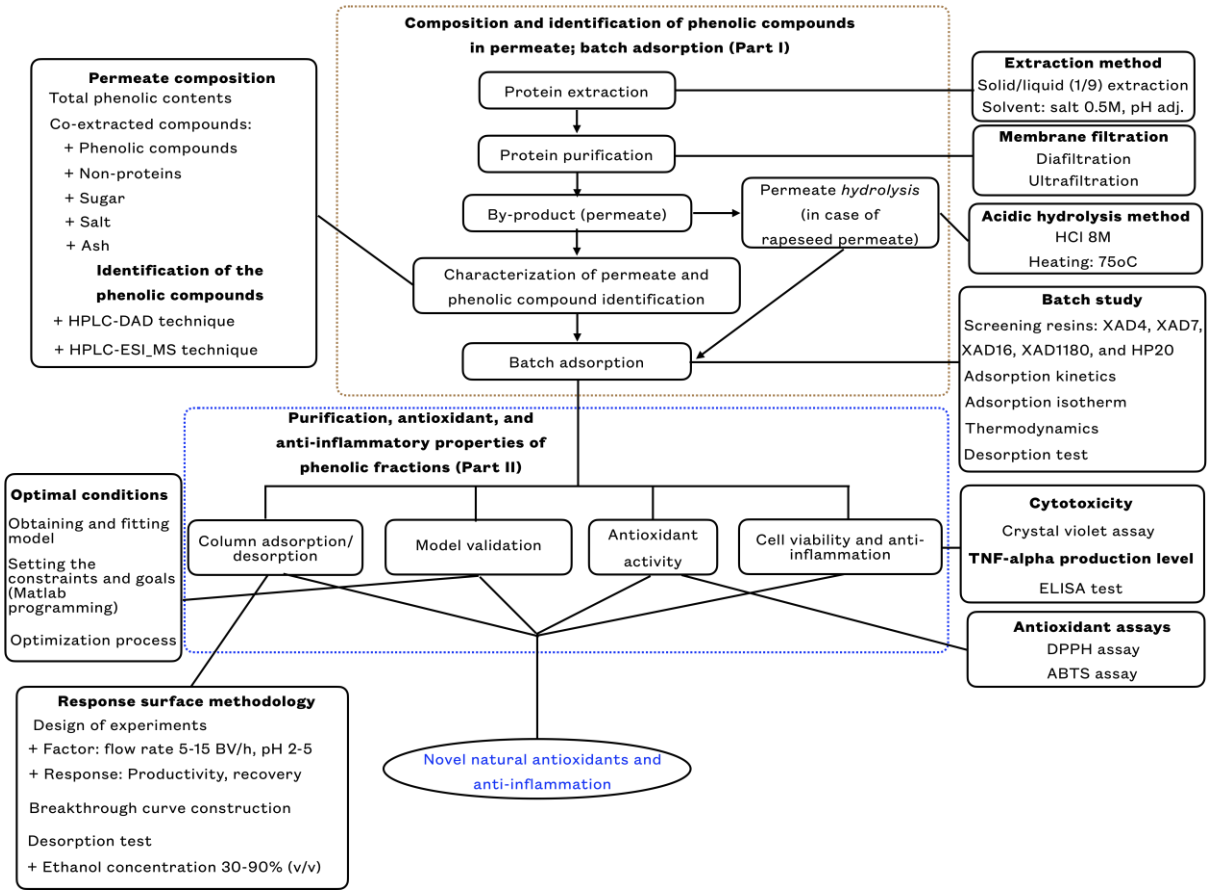

Figure 3.1. Illustration of general scientific approaches.

3.1. Part I: Extraction, characterization, and batch adsorption

In this part, the general scientific approach was illustrated as in the Figure 3.2. The objectives were to: 1) produce the liquid effluent (permeate) as a by-product of proteins isolation/ purification process, 2) identify/determine phenolic compounds in these by-products, 3) select the appropriate macroporous resins for further studies, and 4) understand the mechanism of phenolic compounds adsorption onto selected resin.

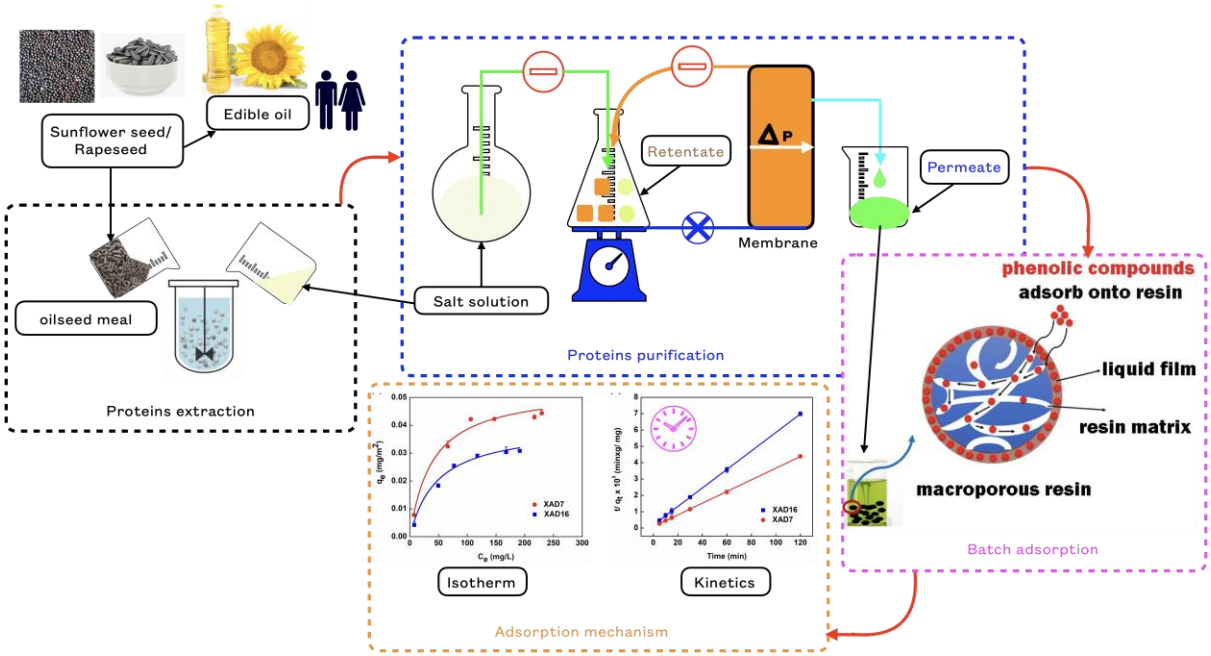

Figure 3.2. General scientific approaches for liquid effluent production and batch adsorption studies.

3.1.1. Aqueous by-product from the oilseeds protein isolate production

Overview of aqueous by-products from oilseed proteins extraction/purification process in this chapter illustrated in Figure 3.3.

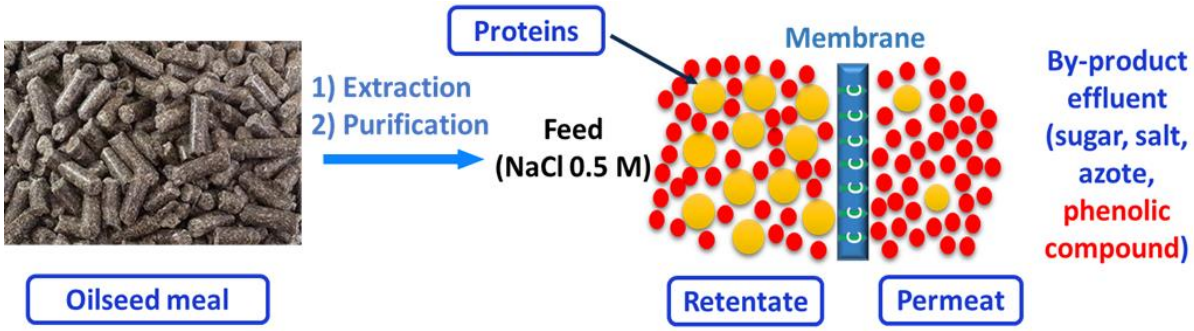

Figure 3.3. Process of aqueous by-product from oilseed protein isolate production.

Oilseed meals used in this project were sunflower meal (SFM) and rapeseed meal (RSM). The aqueous effluent used in this Ph.D. project resulted from SFM and RSM by-products of protein isolate/ purification process (Claire et al., 2019; Albe Slabi et al., 2020). As the reported of the previous studies in our labotatory (Claire et al., 2019; Albe Slabi et al., 2020), the protein isolate process in both materials was carried out in two steps: 1) protein extraction from SFM/ RSM using appropriate concentration of salt solution and pH and 2) protein isolate/ purification using tangential filtration (ultrafiltration, UF). During the process, the retentate compartment was fed with appropriate concentration of salt solution at the same flow rate as the permeate flux in order to keep the volume constant. Six diavolume (DV) of NaCl solution was added. Then, three DV of deionized water was used to flush NaCl from proteins. The permeate containing the phenolic compounds was recovered and adjusted to pH 2 by adding HCl 1M for further studies (Albe Slabi et al., 2020). The liquid effluents obtained after purification using membranes called the permeate (Figure 3.3). These by-products contained a low-molecules weight such

as carbohydrate (sugar), salt, azote, and rich in phenolic compounds. These liquid effluents were used to investigate in the further studies.

3.1.2. Characterization these liquid effluents (permeate)

These phenolic compounds showed a promising candidate for several biological activities such as anti-oxidant and anti-inflammatory properties (Shan et al., 2009; Essafi-Benkhadir et al., 2012; Salgado et al., 2012; Weisz et al., 2013; Žilić et al., 2010). Therefore, in this Ph.D. project, we characterized these permeates and isolated/ purified the targeted compounds (phenolic compounds).

In this part, we used HPLC and HPLC-MS to identify the phenolic compounds in by-products proteins isolate. Previous studies also showed that chlorogenic acid (CGA) was the main phenolic compounds in SFM (Weisz et al., 2009; Weisz et al., 2010; Weisz et al. 2013). In addition, sinapine (SP) was the main phenolic compounds from RSM. In the previous report, Vuorela et al. (Vuorela et al., 2005) demonstrated that sinapic acid showed more potent in antioxidant capacity. Therefore, in this study, permeate from RSM was hydrolyzed to convert sinapine and sinapic acid derivates (sinapic acid in esterfied forms) into sinapic acid using acidic method. This reaction also allowed us to determine the free and esterified phenolic compounds concentration during the reaction. The determination of phenolic compounds was identified by comparing their relative retention time with authentic standards, including chlorogenic acid (CGA) with the phenolic compound froms sunflower meal (SFM) and sinapine (SP) and sinapic acid (SA) with the phenolic compounds from rapeseed meal (RSM). Moreover, the identification of phenolic compounds from sunflower, rapeseed, and hydrolysis permeate expressed based on the *m/z* values and unique fragmentation pattern of the protonated molecules ions $[M-H]^+$ or $[M-H]^-$. The standard phenolic compounds were also used to construc the calibration curves. These calibration curves allowed us to determine the concentration of phenolic compounds in the liquid effluents and in the phenolic fractions as well.

The by-products proteins isolate in RSM contained various phenolic compounds. Therefore, the quantification of total phenolic contents (TPC) in a rapeseed meal was performed by the “sum of phenolic acids” method of Rabie Khattab et al. (Khattab, 2010). TPC was estimated as SA equivalent (SAE, in mg) from the sum area of all peaks of phenolic compounds, including the unidentified ones, which were recorded at 325 nm, based on the SA calibration curve.

Other microsolutes compounds in these permeates were also determined in cluding salt content, total carbohydrate content, non-protein nitrogen content, and dry matter. The salt content was calculated using a NaCl calibration curve by conductimetry technique. Total carbohydrate content in the permeate was measured using anthrone-sulfuric acid presented by Yemm and Willis with some modifications (Yemm & Willis, 1954). In this method, glucose was used to construc the calibration curve. The Kjeldahl method was used to measure the total nitrogen in the permeate (AOCS International., 1995). A nitrogen-to-protein conversion coefficient of 5.6 and 6.25 for SFM and RSM, respectly, was applied as recommended in the previous study (Albe Slabi et al., 2019; Claire et al., 2019).

3.1.3. Adsorption/ desorption batch study

This part was conducted to select the appropriate resins for phenolic compounds adsorption. To do so, five different macroporous resins including non-polar resins such as SDVB resin and mild-polar resins such as acrylic resin were used to screen.

3.1.3.1. Adsorption kinetics

Using HPLC technique, we calculated the phenolic compounds concentration and adsorption/ desorption capacity and ratio for each resin. The best resins were chosen based on the highest adsorption capacity (massic and surface adsorption) for further studies. The adsorption capacity was monitored after certain times. This step allowed us to know the duration of phenolic adsorption reach the equilibrium state. And this duration was applied to further adsorption process.

Several mathematical models were applied to understand the adsorption kinetic mechanisms including pseudo-first-order (PFO), pseudo-second-order (PSO), and intra-particles diffusion model.

3.1.3.2. Adsorption isotherms

Adsorption isotherms expressed the relationship between the adsorption capacity of phenolic compounds and the concentration of phenolic compounds in the permeate at the equilibriumstatus at different temperature. To understand the adsorption behavior of phenolic compounds, several isotherm models were used to monitored such as Langmuir and Freudlich models. And from these models, we calculated the maximal adsorption capacity of phenolic compounds onto the selected resin. This step allowed us to predict the quantity of phenolic compounds adsorbed and understand the mechanisms of adsoprion process. This information was useful for the further studies.

3.1.3.3. Adsorption thermodynamic parameters

The effect of the adsorption temperature was investigated by determining the adsorption isotherms atdifferent temperatures. Several thermodynamic parameters were determined including enthalpy, entropy, and the Gibbs energy change. The values of these parameters allowed us to understand the adsoprion process and to design for further studies on purification process.

3.1.3.4. Batch desorption

Desorption ratios were determined using different ethanol/ water solvents after the adsorption step on selected resins up to equilibrium. Using ethanol solutions were recommended by several research goups because of their non-toxicity with the phenolic samples and eco-frendly (Weisz et al., 2010; Weisz et al. 2013).

3.2. Part II: Dynamic adsorption/ desorption and biomedical valorization of phenolic fractions after desorption process.

The best resins which exhibited the highest adsorption capacity of phenolic compounds in part I was used to investigate the column adsorption/ desorption for purification process and produce the phenolic fractions for biological activities studies in this part of Ph.D. project. The general scientific approaches was illustrated in Figure 3.4. The objectives of this part were to: 1) understand the effect of

adsorption flow rate and pH on dynamic binding capacity, productivity and recovery was investigated by design of experiments (DoE), 2) determine the optimal conditions using the multi-objective optimization method, 3) understand the effect of the ethanol concentrations on phenolic fraction purity and recovery, 4) determine the antioxidant capacity of these phenolic fractions, and 5) evaluate the anti-inflammatory activity of these phenolic compounds. These last studies allowed to demonstrate a protective effect of this fraction against a future inflammation. This property could be valorized in the veterinary and human well-being fields and its antioxidants properties in the food industry.

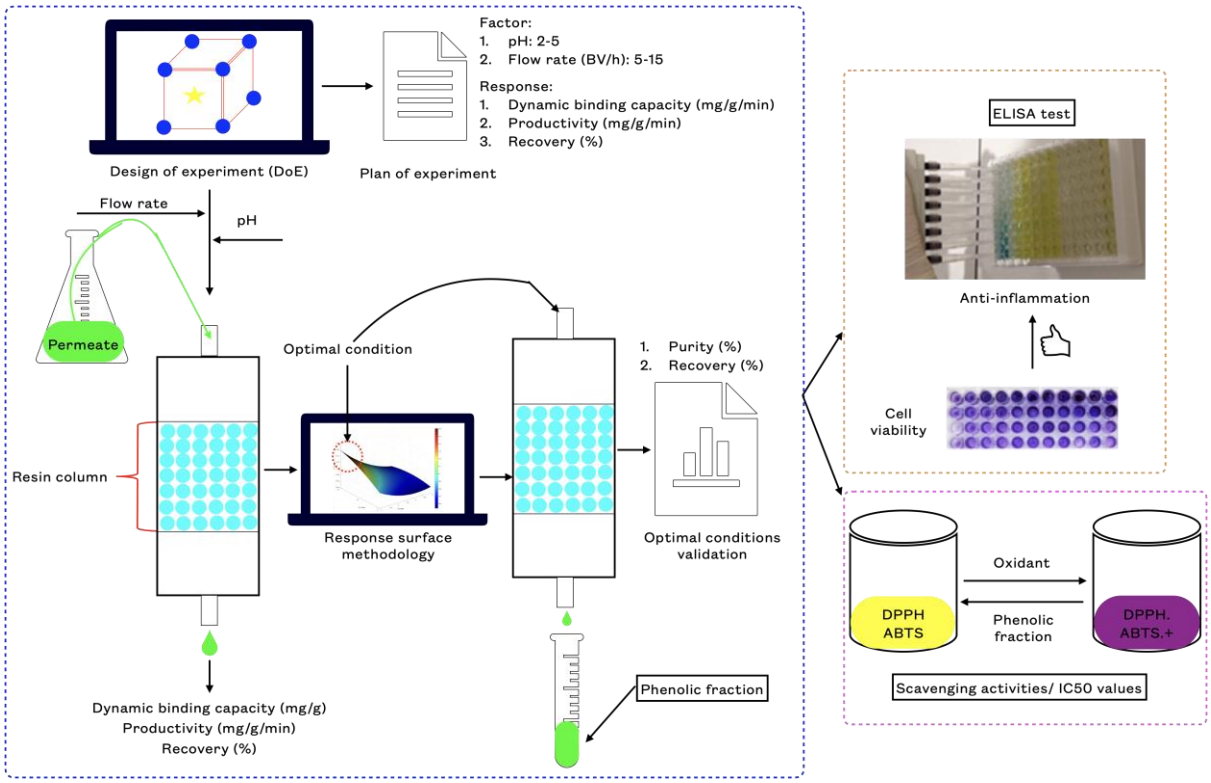

Figure 3.4. General scientific approaches for column adsorption and bioactivity evaluation of phenolic fractions.

3.2.1. Column adsorption and design of experiments

As shown in Figure 3.4., two factors including adsorption flow rate (5-15 BV/ h) and pH (2-5) were considered to study the dynamic binding capacity, productivity, and recovery of column adsorption process. The influence of adsorption flow rate and pH on the adsorption process was investigated by the design of experiments (DoE). The output solutions were collected and phenolic compounds concentration were determined by HPLC. The input permeate solution was stopped when the adsorbance at 325 nm corresponded to a phenolic concentration equal to 10% of its concentration in the feed as recommended (B. Liu et al., 2016; P.-C. Sun et al., 2015). In the desorption step, the column was washed by absoluted ethanol. This step allowed us to calculate the dynamic binding capacity at 10% (DBC10, in mg/g), productivity process (in mg/g/min), and recovery for each condition

(in %). The face-centered central composition design was introduced and analyzed using the MODDE® 7 software. The results obtained from each condition (adsorption flow rate and pH) of experiment were used to determine the best condition for productivity and recovery by multi-optimization method. The objective function corresponded to the simultaneous maximization of productivity and recovery. The multi-objective problem was solved using the model equations and setting two criteria including productivity and recovery. The multilevel algorithm was built and analyzed using the MATLAB® software. The purpose of this step was to determine the optimal conditions for column adsorption. These optimal conditions were used to apply into the column at adsorption step and to study the desorption step.

The summary of multicriteria optimization of phenolic compounds captures from sunflower/ rapeseed proteins isolate production process presented in Figure 3.5.

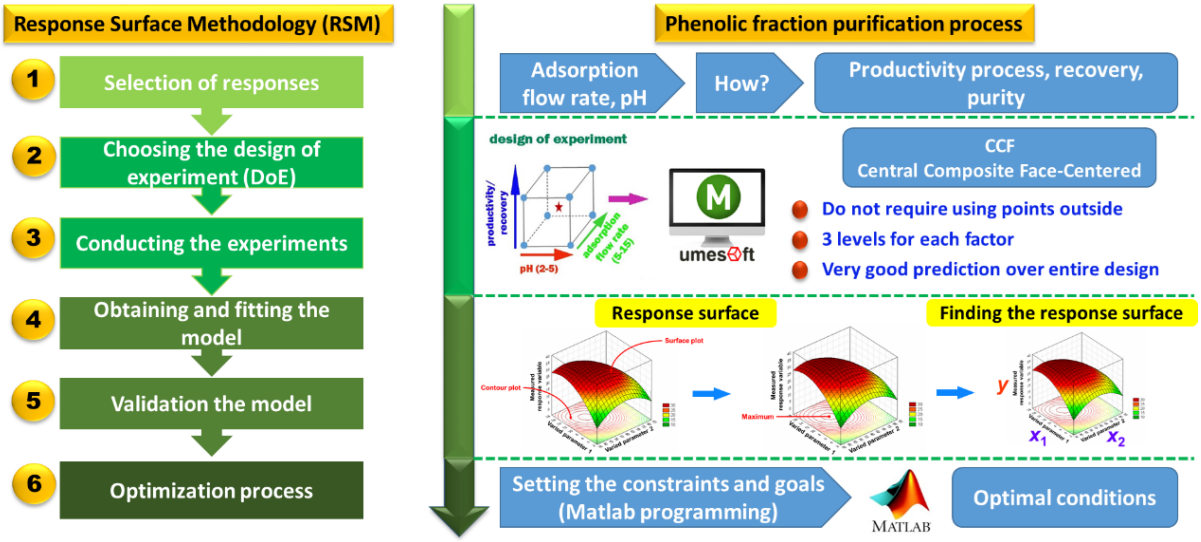

Figure 3.5. The general procedure of multicriteria optimization for phenolic compounds purification.

3.2.2. Column desorption

The optimal conditions for column adsorption were applied to determine the optimal condition for desorption step. To do so, various ethanol concentrations were used to determine the recovery and purity of phenolic fraction. The selected concentration of ethanol solution based on the highest purity and recovery of phenolic compounds. This step allowed us to generate enough amount of phenolic fractions for further studies.

3.2.2. *In vitro* antioxidant activity

Figure 3.8 illustrates the procedure of methods (DPPH and ABTS assays) using for determination the antioxidant capacity of phenolic fractions.

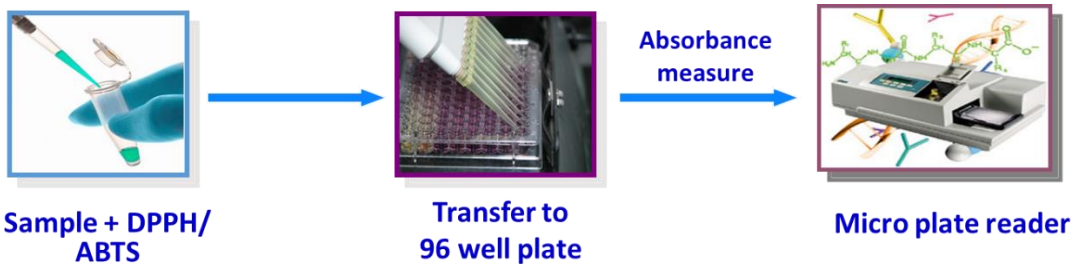

Figure 3.6. The procedure of DPPH and ABTS assays.

The antioxidant capacity of phenolic fractions was measured based on their ability of free radical scavenging (J. Zhu & Wu, 2009; Re et al., 1999). The antioxidant concentration showing 50% maximum antioxidant capavity (IC50) was also calculated in this part. The IC50 values helped us to know the potent of phenolic fractions in antioxidant property. The phenolic fraction show high anti-oxidant activity could consider as a promising candidate for food industry.

3.2.3. Cell viability and anti-inflammatory property

The THP-1 human monocytic leukemia cell line was used in this study. To evaluate the anti-inflammatory property of phenolic fractions, THP-1 was differentiated into macrophages using phorbol myristate acetate (PMA). Then, the differentiated THP-1 cells were treated with lipopolysaccharide (LPS). This step allowed to produce the pro-inflammatory cytokine, tumor necrosis factor alpha (TNF-α). This scientific approach was illustrated in Figure 3.7.

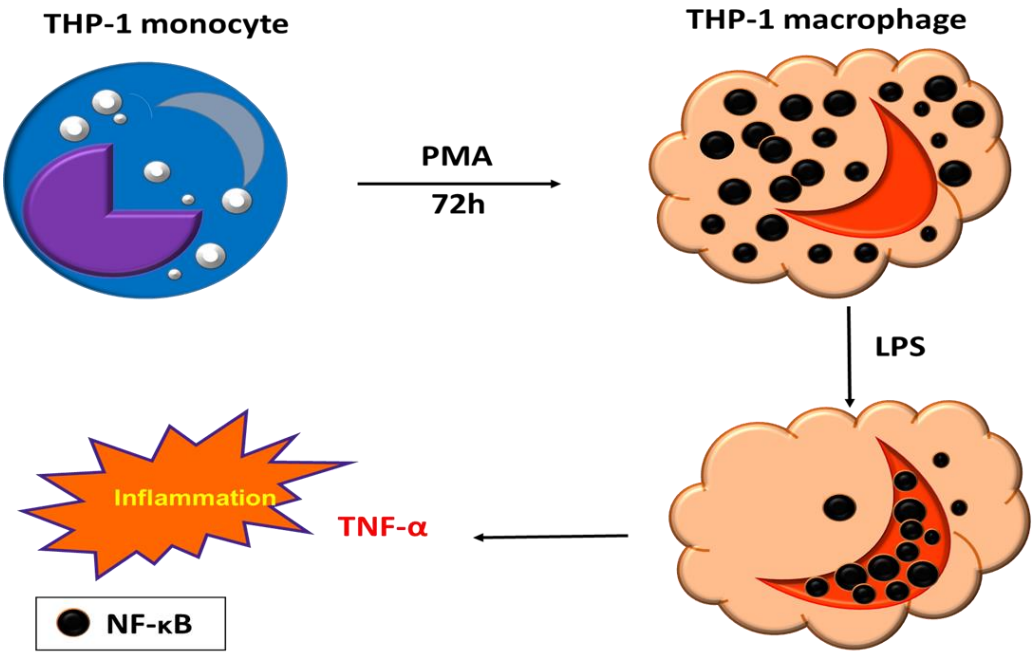

Figure 3.7. Scheme of THP-1 monocyte differentiation and TNF-α secretion.

The phenolic fractions were added into the THP-1 macrophages before or after LPS. The purposes of this step were to evaluate whether these phenolic fraction could act as the agents could prevent THP-1

macrophages from the inflammation or could act as inhibitors of inflammatory process. These results were concluded based on the TNF-α production level using human TNF-α quantikine ELISA kit. In any cases, the differentiated THP-1 cell viability was determined using the crystal violet. The phenolic fractions which show non-cytotoxicty and inhibit the TNF-α production level are promising agents to moderate inflammation.

Chapter 4. Characterization and adsorption mechanism of phenolic compounds from oilseed protein isolate byproducts.

4.1. Introduction

In this chapter, the phenolic compounds in UF permeate from sunflower and rapeseed protein isolate production were characterized HPLC-MS and quantified on the basis of HPLC UV signal. The overall proximal composition was also determined. Then, a screening of resins having different properties was achieved in order to select the most promising one for further investigations. In this study, low to mild apolar resins with various pore size and bead diameters were selected. The selection of resin was classically based on the adsorption capacity. With the selected resin adsorption kinetics and isotherms were studied experimentally and regressed with different models in order to qualify the mass transport phenomena and the thermodynamic properties of the adsorption.

In the first part of the chapter, the strategy explained above is carried out with sunflower meal. This part constitutes a manuscript of a paper published in the journal of *Chromatography and Separation Techniques* in 2020. The second part of the chapter is dedicated to the rapeseed resource. It is a part of a paper published in *Molecules* in 2021.

4.2. Sunflower polyphenols characterization and capture by adsorption.

Adsorption of phenolic compounds from an aqueous by-product of sunflower protein extraction/ purification by macroporous resins

Tuong Thi Le [a,b], Arnaud Aymes [a], Xavier Framboisier [a], Irina Ioannou [a,c], and Romain Kapel [a]*

[a] Laboratoire Réaction et Génie des Procédés, Université de Lorraine, CNRS, LRGP, F-54500, Nancy, France

[b] Laboratoire Stress, Immunité, Pathogènes, Université de Lorraine, EA7300, 9 Avenue de la forêt de haye, 54500 Vandoeuvre-lès-Nancy, France

[c] URD Agro-Biotechnologies Industrielles, AgroParisTech, CEBB, 3 rue des Rouges Terres, 51110 Pomacle, France

Abstract

In this study, adsorption of phenolic compounds from an aqueous by-product of sunflower protein isolate production was investigated. Phenolic compounds in this by-product (ultrafiltration permeate of protein purification step) were almost exclusively CGA (mainly 5-CQA isomer). Five different macroporous resins including XAD4, XAD7, XAD16, XAD1180, and HP20 were screened for CGA capture. XAD16 had the best massic adsorption capacities (15.32 ± 0.04 mg/g), while XAD7 had a better surface adsorption capacity (0.027 ± 0.00146 mg/m²). CGA adsorption on both resins followed both the pseudo-second-order kinetic model with a similar intra diffusional pattern. Adsorption isotherms of the two resins better fitted the Langmuir model with Qmax for XAD7 and

XAD16 of 0.054 and 0.040 (mg/ m²), respectively. The adsorption process of phenolic compounds revealed to be exothermic, physical adsorption, and spontaneous. Better adsorption results were observed at 25°C. Maximal CGA desorption ratio was observed from 70% (v/v) ethanol. The high values were reached with both the two resins (88.09 ± 0.13 and 86.16 ± 0.32% for XAD7 and XAD16, respectively). The CGA purity in the desorption phase was surprisingly high (77.56 ± 0.99% and 74.59 ± 0.12% for XAD7 and XAD16, respectively).

Keywords: Sunflower meal, macroporous resin, adsorption study, chlorogenic acid.

4.2.1. Introduction

Phenolic compounds are a wide group of natural products from plant sources. These molecules are secondary metabolites having one or several benzene ring with hydroxyl groups. They are known to have various bioactivities like anti-oxydant, anti-inflammatory, anti-cancer, anti-ageing or anti-osteoporosis activities (Ren et al., 2017; Wong et al., 2018; H. Zhang & Tsao, 2016). Among phenolic compounds, chlorogenic acid (CGA) revealed particularly attractive. Chemically, CGA is a polar phenolic compound composed of a quinic acid and caffeic acid linked by an ester bond. The position of the quinic acid on the benzene ring define three CGA isomers including 5- O-caffeoylquinic acid i.e 5-CQA, 4-O-caffeoylquinic acid i.e 4-CQA, and 3-O-caffeoylquinic acid i.e 3-CQA. Interestingly, CGA has demonstrated high anti-oxydant, anti-inflammation and anti-tumor effects (P. Li et al., 2011; Tajik et al., 2017).

Some raw materials like coffee beans, low-grade coffee beans, noxious weeds like *Eupatorium adenophorum* Spreng (Crofton weed) (B. Liu et al., 2016) or *Boehmeria* nivea L. Gaud (Ramie) leaves (Tan et al., 2014) revealed to be interesting sources of CGA. Sunflower seed is also rich in phenolic compounds (1 - 4.5% on a dry weight basis) and particularly in CGA. It is the second most cultivated oilseed in Europe with an annual production of about 16 million tons (FAO, US Department of Agriculture) in 2018 (*FAOSTAT*, 2020a). It is mainly processed for oil production. The industrial oil extraction process yields a solid by-product called “meal” composed of up to 50% of proteins (Geneau-Sbartaï et al., 2008; Pickardt et al., 2011), which contains seeds phenolic compounds. Beside CGA, these compounds are mainly CGA isomers, CGA dimers, and caffeic acid.

To date, sunflower meal is mainly used for the feed. For this purpose, phenolic compounds are considered as antinutritionals and need to be eliminated. Many approaches were reported to remove phenolic compounds from the meal. As for other ressources, the most classical way is to use organic solvents like acetone, methanol, ethyl acetate or water/ ethanol mixtures (Canella & Sodini, 1977; Sripad & Rao, 1987). Weizs et al. (Weisz et al., 2009) showed that methanol/ water mixtures 60% (v/v) was suitable for extraction of sunflower phenols from both kernels and shells. Interestingly, they showed that the obtained extract with a phenolic fraction composed of a particularly high proportion of CGA (around 85%). After solvent extraction, phenolic compounds can be further purified by chromatography (Ky et al., 1997), membrane processes (Conidi et al., 2017; Zagklis et al., 2015) or

adsorption on macroporous resins (Jia & Lu, 2008). This last process proved to be particularly efficient for phenolic compounds capture from various plant extracts (Jia & Lu, 2008; B. Liu et al., 2016; Q.-S. Liu et al., 2010). Besides, adsorption processes can easily be scaled up and some resins are food grade (Scordino et al., 2003). Macroporous resins are divided into polar resins, mild polar resins and non-polar resins. The mechanism of separation is based on differential affinity between phenolic compounds, impurities and the adsorbent (P.-C. Sun et al., 2015). Proper resins should be chosen on the basis of both adorption capacities and purity after desorption step, but purity is often not considered. Furthermore, the complex transport phenomenon that are also involved are rarely thoroughly investigated.

Sunflower meal is also considered as an promising source of proteins (González-Pérez & Vereijken, 2007; Hudson, 1994) for food applications under isolate products. The production of sunflower protein isolates is classically achieved in two main steps (aqueous extraction and purification). The extraction step has to be done under pH 8 and at high NaCl concentration (> 0.2 M NaCl) in order to get satisfying protein extraction yield and color (Bongartz et al., 2016; Wildermuth et al., 2016). A large part of sunflower phenolic compounds are extracted alongside with proteins in these conditions. Recently, an integrated process was proposed for both protein and phenolic compounds valorization (Weisz et al., 2010, 2013). This process integrates a capture of phenolic compounds by adsorption from the aqueous extract prior to protein purification by acid precipitation. The resin had to have low protein binding capacity. XAD16 resin revealed to be the most appropriate resin to do so beyond other apolar and ion exchange resins (Weisz et al., 2013). However, CGA purity after adsorption step was not considered and adsorption mechanisms and transport were not investigated and remained unclear. Furthermore, in this approach, protein acid precipitation led to an isolate having a poor solubility which is rather detrimental for food applications.

More recently, we proposed an alternative approach in which sunflower proteins are purified from the aqueous extract by tangential filtration (Albe Slabi et al., 2019). This yielded a highly soluble sunflower protein isolate with high functional properties. Interestingly, phenolic compounds in the extract were only composed of CGA (mainly 5-CQA isomer) (Albe Slabi et al., 2019). The liquid effluent of this process (the UF permeate) was largely depleted in proteins and probably contained the main part of extracted CGA. Hence, the capture of CGA from this side product would constitute an interesting valorization pathway. The aim of this work was to study CGA adsorption from the UF permeate on five macroporous resins including XAD4, XAD7, XAD16, XAD1180 and HP20 having various properties in term of polarity, pore diameters, specific area). On the resins exhibiting the best adsorption capacities, kinetics and isotherms experimental data were regressed at different temperatures in order to elucidate CGA adsorption mechanisms. Desorption by ethanol/ water mixtures was also investigated and the purity was considered in order to choose the most appropriate resin for CGA capture from this effluent.

4.2.2. Materials and methods

4.2.2.1. Chemical and reagents

The sunflower meal used was defatted by *n*-hexane at the industrial scale and provided by Saipol (Bassen, France). Chlorogenic acid (CGA, 5-*O*-caffeoylquinic acid), 4-*O*-caffeoylquinic acid (4-CQA), 3-*O*-caffeoylquinic acid (3-CQA) standards and the five macroporous resins (XAD7, XAD4, XAD16, XAD1180 and HP20) were purchased from Sigma-Aldrich (St. Louis, Missouri, USA). The characteristics of macroporous resins are shown in Table 4.1.

Table 4.1. Properties of XAD 7, XAD 16, XAD 4, XAD 1180 and HP 20

Resins	Material	Polarity	Specific surface (m^2/g)	Pore (Å)
XAD4	SDVB*	Non polar	725	50
XAD7	Acrylate	Polar	450	90
XAD16	SDVB	Non polar	900	100
XAD1180	SDVB	Non polar	600	300
HP20	SDVB	Non polar	500	260

SDVB*: Styrene-divinyl benzene

Sodium chloride (NaCl) and sodium hydroxide (NaOH) pellets were both from VWR (Darmstadt, Germany). Hydrochloric acid (HCl) solution was from Carlo Erba (Milan, Italy). Acetonitrile and formic acid at analytical grade were supplied by Fisher Scientific (Hampton, USA).

4.2.2.2. Sunflower protein extraction/purification process

The process was carried out in two stages as described in (Albe Slabi et al., 2019). The first one was a solid/liquid extraction from the sunflower meal. The second was a protein purification by ultrafiltration (UF). The extraction step was achieved using a 0.5 M NaCl solution at a solid/ liquid ratio of 1:9 (w/w). The pH of the slurry was adjusted at pH 7.5 with HCl 1 M and stirred at room temperature for 30 min. Then the slurry was centrifugated (Thermo Scientific Lynx 6000 centrifuge, USA) at 15 000 *g* and 20°C for 30 min. The purification step was achieved with an Akta Flux 6 ultrafiltration apparatus (GE Healthcare Life Science, USA). The membrane used was a polyethersulfone hollow fiber membrane of 3 kDa cut-off (4800 cm^2 area, UFP-3, C-6A, GE Healthcare, USA). The transmembrane pressure was set at 1.5 bar and the feed rate at 1.5 L/min. In a first stage, six diavolumes (DV, DV = diafiltration solution volume/ initial volume) of 0.5 M NaCl solution was used to flush proteins from micro-solutes (low molar weight carbohydrate, minerals, non-protein nitrogen, and phenolic compounds). Then, NaCl was removed by three diavolumes of deionized water. The retentate compartment contained the purified proteins. The permeate obtained was collected and adjusted at pH 2 (in order to avoid phenol oxidation as recommended (Albe Slabi et al., 2020) and stored at -20°C before use.

4.2.2.3. Adsorption/ desorption study

Before each experiment, resins were washed with methanol for 10 minutes under magnetic stirring (150 rpm) at room temperature and rinsed with ultrapure water as recommended by the manufacturer. For each experiment, 1.5 g resin was mixed with 30 mL of permeate under magnetic stirring (150 rpm) at 25°C. After adsorption, resins were separated from the liquid phase by filtration

(using Millex syringe Filter, PVDF, 0.22µm, non-sterile from ThermoFisher Scientific (USA). Liquid phases were analyzed by HPLC for phenolic compounds characterization and/ or CGA quantification.

4.2.2.3.1. Resin screenings

The resins were screened on the basis of massic (Eq. 4.1) and specific surface (Eq. 4.2) adsorption capacity:

The adsorption capacity (q_e, amount of CGA adsorbed per g of resin, Eq. 4.1) was calculated as:

$$q_e = \frac{(C_0 - C_e)V_i}{W} \quad (4.1)$$

where C_o and C_e are the initial and equilibrium concentrations of CGA in permeate solution respectively (mg/ mL); V_i is the initial volume of permeate added into the resins (mL); and W is the weight of the dried resin (g).

The specific surface adsorption capacity (SA, amount of CGA per m² of resin, equation 4.2) was calculated as:

$$SA = \frac{(C_0 - C_e)V_i}{SS \times W} \quad (4.2)$$

where SA is the surface adsorption capacity (mg / m^2), SS is the resin specific surface (m^2/ g).

4.2.2.3.2. Adsorption kinetics

Adsorption capacity was monitored after 5, 10, 15, 30, 60, 90, and 120 min. To do so, CGA concentration was measured in the liquid phase by HPLC. From the concentration, q_e and/ or SA was deduced. Results were plotted under linearized models (pseudo-first-order, pseudo-second-order, and intra-particle diffusion, Table 4.3).

4.2.2.3.3. Adsorption isotherms

Adsorption isotherms expressed the relationship between CGA adsorption capacity (q_e, mg/g) and the concentration of sample solution in the liquid phase at the equilibrium (C_e, mg/ L). For the adsorption study, a duration of 120 min was chosen. Experiments were carried out at 25°C (298.15 K). Langmuir and Freundlich models were used to regress experimental data (Table 4.4).

4.2.2.3.4. Adsorption thermodynamic parameters

The effect of the adsorption temperature was investigated by determining the adsorption isotherms at 298.15, 308.15, and 318.15 K. Enthalpy and entropy variations were obtained from the slope and intercept of the linear plot $\ln K_{eq}$ *vs* 1/T according to the linear form of Clausius-Clapeyron Eq. 4.3:

$$\ln K_{eq} = -\frac{\Delta H}{RT} + \frac{\Delta S}{R} \quad (4.3)$$

where $\ln K_{eq}$ is the natural logarithm of the constant of adsorption equilibrium (K_{eq}), ΔH is the enthalpy change (J/ mol), ΔS is entropy change (J/ mol), R is the universal gas constant (8.3144 J/ (molK) and T is the absolute temperature in Kelvin (K).

ΔG was determined using Eq. 4.4:

$$\Delta G = - RT \ln K_{eq} \quad (4.4)$$

where ΔG (J/ mol) is the Gibbs energy change.

4.2.2.3.5. Desorption

Desorption ratio were determined using different water/ethanol solvents after the adsorption step on XAD7 and XAD16 up to equilibrium. To do so, 40 mL of 30, 50, 70, and 90%, v/v was added to the resins, and shaken at 150 rpm at 25°C for 2 hours (to reach desorption equilibrium). Resins were washed with deonized water twice prior solvent addition. Resins were separated from the liquid filtration using filter paper. CGA concentration in the liquid was quantified by HPLC. Desorption ratio was calculated using Eq.4.5:

$$Desorption\ ratio\ (\%) = \frac{C_d V_d}{(C_o - C_e) V_i} 100\% \quad (4.5)$$

where C_d is the concentration of CGA in desorption solution (mg/ mL), V_d is the volume of the desorption solution (mL).

The purity of CGA after desorption step was determined using Eq.4.6:

$$\text{Purity of CGA } (\%) = \frac{Amount\ of\ CGA\ after\ desorption\ (mg)}{Total\ total\ mass\ (mg)} 100\% \quad (4.6)$$

4.2.2.4. Analytical methods

4.2.2.4.1. CGA identification and quantification

CGA concentration in the liquid by-product was quantified by HPLC (Shimadzu Corporation, Kyoto, Japan) according to (Albe Slabi et al., 2019) with some modification. The equipment used included a pump with a degasser (LC-20AD), an auto-sampler (SIL-20AC), a column oven (CTO-20A), a diode array detector (CPO-M20A) and a LCSolutions software. The analysis was carried out with a Biosep SEC-s2000 column (300 x 7.8 mm, 5 µm) purchased from Phenomenex (Torrance, CA, USA). The mobile phase consisted of formic acid: ultrapure water: acetonitrile mixture (0.1%: 55%: 45%, v/v). The injection volume was 5 µL. The flow rate was 0.6 mL/min. The detection wavelength was 325 nm. The oven temperature was kept at 35°C. All solutions and samples were filtered through 0.45 µm membranes (Fisher Scientific, Hampton, USA) before injection. CGA identification was done from standards retention time by on-line electrospray ionization mass spectrometry (ESI-MS). Data acquisition and processing were monitored with LabSolution software (Shimadzu Corporation, Kyoto, Japan). Nitrogen was used as drying gas at a flow rate of 21.5 L/ min. The nebulizer temperature was set at 300°C. CGA was searched in positive mode at m/z = 355.3$^+$. A CGA calibration curve with

concentrations ranging from 0.05 to 1.25 mg/mL was used for the quantification (linear regression equation was $y = 25057208.61x$ with $R^2 = 0.9983$).

4.2.2.4.2. NaCl content

NaCl content in the permeate was assessed by conductimetry (Meterlab PHM 210, Radiometer analytical, France). The quantification was done using an NaCl calibration curve ranging from 0.2 to 50 g/L ($y = 1.9054x$ with $R^2 = 0.9908$).

4.2.2.4.3. Total carbohydrate content

Total carbohydrate content in the permeate was measured by the method of anthrone-sulfuric acid presented by Yemm and Willis with some modifications (Yemm & Willis, 1954). Briefly, samples were mixed with 2 g/L anthrone in 98% sulfuric acid in boiling water for 10 min. After cooling, the absorbance of the solution was measured at 620 nm in a multiplate (Multiskan GO, Thermo scientific, Japan). Glucose was used as standard with concentration ranging from 0.1 to 1 mg/ mL ($y = 1.1845x$, $R^2 = 0.9981$).

4.2.2.4.4. Nonprotein nitrogen content

Kjeldahl method was used to measure the total nitrogen in the permeate (AOCS International., 1995). A nitrogen-to-protein conversion coefficient of 5.6 was applied as recommended in (Slabie Albe et al., 2019) for sunflower source.

4.2.2.4.5. Dry matter

1 mL of permeate was put in aluminium dish and left in oven during 24 h at 111°C. Afterward, aluminium dish was weighted regularly until reaching a constant weight.

4.2.2.5. Data analysis

All experiments and analytical measurements were carried out three times. Data displayed corresponded to the average value with the standard deviation. Statistical analysis was performed by Student's *t*-test with Rstudio 3.6.1 (Boston, MA, USA). A *p*-value inferior to 0.05 was considered a significant difference. All figures were designed by OriginPro 8.5 package (MA, USA). The chemical structures of phenolic compounds and CGA interaction forces with selected resins were illustrated using ChemDrawUltra 8.0 software (Cambridge Soft, MA, USA).

4.2.3. Results and Discussion

4.2.3.1. Characterization of the ultrafiltration permeate from sunflower protein purification

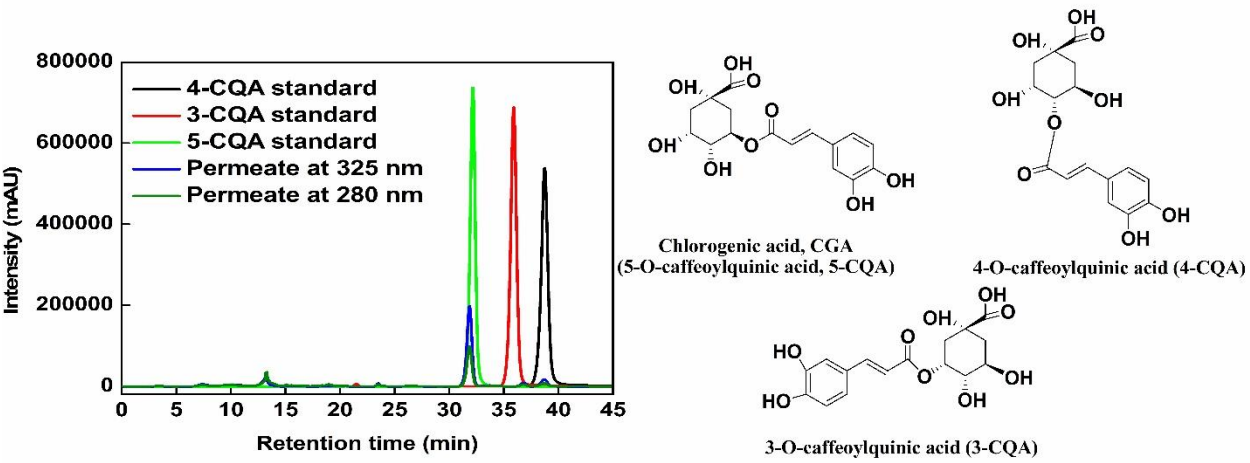

Figure 4.1. SE-HPLC chromatogram and structures of phenolic compounds detected in the UF permeate obtained from sunflower protein purification.

Chromatograms were recorded at 325 and 280 nm. The elution of CGA isomers in the same conditions was also displayed.

Figure 4.1 shows the SE-HPLC chromatogram at 325 nm and 280 nm of ultrafiltration (UF) permeate obtained from the purification of proteins extracted from sunflower meal at pH 7.5, 0.5 M NaCl. This figure shows the main peak at 32 min of retention time. Marginal signals can be observed at 13, 37 and 39 min of retention time. The first minor peak (13 min) corresponded to the column void volume and showed a higher signal at 280 nm rather than 325 nm. SDS-PAGE analysis of this peak revealed the presence of proteins in a molar weight range of sunflower albumins (SFA, 10 – 18 kDa) (Albe Slabi et al., 2019). Hence, the 3 kDa membrane used for the purification probably allowed the transmission of traces of these proteins. SFA is particularly associated with phenolic compounds by covalent bonds. This would explain the signal observed at 325 nm at this retention time. Peaks at 32, 37, and 39 min revealed the presence of molecules with *m/z* of 355 in positive mode ESI-MS. This corresponds to chlorogenic acid (CGA) *m/z*. The figure also shows that standard CGA isomers had the same retention times (5-CQA at 32 min, 3-CQA at 37 min, and 4-CQA at 39 min). This indicated that free polyphenolic fraction in the UF permeate was composed of CGA, mainly in its 5-CQA isomer. The predominance of CGA in sunflower and relative in aqueous extracts of sunflower meal (Albe Slabi et al., 2019; Weisz et al., 2009). The relative absence of caffeic acid and CGA dimers that account for 15 – 20% of total phenolic compounds in the meal according to Weisz et al. (Weisz et al., 2009) are probably less extracted in aqueous solvents due to their polarity lower than CGA. In any cases, it makes this side products of sunflower meal protein purification a particularly attractive source of CGA. Indeed, generally recognized as interesting sources of CGA like low-grade coffee bean, coffee bean methanol extracts or Crafton weed ethanol extracts are composed of many other phenolic compounds (Farah et al., 2008; B. Liu et al., 2016; Ramalakshmi et al., 2011).

Table 4.2. Composition of the liquid by-product.

Component	Compound	Proportion (%)
Liquid by-product (UF permeate)	Chlorogenic acid, CGA (5-CQA) % *dm*	1.13 ± 0.21
	NaCl % *dm*	87.67 ± 11.93
	Total carbohydrates % *dm*	3.53 ± 1.98
	Nitrogen containing molecules (N x 5.6) % *dm*	0.11 ± 0.02
	Ash % *dm*	7.56 ± 0.70

Table 4.2 presents the proximate composition of the permeate dry matter. The high content in NaCl (87 ± 11.93 %) was consistent with a large amount of NaCl either for the protein extraction step and the protein purification. Ash (7.56 ± 0.70%) were minerals extracted from the meal that also highly crossed the membrane. The permeate also contained carbohydrates (3.53 ± 1.98%). These were probably soluble fibers with molar weights low enough to cross the membrane or simple carbohydrates (both contained in the sunflower meal (Bishop, 1955). The nitrogen-containing biomolecules fraction (0.11 ± 0.02 %) is probably not homogeneous. A part of it might be the albumin traces in the permeate. Besides, about 11% of nitrogen assayed by Kjeldahl analysis in the protein extract remained soluble in 10% (v/v) trichloro acitic acid (TCA) (data not shown). These nitrogen containing molecules are classically referred to as 'non-protein' nitrogen and meant to be low molar weight peptides, free amino acids and/ or nucleic acids. These molecules probably constituted the other part of the nitrogen containing molecules observed.

This table also shows that around 25% of the UF permeate organic dry matter is composed of CQA. The rest of the organic matter is composed of polar molecules. Liu et al. (B. Liu et al., 2016) showed that polar resin exhibited higher CGA adsorption capacity than apolar or mildly polar ones. But they observed poor CGA purity after desorption step. This was due to the competitive adsorption of polar molecules on the polar resin. Or it is likely that polarity and affinity characteristic of the elution solution and the adsorbed components may influence the purity of CGA. Hence, for CGA capture from sunflower meal aqueous extract, apolar or mildly polar resin should be more appropriate.

4.2.3.2. Resins screening

Figure 4.2A shows CGA adsorption capacity from XAD4, XAD7, XAD16, XAD1180, and HP20. Those resins were known for their ability to adsorb phenolic compounds from many different plant extract (B. Liu et al., 2016; Weisz et al., 2010, 2013). XAD16, XAD4, XAD1189, and HP20 were apolar resins made of styrene divinylbenzene (SDVB). XAD7 was a slightly polar resin made of an acrylic polymer.

XAD16 and XAD4 showed the highest adsorption capacity at equilibrium (15.32 ± 0.04 mg/g and 14.07 ± 0.01 mg/g respectively). XAD7, XAD1180 and HP20 had lower values (12.03 ± 0.45, 12.62 ± 0.07 and 11.21 ± 0.02 mg/g dried resin, respectively). The very similar CGA adsorption capacity was observed with XAD7 and HP20 (11 mg/g and 15 mg/g, respectively) from craftonweed extract (B. Liu et al., 2016). Besides, XAD16 was shown to be particularly efficient for CGA adsorption from sunflower meal aqueous extracts (Weisz et al., 2010, 2013). The adsorption capacity depends on

adsorption kinetics pattern, molecule affinity toward the material and resin specific area (Z. Xu et al., 1999). It can also be modulated by the pore diameter. Indeed, if the diameter is low enough (≤ 50 Å) it can induce diffusional limitations by steric hindrance (Z. Xu et al., 1999; Q. Yang et al., 2016) or even limit the accessibility of a fraction of the resin area.

Table 4.1 shows material, pore diameters, and specific area of the resins used in the study. Non-polar resins. Among SDVB resins, XAD16 showed the highest specific area (900 m^2/g) followed by XAD4, XAD1180, and HP20. Interestingly, this ranking corresponded to the observed capacity values. XAD4 had the smallest pore diameters (50 Å). This indicated that SDVB resin mass capacities were essentially governed by the contact area. Probably no or few diffusional limitations due to the pore size occurred (Sandhu & Gu, 2013). This was also suggested by B. Liu et al. with CGA capture from *Eupatorium Adenophlorium* extracts (B. Liu et al., 2016).

In order to investigate the effect of a resin material on CGA adsorption, surface capacity had to be compared. Figure 4.2B shows that XAD7 had by far the highest surface capacity (27 µg/m^2 dry resin) whereas its specific area was rather low (450 m^2/g). For SDVB resins the value was close to 20 µg/m^2). This indicated that acrylic material had a better affinity than SDVB toward CGA.

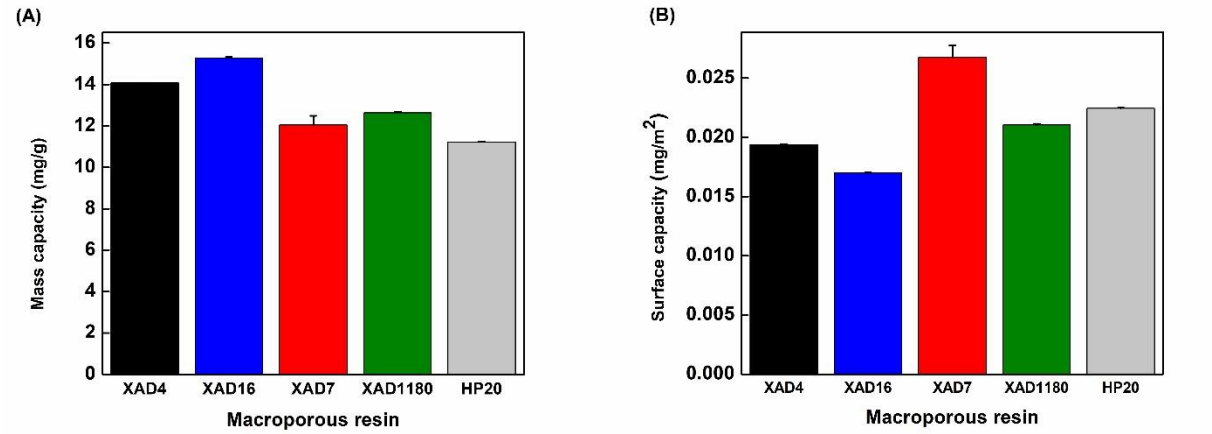

Figure 4.2. Mass (A) and surface (B) adsorption capacity of CGA on XAD4, XAD16, XAD7, XAD1180, and HP20.

L. Lin et al. reported that chemical features of XAD7 and HP20 resins were as important as physical characteristics on phenolic compounds adsorption (L. Lin et al., 2012). The adsorption mechanism remains unclear though. In this study, we propose a possible CGA interaction scheme with acrylic and SDVB resins (Figure 4.3). CGA would interact with XAD7 through hydrogen bonding implying alcohol functions of the caffeic acid part and the acrylate ester bonds of the resin backbone. Hydrophobic interactions between the caffeic part (benzene ring) and acrylate carbon backbone might also take place (Figure 4.3B). Water molecules are probably partly excluded from this backbone, otherwise, they would compete with CGA and no CGA adsorption would occur. It is more likely that the highly hydrophilic quinic acid part interacts more favorably with the bulk water molecules.

In a different way, the interaction of CGA – SDVB resins should rather be through π-π stacking interactions. The highest efficiency of acrylate material to capture CGA could be due to the highest amount of binding sites. But the very high specific area of XAD16 makes it the better resin in terms of massic capacity.

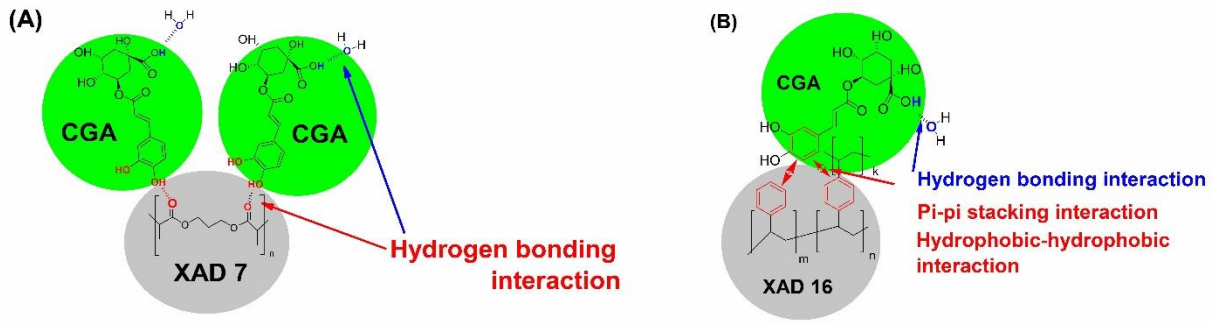

Figure 4.3. Schemes for mechanism proposed of the adsorption process of the phenolic compound onto the different resins.

(A) CGA onto XAD7 resin and (B) CGA onto XAD16 resin.

The adsorption kinetics, isotherms, thermodynamics properties, and CGA desorption were further investigated with XAD7 and XAD16 to better understand the process with these two resins.

4.2.3.3. Adsorption kinetics

Adsorption kinetics of CGA (from UF permeate) on XAD7 and XAD16 were presented in Figure 4.4A. Very similar trends were observed with the two resins. A large part of CGA was quickly adsorbed (up to 80% of the equilibrium capacity in 15 min). Then the adsorption kinetics slowed down and the equilibrium happened between 60 min and 120 min. Thus, the adsorption process should be conducted for 120 min to achieve an equilibrium state. Interestingly, Liu et al. (B. Liu et al., 2016) observed that CGA adsorption equilibrium with a highly polar resin (NKA – II) was reached at 300 min. This resin had an average pore size similar to XAD7 and XAD16 (around 120 Å). So the adsorption process on apolar or slightly polar resin would be quicker.

Adsorption kinetics were regressed with pseudo-first-order (PFO, (Lagergren, 1898)) and pseudo-second-order (PSO, (Ho & Mckay, 1998)) equations in the linearized form (Figure 4.4B – C). Table 4.3 shows the corresponding equations, parameter values of the models, and R^2 of the linear regressions. The R^2 obtained with linearized PFO ($\ln(q_e-q_t)$ *vs.* t) was less than 0.98. Furthermore, the calculated q_e for XAD7 (0.016 mg/m²) and XAD16 (0.010 mg/m²) was found very different from experimental values (0.027 mg/m² for XAD7 and 0.017 mg/m² for XAD16). On the other hand, R^2 of the linear regression of the t/q_t *vs* t plot was very close or equal to 1 (0.999 and 1 for XAD7 and XAD16, respectively). Moreover, the calculated q_e (0.0274 mg/m² for XAD7 and 0.017 mg/m² for XAD16) predicted from PSO model was very near the experimental values of q_e (0.0273 mg/m² for XAD7 and 0.017 mg/m² for XAD16). These results indicate that adsorption kinetics followed a PSO model for the

two resins. This was also observed with adsorption of CGA from *Eupatorium adenophorum* Spreng extracts on NKA-II resin (B. Liu et al., 2016) and *Helianthus tuberosus* L. leaves extracts on ADS-21 resin (P.-C. Sun et al., 2015).

Solute transport phenomena are complex in adsorption processes. In the liquid phase, solutes are transported by convection and diffusion. There is also a diffusive transport from the liquid phase to the bead surface (through a limit liquid film) and a diffusive transport inside the particle pores. Adsorption kinetics may be modulated by several diffusional types of transports. The intra-particle diffusion model (Weber & Morris, 1963) is commonly used to investigate the diffusive rate-controlling phenomenon (Annadurai & Krishnan, 1997; Firdaous et al., 2017; Tran et al., 2017).

Figure 4.4D shows q_t *vs* $t_{1/2}$ plots obtained with XAD7 and XAD16. These plots correspond to the linear form of the intra-particle diffusion model (Table 4.3). For both the two resins, a linear evolution with two slopes is observed. The slopes represent the constant rate (k_i) of each adsorption step while C_i (intercept at y-axis) is related to the thickness of the limiting layer. R^2, k_i, and C_i values obtained from linear regressions are displayed in Table 4.3. In the two cases, k_1 (0.0024 and 0.0017 $m^2/(mgmin^{0.5})$ for XAD7 and XAD16, respectively) are by far higher than k_2 (approximately 0) for the two resins. It can also be noticed that R^2 values for XAD7 and XAD16 are 0.9829 and 0.9848, respectively. This indicates that for both the two resins the adsorption process is limited by two diffusional effects. Very similar results were observed with the adsorption of alfalfa phenolic compounds and on HP20 and AER1 resins (Firdaous et al., 2017). It was interpreted as a two steps adsorption process. The first one is related to the diffusional transport throughout the boundary layer at the liquid/ beads interface. Its high rate constant ($K_{i,1}$ was 0.0024 and 0.0017 (mg/ m^2) for XAD7 and XAD16, respectively) indicates a low diffusional limitation. The second one is due to intraparticle diffusion. The low rate constant ($K_{i,2}$ approximately equal to 0 for both resins) associated indicates a strong diffusional limitation. Such observation and explanation were also made by others (Y. Chen et al., 2016; Dong et al., 2015a; Gök et al., 2008). Curiously, it can be noticed that the first step involved the adsorption of the largest part of the phenolic compounds (more than 90% of the adsorption at the equilibrium). This tends to indicate that the intraparticle diffusion limitation only took place for a small part of phenols adsorption. Since the intraparticle diffusion happens inside bead pores, representing the largest part of the resin surface it can be hypothesized that the limitation only concerns the deepest zone of the pores. The diffusion inside pores near the surface is probably only limited by the boundary layer. This would explain why the intraparticle diffusion limitation affects less than 10% of the overall adsorption. The close pore size of the two resins (around 100 Å) explains their close behavior in terms of diffusional limitations.

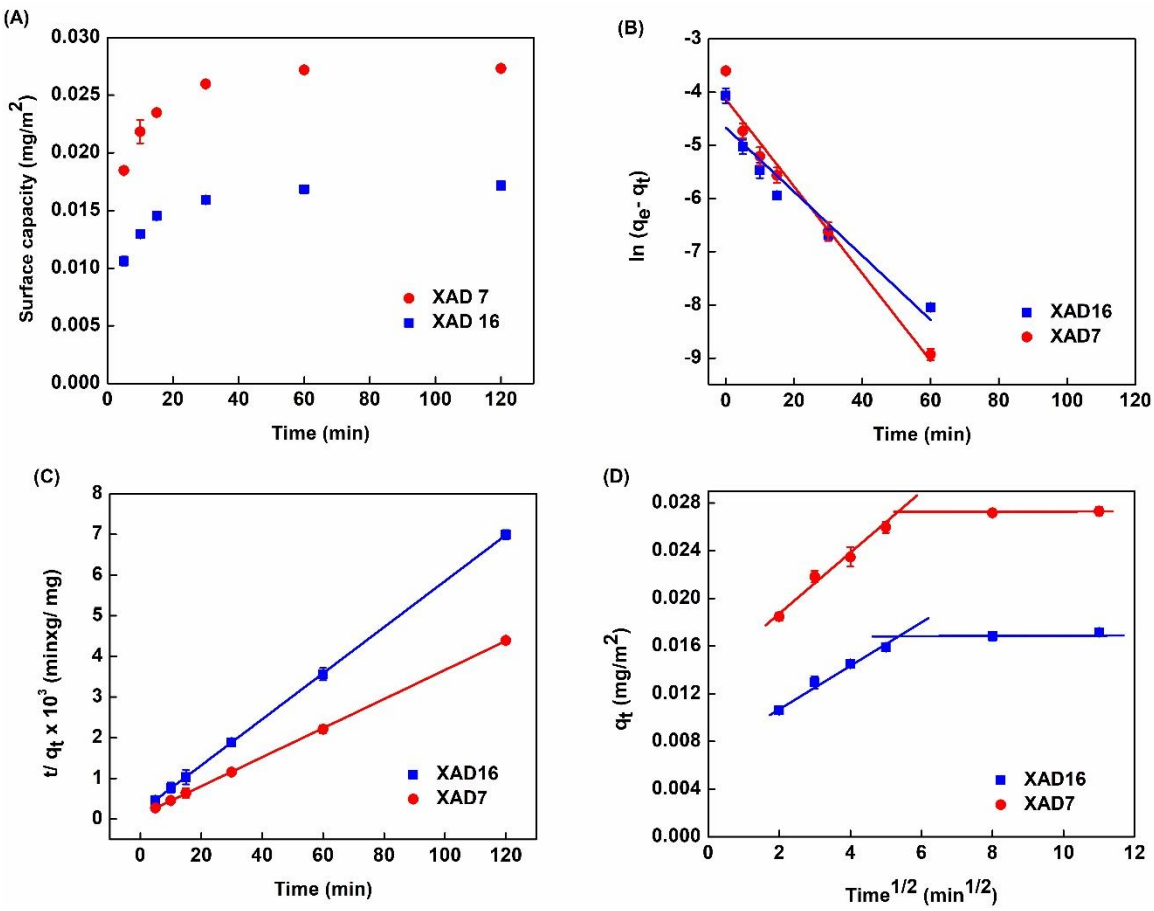

Figure 4.4. Adsorption kinetics of CGA with XAD 7 and XAD 16.

(A) surface adsorption kinetic curves, (B) pseudo-first-order model, (C) pseudo-second-order model, and (D) intra-particle diffusion model (in linearized forms).

Table 4.3. Equations and parameters for the adsorption kinetic models of CGA obtained with the XAD7 and XAD16 resins.

Kinetic model	Linear form	Plot	Parameter	Resin	
				XAD 7	XAD 16
Pseudo-first-order	$\ln(q_e - q_t) = \ln q_e - k_1 t$	$\ln(q_e - q_t)$ vs .t	$k_1(1/min)$	-0.082	-0.053
			$q_{e.exp}(mg/m^2)$	0.0273	0.017
			$q_{e.cal}(mg/m^2)$	0.016	0.01
			R^2	0.971	0.982
Pseudo-second-order	$\frac{1}{q_t} = \frac{1}{k_2 q_e^2} + \frac{t}{q_e}$	$\frac{1}{q_t}\ vs.\ t$	$k_2\ (m^2/\ (mg.min)$	0.036	0.057
			$q_{e.exp}(mg/m^2)$	0.0273	0.017
			$q_{e.cal}(mg/m^2)$	0.0274	0.017
			R^2	0.9999	1
Intra-particle diffusion	$q_t = kt^{\frac{1}{2}} + C$	$q_t\ vs. t^{\frac{1}{2}}$	$K_{i,1}(m^2.mg^{-1}.min^{-1/2})$	0.0024	0.0017
			$C_1(mg/m^2)$	0.014	0.0074
			R^2	0.9829	0.9848
			$K_{i,2}(m^2.mg^{-1}.min^{-1/2})$	0	0
			$C_2(mg/m^2)$	0.027	0.016

4.2.3.4. Adsorption isotherms

Figure 4.5 shows the adsorption isotherms of CGA on XAD7 and XAD16 at 25°C. Data were regressed with Langmuir (Figure 4.5A) and Freundlich (Figure 4.5B) equations as commonly done elsewhere (B. Liu et al., 2016; P.-C. Sun et al., 2015; Weisz et al., 2013). Table 4.4 listed the R^2 of the regression, equations, and model parameters with XAD7 and XAD16. R^2 values indicated that experimental data were better fitted by the Langmuir model (0.9899 and 0.9586 for both XAD7 and XAD16, respectively) than the Freundlich model (0.8690 and 0.9119 for XAD7 and XAD16, respectively). This indicated that the adsorption mechanism was the same for the two studied resins. It consisted in a monolayer adsorption of phenolic compounds at the surface resin (B. Liu et al., 2016; P.-C. Sun et al., 2015; Weisz et al., 2013). These findings also are in agreement with other work on CGA adsorption on XAD16 HP and NKA-II resins from other sources (B. Liu et al., 2016; Weisz et al., 2013).

Table 4.4 indicated that maximum adsorption capacity based on the resin area of XAD7 was higher than XAD16 (0.054 mg/m² *vs.* 0.040 mg/m^2). However, as expected from screening experiments, XAD16 showed higher maximum capacity when results were based on resin amount (36.59 mg/g for XAD16 *vs.* 26.21 mg/g for XAD7). Considering kinetics result with the two resins it can be deduced that XAD7 polymer (acrylate resin) had a better adsorption property than XAD16 polymer (styrene divinyl benzene). The far better specific surface area of XAD16 (900 m²/g *vs.* 450 m²/g) probably made

its highest massic adsorption capacity. In any case, it would confirm the hypothesis of a higher adsorption site density on acrylate material.

Besides, q_{max} value of CGA adsorption from a sunflower (*Helianthus annuus* L.) aqueous extract on XAD16HP was observed at 42.7 mg/g (Weisz et al., 2010). This result is close to what is observed here. The discrepancy may be due to the interference of other organic molecules. Indeed, the above-mentioned article dealt with a raw extract containing proteins. It might also be due to the impact of an ionic strength. In this study a UF permeate was used (vs. a whole extract) and the NaCl content was around 0.5 M. q_{max} observed here were lower than on the highly polar NKA-II resin (66.863 mg/g) (B. Liu et al., 2016). Authors claimed that this high adsorption capacity was due to the resin polarity, but discrepancies are harder to interpret since the starting material was different (Crofton weed extract) (B. Liu et al., 2016).

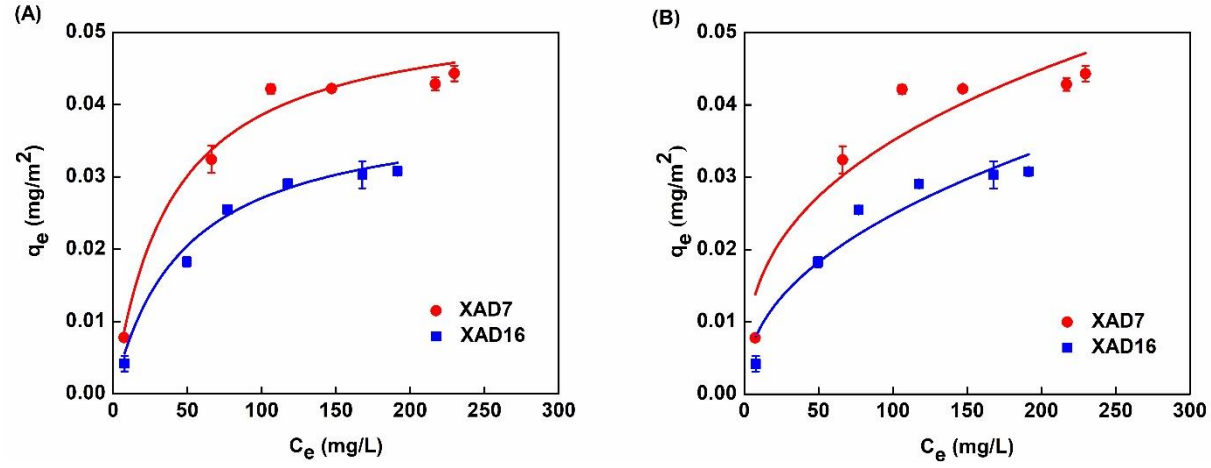

Figure 4.5. Adsorption isotherms non-linear fitting of selected XAD7 and XAD16 resin.
(A) Langmuir model and (B) Freundlich isotherm model.

Table 4.4. Adsorption isotherm models and parameters for the phenolic compound obtained with the two resins selected XAD7 and XAD16.

Isotherm model	Non-linear form	Parameter	Constraint	Resin	
				XAD 7	XAD 16
Langmuir	$q_e = \frac{Q_{max} K_L C_e}{1 + K_L C_e}$	Q_{max} (mg/m^2)		0.054	0.040
		K_L (L/mg)		0.026	0.021
		R^2		0.9899	0.9586
Freundlich	$q_e = K_F C_e^n$	$K_F(\frac{mg}{m^2})/(\frac{mg}{L})^n$		0.007	0.003
		n	$0 < n \leq 1$	0.358	0.445
		R^2		0.8690	0.9119

4.2.3.5. Determination of thermodynamic parameters

The effect of temperature on both resins adsorption capacity of CGA was also investigated in order to get the thermodynamic parameters of adsorption. Figure 4.6A-B shows adsorption isotherms at 25°C, 35°C and 45°C (linearized Langmuir model). Langmuir model parameters and R^2 were listed in Table 4.5. Obviously, the adsorption of phenolic compounds decreased with increasing temperature (Table 4.5). XAD7 Q_{max} ranged from 0.13, to 0.09 mg/m² from 25°C to 45°C while XAD16 Q_{max} value decreased from 0.19, 0.09 and 0.07 mg/m² in the same temperature range. ΔH and ΔS were determined through the slope and intercept of ln K_L against 1/T (Eq. 4.3) (Figure 4.6C) according to Van Hoff's equation. The enthalpy changes (ΔH) for the CGA adsorption process on both XAD7 and XAD16 resin were -37.35 and -22.47 kJ/mol, respectively (Table 4.5). Negative values indicate an exothermic adsorption process. The fact that values were less than 43 kJ/ mol demonstrated that the adsorption process of CGA on the resins was governed by physical rather than chemical interactions (Gökmen & Serpen, 2002; T. Liu et al., 2012; Q. Yang et al., 2016). That demonstrated that XAD7 and XAD16 resins would not undergo structural changes during the CGA adsorption process. Therefore, adsorption of CGA on the resins only takes place through physical mechanism with no chemical reactions. This observation was also reported in the work of Zhen Peng Gao et al. (Z. P. Gao et al., 2013) when they studied the adsorption of polyphenols separation from kiwifruit juice using AB-8 resin. Furthermore, it indicated that the adsorption process of CGA for both resins should be conducted at room temperature (around 25°C). In addition, the entropy changes (ΔS) values of XAD7 and XAD16 were -0.119 and -0.068 kJ/molK, respectively. These negative values suggested a random adsorption process at the solid-liquid interface (Gupta, 1998) which happened owing to the desorption process of water molecules previously adsorbed onto the resins' surface (Z. P. Gao et al., 2013). The negative free energy change (ΔG) deduced from ΔH and ΔS (Table 4.5). suggested that CGA adsorption onto XAD7 and XAD16 was a spontaneous process. Moreover, the absolute value of ΔG < 20 kJ/mol confirmed physical adsorption of CGA onto both resin (Ding et al., 2012; Z. P. Gao et al., 2013). These results are also online with the proposed adsorption scheme in Figure 4.3.

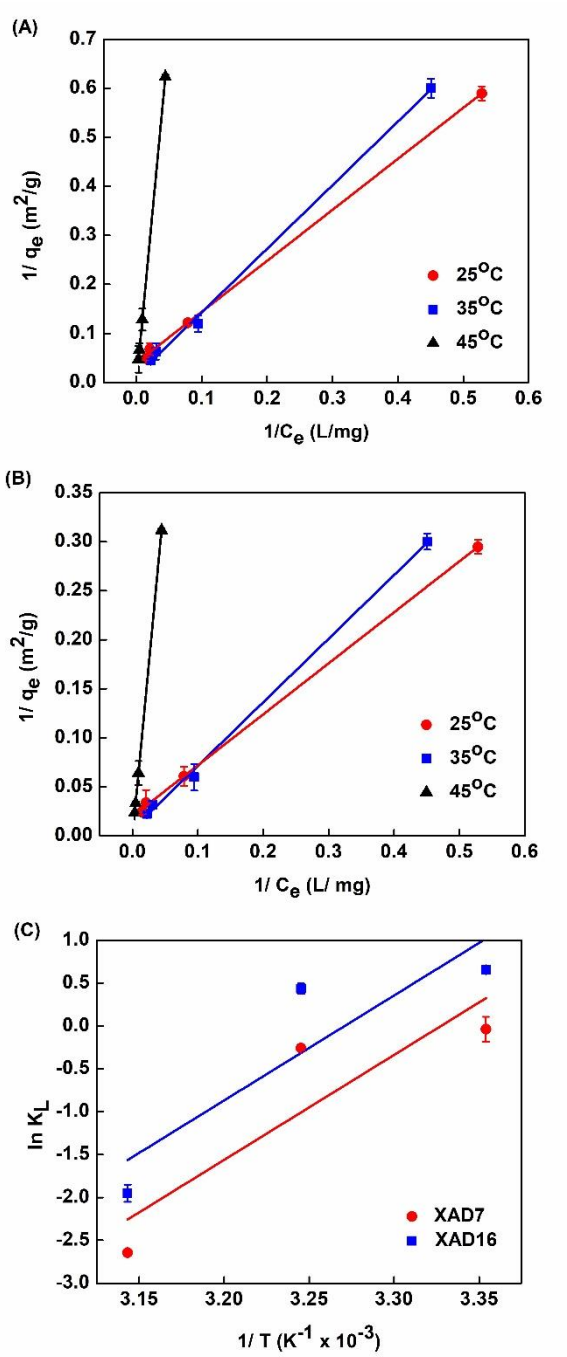

Figure 4.6. Equilibrium adsorption isotherm using the Langmuir model in linear form.

(A) XAD7 and (B) XAD16 at 25°C, 35°C and 45°C; (C) ln K_L vs. 1/T plot of adsorption equilibrium constant K_L using the Langmuir model.

Table 4.5. Isotherm and thermodynamic parameters of phenolic compound adsorption on XAD7 and XAD16 at 25°C, 35°C and 45°C.

Resin	Temperature (^{0}C/ K)	Isotherm parameter			Thermodynamic parameter		
		Langmuir model					
		K_L	Q_{max} (mg/m^2)	R^2	ΔH (kJ/mol)	ΔG (kJ/mol K)	ΔS (kJ/mol K)
XAD7	25/298.15	1.923	0.13	0.9945	-37.75	-2.235	-0.119
	35/308.15	1.543	0.12	0.9994		-1.044	
	45/318.15	0.142	0.09	0.9998		0.147	
XAD16	25/298.15	1.923	0.19	0.9994	-22.47	-1.932	-0.068
	35/308.15	1.543	0.09	0.9982		-1.243	
	45/318.15	0.142	0.07	0.9997		-0.554	

4.2.3.6. Desorption of CGA on XAD7 and XAD16

Ethanol solutions from 30, 50, 70, and 90%, v/v were used to desorb CGA from XAD7 and XAD16. Desorption kinetics showed that 120 min was necessary to reach the equilibrium (data not shown). This observation was in agreement with L. Xi et al. (Xi et al., 2015) that studied the desorption static of polyphenols from sweet potato *Ipomoea batatas* L. leaves on AB-8 resin. Figure 4.7 shows a maximum of CGA desorption ratio from 70% ethanol (v/v) in both the two cases. At this ethanol concentration (and higher), the desorption ratio was around 90%. L. Xi et al. (Xi et al., 2015) also showed that the highest desorption ratio (90.9%) was observed when ethanol concentration was 70% (v/v). Such a maximum ratio was also observed with the desorption of flavonoids from *G. glabra* L. leaf from XAD16 (at ethanol 80%, v/v) (Dong et al., 2015a). Interestingly, for ethanol concentration below 70% (v/v), the desorption ratio of CGA for XAD16 was higher than for XAD7 ($p < 0.05$). Relatively large desorption ratio discrepancies were particularly observed at 30% ethanol (48.08% for XAD7 and 56.03% for XAD16). This may indicate stronger interactions throughout hydrogen bonding (occurring with XAD7) rather than π - π interactions (occurring with XAD16). In the past, B. Liu et al. (B. Liu et al., 2016) reported that the purity of CGA from the organic extract of *Eupatorium adenophorum* Spreng was 22.17% using NKA-II macroporous resin (polar). Meanwhile, P-C. Sun et al. (P.-C. Sun et al., 2015) indicated that CGA separation from *Helianthus tuberosus* L. leaves extract by ADS-21 (polar resin) was 65.2%. On the contrary, in this study, the purity of CGA from sunflower meal when we used XAD7 and XAD16 were 77.56 ± 0.99 and 74.59 ± 0.12%, respectively. It might be the effect of the polarity of macroporous resin on the adsorption selectivity of CGA to some degree. The results in the current study indicated that selected macroporous resins were efficient for separation of CGA notably with XAD7 resin (moderate polar resin).

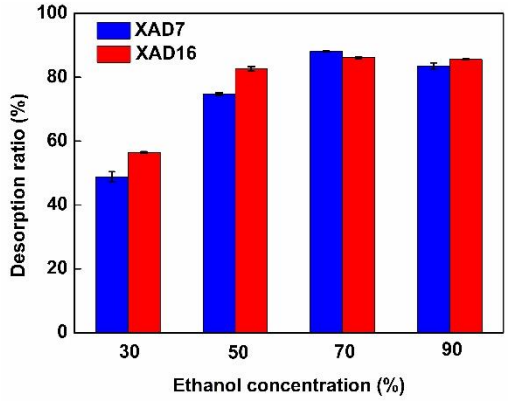

Figure 4.7. Desorption ratio of CGA onto XAD7 and XAD16 with different ethanol concentrations.

4.2.4. Conclusions

XAD7 (mildly polar) and XAD16 (apolar) showed high CGA surface and massic adsorption capacities (from an aqueous by-product of sunflower protein purification process). The adsorption kinetics of polyphenols on the two resins followed a pseudo-second-order model with a similar intraparticle diffusion pattern. The Langmuir model described more accurately the adsorption behavior of phenolic compounds on both the two resins indicating a monolayer adsorption behavior. The negative value of enthalpy, entropy, and Gibbs free energy indicated spontaneous and exothermic processes. Hence, the adsorption process was controlled by a physical mechanism and should be favorably performed at low temperatures. We concluded that the high surface adsorption capacity on XAD 7 was probably due to a high frequency of the binding sites on acrylate polymer. The high massic adsorption capacity observed with XAD16 is due to its very high specific area. In addition, the highest desorption ratio was observed at ethanol solution at 70% (v/v) but slight discrepancies were observed between the two resins. This would be due to the different interactions at stake between CGA and the two resins (hydrogen bond with XAD7 and $\pi - \pi$ stacking with XAD16).

4.3. Rapeseed polyphenols characterization and capture by adsorption

In this part, the same scientific approach has been implemented with rapeseed meal (RSM) protein isolate by-product. As we mentioned in the previous part in this thesis, rapeseed meal is the main by-product of oil industrial extraction processes. Its annual production reached 70 million tons in 2019 (FAOSTAT, 2020a). To date, RSM is used for animal nutrition (Downey & Bell, 1990). However, protein isolates from RSM are protein-based products with a high protein content could be used in human consumption (Tzeng et al., 1990). Rapeseed protein isolate production is classically based on a solid liquid extraction using aqueous solvents (modulated by pH and ionic strength), a clarification step and a protein purification step. The purification is most often achieved either by tangential filtration or isoelectric precipitation (Defaix et al., 2019). Polar phenolic compounds are extracted with proteins during the extraction step and parted from proteins during the protein purification step. At the end of the purification process, phenolic compounds are in an aqueous by-product alongside with soluble low molar weight minerals and non-protein nitrogen containing molecules. The valorization of this by-

product is of a crucial importance for industrial viability of rapeseed protein isolate production. The capture of phenolic compounds could be an interesting valorization strategy.

Therefore, in this study, identification and capture of phenolic compounds from a rapeseed protein isolate by-product obtained by ultrafiltration was also investigated. Phenolic compounds in the aqueous by-product were identified by LC-MS. Five macroporous resins, including XAD4, XAD7, XAD16, XAD1180, and HP20, having various properties were screened for phenolic compounds capture from RSM protein isolate by-product. adsorption kinetics and isotherms of phenolic compounds from RSM protein isolate by-product were studied in order to elucidate phenolic compounds adsorption mechanisms using resin. Desorption by ethanol/water mixtures was investigated and obtained purity considered to choose the most appropriate eluent for phenolic compounds capture from this effluent. The obtained results represented in this part of thesis are a part of our publication which entitled "*Identification and capture of phenolic compounds from a rapeseed meal protein isolate production process by-product by macroporous resin and valorization their antioxidant properties*" on the journal *Molecules*.

4.3.1. Identification of phenolic compounds in the ultrafiltration (UF) permeate

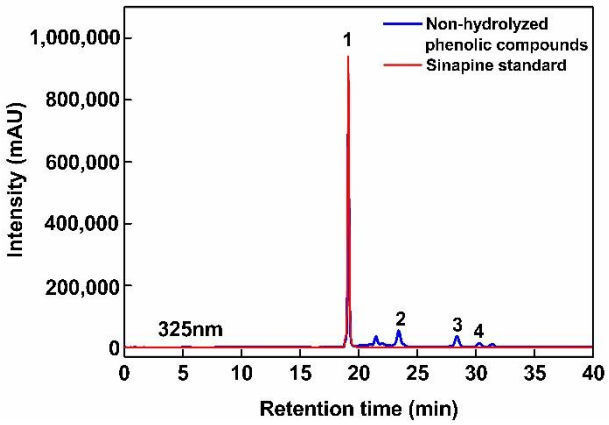

Figure S4.1. SE-HPLC chromatogram and structures of phenolic compounds detected in the UF permeate obtained from rapeseed protein purification**.**

Chromatograms were recorded at 325 nm.

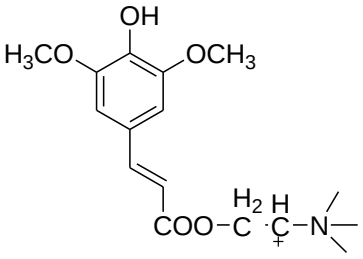

(1) sinapine

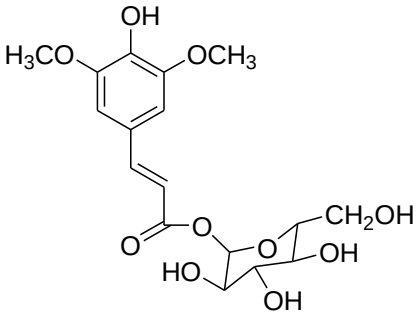

(2) sinapoyl glucose

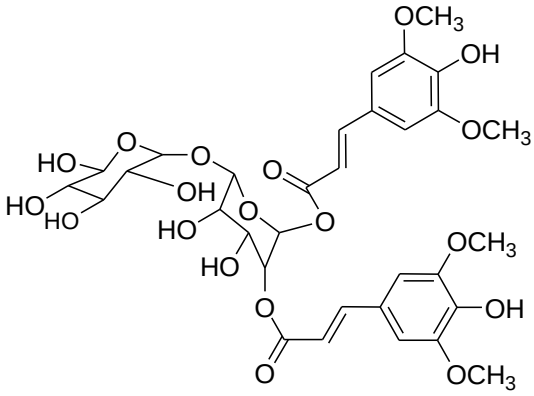

(3) 1,2-di-sinapoyl gentiobise

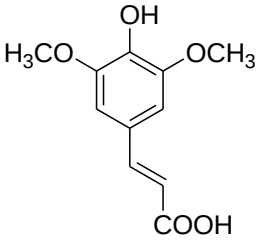

(4) sinapic acid

Figure S4.2. Chemical structures of phenolic compounds (1) Sinapine, (2) sinapoyl glucose, (3) 1,2-disinapoyl gentiobiose, and (4) sinapic acid.

Different numbers indicated the position of phenolic compounds presented in the HPLC chromatogram.

Table S4.1. Retention time (t_R) and MS data of the peaks detected by HPLC-DAD and HPLC-MS in permeate and hydrolyzed permeate from rapeseed meal.

Peak	Compound identity	t_R (min)	m/z	Molecular weight
1	Sinapine	18.94	310 $[M-H]^+$	310
2	Sinapoyl glucose	23.31	385 [M-H]-	386
3	1,2-di-sinapoyl gentiobise	28.33	753 [M-H]-	754
4	Sinapic acid	31.68	223 [M-H]-	224

Figure S4.1 shows the SE-HPLC chromatogram at 325 nm of the ultrafiltration (UF) permeate. Figure S4.2 shows the chemical structures of phenolic compounds represented in permeate.This permeate was obtained from a rapeseed albumin isolate production process recently patented (Albe Slabi et al., 2019; Defaix et al., 2019). A main peak can be observed at 18.94 min of retention time alongside with marginal signals at 23.31, 28.33 and 31.68 min. ESI-MS analysis revealed that this peak contained molecules with m/z of 310 (positive mode), 385, 753, and 223 (negative mode) (Table S4.1). This corresponded to sinapine (SP), sinapoyl glucose (SG), 1,2-di-sinapoyl gentiobise, and sinapic acid (SA), respectively. The identification of sinapine and sinapic acid was confirmed by injection of standards. R. Khattab et al. (Khattab, 2010) also identified SP, SA, and SG from canola / rapeseed organic solvents extracts such as 70% ethanol, 70% methanol, or 70% iso-propanol (v/v). In the UF

permeate, SP, other identified SA esters and SA represented 59.78%, 21.66% and 2.84% in proportion, respectively. Only 15.72% of the phenolic compounds remained unidentified. These observations also agreed with the report from U. Thiyam-Holländer et al. (Thiyam-Holländer et al., 2012). In their study, the de-oil rapeseed were extracted by distilled water with ratio 1:10 (w/v) for 10 min. The unidentified compounds were most probably other polar sinapic acid esters.

4.3.2. Phenolic compounds capture

4.3.2.1. Resin screening

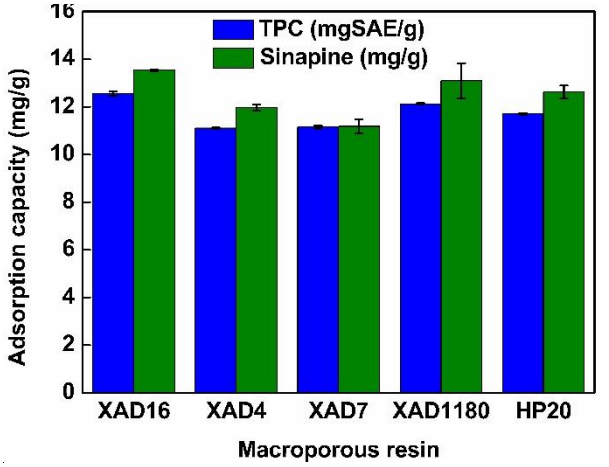

Figure S4.3. Adsorption capacity of phenolic compounds after adsorption of UF permeate using XAD4, XAD16, XAD7, XAD1180, and HP20 resins.
Results are given in terms of total phenolic compounds (TPC) and the main phenolic compound of the starting product (sinapine).

Figure S4.3 shows the adsorption capacity of total phenolic content (TPC) and sinapine, from permeate on XAD4, XAD7, XAD16, XAD1180, and HP20 resins. Table 4.1 displays resins properties. XAD4, XAD16, XAD1180, and HP20 are nonpolar resins made out of SDVB polymers. They differ by bead and pore size (50-300 Å). XAD7 is composed of acrylamide polymer which is considered as mild polar (Tuong Thi Le et al., 2020). All these resins were demonstrated to adsorb phenolic compounds from many different plant extracts (Firdaous et al., 2017; B. Liu et al., 2016). The adsorption of TPC from non-hydrolyzed permeate ranged from about 11 (for XAD4 and XAD7) to 12.5 mgSAE/g (for XAD16) of dry resins. Interestingly, the adsorption of sinapine (main phenolic compound) was similar to TPC, ranging from 11 (for XAD7) to 13.5 mg/g (for XAD16) of dry resin.

The adsorption capacity depends on molecule affinity toward the material and the specific surface (Q. Yang et al., 2016). This last parameter is conditioned by bead size and can be modulated by pore size if it limits the molecule inner accessibility (Tuong Thi Le et al., 2020). Pore ≤ 50 Å were shown to limit the diffusion of phenolic compounds into particle's pores by steric hindrance (Dong et al., 2015a; Q. Yang et al., 2016). Among styrene-divinyl benzene (SDVB) resins, XAD16 showed the highest specific area (900 m^2/g) followed by XAD4, XAD1180, and HP20. Interestingly, this ranking

corresponded to observed capacity values. This indicates that SDVB resin capacities were essentially governed by specific area. It can be hypothesized that XAD4 low pore size (50 Å) did no yield additional diffusion limitation. Probably, the interaction of sinapine (Figure S4.1) (a main phenolic compound) and SDVB resins were through pi-pi stacking interaction (aromatic ring part of phenolic compounds and benzene rings of SDVB resins) (Tuong Thi Le et al., 2020). XAD16 and XAD1180 showed the highest adsorption capacity of TPC. However, XAD16 had the highest adsorption capacity of TPC and sinapine. The very high specific area of XAD16 (900 m^2/g) showed better adsorption in terms of massic capacity than XAD7 or HP20 with a similar specific area (450 or 500 m^2/g). So, the adsorption kinetics, isotherms, thermodynamics properties, and phenolic compounds desorption were further investigated with this resin.

4.3.2.2. Adsorption kinetics

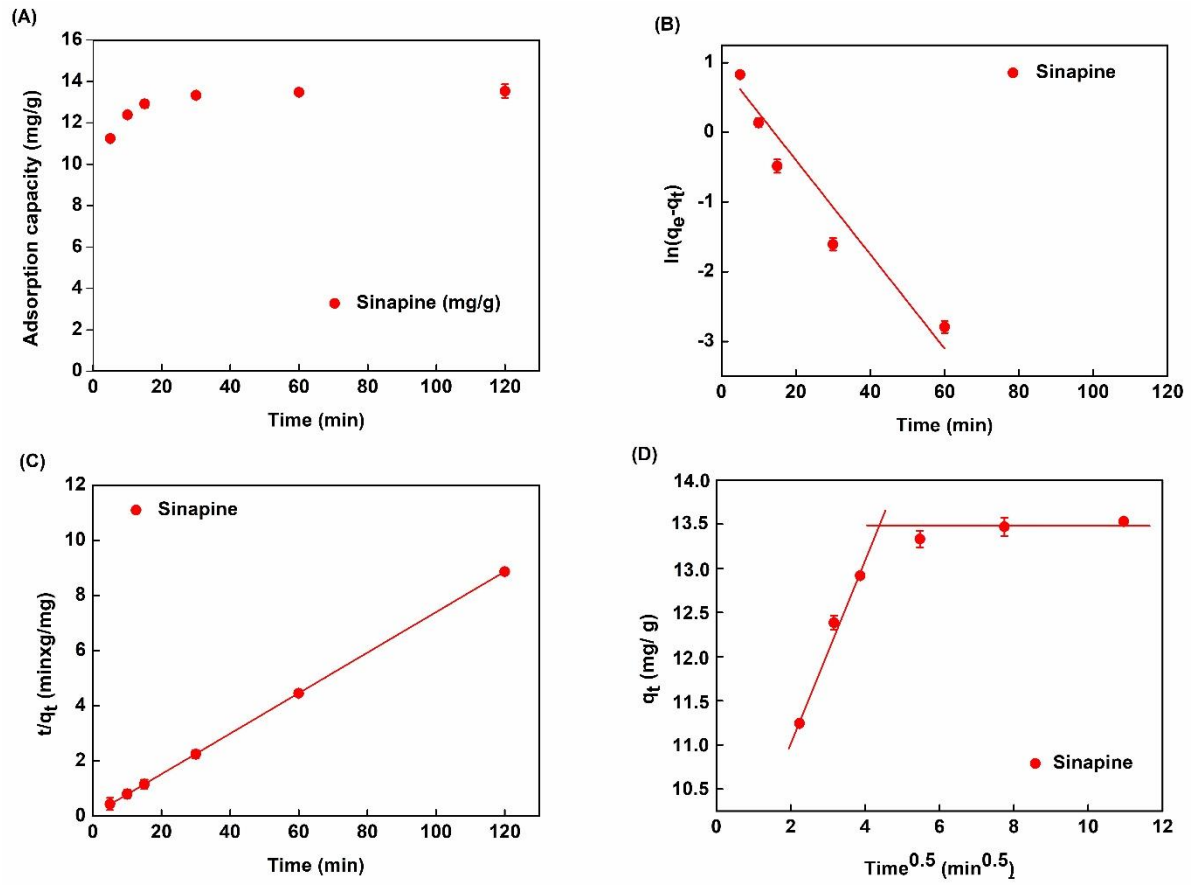

Figure S4.4. Adsorption kinetics with XAD16. (A) adsorption kinetic curve**.**
(B) pseudo-first-order model. (C) pseudo-second-order model. (D) intra-particle diffusion model (in linearized forms) of sinapine.

Adsorption kinetics of the main phenolic compounds from UF permeate with sinapine on XAD16 are presented in Figure S4.4A. Very similar trends were observed. A large part of phenolic compounds was quickly adsorbed (up to 90% of the equilibrium capacity in 30 min). Then, the kinetics slowed down up to the equilibrium observed between 60 min and 120 min. As expected from resin

screening results, this indicated that XAD16 has a strong affinity toward rapeseed phenolic compounds. Such a behavior was also reported for adlay bran phenolic compounds (Q. Yang et al., 2016).

Table S4.2. Kinetic parameters for sinapine adsorption onto XAD16 resin.

Kinetic model	Equation	Parameter	Sinapine
Pseudo-first-order (PFO)	$\ln(q_e - q_t) = \ln(q_e) - k_1 t$	k_1 (1/min)	0.0627
		$q_{e,exp}$ (mg/g)	13.532
		$q_{e,cal}$ (mg/g)	3.83
		R^2	0.9381
Pseudo-second-order (PSO)	$\frac{1}{q_t} = \frac{1}{k_2 q_e^2} + \frac{t}{q_e}$	k_2 (g/mg x min)	0.0733
		$q_{e,exp}$ (mg/g)	13.532
		$q_{e,cal}$ (mg/g)	13.544
		R^2	1
Intra-particle diffusion	$q_t = kt^{0.5} + C$	$k_{i,1}$ (mg/g)/min$^{0.5}$	1.0321
		C_1 (mg/g)	8.9921
		R^2	0.9828
		$k_{i,2}$ (mg/g)/min$^{0.5}$	0
		C_2 (mg/g)	13.532

Adsorption kinetics were regressed with pseudo-first-order (PFO, (Lagergren, 1898)) and pseudo-second-order (PSO, (Ho & Mckay, 1998)) equations in linearized form (Figure S4. B-C-D). Table S4.2 summarizes the corresponding equations, model parameter values and R^2 of the linear regressions.

The R^2 obtained with linearized PFO ($\ln(q_e\text{-}q_t)$ vs. t) was less than 0.94 for sinapine. Furthermore, the calculated q_e for XAD16 3.83 mg/g for sinapine was found very different from experimental values 13.53 mg/g for sinapine. On the other hand, R^2 obtained with PSO was equal to 1. Moreover, the calculated q_e 13.54 for sinapine predicted from PSO model was very near the experimental values of qe 13.53 mg/g. These results indicate that adsorption kinetics followed a PSO model for the XAD16 resin. This was also observed with adsorption of chlorogenic acid from by-product proteins isolates on XAD16 resin (Tuong Thi Le et al., 2020).

Solute transport phenomena are complex in adsorption processes. In the liquid phase, solutes are transported by convection and diffusion. There is also a diffusive transport from the liquid phase to the bead surface (through a limit liquid film) and a diffusive transport inside the particle's pores. Adsorption kinetics may be modulated by several diffusional types of transports. The intra-particle diffusion model (Weber & Morris, 1963) is commonly used to investigate the diffusive rate-controlling phenomenon (Firdaous et al., 2017; Gök et al., 2008).

Figure S4.4D show q_t vs $t^{0.5}$ plots obtained with the XAD16 resin. These plots correspond to the linear form of the intra-particle diffusion model (Table S4.1). The slopes represent the constant rate (k_i) of each adsorption step while C_i (intercept at y-axis) is related to the thickness of the limiting layer. R^2, k_i, and C_i values obtained from linear regressions are displayed in Table S4.1. Interestingly, k_1 1.03 (mg/g)/min$^{0.5}$ for sinapine is by far higher than k_2 (approximately 0). It can also be noticed that R^2 values for sinapine is 0.9828. This indicates that for both liquid effluents, the adsorption process is limited by two diffusional effects. In the previous study, the similar pattern was also observed with the adsorption

of chlorogenic acid onto XAD16 resin (Tuong Thi Le et al., 2020). Very similar results were observed with the adsorption of alfalfa phenolic compounds on HP20 and AER1 resins (Firdaous et al., 2017). It was interpreted as a two steps adsorption process. The first one is related to the diffusional transport throughout the boundary layer at the liquid/beads interface. Its high rate constant $k_{i,1}$ was 1.03 (mg/g)/min$^{0.5}$ for sinapine indicates a low diffusional limitation at this stage. The second one is due to intraparticle diffusion. The low rate constant $k_{i,2}$ approximately equal to 0 indicates a stronger diffusional limitation. Such observation and explanation were also made by others (Y. Chen et al., 2016; Dong et al., 2015a; Gök et al., 2008).

4.3.3. Adsorption isotherms

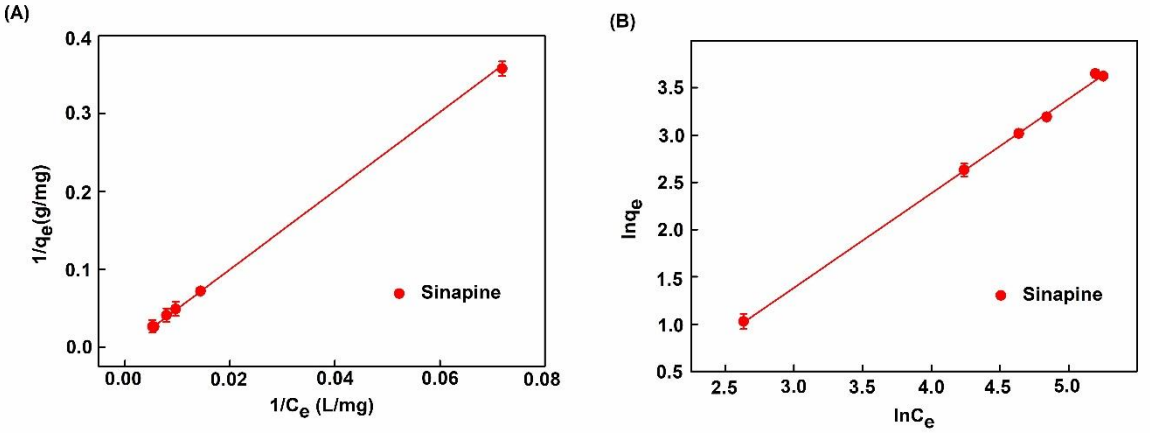

Figure S4.5. Adsorption isotherms of phenolic compounds on XAD16 with (A) Langmuir and (B) Freundlich linear models for sinapine.

Table S4.3. Adsorption isotherm equation and parameters of sinapine adsorption onto XAD16 resin.

Isotherm model	Parameter	Sinapine
Langmuir	Q_{max} (mgSAE/g)	35.93
$q_e = \frac{Q_{max} K_L C_e}{1 + K_L C_e}$	K_L (L/ mg)	124.29
	R^2	0.997
Freundlich	K_F (mg/g)/ (mg/L)^n	0.1988
$q_e = K_F C_e^n$	n	0.9987
	R^2	0.996

Figure S4.5 shows adsorption isotherms of sinapine and sinapic acid onto XAD16 at 25°C. Data were regressed with Langmuir (Figure S4.5A) and Freundlich (Figure S4.5B) equations as commonly done elsewhere (Chang et al., 2014; Y. Chen et al., 2016; P.-C. Sun et al., 2015). Table S4.3 lists the R^2 of the regression, equations, and model parameters with sinapine and sinapic acid. In this case, we observed the R^2 values were equivalent between Freundlich (0.996) and Langmuir (0.997) models. In the literature, the best fit with Langmuir model was found (Moreno-González et al. 2020). This indicated that the same adsorption mechanism took place in any cases. This consisted in a monolayer adsorption of phenolic compounds at the surface of the resin (Chang et al., 2014; Y. Chen et al., 2016; P.-C. Sun et al., 2015). These findings also are in agreement with another work on chlorogenic acid adsorption on XAD16 resin from sunflower meal (Tuong Thi Le et al., 2020; Weisz et al., 2013).

Moreover, this finding is consistent with that of M. Moreno-González et al. (Moreno-González et al., 2020) about the adsorption of sinapic acid from canola/rapeseed meal using the FPX66 resin. The maximum adsorption capacity of sinapine was 35.93 mg/g (0.12 mol/g) of dry resin (Table S4.3). This observation has never been published. Meanwhile, according to M. Moreno-González et al. (Moreno-González et al., 2020), the maximum adsorption capacity for sinapic acid was lower (about 15 mg/g or 0.07 mol/g) onto the non-polar (SDVB) FPX66 resin. The different values might be due to other organic compounds such as carbohydrates, amino acids, and proteins in raw materials. It might also be due to the impact of ionic strength. Moreover, the difference in physical characteristics also caused the difference in adsorption capacity. A. Thiel et al. (Thiel et al., 2015) investigated the adsorption of sinapic acid and other compounds onto zeolites and hydrophobic resins, including XAD16, the resin used in this study. These authors claimed that the adsorption capacity of sinapic acid was higher than the one presented here (44.5 mg/g or 0.20 mol/g of dry resin). However, these authors evaluated the experiments at different pH (pH 5) and used different starting materials; rapeseed meal extracted with heated deionized water at 70°C at a ratio of 1 : 8 (solid : liquid) that might explain the difference in these values.

4.3.4. Determinations of thermodynamic parameters

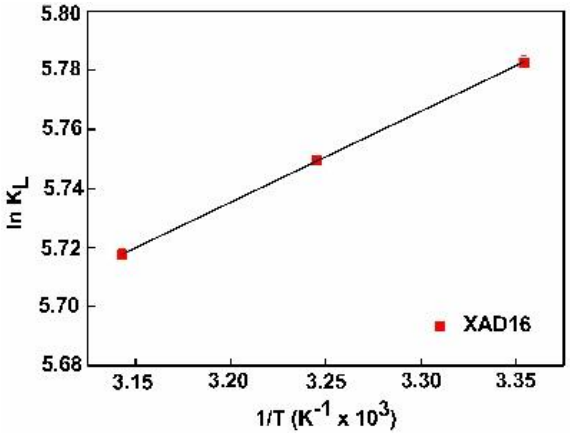

Figure S4.6. ln K_L vs. 1/T plot of adsorption equilibrium constant K_L using Langmuir isotherm of sinapine.

Table S4.4. Thermodynamic parameters of sinapine adsorption onto XAD16 at 25°C, 35°C and 45°C.

Phenolic compound	Temperature (°C/K)	ΔS (kJ/molK)	ΔH (kJ/mol)	ΔG (kJ/mol)
Sinapine	25/ 298.15			-13.34
	35/ 308.15	-55.95	-2.56	-17.28
	45/ 318.15			-15.56

The effect of temperature on the adsorption capacity of phenolic compounds from the XAD16 resin in the two liquid effluents were investigated to obtain the thermodynamic parameters of adsorption. Langmuir model parameters and R^2 are listed in Table S4.4. ΔH and ΔS were determined through the slope and intercept of ln K_L against 1/T (Figure S4.6) according to Van Hoff's equation. Enthalpy changes (ΔH) for sinapine and sinapic acid adsorption process on XAD16 resin were -2.56, and -2.72

kJ/mol, respectively (Table S4.4). Negative values indicate an exothermic adsorption process. The fact that values were less than 43 kJ/mol demonstrates that the adsorption process of phenolic compounds on the XAD16 resin was governed by physical rather than chemical interactions (Tuong Thi Le et al., 2020). This demonstrates that the XAD16 resin would not undergo structural changes during phenolic compounds' adsorption process. Therefore, adsorption of phenolic compounds on the resin only takes place through physical mechanism with no chemical reactions. This observation was also reported by Z. P. Gao et al. (Z. P. Gao et al., 2013) who studied the adsorption of polyphenols from kiwifruit juice using AB-8 resin (Z. P. Gao et al., 2013). In addition, the entropy changes (ΔS) values of XAD16 were -55.95 for sinapine. This negative value suggests a random adsorption process at the solid-liquid interface (Gupta, 1998) which happened owing to the desorption process of water molecules previously adsorbed onto the resins' surface (Z. P. Gao et al., 2013). The negative free energy change (ΔG) deduced from ΔH and ΔS (Table S4) suggests that phenolic compounds adsorption onto the XAD16 resin was a spontaneous process. Moreover, the absolute value of ΔG < 20 kJ/mol confirmed physical adsorption of phenolic compounds onto XAD16 resin (Z. P. Gao et al., 2013; Tuong Thi Le et al., 2020).

4.3.5. Desorption of sinapine from the XAD16 resin

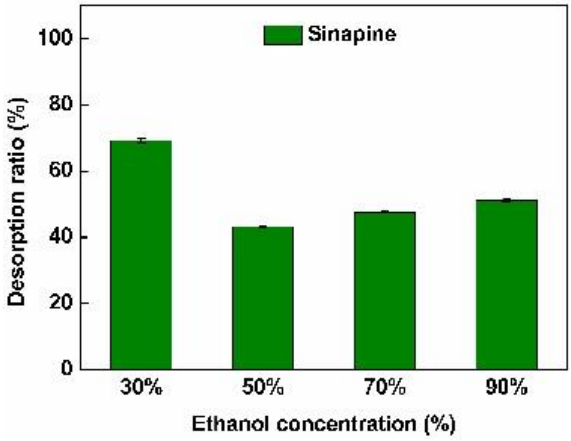

Figure S4.7. Desorption ratio of sinapine from the XAD16 resin at different ethanol concentrations.

To assess the effect of ethanol concentration on desorption, five ethanol concentrations were evaluated: 30, 50, 70 and 90% (v/v). Preliminary results showed that the desorption curve reaches equilibrium after 120 min (data not shown). As shown in Figure S4.7, ethanol concentration significantly influenced on sinapine desorption ratio. The highest of desorption ratio of sinapine was observed with ethanol 30% (v/v) ($p < 0.05$). These results indicate that desorption ratio was influenced by ethanol concentration and the solubility of phenolic compounds in the desorption phase. Indeed, sinapine is a polar compound demonstrating a good desorption ratio with ethanol at a lower concentration. Surprisingly, the desorption ratios of sinapic acid and sinapine in this study were much higher than in the report of A. Thiel et al. (Thiel et al., 2013, 2015) (about 3.7% for sinapine) who used the same macroporous resin (XAD16) and desorption with 70% aqueous ethanol.

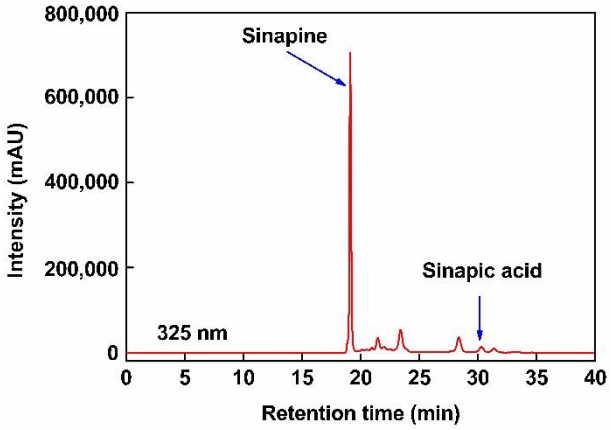

Figure S4.8. HPLC chromatogram of phenolic compounds in desorption fraction.

Figure S4.8 shows the HPLC chromatogram of phenolic compounds after purification with the XAD16 resin. The peaks of sinapine (Figure S4.8) and sinapic acid are highlighted in the desorption fraction. Sinapine (63.31%) is the mains phenolic compound in the fraction after purification. As different compositions of phenolic compounds after purification might lead to different biological actions, we used both fractions to assess the antioxidant and activities in subsequent experiments.

4.3.6. Conclusions of phenolic capture in rapeseed permeate

In conclusion, this study provides insights into determination of phenolic compounds in an aqueous protein extraction/purification by-product (permeate) from rapeseed meal (RSM). We found that sinapine was the main phenolic compound in this permeate. The other compounds were sinapoyl glucose, 1,2-di-sinapoyl gentiobise and sinapic acid. The XAD16 resin showed the highest adsorption capacity. Adsorption behaviors of total phenolic compounds and sinapine were also investigated. Our results revealed that the adsorption of phenolic compounds followed the pseudo-second-order model and presented a very similar pattern of intra-particle diffusion. The Langmuir model was suitable to describe the adsorption process of phenolic compound. Besides, the adsorption process was an exothermic, randomness, and physical adsorption process.

4.4. Conclusion for chapter 4

The main objective of this chapter was to identify the phenolic compounds in SFM and RSM proteins isolate byproducts and understand the mechanisms of phenolic compounds adsorbed onto different macroporous resins such as XAD4, XAD7, XAD16, XAD1180, and HP20. The main phenolic compounds SFM and RSM proteins isolate by-products were CGA and SP, respectively. The macroporous resins with different properties (physical and chemical properties) exhibited different adsorption capacities and desorption capacities.

XAD7 and XAD16 exhibited high CGA surface and massic adsorption capacities from SFM protein isolate by-product. Obviously, the high surface adsorption capacity on XAD7 was probably due to a high frequency of the binding sites on acrylate polymer. Besides, the high massic adsorption capacity observed with XAD16 is owing to its high specific area. On the other hand, the high massic SP and TPC adsorption capacities from RSM protein isolate by-product was observed with XAD16

resin. This would be due to the different interactions at stake between CGA and SP on the two resins. CGA and XAD7 resin interaction is based on hydrogen bonding between hydroxyl group of caffeic acid part and the acrylate ester bonds of the resin backbone. This interaction might be dominant in case of CGA and XAD7. However, the interaction of SP from RSM and XAD16 is based on hydrophobic – hydrophobic interaction. It is more likely that the pi-pi stacking in aromatic ring of SP interacts more favorably with the pi-pi stacking in benzene rings of XAD16 resin backbone.

In addition, the adsorption kinetics of phenolic compounds from SFM and RSM onto XAD7 and XAD16 followed a pseudo-second-order model with a similar intra-particle diffusion. The adsorption isotherms were described by Langmuir model indicating a monolayer adsorption behavior. The adsorption process was controlled by a physical mechanism and it was exothermic processes due to the negative values of thermodynamic parameters. The best eluent for desorption process with ethanol solution at 70% (v/v) was observed in any cases. In summary, these results provided informative content for designing purification system to produce enough phenolic fractions for bioactivity studies such as antioxidant and anti-inflammation.

Chapter 5. Multicriteria optimization of phenolic compounds by adsorption column and assessment of their bioactivities

5.1. Introduction to chapter 5

We previously reported in chapter 4 that CGA and SP were shown to be the main phenolic compounds of SFM and RSM proteins isolate by-product. Batch adsorption study revealed that CGA was most favorably captured by XAD7 resin from aqueous by-product of protein extraction/purification. Besides, XAD16 showed the highest captured capacity of TPC and SP. Therefore, in this chapter, XAD7 and XAD16 were used to pack into column for purification process of CGA and TPC/SP.

There is limited information on CGA/ TPC capture by adsorption column (dynamic adsorption) that are used in industrial applications. Dynamic adsorption is particularly complex since it implies many operating conditions (flow rate, adsorption pH, desorption flow rate, composition of the desorption eluent) and antagonist performance criteria (purity, recovery, and productivity). This makes it difficult to identify the optimal conditions for the CGA/TPC capture. Moreover, the desorption is generally carried out using ethanol – water solvent with different ethanol proportion. Most of these previous studies in the literature were carried out using one factor at a time or design of experiments optimization methods, but were aimed at maximizing a single criterion (most often the dynamic binding capacity). Thus, to our knowledge, no study integrates the productivity as a performance criteria, which is crucial for industrial applications. Considering that productivity is antagonist of the binding capacity, the so-called optimized conditions reported in literature are most probably far from the best trade-off.

The purposes of this chapter was to study and optimize the capture process and investigate their potential of valorization in biomedical (anti-infammation) and food safety (anti-oxidant). The scientific approach followed was divided into three major steps as shown in Figure 3.4.

Firstly, the effect of adsorption flow rate and pH on dynamic binding capacity, productivity and recovery was investigated by design of experiments (DoE). Then, a multiobjective optimization method of this step was proposed based on the DoE models. This step allowed to determine the optimal conditions for column adsorption.

Secondly, concerning the desorption step, the effect of the ethanol concentration on both CGA/TPC purity and recovery was considered. This step allowed to determine the best eluent for desorption step.

Finally, the antioxidant activity of the fraction obtained in the set of optimal conditions was compared to CGA/SP standard and vitamin C. The anti-inflammatory activity was evaluated using a classical model (Chanput et al., 2014); the release of the TNF-α pro-inflammatory cytokine.by lipopolysaccharide (LPS) treated THP-1 macrophages. These last studies allowed to demonstrate a protective effect of this fraction against a future inflammation. This property could be valorized in the veterinary and human well-being fields and its antioxidant properties in the food industry.

The work of this part of the thesis has been valorized in the form of the article "*Multicriteria optimization of phenolic compounds capture from a sunflower protein isolate production process*

byproduct by adsorption column and assessment of their antioxidant and anti-inflammatory effects" published in the journal *Foods* in 2021. The last section of this chapter is dedicated to RSM resource.

5.2. Sunflower phenolic compound adsorption on columns and assessement of their bioactivities

Multicriteria optimization of phenolic compounds capture from a sunflower protein isolate production process byproduct by adsorption column and assessment of their antioxidant and anti-inflammatory effects.

Tuong Thi Le[1,2], Armelle Ropars[2], Arnaud Aymes[1], Jean-Pol Frippiat[2*], and Romain Kapel[1*]

[1] Laboratoire Réactions et Génie des Procédés, Université de Lorraine, Unité Mixte de Recharche CNRS/Ministère (UMR) 7274, LRGP, F-54500 Vandœuvre-lès-Nancy, France

[2] Stress, Immunity, Pathogens Laboratory, SIMPA, Université de Lorraine, F-54000 Nancy, France

* co-supervised this study

Abstract

The aim of this study was to valorize liquid effluent from sunflower protein isolate process by extracting phenolic compounds it contains. To do so XAD7 resin was used. A multicriteria optimization methodology based on Design of Experiments showed the optimal conditions were adsorption flow rate of 15 BV/ h at pH 2.7, a desorption flow rate af 120 BV/h with ethanol / water 50% (v/v). The best trade off between purity and recovery yields resulted in the production of a fraction containing 76% of chlorogenic acid (CGA) whose biological properties were evaluated. DPPH and ABTS tests showed that this fraction had a higher radical scavenging capacity than vitamin C. *In vitro* assays have shown that this fraction, when used at a concentration corresponding to 50 or 100 µM of CGA, does not present any cytotoxicity on human THP-1 cells differentiated into macrophages. In addition, this fraction when added prior to the inflammatory stimulus (LPS), can reduce tumor necrosis factor-alpha (TNF-α) production by 22% thereby highlighting its protective properties against a future inflammation.

Keywords: chlorogenic acid, response surface methodology, THP-1 macrophage, inflammation, antioxidant.

5.2.1. Introduction

Chlorogenic acid (CGA) is a mild polar phenolic compound composed of a quinic acid and a caffeic acid part linked by an ester bond (Kremr et al., 2016; H. J. Park et al., 2010). This compound has antioxidant properties throughout free radical scavenging (Mandrone et al., 2015; Santana-Gálvez et al., 2017; Xi et al., 2015) and metal chelation activities (M.-H. Huang et al., 2010; Kurata et al., 2007, 2011). Besides, CGA has anti-inflammatory effects (Francisco et al., 2013; S. J. Hwang et al., 2014; Shan et al., 2009; Shin et al., 2015, p. 201; Z. Zhao et al., 2008). According to Drugbank (Wishart et al., 2018), CGA can be used in the pharmaceutical field and a recent report suggests that it could be useful for the preservation of food products (Santana-Gálvez et al., 2017). However, the way to use it in the biomedical (human and/or veterinary) field deserves more attention.

CGA can be found in various resources like coffee bean, tea, apple and sweet potato leaves (Meng et al., 2013; L. Sun et al., 2013; Xi et al., 2015). However, these resources are either valorized as commodity or poorly available for CGA production. Sunflower meal (SFM) is also particularly rich in CGA (1.42-4.00% on a dry basis (Pedrosa et al., 2000; Weisz et al., 2009, 2013). SFM is the oil extraction by-product and is largely available (yearly production about 56 million tons worldwide (*FAOSTAT*, 2020a). To date, SFM is mainly used for animal nutrition because of its high content in proteins (Weisz et al., 2010, 2013). Recently, SFM revealed to be a very interesting source for protein isolate production (Albe Slabi et al., 2019; Weisz et al., 2010, 2013). Interestingly, CGA was shown largely predominant in the aqueous by-product yielded by sunflower meal protein isolate production. Such by-products are obtained after saline extraction and a protein purification process either carried out by ultrafiltration or acid precipitation (Albe Slabi et al., 2019; Weisz et al., 2010). Hence, the capture of CGA from these effluents could offer a very promising valorization way.

Many studies report that the use of mild polar macroporous resins, such as AB-8, NKA-II, and ADS-21 resins, is appropriate for CGA capture from plant extracts with maximum adsorption capacity ranging from 9.83 to 26.8 mg/g (B. Liu et al., 2016; P.-C. Sun et al., 2015; Xi et al., 2015). Obviously, the adsorption capacity of CGA is favorable under acidic conditions (pH 2 – 3) because the carboxylic acid function is protonated which limits CGA polarity and increases the adsorption on mild polar resins (P.-C. Sun et al., 2015; Xi et al., 2015). Batch adsorption studies allowed to finely understand transport and adsorption phenomena of CGA on resins (B. Liu et al., 2016; P.-C. Sun et al., 2015). In brief, CGA transport shows rather low diffusional limitations and the adsorption is mainly governed by physic interactions. Thus, resins should be implemented at temperature around 20°C (Tuong Thi Le et al., 2020; Weisz et al., 2013).

However, there are limited information on CGA capture by adsorption column (dynamic adsorption) that are used in industrial applications. Dynamic adsorption is particularly complex since it implies many operating conditions (flow rate, adsorption pH, desorption flow rate, composition of the desorption eluent, etc.) and antagonist performance criteria (purity, recovery and productivity). This makes difficult to identify the optimal conditions for the CGA capture. The few dynamic adsorption studies of CGA on macroporous resins showed that the most favorable adsorption pH and flow rate for maximizing dynamic binding capacities or CGA adsorption ratio ranged from 1 – 3. Bed volume / hour and pH 2 – 3 respectively with dynamic binding capacity or CGA capture rate around 25 mg/g or 80% (Weisz et al., 2010; Xi et al., 2015). The desorption is generally carried out using ethanol – water solvent with ethanol proportion comprising between 40 and 70% (v/v). Polyphenol purity in the fraction varied in a 15 – 65% range depending on the material and the ethanol / water ratio (B. Liu et al., 2016; P.-C. Sun et al., 2015). The recovery was around 80% (B. Liu et al., 2016; P.-C. Sun et al., 2015). Most of these studies were carried out using one factor at a time or design of experiments optimization methods, but were aimed at maximizing a single criterion (most often the dynamic binding capacity). Furthermore, to our knowledge, no study integrates the productivity as a performance criteria, which is crucial for

industrial applications. Considering that productivity is antagonist of the binding capacity, the so-called optimized conditions reported in literature are most probably far from the best trade-off.

We previously reported an optimized process for SFM protein isolate production based on protein saline extraction and purification by tangential filtration (Albe Slabi et al., 2019). In the aqueous by-product, which is the ultrafiltration permeate yielded by the diafiltration step, CGA was shown to be the main phenolic compound (Tuong Thi Le et al., 2020). Batch adsorption study revealed that CGA was most favorably captured by XAD7 resin from this by-product. In this study, the effect of adsorption flow rate and pH on dynamic binding capacity, productivity and recovery was investigated by DoE. Then, a multiobjective optimization method of this step was proposed based on the DoE models. Concerning the desorption step, the effect of the ethanol concentration on both CGA purity and recovery was considered. The antioxidant activity of the fraction obtained in the set of optimal conditions was compared to CGA standard and vitamin C. The anti-inflammatory activity was evaluated using a classical model (Chanput et al., 2014); the release of the TNF-α pro-inflammatory cytokine.by lipopolysaccharide (LPS) treated THP-1 macrophages. These last studies allowed to demonstrate a protective effect of this fraction against a future inflammation. This property could be valorized in the veterinary and human well-being fields and its antioxidant properties in the food industry.

5.2.2. Materials and methods

5.2.2.1. Chemical reagents

Chlorogenic acid standard (purity ≥ 95%), 1,1-diphenyl-2-picrylhydrazyl (DPPH), 2,2'-azino-bis-(3-ethylbenzothiazoline-6-sulfonic acid) (ABTS), potassium persulfate, ascorbic acid (vitamin C), and macroporous resin XAD7 were purchased from Sigma-Aldrich (St. Louis, Missouri, United States). High-performance liquid chromatography (HPLC) grade solvents, including acetonitrile, formic acid, and methanol, were purchased from Fisher chemical (USA). Absolute ethanol was from the DASIT group (France). Sodium chloride was purchased from UWR chemicals prolabo (Belgium).

5.2.2.2. Aqueous by-product from sunflower protein isolate production

The aqueous effluent used in this study resulted from a sunflower protein isolate process (Albe Slabi et al., 2020). Briefly, this process was carried out in two steps: firstly, a protein extraction from sunflower cake and secondly, a protein purification by tangential filtration (diafiltration mode). For protein extraction, the appropriate amount of meal and NaCl 0.5 M were mixed at a solid/liquid ratio of 1/9. Then, the pH was adjusted at 7.5 by adding NaOH 1M. The slurry was agitated (400 rpm) at room temperature during 30 min. The liquid phase was separated from the meal by centrifugation (Thermo Scientific Sorvall LYNX 6000 centrifuge) at 15000*g* and 20°C for 30 min. The aqueous phase was filtered through cellulose filters (Fisherbrand, USA). Proteins from the clarified aqueous phase were purified by diafiltration using an Akta Flux 6 ultrafiltration apparatus (GE Healthcare Life Science, USA) equipped with a 3 kDa PolyEther Sulfone (PES) membrane with a 4800 cm² surface area (UFP-3-C-6A, GE Healthcare, USA). The transmembrane pressure was set at 1.5 bar and the feed rate at 1.5 L/min. The aqueous effluent used in the study was the permeate fraction obtained after flushing the

retentate compartment with 6 diavolumes (DV) of NaCl 0.5M. The generated permeate was acidified to pH 2 by adding HCl 1M and stored at -20°C before use.

5.2.2.3. Column adsorption

For the adsorption, appropriate volumes of effluent adjusted to pH 2, 3.5, or 5 were injected into columns (16 x 50 mm) packed with XAD7 resin equilibrated with deionized water. The elution was done at 15 BV/h (bed volume/hour), 10 BV/h or 5 BV/h using an AKTA Pure system (GE Healthcare, Sweden). The eluate was fractionated into 10 mL fractions. CGA concentration in each fraction was quantified by HPLC. The elution was monitored by UV detection at 325 nm. The column charge step was stopped when the absorbance at 325 nm corresponded to a CGA concentration corresponding to 10% of its concentration in the feed. Then, the column was washed by 25 BV of deionized water at 120 BV/h and eluted by 99.6% (v/v) ethanol at 120 BV/h. CGA concentration was also quantified by HPLC in the desorption fraction in order to calculate, for each condition, the three performance criteria associated to the desorption phase (CGA dynamic binding capacity at 10%, i.e. DBC10, process productivity and CGA recovery).

The dynamic binding capacity at 10% (in mg of CGA/g of resin) was calculated as follows:

$$DBC10 = \frac{m_{CGA\ ads.}}{m_{resin}} \quad (5.1)$$

where $m_{CGA\ ads.}$ is the amount of CGA adsorbed onto the resin, and m_{resin} is the dried resin weight.

The process productivity (in mg of CGA/g of resin/min) was determined as follows:

$$\text{Productivity} = \frac{m_{CGA\ des.}}{m_{resin*t}} \quad (5.2)$$

where $m_{CGA\ des.}$ is the amount of CGA in the desorption fraction (in mg), m_{resin} is the dried resin weight (in g), and t is the total duration of the adsorption + washing + desorption process.

The recovery (expressed in %) was calculated as follows:

$$\text{Recovery (\%)} = \frac{m_{CGA\ out.}}{m_{CGA\ in.}} 100\% \quad (5.3)$$

where $m_{CGA\ in.}$ is the mass of CGA introduced at the column inlet determined by HPLC and $m_{CGA\ out.}$ is the amount of CGA in the desorption fraction.

To define the best desorption conditions, the optimal adsorption conditions were applied (15 BV/h at pH 2.7). Then, the column was washed by 25 BV of deionized water and eluted with 30, 50, 70, and 90% of ethanol in water (v/v) at a flow rate of 120 BV/h as recommended by the manufacturer. The elution was collected every 10 mL and stopped when the UV signal at 325 nm reached the baseline. CGA concentration was determined in each of the 10 mL fractions by HPLC. The ÄKTA Pure system (GE Healthcare, Sweden) performed all dynamic adsorption and desorption steps thanks to the UNICORN software. Fractions containing CGA were pooled and freeze-dried after vacuum

concentration for further analysis (CGA and dry matter amounts) and use (antioxidant or anti-inflammatory assays).

CGA purity in the desorption fraction was calculated as follows:

$$\text{Purity (\%)} = \frac{m_{CGA\ des.}}{\sum m_{total\ mass}} 100\% \qquad (5.4)$$

where $m_{CGA\ des.}$ is the amount of CGA in the desorption fraction and $m_{total\ mass}$ is the amount of the dried product.

5.2.2.4. HPLC analysis

CGA quantification was carried by size exclusion HPLC as recommended by Sara et al. [22]. The system (Shimadzu Corporation, Kyoto, Japan) was composed of a pump, a degasser (LC-20AD), an auto-sampler (SIL-20AC), a column oven (CTO-20A), and a diode array detector (CPO-M20A). The column used was a Biosep 5 µm SEC-s2000 (300 x 7.8 mm; Phenomenex, USA). The mobile phase was composed of formic acid / ultrapure water / acetonitrile (0.1% / 55% / 45%, v/v). The temperature was set at 35°C and the flow rate was 0.6 mL/min. The injection volume was 5 µL. The detection wavelength was 325 nm. Peak identity was confirmed from retention time data with a standard sample to measure CGA concentration and MS analysis. The calibration curve of standard CGA was constructed in a concentration range 0.05-1.25 mg/mL ($y = 2.51x10^7$, $R^2 = 0.9983$).

5.2.2.5. Design of Experiments

Design of experiments was used to investigate the influence of adsorption flow rate and pH. The adsorption flow rate (X1) was studied in the range of 5 to 15 BV/h. pH was studied in the range of 2 to 5. Considered criteria were DBC10 (in mg/g), productivity (in mg/g/min), and recovery (in %). The face-centered central composite design was generated and analyzed using the MODDE® 7 software form Sartorius Stedim Biotech (Göttingen, Germany). The experimental matrix was composed of 11 combinations of adsorption flow rates (ranging from 5 to 15 BV/h) and pH values (ranging from 2 to 5) including three replications at the central point. The coded setting conditions are presented in Table 5.A1.

Table 5.A1. Coded factors and experimental design levels for responses surface.

Factor	Unit	Coded symbol	Coded variable levels		
			-1	0	1
Adsorption flow rate	BV/ h	X_1	5	10	15
pH		X_2	2	3.5	5

The mathematical relationship between factors and responses was described by the following second-degree polynomial equation (Eq. (5.5)):

$$Y = \beta_0 + \beta_1 X_1 + \beta_2 X_2 + \beta_{11} X_1^2 + \beta_{22} X_2^2 + \beta_{12} X_1 X_2 \qquad (5.5)$$

where Y is the response, β_o is the constant, β_1 and β_2 are the coefficients of linear effects, β_{11} and β_{22} are the coefficients of quadratic effects, β_{12} is the coefficient of interaction effect, X_1 and X_2 are the independent factors.

The obtained models were statistically verified by evaluating coefficient of determination (R^2), residual standard deviation (RSD), and analyze of variance (ANOVA) (regression p-value and lack of fit). The significance was considered as statistically significant when p-value was < 0.05.

5.2.2.6. Multi-objective optimization

Multi-optimization was employed to identify the best conditions for productivity and CGA recovery in terms of adsorption flow rate and pH. The objective function corresponded to the simultaneous maximization of productivity and recovery. The multi-objective problem was solved using the model equations and setting two criteria within the following constraints: maximal productivity and 80% recovery. The multilevel algorithm was built and analyzed using the MATLAB® software from MathWorks (Natick, MA, USA). Generally, the optimization process was divided into several steps. First, an initial population representing a group of individuals (n = 2000) was generated. Each individual corresponded to random of dynamic adsorption conditions (adsorption flow rate from 5 to 15 BV/h and pH from 2 to 5) varying by the algorithm. Process performance (dynamic binding capacity, productivity, and recovery) of each individual was calculated on the basis of the model equations. Then, the initial population was evaluated regarding their performances towards fixed criteria. The dominant individuals participated subsequently in the production of a new generation and created solutions were one more time evaluated. Process was repeated until the set of non-dominant solutions was not established.

5.2.3. Antioxidant activity

5.2.3.1. DPPH radical scavenging activity

DPPH free radical scavenging activity was studied according to Wu et al. (J. Zhu & Wu, 2009) with some modifications. One hundred µL of the samples at 40µg/mL were mixed with 100 µL of DPPH 0.2 mM solution, prepared in MeOH, into the wells of a microplate. Theses mixtures were shaken for 30 s and left 30 min in the dark at 25°C. Then, the absorbance was recorded at 517 nm. The inhibition percentage (%) of radical scavenging capacity was expressed as follows:

$$DPPH\ radical\ scavenging\ (\%) = \frac{(A_{DPPH} - A_{blank}) - (A_{sample+DPPH} - A_{sample+blank})}{A_{DPPH} - A_{Blank}} 100\ (\%) \qquad (5.6)$$

where A_{DPPH} is the absorbance of the DPPH solution, A_{blank} is the absorbance of pure methanol, $A_{sample+DPPH}$ is the absorbance of DPPH with the sample, and $A_{sample+blank}$ is the absorbance of pure methanol with the sample.

5.2.3.2. $ABTS^+$ radical scavenging activity

$ABTS^+$ radical scavenging activity was determined using the method described by Re et al. (Re et al., 1999) with some modifications. ABTS+ was prepared by mixing 7 mM ABTS radical cation stock solution with 2.45 mM potassium persulfate in a 1:1 (v/v) ratio. This solution was kept in the dark at room temperature for 16 h and thereafter its absorbance at 734 nm was adjusted to 0.70 ± 0.02 by diluting it with a 90% (v/v) methanol/water. Samples were tested at the following concentrations: 200,

100, 50, 25, and 12.5 µg/mL. 20µL of each sample concentration were mixed with 180 µL of ABTS and incubated 5 min in the dark. Then, the absorbance at 734 nm was read. The following equation was used to calculate the percentage of decrease of the absorbance at 734 nm:

$$ABTS\ inhibited\ rate\ (\%) = \frac{A_{ABTS} - A_{sample+ABTS}}{A_{ABTS}} 100\ (\%) \quad (5.7)$$

where A_{ABTS} is the absorbance of ABTS alone and $A_{sample+ABTS}$ is the absorbance of ABTS+ in the presence of the sample.

The IC50 value (i.e. the antioxidant concentration showing 50% of maximum antioxidant capacity) was calculated by linear regression of the plot of scavenging activity versus sample concentration. Data are expressed as mean ± standard deviation (S.D), and all experiments were run in triplicate.

5.2.4. Cell culture and treatments

The THP-1 human monocytic leukemia cell line was a gift of Dr. E. Emilie (INSERM, Paris, France). THP-1 cells were cultured at 37°C under 5% CO_2 in RPMI 1640 medium supplemented with 10% heat inactivated fetal calf serum, 100 U/mL penicillin, 100 µg/mL streptomycin, 10 mM HEPES, 2 mM L-glutamine, 1 mM sodium pyruvate, and 1x non-essential amino-acids. THP-1 cells, at a density of $0.8x10^6$ cells/mL, were differentiated into macrophages with 20 nM of phorbol myristate acetate (PMA) in 24-wells plates. After 3 days, differentiated THP-1 cells were incubated for 24h with 100 ng/mL of LPS added one hour before or after chlorogenic acid standard (CGA) or CGA fraction. Two concentrations of CGA (50 and 100 µM) and two working concentrations of CGA fraction, corresponding to a content of 50 or 100 µM of CGA, were used. All chemicals were purchased from Sigma-Aldrich (St. Louis, Missouri, USA.

5.2.5. Cell viability

After 24 h of incubation with LPS and CGA, or LPS and CGA fractions, differentiated THP-1 cell viability was determined using the crystal violet assay. Briefly, cells were washed with phosphate buffer saline (PBS) and incubated with 0.1% crystal violet for 20 min at ambient temperature. Then, cells were carefully washed with PBS and lysed with 10% acetic acid for 20 min. Well contents were homogenized and analyzed by spectrophotometry at 595 nm with a multilabel counter (Wallac-1420, Perkin Elmer).

5.2.6. TNF-α quantification

At the end of the 24h of incubation with LPS and CGA, or LPS and CGA fraction, cell culture supernatants were harvested in sterile conditions, centrifuged to remove dead cells, and stored at -80°C until analysis. TNF-α concentrations were determined using the Human TNF-alpha Quantikine ELISA Kit (R&D Systems, BioTechne Brands, Rennes, France). Assays were performed according to the instructions of the manufacturer, in duplicate, and repeated three to five times. Plates were read at 450 nm with a multilabel counter (Wallac-1420, Perkin Elmer, USA).

5.2.7. Data analysis

For the response surface methodology, using the analysis of variance (ANOVA) given by MODDE 7.0, the statistical parameters, including the determination of coefficients (R^2), regression p-value, and lack of fit could be achieved. The mathematical models had criteria R^2 values close to 1. For antioxidant activity, the statistical analysis was performed using Rstudio (version 3.6.1) and *t*-tests. Statistically significant differences were indicated by p value < 0.05. For anti-inflammation studies, six independent experiments were performed in triplicates. *t*-tests were used to identify statistically significant differences ($p \leq 0.05$).

5.3. Results and discussion

5.3.1. Dynamic adsorption step

5.3.1.1. Effect of pH and flow rate on dynamic binding capacity, recovery and process productivity

In a previous study, the XAD7 macroporous resin was reported to be promising for phenolic compounds capture from an aqueous by-product yielded by a sunflower protein isolate process (Tuong Thi Le et al., 2020). In the present study, the dynamic adsorption of the phenolic fraction on XAD7 column from the same by-product was studied using the DoE methodology. The adsorption flow rate and the pH of liquid effluent on the resin dynamic binding capacity (DBC10), process productivity and recovery were considered. The adsorption flow rate was chosen because it is known to strongly impact dynamic adsorption (B. Liu et al., 2016; Weisz et al., 2010). The effect of the pH was considered because it was reported to impact the adsorption of main sunflower phenolic compounds (i.e. chlorogenic acid, CGA) on macroporous resins (L. Sun et al., 2013; P.-C. Sun et al., 2015; Weisz et al., 2010; Xi et al., 2015; B. Zhang et al., 2008). Criteria like DBC and recovery are often included in column adsorption studies but process productivity is more rarely took into consideration whereas it is crucial for industrial applications. The chosen pH ranges from 2 to5 because above pH 5, CGA is known to be converted into its oxidized form (Albe Slabi et al., 2020). The flow rate varied from 5 to 15 BV/h as recommended by the supplier. The results related to polyphenol amounts were expressed in CGA mass because this phenolic compound constitutes 1.13 ± 0.21% of the liquid by-product used in this study (Tuong Thi Le et al., 2020).

The obtained mathematical models are shown in equations (8)-(10). Regression parameters (unscaled and scaled), and statistical verification of model performances using the ANOVA test are presented in Table 5.1.

Table 5.1. Regression coefficients of the predicted polynomial models for productivity and recovery.

Regression coefficient		**Response**		
		Y_1 (Dynamic binding capacity, mg/g)	Y_2 (Productivity, mg/g/min)	Y_3 (Recovery, %)
Unscaled	β_o[a]	109.19	0.10	-139.43
	β_1[b]	-4.31	0.018	-0.68
	β_2[c]	-29.89	-0.05	147.49
	β_{11}[d]	0.085	-0.0003	0.07
	β_{22}[e]	2.39	0.0075	-21.53
	β_{12}[f]	0.44	-0.0023	-0.67
Scaled and centered	β_o	14.71	0.083	89.56
	β_1	-5.35	0.018	-8.38
	β_2	-13.11	-0.032	-14.85
	β_{11}	2.12	-0.0080	1.67
	β_{22}	5.38	0.017	-48.44
	β_{12}	3.30	-0.018	-5.003
Statistic model parameter				
R^2		0.996	0.996	0.93
RSD[g]		1.005	0.003	11.09
Regression *p*-value		0.00	0.00	0.007
Lack of fit		0.28	0.22	0.877

[a] constant[b] coefficient of the linear effect of adsorption flow rate
[c] coefficient of the linear effect of pH
[d] coefficient of the quadratic effect of adsorption flow rate
[e] coefficient of the quadratic effect of pH
[f] interaction coefficient of adsorption flow rate and pH
[g] residual standard deviation

The mathematical models were characterized by high indexes of regression coefficient between predicted and observed values (R^2 = 0.996 for dynamic binding capacity at 10% (DBC10), R^2 = 0.996 for productivity, and R^2 = 0.93 for recovery) (Figure 5.1).

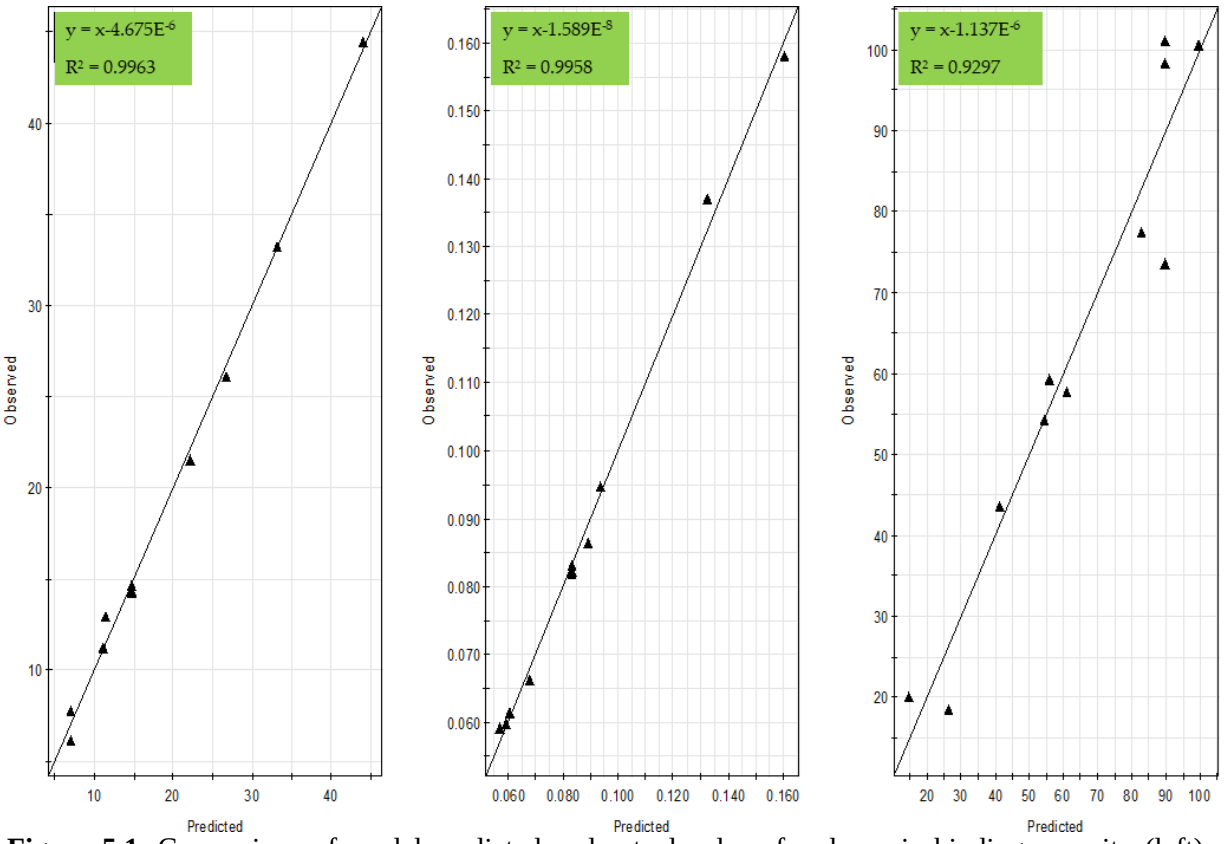

Figure 5.1. Comparison of model-predicted and actual values for dynamic binding capacity (left), productivity (middle), and recovery (right) responses.

These models were also observed with low regression *p*-values (0.00 for dynamic binding capacity, 0.00 for productivity, and 0.007 for recovery) and insignificant lack of fit (0.28 for dynamic binding capacity, 0.22 for productivity, and 0.877 for recovery). The calculated and experimental plots are presented in Figure 5.1. These data suggested a high fitted and reliability of models for the prediction of the assessed process.

$$Y_{1(dynamic\ binding\ capacity\ at\ 10\%,DBC10)} = 109.19 - 4.31X_1 - 29.89X_2 + 0.085X_1^2 + 2.39X_2^2 - 0.44X_1X_2 \quad (5.8)$$

$$Y_{1(productivity)} = 0.10 + 0.018X_1 - 0.05X_2 - 0.0003X_1^2 + 0.0075X_2^2 - 0.0023X_1X_2 \quad (5.9)$$

$$Y_{2(recovery)} = -139.43 - 0.68X_1 + 147.49X_2 + 0.067X_1^2 - 21.53X_2^2 - 0.67X_1X_2 \quad (5.10)$$

where: X_1 is the adsorption flow rate (BV/ h), and X_2 is the pH of the permeate solution.

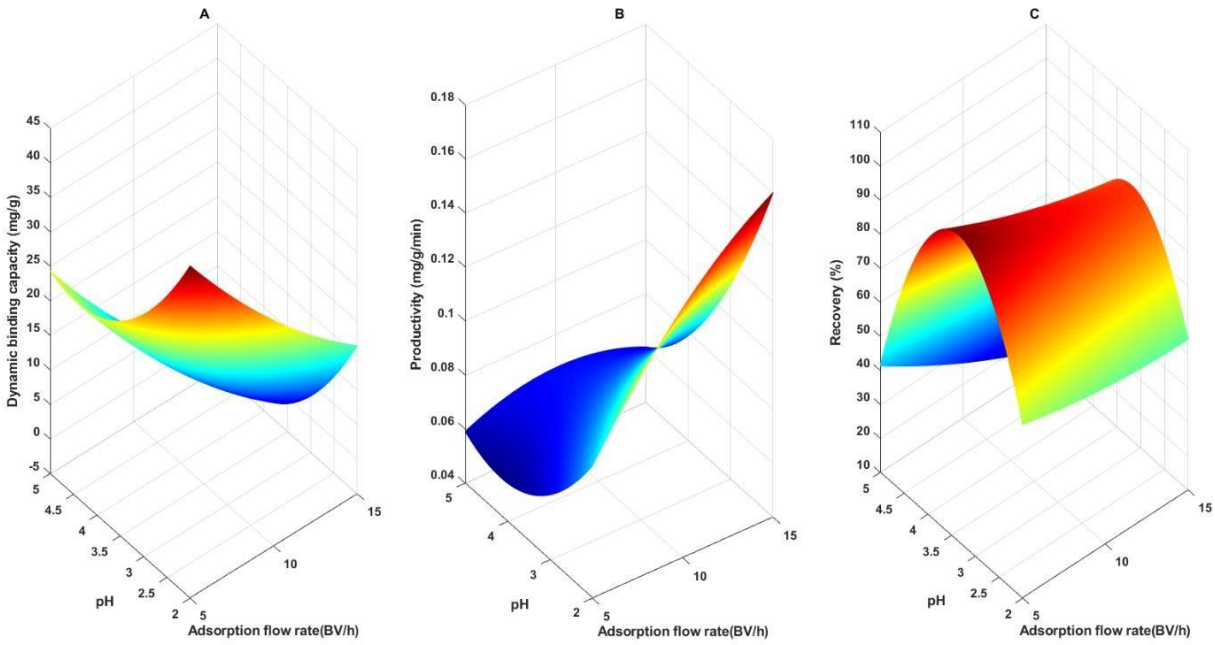

Figure 5.2. 3-dimensional plots presenting the effects of adsorption flow rate and pH on CGA yield. pH versus adsorption flow rate on adsorption binding capacity (A), productivity (B), and recovery (C).

Figure 5.2A shows the effect of pH and flow rate on DBC10. At pH 2, DBC10 increases from 26.1 to 44.47 mg/g when flow rate decreases from 15 to 5 BV/h. This trend is observed whatever the pH value. This behavior is classically explained by reduced diffusional limitations inside resin pores at low flow rate. It has been observed in many reports regarding CGA adsorption onto macroporous resins. Hence, CGA adsorption from *Helianthus tuberosus* L. leaves extract on ADS-21, from potato leaves on AB-8, from *Eupatorium adenophorum* Spreng extract onto NKA-II were recommended to range from 1 to 3 BV/h (B. Liu et al., 2016; P.-C. Sun et al., 2015; Xi et al., 2015). However, it can be noticed that in this case, DBC10 is only increased by 41.5% at pH 2 when the flow rate is decreased from 15 to 5 BV/h while others observed an 80% increase when flow rate was decreased from 7 to 3 BV/h (Weisz et al., 2010). Furthermore, DBC10 at pH 5 and 5 BV/h revealed close (70%) to maximal CGA binding capacity (Tuong Thi Le et al., 2020). Interestingly, kinetic study of batch CGA adsorption on XAD7 revealed that a strong intra-pore diffusional limitation was observed for only 10-15% of the total resin area. This could explain the mild effect of the flow rate on CGA DBC10 on XAD7.

A pH decrease clearly had a positive effect on DBC10 (increase from 11.28 mg/g to 44.47 mg/g when decreasing pH from 5 to 2 at 5 BV/h). This is consistent with other CGA adsorption studies from various sources (sweet potato leaves and sunflower meal) on other macroporous resins (XAD16, AB-8) (B. Liu et al., 2016; P.-C. Sun et al., 2015; Xi et al., 2015). This can be explained by a strong reduction of polarity at pH < 4 due to the ionization of the carboxylic acid function of CGA quinic acid part (pK_a = 3.95). This polarity reduction would improve the association constant with mild apolar resins like XAD7. Hence, most of the authors recommended to perform CGA adsorption at pH 2.

Figure 5.2B shows the impact of pH and flow rate on process productivity. The positive effect of pH decrease on productivity was expected. It results from the above observed increase in CGA

affinity for XAD7. Most interestingly, the productivity was increased by 45.57% (from 0.086 to 0.158 mg/g/min) when the flow rate was increased from 5 to 15 BV/h. It indicates that highest adsorption velocity at high flow rate largely compensates lower binding capacity. To our knowledge, this has never been observed yet. It clearly shows that high flow rate should be recommended contrarily to other reports (B. Liu et al., 2016; P.-C. Sun et al., 2015; Weisz et al., 2010; Xi et al., 2015).

CGA recovery is a crucial performance criterion for industrial applications. In this study, recovery represents the ratio of desorbed CGA after the adsorption process (using 100% ethanol) over the amount of injected CGA. Hence, this term lumps both CGA desorption yield and CGA loss during column washing prior desorption. Figure 5.2C shows the effect of adsorption pH and flow rate on recovery. Above pH 3.5, a positive effect of decreasing pH and flow rate was observed as with DBC10. Below pH 3.5, a strong negative effect with no or few desorption flow rate can be noticed. To our knowledge, such a parabolic effect of adsorption pH on the recovery of a phenolic compound after desorption on macroporous resin has never been observed. The effect of the flow rate above pH 3.5 was also surprising because this condition should only impact criteria related to the adsorption.

As mentioned above, the effect of the pH and flow rate on CGA recovery seems strongly related to its dynamic adsorption. In these conditions, DBC10 remained rather low (between 6.13 and 14.67 mg/g, but mostly around 10 mg/g while the maximum DBC10 value was higher than 40 mg/g). Hence, in this range of poor CGA adsorption, the CGA content in the mobile phase at the end of the adsorption step that was flushed by the washing step was not negligible and impacted the overall recovery. This probably explains the observed effect on CGA recovery. Obviously, it can be assumed that this bias had a poor impact at DBC10 values above 20 mg/g that were reached under pH 4.

The negative effect of pH under 3.5 was more puzzling. As explained above, in this pH range, the DBC10 value was high enough for neglecting CGA loss during the washing step. Hence, the recovery was only impacted by CGA desorption yield. We suggested that the increased CGA adsorption capacity in this pH condition was due to a predominance of its deionized form. We can therefore further hypothesize that the deionized form needs a less polar solvent than ethanol for full desorption.

In any cases, previous studies suggested to implement CGA adsorption at low pH (around 2) and adsorption flow rate (less than 5 BV/h) (B. Liu et al., 2016; P.-C. Sun et al., 2015; Weisz et al., 2010; Xi et al., 2015). Our results indicate that this should be reassessed. We therefore used the mathematical models of the DoE regression tools to carry out a multicriteria optimization of the process.

5.3.1.2. Multi-objective optimization

Table 5.2. Comparison between the predicted and experimental values in the dynamic adsorption process.

Condition	Response value	
	Productivity (mg/g/min)	**Recovery (%)**
Predicted values	0.125	79.66
Experimental values	0.128 ± 0.19	78.77 ± 3.61

Multi-objective optimization was used to identify optimal conditions of the adsorption process, i.e. that give the maximum yield of CGA. The best conditions were identified based on the highest productivity at a fixed recovery of 80%. These studies indicated that the optimum is reached with an adsorption flow rate of 15 BV/h at pH 2.7. Experimental results were then compared to predicted values given by modeling (Table 5.2). Experimentally-determined productivity and recovery were 0.128 ± 0.19 mg/g/min and 78.77 ± 3.61%, respectively. Predicted values were quite comparable to observed values as they were within the 95% confidence level. These results indicate that the regression models appropriately fitted experimental data. Therefore, the adsorption flow rate of 15 BV/ h and the pH value of 2.7 were chosen as optimal for the dynamic adsorption process.

5.3.1.3. Dynamic desorption step

The last criterion to integrate for optimization of adsorption is the purity of the fraction. This criterion is known to depend essentially on desorption conditions (i.e. the desorption solvent composition). Therefore, an appropriate solvent for CGA desorption had to be evaluated and selected after optimization of dynamic adsorptions. Ethanol has the advantages of being low-cost and eco-friendly. It was therefore used as eluent in this study. During the desorption process, ethanol concentration varied from 30% to 90%. The desorption flow rate was fixed at 120 BV/h as recommended by the manufacturer.

Table 5.3. Purity and recovery of chlorogenic acid with different ethanol concentrations.

EtOH concentration (%)	Purity (%)	Recovery (ads.+des.) (%)
30	53.29 ± 0.12	60.05 ± 0.32
50	76.05 ± 0.004	71.38 ± 1.59
70	71.89 ± 0.07	71.77 ± 1.71
90	72.31 ± 1.21	74.22 ± 0.95

Table 5.3 shows that the highest purity of CGA was obtained when elution was performed using EtOH 50% (v/v) (76.05 ± 0.004%), followed by EtOH 70% (v/v) (71.89 ± 0.07%) and EtOH 90% (v/v) (72.31 ± 1.21%). The highest recovery was reached with EtOH 90% (v/v) (74.22 ± 0.95%). EtOH 70% (v/v) and EtOH 50% (v/v) showed slightly lower purity (around 71%) Lowest purity and recovery was noted with EtOH 30% (v/v) (60.05 ± 0.32%). As suggested by Sun et al. (P.-C. Sun et al., 2015), it is likely that CGA is not fully desorbed by low ethanol concentration like 30% (v/v) contrarily to other minor polar impurities.

In any cases, the best compromise between purity and recovery was observed with EtOH 50% (v/v) (76.05 ± 0.004%). In this set of conditions, the purity was better than reported by Sun et al. (P.-C. Sun et al., 2015) and Liu et al. (B. Liu et al., 2016) (65.2% and 22.17% respectively at 60% and 40% (v/v) ethanol) (P.-C. Sun et al., 2015) CGA overall recovery was slightly lower though (71.38 ± 1.59%). Weisz et al. (Weisz et al., 2013) also showed slightly higher recovery (84.3%) using 50% (v/v) 2-propanol elution. But these three studies reported flow rates that are far from those recommended by the manufacturers for industrial applications and used in this study (i.e. 2BV/h vs 15BV/h). This most probably explains the observed discrepancies.

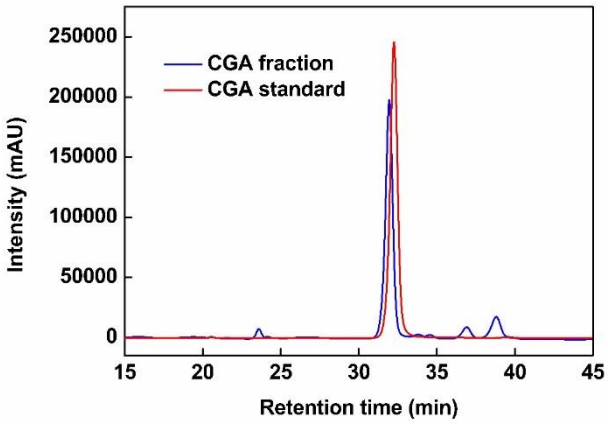

Figure 5.3. HPLC chromatogram of the sample after passing through the XAD7 resin column (fraction), and of pure chlorogenic acid (standard).

Figure 5.3 shows the size exclusion HPLC chromatogram at 325 nm of standard CGA (5-CQA) and of the desorbed fraction obtained at 50% (v/v) ethanol. Standard CGA shows a single peak at 32 minutes of elution time analyzed by mass spectrometry as CGA (5-CQA). The fraction shows a main peak at the elution time and two minor peaks at 37 and 38.5 minutes of elution times identified by MS as 3- and 4-CQA i.e. the two other CGA isomers. Traces of caffeic acid were also detected at 23 minutes. Hence, the largest part of the UV signal at 325 nm (80.69%) was CGA and 5-CQA was the major component (76.05%). To our knowledge, such characterization of CGA fraction has never been reported. Obviously, CGA fraction differed from the standard and is composed of unidentified minor components that could interfere with its reported bioactivity. Hence, the antioxidant effect of the fraction was compared to CGA standard reference and vitamin C.

5.3.2. *In vitro* antioxidant activity

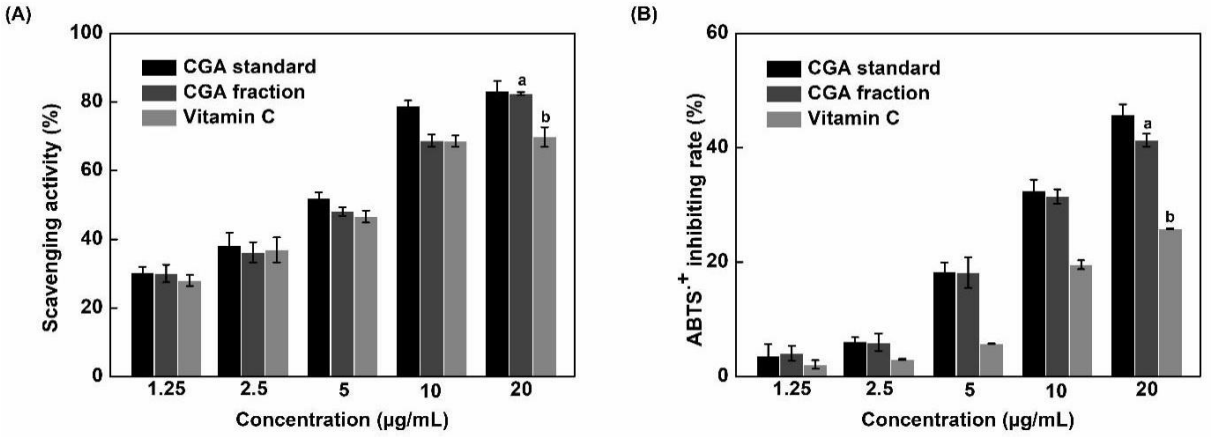

Figure 5.4. Scavenging activity of the CGA fraction compared to pure CGA (standard) and vitamin C determined using DPPH (A) and ABTS (B) assays.
Bars labeled with different letters are significantly different ($p < 0.05$).

Table 5.4. IC50 values deduced from the DPPH and ABTS assays.

Compound	IC50/ DPPH (µg/mL)	IC50/ ABTS (µg/mL)
Pure CGA (standard)	5.76 ± 0.02a	20.38 ± 0.02a
CGA fraction	7.05 ± 0.01b	22.52 ± 0.03b
Vitamin C	7.26 ± 0.02c	36.31 ± 0.01c

Different letters in the same column for the IC50/DPPH and IC50/ABTS indicate significant differences ($p < 0.05$) between individual sample treatments.

To evaluate the scavenging potential of the CGA fraction by comparison to pure CGA and vitamin C at the same concentrations, DPPH and ABTS assays were conducted (Brand-Williams et al., 1995; C.-W. Chen & Ho, 1995). As shown in Figure 5.4, the scavenging potential of all samples gradually increased with concentration, regardless of the method used. At the highest concentration (20 µg/mL), CGA fraction and pure CGA had the same scavenging activity, as revealed by the DPPH assay (83.01 ± 0.16% and 82.36 ± 0.38%), and their antioxidant activity was 1.2 times higher than vitamin C. Besides, Figure 5.4B shows that the ABTS+ inhibition rate of the CGA fraction, pure CGA, and vitamin C at 20 µg/mL were 41.32 ± 0.12, 45.81 ± 0.06, and 25.85 ± 0.13%, respectively. The antioxidant activity of vitamin C, as determined using the ABTS assay, was weaker than that of the CGA fraction and pure CGA (1.60-1.78 times lower). Furthermore, as shown in Table 5.4, very interestingly, vitamin C IC50 values were always higher than those obtained using the CGA fraction or pure CGA thereby showing that the order of antioxidant capacity was: pure CGA ≥ CGA fraction > vitamin C ($p < 0.05$). The antioxidant properties of our fraction is therefore much higher than the one of vitamin C which is frequently used as reference in the literature.

As shown in Table 5.3, the fraction used in antioxidant tests contained 76% of CGA. In both assays, this fraction and pure CGA showed a similar antioxidant activity. This observation indicates that CGA strongly contributed to radical scavenging activity in the CGA fraction. This activity is related

to structure characteristics such as the number of hydroxyl groups (-OHs), and electron-donating activity (Montoro et al., 2005). As shown in Figure 5.5A, CGA is formed by an ester bond between caffeic acid and quinic acid. According to Natella et al. (Natella et al., 1999), the number of hydroxyl groups on phenolic acids contributes as positive moieties to their antioxidant effects. These authors found that the antioxidant activity depends of the number of hydroxyl groups with the following priority: tri-hydroxyl phenolic acids > di-hydroxyl phenolic acids (catechol group) > mono-hydroxyl phenolic acids. The presence of two hydroxyl groups (catechol group) in the caffeic acid part of CGA agrees with this rule and contributes to explain its strong antioxidant activity.

5.3.3. Cytotoxicity and anti-inflammatory activity of the CGA fraction

THP-1 cells differentiated into macrophages were used to analyze the effects of the CGA fraction on cell viability and LPS-induced pro-inflammatory response. Chlorogenic acid was used as reference in these experiments because it is the major compound found in this fraction (see Table 5.3). Two conditions were used to mimic two different cellular states. First condition consisted in pre-incubating differentiated THP-1 cells with 100 ng/mL of LPS to induce a pro-inflammatory state and, one hour later, to add the CGA fraction at working concentrations corresponding to 50 or 100 µM of CGA. The purpose of this approach was to determine if this fraction was able to counter the LPS-induced pro-inflammatory response. The second condition was the opposite, it consisted in incubating THP-1 cells with the CGA fraction, to potentially promote an anti-inflammatory cellular state, and one hour later to add 100 ng/mL of LPS. In both cases, cell viability and TNF-α production, a major pro-inflammatory cytokine, were analyzed after 24 h of treatment.

5.3.3.1. Cytotoxicity

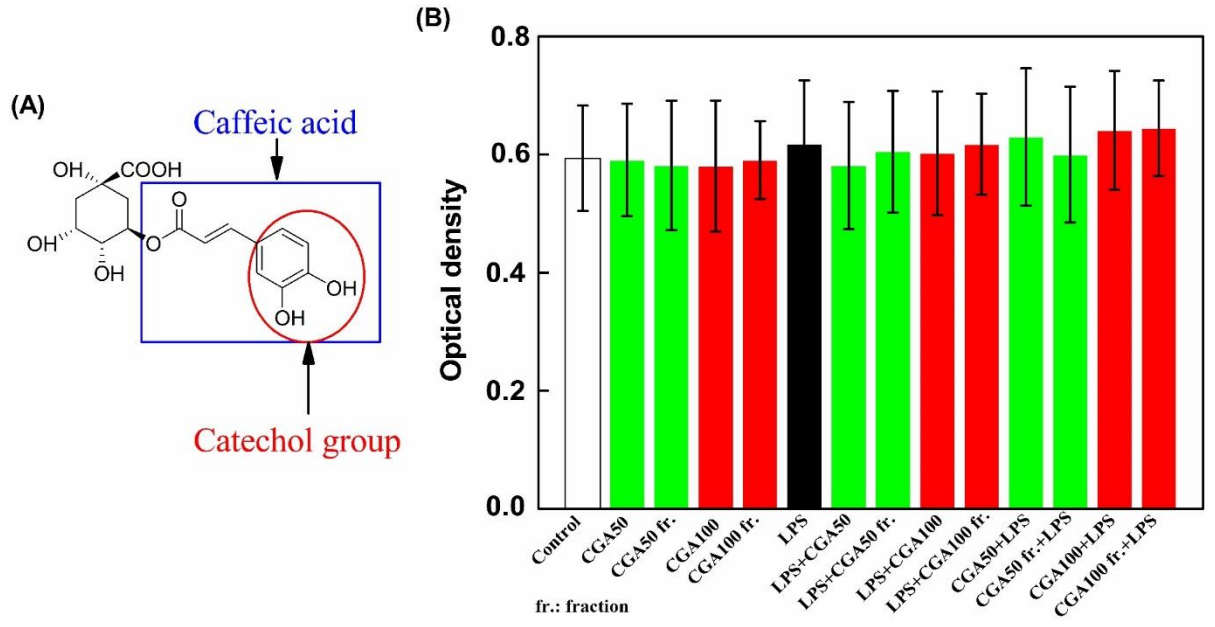

Figure 5.5. Chlorogenic acid (CGA) structure (A) and effects of this pure compound or of the CGA fraction on the viability of differentiated THP-1 cells (B).

Two concentrations (50 and 100 µM) of pure chlorogenic acid used as references and two working concentrations of the fraction corresponding to a content of 50 or 100 µM of CGA (CGA50 fr and CGA100 fr) were used. Differentiated THP-1 cells were incubated for 24h either with these products alone or with 100 ng/mL of LPS added one hour before or after the addition of pure CGA or CGA fraction. Then, cell viability was analyzed by crystal violet assay and optical density (O.D.) was measured at 595 nm. Data are presented as mean ± S.D. This figure is representative of six independent experiments realized in triplicates. "Control" corresponds to a culture in which no product was added. "LPS+CGA50" indicates that LPS was added before CGA at the concentration of 50 µM while "CGA50+LPS' indicates that CGA at the concentration of 50 µM was added before LPS.

As shown in Figure 5.5B, whatever the treatment, no alteration of cell viability was detected using the crystal violet assay. Pure CGA and the CGA fraction, at the two tested concentrations, had no impact on cell viability (cell viability > 97%). Thus, impurities remaining in the fraction did not affect cell viability. Consequently, these experimental settings and concentrations were used to evaluate the production of TNF-α by THP-1 macrophages.

5.3.3.2. Anti-inflammatory activity of the CGA fraction

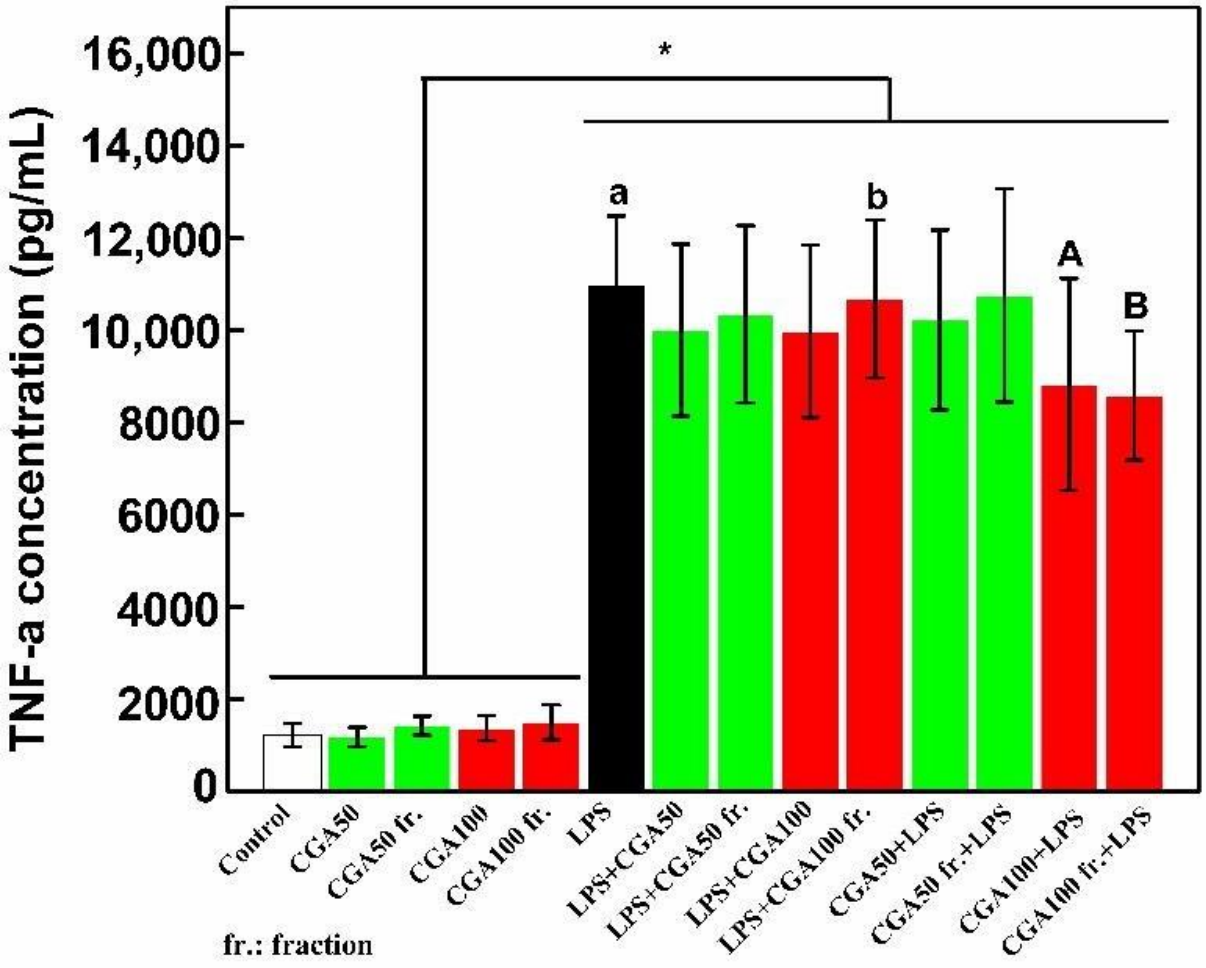

Figure 5.6. When added before LPS, CGA and the CGA fraction reduce the production of TNF-α by differentiated THP-1 cells.

Two concentrations (50 and 100 µM) of pure CGA, used as references, and two working concentrations of the CGA fraction corresponding to a content of 50 or 100 µM of CGA (CGA50 fr. and CGA100 fr.) were used. Differentiated THP-1 cells were incubated for 24 h either with these products alone or with 100 ng/mL of LPS added one hour before or after the addition of pure CGA or the CGA fraction. Cell culture supernatants were then collected and used to quantify TNF-α production by ELISA. This figure is representative of six independent experiments performed in triplicates. Data are presented as mean ± S.D. t-tests were used to identify statistically significant differences. Asterisk indicates a significant difference between samples with and without LPS treatment groups (* $p < 0.05$). Bars labeled with the different lowercase letters and uppercase letters are significantly different ($p < 0.05$). "Control" corresponds to a culture in which no product was added. "LPS + CGA50" indicates that LPS was added before CGA at the concentration of 50 µM while "CGA50 + LPS" indicates that CGA at the concentration of 50 µM was added before LPS.

As shown in Figure 5.6, pure CGA and the CGA fraction had no pro-inflammatory effects when added alone on THP-1 cells differentiated in macrophages. The fact that the CGA fraction is neither cytotoxic nor pro-inflammatory on its own is interesting in term of future potential biomedical valorization. When LPS was added, as expected, a strong increase of TNF-α secretion was observed (indicated by "a" in Figure 5.6). Furthermore, and very interestingly, we noted that when pretreated with CGA or the CGA fraction at 100 µM, cells produced less TNF-α in response to LPS by comparison to cells receiving only LPS (statistically significant reductions of 20 and 22%, respectively indicated by "c" and "d" in Figure 5.6). This means that pure CGA and the CGA fraction at 100 µM are able to induce an anti-inflammatory state in THP-1 cells differentiated in macrophages and that impurities remaining in the CGA fraction did not affect this capacity. This effect was not observed when pure CGA or the CGA fraction at 100 µM was added one hour after LPS indicating that if the pro-inflammatory process is initiated, CGA or the CGA fraction is unable to counter this phenomenon.

These results show that a fraction obtained from a low value industrial liquid effluent possesses preventive functions against inflammation thereby potentially allowing its valorization as a food complement in the biomedical (human and/or veterinary) field. Indeed, intensive breeding is a source of stress leading to an increase of inflammation that affects health and well-being thereby impacting products quality (Gessner et al., 2017; Liehr et al., 2017). Acute and chronic stress, two characteristics of our actual life style, also induce inflammation (Godbout & Glaser, 2006). Thus, the properties of this fraction could be of interest for humans (F. Cardona et al., 2013; Marín et al., 2015). Indeed, macrophages are part of the first line of defense against infection and/or tissue injury, and are key actors of the inflammatory process through the production of various mediators such as the pro-inflammatory cytokine TNF-α. Thus, phenolic compounds reducing TNF-α production are promising agents to moderate inflammation. Of course, this effect will have to be confirmed in *in vivo* studies using stress murine models.

5.3.4. Conclusions

This study presents an effective way to separate and purify CGA from an industrial liquid by-product resulting from a sunflower protein isolate process. Optimal conditions, based on the response surface methodology for the enrichment of phenolic compounds from sunflower meal, were defined as follows using the XAD7 resin: adsorption flow rate of 15 BV/h, pH 2.7, desorption with EtOH 50%. These conditions successfully generated enough product, with a purity of 76.05 ± 0.004% and without using toxic solvents, to evaluate its antioxidant and anti-inflammation properties. The DPPH and ABTS assays showed that the obtained fraction was a more powerful radical scavenger than vitamin C. Furthermore, this fraction showed no cytotoxicity on a human macrophage cell line and reduced LPS-induced TNF-α production by 22%. We therefore propose valorizing this abundant effluent to produce a natural phenolic compound, CGA, which possesses antioxidant and anti-inflammatory properties, but no cytotoxic effects.

5.4. Rapeseed phenolic compound adsorption on columns and assessement of their bioactivities

We previously reported that macroporous XAD16 resin was the most suitable for capturing sinapine and total phenolic contents in the by-product protein isolate. Similarly, the effect of adsorption flow rate and pH on dynamic binding capacity, productivity, and recovery of phenolic compounds was investigated by design of experiments (DoE). Then, modeling to find the optimal condition for the adsorption process by DoE models. Regarding the desorption step, the effect of ethanol concentration in both phenolic compounds purity and recovery was also evaluated. The obtaining phenolic fraction based on the optimal adsorption conditions was used to test antioxidant activity compared to pure sinapine (standard) and vitamin C. The anti-inflammatory activity was investigated by measuring the tumor necrosis factor alpha (TNF-α) production by lipopolysaccharide (LPS) treated THP-1 macrophages (Chanput et al., 2014). The biological properties of phenolic compounds could be valorized in the food industry.

5.4.1. Dynamic adsorption step

5.4.1.1. Effect of pH and flow rate on dynamic binding capacity, recovery, and process productivity

In a previous report, XAD16 macroporous resin showed the best resin for phenolic compounds capture from an aqueous by-product yielded by a rapeseed protein isolate process (Le, Framboisier, et al., 2021). In the current study, the dynamic adsorption of phenolic compounds on XAD16 column from the same by-product was investigated using the design of experiment (DoE) methodology. The effects of adsorption flow rate and the pH of liquid effluent on the resin dynamic binding capacity (DBC10), process productivity, and recovery were taken into account. The adsorption flow rate was taken into consideration because it is reported to impact dynamic adsorption (B. Liu et al., 2016; Weisz et al., 2010; S.-C. Yang et al., 2015). The effect of pH was also reported as a factor impacting the adsorption of phenolic compounds from RSM onto the hydrophobic bed (Moreno-González et al., 2020). Therefore,

the effect of pH was investigated in this study. In the literature, the criteria like DBC and recovery were widely studied in column adsorption studies (B. Liu et al., 2016; Weisz et al., 2010; S.-C. Yang et al., 2015). However, the process productivity, a crucial characteristic for industrial application, was not considered. The chosen pH ranges from 2 to 5 because of above pH 5, the phenolic compounds in liquid effluent can be converted into its oxidized form (Smyk & Drabent, 1989). As recommended from the provider, the flow rate varied from 5 to 15 BV/ h was investigated in this study. The results involved in phenolic compounds quantity or total phenolic content (TPC) were expressed in mg sinapic acid equivalent (mgSAE) because this is phenolic compounds consisted in the liquid effluent used in this work (Le, et al., 2021). We used TPC adsorption capacity as a criterion to determine the optimal condition of column adsorption because there were several phenolic compounds represented in RSM protein isolate by-product besides sinapine (main phenolic compound) such as sinapoyl glucose, 1,2-di-sinapoyl gentiobise, and sinapic acid (Le, et al., 2021).

The obtained mathematical models are expressed in equation (S5.1-3). Regression parameters (unscaled and scaled), and statistical verification of model performances using ANOVA test are listed in Table S5.1.

$Y_{1(dynamic\ binding\ capacity\ at\ 10\%,DBC10)} = 94.446 + 1.36117X_1 - 38.8971X_2 - 0.1308X_1^2 + 5.5902X_2^2 - 0.1304X_1X_2$ (S5.1)

$Y_{2(productivity)} = 0.00385 + 0.0116X_1 - 0.00052X_1^2$ (S5.2)

$Y_{3(recovery)} = 59.281 + 1.70802X_1$ (S5.3)

where:

X_1 is the adsorption flow rate (BV/ h)

X_2 is pH

Table S5.1. Regression coefficients of the predicted polynomial models for dynamic binding capacity, productivity, and recovery.

Regression coefficient		**Response**		
		Y_1 (Dynamic binding capacity, mg/g)	Y_2 (Productivity, mg/g/min)	Y_3 (Recovery, %)
Unscaled	β_o[a]	94.466	0.00385	59.281
	β_1[b]	1.36117	0.0116	1.70802
	β_2[c]	-38.8971	-	-
	β_{11}[d]	-0.130766	-0.00052	-
	β_{22}[e]	5.59018	-	-
	β_{12}[f]	-0.130436	-	-
Scaled and centered	β_o	22.7756	0.07065	76.6819
	β_1	-8.55335	0.006	8.54012
	β_2	-1.60539	-	-
	β_{11}	-3.26915	-0.01148	-
	β_{22}	12.5779	-	-
	β_{12}	-0.978272	-	-
Statistic model parameter				
R^2		0.83	0.72	0.73
RSD[g]		5.8886	0.00426	4.454
Regression *p*-value		0.025	0.01	0.001
Lack of fit		0.09	0.156	0.466

[a] constant, [b] coefficient of the linear effect of adsorption flow rate, [c] coefficient of the linear effect of pH, [d] coefficient of the quadratic effect of adsorption flow rate, [e] coefficient of the quadratic effect of pH, [f] interaction coefficient of adsorption flow rate and pH, [g] residual standard deviation

The mathematical models were characterized by the indexes of regression coefficient between predicted and observed values (R^2 = 0.83 for dynamic binding capacity at 10% (DBC10), R^2 = 0.72 for productivity, and R^2 = 0.73 for recovery) (Figure S5.1). The closer the R^2 values to 1, the more accurate the models were L.A.Sarabia and M.C.Ortiz (Sarabia & Ortiz, 2009). The calculated values and observed values are presented in Figure S5.1.

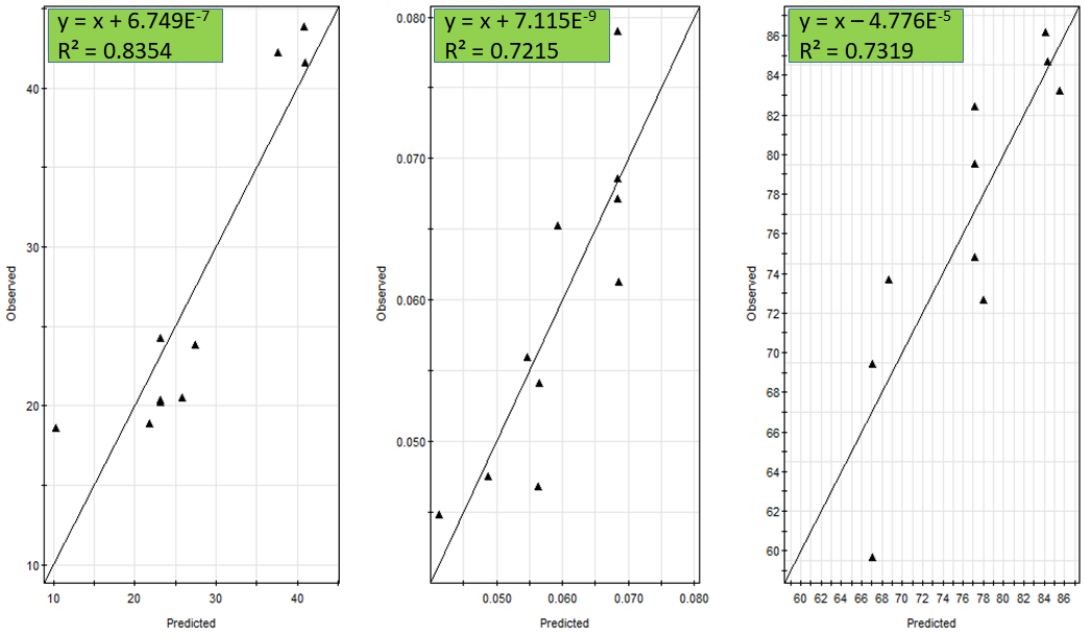

Figure S5.1. Comparison of model-predicted and actual values for dynamic binding capacity (left), productivity (middle), and recovery (right) responses.

Besides, regression p-values (0.025 for dynamic binding capacity, 0.01 for productivity, and 0.001 for recovery, < 0.05) and lack of fit (with p > 0.05) confirmed the high accuracy for predictive these models. These results suggested a good fitted and reliability of models for prediction of the assessed process.

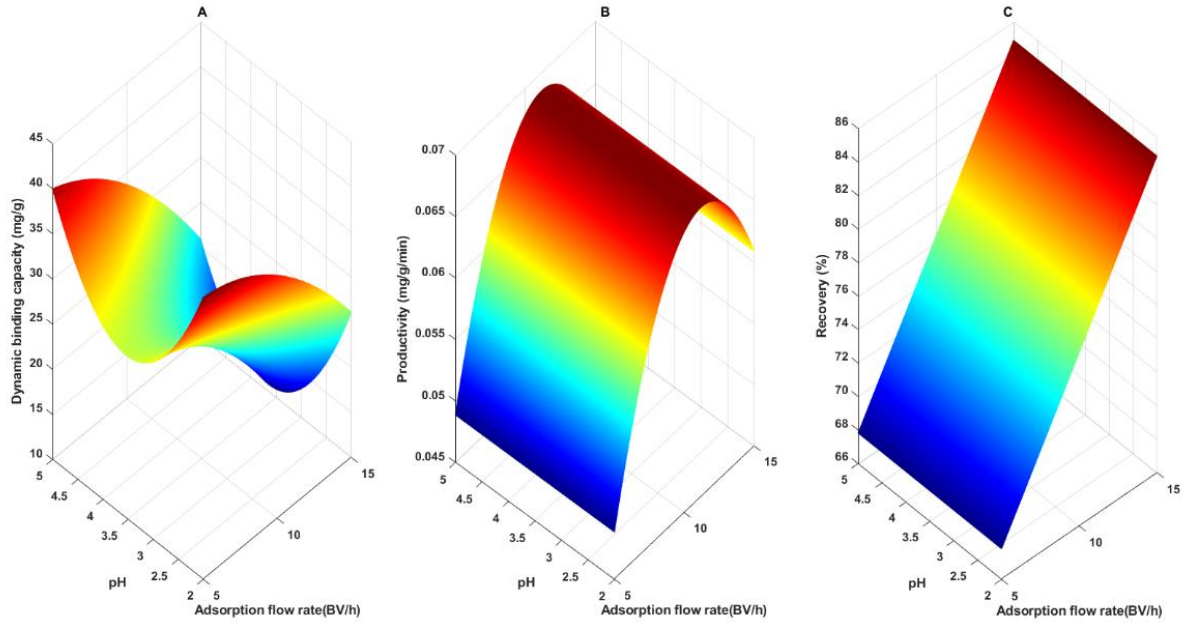

Figure S5.2. 3-dimensional plots representing the effects of adsorption flow rate and pH on TPC yield. pH versus adsorption flow rate on adsorption binding capacity (A), productivity (B), and recovery (C).

The effect of pH and flow rate on DBC10 is shown in Figure S5.2A. DBC10 values of TPC increase from 20.51 to 43.88 mgSAE/ g when flow rate decreases from 15 to 5 BV/h. Whatever the pH value, this trend is observed (Le, et al., 2021). This phenomenon can be explained by the reduced diffusional limitations inside resin pores at low flow rate (Le, , et al., 2021). In the past, the adsorption of chlorogenic acid onto macroporous resin has been observed at flow rate ranging from 1 to 3 BV/h because of highest dynamic binding capacity (B. Liu et al., 2016; Xi et al., 2015). However, it can be highlighted that in this case, DBC10 is only increased by 53.26% at pH 2 when the flow rate is varied from 15 to 5 BV/h. In the previous study, we observed a 41.5% increase with chlorogenic acid from sunflower meal (Le, , et al., 2021; Le,, et al., 2021). Meanwhile, according to Weisz et al. (Weisz et al., 2010), the increasing is observed by 80% when flow rate was decreased from 7 to 3 BV/h. Moreover, DBC10 at pH 5 and 5BV/h reached close (61.43%) to maximal TPC binding capacity (Le, et al., 2021; Le, et al., 2021). Interestingly, the kinetic adsorption of TPC on XAD16 resin showed a strong intra particle diffusion (diffusional limitation was observed for about 16% of the total resin (Le, et al., 2021; Le, et al., 2021). This behavior could explain the slightly effect of the flow rate on TPC DBC10 on XAD16 resin.

A pH decrease showed slightly effect on DBC10 (increase from 41.61 mgSAE/g to 43.88 mg SAE/g when increasing pH from 2 to 5 at 5BV/h; decrease from 20.51 mgSAE/g to 18.86 mgSAE/ g when increasing pH from 2 to 5 at 15BV/h). As shown in Figure S5.2, the maximal dynamic binding capacity (DBC10) was found at pH ranging from 4.5-5 or 2-2.5. These results can be explained by the stability of phenolic compounds presented in RSM in these pH ranges. At pH from 2-2.5, the highest DBC10 was observed that agreed with chlorogenic acid adsorption onto XAD16 (Weisz et al., 2010) or XAD7 (Le, et al., 2021; Le, et al., 2021) resin from sunflower meal. In those cases, the authors recommended performing chlorogenic acid adsorption at about pH 2 (Le, et al., 2021; B. Liu et al., 2016; P.-C. Sun et al., 2015; Xi et al., 2015, p. 201).

Figure S5.2B illustrates the effect of pH and flow rate on process productivity. Interestingly, the pH at 2-5 did not influence productivity. The minimal productivity was observed at 5 BV/h adsorption flow rate (ranged from 0.04-0.05 mg/g/min) at the pH ranged 2-5. The process productivity was increased by 34.78% (from 0.044 to 0.065 mgSAE/g/min) when the flow rate was increased from 5 to 15 BV/h. This result suggests the highest adsorption velocity at a high flow rate widely contributes for lower binding capacity. Obviously, the high flow rate should be recommended contrarily to other reports (P.-C. Sun et al., 2015; Weisz et al., 2010; Xi et al., 2015, p. 20). Surprisingly, the productivity obtained the maximum value (about 0.07 mg/g/min) when the adsorption flow rate was about 11-13 BV/h and pH range from 2 to 5. These results suggested that at these adsorption flow rate values, the phenolic compounds had a sufficient contact time requiring their diffusion into the resin pores. However, as the adsorption flow rate increased to 15BV/h, the productivity slightly decreased (0.05-0.06 mg/g/min). This phenomenon can explain that at a too high adsorption flow rate (15 BV/h), the adsorption of phenolic compounds onto XAD16 resin would be incomplete. Interestingly, this finding was not observed with CGA from SFM on XAD7 resin. This difference in productivity process might come from different starting material and adsorbant. Indeed, there are various phenolic compounds in RSM with different polarities (Le, et al., 2021). Besides, in SFM, we observed only CGA with a minor quantity of CGA isomers (Tuong Thi Le et al., 2020).

TPC recovery is a vital criterion for industrial scale-up. In current work, recovery of phenolic compounds presents the ratio of desorbed TPC after the adsorption process with absolute ethanol as an elute solution over the amount of charged TPC. This process was combined the TPC desorption yield and TPC desorbed during column washing in the previous step. Figure 2C proved that pH did not affect the recovery of TPC. In contrast, the adsorption flow rate had a strong effect on these responses. As the flow rate increased, the recovery obtained a maximal value (74.83-86.15%) at a flow rate around 11 to 15 BV/h.

According to MATLAB programming, the maximal values of the productivity (0.069 mg/g/min) and recovery yield of TPC (62.69%) were observed under the conditions of adsorption flow rate at 13.3 BV/h and pH in the investigated range (2-5). In this study, we set the pH at 2 for further studies. To the best of our knowledge, the effect of pH on TPC from rapeseed meal adsorption has never

been observed yet. Our previous study showed that pH strongly impacted the adsorption of chlorogenic acid on XAD7 (Le, et al., 2021). We observed the flow rate impacted on DBC10 and the process productivity of chlorogenic acid adsorption (Le, et al., 2021). In that study, the optimal flow rate for chlorogenic acid purification was 15 BV/h (Le, et al., 2021). However, in most cases, the previous works recommended conducting phenolic compounds at a low adsorption flow rate (under 5 BV/h) (B. Liu et al., 2016; P.-C. Sun et al., 2015; Xi et al., 2015). Our findings demonstrate that this should be re-considered. Thus, in this study, we used the mathematical models of the DoE regression method to perform a multicriteria optimization of the process. This step allows defining the optimal conditions for the phenolic compounds purification process.

5.4.1.2. Multi-objective optimization

Table S5.2. Comparison between the predicted and experimental values in the dynamic adsorption process.

Condition	Response value	
	Productivity (mgSAE/g/min)	Recovery (%)
Predicted value	0.069	62.69
Experimental value	0.06 ± 0.0002	67.88 ± 3.45

The polynomial equations of models were used to determine the most suitable conditions for phenolic purification. The optimization aimed to maximize both criteria, which are productivity and recovery. These models were verified based on the results obtained from response surface analysis. According to these findings above, The optimal adsorption flow rate was 13.3 BV/h, and at pH range 2-5 (in this study, we used pH 2). The accuracy of models to predict the process performance in the selected conditions was verified by comparing the predicted and experimental values. Table 4 presented all the results of model validation. Under these optimal conditions, the predicted productivity and recovery were 0.069 (mg/g/min) and 62.69 (%), respectively. The validation was conducted under these conditions, obtaining the value of productivity and recovery were 0.06 ± 0.0002 (mg/g/min) and 67.88 ± 3.45%, respectively, as listed in Table S5.2. These results confirmed that these models were adequate and accurate for this study. Hence, the adsorption flow rate of 13.3 BV/h and the pH value of 2 were selected as optimal conditions for the dynamic adsorption process. These results were consistent with the finding of our previous study regarding the adsorption of chlorogenic acid on XAD7, that the optimal condition for dynamic adsorption should be conducted at a high flow rate (Le, et al., 2021).

5.4.1.3. Dynamic desorption step

The last criterion to combine for optimization of adsorption is the purity of the phenolic fraction after desorption. This criterion depends on the desorption conditions, such as the composition of an eluent. Hence, the appropriate elute concentration had to be assessed and selected after optimization of dynamic adsorption. Ethanol has widely used in the desorption process because of being low-cost, non-toxic, and eco-friendly. Thus, ethanol was selected to be an eluent in this study. In our previous study, ethanol with a concentration ranging from 30-90% (v/v) affected the purity and recovery

of chlorogenic acid (Le, et al., 2021). In this study, the same conditions of ethanol was applied in the desorption step.

Desorption flow rate fixed at 120 BV/h as recommended by the provider with 40 BV after washing the column with 20 BV by deionized water. Preliminary experiments showed that ethanol concentration at 30% (v/v), the highest purity and recovery of TPC observed in permeate solution. These results also agreed with the static desorption study in the previous report (Le, et al., 2021). XAD16 resin was preferred the higher ethanol concentration for the desorption process (Moreno-González et al., 2020). After the desorption process, the purity of TPC in the desorption fraction (N fraction) was 20.68 ± 1.94%. The recovery of TPC was 76.90 ± 4.24%. This fraction was used to investigate the biological activities, including antioxidant and anti-inflammatory properties in this study.

5.4.2. *In vitro* antioxidant activity

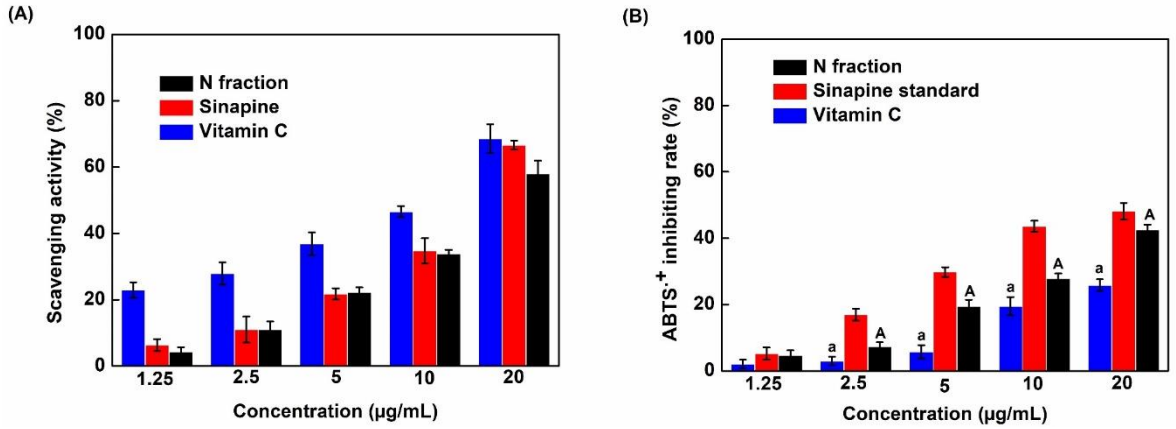

Figure S5.3. Scavenging activity of the phenolic fraction (N fraction) compared to pure sinapine (standard) and vitamin C determined using DPPH (A) and ABTS (B) assays.
Bars labeled with different letters are significantly different ($p < 0.05$).

To evaluate the radical scavenging capacity of the N fraction by comparison to pure sinapine and vitamin C at the same concentrations, DPPH and ABTS assays were implemented (Brand-Williams et al., 1995; C.-W. Chen & Ho, 1995). As shown in Figure S5.3, the free radical scavenging potential gradually increased when the concentration of samples was increased in both methods. At the concentration range 1.25-10 µg/mL, DPPH assay revealed that N fraction and pure sinapine had the same scavenging capacity (Figure S5.3A). This observation can be explained that sinapine is a main phenolic compound in the N fraction (Le, et al., 2021). Surprisingly, at the highest concentration (20µg/mL), pure sinapine and vitamin C showed slightly higher than N fraction (68% and 58% of scavenging activity, respectively, Figure S5.3A). Table S5.3 showed the IC50 value of N fraction and vitamin C were 10.05 µg/mL and 7.27 µg/mL, respectively. Therefore, by this test, the phenolic fraction had slightly weaker than vitamin C. The presented different phenolic compounds might explain this phenomenon in the N fraction (Le, et al., 2021).

Table S5.3. IC50 values deduced from the DPPH and ABTS assays.

Antioxidant	IC50/ DPPH (µg/mL)	IC50/ ABTS (µg/mL)
N fraction	10.05 ± 0.15	22.70 ± 0.11a
Sinapine standard	7.58 ± 0.19	17.98 ± 0.13b
Vitamin C	7.27 ± 0.20	36.31 ± 0.19c

Different letters in the same column for the IC50/DPPH and IC50/ABTS indicate significant differences ($p < 0.05$) between individual sample treatments.

On the other hand, the antioxidant of N fraction showed 1.6 times higher than the antioxidant of vitamin C at 20µg/mL, as determined by ABTS assay (Figure S5.3B). Moreover, as shown in Table S5.3, the IC50 scavenging capacities of N fraction, pure sinapine, and vitamin C were 10.60, 17.98, and 36.31 µg/mL, respectively. Results showed that the anti-oxidant ability of N fraction > pure sinapine > vitamin C (*$p < 0.05$). The results finding in this study showed the potential of phenolic compounds of by-product protein isolate from rapeseed meal in the free radical scavenging activities. This antioxidant activity can be explained by the presence of the number of hydroxyl groups (-OHs) directly attached to the aromatic ring and the electron-donating activity of the phenolic compounds (Le, et al., 2021; Le, et al., 2021; Montoro et al., 2005). The antioxidant activity of phenolic compounds in rapeseed oil had been found in the report of Satu Vourela et al. (Vuorela et al., 2004). However, the antioxidant properties of phenolic compounds from rapeseed meal have never been published in our knowledge (Le, et al., 2021). Our previous study also showed the potential of phenolic compounds from by-product protein isolate from rapeseed meal (Le, et al., 2021). Thus, these compounds can be considered as natural antioxidants in food applications.

5.4.3. Cytotoxicity and anti-inflammatory activity of the phenolic fraction

THP-1 cells differentiation into macrophages was used to investigate the phenolic fraction (N fraction) effects on cell viability and LPS-induced pro-inflammatory response as in our previous study with phenolic compounds from sunflower meal (Le, et al., 2021). Sinapine (SP) was used as the reference in these biological experiments due to their major component (50.81% SP in N fraction (Le, et al., 2021). The experiments were divided into two conditions. First, pre-incubating differentiated THP-1 cells with 100 ng/ mL of LPS to induce a pro-inflammatory cytokine such as TNF-α and add the N fraction after 1h concentrations corresponding to 50 or 100 µM of SP. Second, to investigate an anti-inflammatory potential, we incubated THP-1 cells with N fraction corresponding to 50 or 100 µM of SP and added 100 ng/ mL of LPS after 1h. In both cases, cells viability and TNF- α production level was estimated after 24h treatment.

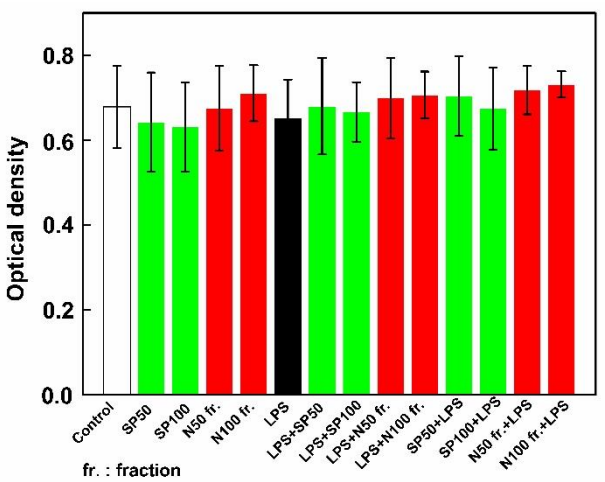

Figure S5.4. Effects of pure sinapine (SP) or phenolic fraction (N fraction) on the viability of differentiated THP-1 cells.

Two concentrations (50 and 100 µM) of pure sinapine (SP) used as references and two working concentrations of the fraction corresponding to a content of 50 or 100 µM of SP (N50 fr. and N100 fr.) were used. Differentiated THP-1 cells were incubated for 24h either with these products alone or with 100 ng/mL of LPS added one hour before or after the addition of pure SP or N fraction. Then, cell viability was evaluated by crystal violet assay and optical density (O.D.) was measured at 595 nm. Data are presented as mean ± S.D. This figure is representative of four independent experiments realized in triplicates. "Control" corresponds to a culture in which no product was added. "LPS+SP50" indicates that LPS was added before SP at the concentration of 50 µM while "SP50+LPS" indicates that SP at the concentration of 50 µM was added before LPS. "LPS+N50 fr." indicates that LPS was added before N fraction containing 50µM of SP. "N50 fr. + LPS" indicates that LPS was added after N fraction containing 50µM of SP.

First, we investigated the effect of N fraction on cell viability. As shown in Figure S5.4, the sample concentration resulting in over 90% of cell viability was considered to show no cytotoxicity. Thus, phenolic fractions did not affect cell viability up to a concentration of 100µM (of SP in N fraction). Notably, the "impurities" present in these two fractions did not affect cell viability. Moreover, no phenolic components in obtained fraction showed cytotoxicity. The results suggested that phenolic compounds in rapeseed meal after purification have no cytotoxicity at a concentration ranging from 50 to 100µM of SP in N fraction. This finding also was in agreement with the chlorogenic fraction in sunflower meal in our previous study (Le, et al., 2021). Based on this result, these concentrations of pure SP and SP in N fraction (at 50 and 100µM) were used to analyzed the production level of TNF-α by THP-1 macrophage.

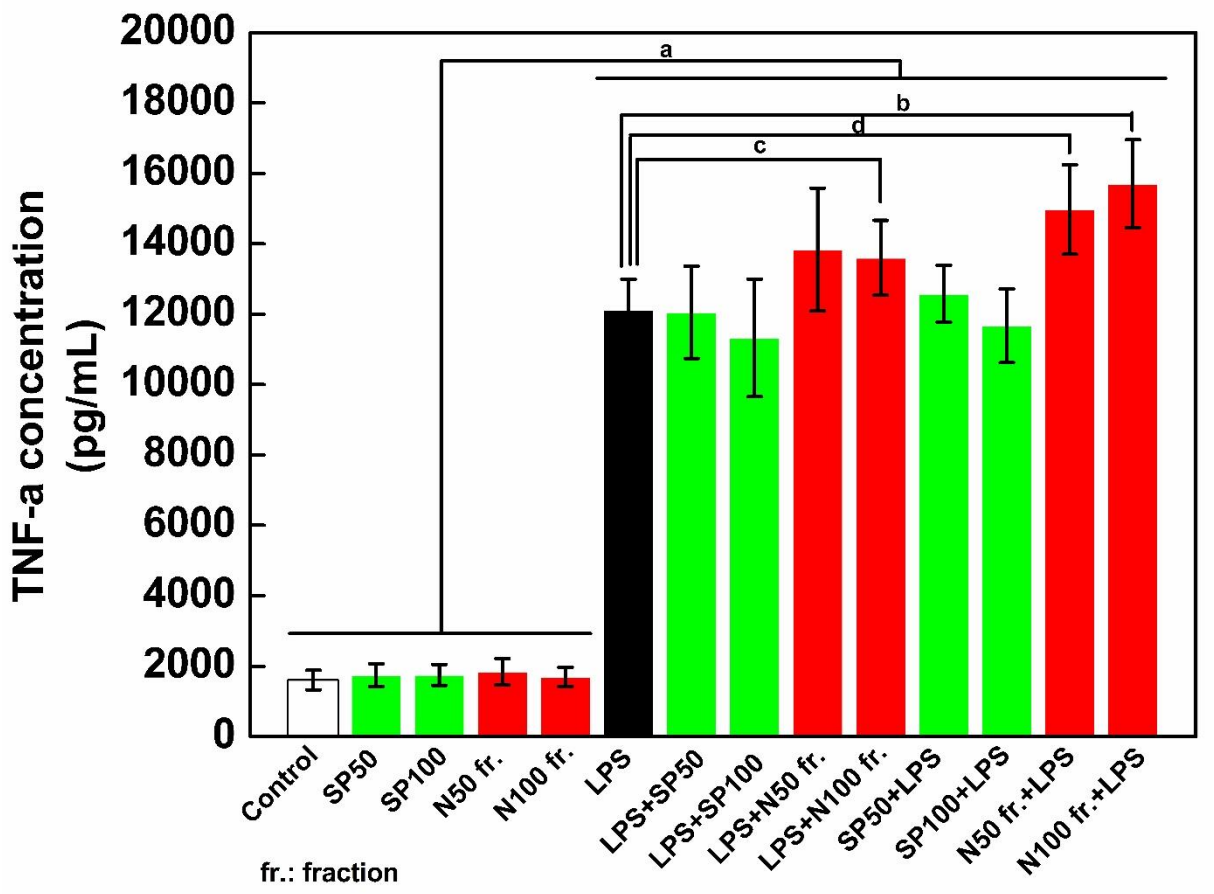

Figure S5.5. Effect of pure sinapine (SP) and N fraction when added before and after LPS on TNF-α production by differentiated THP-1 cells.

Two concentrations (50 and 100 µM) of pure sinapine (SP), used as references, and two working concentrations of rapeseed phenolic fraction (N fraction), corresponding to a content of 50 or 100 µM of SP, were used. Differentiated THP-1 cells were incubated for 24h either with these products alone or with 100 ng/mL of LPS added one hour before or after SP or rapeseed phenolic fraction. Cell culture supernatants were then collected and used to quantify TNF-α production by ELISA. This figure is representative of four independent experiments performed in triplicates. Data are presented as mean ± S.D. *t*-tests were used to identify statistically significant differences. $^{a}p < 0.05$ vs conditions without LPS. $^{b,c,d}p < 0.05$ vs LPS alone. "Control" corresponds to a culture in which no product was added. "LPS+SP50" indicates that LPS was added before SP at the concentration of 50 µM while "SP50+LPS" indicates that SP at the concentration of 50 µM was added before LPS. "LPS+N50 fr." indicates that LPS was added before N fraction containing 50µM of SP. "N50 fr. + LPS" indicates that LPS was added after N fraction containing 50µM of SP.

Second, we investigated the phenolic fraction effect on LPS-induced TNF-α production in THP-1 macrophages. The preliminary results showed that N phenolic fraction had non-cytotoxicity. Thus, this phenolic fraction was used to test the potential anti-inflammatory effect.

As shown in Figure S5.5, when all sample solutions were treated with LPS, the TNF-α production increased dramatically (indicated by "a" in Figure S5.5) as expected. Surprisingly, we noted that this fraction at 50/ 100 µM of SP concentration treated with LPS alone produced more TNF-α in response

to LPS by comparison with cells treated with LPS only (statistically significant increase of 29, 12, and 24% indicated by “b”, “c”, and “d” in Figure S5.5, respectively). These results suggested that the N fraction had pro-inflammatory effects on THP-1 differentiated cells (Figure S5.5). This effect was also observed when pure sinapine (SP) at 50µM added one hour before/ after LPS but slightly inhibited the TNF-α production (about 6%) when treated with pure SP at 100µM. This phenomenon can be explained that the impurities in the N fraction might cause the pro-inflammatory effect. In the past, Satu Vuorela et al. (Vuorela et al., 2005) also reported that rapeseed phenolic extracted had no anti-inflammatory effect after hydrolyzed with ferulic acid esterase (sinapic acid, in this case, proportioned 64%). Hence, the conclusion in this study was consistent with the previous report (Vuorela et al., 2005).

5.4.4. Conclusions

In this study, an effective method for purifying phenolic compounds by XAD16 resin from byproduct protein isolate from rapeseed meal was established using the design of experiments (DoE). High productivity and recovery can be observed with the adsorption flow rate of 13.3 BV/h and at pH ranging from 2 to 5. The high purity and recovery of phenolic compound in the by-product protein isolation/ purification was found in the case of desorption with ethanol concentration at 30% (v/v). Phenolic fraction showed a higher antioxidant capacity than vitamin C in ABTS assay (IC50/phenolic N fraction < IC50 vitamin C, $p < 0.05$). Phenolic fraction after desorption process did not show the cell cytotoxicity on THP-1 macrophages. Furthermore, this phenolic fraction did not affect anti-inflammatory through inhibition of the TNF-α production in LPS-induced macrophages. This study can provide useful information concerning searching for natural antioxidants that can use in the food domain.

5.5. Conclusion for chapter 5

The main objective of this chapter was to establish an effective way to separate and purify CGA and sinapine from sunflower and rapeseed proteins isolate process. Optimal conditions were determined based on the response surface methodology for enrichment of phenolic compounds from SFM and RSM. The obtained conditions successfully generated enough product to evaluate its antioxidant and anti-inflammatory properties. CGA and sinapine fractions showed a good radical scavenging activities and more powerful than vitamin C. These antioxidant properties of CGA and sinapine fraction could be used in the food antioxidant application. CGA and sinapine fraction showed no cytotoxicity on a human macrophage cell line. Interestingly, the CGA fraction exhibited an anti-inflammatory property via inhibition the LPS-induced TNF-α production. In view of these results, we therefore propose valorizing this abundant effluent to produce a natural antioxidant and anti-inflammatory agent.

Note: Kindly note that the term: “Vitamin C” using in this thesis was ascorbic acid.

Chapter 6. Effect of hydrolysis on capture of phenolic compounds from rapeseed and assessment their antioxidant

6.1. Introduction

We previously introduced in the chapter 5 that rapeseed phenolic compounds are mainly composed of sinapic acid esters. Sinapic acid is a hydroxycinnamic acid widespread in plants (Nićiforović & Abramovič, 2014). The most aboudant rapeseed phenolic compound is an ester of sinapic acid and choline called sinapine (Bell, 1993; Kozlowska et al., 1983). Other hydrophilic non phenolic part may be associated to sinapic acid like glucose-based osides (like sinapoyl glucose) associated. Rapeseed also contain minor phenolic compounds like free sinapic acid (Naczk et al., 1998; Siger et al., 2013). These phenolic compounds are extractible using mild polar solvents like ethanol, isopropanol or methanol (Engels et al., 2012). A previous study showed that rapeseed phenolic compounds possessed interesting antioxidant effects (U. N. Wanasundara et al., 1995). However, other authors reported a weak antioxidant effect of sinapine (Krygier et al., 1982; Thiyam et al., 2006). Interestingly, the antioxidant capacity of rapeseed phenolic extracts was reported to by higher after acid or basic treatment (Siger et al., 2013, p. 20; Thiel et al., 2015). These observations suggest that sinapic acid would be far more antioxidant than its esters but there is a lack of comparative data on that point.

The previous study was focused on rapeseed phenolic capture from an aqueous extract (Moreno-González et al., 2020). Therefore, in this chapter, we presented the adsorption of phenolic compounds with non-hydrolyzed and hydrolyzed permate onto different resins such as XAD4, XAD7, XAD16, XAD1180, and HP20 resins and assess their antioxidant properties. The approach scientific is illustrated in Figure 6.1. First, we produced the rapeseed permate. Then, this permeate was hydrolyzed by acidic method for further studies. In this study, we used chemical (acid) hydrolyse since this method was one of the effective method in increasing the release rate of free phenolic acids (Siger et al., 2013). Therefore, the acidic hydrolysis of this permeate allowed the efficient conversion of sinapine into sinapic acid. In addition, the stability of phenolic acids should be considered during hydrolyzed reaction. According to study of A. Siger et al. (Siger et al., 2013), acidic hydrolysis exhibited the highest recovery of free phenolic acids in comparison with basic method. Finally, the batch adsorption and desorption allowed to obtain phenolic fractions for antioxidant tests.

The purposes of this chapter were therefore to investigate the capture of phenolic compounds from a rapeseed protein isolate by-product obtained by ultrafiltration with or without acidic treatment and to assess their antioxidant activities compared to market references. Phenolic compounds in the aqueous by-product after and before acidic hydrolysis were identified by LC-MS. Five macroporous resins as used in chapter 4 were screened for phenolic compounds capture. Adsorption kinetics and isotherms were studied in order to elucidate phenolic compounds adsorption mechanisms with the more efficient resin. Desorption by ethanol/water mixtures was investigated and obtained purity considered to choose the most appropriate eluent for phenolic compounds capture from this effluent. Finally, the

antioxidant activity of the phenolic fractions obtained after desorption was assessed and compared to sinapine, sinapic acid, and vitamin C standards.

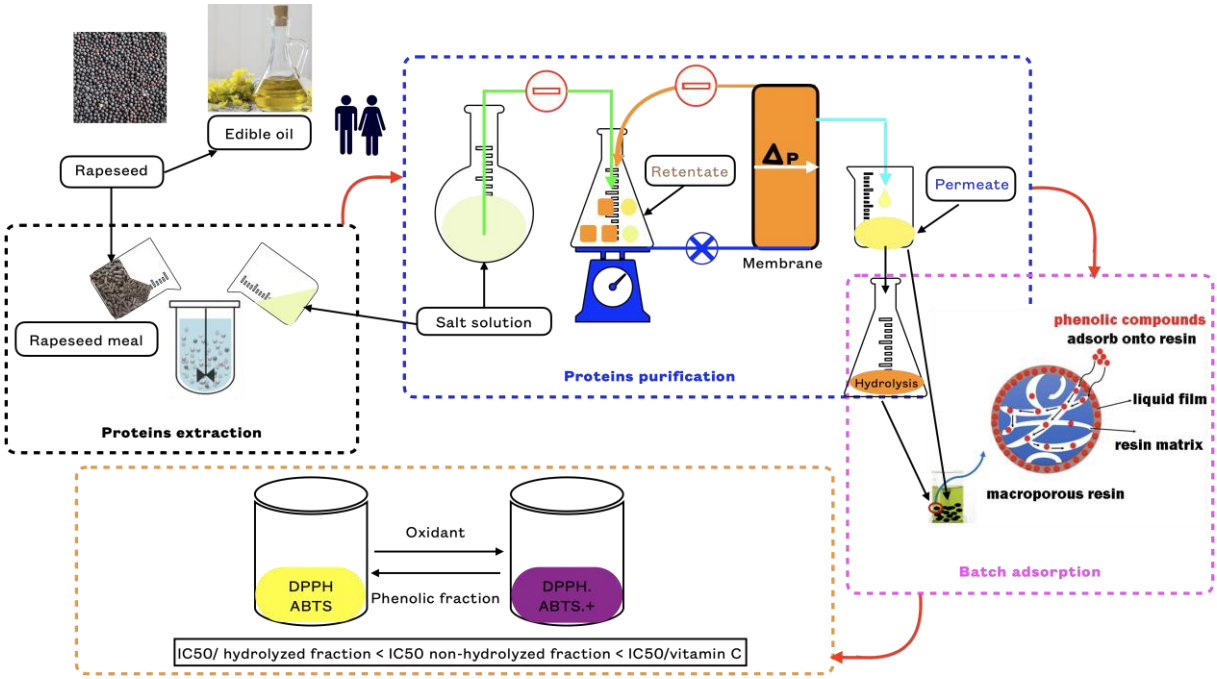

Figure 6.1. Scientific approaches in chapter 6

This chapter of the thesis has been published on the journal *Molecules* (IF = 4.4) with the title: "Identification and capture of phenolic compounds from a rapeseed meal protein isolate production process by-product by macroporous resin and valorization their antioxidant properties" in 2021.

The last section of this chapter, we presented the supporting information regarding the anti-inflammatory property of non-hydrolyzed and hydrolyzed phenolic fraction.

6.2. Manuscript

Identification and capture of phenolic compounds from a rapeseed meal protein isolate production process by-product by macroporous resin and valorization their antioxidant properties

Tuong Thi Le[1,2], Xavier Framboisier [1], Arnaud Aymes [1], Armelle Ropars[2], Jean-Pol Frippiat[2] and Romain Kapel [1]

[1] Laboratoire Réactions et Génie des Procédés, Université de Lorraine, Unité Mixte de Recherche CNRS/Ministère (UMR) 7274, LRGP, F-54500 Vandœuvre-lès-Nancy, France

[2] Stress, Immunity, Pathogens Laboratory, SIMPA UR7300, Université de Lorraine, F-54000 Nancy, France

Abstract

In this study, phenolic compounds from an aqueous protein by-product from rapeseed meal (RSM) were identified by HPLC-DAD and HPLC-ESI-MS, including sinapine, sinapic acid, sin-apoyl glucose, and 1,2-di-sinapoyl gentibiose. The main phenolic compound in this by-product was sinapine.

We also performed acid hydrolysis to convert sinapine, and sinapic acid deriva-tives present in the permeate, to sinapic acid. The adsorption of phenolic compounds was inves-tigated using five macroporous resins, including XAD4, XAD7, XAD16, XAD1180, and HP20. Among them, XAD16 showed the highest total phenolic contents adsorption capacities. The ad-sorption behavior of phenolic compounds was described by pseudo-second-order and Langmuir models. Besides, thermodynamics tests demonstrated that the adsorption process of phenolic compounds was exothermic and spontaneous. The highest desorption ratio was obtained with 30% (v/v) and 70% (v/v) ethanol for sinapine and sinapic acid, respectively, with a desorption ra-tio of 63.19 ± 0.03 % and 94.68 ± 0.013 %. DPPH and ABTS tests revealed that the antioxidant ac-tivity of the hydrolyzed fraction was higher than the one of the non-hydrolyzed fraction, and higher than the one of vitamin C. Antioxidant tests demonstrated that these phenolic com-pounds could be used as natural antioxidants, which can be applied in the food industry.

Keywords

Macroporous resin, adsorption, rapeseed meal, phenolic compounds, sinapine, sinapic acid

6.2.1. Introduction

Rapeseed (*Brassica napus* L.) is an oilseed cultivated worldwide, particularly in Europe and China (11.684 and 11.760 tons/year, respectively) (*FAOSTAT*, 2020a). This resource shows content of phenolic compounds as high as 1.705g of sinapic acid equivalent (SAE)/ 100g of dry matter (Lomascolo et al., 2012). Naczk et al. found that the proportion of rapeseed polar phenolic compounds was ten times higher than other oilseeds (Naczk et al., 1998). Rapeseed phenolic compounds are mainly composed of sinapic acid esters. Sinapic acid is a hydroxycinnamic acid widespread in plants (Nićiforović & Abramovič, 2014). The most aboudant rapeseed phenolic compound is an ester of sinapic acid and choline called sinapine (Bell, 1993; Kozlowska et al., 1983). Other hydrophilic non phenolic part may be associated to sinapic acid like glucose-based osides (like sinapoyl glucose) associated or not with keampferol (like kaempferol-sinapoyl-trihexoside) (Engels et al., 2012; Khattab, 2010; Thiyam et al., 2006). Rapeseed also contain minor phenolic compounds like free sinapic acid, ferulic acid, vanillic acid or syringic acid (Naczk et al., 1998; Siger et al., 2013). These phenolic compounds are extractible using mild polar solvents like ethanol, isopropanol or methanol (Engels et al., 2012). A previous study showed that rapeseed phenolic compounds possessed interesting antioxidant effects (U. Wanasundara et al., 1994). However, other authors reported a weak antioxidant effect of sinapine (Vuolera et al., 2003). Interestingly, the antioxidant capacity of rapeseed phenolic extracts was reported to by higher after acid or basic treatment (Siger et al., 2013, p. 20; Thiel et al., 2015). These observations suggest that sinapic acid would be far more antioxidant than its esters but there is a lack of comparative data on that point.

Rapeseed meal is the main by-product of oil industrial extraction processes. Its annual production reached 70 million tons in 2019 (*FAOSTAT*, 2020a). Rapeseed meal contains around 30% protein, 16% carbohydrates, and 3% of phenolic compounds (Nadathur et al., 2016). The phenolic

fraction is composed of polar phenolic compounds, sinapic acid esters (61-70% sinapine, 14-27% SG) and sinapic acid (7-10% SA) (Thiyam-Holländer et al., 2012). To date, rapeseed meal is used for animal nutrition (Downey & Bell, 1990). Many reports showed the possibility to use it as a resource for protein isolate production (Quinn et al., 2017). Protein isolates are protein-based products with a high protein content (>90% on a dry mater basis) used in human nutrition (Tzeng et al., 1990). Rapeseed protein isolate production is classically based on a solid liquid extraction using aqueous solvents (modulated by pH and ionic strength), a clarification step and a protein purification step. The purification is most often achieved either by tangential filtration or isoelectric precipitation (Defaix et al., 2019). Polar phenolic compounds are extracted with proteins during the extraction step and parted from proteins during the protein purification step. At the end of the purification process, phenolic compounds are in an aqueous by-product alongside with soluble low molar weight osides, minerals and non-protein nitrogen containing molecules. The valorization of this by-product is of a crucial importance for industrial viability of rapeseed protein isolate production. The capture of phenolic compounds could be an interesting valorization strategy.

Macroporous resins are particularly promising for phenolic compounds capture from plant extracts (Moreno-González et al., 2020; Weisz et al., 2010). Indeed, it can be easily scaled up and some resins are food grade (Scordino et al., 2003). The separation with adsorption resins is based on differential affinity between phenolic compounds, impurities and the adsorbent (P.-C. Sun et al., 2015). The process is also impacted by complex transport phenomenon (diffusive and convective transport in the liquid phase, diffusive transport from the liquid phase to the solid adsorbant throughout a limit layer and diffusive transport inside the adsorbant pores) (Firdaous et al., 2017; Tuong Thi Le et al., 2020). Some study reports the adsorption of rapeseed phenolic compounds on macroporous resins. Most of them used solvent extracts from seeds or meals (Khattab, 2010; Siger et al., 2013).

A recent study was focused on rapeseed phenolic capture from an aqueous extract (Moreno-González et al., 2020). However, the transport mechanism were not investigated. Furthermore there is a lack of comparative data concerning the adsorption of rapeseed phenolic compounds with and without hydrolysis (i.e esterified sinapic acid and free sinapic acid) and their antioxidant activities.

The aim of this work was therefore to investigate the capture of phenolic compounds from a rapeseed protein isolate by-product obtained by ultrafiltration with or without acidic treatment and to assess their antioxidant activities compared to market references. Phenolic compounds in the aqueous by-product after and before acidic hydrolysis were identified by LC-MS. Five macroporous resins having various properties were screened for phenolic compounds capture. Adsorption kinetics and isotherms were studied in order to elucidate phenolic compounds adsorption mechanisms with the more efficient resin. Desorption by ethanol/water mixtures was investigated and obtained purity considered to choose the most appropriate eluent for phenolic compounds capture from this effluent. Finally, the antioxidant activity of the phenolic fractions obtained after desorption was assessed and compared to sinapine, sinapic acid, and vitamin C standards.

6.2.2. Results and discussion

6.2.2.1. Characterization of the ultrafiltration (UF) permeate from rapeseed protein isolate production and effect of the acidic hydrolysis

6.2.2.1.1. Identification of phenolic compounds in the ultrafiltration (UF) permeate

Figure 6.2A shows the SE-HPLC chromatogram at 325 nm of the ultrafiltration (UF) permeate. This permeate was obtained from a rapeseed albumin isolate production process recently patented (Albe-Slabi et al., 2021; Defaix et al., 2020). A main peak can be observed at 18.94 min of retention time alongside with marginal signals at 23.31, 28.33 and 31.68 min. ESI-MS analysis revealed that this peak contained molecules with *m/z* of 310 (positive mode), 385, 753, and 223 (negative mode) (Table 6.1). This corresponded to sinapine (SP), sinapoyl glucose (SG), 1,2-di-sinapoyl gentiobise, and sinapic acid (SA) respectively. The identification of sinapine and sinapic acid was confirmed by injection of standards. Khattab et al. (Khattab, 2010) also identified SP, SA, and SG from canola / rapeseed organic solvents extracts such as 70% ethanol, 70% methanol, or 70% iso-propanol (v/v). In the UF permeate, SP, other identified SA esters and SA represented 59.78%, 21.66% and 2.84% in proportion respectively. Only 15.72% of the phenolic compounds remained unidentified. These observations also agreed with the report from Thiyam-Holländer et al. (Thiyam-Holländer et al., 2012). In their study, the de-oil rapeseed were extracted by distilled water with ratio 1:10 (w/v) for 10 min. The unidentified compounds were most probably other polar sinapic acid esters.

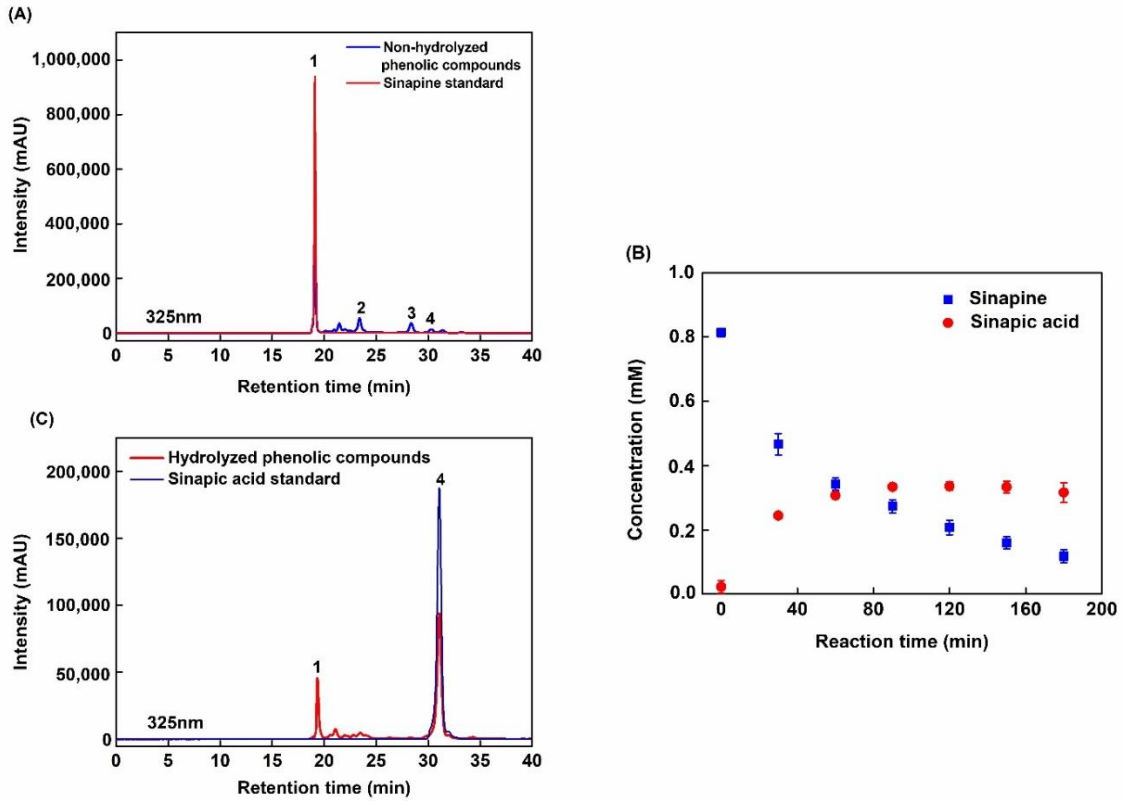

Figure 6.2. SE-HPLC chromatogram and structures of phenolic compounds detected in the UF permeate obtained from rapeseed protein purification.

Chromatograms were recorded at 325 nm. (A) Non-hydrolyzed phenolic compounds. (B) Kinetic curve of permeate hydrolysis reaction. (C) Hydrolyzed phenolic compounds.

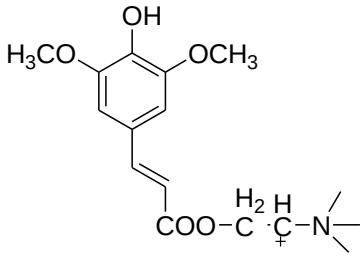

(1) sinapine

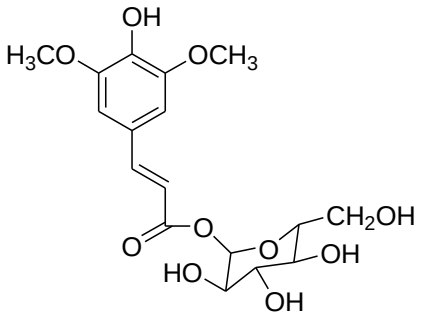

(2) sinapoyl glucose

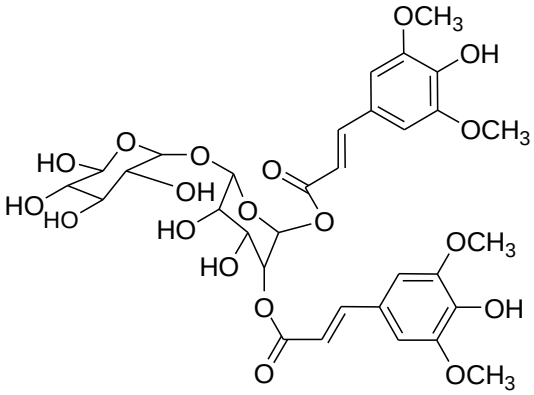

(3) 1,2-di-sinapoyl gentiobise

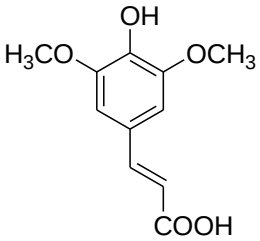

(4) sinapic acid

Figure 6.3. Chemical structures of phenolic compounds (1) Sinapine, (2) sinapoyl glucose, (3) 1,2-disinapoyl gen-tiobiose, and (4) sinapic acid. Different numbers indicated the position of phenolic compounds presented in the HPLC chromatogram.

Table 6.1. Retention time (t_R) and MS data of the peaks detected by HPLC-DAD and HPLC-MS in permeate and hydrolyzed permeate from rapeseed meal.

Peak	Compound identity	t_R (min)	m/z	Molecular weight
1	Sinapine	18.94	310 $[M-H]^+$	310
2	Sinapoyl glucose	23.31	385 [M-H]-	386
3	1,2-di-sinapoyl gentiobise	28.33	753 [M-H]-	754
4	Sinapic acid	31.68	223 [M-H]-	224

6.2.2.1.2. Kinetics of sinapine acid hydrolysis in the UF permeate

Figure 6.2B shows SP and SA kinetics during acidic hydrolysis of the UF permeate. Initial SP concentration was around 0.8 mM (i.e 0.25 g/L) and continuously decreased during 180 min to reach less than 0.1 mM. SA concentration increased dramatically during the first 60 min and get stabilized after 90 min at around 0.35 mM. During this period, the amount of SA increased from 23.35 mg/100 g to 135.18 mg/100 g rapeseed meal. This suggests that the chemical hydrolysis of SP ester bond into SA

reached an equilibrium. Hence, the SP concentration decrease after 90 min was surprising. This indicated a degradation into other molecules with no UV property at 325 nm. It can be hypothesized a degradation of the benzene ring. Interestingly, at 180 min the purity of SA was the highest (63.66%). SP was still present but at a low proportion (17.44%). So, this reaction duration was chosen for further study of phenolic compounds capture and bioactivity characterization.

A. Siger et al. (Siger et al., 2013) found that the contents of sinapic acid after acidic hydrolysis of in two rapeseed extracts from two cultivars were 93.2 mg/100 g (cv. Visby) and 89.4 mg/100 g (cv. Bellevue). The SA content observed in our study is slightly higher (135.18 mg/100 g). This could be due to a difference in starting material or to the solvent used for extraction. Indeed, these authors used methanol while we used an aqueqous solvent (NaCl 0.11 M at pH 2). This could also be due to a difference in hydrolysis step duration (during 20 min at 90°C).

6.2.2.1.3. Method validation

The validation of the SE-HPLC method was performed according to the International Conference on Harmonisation (ICH) of technical requirements for registration of pharmaceuticals for human use (Tietje & Brouder, 2010) recommendations. All experiments were conducted in triplicate. The parameters such as LOD (limit of detection), LOQ (limit of quantification), and standard deviation (SD) values were determined and are summarized in Table 6.2 using pure standards such as sinapine and sinapic acid.

Table 6.2. Parameters of the calibration curves for pure sinapine and sinapic acid.

Phenolic Compounds	Regression Coefficient (R^2)	LOD (µg/mL)	LOQ (µg/mL)
Sinapine	0.9998	0.25	0.60
Sinapic acid	0.9984	0.25	0.60

As listed in Table 6.2, the LODs of sinapine and sinapic acid were 0.25 µg/mL. The LOQs of sinapine and sinapic acid were 0.6 µg/mL. These low values of LOD and LOQ demonstrated a high sensitivity of the developed SE-HPLC technical method. The linearity of calibration curves was constructed with three measurements for each calibration point ranging from 0.05 to 1.25 mg/mL. A strong linear correlation ($R^2 > 0.99$) between the concentration and the peak area was observed. Preliminary results showed that the retention time and peak area were almost similar with intra- and inter-day standard deviation (SD) values less than 0.12 and 1.9 for the retention time and peak area, respectively. These results revealed the good performance of the developed analytical method for quantification of phenolic compounds such as sinapine and sinapic acid within the permeate with and without hydrolysis.

6.2.2.2. Phenolic componds capture

6.2.2.2.1. Resin screening

Figure 6.4 shows the adsorption capacity of total phenolic content (TPC), sinapine, and sinapic acid from permeate and hydrolyzed permeate on XAD4, XAD7, XAD16, XAD1180, and HP20 resins. Table 7 displays resins properties. XAD4, XAD16, XAD1180, and HP20 are nonpolar resins made out

of SDVB polymers. They differ by bead and pore size (50-300 Å). XAD7 is composed of acrylamide polymer which is considered as mild polar (Tuong Thi Le et al., 2020). All these resins were demonstrated to adsorb phenolic compounds from many different plant extracts (Dong et al., 2015b; Q. Yang et al., 2016). The adsorption of TPC from non-hydrolyzed permeate ranged from about 11 (for XAD4 and XAD7) to 12.5 mgSAE/g (for XAD16) of dry resins (Figure 6.4A). Interestingly, the adsorption of sinapine (main phenolic compound in non-hydrolyzed permeate) was similar to TPC, ranging from 11 (for XAD7) to 13.5 mg/g (for XAD16) of dry resin (Figure 6.4A).

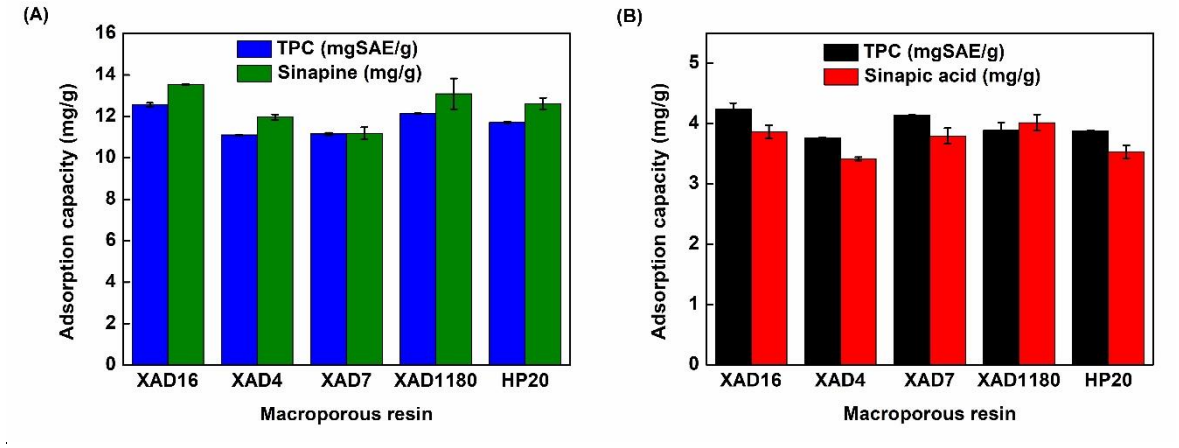

Figure 6.4. Adsorption capacity of phenolic compounds after adsorption of UF permeate without (A) or with acidic hydrolysis (B) using XAD4, XAD16, XAD7, XAD1180, and HP20 resins.

Results are given in terms of total phenolic compounds and the main phenolic compound of the starting product (sinapine and sinapic acid without and with hydrolysis respectively).

Notably, XAD4 showed the lowest adsorption capacity of TPC (about 3.7 mgSAE/g of dry resin) and of sinapic acid (about 3.25 mg/g of dry resin) in hydrolyzed permeate (Figure 6.3B). On the other hand, XAD16 showed the highest adsorption capacity of TPC (4.1 mgSAE/g of dry resin) and of sinapic acid (3.9 mg/g of dry resin) (Figure 6.3B).

The adsorption capacity depends on molecule affinity toward the material and the specific surface (Z. Xu et al., 1999). This last parameter is conditioned by bead size and can be modulated by pore size if it limits the molecule inner accessibility (Tuong Thi Le et al., 2020). Pore ≤ 50 Å were shown to limit the diffusion of phenolic compounds into particle's pores by steric hindrance (Dong et al., 2015b; Z. Xu et al., 1999). Among SDVB resins, XAD16 showed the highest specific area (900 m^2/g) followed by XAD4, XAD1180, and HP20. Interestingly, this ranking corresponded to observed capacity values. This indicates that SDVB resin capacities were essentially governed by specific area. It can be hypothesized that XAD4 low pore size (50 Å) did no yield additional diffusion limitation. The adsorption behavior of phenolic compounds in non-hydrolyzed and hydrolyzed permeates onto SDVB resins and mild polar resin (XAD7) had the same pattern. Probably, the interaction of sinapine (Figure 6.2) (a main phenolic compound in non-hydrolyzed permeate) and sinapic acid (a main phenolic

compound in hydrolyzed permeate) (Figure 6.3) and SDVB resins were through pi-pi stacking interaction (aromatic ring part of phenolic compounds and benzene rings of SDVB resins) (Tuong Thi Le et al., 2020). XAD16 and XAD1180 showed the highest adsorption capacity of TPC from non-hydrolyzed and hydrolyzed permeates. However, XAD16 had the highest adsorption capacity of sinapine and sinapic acid. The very high specific area of XAD16 (900 m^2/g) showed better adsorption in terms of massic capacity than XAD7 or HP20 with a similar specific area (450 or 500 m^2/g). So, the adsorption kinetics, isotherms, thermodynamics properties, and phenolic compounds desorption were further investigated with this resin.

6.2.2.2.2. Adsorption kinetics

Adsorption kinetics of the main phenolic compounds from UF permeate with (sinapic acid) or without hydrolysis (sinapine) on XAD16 are presented in Figure 6.5A-B. Very similar trends were observed. A large part of phenolic compounds was quickly adsorbed (up to 90% of the equilibrium capacity in 30 min). Then, the kinetics slowed down up to the equilibrium observed between 60 min and 120 min. As expected from resin screening results, this indicated that XAD16 has a strong affinity toward rapeseed phenolic compounds. Such a behavior was also reported for *adlay bran* phenolic compounds (Q. Yang et al., 2016).

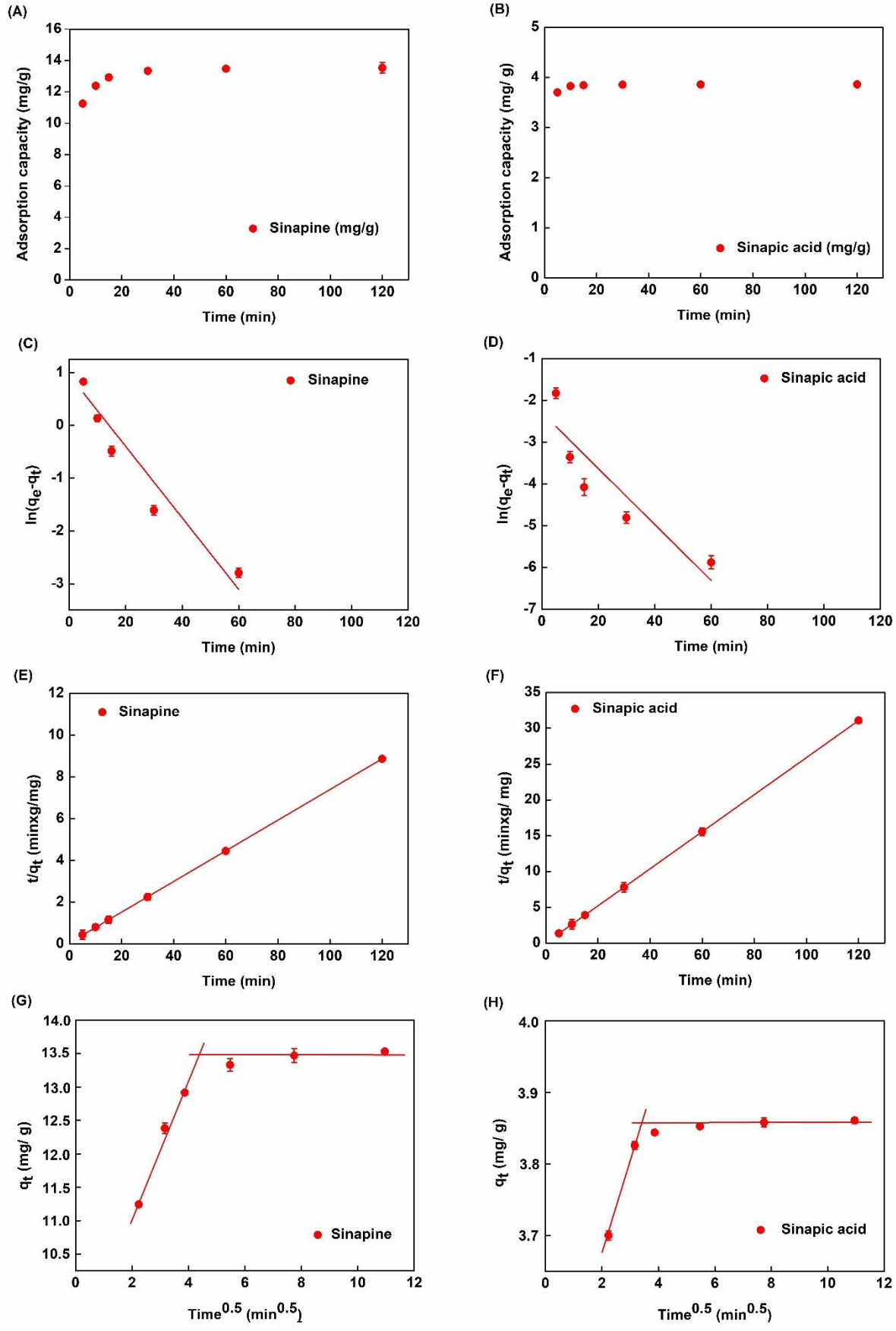

Figure 6.5. Adsorption kinetics with XAD16.

(A, B) adsorption kinetic curve. (C, D) pseudo-first-order model. (E, F) pseudo-second-order model. (G, H) intra-particle diffusion model (in linearized forms) of SP and SA in non-hydrolyzed and hydrolyzed permeates, respectively.

Adsorption kinetics were regressed with pseudo-first-order (PFO, (Lagergren, 1898)) and pseudo-second-order (PSO, (Ho & Mckay, 1998)) equations in linearized form (Figure 6.5C – F). Table 6.3 summarizes the corresponding equations, model parameter values and R^2 of the linear regressions.

Table 6.3. Kinetic parameters for sinapine and sinapic acid adsorption onto XAD16 resin in non-hydrolyzed and hydrolyzed permeates.

Kinetic model	**Equation**	**Parameter**	**Phenolic compound**	
			Sinapine	**Sinapic acid**
Pseudo-first-order (PFO)	$\ln(q_e - q_t) = \ln(q_e) - k_1 t$	k_1 (1/min)	0.0627	0.0619
		$q_{e,exp}$ (mg/ g)	13.532	3.861
		$q_{e,cal}$ (mg/ g)	3.83	0.29
		R^2	0.9381	0.8113
Pseudo-second-order (PSO)	$\frac{1}{q_t} = \frac{1}{k_2 q_e^2} + \frac{t}{q_e}$	k_2 (g/mg x min)	0.0733	0.2587
		$q_{e,exp}$ (mg/ g)	13.532	3.861
		$q_{e,cal}$ (mg/ g)	13.544	3.861
		R^2	1	1
Intra-particle diffusion	$q_t = kt^{0.5} + C$	$k_{i,1}$ (mg/g)/min$^{0.5}$	1.0321	0.09
		C_1 (mg/g)	8.9921	3.5118
		R^2	0.9828	0.9639
		$k_{i,2}$ (mg/g)/min$^{0.5}$	0	0
		C_2 (mg/g)	13.532	3.861

The R^2 obtained with linearized PFO ($\ln(q_e\text{-}q_t)$ *vs.* t) was less than 0.94 for both sinapine and sinapic acid. Furthermore, the calculated q_e for XAD16 (0.32 mg/g and 0.29 mg/g for sinapine and sinapic acid, respectively) was found very different from experimental values (13.52 and 3.86 for sinapine and sinapic acid, respectively). On the other hand, R^2 of the linear regression of the t/q_t *vs* t plot was very close or equal to 1 (0.999 and 1). Moreover, the calculated q_e (13.54 and 3.86 mg/g for sinapine and sinapic acid) predicted from PSO model was very near the experimental values of q_e (13.53 and 3.86 mg/g for sinapine and sinapic acid). These results indicate that adsorption kinetics followed a PSO model for the XAD16 resin. This was also observed with adsorption of chlorogenic acid from by-product proteins isolates on XAD16 resin (Tuong Thi Le et al., 2020).

Solute transport phenomena are complex in adsorption processes. In the liquid phase, solutes are transported by convection and diffusion. There is also a diffusive transport from the liquid phase to the bead surface (through a limit liquid film) and a diffusive transport inside the particle's pores. Adsorption kinetics may be modulated by several diffusional types of transports. The intra-particle diffusion model (Weber & Morris, 1963) is commonly used to investigate the diffusive rate-controlling phenomenon (Annadurai & Krishnan, 1997; Firdaous et al., 2017).

Figure 6.5G - H show q_t *vs* $t_{1/2}$ plots obtained with the XAD16 resin. These plots correspond to the linear form of the intra-particle diffusion model (Table 6.2). The slopes represent the constant rate (k_i) of each adsorption step while C_i (intercept at y-axis) is related to the thickness of the limiting layer. R^2, k_i, and C_i values obtained from linear regressions are displayed in Table 6.3. Interestingly, k_1 (0.103

and 0.09 (mg/g)/min$^{0.5}$) for sinapine and sinapic acid, respectively) are by far higher than k_2 (approximately 0). These differences might come from the smaller molecular size of sinapic acid than sinapine. It can also be noticed that R^2 values for sinapine and sinapic acid are 0.9828 and 0.9639, respectively. This indicates that for both liquid effluents, the adsorption process is limited by two diffusional effects. In the previous study, the similar pattern was also observed with the adsorption of chlorogenic acid onto XAD16 resin (Tuong Thi Le et al., 2020). Very similar results were observed with the adsorption of alfalfa phenolic compounds on HP20 and AER1 resins (Firdaous et al., 2017). It was interpreted as a two steps adsorption process. The first one is related to the diffusional transport throughout the boundary layer at the liquid/beads interface. Its high rate constant ($K_{i,1}$ was 1.03 and 0.09 (mg/g)/min$^{0.5}$) for sinapine and sinapic acid, respectively) indicates a low diffusional limitation at this stage. The second one is due to intraparticle diffusion. The low rate constant ($K_{i,2}$ approximately equal to 0 for both liquid effluents) indicates a stronger diffusional limitation. Such observation and explanation were also made by others (Y. Chen et al., 2016; Dong et al., 2015b).

6.2.2.3. Adsorption isotherms

Figure 6.6 shows adsorption isotherms of sinapine and sinapic acid onto XAD16 at 25°C. Data were regressed with Langmuir (Figure 6.4A,C) and Freundlich (Figure 6.4B,D) equations as commonly done elsewhere (B. Liu et al., 2016; P.-C. Sun et al., 2015; Weisz et al., 2013). Table 6.4 lists the R^2 of the regression, equations, and model parameters with sinapine and sinapic acid. R^2 values indicated that experimental data were better fitted by the Langmuir model (0.997 and 0.9999 for sinapine and sinapic acid, respectively) than by the Freundlich model (0.996 and 0.9978 for sinapine and sinapic acid, respectively). This indicated that the same adsorption mechanism took place in any cases. This consisted in a monolayer adsorption of phenolic compounds at the surface of the resin (B. Liu et al., 2016; P.-C. Sun et al., 2015; Weisz et al., 2013). These findings also are in agreement with another work on chlorogenic acid adsorption on XAD16 resin from sunflower meal (Tuong Thi Le et al., 2020).

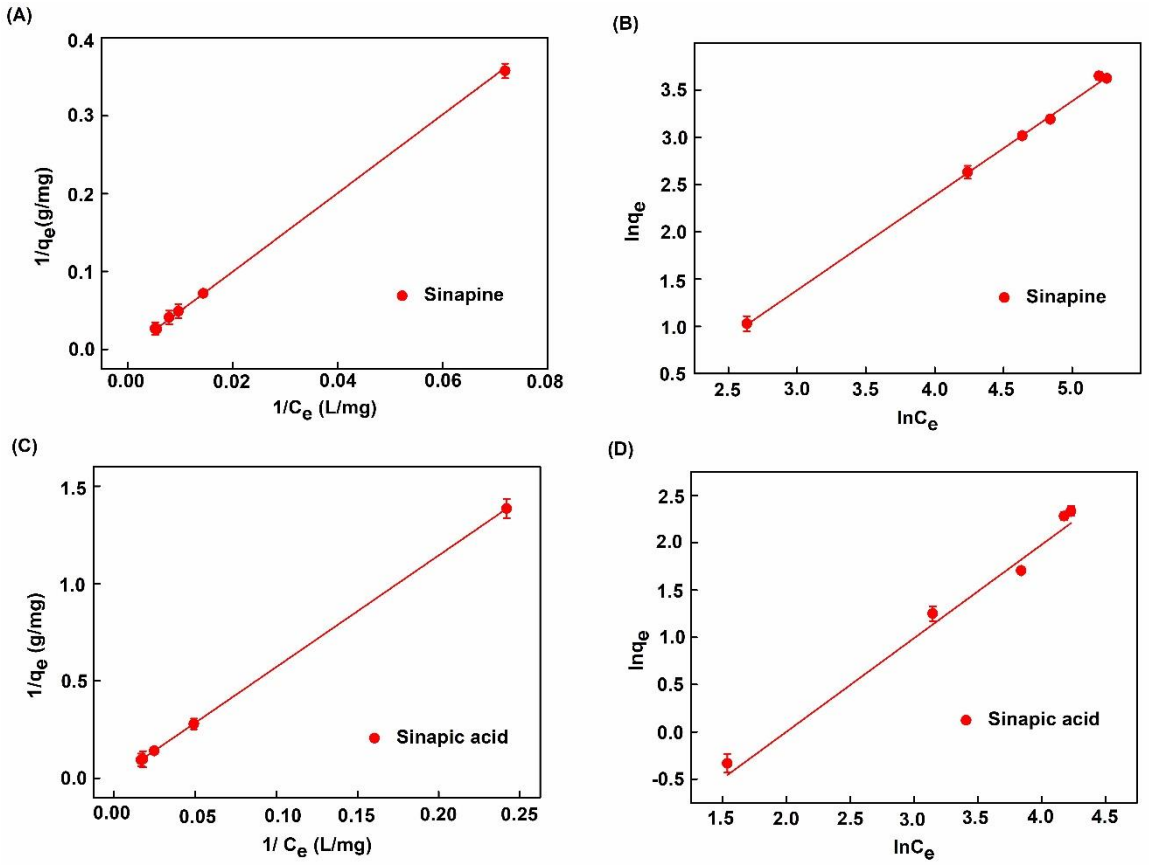

Figure 6.6. Adsorption isotherms of phenolic compounds on XAD16 with Langmuir and Freundlich linear models.

(A, B) Langmuir and Freundlich models for sinapine. (C, D) Langmuir and Freundlich models for sinapic acid

Table 6.4. Adsorption isotherm equation and parameters of sinapine, and sinapic acid adsorption onto XAD16 resin.

Isotherm model	**Parameter**	**Phenolic compound**	
		Sinapine	**Sinapic acid**
Langmuir $q_e = \frac{Q_{max} K_L C_e}{1 + K_L C_e}$	Q_{max} (mgSAE/ g)	35.93	23.96
	K_L (L/ mg)	124.29	0.076
	R^2	0.997	0.9999
Freundlich $q_e = K_F C_e^n$	K_F (mg/g)/ (mg/L)^n	0.1988	0.1562
	n	0.9987	0.9892
	R^2	0.996	0.9978

Moreover, this finding is consistent with that of Moreno-González et al. (Moreno-González et al., 2020) about the adsorption of sinapic acid from canola/rapeseed meal using the FPX66 resin. The maximum adsorption capacity of sinapine and sinapic acid was 35.93 mg/g (0.12 mol/g) and 23.96 mg/g (0.11 mol/g) of dry resin, respectively (Table 6.4). The values obtained in this study suggest that the adsorption onto resin material implies interaction with the same part of the molecule (sinapine and sinapic acid) without the interference of the choline part (quaternary ammonium group, Figure 6.3).

This observation has never been published. Meanwhile, according to Moreno-González et al. (Moreno-González et al., 2020), the maximum adsorption capacity for sinapic acid was lower (about 15 mg/g or 0.07 mol/g) onto the non-polar (SDVB) FPX66 resin. The different values might be due to other organic compounds such as carbohydrates, amino acids, and proteins in raw materials. It might also be due to the impact of ionic strength. Moreover, the difference in physical characteristics also caused the difference in adsorption capacity. Thiel et al. (Thiel et al., 2013) investigated the adsorption of sinapic acid and other compounds onto zeolites and hydrophobic resins, including XAD16, the resin used in this study. These authors claimed that the adsorption capacity of sinapic acid was higher than the one presented here (44.5 mg/g or 0.20 mol/g of dry resin). However, these authors evaluated the experiments at different pH (pH 5) and used different starting materials; rapeseed meal extracted with heated deionized water at 70°C at a ratio of 1 : 8 (solid : liquid) that might explain the difference in these values.

6.2.2.4. Determinations of thermodynamic parameters

The effect of temperature on the adsorption capacity of phenolic compounds from the XAD16 resin in the two liquid effluents were investigated to obtain the thermodynamic parameters of adsorption. Langmuir model parameters and R^2 are listed in Table 6.5. ΔH and ΔS were determined through the slope and intercept of ln K_L against 1/T (Eq. 6.2,3) (Figure 6.7A-B) according to Van Hoff's equation. Enthalpy changes (ΔH) for sinapine and sinapic acid adsorption process on XAD16 resin were -2.56, and -2.72 kJ/mol, respectively (Table 6.5). Negative values indicate an exothermic adsorption process. The fact that values were less than 43 kJ/mol demonstrates that the adsorption process of phenolic compounds on the XAD16 resin was governed by physical rather than chemical interactions (Q. Yang et al., 2016). This demonstrates that the XAD16 resin would not undergo structural changes during phenolic compounds' adsorption process. Therefore, adsorption of phenolic compounds on the resin only takes place through physical mechanism with no chemical reactions. This observation was also reported by Z. P. Gao et al. (Z. P. Gao et al., 2013) who studied the adsorption of polyphenols from kiwifruit juice using AB-8 resin (Guo, Qiao, et al., 2018). In addition, the entropy changes (ΔS) values of XAD16 were -55.95 and -8.37 kJ/molK for sinapine and sinapic acid, respectively. These negative values suggest a random adsorption process at the solid-liquid interface (Gupta, 1998) which happened owing to the desorption process of water molecules previously adsorbed onto the resins' surface (Z. P. Gao et al., 2013). The negative free energy change (ΔG) deduced from ΔH and ΔS (Table 6.4) suggests that phenolic compounds adsorption onto the XAD16 resin was a spontaneous process. Moreover, the absolute value of $\Delta G < 20$ kJ/mol confirmed physical adsorption of phenolic compounds onto XAD16 resin (Ding et al., 2012; Z. P. Gao et al., 2013).

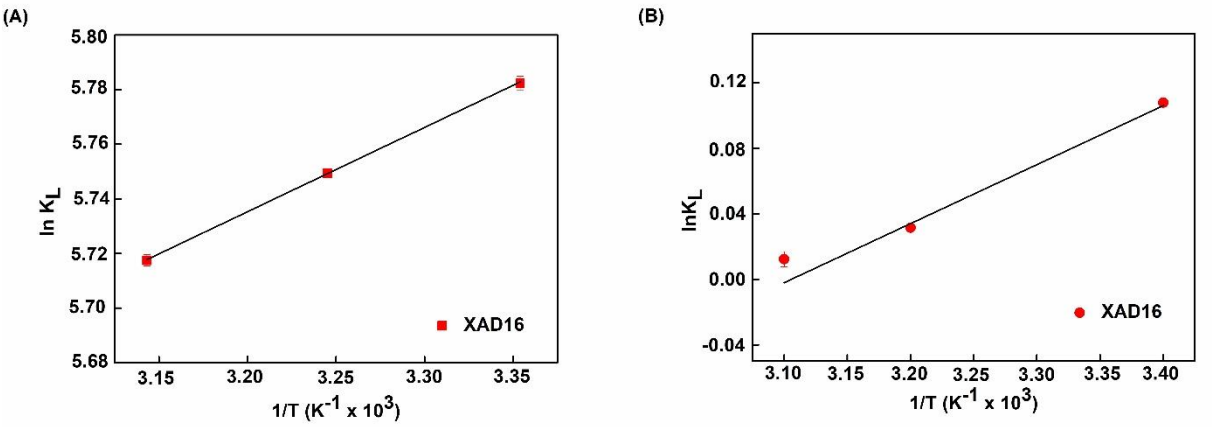

Figure 6.7. ln K_L vs. 1/T plot of adsorption equilibrium constant K_L using Langmuir isotherm of (A) Sinapine and (B) Sinapic acid.

Table 6.5. Thermodynamic parameters of sinapine and sinapic acid adsorption onto XAD16 at 25°C, 35°C and 45°C.

Non-hydrolyzed permeate	Temperature (°C/K)	ΔS (kJ/molK)	ΔH (kJ/mol)	ΔG (kJ/mol)
Sinapine	25/ 298.15			-13.34
	35/ 308.15	-55.95	-2.56	-17.28
	45/ 318.15			-15.56
Sinapic acid	25/ 298.15			-0.267
	35/ 308.15	-8.37	-2.72	-0.08
	45/ 318.15			-0.03

6.2.2.5. Desorption of phenolic compounds from the XAD16 resin

To assess the effect of ethanol concentration on desorption, five ethanol concentrations were evaluated: 30, 50, 70 and 90% (v/v). Preliminary results showed that the desorption curve reaches equilibrium after 120 min (data not shown). As shown in Figure 6.8, ethanol concentration significantly influenced SP and SA desorption ratio. The highest of desorption ratio of sinapine and sinapic acid was observed with ethanol 30% and 70% (v/v) ($p < 0.05$), respectively. These results indicate that desorption ratio was influenced by ethanol concentration and the solubility of phenolic compounds in the desorption phase. Indeed, sinapine is a polar compound demonstrating a good desorption ratio with ethanol at a lower concentration. Sinapic acid is by far less polar therefore presenting the higher desorption ratio at a higher ethanol concentration. Surprisingly, the desorption ratios of sinapic acid and sinapine in this study were much higher than in the report of Thiel et al. (Thiel et al., 2013, 2015) (about 44% and 3.7% for SA and SP) who used the same macroporous resin (XAD16) and desorption with 70% aqueous ethanol. However, a high desorption ratio of sinapic acid was also found by Moreno-González et al. (Moreno-González et al., 2020) with 70% (v/v) of ethanol.

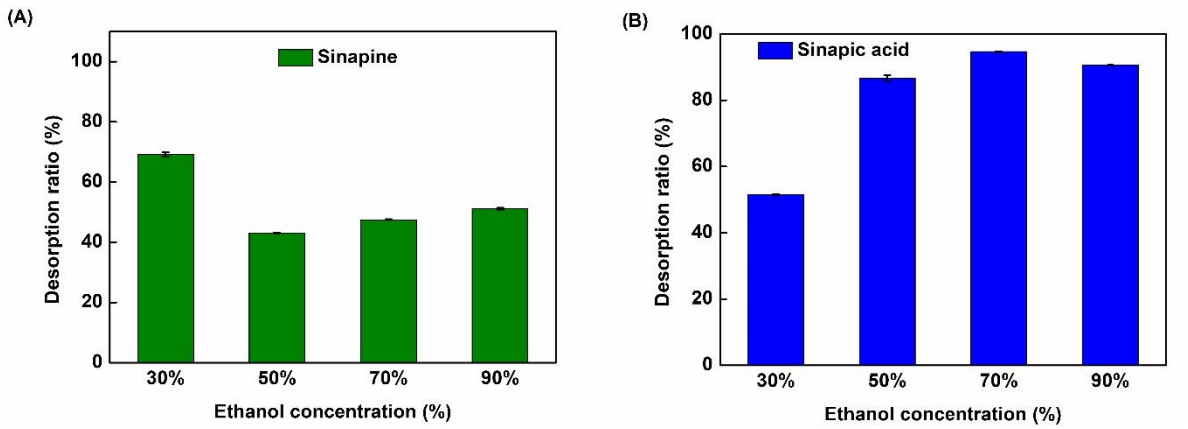

Figure 6.8. Desorption ratio of sinapine (A) and sinapic acid (B) from the XAD16 resin at different ethanol concentrations.

Figure 6.9 shows the HPLC chromatogram of phenolic compounds after purification with the XAD16 resin. The peaks of sinapine (Figure 6.9A) and sinapic acid (Figure 6.9B) are highlighted in the desorption fractions. Sinapine (63.31%) and sinapic acid (73.00%) are the mains phenolic compounds in the hydrolyzed fraction after purification. As different compositions of phenolic compounds after purification might lead to different biological actions, we used both fractions to assess the antioxidant activity in subsequent experiments.

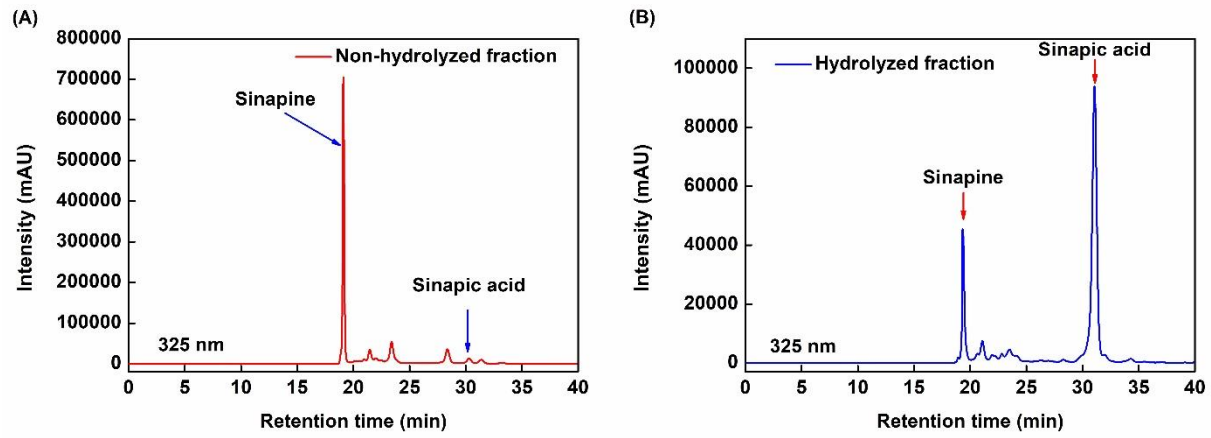

Figure 6.9. HPLC chromatogram of phenolic compounds in (A) the non-hydrolyzed fraction after desorption with ethanol 30% (v/v) and (B) the hydrolyzed fraction after desorption with ethanol 70% (v/v).

6.2.2.6. *In vitro* antioxidant activity

The free radical scavenging rate of DPPH was determined to assess the antioxidant activity of the non-hydrolyzed and hydrolyzed fractions by comparison to pure SP, SA and vitamin C. As shown in Figure 6.10A, scavenging rate increased with the concentration of non-hydrolyzed fraction (N fraction). The same was observed for the hydrolyzed fraction (H fraction) but in this case, interestingly, we observed scavenging rates higher than the ones obtained with vitamin C at 5, 10 and 20 µg/mL. These results were confirmed by the ABTS assay (Figure 6.10B).

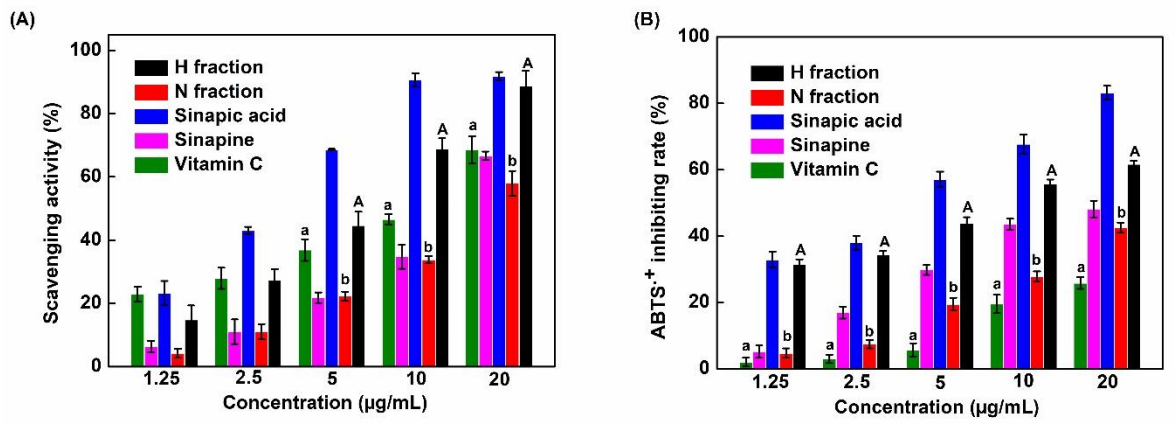

Figure 6.10. Scavenging activity of the non-hydrolyzed (N fraction) and hydrolyzed (H fraction) fractions compared to pure sinapine, sinapic acid and vitamin C determined using (A) DPPH assay and (B) ABTS assay.

Bars labeled with the different lowercase letters and uppercase letters are significantly different ($p < 0.05$).

Table 6.6 presents IC50 values of compounds tested using DPPH and ABTS assays. These data demonstrate that the antioxidant activity of the hydrolyzed phenolic fraction was stronger than the one of the non-hydrolyzed fraction and vitamin C in both assays. These findings are likely due to the enrichment of the hydrolyzed fraction in sinapic acid as this compound exhibited the lowest IC50 values.

Table 6.6. IC50 values of compounds tested using the DPPH and ABTS assays

Antioxidant	IC50/ DPPH (µg/mL)	IC50/ ABTS (µg/mL)
N fraction	10.05 ± 0.025a	22.70 ± 0.021a
H fraction	4.26 ± 0.012b	10.60 ± 0.029b
Sinapine standard	7.58 ± 0.017c	17.98 ± 0.016c
Sinapic acid standard	2.16 ± 0.001d	5.51 ± 0.010d
Vitamin C	7.27 ± 0.019e	36.31 ± 0.021e

Different letters in the same column for the IC50/ DPPH and IC50/ ABTS indicate significant differences ($p < 0.005$) between individual sample treatments.

It has already shown that phenolic compounds found in RSM are excellent antioxidants. Previous studies showed that the antioxidant activity is most likely due to vinylsyringol found in rapeseed oil (Ding et al., 2012; Thiyam-Holländer et al., 2012). In this study, we show that sinapic acid has also strong antioxidant properties. Interestingly, the hydrolyzed fraction (containing mainly SA) was more effective than the non-hydrolyzed fraction (mainly containing SP) and vitamin C. These observations are in accordance with the report of Vourela et al. (Vuorela et al., 2003) who investigated the antioxidant function of phenolic compounds in rapeseed oil. Other researchers also indicated that the high concentration of phenolic compounds is related to a high antioxidant capacity (Leyton et al., 2017; Siger et al., 2013; Thiyam et al., 2006) and our previous study (Le et al., 2021) also indicated that the high concentration of phenolic com-pounds is related to a high antioxidant capacity. Taken together, these data indicate that phenolic compounds isolated from RSM are interesting natural antioxidants that could be used in food industry or other applications (Le et al., 2020).

6.2.3. Materials and methods

6.2.3.1. Materials

The rapeseed meal was provided by Olead (Pessac, Bordeaux,France). Sinapine standard was purchased from ChemScience (JJ08852, Monmouth JunctionCity, NJ, USA). Sinapic acid and formic acid (FA) were obtained from Sigma-Aldrich (St. Louis, Missouri, USA). Sodium chloride (NaCl) and sodium hydroxide (NaOH) pellets were purchased from VWR (Radnor, Pennsylvania, USA). Chlorohydric acid (HCl) 37% was from CarloErba (Val-de-Reuil, France). Acetonitrile (ACN) solution was provided by Biosolve BV (Valkensward, the Netherlands). Absolute ethanol (EtOH) was purchased from DASIT (France). All solvents and chemical reagents used in this study were analytical and high-performance liquid chromatography (HPLC)-grade. 1,1-diphenyl-2-picrylhydrazyl (DPPH), 2,2'-azino-bis-(3-ethylbenzothiazoline-6-sulfonic acid) (ABTS), potassium persulfate, and ascorbic acid (vitamin C) were provided by Sigma-Aldrich (St. Louis, Missouri, United States).

Five macroporous resins (XAD7, XAD4, XAD16, XAD1180, and HP20) were purchased from Sigma-Aldrich (St. Louis, Missouri, USA). The characteristics of these macroporous resins are shown in Table 6.7.

Table 6.7. Characteristics of the resins used in this study.

Resins	Material	Polarity	Specific surface (m^2/g)	Pore (Å)
XAD 4	SDVB*	Non-polar	725	50
XAD 7	Acrylate	Polar	450	90
XAD 16	SDVB	Non-polar	900	100
XAD 1180	SDVB	Non-polar	600	300
HP 20	SDVB	Non-polar	500	260

SDVB*: Styrene-divinyl benzene

6.2.3.2. Rapeseed protein isolate and its aqueous by-product production

The protein isolate/purification process was performed in two steps: first, protein extraction from rapeseed meal (RSM) and second, protein purification by ultrafiltration as recommended in (Defaix et al., 2020; Sara et al., 2020). For protein extraction, the appropriate amount of RSM and NaCl 0.1M solution was mixed at a solid/liquid ratio of 1:9 (w/w). The extraction step was performed at pH 2 under agitation at 400 rpm for 30 min. Then, the liquid extract was clarified by centrifugation at 10 000 *g* for 30 min at 20°C (Heraeus Megafuge 16R centrifugation system, ThermoScientific, Waltham, Massachusets, USA). The supernatant was further clarified by tangential microfiltration using a 0.22 µm membrane at 0.2 bar of transmembrane pressure (0.1 m² area, Pellicon Mini Cassette Durapore, polyvinylidene difluoride (PVDF) membrane, MA, USA). The protein purification was achieved by diafiltration using an Akta Flux 6 device (GE Healthcare, Chicago, Illinois, USA) at a feed flow of 2 L/min and a transmembrane pressure of 1.5 bars. During the process, the retentate compartment was fed with 0.5 M salt solution at the same flow rate as the permeate flux in order to keep the volume constant. Six diavolume (DV, $DV = V_{NaCl}/V_0$) of NaCl solution were poured. Then, 3 DV of deionized water were used to flush NaCl from proteins. The permeate containing the phenolic compounds was recovered and adjusted to pH 2 by adding HCl 1M for further studies.

6.2.3.3. Phenolic compounds hydrolysis

Phenolic compounds contained in the UF permeate were hydrolyzed under acidic conditions as suggested by A. Siger et al. (Siger et al., 2013). To do so, 350 mL of permeate were mixed with 70 mL of HCl 37% (v/v). The reaction was carried out at 75°C with agitation at 150 rpm for 3h. During the reaction, 600 µL samples were taken at 30, 60, 90, 120, 150, and 180 min for phenolic compounds analysis and quantification by SEC-HPLC.

6.2.3.4. Analytical methods

6.2.3.4.1. Phenolic compounds identification by HPLC-MS

Phenolic compounds from UF permeate with or without acidic hydrolysis were separated by SE-HPLC and identified by ESI-MS as T. T. Le et al. (Le, et al., 2021; Tuong Thi Le et al., 2020). The HPLC system used was from Shimadzu Corporation (Kyoto, Japan). It was equipped with a pump and degasser (LC-20AD), a column oven (CTO-20A), and a diode array detector (CPO-M20A). The analysis was done using a size exclusion (SE) column Biosep 5µm SEC-s2000 145 Å column (300 x 7.5mm, 5µm) purchased from Phenomenex (Torrance, USA). The elution was performed during 40 min at 35°C using ACN : UltraPure Water : formic acid with a 10 : 90 : 0.1 (v/v) composition. The flow rate was 0.6 mL/min. The injection volume was 5 µL. ESI-MS analysis was performed on line with an ion trap (IT) mass spectrometer apparatus LC-MS2020 (Shimadzu Corporation, Kyoto, Japan). Nitrogen flow rate was set at 21.5 L/min. Data were analyzed using the LabSolution package. Qualitative identification of phenolic compounds from permeate and hydrolyzed permeate were based on *m/z* values and unique fragmentation pattern of the protonated molecules ions $[M-H]^+$ or $[M-H]^-$.

6.2.3.4.2. Sinapic acid (SA) and sinapine (SP) quantification by SE-HPLC

SA and SP were quantified from UF permeate with or without acidic hydrolysis by the above described SE-HPLC method using their UV signal at 325 nm. To do so, calibration curves were established by quantifying peak area of standard SA and SP at concentrations ranging from 0.05 to 1.25 mg/mL. The linear regression equations of the calibration curves were $y = 2.9.10^7x$ and $y = 5.31.10^7x$ with $R^2 = 0.9998$ and $R^2 = 0.9984$ of SP and SA, respectively.

6.2.3.4.3. Method validation

Validation of this method was conducted according to the International Conference on Harmonization (ICH) (Tietje & Brouder, 2010). Linearity of the detector responses and limits were performed in the range 0.05–1.25 mg/mL. Each calibration plot performs an average of three independent repetitions for five different concentration levels. Linear regression analysis was used to determine the slope and correlation coefficient (R^2). All experiments were test-ed three times for phenolic compounds standards and the phenolic compounds presenting in samples solution in this study.

6.2.3.4.4. Total phenolic contents (TPC)

The quantification of total phenolic contents (TPC) was performed by the "sum of phenolic acids" method of Rabie Khattab et al. (Khattab, 2010). TPC was estimated as SA equivalent (SAE) from the sum area of all peaks of phenolic compounds at 325 nm using the above described SE-HPLC method.

6.2.3.4.5. NaCl content

NaCl content in UF permeate was evaluated by measuring each sample's conductivity using a conduct meter (MeterLab HPM210, Radiometer analytical, France). NaCl solutions with concentrations ranging from 0.2 to 50 g/L were used to establish the calibration curve. The calibration equation was y = 1.4088x and the coefficient of determination was 0.993.

6.2.3.4.6. Total carbohydrate content

Total carbohydrate content in UF permeate and hydrolyzed permeate was determined according to the anthrone-sulfuric acid method of Yemm and Wilis (Yemm & Willis, 1954). Glucose was used as standard and glucose solutions with concentration ranging from 0.1 to 1 mg/mL were used to construct the calibration curve (y = 1.1845x, R^2 = 0.9981).

6.2.3.4.7. Protein content

Protein content in UF permeate was assessed using the Kjeldahl method (AOCS International., 1995). These compounds were low molar weight peptides or free amino acids since proteins were fully retained by the membrane. A nitrogen-to-protein factor of 6.25 was used as frequently used for rapeseed meal.

6.2.3.5. Adsorption / desorption study

6.2.3.5.1. Resin screenings

The resins were screened on the basis of massic adsorption capacity (q_e, amount of phenolic compounds adsorbed per g of resin) calculated as:

$$q_e = \frac{(C_0 - C_e)V_i}{W} \qquad (6.1)$$

where C_o and C_e are the initial and equilibrium concentrations of phenolic compounds in non-hydrolyzed and hydrolyzed permeate solution respectively (mg/mL); V_i is the initial volume of permeate added onto the resins (mL); and W is the weight of the dried resin (g).

6.2.3.5.2. Adsorption kinetics

Adsorption capacity was monitored after 5, 10, 15, 30, 60, 90, and 120 min. To do so, phenolic compounds concentration was measured in the liquid phase by HPLC. q_e was deduced from the concentration. Results were plotted under linearized models (pseudo-first-order, pseudo-second-order, and intra-particle diffusion).

6.2.3.5.3. Adsorption isotherms

Adsorption isotherms expressed the relationship between phenolic compounds adsorption capacity (q_e, mg/g) and the concentration of sample solution in the liquid phase at the equilibrium (C_e, mg/ L). For the adsorption study, a duration of 120 min was chosen. Experiments were carried out at 25°C - Langmuir and Freundlich models were used to regress experimental data.

6.2.3.5.4. Adsorption thermodynamic parameters

The effect of the temperature was investigated by determining the adsorption isotherms at 298.15, 308.15, and 318.15 K. Enthalpy and entropy variations were obtained from the slope and intercept of the linear plot $\ln K_{eq}$ *vs* 1/T according to the linear form of Clausius-Clapeyron Eq. 6.2:

$$\ln K_{eq} = -\frac{\Delta H}{RT} + \frac{\Delta S}{R} \qquad (6.2)$$

where $\ln K_{eq}$ is the natural logarithm of the constant of adsorption equilibrium (K_{eq}), ΔH is the enthalpy change (J/ mol), ΔS is entropy change (J/ mol), R is the universal gas constant (8.3144 J/molK) and T is the absolute temperature in Kelvin (K).

ΔG was determined using Eq. 6.3:

$$\Delta G = - RT \ln K_{eq} \quad (6.3)$$

where ΔG (J/mol) is the Gibbs energy change.

6.2.3.5.5. Desorption

Desorption ratios were determined using different water/ethanol solutions after the adsorption step on XAD16 up to equilibrium. 40 mL of 30, 50, 70, and 90% water/ethanol (v/v) were added to the resin, and shaken at 150 rpm and 25°C for 2 hours to reach desorption equilibrium. Resins were washed twice with deionized water prior solvent addition. Resins were separated from the liquid filtration using filter paper. Phenolic compounds concentration in the liquid was quantified by HPLC. Desorption ratio was calculated using Eq.6.4:

$$Desorption\ ratio\ (\%) = \frac{C_d V_d}{(C_o - C_e) V_i} 100\% \ (6.4)$$

where C_d is the concentration of CGA in desorption solution (mg/mL) and V_d is the volume of the desorption solution (mL).

6.2.3.6. Antioxidant activity

6.2.3.6.1. DPPH radical scavenging assay

DPPH free radical scavenging activity was carried on according to Wu et al. (J. Zhu & Wu, 2009) with some modifications. Briefly, DPPH 0.2 mM in MeOH was prepared. 100 µL of samples at 1.25, 2.5, 5, 10 and 20 µg/mL were mixed with 100µL of DPPH 0.2mM and added to the wells of a microplate. The mixtures were kept at 25°C for 30 min in the dark and then shaken for 30 s. The absorbance was measured at 517 nm. The inhibition percentage (%) of radical scavenging capacity was expressed as follows:

$$DPPH\ radical\ scavenging\ (\%) = \frac{(A_{DPPH} - A_{blank}) - (A_{sample+DPPH} - A_{sample+blank})}{A_{DPPH} - A_{Blank}} 100\ (\%)\ (6.5)$$

where A_{DPPH} is the absorbance of the DPPH solution, A_{blank} is the absorbance of pure methanol, $A_{sample+DPPH}$ is the absorbance of DPPH with the sample, and $A_{sample+blank}$ is the absorbance of pure methanol with the sample.

6.2.3.6.2. ABTS radical scavenging assay

The ABTS assay was used according to the procedure described by Re et al. (Re et al., 1999) with some modifications. 3.5 mM ABTS solution and potassium persulfate 1.225 mM were mixed to produce the $ABTS^+$ solution. This solution was kept at room temperature in the dark for 16 h before use. When the radical had formed, the absorbance of $ABTS^+$ solution at 734 nm was adjusted to 0.7 ± 0.02 by dilution with 95% (v/v) methanol solution with a 1/32 ratio (v/v). 20 µL samples at different concentrations (20, 10, 5, 2.5, and 1.25 µg/mL) were mixed with 180 µL $ABTS^+$ solution and added into each well of a 96-well plate. After 5 min of incubation in the dark at 25°C, the plate was shaken for 20 seconds and the absorbance was measured at 734 nm. Ascorbic acid (vitamin C), SP, and SA were used as references. The following equation was used to calculate $ABTS^{\cdot+}$ inhibition rate (%):

$$ABTS^{\cdot+} inhibition\ rate\ (\%) = \frac{A_{ABTS} - A_{sample+ABTS}}{A_{ABTS}} 100\ (\%)\ \ (6.6)$$

where A_{ABTS} is the absorbance of $ABTS^+$ and $A_{sample+ABTS}$ is the absorbance of $ABTS^+$ with the sample. All measurements for all samples solution at each concentration were performed in triplicate.

6.2.3.6.3. Calculation of IC_{50}

The IC50 (inhibitory concentration) value is the antioxidant concentration required to scavenge 50% of DPPH and ABTS free radical. These values were calculated from the graph of radical scavenging activity against the different concentrations of tested samples. The concentration of the sample solution at IC_{50} (µg/mL) was determined by regression.

6.2.3.7. Data analysis

Results are presented as means ± S.D. (standard deviation) from three replicates of each experiment. All tests were considered significant at $p < 0.05$. Statistical analyses were performed using Rstudio 3.6.1 (Boston, MA, USA) open-source code. All figures were implemented by using the OriginPro 8.5 software (Northampton, MA, USA). The chemical structures of phenolic compounds were represented using the ChemDrawUltra 8.0 package (Cambridge Soft, MA, USA).

6.2.4. Conclusion

In conclusion, this study provides insights into determination of phenolic compounds in an aqueous protein extraction/purification by-product (permeate) from rapeseed meal (RSM). We found that sinapine was the main phenolic compound in this permeate. The other compounds were sinapoyl glucose, 1,2-di-sinapoyl gentiobise and sinapic acid. The acidic hydrolysis of this permeate allowed the

efficient conversion of sinapine into sinapic acid. The XAD16 resin showed the highest adsorption capacity. Adsorption behaviors of total phenolic compounds, sinapine, and sinapic acid were also investigated. Our results revealed that the adsorption of phenolic compounds in both the hydrolyzed and non-hydrolyzed fractions followed the pseudo-second-order model and presented a very similar pattern of intra-particle diffusion. The Langmuir model was suitable to describe the adsorption process of phenolic compounds. Besides, the adsorption process was an exothermic, randomness, and physical adsorption process. Finally, we showed that the hydrolyzed fraction has the potential to become an interesting natural antioxidant, by comparison to vitamin C, that could find applications in food preservation or other domains.

6.3. Supporting informations

In this part of the thesis, the cytotoxicity and anti-inflammatory activities of both phenolic fractions (N and H fractions) were assessed. As presented in the chapter 4, the THP-1 cells differentiated into macrophages were also used to analyze the effects of the N and H fraction on cell viability and LPS-induced pro-inflammatory response.

Two conditions were used to mimic two different cellular states. First condition consisted in pre-incubating differentiated THP-1 cells with 100 ng/mL of LPS to induce a pro-inflammatory state and, one hour later, to add the N and H phenolic fractions at working concentrations corresponding to 50 or 100 µM of SP/SA. The purpose of this approach was to determine if this fraction was able to counter the LPS-induced pro-inflammatory response. The second condition was the opposite, it consisted in incubating THP-1 cells with the N and H phenolic fractions, to potentially promote an anti-inflammatory cellular state, and one hour later to add 100 ng/mL of LPS. In both cases, cell viability and TNF-α production, a major pro-inflammatory cytokine, were analyzed after 24 h of treatment.

6.3.1. Cytotoxicity

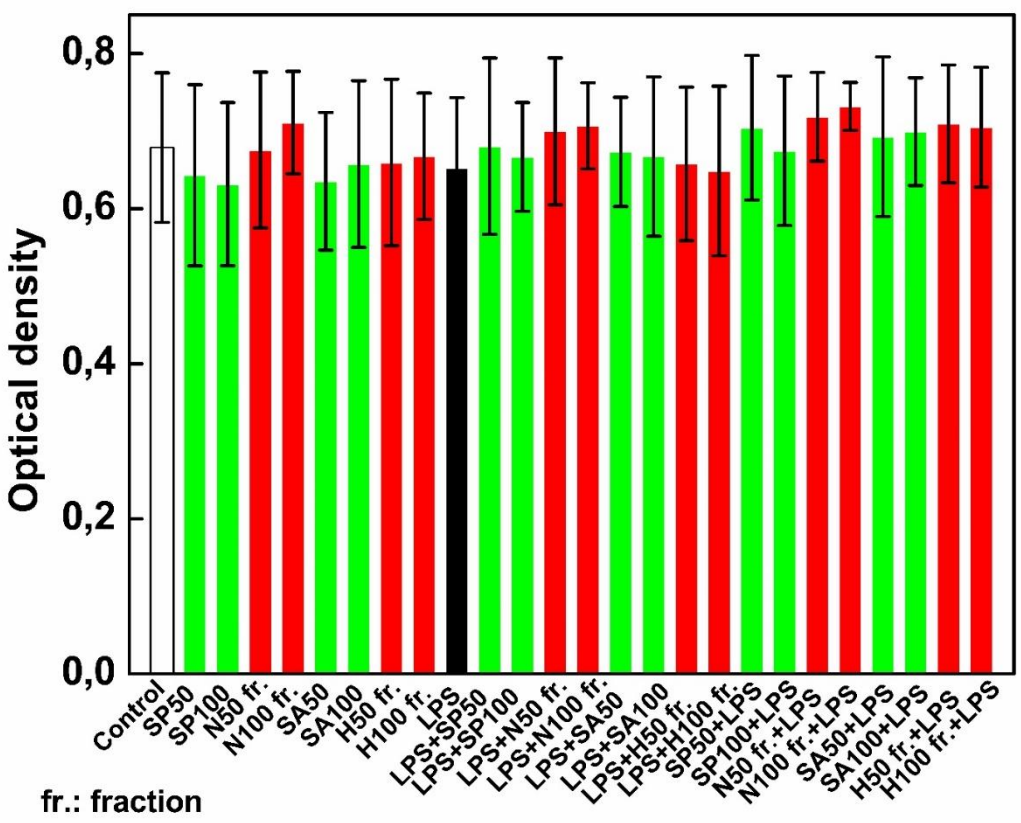

Figure S6.1. SP, SA, N-fraction, and H-fraction rapeseed fractions do not affect differentiated THP-1 cells' viability.

Two concentrations (50 and 100 µM) of SP/ SA, used as reference compounds, and two working concentrations of each rapeseed fraction, corresponding to a content of 50 or 100 µM of SP/ SA, were used. Differentiated THP-1 cells were incubated for 24h either with these products alone or with 100 ng/mL of LPS added one hour before or after SP/ SA or rapeseed fractions (N or H). Then, cell viability was evaluated by crystal violet assay, and optical density (O.D.) was measured at 595 nm. Data are presented as mean ± S.D. This Figureure is representative of three independent experiments realized in triplicates. 'Control' corresponds to a culture in which no product was added. "LPS+SP50" or "LPS+SA50" indicates that LPS was added before SP/ SA at the concentration of 50 µM while "SP50+LPS" or "SA50+LPS" indicates that SP/ SA at the concentration of 50 µM was added before LPS.

THP-1 macrophages were used to estimate the effects of two rapeseed fractions (N and H fractions) on cell viability and LPS induced pro-inflammatory response. Sinapine (SP) and Sinapic acid (SA) were used as the references in these biological experiments due to their major component (63.31% SP in N-fraction and 73.00% SA in H-fraction). The experiments were divided into two conditions. First, pre-incubating differentiated THP-1 cells with 100 ng/ mL of LPS to induce a pro-inflammatory cytokine such as TNF-α and add the N or H fraction after 1h concentrations corresponding to 50 or 100 µM of SP or SA, respectively. Second, to investigate an anti-inflammatory potential, we incubated THP-1 cells with N or H fraction corresponding to 50 or 100 µM of SP or SA and added 100 ng/ mL

of LPS after 1h. In both cases, cells viability and TNF- α production level was estimated after 24h treatment.

First, we investigated the effects of N-fraction and H-fraction on cell viability. As shown in Figure S6.1, the sample concentration resulting in over 90% of cell viability was considered to show no cytotoxicity. Thus, phenolic fractions did not affect cell viability up to a concentration of 100µM (of SP or SA in N and H fraction). Notably, the "impurities" present in these two fractions did not affect cell viability. Moreover, all the phenolic components in both fractions did not show cytotoxicity. The results suggested that phenolic compounds in rapeseed meal after purification have no cytotoxicity at a concentration ranging from 50 to 100µM of SP or SA in N and H fraction, respectively.

6.3.2. Anti-inflammatory activity of the phenolic fractions before and after hydrolysis

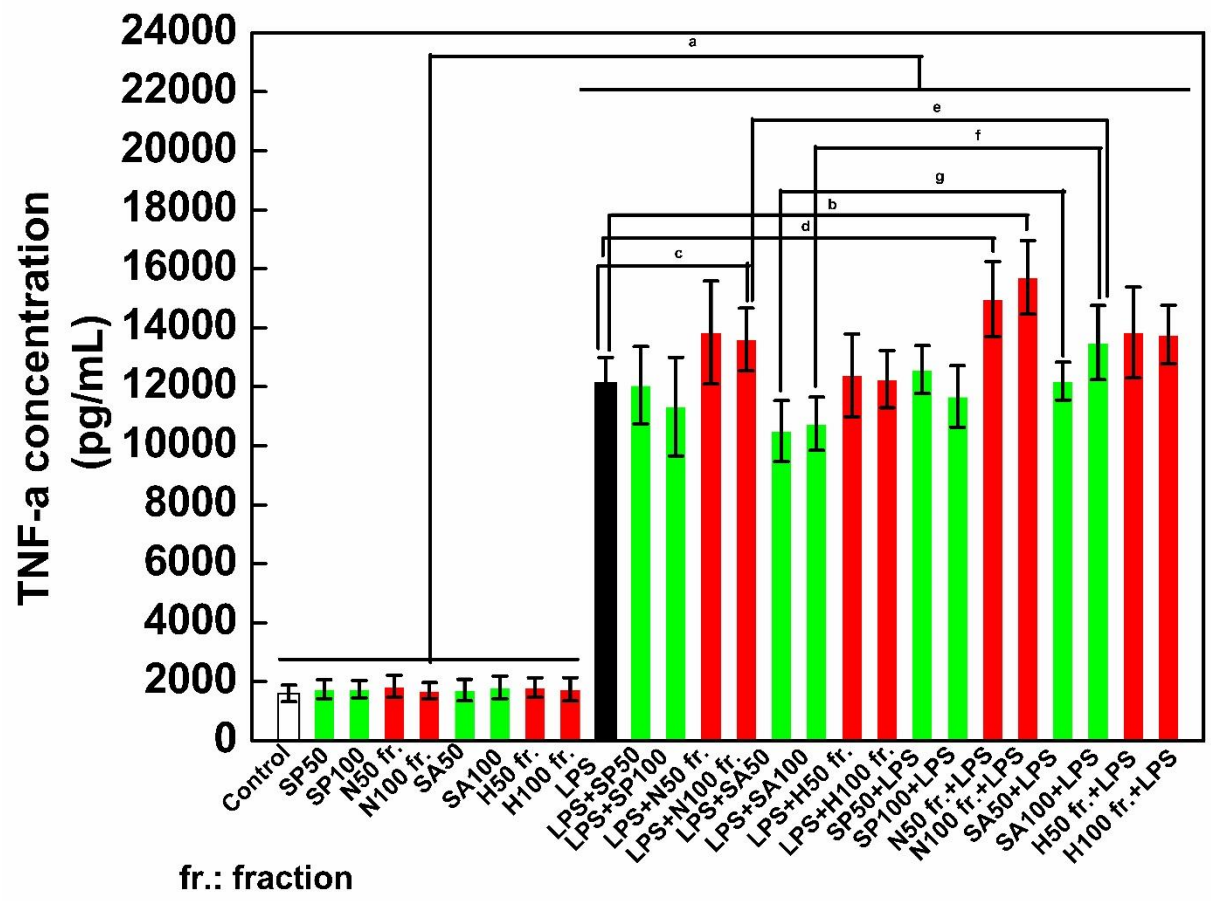

Figure S6.2. Effect of SP, SA, and rapeseed fraction reduces TNF alpha production by differentiated THP-1 cells.

Two concentrations (50 and 100 µM) of sinapine (SP) or sinapic acid (SA), used as reference compounds, and two working concentrations of each rapeseed fraction, corresponding to a content of 50 or 100 µM of SP/ SA, were used. Differentiated THP-1 cells were incubated for 24h either with these products alone or with 100 ng/mL of LPS added one hour before or after SP/ SA or rapeseed fractions (N or H). Cell culture supernatants were then collected and used to quantify TNF alpha production by ELISA. This Figureure is representative of two independent experiments performed in triplicates. Data are presented as mean ± S.D. *t*-tests were used to identify statistically significant differences. $^{a}p < 0.05$ vs conditions without LPS. $^{b,c,d}p < 0.05$ vs LPS alone. $^{g}p < 0.05$ vs

"SA50+LPS". $^{e,f}p < 0.05$ vs "SA100+LPS". $^{e}p < 0.05$ vs "LPS+N100 fr.". "Control" corresponds to a culture in which no product was added. "LPS+SP/SA50" indicates that LPS was added before SP/SA at the concentration of 50 µM while "SP/SA50+LPS" indicates that SP/SA at the concentration of 50 µM was added before LPS.

Second, we investigated N fraction and H fraction effects on LPS-induced TNF-α production in THP-1 macrophages. Surprisingly, we noted that N fraction at SP concentration at 50/ 100 µM treated with LPS alone had pro-inflammatory effects on THP-1 differentiated cells (Figure S6.2). On the contrary, its can cause the pro-inflammatory effect ($^{b,c,d}p < 0.05$) when treated with N fraction. As shown in Figure S6.2, when all sample solutions were treated with LPS, the TNF-α production increased dramatically ($^{a}p < 0.05$). Moreover, when LPS was added after 1h with SA at a concentration of 100µM caused pro-inflammatory effects.

In contrast, when LPS was added before SA at 50 and 100µM 1h, there was an inhibitory TNF-α production level compared with LPS only ($^{b,c,d}p < 0.05$). However, when we replaced SA into H fraction (corresponding SA concentration was 50 or 100µM), There was no TNF-α production level activity. The results suggested that might all phenolic compounds in the H fraction participated in this activity. The difference might come from the difference in SA purity degree. Furthermore, and very interestingly, we observed that when pretreated with SA or H fraction in both concentrations 50 and 100 µM, the macrophages cells produced less TNF-α level than N fraction at the same concentration ($^{e}p < 0.05$). These results suggested that phenolic fraction after hydrolyzed, which mainly contains SA 73.00%, had an inhibitory effect on TNF-α production level without cell toxicity. In the past, Satu Vourela et al. (Satu Vourela et al., 2005) also found that rapeseed phenolic extracted showed no anti-inflammatory properties after hydrolyzed with ferulic acid esterase (SA, in this case, proportioned 64%). Hence, the conclusion in this study was consistent with the previous report. Notably, hydrolyzed permeate in the current study showed a weaker effect on pro-inflammatory effect than non-hydrolyzed permeate.

6.3.3. Conclusion

Both phenolic fractions did not affect cytotoxicity. Furthermore, it did not affect anti-inflammatory through inhibition of the TNF-α production in LPS-induced macrophages.

6.4. Conclusion for chapter 6

These results of this chapter provided insights into determination of phenolic compounds in an aqueous protein extraction/purification by-product (permeate) from rapeseed meal (RSM). This liquid effluent consisted of sinapine (the main phenolic compound) and the other compounds were sinapoyl glucose, 1,2-di-sinapoyl gentiobise (esters of sinapic acid) and free sinapic acid. To convert the sinpaine and other ester of sinapic acid, the acidic hydrolysis of this permeate has successfully implemented. Our results revealed that the adsorption of phenolic compounds in both the hydrolyzed and non-hydrolyzed fractions followed the pseudo-second-order model and presented a very similar pattern of intra-particle diffusion. The Langmuir model was suitable to describe the adsorption process of phenolic compounds. Besides, the adsorption process was an exothermic, randomness, and physical

adsorption process. Finally, we showed that the hydrolyzed fraction (H fraction) has the potential to become an interesting natural antioxidant, by comparison to vitamin C, that could find applications in food preservation or other domains. The both phenolic fraction, non-hyrolyzed (N fraction) and hydrolyzed fraction (H fraction) showed a high potential to become a natural antioxidant source based on radical scavenging inhibition capacity. Furthermore, both phenolic fractions did not affect cytotoxicity. In addition, it did not affect anti-inflammatory through inhibition of the TNF-α production in LPS-induced macrophages. In summary, this study can provide useful information concerning searching for natural antioxidants that can use in the food domain.

Note: Kindly note that the term “Vitamin C” using in this thesis was ascorbic acid.

Chapter 7. Conclusions et perspectives

7.1. Conclusions

Les principaux objectifs de ce travail étaient : 1) caractériser et identifier les composés phénoliques des effluents liquides issus de la production d'isolats protéiques à partir de tourteaux de tournesol et de colza; 2) sélectionner les meilleures résines macroporeuses et étudier le mécanisme d'adsorption des composés phénoliques ; 3) optimiser les conditions dans la colonne d'adsorption des composés phénoliques ; et 4) évaluer les activités biologiques des fractions phénoliques obtenues, notamment les propriétés antioxydantes et anti-inflammatoires.

Les résultats obtenus ont permi de montrer que des résines macroporeuses permettent d'isoler les composés phénoliques des sels, des sucres, des composés non protéiques en raison de leur sélectivité d'adsorption. Une méthode originale basée sur des téchniques d'HPLC et HPLC-MS ont permi d'établir que le principal composé phénolique identifié dans les permeats issus de SFM était l'acide chlorogénique (CGA). La sinapine (SP) était le composé phénolique prédominant dans les permeats issus de RSM, suivi de l'acide sinapique (SA) et des formes esters de l'acide sinapique, notamment le sinapoyl glucose et le 1,2-di-sinapoyl gentiobise. Ces esters d'acide sinapiques peuvent être hydrolysés à plus de 75% en acide sinapique en conditions acide.

L'adsorption sur résines macroporeuses adsorbantes a été étudiée en mode batch dans un premier temps. Cinq résines macroporeuses différentes, dont le SDVB (XAD4, XAD16, XAD1180 et HP20) et la résine acrylique (XAD7), ont été utilisées. Ces résines possèdent différents diamètre des pores, surface spécifique et les propriétés de surface. La meilleure résine pour l'adsorption du CGA dans le SFM était la XAD7, et pour l'adsorption de la Sinapine et des composés phénoliques totaux (TPC) dans le perméat non hydrolysé et hydrolysé était la XAD16. Ceci a indiqué que l'adsorption était basée principalement sur une interaction hydrophobe-hydrophobe et un empilement π-π entre le cycle benzénique des composés phénoliques (partie acide sinapique) et le cycle benzénique des résines macroporeuses. Au contraire, cette interaction était plutôt des ponts hydrogènes dans le cas du CGA dans le SFM avec XAD7. Cette interaction se produit au niveau de la partie acide caféique (dans la structure du CGA, donneur d'électrons) et du groupe acyle (dans le squelette de la résine XAD7, accepteur d'électrons).

XAD7 et XAD16 ont donc été selectionnées pour réaliser caractériser la cinétique d'adsorption, les isothermes ainsi que la mise en œuvre en colonne. Les cinétiques d'adsorption des composés phénoliques adsorbés par SFM/ RSM sur les résines XAD7 et XAD16 s'adaptaient bien au modèle de pseudo-second ordre. En outre, ces données ont montré un schéma de diffusion intra-particulaire similaire dans tous les cas. Par conséquent, nous avons conclu que la cinétique d'adsorption des composés phénoliques est essentiellement limité par la diffusion à l'intérieur des pores de la particule. Le modèle de Langmuir décrit le plus précisément le mécanisme d'adsorption des composés phénoliques dans les deux résines, indiquant un comportement d'adsorption monocouche.

De plus, sur la base des paramètres thermodynamiques, ce travail a montré que le processus d'adsorption était contrôlé par un mécanisme physique et devait être favorablement mené à basse température. Ensuite, la désorption statique avec l'éluant à différentes concentrations d'éthanol peut affecter le ratio de désorption des composés phénoliques. Selon les résultats du ratio de désorption, une solution d'éthanol à 50% (v/v) a été confirmée comme étant la meilleure solution de compromis avec le CGA et des solutions d'éthanol à 30% (v/v) et 70% (v/v) pour la sinapine et l'acide sinapique, respectivement.

Dans cette étude, un processus efficace pour la purification des composés phénoliques et des composés phénoliques totaux à partir du SFM/ RSM a été établi en utilisant une méthodologie plan d'expériences (DoE) couplé à une optimisation multicritères. La condition optimale basée sur la méthodologie de surface de réponse pour l'enrichissement des composés phénoliques à partir de la GDF en utilisant la résine XAD7 était un débit d'adsorption de 15BV/h, un pH de 2,7 et une désorption avec de l'EtOH à 50 % (v/v). De plus, la condision optimale pour le RSM était un débit d'adsorption de 13.30 BV/ h, pH 2-5, et une désorption avec 30% (v/v). Ces conditions ont permis de générer suffisamment de produit pour évaluer ses propriétés antioxydantes et anti-inflammatoires.

Les tests DPPH et ABTS ont montré que les fractions obtenues (fraction CGA, fraction sinapine et fraction acide sinapique) avaient une activité de piégeage des radicaux plus puissante que la vitamine C, ce qui pourrait trouver des applications dans la conservation des aliments ou d'autres domaines. En outre, la fraction CGA et les fractions sinapine/acide sinapique n'ont révélé aucune cytotoxicité sur une lignée cellulaire de macrophages humains. En particulier, la fraction CGA a réduit de 22 % le niveau de production de TNF-α induit par le LPS.

Ces études ont fourni une base nécessaire pour le développement futur de la séparation et de la purification des composés phénoliques à partir du SFM et du RSM. Plus important encore, les résultats obtenus dans le cadre de ce projet de doctorat suggèrent que nous pouvons développer les antioxydants naturels dérivés du SFM et du RSM pour l'industrie alimentaire et cosmétique. Comme démontré dans ce travail de doctorat, le SFM contenant du CGA a une application potentielle dans la préparation pharmaceutique en raison de sa fonction anti-inflammatoire.

7.2. Perspectives

Ce travail a montré un potentiel applicatif interessant des composés phénoliques de tournesol et de colza en utilisant des systèmes de criblage *in vitro* et des tests cellulaires (cytotoxicité et activités antiinflammatoires). Une première perspective de ce travail consisterait à valider l'interêt de ces molécules avec des systèmes proches des systèmes réels. Ainsi, l'évaluation du potentiel antioxydant pourrait être évalué sur des matrices alimentaires (ex. mayonnaises) pour les applications en sécurité alimentaire en utilisant des témoins mis en œuvre pour ces applications. Il faudrait également integrer des études organoleptiques car l'utilisation de composés phénoliques peut entraîner des problèmes de couleur et / ou impacter le goût des matrices. Une démarche similaire peut être réalisée pour valider l'activité protective sur l'inflammation *in vivo* sur des modèles animaux. Il est également envisageable

d’étudier des effets synergiques de composés phénoliques en mélanges pour ces applications. Principalement concernant les activités antiinflammatoires.

Par ailleurs, les effluents liquides contiennent potentiellement d’autres biomolécules d’interêt tels que les oligosides et composés azotés qui peuvent être utilisés comme liqueurs pour la fabrication d’énergie et / ou de molécules plateformes biosourcées où encore l’acide phytique qui présentent un potentiel d’application important en industrie cosmetique comme agent chelateur d’ions métaliques divalents. Une étude plus globale de fractionnement peut donc être envisagée. Cette démarche peut integrer les procédés d’adsorption et / ou integrer des procédés membranaires (nanofiltration et / ou procédés électromembranaires) plus ecocompatibles. Cette étude doit integrer des démarches d’optimisation systémiques (multi-étapes) afin d’évaluer les optimums de fonctionnement integrant l’utilisation des intrants (eau, sel, soude et acide) et leur recyclage de sorte à évaluer de manière rationnelle cette nouvelle filière.

L'hydrolyse des esters d’acide sinapique présents dans les effluents de production d’isolats de protéines de colza a montré une liberation de composés présentant une activité antioxydante particulièrement importante. Toutefois, l’hydrolyse acide réalisée dans le cadre de ce travail de thèse nécessite de grandes quantités d’acide et a probablement détruit d’autres molécules potentiellement valorisables. Des travaux récents montrent qu’il est possible d’hydrolyser la sinapine en acide sinapique par bioconversion enzymatique (Thiel et al., 2015). Une autre perspective de ce travail pourrait donc être l’étude de systèmes d’hydrolyse enzymatique en batch ou en continu dans le cadre de couplages avec des procédés de séparation afin de compartimenter l’enzyme et le substrat et soutirer les produits (acide sinapique).

References

A. Fungaro, D., I. Borrely, S., & E.M. Carvalho, T. (2013). Surfactant Modified Zeolite from Cyclone Ash as Adsorbent for Removal of Reactive Orange 16 from Aqueous Solution. *American Journal of Environmental Protection*, *1*(1), 1–9. https://doi.org/10.12691/env-1-1-1

Abburi, K. (2003). Adsorption of phenol and p-chlorophenol from their single and bisolute aqueous solutions on Amberlite XAD-16 resin. *Journal of Hazardous Materials*, *105*(1–3), 143–156. https://doi.org/10.1016/j.jhazmat.2003.08.004

Abrams, I. M., & Millar, J. R. (1997). A history of the origin and development of macroporous ion-exchange resins. *Reactive and Functional Polymers*, *35*(1–2), 7–22. https://doi.org/10.1016/S1381-5148(97)00058-8

Aehle, E., Raynaud-Le Grandic, S., Ralainirina, R., Baltora-Rosset, S., Mesnard, F., Prouillet, C., Mazière, J.-C., & Fliniaux, M.-A. (2004). Development and evaluation of an enriched natural antioxidant preparation obtained from aqueous spinach (Spinacia oleracea) extracts by an adsorption procedure. *Food Chemistry*, *86*(4), 579–585. https://doi.org/10.1016/j.foodchem.2003.10.006

Agalias, A., Magiatis, P., Skaltsounis, A.-L., Mikros, E., Tsarbopoulos, A., Gikas, E., Spanos, I., & Manios, T. (2007). A New Process for the Management of Olive Oil Mill Waste Water and Recovery of Natural Antioxidants. *Journal of Agricultural and Food Chemistry*, *55*(7), 2671–2676. https://doi.org/10.1021/jf063091d

Aharoni, C., & Ungarish, M. (1977). Kinetics of activated chemisorption. Part 2.Theoretical models. *Journal of the Chemical Society, Faraday Transactions 1: Physical Chemistry in Condensed Phases*, *73*(0), 456. https://doi.org/10.1039/f19777300456

Ahmaruzzaman, Md. (2008). Adsorption of phenolic compounds on low-cost adsorbents: A review. *Advances in Colloid and Interface Science*, *143*(1–2), 48–67. https://doi.org/10.1016/j.cis.2008.07.002

Ahmed, Z. M., Lyne, S., & Shahrabani, R. (2000). Removal and Recovery of Phenol From Phenolic Wastewater Via Ion Exchange and Polymeric Resins. *Environmental Engineering Science*, *17*(5), 245–255. https://doi.org/10.1089/ees.2000.17.245

Alam, Md. N., Bristi, N. J., & Rafiquzzaman, Md. (2013). Review on in vivo and in vitro methods evaluation of antioxidant activity. *Saudi Pharmaceutical Journal*, *21*(2), 143–152. https://doi.org/10.1016/j.jsps.2012.05.002

Albe Slabi, S., Mathe, C., Basselin, M., Framboisier, X., Ndiaye, M., Galet, O., & Kapel, R. (2020). Multi-objective optimization of solid/liquid extraction of total sunflower proteins from cold press meal. *Food Chemistry*, *317*, 126423. https://doi.org/10.1016/j.foodchem.2020.126423

Albe Slabi, S., Mathé, C., Framboisier, X., Defaix, C., Mesieres, O., Galet, O., & Kapel, R. (2019). A new SE-HPLC method for simultaneous quantification of proteins and main phenolic compounds from sunflower meal aqueous extracts. *Analytical and Bioanalytical Chemistry*, *411*(10), 2089–2099. https://doi.org/10.1007/s00216-019-01635-2

Albe-Slabi, S., Defaix, C., Beaubier, S., Galet, O., & Kapel, R. (2021). Selective extraction of napins: Process optimization and impact on structural and functional properties. *Food Hydrocolloids*, 107105. https://doi.org/10.1016/j.foodhyd.2021.107105

Alho, H., & Leinonen, J. (1999). [1] Total antioxidant activity measured by chemiluminescence methods. In *Methods in Enzymology* (Vol. 299, pp. 3–15). Elsevier. https://doi.org/10.1016/S0076-6879(99)99004-3

Al-Malah, K., Azzam, M. O. J., & Abu-Lail, N. I. (2000). Olive mills effluent (OME) wastewater post-treatment using activated clay. *Separation and Purification Technology*, *20*(2–3), 225–234. https://doi.org/10.1016/S1383-5866(00)00114-3

Alonso, Á. M., Domínguez, C., Guillén, D. A., & Barroso, C. G. (2002). Determination of Antioxidant Power of Red and White Wines by a New Electrochemical Method and Its Correlation with Polyphenolic Content. *Journal of Agricultural and Food Chemistry*, *50*(11), 3112–3115. https://doi.org/10.1021/jf0116101

Al-Sayed, E., & Abdel-Daim, M. M. (2018). Analgesic and anti-inflammatory activities of epicatechin gallate from Bauhinia hookeri. *Drug Development Research*, *79*(4), 157–164. https://doi.org/10.1002/ddr.21430

Amarowicz, R., Fornal, J., Karamać, M., & Shahidi, F. (2001). Antioxidant activity of extracts of phenolic compounds from rapeseed oil cakes. *Journal of Food Lipids*, *8*(1), 65–74. https://doi.org/10.1111/j.1745-4522.2001.tb00184.x

Amarowicz, R., Karamac, M., Kmita-Glazewska, H., Troszynaska, A., & Kozlowska, H. (1996). Antioxidant activity of phenolic fractions of everlasting pea, faba bean and broad bean. *Journal of Food Lipids*, *3*(3), 199–211. https://doi.org/10.1111/j.1745-4522.1996.tb00067.x

Amarowicz, R., Naczk, M., & Shahidi, F. (2000). Antioxidant Activity of Various Fractions of Non-Tannin Phenolics of Canola Hulls. *Journal of Agricultural and Food Chemistry*, *48*(7), 2755–2759. https://doi.org/10.1021/jf9911601

Amarowicz, R., Pegg, R. B., Rahimi-Moghaddam, P., Barl, B., & Weil, J. A. (2004). Free-radical scavenging capacity and antioxidant activity of selected plant species from the Canadian prairies. *Food Chemistry*, *84*(4), 551–562. https://doi.org/10.1016/S0308-8146(03)00278-4

Amarowicz, R., Wanasundara, P. K. J. P. D., & Shahidi, F. (1994). Chromatographic separation of flaxseed phenolics. *Food / Nahrung*, *38*(5), 520–526. https://doi.org/10.1002/food.19940380508

Ambriz-Pérez, D. L., Leyva-López, N., Gutierrez-Grijalva, E. P., & Heredia, J. B. (2016). Phenolic compounds: Natural alternative in inflammation treatment. A Review. *Cogent Food & Agriculture*, *2*(1), 1131412.

Andreasen, M. F., Landbo, A.-K., Christensen, L. P., Hansen, Å., & Meyer, A. S. (2001). Antioxidant Effects of Phenolic Rye (*Secale cereale* L.) Extracts, Monomeric Hydroxycinnamates, and Ferulic Acid Dehydrodimers on Human Low-Density Lipoproteins. *Journal of Agricultural and Food Chemistry*, *49*(8), 4090–4096. https://doi.org/10.1021/jf0101758

Aneja, R., Hake, P. W., Burroughs, T. J., Denenberg, A. G., Wong, H. R., & Zingarelli, B. (2004). Epigallocatechin, a green tea polyphenol, attenuates myocardial ischemia reperfusion injury in rats. *Molecular Medicine*, *10*(1–6), 55–62.

Anirudhan, T. S., & Ramachandran, M. (2006). Adsorptive removal of tannin from aqueous solutions by cationic surfactant-modified bentonite clay. *Journal of Colloid and Interface Science*, *299*(1), 116–124. https://doi.org/10.1016/j.jcis.2006.01.056

Annadurai, G., & Krishnan, M. R. V. (1997). Adsorption of acid dye from aqueous solution by chitin: Equilibrium studies. *Indian J. of Chem.Technol*, *04(5)*, 217–222.

AOCS International. (1995). Official method 991.20. Nitrogen (total) in milk. Official methods of analysis, 19th edition. *Gaithersburg: AOCS International*.

Arafat, H. A., Franz, M., & Pinto, N. G. (1999). Effect of Salt on the Mechanism of Adsorption of Aromatics on Activated Carbon. *Langmuir*, *15*(18), 5997–6003. https://doi.org/10.1021/la9813331

Arai, S., Suzuki, H., Fujimaki, M., & Sakurai, Y. (1966). Studies on Flavor Components in Soybean: Part II. Phenolic Acids in Defatted Soybean Flour. *Agricultural and Biological Chemistry*, *30*(4), 364–369. https://doi.org/10.1080/00021369.1966.10858609

Arrutia, F., Binner, E., Williams, P., & Waldron, K. W. (2020). Oilseeds beyond oil: Press cakes and meals supplying global protein requirements. *Trends in Food Science & Technology*, *100*, 88–102. https://doi.org/10.1016/j.tifs.2020.03.044

Ayawei, N., Ebelegi, A. N., & Wankasi, D. (2017). Modelling and Interpretation of Adsorption Isotherms. *Journal of Chemistry*, *2017*, 1–11. https://doi.org/10.1155/2017/3039817

Balasundram, N., Sundram, K., & Samman, S. (2006). Phenolic compounds in plants and agri-industrial by-products: Antioxidant activity, occurrence, and potential uses. *Food Chemistry*, *99*(1), 191–203. https://doi.org/10.1016/j.foodchem.2005.07.042

Ballester, D., Rodrigo, R., Nakouzi, J., Chichester, C. O., Yanez, E., & Mönckeberg, F. (1970). Rapeseed meal II. Chemical composition and biological quality of the protein. *Journal of the Science of Food and Agriculture*, *21*(3), 140–142.

Banat, F. A., Al-Bashir, B., Al-Asheh, S., & Hayajneh, O. (2000). Adsorption of phenol by bentonite. *Environmental Pollution*, *107*(3), 391–398. https://doi.org/10.1016/S0269-7491(99)00173-6

Basaga, H., Tekkaya, C., & Acikel, F. (1997). Antioxidative and Free Radical Scavenging Properties of Rosemary Extract. *LWT - Food Science and Technology*, *30*(1), 105–108. https://doi.org/10.1006/fstl.1996.0127

Baublis, A. J., Lu, C., Clydesdale, F. M., & Decker, E. A. (2000). Potential of Wheat-Based Breakfast Cereals as a Source of Dietary Antioxidants. *Journal of the American College of Nutrition*, *19*(sup3), 308S-311S. https://doi.org/10.1080/07315724.2000.10718965

Bautista, J., Parrado, J., & Machado, A. (1990). Composition and fractionation of sunflower meal: Use of the lignocellulosic fraction as substrate in solid-state fermentation. *Biological Wastes*, *32*(3), 225–233.

Bell, J. M. (1984). Nutrients and toxicants in rapeseed meal: A review. *Journal of Animal Science*, *58*(4), 996–1010. https://doi.org/10.2527/jas1984.584996x

Bell, J. M. (1993). Factors affecting the nutritional value of canola meal: A review. *Canadian Journal of Animal Science*, *73*(4), 689–697.

Bell, J. M., & Jeffers, H. F. (1976). Variability in the chemical composition of rapeseed meal. *Canadian Journal of Animal Science*, *56*(2), 269–273.

Benavente-García, O., & Castillo, J. (2008). Update on Uses and Properties of Citrus Flavonoids: New Findings in Anticancer, Cardiovascular, and Anti-inflammatory Activity. *Journal of Agricultural and Food Chemistry*, *56*(15), 6185–6205. https://doi.org/10.1021/jf8006568

BenSaad, L. A., Kim, K. H., Quah, C. C., Kim, W. R., & Shahimi, M. (2017). Anti-inflammatory potential of ellagic acid, gallic acid and punicalagin A&B isolated from Punica granatum. *BMC Complementary and Alternative Medicine*, *17*(1), 47. https://doi.org/10.1186/s12906-017-1555-0

Benzaoui, T., Selatnia, A., & Djabali, D. (2018). Adsorption of copper (II) ions from aqueous solution using bottom ash of expired drugs incineration. *Adsorption Science & Technology*, *36*(1–2), 114–129. https://doi.org/10.1177/0263617416685099

Benzie, I. F. F., & Strain, J. J. (1996). The Ferric Reducing Ability of Plasma (FRAP) as a Measure of "Antioxidant Power": The FRAP Assay. *Analytical Biochemistry*, *239*(1), 70–76. https://doi.org/10.1006/abio.1996.0292

Berardini, N., Knödler, M., Schieber, A., & Carle, R. (2005). Utilization of mango peels as a source of pectin and polyphenolics. *Innovative Food Science & Emerging Technologies*, *6*(4), 442–452. https://doi.org/10.1016/j.ifset.2005.06.004

Berdahl, D. R., Nahas, R. I., & Barren, J. P. (2010). Synthetic and natural antioxidant additives in food stabilization: Current applications and future research. In *Oxidation in Foods and Beverages and Antioxidant Applications* (pp. 272–320). Elsevier. https://doi.org/10.1533/9780857090447.2.272

Berk, M., Kapczinski, F., Andreazza, A. C., Dean, O. M., Giorlando, F., Maes, M., Yücel, M., Gama, C. S., Dodd, S., Dean, B., Magalhães, P. V. S., Amminger, P., McGorry, P., & Malhi, G. S. (2011). Pathways underlying neuroprogression in bipolar disorder: Focus on inflammation, oxidative stress and neurotrophic factors. *Neuroscience & Biobehavioral Reviews*, *35*(3), 804–817. https://doi.org/10.1016/j.neubiorev.2010.10.001

Bertin, L., Ferri, F., Scoma, A., Marchetti, L., & Fava, F. (2011). Recovery of high added value natural polyphenols from actual olive mill wastewater through solid phase extraction. *Chemical Engineering Journal*, *171*(3), 1287–1293. https://doi.org/10.1016/j.cej.2011.05.056

Bezerra, M. A., Santelli, R. E., Oliveira, E. P., Villar, L. S., & Escaleira, L. A. (2008). Response surface methodology (RSM) as a tool for optimization in analytical chemistry. *Talanta*, *76*(5), 965–977. https://doi.org/10.1016/j.talanta.2008.05.019

Bian, Y., Liu, P., Zhong, J., Hu, Y., Fan, Y., Zhuang, S., & Liu, Z. (2018). Kaempferol inhibits multiple pathways involved in the secretion of inflammatory mediators from LPS-induced rat intestinal microvascular endothelial cells. *Molecular Medicine Reports*. https://doi.org/10.3892/mmr.2018.9777

Bilgili, M. S. (2006). Adsorption of 4-chlorophenol from aqueous solutions by xad-4 resin: Isotherm, kinetic, and thermodynamic analysis. *Journal of Hazardous Materials*, *137*(1), 157–164. https://doi.org/10.1016/j.jhazmat.2006.01.005

Biparva, P., Ehsani, M., & Hadjmohammadi, M. R. (2012). Dispersive liquid–liquid microextraction using extraction solvents lighter than water combined with high performance liquid chromatography for determination of synthetic antioxidants in fruit juice samples. *Journal of Food Composition and Analysis*, *27*(1), 87–94. https://doi.org/10.1016/j.jfca.2012.04.002

Bishop, C. T. (1955). Carbohydrates of sunflower heads. *Canadian Journal of Chemistry*, *33*(10), 1521–1529. https://doi.org/10.1139/v55-186

Bjarnason, I., Hayllar, J., Macpherson, A. N. drew J., & Russell, A. N. thony S. (1993). Side effects of nonsteroidal anti-inflammatory drugs on the small and large intestine in humans. *Gastroenterology*, *104*(6), 1832–1847. https://doi.org/10.1016/0016-5085(93)90667-2

Blair, R., & Scougall, R. K. (1975). Chemical composition, nutritive values of rapeseed meals. *Feedstuffs*, *47*(6), 26–27.

Blanchard, G., Maunaye, M., & Martin, G. (1984). Removal of heavy metals from waters by means of natural zeolites. *Water Research*, *18*(12), 1501–1507. https://doi.org/10.1016/0043-1354(84)90124-6

Blois, M. S. (1958). Antioxidant Determinations by the Use of a Stable Free Radical. *Nature*, *181*(4617), 1199–1200. https://doi.org/10.1038/1811199a0

Bonfili, L., Cecarini, V., Amici, M., Cuccioloni, M., Angeletti, M., Keller, J. N., & Eleuteri, A. M. (2008). Natural polyphenols as proteasome modulators and their role as anti-cancer compounds: Antioxidants and proteasome in cancer treatment. *FEBS Journal*, *275*(22), 5512–5526. https://doi.org/10.1111/j.1742-4658.2008.06696.x

Bongartz, V., Brandt, L., Gehrmann, M., Zimmermann, B., Schulze-Kaysers, N., & Schieber, A. (2016). Evidence for the Formation of Benzacridine Derivatives in Alkaline-Treated Sunflower Meal and Model Solutions. *Molecules*, *21*(1), 91. https://doi.org/10.3390/molecules21010091

Boni, R., Assogna, A., Grillo, F., Robertiello, A., Petrucci, F., Giacomozzi, E., & Patricelli, A. (1987). Method for preparing protein hydrolysates soluble in an acid environment, and the hydrolysates obtained. *European Patent EP0*, *271*(964), A2.

Borek, C. (1991). Free-Radical Processes in Multistage Carcinogenesis. *Free Radical Research Communications*, *13*(1), 745–750. https://doi.org/10.3109/10715769109145854

Boudet, A.-M. (2007). Evolution and current status of research in phenolic compounds. *Phytochemistry*, *68*(22–24), 2722–2735. https://doi.org/10.1016/j.phytochem.2007.06.012

Box, G. E. P., & Behnken, D. W. (1960). Some New Three Level Designs for the Study of Quantitative Variables. *Technometrics*, *2*(4), 455–475. https://doi.org/10.1080/00401706.1960.10489912

Box, G. E. P., & Wilson, K. B. (1951). On the Experimental Attainment of Optimum Conditions. *Journal of the Royal Statistical Society: Series B (Methodological)*, *13*(1), 1–38. https://doi.org/10.1111/j.2517-6161.1951.tb00067.x

Brand-Williams, W., Cuvelier, M. E., & Berset, C. (1995). Use of a free radical method to evaluate antioxidant activity. *LWT - Food Science and Technology*, *28*(1), 25–30. https://doi.org/10.1016/S0023-6438(95)80008-5

Branen, A. L. (1975). Toxicology and biochemistry of butylated hydroxyanisole and butylated hydroxytoluene. *Journal of the American Oil Chemists' Society*, *52*(2), 59. https://doi.org/10.1007/BF02901825

Bravo, L. (1998). Polyphenols: Chemistry, dietary sources, metabolism, and nutritional significance. *Nutrition Reviews*, *56*(11), 317–333.

Breitbach, M., Bathen, D., & Schmidt-Traub, H. (2003). Effect of Ultrasound on Adsorption and Desorption Processes. *Industrial & Engineering Chemistry Research*, *42*(22), 5635–5646. https://doi.org/10.1021/ie030333f

Bretag, J., Kammerer, D. R., Jensen, U., & Carle, R. (2009). Evaluation of the adsorption behavior of flavonoids and phenolic acids onto a food-grade resin using a D-optimal design. *European Food Research and Technology*, *228*(6), 985–999. https://doi.org/10.1007/s00217-009-1017-0

Briones, R., Serrano, L., & Labidi, J. (2012). Valorization of some lignocellulosic agro-industrial residues to obtain biopolyols. *Journal of Chemical Technology & Biotechnology*, *87*(2), 244–249.

Broom, O. J., Widjaya, B., Troelsen, J., Olsen, J., & Nielsen, O. H. (2009). Mitogen activated protein kinases: A role in inflammatory bowel disease? *Clinical & Experimental Immunology*, *158*(3), 272–280. https://doi.org/10.1111/j.1365-2249.2009.04033.x

Buran, T. J., Sandhu, A. K., Li, Z., Rock, C. R., Yang, W. W., & Gu, L. (2014). Adsorption/desorption characteristics and separation of anthocyanins and polyphenols from blueberries using macroporous adsorbent resins. *Journal of Food Engineering*, *128*, 167–173. https://doi.org/10.1016/j.jfoodeng.2013.12.029

Burns, J., Yokota, T., Ashihara, H., Lean, M. E. J., & Crozier, A. (2002). Plant Foods and Herbal Sources of Resveratrol. *Journal of Agricultural and Food Chemistry*, *50*(11), 3337–3340. https://doi.org/10.1021/jf0112973

Byun, S., Lee, K. W., Jung, S. K., Lee, E. J., Hwang, M. K., Lim, S. H., Bode, A. M., Lee, H. J., & Dong, Z. (2010). Luteolin Inhibits Protein Kinase Cε and c-Src Activities and UVB-Induced Skin Cancer. *Cancer Research*, *70*(6), 2415–2423. https://doi.org/10.1158/0008-5472.CAN-09-4093

Cai, R., & Arntfield, S. D. (2001). A rapid high-performance liquid chromatographic method for the determination of sinapine and sinapic acid in canola seed and meal. *Journal of the American Oil Chemists' Society*, *78*(9), 903–910. https://doi.org/10.1007/s11746-001-0362-4

Camacho-Barquero, L., Villegas, I., Sánchez-Calvo, J. M., Talero, E., Sánchez-Fidalgo, S., Motilva, V., & Alarcón de la Lastra, C. (2007). Curcumin, a Curcuma longa constituent, acts on MAPK p38 pathway modulating COX-2 and iNOS expression in chronic experimental colitis. *International Immunopharmacology*, *7*(3), 333–342. https://doi.org/10.1016/j.intimp.2006.11.006

Canella, M., & Sodini, G. (1977). Extraction of gossypol and oligosaccharides from oilseed meals. *Journal of Food Science*, *42*(5), 1218–1219. https://doi.org/10.1111/j.1365-2621.1977.tb14463.x

Cano, A., Hernández-Ruíz, J., García-Cánovas, F., Acosta, M., & Arnao, M. B. (1998). An end-point method for estimation of the total antioxidant activity in plant material. *Phytochemical Analysis*, *9*(4), 196–202. https://doi.org/10.1002/(SICI)1099-1565(199807/08)9:4-196::AID-PCA395>3.0.CO;2-W

Cao, G., & Prior, R. L. (1999). Measurement of oxygen radical absorbance capacity in biological samples. In *Methods in Enzymology* (Vol. 299, pp. 50–62). Elsevier. https://doi.org/10.1016/S0076-6879(99)99008-0

Cao, G., Sofic, E., & Prior, R. L. (1997). Antioxidant and Prooxidant Behavior of Flavonoids: Structure-Activity Relationships. *Free Radical Biology and Medicine*, *22*(5), 749–760. https://doi.org/10.1016/S0891-5849(96)00351-6

Cardona, F., Andrés-Lacueva, C., Tulipani, S., Tinahones, F. J., & Queipo-Ortuño, M. I. (2013). Benefits of polyphenols on gut microbiota and implications in human health. *The Journal of Nutritional Biochemistry*, *24*(8), 1415–1422. https://doi.org/. https://doi. org/10.1016/j.jnutbio.2013.05.001

Cardona, J. A., Lee, J.-H., & Talcott, S. T. (2009). Color and Polyphenolic Stability in Extracts Produced from Muscadine Grape (Vitis rotundifolia) Pomace. *Journal of Agricultural and Food Chemistry*, *57*(18), 8421–8425. https://doi.org/10.1021/jf901840t

Carluccio, M. A., Siculella, L., Ancora, M. A., Massaro, M., Scoditti, E., Storelli, C., Visioli, F., Distante, A., & De Caterina, R. (2003). Olive oil and red wine antioxidant polyphenols inhibit endothelial activation: Antiatherogenic properties of Mediterranean diet phytochemicals. *Arteriosclerosis, Thrombosis, and Vascular Biology*, *23*(4), 622–629. https://doi.org/10.1161/01.ATV.0000062884.69432.A0

Catena, G. C., & Bright, F. V. (1989). Thermodynamic study on the effects of .beta.-cyclodextrin inclusion with anilinonaphthalenesulfonates. *Analytical Chemistry*, *61*(8), 905–909. https://doi.org/10.1021/ac00183a024

Çelik, H., Kucukler, S., Çomaklı, S., Özdemir, S., Caglayan, C., Yardım, A., & Kandemir, F. M. (2020). Morin attenuates ifosfamide-induced neurotoxicity in rats via suppression of oxidative stress, neuroinflammation and neuronal apoptosis. *NeuroToxicology*, *76*, 126–137. https://doi.org/10.1016/j.neuro.2019.11.004

Chan, M. M.-Y. (1995). Inhibition of tumor necrosis factor by curcumin, a phytochemical. *Biochemical Pharmacology*, *49*(11), 1551–1556. https://doi.org/10.1016/0006-2952(95)00171-U

Chan, M. M.-Y., Huang, H.-I., Fenton, M. R., & Fong, D. (1998). In Vivo Inhibition of Nitric Oxide Synthase Gene Expression by Curcumin, a Cancer Preventive Natural Product with Anti-Inflammatory Properties. *Biochemical Pharmacology*, *55*(12), 1955–1962. https://doi.org/10.1016/S0006-2952(98)00114-2

Chang, X.-L., Wang, D., Chen, B.-Y., Feng, Y.-M., Wen, S.-H., & Zhan, P.-Y. (2012). Adsorption and Desorption Properties of Macroporous Resins for Anthocyanins from the Calyx Extract of Roselle (Hibiscus sabdariffa L.). *Journal of Agricultural and Food Chemistry*, *60*(9), 2368–2376. https://doi.org/10.1021/jf205311v

Chang, X.-L., Zhao, Z.-L., Li, X.-L., Xu, H., Sun, Y., & Wang, W.-H. (2014). Extraction and Advanced Adsorbents for the Separation of Perillaldehyde from Perilla frutescens (L.) Britton var. Crispa f. Viridis Leaves. *Food Science and Technology Research*, *20*(2), 189–199. https://doi.org/10.3136/fstr.20.189

Chanput, W., Mes, J. J., & Wichers, H. J. (2014). THP-1 cell line: An in vitro cell model for immune modulation approach. *International Immunopharmacology*, *23*(1), 37–45. https://doi.org/10.1016/j.intimp.2014.08.002

Chao, L., Hong, Z., Li, Z., & Gang, Z. (2010). Study on adsorption characteristic of macroporous resin to phenol in wastewater. *The Canadian Journal of Chemical Engineering*, n/a-n/a. https://doi.org/10.1002/cjce.20289

Chemat, F., Vian, M. A., & Cravotto, G. (2012). Green Extraction of Natural Products: Concept and Principles. *International Journal of Molecular Sciences*, *13*(7), 8615–8627. https://doi.org/10.3390/ijms13078615

Chen, C.-C., Chow, M.-P., Huang, W.-C., Lin, Y.-C., & Chang, Y.-J. (2004). Flavonoids inhibit tumor necrosis factor-α-induced up-regulation of intercellular adhesion molecule-1 (ICAM-1) in respiratory epithelial cells through activator protein-1 and nuclear factor-κB: structure-activity relationships. *Molecular Pharmacology*, *66*(3), 683–693.

Chen, C.-W., & Ho, C.-T. (1995). Antioxidant properties of polyphenols extracted from green and black teas. *Journal of Food Lipids*, *2*(1), 35–46. https://doi.org/10.1111/j.1745-4522.1995.tb00028.x

Chen, D., Daniel, K. G., Chen, M. S., Kuhn, D. J., Landis-Piwowar, K. R., & Dou, Q. P. (2005). Dietary flavonoids as proteasome inhibitors and apoptosis inducers in human leukemia cells. *Biochemical Pharmacology*, *69*(10), 1421–1432. https://doi.org/10.1016/j.bcp.2005.02.022

Chen, J.-C., Ho, F.-M., Pei-Dawn Lee Chao, Chen, C.-P., Jeng, K.-C. G., Hsu, H.-B., Lee, S.-T., Wen Tung Wu, & Lin, W.-W. (2005). Inhibition of iNOS gene expression by quercetin is mediated by the inhibition of IκB kinase, nuclear factor-kappa B and STAT1, and depends on heme oxygenase-1 induction in mouse BV-2 microglia. *European Journal of Pharmacology*, *521*(1–3), 9–20. https://doi.org/10.1016/j.ejphar.2005.08.005

Chen, S.-R., Xu, X.-Z., Wang, Y.-H., Chen, J.-W., Xu, S.-W., Gu, L.-Q., & Liu, P.-Q. (2010). Icariin Derivative Inhibits Inflammation through Suppression of p38 Mitogen-Activated Protein Kinase and Nuclear Factor-.κB Pathways. *Biological and Pharmaceutical Bulletin*, *33*(8), 1307–1313. https://doi.org/10.1248/bpb.33.1307

Chen, Y., Chen, W.-N., Hu, N., Banwell, M. G., Ma, C., Gardiner, M. G., & Lan, P. (2019). Cytotoxicity and Anti-inflammatory Properties of Apigenin-Derived Isolaxifolin. *Journal of Natural Products*, *82*(9), 2451–2459. https://doi.org/10.1021/acs.jnatprod.9b00113

Chen, Y., & Zhang, D. (2014). Adsorption kinetics, isotherm and thermodynamics studies of flavones from Vaccinium Bracteatum Thunb leaves on NKA-2 resin. *Chemical Engineering Journal*, *254*, 579–585.

Chen, Y., Zhang, W., Zhao, T., Li, F., Zhang, M., Li, J., Zou, Y., Wang, W., Cobbina, S. J., & Wu, X. (2016). Adsorption properties of macroporous adsorbent resins for separation of anthocyanins from mulberry. *Food Chemistry*, *194*, 712–722.

Chen, Y.-C., Shen, S.-C., Lee, W.-R., Hou, W.-C., Yang, L.-L., & Lee, T. J. F. (2001). Inhibition of nitric oxide synthase inhibitors and lipopolysaccharide induced inducible NOS and cyclooxygenase-2 gene expressions by rutin, quercetin, and quercetin pentaacetate in RAW 264.7 macrophages. *Journal of Cellular Biochemistry*, *82*(4), 537–548. https://doi.org/10.1002/jcb.1184

Cheng, S.-C., Wu, Y.-H., Huang, W.-C., Pang, J.-H. S., Huang, T.-H., & Cheng, C.-Y. (2019). Anti-inflammatory property of quercetin through downregulation of ICAM-1 and MMP-9 in TNF-α-activated retinal pigment epithelial cells. *Cytokine*, *116*, 48–60. https://doi.org/10.1016/j.cyto.2019.01.001

Chien, T. Y., Chen, L. G., Lee, C. J., Lee, F. Y., & Wang, C. C. (2008). Anti-inflammatory constituents of Zingiber zerumbet. *Food Chemistry*, *110*(3), 584–589. https://doi.org/10.1016/j.foodchem.2008.02.038

Cho, S., Park, S., Kwon, M., Jeong, T., Bok, S., Choi, W., Jeong, W., Ryu, S., Do, S., Lee, C., Song, J., & Jeong, K. (2003). Quercetin suppresses proinflammatory cytokines production through MAP kinases and NF-κB pathway in lipopolysaccharide-stimulated macrophage. *Molecular and Cellular Biochemistry*, *243*(1/2), 153–160. https://doi.org/10.1023/A:1021624520740

Choi, H. G., Tran, P. T., Lee, J.-H., Min, B. S., & Kim, J. A. (2018). Anti-inflammatory activity of caffeic acid derivatives isolated from the roots of Salvia miltiorrhiza Bunge. *Archives of Pharmacal Research*, *41*(1), 64–70. https://doi.org/10.1007/s12272-017-0983-1

Choi, J.-S., Choi, Y.-J., Park, S.-H., Kang, J.-S., & Kang, Y.-H. (2004). Flavones mitigate tumor necrosis factor-α-induced adhesion molecule upregulation in cultured human endothelial cells: Role of nuclear factor-κB. *The Journal of Nutrition*, *134*(5), 1013–1019.

Clandinin, D. R. (1961). Rapeseed Oil Meal Studies: 4. Effect of Sinapin, the Bitter Substance in Rapeseed Oil Meal, on the Growth of Chickens. *Poultry Science*, *40*(2), 484–487. https://doi.org/10.3382/ps.0400484

Colombo, F., Lorenzo, C. D., Regazzoni, L., Fumagalli, M., Sangiovanni, E., Sousa, L. P. de, Bavaresco, L., Tomasi, D., Bosso, A., Aldini, G., Restani, P., & Dell'Agli, M. (2019). Phenolic profiles and anti-inflammatory activities of sixteen table grape (Vitis vinifera L.) varieties. *Food & Function*, *10*(4), 1797–1807. https://doi.org/10.1039/C8FO02175A

Conde, E., Moure, A., & Domínguez, H. (2017). Recovery of phenols from autohydrolysis liquors of barley husks: Kinetic and equilibrium studies. *Industrial Crops and Products*, *103*, 175–184. https://doi.org/10.1016/j.indcrop.2017.03.048

Conidi, C., Cassano, A., Caiazzo, F., & Drioli, E. (2017). Separation and purification of phenolic compounds from pomegranate juice by ultrafiltration and nanofiltration membranes. *Journal of Food Engineering*, *195*, 1–13. https://doi.org/10.1016/j.jfoodeng.2016.09.017

Contescu, A., Vass, M., Contescu, C., Putyera, K., & Schwarz, J. A. (1998). Acid buffering capacity of basic carbons revealed by their continuous pK distribution. *Carbon*, *36*(3), 247–258. https://doi.org/10.1016/S0008-6223(97)00168-1

Costa, G., Francisco, V., C. Lopes, M., T. Cruz, M., & T. Batista, M. (2012). Intracellular Signaling Pathways Modulated by Phenolic Compounds: Application for New Anti-Inflammatory Drugs Discovery. *Current Medicinal Chemistry*, *19*(18), 2876–2900. https://doi.org/10.2174/092986712800672049

Dąbrowski, A., Podkościelny, P., Hubicki, Z., & Barczak, M. (2005). Adsorption of phenolic compounds by activated carbon—A critical review. *Chemosphere*, *58*(8), 1049–1070. https://doi.org/10.1016/j.chemosphere.2004.09.067

Dabrowski, K. J., & Sosulski, F. W. (1984). Composition of free and hydrolyzable phenolic acids in defatted flours of ten oilseeds. *Journal of Agricultural and Food Chemistry*, *32*(1), 128–130. https://doi.org/10.1021/jf00121a032

de la Puerta, R., Gutierrez, V. R., & Hoult, J. R. S. (1999). Inhibition of leukocyte 5-lipoxygenase by phenolics from virgin olive oil. *Biochemical Pharmacology*, *57*(4), 445–449. https://doi.org/10.1016/S0006-2952(98)00320-7

De Stefano, D., Maiuri, M. C., Simeon, V., Grassia, G., Soscia, A., Cinelli, M. P., & Carnuccio, R. (2007). Lycopene, quercetin and tyrosol prevent macrophage activation induced by gliadin and IFN-γ. *European Journal of Pharmacology*, *566*(1–3), 192–199.

Defaix, C., Aymes, A., Albe Slabi, S., Basselin, M., Mathé, C., Galet, O., & Kapel, R. (2019). A new size-exclusion chromatography method for fast rapeseed albumin and globulin quantification. *Food Chemistry*, *287*, 151–159. https://doi.org/10.1016/j.foodchem.2019.01.209

Defaix, C., Kapel, R., & Galet, O. (2020). *Protein isolate and process for the production thereof*. https://patents.justia.com/inventor/claire-defaix

Dey, P. M., & Harborne, J. B. (1997). *Plant Biochemistry*. Elsevier.

Ding, L., Deng, H., Wu, C., & Han, X. (2012). Affecting factors, equilibrium, kinetics and thermodynamics of bromide removal from aqueous solutions by MIEX resin. *Chemical Engineering Journal*, *181–182*, 360–370. https://doi.org/10.1016/j.cej.2011.11.096

Dominguez, H., Núnẽz, M. J., & Lema, J. M. (1995). Aqueous processing of sunflower kernels with enzymatic technology. *Food Chemistry*, *53*(4), 427–434.

Doner, L. W., Becard, Guillaume., & Irwin, P. L. (1993). Binding of flavonoids by polyvinylpolypyrrolidone. *Journal of Agricultural and Food Chemistry*, *41*(5), 753–757. https://doi.org/10.1021/jf00029a014

Dong, Y., Zhao, M., Sun-Waterhouse, D., Zhuang, M., Chen, H., Feng, M., & Lin, L. (2015a). Absorption and desorption behaviour of the flavonoids from Glycyrrhiza glabra L. leaf on macroporous adsorption resins. *Food Chemistry*, *168*, 538–545.

Dong, Y., Zhao, M., Sun-Waterhouse, D., Zhuang, M., Chen, H., Feng, M., & Lin, L. (2015b). Absorption and desorption behaviour of the flavonoids from Glycyrrhiza glabra L. leaf on macroporous adsorption resins. *Food Chemistry*, *168*, 538–545. https://doi.org/10.1016/j.foodchem.2014.07.109

Donnelly, L. E., Newton, R., Kennedy, G. E., Fenwick, P. S., Leung, R. H. F., Ito, K., Russell, R. E. K., & Barnes, P. J. (2004). Anti-inflammatory effects of resveratrol in lung epithelial cells: Molecular mechanisms. *American Journal of Physiology-Lung Cellular and Molecular Physiology*, *287*(4), L774–L783. https://doi.org/10.1152/ajplung.00110.2004

Dorrell, D. G. (1976). Chlorogenic Acid Content of Meal from Cultivated and Wild Sunflowers. *Crop Science*, *16*(3), 422–424. https://doi.org/10.2135/cropsci1976.0011183X001600030028x

Downey, R. K., & Bell, J. M. (1990). New Developments in Canola Research. In F. Shahidi (Ed.), *Canola and Rapeseed: Production, Chemistry, Nutrition and Processing Technology* (pp. 37–46). Springer US. https://doi.org/10.1007/978-1-4615-3912-4_4

Dreiseitel, A., Korte, G., Schreier, P., Oehme, A., Locher, S., Hajak, G., & Sand, P. G. (2009). SPhospholipase A2 is inhibited by anthocyanidins. *Journal of Neural Transmission*, *116*(9), 1071–1077. https://doi.org/10.1007/s00702-009-0268-z

Dziezak, J. D. (1986). Preservatives: Antioxidants. The ultimate answer to oxidation. *Preservatives: Antioxidants. The Ultimate Answer to Oxidation*, *40*(9), 94–102.

Egües, I., Alriols, M. G., Herseczki, Z., Marton, G., & Labidi, J. (2010). Hemicelluloses obtaining from rapeseed cake residue generated in the biodiesel production process. *Journal of Industrial and Engineering Chemistry*, *16*(2), 293–298.

Eler, G. J., Peralta, R. M., & Bracht, A. (2009). The action of n-propyl gallate on gluconeogenesis and oxygen uptake in the rat liver. *Chemico-Biological Interactions*, *181*(3), 390–399. https://doi.org/10.1016/j.cbi.2009.07.006

El-Shitany, N. A., & Eid, B. G. (2019). Icariin modulates carrageenan-induced acute inflammation through HO-1/Nrf2 and NF-kB signaling pathways. *Biomedicine & Pharmacotherapy*, *120*, 109567. https://doi.org/10.1016/j.biopha.2019.109567

Engels, C., Schieber, A., & Gänzle, M. G. (2012). Sinapic acid derivatives in defatted Oriental mustard (Brassica juncea L.) seed meal extracts using UHPLC-DAD-ESI-MS n and identification of compounds with antibacterial activity. *European Food Research and Technology*, *234*(3), 535–542.

Erdelyi, K., Kiss, A., Bakondi, E., Bai, P., Szabo, C., Gergely, P., Erdödi, F., & Virag, L. (2005). Gallotannin inhibits the expression of chemokines and inflammatory cytokines in A549 cells. *Molecular Pharmacology*, *68*(3), 895–904.

Erdèlyi, K., Kiss, A., Bakondi, E., Bai, P., Szabó, C., Gergely, P., Erdödi, F., & Virág, L. (2005). Gallotannin Inhibits the Expression of Chemokines and Inflammatory Cytokines in A549 Cells. *Molecular Pharmacology*, *68*(3), 895–904. https://doi.org/10.1124/mol.105.012518

Eriksson, G., Hedman, H., Boström, D., Pettersson, E., Backman, R., & Ohman, M. (2009). Combustion characterization of rapeseed meal and possible combustion applications. *Energy & Fuels*, *23*(8), 3930–3939.

Essafi-Benkhadir, K., Refai, A., Riahi, I., Fattouch, S., Karoui, H., & Essafi, M. (2012). Quince (Cydonia oblonga Miller) peel polyphenols modulate LPS-induced inflammation in human THP-1-derived macrophages through NF-κB, p38MAPK and Akt inhibition. *Biochemical and Biophysical Research Communications*, *418*(1), 180–185. https://doi.org/10.1016/j.bbrc.2012.01.003

Fang, J., Reichelt, M., Hidalgo, W., Agnolet, S., & Schneider, B. (2012). Tissue-Specific Distribution of Secondary Metabolites in Rapeseed (Brassica napus L.). *PLoS ONE*, *7*(10), e48006. https://doi.org/10.1371/journal.pone.0048006

FAOSTAT. (2020a, July 1). http://www.fao.org/faostat/en/#data/QC/visualize

FAOSTAT. (2020b, September 7). http://www.fao.org/faostat/en/#data/QC

Farah, A., Monteiro, M., Donangelo, C. M., & Lafay, S. (2008). Chlorogenic Acids from Green Coffee Extract are Highly Bioavailable in Humans. *The Journal of Nutrition*, *138*(12), 2309–2315. https://doi.org/10.3945/jn.108.095554

Farkhondeh, T., Abedi, F., & Samarghandian, S. (2019). Chrysin attenuates inflammatory and metabolic disorder indices in aged male rat. *Biomedicine & Pharmacotherapy*, *109*, 1120–1125. https://doi.org/10.1016/j.biopha.2018.10.059

Fechtner, S., Singh, A., Chourasia, M., & Ahmed, S. (2017). Molecular insights into the differences in anti-inflammatory activities of green tea catechins on IL-1β signaling in rheumatoid arthritis synovial fibroblasts. *Toxicology and Applied Pharmacology*, *329*, 112–120. https://doi.org/10.1016/j.taap.2017.05.016

Fernández-Bolaños, J., Rodríguez, G., Rodríguez, R., Heredia, A., Guillén, R., & Jiménez, A. (2002). Production in Large Quantities of Highly Purified Hydroxytyrosol from Liquid−Solid Waste of Two-Phase Olive Oil Processing or "Alperujo." *Journal of Agricultural and Food Chemistry*, *50*(23), 6804–6811. https://doi.org/10.1021/jf011712r

Fernandez-Panchon, M. S., Villano, D., Troncoso, A. M., & Garcia-Parrilla, M. C. (2008a). Antioxidant Activity of Phenolic Compounds: From *In Vitro* Results to *In Vivo* Evidence. *Critical Reviews in Food Science and Nutrition*, *48*(7), 649–671. https://doi.org/10.1080/10408390701761845

Fernandez-Panchon, M. S., Villano, D., Troncoso, A. M., & Garcia-Parrilla, M. C. (2008b). Antioxidant Activity of Phenolic Compounds: From In Vitro Results to In Vivo Evidence. *Critical Reviews in Food Science and Nutrition*, *48*(7), 649–671. https://doi.org/10.1080/10408390701761845

Ferreira, D., & Li, X.-C. (2000). Oligomeric proanthocyanidins: Naturally occurring O-heterocycles (January 1996 to December 1998). *Natural Product Reports*, *17*(2), 193–212. https://doi.org/10.1039/a705728h

Figueirinha, A., Cruz, M. T., Francisco, V., Lopes, M. C., & Batista, M. T. (2010). Anti-Inflammatory Activity of *Cymbopogon citratus* Leaf Infusion in Lipopolysaccharide-Stimulated Dendritic Cells: Contribution of the Polyphenols. *Journal of Medicinal Food*, *13*(3), 681–690. https://doi.org/10.1089/jmf.2009.0115

Firdaous, L., Fertin, B., Khelissa, O., Dhainaut, M., Nedjar, N., Chataigné, G., Ouhoud, L., Lutin, F., & Dhulster, P. (2017). Adsorptive removal of polyphenols from an alfalfa white proteins concentrate: Adsorbent screening, adsorption kinetics and equilibrium study. *Separation and Purification Technology*, *178*, 29–39. https://doi.org/10.1016/j.seppur.2017.01.009

Flower, R. J., & Vane, J. R. (1972). Inhibition of Prostaglandin Synthetase in Brain explains the Anti-pyretic Activity of Paracetamol (4-Acetamidophenol). *Nature*, *240*(5381), 410–411. https://doi.org/10.1038/240410a0

Foo, K. Y., & Hameed, B. H. (2010). Insights into the modeling of adsorption isotherm systems. *Chemical Engineering Journal*, *156*(1), 2–10. https://doi.org/10.1016/j.cej.2009.09.013

Fougerat, A., Gayral, S., Malet, N., Briand-Mesange, F., Breton-Douillon, M., & Laffargue, M. (2009). Phosphoinositide 3-kinases and their role in inflammation: Potential clinical targets in atherosclerosis? *Clinical Science*, *116*(11), 791–804. https://doi.org/10.1042/CS20080549

Francisco, V., Costa, G., Figueirinha, A., Marques, C., Pereira, P., Miguel Neves, B., Celeste Lopes, M., García-Rodríguez, C., Teresa Cruz, M., & Teresa Batista, M. (2013). Anti-inflammatory activity of Cymbopogon citratus leaves infusion via proteasome and nuclear factor-κB pathway inhibition: Contribution of chlorogenic acid. *Journal of Ethnopharmacology*, *148*(1), 126–134. https://doi.org/10.1016/j.jep.2013.03.077

Francisco, V., Figueirinha, A., Neves, B. M., García-Rodríguez, C., Lopes, M. C., Cruz, M. T., & Batista, M. T. (2011). Cymbopogon citratus as source of new and safe anti-inflammatory drugs: Bio-guided assay using lipopolysaccharide-stimulated macrophages. *Journal of Ethnopharmacology*, *133*(2), 818–827. https://doi.org/10.1016/j.jep.2010.11.018

Frankel, E. N. (1996). Antioxidants in lipid foods and their impact on food quality. *Food Chemistry*, *57*(1), 51–55. https://doi.org/10.1016/0308-8146(96)00067-2

Franz, M., Arafat, H. A., & Pinto, N. G. (2000). Effect of chemical surface heterogeneity on the adsorption mechanism of dissolved aromatics on activated carbon. *Carbon*, *38*(13), 1807–1819. https://doi.org/10.1016/S0008-6223(00)00012-9

Fu, B., Liu, J., Li, H., Li, L., Lee, F. S. C., & Wang, X. (2005). The application of macroporous resins in the separation of licorice flavonoids and glycyrrhizic acid. *Journal of Chromatography A*, *1089*(1–2), 18–24. https://doi.org/10.1016/j.chroma.2005.06.051

Fu, Y., Zu, Y., Liu, W., Efferth, T., Zhang, N., Liu, X., & Kong, Y. (2006). Optimization of luteolin separation from pigeonpea [Cajanus cajan (L.) Millsp.] leaves by macroporous resins. *Journal of Chromatography A*, *1137*(2), 145–152. https://doi.org/10.1016/j.chroma.2006.08.067

Fuccelli, R., Fabiani, R., & Rosignoli, P. (2018). Hydroxytyrosol Exerts Anti-Inflammatory and Anti-Oxidant Activities in a Mouse Model of Systemic Inflammation. *Molecules*, *23*(12), 3212. https://doi.org/10.3390/molecules23123212

Gao, M., Huang, W., & Liu, C.-Z. (2007). Separation of scutellarin from crude extracts of Erigeron breviscapus (vant.) Hand. Mazz. By macroporous resins. *Journal of Chromatography B*, *858*(1–2), 22–26. https://doi.org/10.1016/j.jchromb.2007.07.046

Gao, X.-H., Zhang, S.-D., Wang, L.-T., Yu, L., Zhao, X.-L., Ni, H.-Y., Wang, Y.-Q., Wang, J.-D., Shan, C.-H., & Fu, Y.-J. (2020). Anti-Inflammatory Effects of Neochlorogenic Acid Extract from Mulberry Leaf (Morus alba L.) Against LPS-Stimulated Inflammatory Response through Mediating the AMPK/Nrf2

Signaling Pathway in A549 Cells. *Molecules (Basel, Switzerland)*, *25*(6), Article 6. https://doi.org/10.3390/molecules25061385
Gao, Z. P., Yu, Z. F., Yue, T. L., & Quek, S. Y. (2013). Adsorption isotherm, thermodynamics and kinetics studies of polyphenols separation from kiwifruit juice using adsorbent resin. *Journal of Food Engineering*, *116*(1), 195–201. https://doi.org/10.1016/j.jfoodeng.2012.10.037
Garcia, J. C., & Takashima, K. (2003). Photocatalytic degradation of imazaquin in an aqueous suspension of titanium dioxide. *Journal of Photochemistry and Photobiology A: Chemistry*, *155*(1–3), 215–222. https://doi.org/10.1016/S1010-6030(02)00370-2
Gautam, R., & Jachak, S. M. (2009). Recent developments in anti-inflammatory natural products. *Medicinal Research Reviews*, *29*(5), 767–820. https://doi.org/10.1002/med.20156
Geller, D. A., & Billiar, T. R. (1998). Molecular biology of nitric oxide synthases. *Cancer and Metastasis Reviews*, *17*(1), 7–23. https://doi.org/10.1023/A:1005940202801
Geneau-Sbartaï, C., Leyris, J., Silvestre, F., & Rigal, L. (2008). Sunflower Cake as a Natural Composite: Composition and Plastic Properties. *Journal of Agricultural and Food Chemistry*, *56*(23), 11198–11208. https://doi.org/10.1021/jf8011536
Gennaro, L., Bocca, A. P., Modesti, D., Masella, R., & Coni, E. (1998). Effect of Biophenols on Olive Oil Stability Evaluated by Thermogravimetric Analysis. *Journal of Agricultural and Food Chemistry*, *46*(11), 4465–4469. https://doi.org/10.1021/jf980562q
Gerritsen, M. E., Carley, W. W., Ranges, G. E., Shen, C. P., Phan, S. A., Ligon, G. F., & Perry, C. A. (1995). Flavonoids inhibit cytokine-induced endothelial cell adhesion protein gene expression. *The American Journal of Pathology*, *147*(2), 278–292.
Gessner, D. K., Ringseis, R., & Eder, K. (2017). Potential of plant polyphenols to combat oxidative stress and inflammatory processes in farm animals. *Journal of Animal Physiology and Animal Nutrition*, *101*(4), 605–628. https://doi.org/10.1111/jpn.12579
Ghafourifar, P., & Cadenas, E. (2005). Mitochondrial nitric oxide synthase. *Trends in Pharmacological Sciences*, *26*(4), 190–195. https://doi.org/10.1016/j.tips.2005.02.005
Godbout, J. P., & Glaser, R. (2006). Stress-induced immune dysregulation: Implications for wound healing, infectious disease and cancer. *Journal of Neuroimmune Pharmacology*, *1*(4), 421–427. https://doi.org/10.1007/s11481-006-9036-0.
Gök, Ö., Özcan, A., Erdem, B., & Özcan, A. S. (2008). Prediction of the kinetics, equilibrium and thermodynamic parameters of adsorption of copper(II) ions onto 8-hydroxy quinoline immobilized bentonite. *Colloids and Surfaces A: Physicochemical and Engineering Aspects*, *317*(1–3), 174–185. https://doi.org/10.1016/j.colsurfa.2007.10.009
Gökmen, V., & Serpen, A. (2002). Equilibrium and kinetic studies on the adsorption of dark colored compounds from apple juice using adsorbent resin. *Journal of Food Engineering*, *53*(3), 221–227. https://doi.org/10.1016/S0260-8774(01)00160-1
Goli, A. H., Barzegar, M., & Sahari, M. A. (2005). Antioxidant activity and total phenolic compounds of pistachio (Pistachia vera) hull extracts. *Food Chemistry*, *92*(3), 521–525. https://doi.org/10.1016/j.foodchem.2004.08.020
González, R., Ballester, I., López-Posadas, R., Suárez, M. D., Zarzuelo, A., Martínez-Augustin, O., & Medina, F. S. D. (2011). Effects of Flavonoids and other Polyphenols on Inflammation. *Critical Reviews in Food Science and Nutrition*, *51*(4), 331–362. https://doi.org/10.1080/10408390903584094
González-Pérez, S., & Vereijken, J. M. (2007). Sunflower proteins: Overview of their physicochemical, structural and functional properties. *Journal of the Science of Food and Agriculture*, *87*(12), 2173–2191. https://doi.org/10.1002/jsfa.2971
Grohmann, K., Manthey, J. A., Cameron, R. G., & Buslig, B. S. (1999). Purification of Citrus Peel Juice and Molasses. *Journal of Agricultural and Food Chemistry*, *47*(12), 4859–4867. https://doi.org/10.1021/jf9903049
Gülçin, İ., Elias, R., Gepdiremen, A., Chea, A., & Topal, F. (2010). Antioxidant activity of bisbenzylisoquinoline alkaloids from Stephania rotunda: Cepharanthine and fangchinoline. *Journal of Enzyme Inhibition and Medicinal Chemistry*, *25*(1), 44–53. https://doi.org/10.3109/14756360902932792
Gunay, A. (2007). Application of nonlinear regression analysis for ammonium exchange by natural (Bigadiç) clinoptilolite. *Journal of Hazardous Materials*, *148*(3), 708–713. https://doi.org/10.1016/j.jhazmat.2007.03.041
Guo, C., Guo, M., Zhang, S., Qin, D., Yang, Y., & Li, M. (2018). Assessment of patulin adsorption efficacy from aqueous solution by water-insoluble corn flour. *Journal of Food Safety*, *38*(1), Article 1. https://doi.org/10.1111/jfs.12397

Guo, C., Qiao, J., Zhang, S., Ren, X., & Li, M. (2018). Purification of polyphenols from kiwi fruit peel extracts using macroporous resins and high-performance liquid chromatography analysis. *International Journal of Food Science & Technology*, *53*(6), 1486–1493. https://doi.org/10.1111/ijfs.13729

Gupta, V. K. (1998). Equilibrium Uptake, Sorption Dynamics, Process Development, and Column Operations for the Removal of Copper and Nickel from Aqueous Solution and Wastewater Using Activated Slag, a Low-Cost Adsorbent. *Industrial & Engineering Chemistry Research*, *37*(1), 192–202. https://doi.org/10.1021/ie9703898

Güran, M., Şanlıtürk, G., Kerküklü, N. R., Altundağ, E. M., & Süha Yalçın, A. (2019). Combined effects of quercetin and curcumin on anti-inflammatory and antimicrobial parameters in vitro. *European Journal of Pharmacology*, *859*, 172486. https://doi.org/10.1016/j.ejphar.2019.172486

Gururajan, M., Dasu, T., Shahidain, S., Jennings, C. D., Robertson, D. A., Rangnekar, V. M., & Bondada, S. (2007). Spleen Tyrosine Kinase (Syk), a Novel Target of Curcumin, Is Required for B Lymphoma Growth. *The Journal of Immunology*, *178*(1), 111–121. https://doi.org/10.4049/jimmunol.178.1.111

Gyamfi, M. A., & Aniya, Y. (2002). Antioxidant properties of Thonningianin A, isolated from the African medicinal herb, Thonningia sanguinea. *Biochemical Pharmacology*, *63*(9), 1725–1737. https://doi.org/10.1016/S0006-2952(02)00915-2

Ha, S. K., Park, H.-Y., Eom, H., Kim, Y., & Choi, I. (2012). Narirutin fraction from citrus peels attenuates LPS-stimulated inflammatory response through inhibition of NF-κB and MAPKs activation. *Food and Chemical Toxicology*, *50*(10), 3498–3504. https://doi.org/10.1016/j.fct.2012.07.007

Hagiu, A., Attin, T., Schmidlin, P. R., & Ramenzoni, L. L. (2020). Dose-dependent green tea effect on decrease of inflammation in human oral gingival epithelial keratinocytes: In vitro study. *Clinical Oral Investigations*, *24*(7), 2375–2383. https://doi.org/10.1007/s00784-019-03096-4

Hajimahmoodi, M., Moghaddam, G., Mousavi, S., Sadeghi, N., Oveisi, M., & Jannat, B. (2014). Total Antioxidant Activity, and Hesperidin, Diosmin, Eriocitrin and Quercetin Contents of Various Lemon Juices. *Tropical Journal of Pharmaceutical Research*, *13*(6), 951. https://doi.org/10.4314/tjpr.v13i6.18

Halhouli, K. A., Darwish, N. A., & Al-Dhoon, N. M. (1995). Effects of pH and Inorganic Salts on the Adsorption of Phenol from Aqueous Systems on Activated Decolorizing Charcoal. *Separation Science and Technology*, *30*(17), 3313–3324. https://doi.org/10.1080/01496399508013147

Halliwell, B. (1996). Commentary Oxidative Stress, Nutrition and Health. Experimental Strategies for Optimization of Nutritional Antioxidant Intake in Humans. *Free Radical Research*, *25*(1), 57–74. https://doi.org/10.3109/10715769609145656

Hamdaoui, O., & Naffrechoux, E. (2007). Modeling of adsorption isotherms of phenol and chlorophenols onto granular activated carbonPart I. Two-parameter models and equations allowing determination of thermodynamic parameters. *Journal of Hazardous Materials*, *147*(1–2), 381–394. https://doi.org/10.1016/j.jhazmat.2007.01.021

Hameed, B. H., & El-Khaiary, M. I. (2008). Malachite green adsorption by rattan sawdust: Isotherm, kinetic and mechanism modeling. *Journal of Hazardous Materials*, *159*(2–3), 574–579. https://doi.org/10.1016/j.jhazmat.2008.02.054

Hamid, A. A., Aiyelaagbe, O. O., Usman, L. A., Ameen, O. M., & Lawal, A. (2010). Antioxidants: Its medicinal and pharmacological applications. *African Journal of Pure and Applied Chemistry*, *4*(8), 142–151. https://doi.org/10.5897/AJPAC.9000020

Han, R.-M., Zhang, J.-P., & Skibsted, L. H. (2012). Reaction Dynamics of Flavonoids and Carotenoids as Antioxidants. *Molecules*, *17*(2), 2140–2160. https://doi.org/10.3390/molecules17022140

Hararah, M. A., Ibrahim, K. A., Al-Muhtaseb, A. H., Yousef, R. I., Abu-Surrah, A., & Qatatsheh, A. (2010). Removal of phenol from aqueous solutions by adsorption onto polymeric adsorbents. *Journal of Applied Polymer Science*, *117*(4), 1908–1913. https://doi.org/10.1002/app.32107

Harirforoosh, S., & Jamali, F. (2009). Renal adverse effects of nonsteroidal anti-inflammatory drugs. *Expert Opinion on Drug Safety*, *8*(6), 669–681. https://doi.org/10.1517/14740330903311023

Hawkey, C. J. (2003). Non-steroidal anti-inflammatory drugs: Overall risks and management. Complementary roles for COX-2 inhibitors and proton pump inhibitors. *Gut*, *52*(4), 600–608. https://doi.org/10.1136/gut.52.4.600

He, Z., Xia, W., & Chen, J. (2008). Isolation and structure elucidation of phenolic compounds in Chinese olive (Canarium album L.) fruit. *European Food Research and Technology*, *226*(5), 1191–1196. https://doi.org/10.1007/s00217-007-0653-5

Heijnen, C. G. M., Haenen, G. R. M. M., van Acker, F. A. A., van der Vijgh, W. J. F., & Bast, A. (2001). Flavonoids as peroxynitrite scavengers: The role of the hydroxyl groups. *Toxicology in Vitro*, *15*(1), 3–6. https://doi.org/10.1016/S0887-2333(00)00053-9

Heim, K. E., Tagliaferro, A. R., & Bobilya, D. J. (2002). Flavonoid antioxidants: Chemistry, metabolism and structure-activity relationships. *The Journal of Nutritional Biochemistry*, *13*(10), 572–584. https://doi.org/10.1016/S0955-2863(02)00208-5

Herrera, E., & Barbas, C. (2001). Vitamin E: Action, metabolism and perspectives. *Journal of Physiology and Biochemistry*, *57*(1), 43–56. https://doi.org/10.1007/BF03179812

Hettiarachchy, N. S., Glenn, K. C., Gnanasambandam, R., & Johnson, M. G. (1996). Natural Antioxidant Extract from Fenugreek (Trigonella foenumgraecum) for Ground Beef Patties. *Journal of Food Science*, *61*(3), 516–519. https://doi.org/10.1111/j.1365-2621.1996.tb13146.x

Hirano, T., Higa, S., Arimitsu, J., Naka, T., Ogata, A., Shima, Y., Fujimoto, M., Yamadori, T., Ohkawara, T., Kuwabara, Y., Kawai, M., Matsuda, H., Yoshikawa, M., Maezaki, N., Tanaka, T., Kawase, I., & Tanaka, T. (2006). Luteolin, a flavonoid, inhibits AP-1 activation by basophils. *Biochemical and Biophysical Research Communications*, *340*(1), 1–7. https://doi.org/10.1016/j.bbrc.2005.11.157

Ho, Y. S., & Mckay, G. (1998). Kinetic Models for the Sorption of Dye from Aqueous Solution by Wood. *Process Safety and Environmental Protection*, *76*(2), 183–191. https://doi.org/10.1205/095758298529326

Hoppe, M. B., Jha, H. C., & Egge, H. (1997). Structure of an antioxidant from fermented soybeans (tempeh). *Journal of the American Oil Chemists' Society*, *74*(4), 477–479. https://doi.org/10.1007/s11746-997-0110-4

Huang, D., Ou, B., & Prior, R. L. (2005). The Chemistry behind Antioxidant Capacity Assays. *Journal of Agricultural and Food Chemistry*, *53*(6), 1841–1856. https://doi.org/10.1021/jf030723c

Huang, M.-H., Chu, H.-L., Juang, L.-J., & Wang, B.-S. (2010). Inhibitory effects of sweet potato leaves on nitric oxide production and protein nitration. *Food Chemistry*, *121*(2), 480–486.

Huang, X., Liu, Y., Song, F., Liu, Z., & Liu, S. (2009). Studies on principal components and antioxidant activity of different Radix Astragali samples using high-performance liquid chromatography/electrospray ionization multiple-stage tandem mass spectrometry. *Talanta*, *78*(3), 1090–1101. https://doi.org/10.1016/j.talanta.2009.01.021

Huang, X., Pan, Q., Mao, Z., Zhang, R., Ma, X., Xi, Y., & You, H. (2018). Sinapic Acid Inhibits the IL-1β-Induced Inflammation via MAPK Downregulation in Rat Chondrocytes. *Inflammation*, *41*(2), 562–568. https://doi.org/10.1007/s10753-017-0712-4

Hudson, B. J. F. (Ed.). (1994). *New and Developing Sources of Food Proteins*. Springer US. https://doi.org/10.1007/978-1-4615-2652-0

Hurrell, R. F. (2003). Influence of Vegetable Protein Sources on Trace Element and Mineral Bioavailability. *The Journal of Nutrition*, *133*(9), 2973S-2977S. https://doi.org/10.1093/jn/133.9.2973S

Hwang, M. K., Song, N. R., Kang, N. J., Lee, K. W., & Lee, H. J. (2009). Activation of phosphatidylinositol 3-kinase is required for tumor necrosis factor-α-induced upregulation of matrix metalloproteinase-9: Its direct inhibition by quercetin. *The International Journal of Biochemistry & Cell Biology*, *41*(7), 1592–1600. https://doi.org/10.1016/j.biocel.2009.01.014

Hwang, S. J., Kim, Y.-W., Park, Y., Lee, H.-J., & Kim, K.-W. (2014). Anti-inflammatory effects of chlorogenic acid in lipopolysaccharide-stimulated RAW 264.7 cells. *Inflammation Research*, *63*(1), 81–90. https://doi.org/10.1007/s00011-013-0674-4

Ichikawa, D., Matsui, A., Imai, M., Sonoda, Y., & Kasahara, T. (2004). Effect of various catechins on the IL-12p40 production by murine peritoneal macrophages and a macrophage cell line, J774.1. *Biological & Pharmaceutical Bulletin*, *27*(9), 1353–1358. https://doi.org/10.1248/bpb.27.1353

Idris, Z. M., Dzahir, M. I. H. M., Jamal, P., Barkat, A. A., & Xian, R. L. W. (2017). Purification of bioactive phenolics from Phanerochaete chysosporium biomass extract on selected macroporous resins. *IOP Conference Series: Materials Science and Engineering*, *206*, 012070. https://doi.org/10.1088/1757-899x/206/1/012070

Ihara, Y. (1988). Effect of inorganic salt on adsorption of sodium alkyl sulfates and fatty acid sodium salts from aqueous solution onto ion exchange resins. *Journal of Applied Polymer Science*, *36*(4), 891–897. https://doi.org/10.1002/app.1988.070360412

Ismail, T., Sestili, P., & Akhtar, S. (2012). Pomegranate peel and fruit extracts: A review of potential anti-inflammatory and anti-infective effects. *Journal of Ethnopharmacology*, *143*(2), 397–405. https://doi.org/10.1016/j.jep.2012.07.004

Jacobi, H. (1998). DNA Strand Break Induction and Enhanced Cytotoxicity of Propyl Gallate in the Presence of Copper(II). *Free Radical Biology and Medicine*, *24*(6), 972–978. https://doi.org/10.1016/S0891-5849(97)00400-0

Jacobi, H., Hinrichsen, M.-L., Weß, D., & Witte, I. (1999). Induction of lipid peroxidation in human fibroblasts by the antioxidant propyl gallate in combination with copper(II). *Toxicology Letters*, *110*(3), 183–190. https://doi.org/10.1016/S0378-4274(99)00156-3

Jayaprakasha, G. K., Singh, R. P., & Sakariah, K. K. (2001). Antioxidant activity of grape seed (Vitis vinifera) extracts on peroxidation models in vitro. *Food Chemistry*, *73*(3), 285–290. https://doi.org/10.1016/S0308-8146(00)00298-3

Jia, G., & Lu, X. (2008). Enrichment and purification of madecassoside and asiaticoside from Centella asiatica extracts with macroporous resins. *Journal of Chromatography A*, *1193*(1–2), 136–141. https://doi.org/10.1016/j.chroma.2008.04.024

Jin, Q., Yue, J., Shan, L., Tao, G., Wang, X., & Qiu, A. (2008). Process research of macroporous resin chromotography for separation of N-(p-coumaroyl) serotonin and N-feruloylserotonin from Chinese safflower seed extracts. *Separation and Purification Technology*, *62*(2), 370–375. https://doi.org/10.1016/j.seppur.2008.02.007

Joseph, S. V., Edirisinghe, I., & Burton-Freeman, B. M. (2016). Fruit Polyphenols: A Review of Anti-inflammatory Effects in Humans. *Critical Reviews in Food Science and Nutrition*, *56*(3), 419–444. https://doi.org/10.1080/10408398.2013.767221

Juang, R.-S., & Shiau, J.-Y. (1999). Adsorption isotherms of phenols from water onto macroreticular resins. *Journal of Hazardous Materials*, *70*(3), 171–183. https://doi.org/10.1016/S0304-3894(99)00152-1

Kamble, S. P., Jagtap, S., Labhsetwar, N. K., Thakare, D., Godfrey, S., Devotta, S., & Rayalu, S. S. (2007). Defluoridation of drinking water using chitin, chitosan and lanthanum-modified chitosan. *Chemical Engineering Journal*, *129*(1–3), 173–180. https://doi.org/10.1016/j.cej.2006.10.032

Kammerer, D., Gajdos Kljusuric, J., Carle, R., & Schieber, A. (2005). Recovery of anthocyanins from grape pomace extracts (Vitis vinifera L. cv. Cabernet Mitos) using a polymeric adsorber resin. *European Food Research and Technology*, *220*(3–4), 431–437. https://doi.org/10.1007/s00217-004-1078-z

Kammerer, D. R., Saleh, Z. S., Carle, R., & Stanley, R. A. (2007). Adsorptive recovery of phenolic compounds from apple juice. *European Food Research and Technology*, *224*(5), 605–613. https://doi.org/10.1007/s00217-006-0346-5

Kang, G., Kong, P.-J., Yuh, Y.-J., Lim, S.-Y., Yim, S.-V., Chun, W., & Kim, S.-S. (2004). Curcumin Suppresses Lipopolysaccharide-Induced Cyclooxygenase-2 Expression by Inhibiting Activator Protein 1 and Nuclear Factor κB Bindings in BV2 Microglial Cells. *Journal of Pharmacological Sciences*, *94*(3), 325–328. https://doi.org/10.1254/jphs.94.325

Kang, J., Xie, C., Li, Z., Nagarajan, S., Schauss, A. G., Wu, T., & Wu, X. (2011). Flavonoids from acai (Euterpe oleracea Mart.) pulp and their antioxidant and anti-inflammatory activities. *Food Chemistry*, *128*(1), 152–157. https://doi.org/10.1016/j.foodchem.2011.03.011

Karadag, A., Ozcelik, B., & Saner, S. (2009). Review of Methods to Determine Antioxidant Capacities. *Food Analytical Methods*, *2*(1), 41–60. https://doi.org/10.1007/s12161-008-9067-7

Karamać, M., Kosińska, A., Estrella, I., Hernández, T., & Dueñas, M. (2012). Antioxidant activity of phenolic compounds identified in sunflower seeds. *European Food Research and Technology*, *235*(2), 221–230. https://doi.org/10.1007/s00217-012-1751-6

Karimifard, S., & Alavi Moghaddam, M. R. (2018). Application of response surface methodology in physicochemical removal of dyes from wastewater: A critical review. *Science of The Total Environment*, *640–641*, 772–797. https://doi.org/10.1016/j.scitotenv.2018.05.355

Kaya, Z., Yayla, M., Cinar, I., Atila, N. E., Ozmen, S., Bayraktutan, Z., & Bilici, D. (2019). Epigallocatechin-3-gallate (EGCG) exert therapeutic effect on acute inflammatory otitis media in rats. *International Journal of Pediatric Otorhinolaryngology*, *124*, 106–110. https://doi.org/10.1016/j.ijporl.2019.05.012

Khan, M. A., & Shahidi, F. (2001). Effects of natural and synthetic antioxidants on the oxidative stability of borage and evening primrose triacylglycerols. *Food Chemistry*, *75*(4), 431–437. https://doi.org/10.1016/S0308-8146(01)00232-1

Khan, N., & Mukhtar, H. (2010). Cancer and metastasis: Prevention and treatment by green tea. *Cancer and Metastasis Reviews*, *29*(3), 435–445. https://doi.org/10.1007/s10555-010-9236-1

Khattab, R. (2010). Determination of Sinapic Acid Derivatives in Canola Extracts Using High-Performance Liquid Chromatography (R. Khattab, M. Eskin, M. Aliani, & U. Thiyam, Trans.). *Journal of the American Oil Chemists' Society*, *v. 87*(2), 147–155. PubAg. https://doi.org/10.1007/s11746-009-1486-0

Khuri, A. I., & Mukhopadhyay, S. (2010). Response surface methodology. *Wiley Interdisciplinary Reviews: Computational Statistics*, *2*(2), 128–149. https://doi.org/10.1002/wics.73

Kim, H. Y., Park, E. J., Joe, E., & Jou, I. (2003). Curcumin Suppresses Janus Kinase-STAT Inflammatory Signaling through Activation of Src Homology 2 Domain-Containing Tyrosine Phosphatase 2 in Brain Microglia. *The Journal of Immunology*, *171*(11), 6072–6079. https://doi.org/10.4049/jimmunol.171.11.6072

Kim, J., Yoon, M., Yang, H., Jo, J., Han, D., Jeon, Y.-J., & Cho, S. (2014). Enrichment and purification of marine polyphenol phlorotannins using macroporous adsorption resins. *Food Chemistry*, *162*, 135–142. https://doi.org/10.1016/j.foodchem.2014.04.035

Kim, K. H., Lee, K. W., Kim, D. Y., Park, H. H., Kwon, I. B., & Lee, H. J. (2004). Extraction and fractionation of glucosyltransferase inhibitors from cacao bean husk. *Process Biochemistry*, *39*(12), 2043–2046. https://doi.org/10.1016/j.procbio.2003.10.006

Kim, M.-R., Kim, W.-C., Lee, D.-Y., & Kim, C.-W. (2007). Recovery of narirutin by adsorption on a non-ionic polar resin from a water-extract of Citrus unshiu peels. *Journal of Food Engineering*, *78*(1), 27–32. https://doi.org/10.1016/j.jfoodeng.2005.09.004

Kim, S.-J., Kim, M.-C., Lee, B.-J., Park, D.-H., Hong, S.-H., & Um, J.-Y. (2010). Anti-Inflammatory activity of chrysophanol through the suppression of NF-kB/caspase-1 activation in vitro and in vivo. *Molecules*, *15*(9), 6436–6451.

Klaus, S., Pültz, S., Thöne-Reineke, C., & Wolfram, S. (2005). Epigallocatechin gallate attenuates diet-induced obesity in mice by decreasing energy absorption and increasing fat oxidation. *International Journal of Obesity*, *29*(6), 615–623. https://doi.org/10.1038/sj.ijo.0802926

Kobayashi-Hattori, K., Mogi, A., Matsumoto, Y., & Takita, T. (2005). Effect of Caffeine on the Body Fat and Lipid Metabolism of Rats Fed on a High-Fat Diet. *Bioscience, Biotechnology, and Biochemistry*, *69*(11), 2219–2223. https://doi.org/10.1271/bbb.69.2219

Koble, R. A., & Corrigan, T. E. (1952). Adsorption isotherms for pure hydrocarbons. *Industrial & Engineering Chemistry*, *44*(2), 383–387. https://doi.org/10.1021/ie50506a049

Kooy, N., Royall, J., Ischiropoulos, H., & Beckman, J. (1994). Peroxynitrite-mediated oxidation of dihydrorhodamine 123. *Free Radical Biology and Medicine*, *16*(2), 149–156. https://doi.org/10.1016/0891-5849(94)90138-4

Koski, A., Pekkarinen, S., Hopia, A., K., & Heinonen, M. (2003). Processing of rapeseed oil: Effects on sinapic acid derivative content and oxidative stability. *European Food Research and Technology*, *217*(2), 110–114. https://doi.org/10.1007/s00217-003-0721-4

Kozlowska, H., Naczk, M., Shahidi, F., & Zadernowski, R. (1990a). Phenolic Acids and Tannins in Rapeseed and Canola. In F. Shahidi (Ed.), *Canola and Rapeseed* (pp. 193–210). Springer US. https://doi.org/10.1007/978-1-4615-3912-4_11

Kozlowska, H., Naczk, M., Shahidi, F., & Zadernowski, R. (1990b). Phenolic Acids and Tannins in Rapeseed and Canola. In F. Shahidi (Ed.), *Canola and Rapeseed: Production, Chemistry, Nutrition and Processing Technology* (pp. 193–210). Springer US. https://doi.org/10.1007/978-1-4615-3912-4_11

Kozlowska, H., Zadernowski, R., & Sosulski, F. W. (1983). Phenolic acids in oilseed flours. *Food/Nahrung*, *27*(5), 449–453.

Kremr, D., Bajer, T., Bajerová, P., Surmová, S., Ventura, K., Kremr, D., Bajer, T., Bajerová, P., Surmová, S., & Ventura, K. (2016). Unremitting problems with chlorogenic acid Nomenclature: A review. *Química Nova*, *39*(4), 530–533. https://doi.org/10.5935/0100-4042.20160063

Krishnaiah, D., Sarbatly, R., & Nithyanandam, R. (2011). A review of the antioxidant potential of medicinal plant species. *Food and Bioproducts Processing*, *89*(3), 217–233. https://doi.org/10.1016/j.fbp.2010.04.008

Krygier, K., Sosulski, F., & Hogge, L. (1982). Free, esterified, and insoluble-bound phenolic acids. 1. Extraction and purification procedure. *Journal of Agricultural and Food Chemistry*, *30*(2), 330–334. https://doi.org/10.1021/jf00110a028

Ku, Y., & Lee, K.-C. (2000). Removal of phenols from aqueous solution by XAD-4 resin. *Journal of Hazardous Materials*, *80*(1–3), 59–68. https://doi.org/10.1016/S0304-3894(00)00275-2

Ku, Y., Lee, K.-C., & Wang, W. (2005). Removal of Phenols from Aqueous Solutions by Purolite A-510 Resin. *Separation Science and Technology*, *39*(4), 911–923.

Kumar, K. S., Sabu, V., Sindhu, G., Rauf, A. A., & Helen, A. (2018). Isolation, identification and characterization of apigenin from Justicia gendarussa and its anti-inflammatory activity. *International Immunopharmacology*, *59*, 157–167. https://doi.org/10.1016/j.intimp.2018.04.004

Kundu, J. K., & SURH, Y.-J. (2007). Epigallocatechin Gallate Inhibits Phorbol Ester-Induced Activation of NF-κB and CREB in Mouse Skin: Role of p38 MAPK. *Annals of the New York Academy of Sciences*, *1095*(1), 504–512.

Kundu, J. K., & Surh, Y.-J. (2007). Epigallocatechin Gallate Inhibits Phorbol Ester-Induced Activation of NF-B and CREB in Mouse Skin: Role of p38 MAPK. *Annals of the New York Academy of Sciences*, *1095*(1), 504–512. https://doi.org/10.1196/annals.1397.054

Kurata, R., Adachi, M., Yamakawa, O., & Yoshimoto, M. (2007). Growth suppression of human cancer cells by polyphenolics from sweetpotato (Ipomoea batatas L.) leaves. *Journal of Agricultural and Food Chemistry*, *55*(1), 185–190.

Kurata, R., Yahara, S., Yamakawa, O., & Yoshimoto, M. (2011). Simple high-yield purification of 3, 4, 5-tri-O-caffeoylquinic acid from sweetpotato (Ipomoea batatas L.) leaf and its inhibitory effects on aldose reductase. *Food Science and Technology Research*, *17*(2), 87–92.

Ky, C.-L., Noirot, M., & Hamon, S. (1997). Comparison of Five Purification Methods for Chlorogenic Acids in Green Coffee Beans (*Coffea* sp.). *Journal of Agricultural and Food Chemistry*, *45*(3), 786–790. https://doi.org/10.1021/jf9605254

Lagergren, S. (1898). About the Theory of So-Called Adsorption of Soluble Substances. *Kungliga Svenska Vetenskapsakademiens Handlingar*, *24*, 1–39.
Laguna, O., Barakat, A., Alhamada, H., Durand, E., Baréa, B., Fine, F., Villeneuve, P., Citeau, M., Dauguet, S., & Lecomte, J. (2018). Production of proteins and phenolic compounds enriched fractions from rapeseed and sunflower meals by dry fractionation processes. *Industrial Crops and Products*, *118*, 160–172. https://doi.org/10.1016/j.indcrop.2018.03.045
Lakshmi, S. P., Reddy, A. T., Kodidhela, L. D., & Varadacharyulu, N. Ch. (2020). The tea catechin epigallocatechin gallate inhibits NF-κB-mediated transcriptional activation by covalent modification. *Archives of Biochemistry and Biophysics*, *695*, 108620. https://doi.org/10.1016/j.abb.2020.108620
Langmuir, I. (1918). A new adsorption isotherm. *J. Am. Chem. Soc.*, *40*, 1361–1403.
Lau, F. C., Bielinski, D. F., & Joseph, J. A. (2007). Inhibitory effects of blueberry extract on the production of inflammatory mediators in lipopolysaccharide-activated BV2 microglia. *Journal of Neuroscience Research*, *85*(5), 1010–1017. https://doi.org/10.1002/jnr.21205
Le, T. T., Framboisier, X., Aymes, A., Ropars, A., Frippiat, J.-P., & Kapel, R. (2021). Identification and Capture of Phenolic Compounds from a Rapeseed Meal Protein Isolate Production Process By-Product by Macroporous Resin and Valorization Their Antioxidant Properties. *Molecules*, *26*(19), 5853. https://doi.org/10.3390/molecules26195853
Le, T. T., Ropars, A., Aymes, A., Frippiat, J.-P., & Kapel, R. (2021). Multicriteria Optimization of Phenolic Compounds Capture from a Sunflower Protein Isolate Production Process by-Product by Adsorption Column and Assessment of Their Antioxidant and Anti-Inflammatory Effects. *Foods*, *10*(4), 760. https://doi.org/10.3390/foods10040760
Le, T. T., Ropars, A., Sundaresan, A., Crucian, B., Choukér, A., & Frippiat, J.-P. (2020). Pharmacological Countermeasures to Spaceflight-Induced Alterations of the Immune System. In A. Choukèr (Ed.), *Stress Challenges and Immunity in Space* (pp. 637–657). Springer International Publishing. https://doi.org/10.1007/978-3-030-16996-1_35
Lee, S., & Seo, E. (2019). Effects of Rutin on Anti-inflammatory in Adipocyte 3T3-L1 and Colon Cancer Cell SW-480. *Journal of the Korean Society of Food Culture*, *34*(1), 84–92. https://doi.org/10.7318/KJFC/2019.34.1.84
Leung, J., Fenton, T. W., & Clandinin, D. R. (1981). Phenolic Components of Sunflower Flour. *Journal of Food Science*, *46*(5), 1386–1388. https://doi.org/10.1111/j.1365-2621.1981.tb04180.x
Leyton, A., Vergara-Salinas, J. R., Pérez-Correa, J. R., & Lienqueo, M. E. (2017). Purification of phlorotannins from Macrocystis pyrifera using macroporous resins. *Food Chemistry*, *237*, 312–319. https://doi.org/10.1016/j.foodchem.2017.05.114
Li, A., Zhang, Q., Chen, J., Fei, Z., Long, C., & Li, W. (2001). Adsorption of phenolic compounds on Amberlite XAD-4 and its acetylated derivative MX-4. *Reactive and Functional Polymers*, *49*(3), 225–233. https://doi.org/10.1016/S1381-5148(01)00080-3
Li, J., & Chase, H. A. (2009). Characterization and evaluation of a macroporous adsorbent for possible use in the expanded bed adsorption of flavonoids from Ginkgo biloba L. *Journal of Chromatography A*, *1216*(50), 8730–8740. https://doi.org/10.1016/j.chroma.2009.02.092
Li, J., & Chase, H. A. (2010). Development of adsorptive (non-ionic) macroporous resins and their uses in the purification of pharmacologically-active natural products from plant sources. *Natural Product Reports*, *27*(10), 1493–1510.
Li, J., & El Rassi, Z. (2002). High Performance Liquid Chromatography of Phenolic Choline Ester Fragments Derived by Chemical and Enzymatic Fragmentation Processes: Analysis of Sinapine in Rape Seed. *Journal of Agricultural and Food Chemistry*, *50*(6), 1368–1373. https://doi.org/10.1021/jf011334q
Li, P., Huo, L., Su, W., Lu, R., Deng, C., Liu, L., Deng, Y., Guo, N., Lu, C., & He, C. (2011). Free radical-scavenging capacity, antioxidant activity and phenolic content of Pouzolzia zeylanica. *Journal of the Serbian Chemical Society*, *76*(5), 709–717. https://doi.org/10.2298/JSC100818063L
Li, P., Wang, Y., Ma, R., & Zhang, X. (2005). Separation of tea polyphenol from Green Tea Leaves by a combined CATUFM-adsorption resin process. *Journal of Food Engineering*, *67*(3), 253–260. https://doi.org/10.1016/j.jfoodeng.2004.04.009
Li, Y., Liu, J., Cao, R., Deng, S., & Lu, X. (2013). Adsorption of Myricetrin, Puerarin, Naringin, Rutin, and Neohesperidin Dihydrochalcone Flavonoids on Macroporous Resins. *Journal of Chemical & Engineering Data*, *58*(9), 2527–2537. https://doi.org/10.1021/je400416j
Li, Y., Lu, G., & Li, S. (2003). Photocatalytic production of hydrogen in single component and mixture systems of electron donors and monitoring adsorption of donors by in situ infrared spectroscopy. *Chemosphere*, *52*(5), 843–850. https://doi.org/10.1016/S0045-6535(03)00297-2
Li, Y., Zhang, X., Yang, W., Li, C., Chu, Y., Jiang, H., & Shen, Z. (2017). Mechanism of the protective effects of the combined treatment with rhynchophylla total alkaloids and sinapine thiocyanate against a

prothrombotic state caused by vascular endothelial cell inflammatory damage. *Experimental and Therapeutic Medicine*, *13*(6), 3081–3088. https://doi.org/10.3892/etm.2017.4357
Liang, Y.-C., Huang, Y.-T., Tsai, S.-H., Lin-Shiau, S.-Y., Chen, C.-F., & Lin, J.-K. (1999a). Suppression of inducible cyclooxygenase and inducible nitric oxide synthase by apigenin and related flavonoids in mouse macrophages. *Carcinogenesis*, *20*(10), 1945–1952.
Liang, Y.-C., Huang, Y.-T., Tsai, S.-H., Lin-Shiau, S.-Y., Chen, C.-F., & Lin, J.-K. (1999b). Suppression of inducible cyclooxygenase and inducible nitric oxide synthase by apigenin and related flavonoids in mouse macrophages. *Carcinogenesis*, *20*(10), 1945–1952. https://doi.org/10.1093/carcin/20.10.1945
Liehr, M., Mereu, A., Pastor, J. J., Quintela, J. C., Staats, S., Rimbach, G., & Ipharraguerre, I. R. (2017). Olive oil bioactives protect pigs against experimentally-induced chronic inflammation independently of alterations in gut microbiota. *PLoS One*, *12*(3), e0174239. https://doi.org/10.1371/journal.pone.0174239
Lien, E. J., Ren, S., Bui, H.-H., & Wang, R. (1999). Quantitative structure-activity relationship analysis of phenolic antioxidants. *Free Radical Biology and Medicine*, *26*(3–4), 285–294. https://doi.org/10.1016/S0891-5849(98)00190-7
Lim, J. H., & Kwon, T. K. (2010). Curcumin inhibits phorbol myristate acetate (PMA)-induced MCP-1 expression by inhibiting ERK and NF-κB transcriptional activity. *Food and Chemical Toxicology*, *48*(1), 47–52. https://doi.org/10.1016/j.fct.2009.09.013
Lin, L., Zhao, H., Dong, Y., Yang, B., & Zhao, M. (2012). Macroporous resin purification behavior of phenolics and rosmarinic acid from Rabdosia serra (MAXIM.) HARA leaf. *Food Chemistry*, *130*(2), 417–424. https://doi.org/10.1016/j.foodchem.2011.07.069
Lin, M. J. Y., Humbert, E. S., & Sosulski, F. W. (1974). Certain functional properties of sunflower meal products. *Journal of Food Science*, *39*(2), 368–370. https://doi.org/10.1111/j.1365-2621.1974.tb02896.x
Lin, S.-H., & Juang, R.-S. (2009). Adsorption of phenol and its derivatives from water using synthetic resins and low-cost natural adsorbents: A review. *Journal of Environmental Management*, *90*(3), 1336–1349. https://doi.org/10.1016/j.jenvman.2008.09.003
Lindenschmidt, R., Tryka, A. F., Goad, M., & Witschi, H. (1986). The effects of dietary butylated hydroxytoluene on liver and colon tumor development in mice. *Toxicology*. https://doi.org/10.1016/0300-483X(86)90116-2
Liu, B., Dong, B., Yuan, X., Kuang, Q., Zhao, Q., Yang, M., Liu, J., & Zhao, B. (2016). Enrichment and separation of chlorogenic acid from the extract of Eupatorium adenophorum Spreng by macroporous resin. *Journal of Chromatography B*, *1008*, 58–64. https://doi.org/10.1016/j.jchromb.2015.10.026
Liu, C.-C., Zhang, Y., Dai, B.-L., Ma, Y.-J., Zhang, Q., Wang, Y., & Yang, H. (2017). Chlorogenic acid prevents inflammatory responses in IL-1β-stimulated human SW-1353 chondrocytes, a model for osteoarthritis. *Molecular Medicine Reports*, *16*(2), 1369–1375. https://doi.org/10.3892/mmr.2017.6698
Liu, F.-C., Wang, C.-C., Lu, J.-W., Lee, C.-H., Chen, S.-C., Ho, Y.-J., & Peng, Y.-J. (2019). Chondroprotective Effects of Genistein against Osteoarthritis Induced Joint Inflammation. *Nutrients*, *11*(5), 1180. https://doi.org/10.3390/nu11051180
Liu, L., Zubik, L., Collins, F. W., Marko, M., & Meydani, M. (2004). The antiatherogenic potential of oat phenolic compounds. *Atherosclerosis*, *175*(1), 39–49. https://doi.org/10.1016/j.atherosclerosis.2004.01.044
Liu, Q., Wu, L., Pu, H., Li, C., & Hu, Q. (2012). Profile and distribution of soluble and insoluble phenolics in Chinese rapeseed (Brassica napus). *Food Chemistry*, *135*(2), 616–622. https://doi.org/10.1016/j.foodchem.2012.04.142
Liu, Q.-S., Zheng, T., Wang, P., Jiang, J.-P., & Li, N. (2010). Adsorption isotherm, kinetic and mechanism studies of some substituted phenols on activated carbon fibers. *Chemical Engineering Journal*, *157*(2–3), 348–356. https://doi.org/10.1016/j.cej.2009.11.013
Liu, T., Li, Y., Du, Q., Sun, J., Jiao, Y., Yang, G., Wang, Z., Xia, Y., Zhang, W., Wang, K., Zhu, H., & Wu, D. (2012). Adsorption of methylene blue from aqueous solution by graphene. *Colloids and Surfaces B: Biointerfaces*, *90*, 197–203. https://doi.org/10.1016/j.colsurfb.2011.10.019
Lomascolo, A., Uzan-Boukhris, E., Sigoillot, J.-C., & Fine, F. (2012). Rapeseed and sunflower meal: A review on biotechnology status and challenges. *Applied Microbiology and Biotechnology*, *95*(5), 1105–1114. https://doi.org/10.1007/s00253-012-4250-6
Lu, J.-L., Wu, M.-Y., Yang, X.-L., Dong, Z.-B., Ye, J.-H., Borthakur, D., Sun, Q.-L., & Liang, Y.-R. (2010). Decaffeination of tea extracts by using poly(acrylamide-co-ethylene glycol dimethylacrylate) as adsorbent. *Journal of Food Engineering*, *97*(4), 555–562. https://doi.org/10.1016/j.jfoodeng.2009.11.018

Lu, Q., & Sorial, G. A. (2007). The effect of functional groups on oligomerization of phenolics on activated carbon. *Journal of Hazardous Materials*, *148*(1–2), 436–445. https://doi.org/10.1016/j.jhazmat.2007.02.058

Lussignoli, S., Fraccaroli, M., Andrioli, G., Brocco, G., & Bellavite, P. (1999). A Microplate-Based Colorimetric Assay of the Total Peroxyl Radical Trapping Capability of Human Plasma. *Analytical Biochemistry*, *269*(1), 38–44. https://doi.org/10.1006/abio.1999.4010

Lv, L., Tang, J., & Ho, C.-T. (2008). Selection and optimisation of macroporous resin for separation of stilbene glycoside from *Polygonum multiflorum* Thunb. *Journal of Chemical Technology & Biotechnology*, *83*(10), 1422–1427. https://doi.org/10.1002/jctb.1964

Ma, C., Tao, G., JianTang, Lou, Z., Wang, H., Gu, X., Hu, L., & Yin, M. (2009). Preparative separation and purification of rosavin in Rhodiola rosea by macroporous adsorption resins. *Separation and Purification Technology*, *69*(1), 22–28. https://doi.org/10.1016/j.seppur.2009.06.002

Ma, Q. (2013). Role of Nrf2 in Oxidative Stress and Toxicity. *Annual Review of Pharmacology and Toxicology*, *53*(1), 401–426. https://doi.org/10.1146/annurev-pharmtox-011112-140320

MacDonald-Wicks, L. K., Wood, L. G., & Garg, M. L. (2006). Methodology for the determination of biological antioxidant capacityin vitro: A review. *Journal of the Science of Food and Agriculture*, *86*(13), 2046–2056. https://doi.org/10.1002/jsfa.2603

Mackenzie, G. G., Carrasquedo, F., Delfino, J. M., Keen, C. L., Fraga, C. G., & Oteiza, P. I. (2004). Epicatechin, catechin, and dimeric procyanidins inhibit PMA-induced NF-κB activation at multiple steps in Jurkat T cells. *The FASEB Journal*, *18*(1), 167–169.

Maggi-Capeyron, M.-F., Ceballos, P., Cristol, J.-P., Delbosc, S., Le Doucen, C., Pons, M., Léger, C. L., & Descomps, B. (2001). Wine Phenolic Antioxidants Inhibit AP-1 Transcriptional Activity. *Journal of Agricultural and Food Chemistry*, *49*(11), 5646–5652. https://doi.org/10.1021/jf010595x

Mah, S. H., Teh, S. S., & Ee, G. C. L. (2017). Anti-inflammatory, anti-cholinergic and cytotoxic effects of Sida rhombifolia. *Pharmaceutical Biology*, *55*(1), 920–928. https://doi.org/10.1080/13880209.2017.1285322

Makahleh, A., Saad, B., & Bari, M. F. (2015). Synthetic phenolics as antioxidants for food preservation. In *Handbook of Antioxidants for Food Preservation* (pp. 51–78). Elsevier. https://doi.org/10.1016/B978-1-78242-089-7.00003-8

Manach, C., Mazur, A., & Scalbert, A. (2005). Polyphenols and prevention of cardiovascular diseases. *Current Opinion in Lipidology*, *16*(1), 77–84.

Mandrone, M., Lorenzi, B., Venditti, A., Guarcini, L., Bianco, A., Sanna, C., Ballero, M., Poli, F., & Antognoni, F. (2015). Antioxidant and anti-collagenase activity of Hypericum hircinum L. *Industrial Crops and Products*, *76*, 402–408. https://doi.org/10.1016/j.indcrop.2015.07.012

Manna, S. K., Aggarwal, R. S., Sethi, G., Aggarwal, B. B., & Ramesh, G. T. (2007). Morin (3, 5, 7, 2′, 4′-pentahydroxyflavone) abolishes nuclear factor-κB activation induced by various carcinogens and inflammatory stimuli, leading to suppression of nuclear factor-κB–regulated gene expression and up-regulation of apoptosis. *Clinical Cancer Research*, *13*(7), 2290–2297.

Manna, S. K., Mukhopadhyay, A., & Aggarwal, B. B. (2000). Resveratrol suppresses TNF-induced activation of nuclear transcription factors NF-κB, activator protein-1, and apoptosis: Potential role of reactive oxygen intermediates and lipid peroxidation. *The Journal of Immunology*, *164*(12), 6509–6519.

Manthey, J. A. (2004). Fractionation of Orange Peel Phenols in Ultrafiltered Molasses and Mass Balance Studies of Their Antioxidant Levels. *Journal of Agricultural and Food Chemistry*, *52*(25), 7586–7592. https://doi.org/10.1021/jf049083j

Marcocci, L., Maguire, J. J., Droylefaix, M. T., & Packer, L. (1994). The Nitric Oxide-Scavenging Properties of Ginkgo Biloba Extract EGb 761. *Biochemical and Biophysical Research Communications*, *201*(2), 748–755. https://doi.org/10.1006/bbrc.1994.1764

Marín, L., Miguélez, E. M., Villar, C. J., & Lombó, F. (2015). Bioavailability of dietary polyphenols and gut microbiota metabolism: Antimicrobial properties. *BioMed Research International*, *2015*. https://doi.org/10.1155/

Marone, R., Cmiljanovic, V., Giese, B., & Wymann, M. P. (2008). Targeting phosphoinositide 3-kinase—Moving towards therapy. *Biochimica et Biophysica Acta (BBA) - Proteins and Proteomics*, *1784*(1), 159–185. https://doi.org/10.1016/j.bbapap.2007.10.003

Marques, F. Z., Markus, M. A., & Morris, B. J. (2009). Resveratrol: Cellular actions of a potent natural chemical that confers a diversity of health benefits. *The International Journal of Biochemistry & Cell Biology*, *41*(11), 2125–2128. https://doi.org/10.1016/j.biocel.2009.06.003

Matioli, G., & Rodriguez-Amaya, D. B. (2003). Microencapsulação do licopeno com ciclodextrinas. *Ciência e Tecnologia de Alimentos*, *23*. https://doi.org/10.1590/S0101-20612003000400019

Matthäus, B. (2002). Antioxidant Activity of Extracts Obtained from Residues of Different Oilseeds. *Journal of Agricultural and Food Chemistry*, *50*(12), 3444–3452. https://doi.org/10.1021/jf011440s

Meng, S., Cao, J., Feng, Q., Peng, J., & Hu, Y. (2013). Roles of chlorogenic acid on regulating glucose and lipids metabolism: A review. *Evidence-Based Complementary and Alternative Medicine*, *2013*.

Middleton, E., Kandaswami, C., & Theoharides, T. C. (2000). The Effects of Plant Flavonoids on Mammalian Cells:Implications for Inflammation, Heart Disease, and Cancer. *Pharmacological Reviews*, *52*(4), 673–751.

Miles, E. A., Zoubouli, P., & Calder, P. C. (2005). Differential anti-inflammatory effects of phenolic compounds from extra virgin olive oil identified in human whole blood cultures. *Nutrition*, *21*(3), 389–394. https://doi.org/10.1016/j.nut.2004.06.031

Miller, H. E. (1971). A simplified method for the evaluation of antioxidants. *Journal of the American Oil Chemists Society*, *48*(2), 91–91. https://doi.org/10.1007/BF02635693

Miller, N. J., & Rice-Evans, C. A. (1997). The relative contributions of ascorbic acid and phenolic antioxidants to the total antioxidant activity of orange and apple fruit juices and blackcurrant drink. *Food Chemistry*, *60*(3), 331–337. https://doi.org/10.1016/S0308-8146(96)00339-1

Min, Y.-D., Choi, C.-H., Bark, H., Son, H.-Y., Park, H.-H., Lee, S., Park, J.-W., Park, E.-K., Shin, H.-I., & Kim, S.-H. (2007). Quercetin inhibits expression of inflammatory cytokines through attenuation of NF-κB and p38 MAPK in HMC-1 human mast cell line. *Inflammation Research*, *56*(5), 210–215.

Mishra, A., Sharma, A. K., Kumar, S., Saxena, A. K., & Pandey, A. K. (2013). *Bauhinia variegata* Leaf Extracts Exhibit Considerable Antibacterial, Antioxidant, and Anticancer Activities. *BioMed Research International*, *2013*, 1–10. https://doi.org/10.1155/2013/915436

Montoro, P., Braca, A., Pizza, C., & Detommasi, N. (2005). Structure-antioxidant activity relationships of flavonoids isolated from different plant species. *Food Chemistry*, *92*(2), 349–355. https://doi.org/10.1016/j.foodchem.2004.07.028

Moon, M. K., Lee, Y. J., Kim, J. S., Kang, D. G., & Lee, H. S. (2009). Effect of caffeic acid on tumor necrosis factor-alpha-induced vascular inflammation in human umbilical vein endothelial cells. *Biological and Pharmaceutical Bulletin*, *32*(8), 1371–1377.

Moreno-Castilla, C. (2004). Adsorption of organic molecules from aqueous solutions on carbon materials. *Carbon*, *42*(1), 83–94. https://doi.org/10.1016/j.carbon.2003.09.022

Moreno-Castilla, C., Rivera-Utrilla, J., López-Ramón, M. V., & carrasco-Marín, F. (1995). Adsorption of some substituted phenols on activated carbons from a bituminous coal. *Carbon*, *33*(6), 845–851. https://doi.org/10.1016/0008-6223(94)00182-Y

Moreno-González, M., Girish, V., Keulen, D., Wijngaard, H., Lauteslager, X., Ferreira, G., & Ottens, M. (2020). Recovery of sinapic acid from canola/rapeseed meal extracts by adsorption. *Food and Bioproducts Processing*, *120*, 69–79. https://doi.org/10.1016/j.fbp.2019.12.002

Morikawa, K., Nonaka, M., Narahara, M., Torii, I., Kawaguchi, K., Yoshikawa, T., Kumazawa, Y., & Morikawa, S. (2003). Inhibitory effect of quercetin on carrageenan-induced inflammation in rats. *Life Sciences*, *74*(6), 709–721. https://doi.org/10.1016/j.lfs.2003.06.036

Murakami, H., Asakawa, T., Terao, J., & Matsushita, S. (1984). Antioxidative Stability of Tempeh and Liberation of Isoflavones by Fermentation. *Agricultural and Biological Chemistry*, *48*(12), 2971–2975. https://doi.org/10.1080/00021369.1984.10866635

Muriana, F. J. G., Paz, S. M. la, Lucas, R., Bermudez, B., Jaramillo, S., Morales, J. C., Abia, R., & Lopez, S. (2017). Tyrosol and its metabolites as antioxidative and anti-inflammatory molecules in human endothelial cells. *Food & Function*, *8*(8), 2905–2914. https://doi.org/10.1039/C7FO00641A

Myers, R. H., Montgomery, D. C., & Anderson-Cook, C. M. (2016). *Response Surface Methodology: Process and Product Optimization Using Designed Experiments*. John Wiley & Sons.

Naczk, M., Amarowicz, R., Pink, D., & Shahidi, F. (2000). Insoluble condensed tannins of canola/rapeseed. *Journal of Agricultural and Food Chemistry*, *48*(5), 1758–1762.

Naczk, M., Amarowicz, R., Sullivan, A., & Shahidi, F. (1998). Current research developments on polyphenolics of rapeseed/canola: A review. *Food Chemistry*, *62*(4), 489–502.

Naczk, M., & Shahidi, F. (2004a). Extraction and analysis of phenolics in food. *Journal of Chromatography A*, *1054*(1–2), 95–111. https://doi.org/10.1016/S0021-9673(04)01409-8

Naczk, M., & Shahidi, F. (2004b). Extraction and analysis of phenolics in food. *Journal of Chromatography A*, *1054*(1–2), 95–111. https://doi.org/10.1016/S0021-9673(04)01409-8

Naczk, M., Wanasundara, P., & Shahidi, F. (1992). Facile spectrophotometric quantification method of sinapic acid in hexane-extracted and methanol-ammonia-water-treated mustard and rapeseed meals. *Journal of Agricultural and Food Chemistry*, *40*(3), 444–448.

Nadathur, S., Wanasundara, J. P., & Scanlin, L. (2016). *Sustainable protein sources*. Academic Press.

Naik, E., & Dixit, V. M. (2011). Mitochondrial reactive oxygen species drive proinflammatory cytokine production. *Journal of Experimental Medicine*, *208*(3), 417–420. https://doi.org/10.1084/jem.20110367

Nair, A. T., Makwana, A. R., & Ahammed, M. M. (2014). The use of response surface methodology for modelling and analysis of water and wastewater treatment processes: A review. *Water Science and Technology*, *69*(3), 464–478. https://doi.org/10.2166/wst.2013.733

Nanditha, B., & Prabhasankar, P. (2008). Antioxidants in Bakery Products: A Review. *Critical Reviews in Food Science and Nutrition*, *49*(1), 1–27. https://doi.org/10.1080/10408390701764104

Natella, F., Nardini, M., Di Felice, M., & Scaccini, C. (1999). Benzoic and Cinnamic Acid Derivatives as Antioxidants: Structure−Activity Relation. *Journal of Agricultural and Food Chemistry*, *47*(4), 1453–1459. https://doi.org/10.1021/jf980737w

Nenadis, N., Zafiropoulou, I., & Tsimidou, M. (2003). Commonly used food antioxidants: A comparative study in dispersed systems. *Food Chemistry*, *82*(3), 403–407. https://doi.org/10.1016/S0308-8146(02)00579-4

Nićiforović, N., & Abramovič, H. (2014). Sinapic acid and its derivatives: Natural sources and bioactivity. *Comprehensive Reviews in Food Science and Food Safety*, *13*(1), 34–51.

Nowak, H., Kujawa, K., Zadernowski, R., Roczniak, B., & KozŁowska, H. (1992). Antioxidative and Bactericidal Properties of Phenolic Compounds in Rapeseeds. *Fett Wissenschaft Technologie/Fat Science Technology*, *94*(4), 149–152. https://doi.org/10.1002/lipi.19920940406

Okubo, T., Yokoyama, Y., Kano, K., & Kano, I. (2003). Cell death induced by the phenolic antioxidant tert-butylhydroquinone and its metabolite tert-butylquinone in human monocytic leukemia U937 cells. *Food and Chemical Toxicology*, *41*(5), 679–688. https://doi.org/10.1016/S0278-6915(03)00002-4

Olthof, M. R., Katan, M. B., & Hollman, P. C. H. (2001). *Bioavailability of flavonoids and cinnamic acids and their effect on plasma homosysteine in humans*. http://edepot.wur.nl/197620

Ou, B., Huang, D., Hampsch-Woodill, M., Flanagan, J. A., & Deemer, E. K. (2002). Analysis of Antioxidant Activities of Common Vegetables Employing Oxygen Radical Absorbance Capacity (ORAC) and Ferric Reducing Antioxidant Power (FRAP) Assays: A Comparative Study. *Journal of Agricultural and Food Chemistry*, *50*(11), 3122–3128. https://doi.org/10.1021/jf0116606

Ozgen, S., Kilinc, O. K., & Selamoğlu, Z. (2016). Antioxidant Activity of Quercetin: A Mechanistic Review. *Turkish Journal of Agriculture - Food Science and Technology*, *4*(12), 1134. https://doi.org/10.24925/turjaf.v4i12.1134-1138.1069

Padmesh, T. V. N., Vijayaraghavan, K., Sekaran, G., & Velan, M. (2006). Application of Two-and Three-Parameter Isotherm Models: Biosorption of Acid Red 88 onto *Azolla microphylla*. *Bioremediation Journal*, *10*(1–2), 37–44. https://doi.org/10.1080/10889860600842746

Page, T. H., Smolinska, M., Gillespie, J., Urbaniak, A. M., & Foxwell, B. M. J. (2009). Tyrosine Kinases and Inflammatory Signalling. *Current Molecular Medicine*, *9*(1), 69–85. https://doi.org/10.2174/156652409787314507

Palungwachira, P., Tancharoen, S., Phruksaniyom, C., Klungsaeng, S., Srichan, R., Kikuchi, K., & Nararatwanchai, T. (2019, July 31). *Antioxidant and Anti-Inflammatory Properties of Anthocyanins Extracted from Oryza sativa L. in Primary Dermal Fibroblasts* [Research Article]. Oxidative Medicine and Cellular Longevity; Hindawi. https://doi.org/10.1155/2019/2089817

Pan, B., Pan, B., Zhang, W., Zhang, Q., Zhang, Q., & Zheng, S. (2008). Adsorptive removal of phenol from aqueous phase by using a porous acrylic ester polymer. *Journal of Hazardous Materials*, *157*(2–3), 293–299. https://doi.org/10.1016/j.jhazmat.2007.12.102

Pan, M.-H., Lai, C.-S., Wang, Y.-J., & Ho, C.-T. (2006). Acacetin suppressed LPS-induced up-expression of iNOS and COX-2 in murine macrophages and TPA-induced tumor promotion in mice. *Biochemical Pharmacology*, *72*(10), 1293–1303.

Pan, Z., Zhou, Y., Luo, X., Ruan, Y., Zhou, L., Wang, Q., Yan, Y. jie, Liu, Q., & Chen, J. (2018). Against NF-κB/thymic stromal lymphopoietin signaling pathway, catechin alleviates the inflammation in allergic rhinitis. *International Immunopharmacology*, *61*, 241–248. https://doi.org/10.1016/j.intimp.2018.06.011

Park, H. J., Davis, S. R., Liang, H.-Y., Rosenberg, D. W., & Bruno, R. S. (2010). Chlorogenic Acid Differentially Alters Hepatic and Small Intestinal Thiol Redox Status Without Protecting Against Azoxymethane-Induced Colon Carcinogenesis in Mice. *Nutrition and Cancer*, *62*(3), 362–370. https://doi.org/10.1080/01635580903407239

Park, M. J., Lee, J., Suh, Y., Kim, J., & Nam, W. (2006). Reactivities of Mononuclear Non-Heme Iron Intermediates Including Evidence that Iron(III)−Hydroperoxo Species Is a Sluggish Oxidant. *Journal of the American Chemical Society*, *128*(8), 2630–2634. https://doi.org/10.1021/ja055709q

Parrado, J., & Bautista, J. (1993). Protein enrichment of sunflower lignocellulosic fraction by Trichoderma harzianum S/G 2431 in low moisture content media. *Bioscience, Biotechnology, and Biochemistry*, *57*(2), 317–318.

Parry, J., Su, L., Moore, J., Cheng, Z., Luther, M., Rao, J. N., Wang, J.-Y., & Yu, L. L. (2006). Chemical Compositions, Antioxidant Capacities, and Antiproliferative Activities of Selected Fruit Seed Flours. *Journal of Agricultural and Food Chemistry*, *54*(11), 3773–3778. https://doi.org/10.1021/jf060325k

Pedrosa, M. M., M., M., C., G., C., B., G., A., & L.M., R. (2000). Determination of caffeic and chlorogenic acids and their derivatives in different sunflower seeds. *J. Sci. Food Agric.*, *80*, 459–464. https://doi.org/10.1002/(SICI)1097-0010(200003)80:4<459::AID-JSFA549>3.0.CO;2-O

Pellegrini, N., Simonetti, P., Gardana, C., Brenna, O., Brighenti, F., & Pietta, P. (2000). Polyphenol Content and Total Antioxidant Activity of *Vini Novelli* (Young Red Wines). *Journal of Agricultural and Food Chemistry*, *48*(3), 732–735. https://doi.org/10.1021/jf990251v

Pérez-Marín, A. B., Zapata, V. M., Ortuño, J. F., Aguilar, M., Sáez, J., & Lloréns, M. (2007). Removal of cadmium from aqueous solutions by adsorption onto orange waste. *Journal of Hazardous Materials*, *139*(1), 122–131. https://doi.org/10.1016/j.jhazmat.2006.06.008

Petroni, A., Blasevich, M., Papini, N., Salami, M., Sala, A., & Galli, C. (1997). Inhibition of leukocyte leukotriene B4 production by an olive oil-derived phenol identified by mass-spectrometry. *Thrombosis Research*, *87*(3), 315–322. https://doi.org/10.1016/S0049-3848(97)00133-3

Phenrat, T., Saleh, N., Sirk, K., Kim, H.-J., Tilton, R. D., & Lowry, G. V. (2008). Stabilization of aqueous nanoscale zerovalent iron dispersions by anionic polyelectrolytes: Adsorbed anionic polyelectrolyte layer properties and their effect on aggregation and sedimentation. *Journal of Nanoparticle Research*, *10*(5), 795–814. https://doi.org/10.1007/s11051-007-9315-6

Pickardt, C., Weisz, G. M., Eisner, P., Kammerer, D. R., Neidhart, S., & Carle, R. (2011). Processing of low polyphenol protein isolates from residues of sunflower seed oil production. *Procedia Food Science*, *1*, 1417–1424. https://doi.org/10.1016/j.profoo.2011.09.210

Plastina, P., Benincasa, C., Perri, E., Fazio, A., Augimeri, G., Poland, M., Witkamp, R., & Meijerink, J. (2019). Identification of hydroxytyrosyl oleate, a derivative of hydroxytyrosol with anti-inflammatory properties, in olive oil by-products. *Food Chemistry*, *279*, 105–113. https://doi.org/10.1016/j.foodchem.2018.12.007

Pompeu, D. R., Moura, F. G., Silva, E. M., & Rogez, H. (2010). Equilibria, Kinetics, and Mechanisms for the Adsorption of Four Classes of Phenolic Compounds onto Synthetic Resins. *Separation Science and Technology*, *45*(5), 700–709. https://doi.org/10.1080/01496390903562274

Porro, C., Cianciulli, A., Trotta, T., Lofrumento, D. D., & Panaro, M. A. (2019). Curcumin Regulates Anti-Inflammatory Responses by JAK/STAT/SOCS Signaling Pathway in BV-2 Microglial Cells. *Biology*, *8*(3), 51. https://doi.org/10.3390/biology8030051

Porter, L. J. (1989). 11—Tannins. In J. B. Harborne (Ed.), *Methods in Plant Biochemistry* (Vol. 1, pp. 389–419). Academic Press. https://doi.org/10.1016/B978-0-12-461011-8.50017-2

Prasad, A. L., Santhi, T., & Manonmani, S. (2015). Recent developments in preparation of activated carbons by microwave: Study of residual errors. *Arabian Journal of Chemistry*, *8*(3), 343–354. https://doi.org/10.1016/j.arabjc.2011.01.020

Prince, P. D., Fischerman, L., Toblli, J. E., Fraga, C. G., & Galleano, M. (2017). LPS-induced renal inflammation is prevented by (−)-epicatechin in rats. *Redox Biology*, *11*, 342–349. https://doi.org/10.1016/j.redox.2016.12.023

Prior, R. L., Wu, X., & Schaich, K. (2005). Standardized Methods for the Determination of Antioxidant Capacity and Phenolics in Foods and Dietary Supplements. *Journal of Agricultural and Food Chemistry*, *53*(10), 4290–4302. https://doi.org/10.1021/jf0502698

Prousek, J. (2007). Fenton chemistry in biology and medicine. *Pure and Applied Chemistry*, *79*(12), 2325–2338. https://doi.org/10.1351/pac200779122325

Qian, J., Chen, X., Chen, X., Sun, C., Jiang, Y., Qian, Y., Zhang, Y., Khan, Z., Zhou, J., Liang, G., & Zheng, C. (2019). Kaempferol reduces K63-linked polyubiquitination to inhibit nuclear factor-κB and inflammatory responses in acute lung injury in mice. *Toxicology Letters*, *306*, 53–60. https://doi.org/10.1016/j.toxlet.2019.02.005

Quinn, L., Gray, S. G., Meaney, S., Finn, S., Kenny, O., & Hayes, M. (2017). Sinapinic and protocatechuic acids found in rapeseed: Isolation, characterisation and potential benefits for human health as functional food ingredients. *Irish Journal of Agricultural and Food Research*, *56*(1), 104–119. https://doi.org/10.1515/ijafr-2017-0012

Ramachandran, S., Singh, S. K., Larroche, C., Soccol, C. R., & Pandey, A. (2007). Oil cakes and their biotechnological applications – A review. *Bioresource Technology*, *98*(10), 2000–2009. https://doi.org/10.1016/j.biortech.2006.08.002

Ramalakshmi, K., Hithamani, G., Asha, K. R., & Jagan Mohan Rao, L. (2011). Separation and characterisation of chlorogenic acid-rich conserves from green coffee beans and their radical scavenging potential: Separation and characterisation of chlorogenic acid. *International Journal of Food Science & Technology*, *46*(1), 109–115. https://doi.org/10.1111/j.1365-2621.2010.02464.x

Rathee, P., Chaudhary, H., Rathee, S., Rathee, D., Kumar, V., & Kohli, K. (2009). Mechanism of Action of Flavonoids as Anti-inflammatory Agents: A Review. *Inflammation & Allergy - Drug Targets (Formerly Current Drug Targets - Inflammation & Allergy)*, *8*(3), 229–235. https://doi.org/10.2174/187152809788681029

Rayalam, S., Yang, J.-Y., Ambati, S., Della-Fera, M. A., & Baile, C. A. (2008). Resveratrol induces apoptosis and inhibits adipogenesis in 3T3-L1 adipocytes: Resveratrol effects on 3T3-L1 adipocytes. *Phytotherapy Research*, *22*(10), 1367–1371. https://doi.org/10.1002/ptr.2503

Re, R., Pellegrini, N., Proteggente, A., Pannala, A., Yang, M., & Rice-Evans, C. (1999). Antioxidant activity applying an improved ABTS radical cation decolorization assay. *Free Radical Biology and Medicine*, *26*(9–10), 1231–1237. https://doi.org/10.1016/S0891-5849(98)00315-3

Reddy, A. T., Lakshmi, S. P., Maruthi Prasad, E., Varadacharyulu, N. Ch., & Kodidhela, L. D. (2020). Epigallocatechin gallate suppresses inflammation in human coronary artery endothelial cells by inhibiting NF-κB. *Life Sciences*, *258*, 118136. https://doi.org/10.1016/j.lfs.2020.118136

Redlich, O., & Peterson, D. L. (1959). A Useful Adsorption Isotherm. *The Journal of Physical Chemistry*, *63*(6), 1024–1024. https://doi.org/10.1021/j150576a611

Remón, J., Matharu, A. S., & Clark, J. H. (2018). Simultaneous production of lignin and polysaccharide rich aqueous solutions by microwave-assisted hydrothermal treatment of rapeseed meal. *Energy Conversion and Management*, *165*, 634–648. https://doi.org/10.1016/j.enconman.2018.03.091

Ren, J., Zheng, Y., Lin, Z., Han, X., & Liao, W. (2017). Macroporous resin purification and characterization of flavonoids from Platycladus orientalis (L.) Franco and their effects on macrophage inflammatory response. *Food & Function*, *8*(1), 86–95. https://doi.org/10.1039/C6FO01474G

Ribeiro, M., Silveira, D., & Ferreira-Dias, S. (2002). Selective adsorption of limonin and naringin from orange juice to natural and synthetic adsorbents. *European Food Research and Technology*, *215*(6), 462–471. https://doi.org/10.1007/s00217-002-0592-0

Rice-Evans, C. A., Miller, N. J., & Paganga, G. (1996). Structure-antioxidant activity relationships of flavonoids and phenolic acids. *Free Radical Biology and Medicine*, *20*(7), 933–956. https://doi.org/10.1016/0891-5849(95)02227-9

Robbins, R. J. (2003). Phenolic Acids in Foods: An Overview of Analytical Methodology. *Journal of Agricultural and Food Chemistry*, *51*(10), 2866–2887. https://doi.org/10.1021/jf026182t

Rodrigues, J., Miranda, I., Gominho, J., Vasconcelos, M., Barradas, G., Pereira, H., Bianchi-de-Aguiar, F., & Ferreira-Dias, S. (2016). Modeling and optimization of laboratory-scale conditioning of Jatropha curcas L. seeds for oil expression. *Industrial Crops and Products*, *83*, 614–619. https://doi.org/10.1016/j.indcrop.2015.12.062

Rodriguez-Reinoso, F. (1989). An overview of methods for the characterization of activated carbons. *Pure and Applied Chemistry*, *61*(11), 1859–1866. https://doi.org/10.1351/pac198961111859

Romani, A., Pinelli, P., Moschini, V., & Heimler, D. (2017). Seeds and oil polyphenol content of sunflower (Helianthus annuus L.) grown with different agricultural management. *Advances in Horticultural Science*, 85-88 Pages. https://doi.org/10.13128/AHS-20608

Romier, B., Van De Walle, J., During, A., Larondelle, Y., & Schneider, Y.-J. (2008). Modulation of signalling nuclear factor-kappaB activation pathway by polyphenols in human intestinal Caco-2 cells. *The British Journal of Nutrition*, *100*(3), 542–551. https://doi.org/10.1017/S0007114508966666

Ruch, R. J., Cheng, S., & Klaunig, J. E. (1989). Prevention of cytotoxicity and inhibition of intercellular communication by antioxidant catechins isolated from Chinese green tea. *Carcinogenesis*, *10*(6), 1003–1008. https://doi.org/10.1093/carcin/10.6.1003

Ruthven, D. M. (1984). *Principles of Adsorption and Adsorption Processes*. John Wiley & Sons.

Saad, B., Sing, Y., Nawi, M., Hashim, N., Mohamedali, A., Saleh, M., Sulaiman, S., Talib, K., & Ahmad, K. (2007). Determination of synthetic phenolic antioxidants in food items using reversed-phase HPLC. *Food Chemistry*, *105*(1), 389–394. https://doi.org/10.1016/j.foodchem.2006.12.025

Sabir, M. A., Sosulski, F. W., & Finlayson, A. J. (1974). Chlorogenic acid-protein interactions in sunflower. *Journal of Agricultural and Food Chemistry*, *22*(4), 575–578.

Saito, M., Hosoyama, H., Ariga, T., Kataoka, S., & Yamaji, N. (1998). Antiulcer Activity of Grape Seed Extract and Procyanidins. *Journal of Agricultural and Food Chemistry*, *46*(4), 1460–1464. https://doi.org/10.1021/jf9709156

Salah, N., Miller, N. J., Paganga, G., Tijburg, L., Bolwell, G. P., & Riceevans, C. (1995). Polyphenolic Flavanols as Scavengers of Aqueous Phase Radicals and as Chain-Breaking Antioxidants. *Archives of Biochemistry and Biophysics*, *322*(2), 339–346. https://doi.org/10.1006/abbi.1995.1473

Salaverry, L. S., Parrado, A. C., Mangone, F. M., Dobrecky, C. B., Flor, S. A., Lombardo, T., Sotelo, A. D., Saccodossi, N., Rugna, A. Z., Blanco, G., Canellada, A., & Rey-Roldán, E. B. (2020). In vitro anti-inflammatory properties of Smilax campestris aqueous extract in human macrophages, and

characterization of its flavonoid profile. *Journal of Ethnopharmacology*, *247*, 112282. https://doi.org/10.1016/j.jep.2019.112282
Salgado, P. R., López-Caballero, M. E., Gómez-Guillén, M. C., Mauri, A. N., & Montero, M. P. (2012). Exploration of the antioxidant and antimicrobial capacity of two sunflower protein concentrate films with naturally present phenolic compounds. *Food Hydrocolloids*, *29*(2), 374–381. https://doi.org/10.1016/j.foodhyd.2012.03.006
Sánchez-Moreno, C., Larrauri, J. A., & Saura-Calixto, F. (1998). A procedure to measure the antiradical efficiency of polyphenols. *Journal of the Science of Food and Agriculture*, *76*(2), 270–276. https://doi.org/10.1002/1097-0010(199802)76
Sandhu, A. K., & Gu, L. (2013). Adsorption/Desorption Characteristics and Separation of Anthocyanins from Muscadine (Vitis rotundifolia) Juice Pomace by Use of Macroporous Adsorbent Resins. *Journal of Agricultural and Food Chemistry*, *61*(7), 1441–1448. https://doi.org/10.1021/jf3036148
Santana-Gálvez, J., Cisneros-Zevallos, L., & Jacobo-Velázquez, D. (2017). Chlorogenic Acid: Recent Advances on Its Dual Role as a Food Additive and a Nutraceutical against Metabolic Syndrome. *Molecules*, *22*(3), 358. https://doi.org/10.3390/molecules22030358
Sara, A. S., Mathé, C., Basselin, M., Fournier, F., Aymes, A., Bianeis, M., Galet, O., & Kapel, R. (2020). Optimization of sunflower albumin extraction from oleaginous meal and characterization of their structure and properties. *Food Hydrocolloids*, *99*, 105335. https://doi.org/10.1016/j.foodhyd.2019.105335
Sarabia, L. A., & Ortiz, M. C. (2009). 1.12—Response Surface Methodology. In S. D. Brown, R. Tauler, & B. Walczak (Eds.), *Comprehensive Chemometrics* (pp. 345–390). Elsevier. https://doi.org/10.1016/B978-044452701-1.00083-1
Sarkar, M., & Majumdar, P. (2011). Application of response surface methodology for optimization of heavy metal biosorption using surfactant modified chitosan bead. *Chemical Engineering Journal*, *175*, 376–387. https://doi.org/10.1016/j.cej.2011.09.125
Sastry, M. C. S., & Rao, M. S. N. (1990). Binding of chlorogenic acid by the isolated polyphenol-free 11 S protein of sunflower (Helianthus annuus) seed. *Journal of Agricultural and Food Chemistry*, *38*(12), 2103–2110. https://doi.org/10.1021/jf00102a001
Schieber, A., Hilt, P., Streker, P., Endreß, H.-U., Rentschler, C., & Carle, R. (2003). A new process for the combined recovery of pectin and phenolic compounds from apple pomace. *Innovative Food Science & Emerging Technologies*, *4*(1), 99–107. https://doi.org/10.1016/S1466-8564(02)00087-5
Schmidt, Š., & Pokorný, J. (2011). Potential application of oilseeds as sources of antioxidants for food lipids – a review. *Czech Journal of Food Sciences*, *23*(No. 3), 93–102. https://doi.org/10.17221/3377-CJFS
Schonthaler, H. B., Guinea-Viniegra, J., & Wagner, E. F. (2011). Targeting inflammation by modulating the Jun/AP-1 pathway. *Annals of the Rheumatic Diseases*, *70*(Suppl 1), i109–i112. https://doi.org/10.1136/ard.2010.140533
Schueller, B. S., & Yang, R. T. (2001). Ultrasound Enhanced Adsorption and Desorption of Phenol on Activated Carbon and Polymeric Resin. *Industrial & Engineering Chemistry Research*, *40*(22), 4912–4918. https://doi.org/10.1021/ie010490j
Scordino, M., Di Mauro, A., Passerini, A., & Maccarone, E. (2003). Adsorption of Flavonoids on Resins: Hesperidin. *Journal of Agricultural and Food Chemistry*, *51*(24), 6998–7004. https://doi.org/10.1021/jf034496q
Scordino, M., Di Mauro, A., Passerini, A., & Maccarone, E. (2004). Adsorption of Flavonoids on Resins: Cyanidin 3-Glucoside. *Journal of Agricultural and Food Chemistry*, *52*(7), 1965–1972. https://doi.org/10.1021/jf035220l
Seeram, N. P., & Nair, M. G. (2002). Inhibition of Lipid Peroxidation and Structure−Activity-Related Studies of the Dietary Constituents Anthocyanins, Anthocyanidins, and Catechins. *Journal of Agricultural and Food Chemistry*, *50*(19), 5308–5312. https://doi.org/10.1021/jf025671q
Seeram, N. P., Zhang, Y., & Nair, M. G. (2003). Inhibition of Proliferation of Human Cancer Cells and Cyclooxygenase Enzymes by Anthocyanidins and Catechins. *Nutrition and Cancer*, *46*(1), 101–106. https://doi.org/10.1207/S15327914NC4601_13
Serrano, J., Puupponen-Pimiä, R., Dauer, A., Aura, A.-M., & Saura-Calixto, F. (2009). Tannins: Current knowledge of food sources, intake, bioavailability and biological effects. *Molecular Nutrition & Food Research*, *53*(S2), S310–S329. https://doi.org/10.1002/mnfr.200900039
Sevillano, D. M., van der Wielen, L. A. M., Trifunovic, O., & Ottens, M. (2013). Model Comparison for the Prediction of the Solubility of Green Tea Catechins in Ethanol/Water Mixtures. *Industrial & Engineering Chemistry Research*, *52*(17), 6039–6048. https://doi.org/10.1021/ie400113t
Shahidi, F. (2000). Antioxidants in food and food antioxidants. *Nahrung/Food*, *44*(3), 158–163. https://doi.org/10.1002/1521-3803(20000501)44

Shahidi, F. (2015). Antioxidants. In *Handbook of Antioxidants for Food Preservation* (pp. 1–14). Elsevier. https://doi.org/10.1016/B978-1-78242-089-7.00001-4

Shahidi, F., Janitha, P. K., & Wanasundara, P. D. (1992). Phenolic antioxidants. *Critical Reviews in Food Science & Nutrition*, *32*(1), 67–103.

Shamanthaka Sastry, M. C., & Subramanian, N. (1984). Preliminary studies on processing of sunflower seed to obtain edible protein concentrates. *Journal of the American Oil Chemists' Society*, *61*(6), 1039. https://doi.org/10.1007/BF02636213

Shan, J., Fu, J., Zhao, Z., Kong, X., Huang, H., Luo, L., & Yin, Z. (2009). Chlorogenic acid inhibits lipopolysaccharide-induced cyclooxygenase-2 expression in RAW264.7 cells through suppressing NF-κB and JNK/AP-1 activation. *International Immunopharmacology*, *9*(9), 1042–1048. https://doi.org/10.1016/j.intimp.2009.04.011

Shen, L., & Ji, H.-F. (2009). Insights into the inhibition of xanthine oxidase by curcumin. *Bioorganic & Medicinal Chemistry Letters*, *19*(21), 5990–5993. https://doi.org/10.1016/j.bmcl.2009.09.076

Shen, S.-C., Lee, W.-R., Lin, H.-Y., Huang, H.-C., Ko, C.-H., Yang, L.-L., & Chen, Y.-C. (2002). In vitro and in vivo inhibitory activities of rutin, wogonin, and quercetin on lipopolysaccharide-induced nitric oxide and prostaglandin E2 production. *European Journal of Pharmacology*, *446*(1), 187–194. https://doi.org/10.1016/S0014-2999(02)01792-2

Shichijo, M., Yamamoto, N., Tsujishita, H., Kimata, M., Nagai, H., & Kokubo, T. (2003). Inhibition of Syk Activity and Degranulation of Human Mast Cells by Flavonoids. *Biological and Pharmaceutical Bulletin*, *26*(12), 1685–1690. https://doi.org/10.1248/bpb.26.1685

Shie, J.-J., Chen, C.-A., Lin, C.-C., Ku, A. F., Cheng, T.-J. R., Fang, J.-M., & Wong, C.-H. (2010). Regioselective synthesis of di-C-glycosylflavones possessing anti-inflammation activities. *Organic & Biomolecular Chemistry*, *8*(19), 4451. https://doi.org/10.1039/c0ob00011f

Shin, H. S., Satsu, H., Bae, M.-J., Zhao, Z., Ogiwara, H., Totsuka, M., & Shimizu, M. (2015). Anti-inflammatory effect of chlorogenic acid on the IL-8 production in Caco-2 cells and the dextran sulphate sodium-induced colitis symptoms in C57BL/6 mice. *Food Chemistry*, *168*, 167–175.

Siddiqui, I. R., & Wood, P. J. (1977). Carbohydrates of rapeseed: A review. *Journal of the Science of Food and Agriculture*, *28*(6), 530–538.

Sies, H. (1997). Oxidative stress: Oxidants and antioxidants. *Experimental Physiology*, *82*(2), 291–295. https://doi.org/10.1113/expphysiol.1997.sp004024

Siger, A., Czubinski, J., Dwiecki, K., Kachlicki, P., & Nogala-Kalucka, M. (2013). Identification and antioxidant activity of sinapic acid derivatives in *Brassica napus* L. seed meal extracts: Main phenolic compounds in rapeseed. *European Journal of Lipid Science and Technology*, n/a-n/a. https://doi.org/10.1002/ejlt.201300077

Siger, A., Gawrysiak-Witulska, M., & Bartkowiak-Broda, I. (2017). Antioxidant (Tocopherol and Canolol) Content in Rapeseed Oil Obtained from Roasted Yellow-Seeded Brassica napus. *Journal of the American Oil Chemists' Society*, *94*(1), 37–46. PubMed. https://doi.org/10.1007/s11746-016-2921-7

Silva, A. M., Martins-Gomes, C., Souto, E. B., Schäfer, J., Santos, J. A., Bunzel, M., & Nunes, F. M. (2020). Thymus zygis subsp. zygis an Endemic Portuguese Plant: Phytochemical Profiling, Antioxidant, Anti-Proliferative and Anti-Inflammatory Activities. *Antioxidants (Basel, Switzerland)*, *9*(6), Article 6. https://doi.org/10.3390/antiox9060482

Silva, E., Pompeu, D., Larondelle, Y., & Rogez, H. (2007). Optimisation of the adsorption of polyphenols from Inga edulis leaves on macroporous resins using an experimental design methodology. *Separation and Purification Technology*, *53*(3), 274–280. https://doi.org/10.1016/j.seppur.2006.07.012

Sips, R. (1948). On the Structure of a Catalyst Surface. *The Journal of Chemical Physics*, *16*(5), 490–495. https://doi.org/10.1063/1.1746922

Slejko, Frank L., ed. (1985). Adsorption technology: A step-by-step approach to process evaluation and application. *New York: M. Dekker*.

Smyk, B., & Drabent, R. (1989). Spectroscopic investigation of the equilibria of the ionic forms of sinapic acid. *Analyst*, *114*(6), 723–726. https://doi.org/10.1039/AN9891400723

Song, G., Zhang, Y., Yu, S., Lv, W., Guan, Z., Sun, M., & Wang, J. (2019). Chrysophanol attenuates airway inflammation and remodeling through nuclear factor-kappa B signaling pathway in asthma. *Phytotherapy Research*, *33*(10), 2702–2713. https://doi.org/10.1002/ptr.6444

Soto, M. L., Moure, A., Domínguez, H., & Parajó, J. C. (2011). Recovery, concentration and purification of phenolic compounds by adsorption: A review. *Journal of Food Engineering*, *105*(1), 1–27. https://doi.org/10.1016/j.jfoodeng.2011.02.010

Sporn, M. B., & Liby, K. T. (2012). NRF2 and cancer: The good, the bad and the importance of context. *Nature Reviews Cancer*, *12*(8), 564–571. https://doi.org/10.1038/nrc3278

Sripad, G., Prakash, V., & Rao, M. S. N. (1982). Extractability of polyphenols of sunflower seed in various solvents. *Journal of Biosciences*, *4*(2), 145–152. https://doi.org/10.1007/BF02702723

Sripad, G., & Rao, M. S. N. (1987). Effect of methods to remove polyphenols from sunflower meal on the physicochemical properties of the proteins. *Journal of Agricultural and Food Chemistry*, *35*(6), 962–967. https://doi.org/10.1021/jf00078a025

Stanford, J. P., Hall, P. H., Rover, M. R., Smith, R. G., & Brown, R. C. (2018). Separation of sugars and phenolics from the heavy fraction of bio-oil using polymeric resin adsorbents. *Separation and Purification Technology*, *194*, 170–180. https://doi.org/10.1016/j.seppur.2017.11.040

Stein, B., Baldwin, A. S., Ballard, D. W., Greene, W. C., Angel, P., & Herrlich, P. (1993). Cross-coupling of the NF-kappa B p65 and Fos/Jun transcription factors produces potentiated biological function. *The EMBO Journal*, *12*(10), 3879–3891. https://doi.org/10.1002/j.1460-2075.1993.tb06066.x

Suhas, Carrott, P. J. M., & Ribeiro Carrott, M. M. L. (2007). Lignin – from natural adsorbent to activated carbon: A review. *Bioresource Technology*, *98*(12), 2301–2312. https://doi.org/10.1016/j.biortech.2006.08.008

Sun, L., Guo, Y., Fu, C., Li, J., & Li, Z. (2013). Simultaneous separation and purification of total polyphenols, chlorogenic acid and phlorizin from thinned young apples. *Food Chemistry*, *136*(2), 1022–1029.

Sun, L.-M., & Meunier, F. (2003). Adsorption: Aspects théoriques. *Adsorption : Aspects Théoriques*, *W2*(J2730), J2730.1-J2730.16.

Sun, P.-C., Liu, Y., Yi, Y.-T., Li, H.-J., Fan, P., & Xia, C.-H. (2015). Preliminary enrichment and separation of chlorogenic acid from Helianthus tuberosus L. leaves extract by macroporous resins. *Food Chemistry*, *168*, 55–62. https://doi.org/10.1016/j.foodchem.2014.07.038

Szydłowska-Czerniak, A., Amarowicz, R., & Szłyk, E. (2010). Antioxidant capacity of rapeseed meal and rapeseed oils enriched with meal extract. *European Journal of Lipid Science and Technology*, *112*(7), 750–760. https://doi.org/10.1002/ejlt.200900292

Szymanowska, U., Baraniak, B., & Bogucka-Kocka, A. (2018). Antioxidant, Anti-Inflammatory, and Postulated Cytotoxic Activity of Phenolic and Anthocyanin-Rich Fractions from Polana Raspberry (Rubus idaeus L.) Fruit and Juice—In Vitro Study. *Molecules*, *23*(7), 1812. https://doi.org/10.3390/molecules23071812

Tajik, N., Tajik, M., Mack, I., & Enck, P. (2017). The potential effects of chlorogenic acid, the main phenolic components in coffee, on health: A comprehensive review of the literature. *European Journal of Nutrition*, *56*(7), 2215–2244. https://doi.org/10.1007/s00394-017-1379-1

Tamblyn, R. (1997). Unnecessary Prescribing of NSAIDs and the Management of NSAID-Related Gastropathy in Medical Practice. *Annals of Internal Medicine*, *127*(6), 429. https://doi.org/10.7326/0003-4819-127-6-199709150-00003

Tan, Z., Wang, C., Yi, Y., Wang, H., Li, M., Zhou, W., Tan, S., & Li, F. (2014). Extraction and purification of chlorogenic acid from ramie (Boehmeria nivea L. Gaud) leaf using an ethanol/salt aqueous two-phase system. *Separation and Purification Technology*, *132*, 396–400. https://doi.org/10.1016/j.seppur.2014.05.048

Tang, D., Zheng, Z., Lin, K., Luan, J., & Zhang, J. (2007). Adsorption of p-nitrophenol from aqueous solutions onto activated carbon fiber. *Journal of Hazardous Materials*, *143*(1–2), 49–56. https://doi.org/10.1016/j.jhazmat.2006.08.066

Tang, J., Diao, P., Shu, X., Li, L., & Xiong, L. (2019, October 28). Quercetin and Quercitrin Attenuates the Inflammatory Response and Oxidative Stress in LPS-Induced RAW264.7 Cells: In Vitro Assessment and a Theoretical Model. *BioMed Research International*; Hindawi. https://doi.org/10.1155/2019/7039802

Tang, S., Kerry, J. P., Sheehan, D., & Buckley, J. D. (2001). A comparative study of tea catechins and α-tocopherol as antioxidants in cooked beef and chicken meat. *European Food Research and Technology*, *213*(4–5), 286–289. https://doi.org/10.1007/s002170100311

Temkin, M. J., and V. Pyzhe. (1940). *Recent modifications to Langmuir isotherms.* 217-222.

Terra, X., Valls, J., Vitrac, X., Mérrillon, J.-M., Arola, L., Ardèvol, A., Bladé, C., Fernández-Larrea, J., Pujadas, G., Salvadó, J., & Blay, M. (2007). Grape-Seed Procyanidins Act as Antiinflammatory Agents in Endotoxin-Stimulated RAW 264.7 Macrophages by Inhibiting NFkB Signaling Pathway. *Journal of Agricultural and Food Chemistry*, *55*(11), 4357–4365. https://doi.org/10.1021/jf0633185

Theander, O., Aman, P., Miksche, G. E., & Yasuda, S. (1977). Carbohydrates, polyphenols, and lignin in seed hulls of different colors from turnip rapeseed. *Journal of Agricultural and Food Chemistry*, *25*(2), 270–273. https://doi.org/10.1021/jf60210a042

Thibault, J. F., Crepeau, M. J., & Quéméner, B. (1989). Composition glucidique des graines de colza et de tournesol. *Sciences Des Aliments*, *9*(2), 405–412.

Thiel, A., Muffler, K., Tippkötter, N., Suck, K., Sohling, U., Hruschka, S. M., & Ulber, R. (2015). A novel integrated downstream processing approach to recover sinapic acid, phytic acid and proteins from rapeseed meal: A novel downstream processing approach for rapeseed meal. *Journal of Chemical Technology & Biotechnology*, *90*(11), 1999–2006. https://doi.org/10.1002/jctb.4664

Thiel, A., Tippkötter, N., Suck, K., Sohling, U., Ruf, F., & Ulber, R. (2013, May 1). New zeolite adsorbents for downstream processing of polyphenols from renewable resources. *Engineering in Life Sciences; John Wiley & Sons, Ltd.* https://onlinelibrary.wiley.com/doi/abs/10.1002/elsc.201200188

Thies, W. (1991). Determination of the phytic acid and sinapic acid esters in seeds of rapeseed and selection of genotypes with reduced concentrations of these compounds. *Lipid/Fett*, *93*(2), 49–52.

Thiyam, U., Claudia, P., Jan, U., & Alfred, B. (2009). De-oiled rapeseed and a protein isolate: Characterization of sinapic acid derivatives by HPLC–DAD and LC–MS. *European Food Research and Technology*, *229*(5), 825–831.

Thiyam, U., Stöckmann, H., & Schwarz, K. (2006). Antioxidant activity of rapeseed phenolics and their interactions with tocopherols during lipid oxidation. *Journal of the American Oil Chemists' Society*, *83*(6), 523–528. https://doi.org/10.1007/s11746-006-1235-6

Thiyam-Holländer, U., Eskin, N. A. M., & Matthäus, B. (2012). Canola and Rapeseed: Production, Processing, Food Quality, and Nutrition. *CRC Press.*

tian, chunlian, guo, yuru, chang, yu, zhao, jihang, cui, cancan, & liu, mingchun. (2019). Dose-effect relationship on anti-inflammatory activity on LPS induced RAW 264.7 cells and antioxidant activity of rutin in vitro. *Acta Poloniae Pharmaceutica - Drug Research*, *76*(3), 511–522. https://doi.org/10.32383/appdr/102677

Tietje, C., & Brouder, A. (Eds.). (2010). International Conference On Harmonisation Of Technical Requirements For Registration Of Pharmaceuticals For Human Use. In *Handbook of Transnational Economic Governance Regimes* (pp. 1041–1053). https://doi.org/10.1163/ej.9789004163300.i-1081.897

Tilman, D., & Clark, M. (2015). Food, Agriculture & the Environment: Can We Feed the World & Save the Earth? *Daedalus*, *144*(4), 8–23. https://doi.org/10.1162/DAED_a_00350

Torres, P., Poveda, A., Jimenez-Barbero, J., Ballesteros, A., & Plou, F. J. (2010). Regioselective Lipase-Catalyzed Synthesis of 3- *O* -Acyl Derivatives of Resveratrol and Study of Their Antioxidant Properties. *Journal of Agricultural and Food Chemistry*, *58*(2), 807–813. https://doi.org/10.1021/jf903210q

Toth, J. (1971). State Equation of the Solid-Gas Interface Layers. *Acta Chim. Hung.*, *69*, 311–328.

Univia. (2020, September 20). Tourteaux d'oléagineux—Alimentation animale—Produits/Débouchés—Terres. http://www.terresunivia.fr/produitsdebouches/alimentation-animale/tourteaux-d-oleagineux

Tran, H. N., You, S.-J., Hosseini-Bandegharaei, A., & Chao, H.-P. (2017). Mistakes and inconsistencies regarding adsorption of contaminants from aqueous solutions: A critical review. *Water Research*, *120*, 88–116. https://doi.org/10.1016/j.watres.2017.04.014

Tremblay, A., Masson, E., Leduc, S., Houde, A., & Després, J.-P. (1988). Caffeine reduces spontaneous energy intake in men but not in women. *Nutrition Research*, *8*(5), 553–558. https://doi.org/10.1016/S0271-5317(88)80077-0

Tripathi, P., Srivastava, V. C., & Kumar, A. (2009). Optimization of an azo dye batch adsorption parameters using Box–Behnken design. *Desalination*, *249*(3), 1273–1279. https://doi.org/10.1016/j.desal.2009.03.010

Tuck, K. L., & Hayball, P. J. (2002). Major phenolic compounds in olive oil: Metabolism and health effects. *The Journal of Nutritional Biochemistry*, *13*(11), 636–644. https://doi.org/10.1016/S0955-2863(02)00229-2

Tung, Y.-T., Wu, J.-H., Kuo, Y.-H., & Chang, S.-T. (2007). Antioxidant activities of natural phenolic compounds from Acacia confusa bark. *Bioresource Technology*, *98*(5), 1120–1123. https://doi.org/10.1016/j.biortech.2006.04.017

Tuong, T. L., Aymes, A., Framboisier, X., Ioannou, I., & Kapel, R. (2020). Adsorption of Phenolic Compounds from an Aqueous By-product of Sunflower Protein Extraction/Purification by Macroporous Resins. *Journal of Chromatography & Separation Techniques*, *11*(6), 435. https://doi.org/10.35248/2157-7064.20.11.435

Tzeng, Y.-M., Diosady, L. L., & Rubin, L. J. (1990). Production of Canola Protein Materials by Alkaline Extraction, Precipitation, and Membrane Processing. *Journal of Food Science*, *55*(4), 1147–1151. https://doi.org/10.1111/j.1365-2621.1990.tb01619.x

Ueda, H., Yamazaki, C., & Yamazaki, M. (2004). A Hydroxyl Group of Flavonoids Affects Oral Anti-inflammatory Activity and Inhibition of Systemic Tumor Necrosis Factor-α Production. *Bioscience, Biotechnology, and Biochemistry*, *68*(1), 119–125. https://doi.org/10.1271/bbb.68.119

Ugurlu, M., & Hazirbulan, S. (2007). *Removal of some organic compounds from pre-treated olive mill wastewater by sepiolite*. http://acikerisim.mu.edu.tr/xmlui/handle/20.500.12809/5137

United Nations, Department of Economic and Social Affairs, Population Division, & United Nations. (2019). *World population prospects 2019. Volume II, Volume II,*.

Valkonen, M., & Kuusi, T. (1997). Spectrophotometric assay for total peroxyl radical-trapping antioxidant potential in human serum. *Journal of Lipid Research*, *38*(4), 823–833. https://doi.org/10.1016/S0022-2275(20)37249-7

Van Acker, S. A. B. E., Van Den Berg, D., Tromp, M. N. J. L., Griffioen, D. H., Van Bennekom, W. P., Van Der Vijgh, W. J. F., & Bast, A. (1996). Structural aspects of antioxidant activity of flavonoids. *Free Radical Biology and Medicine*, *20*(3), 331–342. https://doi.org/10.1016/0891-5849(95)02047-0

van Meeteren, M. E., Hendriks, J. J. A., Dijkstra, C. D., & van Tol, E. A. F. (2004). Dietary compounds prevent oxidative damage and nitric oxide production by cells involved in demyelinating disease. *Biochemical Pharmacology*, *67*(5), 967–975. https://doi.org/10.1016/j.bcp.2003.10.018

Vera Candioti, L., De Zan, M. M., Cámara, M. S., & Goicoechea, H. C. (2014). Experimental design and multiple response optimization. Using the desirability function in analytical methods development. *Talanta*, *124*, 123–138. https://doi.org/10.1016/j.talanta.2014.01.034

Verhagen, H., Schilderman, P. A. E. L., & Kleinjans, J. C. S. (1991). Butylated hydroxyanisole in perspective. *Chemico-Biological Interactions*, *80*(2), 109–134. https://doi.org/10.1016/0009-2797(91)90019-4

Verma, V. K., Malik, S., Narayanan, S. P., Mutneja, E., Sahu, A. K., Bhatia, J., & Arya, D. S. (2019). Role of MAPK/NF-κB pathway in cardioprotective effect of Morin in isoproterenol induced myocardial injury in rats. *Molecular Biology Reports*, *46*(1), 1139–1148. https://doi.org/10.1007/s11033-018-04575-9

Vuorela, S., Kreander, K., Karonen, M., Nieminen, R., Hämäläinen, M., Galkin, A., Laitinen, L., Salminen, J.-P., Moilanen, E., Pihlaja, K., Vuorela, H., Vuorela, P., & Heinonen, M. (2005). Preclinical Evaluation of Rapeseed, Raspberry, and Pine Bark Phenolics for Health Related Effects. *Journal of Agricultural and Food Chemistry*, *53*(15), 5922–5931. https://doi.org/10.1021/jf050554r

Vuorela, S., Meyer, A. S., & Heinonen, M. (2003). Quantitative analysis of the main phenolics in rapeseed meal and oils processed differently using enzymatic hydrolysis and HPLC. *European Food Research and Technology*, *217*(6), 517–523. https://doi.org/10.1007/s00217-003-0811-3

Vuorela, S., Meyer, A. S., & Heinonen, M. (2004). Impact of isolation method on the antioxidant activity of rapeseed meal phenolics. *Journal of Agricultural and Food Chemistry*, *52*(26), 8202–8207.

Wadsworth, T. L., McDonald, T. L., & Koop, D. R. (2001). Effects of Ginkgo biloba extract (EGb 761) and quercetin on lipopolysaccharide-induced signaling pathways involved in the release of tumor necrosis factor-α 1. *Biochemical Pharmacology*, *62*(7), 963–974. https://doi.org/10.1016/S0006-2952(01)00734-1

Walker, M. E., Gaines, T. P., & Henning, R. J. (1982). Foliar Fertilization Effects on Yield, Quality, Nutrient Uptake, and Vegetative Characteristics of Florunner Peanuts.1,2. *Peanut Science*, *9*(2), 53–57. https://doi.org/10.3146/i0095-3679-9-2-1

Walter, E. D. (1941). Genistin (an Isoflavone Glucoside) and its Aglucone, Genistein, from Soybeans. *Journal of the American Chemical Society*, *63*(12), 3273–3276. https://doi.org/10.1021/ja01857a013

Walters, R. W., & Luthy, R. G. (1984). Equilibrium adsorption of polycyclic aromatic hydrocarbons from water onto activated carbon. *Environmental Science & Technology*, *18*(6), 395–403. https://doi.org/10.1021/es00124a002

Wanasundara, J. P. D., McIntosh, T. C., Perera, S. P., Withana-Gamage, T. S., & Mitra, P. (2016). Canola/rapeseed protein-functionality and nutrition. *OCL*, *23*(4), D407. https://doi.org/10.1051/ocl/2016028

Wanasundara, U., Amarowicz, R., & Shahidi, F. (1994). Isolation and Identification of an Antioxidative Component in Canola Meal. *Journal of Agricultural and Food Chemistry*, *42*(6), 1285–1290. https://doi.org/10.1021/jf00042a006

Wanasundara, U. N., Amarowicz, R., & Shahidi, F. (1995). Partial characterization of natural antioxidants in canola meal. *Food Research International*, *28*(6), 525–530. https://doi.org/10.1016/0963-9969(96)87362-5

Wanasundara, U. N., & Shahidi, F. (1998). Antioxidant and pro-oxidant activity of green tea extracts in marine oils. *Food Chemistry*, *63*(3), 335–342. https://doi.org/10.1016/S0308-8146(98)00025-9

Wang, A., Wei, J., Lu, C., Chen, H., Zhong, X., Lu, Y., Li, L., Huang, H., Dai, Z., & Han, L. (2019). Genistein suppresses psoriasis-related inflammation through a STAT3–NF-κB-dependent mechanism in keratinocytes. *International Immunopharmacology*, *69*, 270–278. https://doi.org/10.1016/j.intimp.2019.01.054

Wang, H., Cao, G., & Prior, R. L. (1997). Oxygen Radical Absorbing Capacity of Anthocyanins. *Journal of Agricultural and Food Chemistry*, *45*(2), 304–309. https://doi.org/10.1021/jf960421t

Wang, H., Gao, X. D., Zhou, G. C., Cai, L., & Yao, W. B. (2008). In vitro and in vivo antioxidant activity of aqueous extract from Choerospondias axillaris fruit. *Food Chemistry*, *106*(3), 888–895. https://doi.org/10.1016/j.foodchem.2007.05.068

Wang, J.-P., Feng, H.-M., & Yu, H.-Q. (2007). Analysis of adsorption characteristics of 2,4-dichlorophenol from aqueous solutions by activated carbon fiber. *Journal of Hazardous Materials*, *144*(1–2), 200–207. https://doi.org/10.1016/j.jhazmat.2006.10.003

Wang, S. X., Oomah, B. D., & McGregor, D. I. (1998). Application and evaluation of ion-exchange UV spectrophotometric method for determination of sinapine in Brassica seeds and meals. *Journal of Agricultural and Food Chemistry*, *46*(2), 575–579.

Wang, X. S., Zhou, Y., Jiang, Y., & Sun, C. (2008). The removal of basic dyes from aqueous solutions using agricultural by-products. *Journal of Hazardous Materials*, *157*(2), 374–385. https://doi.org/10.1016/j.jhazmat.2008.01.004

Wang, X., Zhao, J., Xia, S., Li, A., & Chen, L. (2004). Adsorption mechanism of phenolic compounds from aqueous solution on hypercrosslinked polymeric adsorbent. *Journal of Environmental Sciences*, *16*(6), 919–924.

Wang, Y.-J., Wu, Y.-F., Xue, F., Wu, Z.-X., Xue, Y.-P., Zheng, Y.-G., & Shen, Y.-C. (2012). Isolation of brefeldin A from Eupenicillium brefeldianum broth using macroporous resin adsorption chromatography. *Journal of Chromatography B*, *895–896*, 146–153. https://doi.org/10.1016/j.jchromb.2012.03.033

Wang, Z., Wang, C., Yuan, J., & Zhang, C. (2017a). Adsorption characteristics of adsorbent resins and antioxidant capacity for enrichment of phenolics from two-phase olive waste. *Journal of Chromatography B*, *1040*, 38–46. https://doi.org/10.1016/j.jchromb.2016.11.023

Wang, Z., Wang, C., Yuan, J., & Zhang, C. (2017b). Adsorption characteristics of adsorbent resins and antioxidant capacity for enrichment of phenolics from two-phase olive waste. *Journal of Chromatography B*, *1040*, 38–46. https://doi.org/10.1016/j.jchromb.2016.11.023

Wanjari, N., & Waghmare, J. (n.d.). Extraction of Antioxidants from Deoiled Sunflower Cake. *Journal of Lipid Science and Technology*.

Wayner, D. D. M., Burton, G. W., Ingold, K. U., & Locke, S. (1985). Quantitative measurement of the total, peroxyl radical-trapping antioxidant capability of human blood plasma by controlled peroxidation: The important contribution made by plasma proteins. *FEBS Letters*, *187*(1), 33–37. https://doi.org/10.1016/0014-5793(85)81208-4

Weber, W. J., & Morris, J. C. (1963). Kinetics of adsorption on carbon from solution. *Journal of the Sanitary Engineering Division*, *89*(2), 31–60.

Weber, W. J., & Smith, E. H. (1986). Activated Carbon Adsorption: The State of the Art. In *Studies in Environmental Science* (29), 455–492. Elsevier. https://doi.org/10.1016/S0166-1116(08)70958-0

Weber, W. J., & Smith, E. H. (1987). Simulation and design models for adsorption processes. *Environmental Science & Technology*, *21*(11), 1040–1050. https://doi.org/10.1021/es00164a002

Weisz, G. M., Carle, R., & Kammerer, D. R. (2013). Sustainable sunflower processing-II. Recovery of phenolic compounds as a by-product of sunflower protein extraction. *Innovative Food Science & Emerging Technologies*, *17*, 169–179. https://doi.org/10.1016/j.ifset.2012.09.009

Weisz, G. M., Kammerer, D. R., & Carle, R. (2009). Identification and quantification of phenolic compounds from sunflower (Helianthus annuus L.) kernels and shells by HPLC-DAD/ESI-MSn. *Food Chemistry*, *115*(2), 758–765. https://doi.org/10.1016/j.foodchem.2008.12.074

Weisz, G. M., Schneider, L., Schweiggert, U., Kammerer, D. R., & Carle, R. (2010). Sustainable sunflower processing—I. Development of a process for the adsorptive decolorization of sunflower [Helianthus annuus L.] protein extracts. *Innovative Food Science & Emerging Technologies*, *11*(4), 733–741. https://doi.org/10.1016/j.ifset.2010.05.005

Wildermuth, S. R., Young, E. E., & Were, L. M. (2016). Chlorogenic Acid Oxidation and Its Reaction with Sunflower Proteins to Form Green-Colored Complexes: Chlorogenic acid oxidation…. *Comprehensive Reviews in Food Science and Food Safety*, *15*(5), 829–843. https://doi.org/10.1111/1541-4337.12213

Willcox, J. K., Ash, S. L., & Catignani, G. L. (2004). Antioxidants and Prevention of Chronic Disease. *Critical Reviews in Food Science and Nutrition*, *44*(4), 275–295. https://doi.org/10.1080/10408690490468489

Williams, C. S., Mann, M., & DuBois, R. N. (1999). The role of cyclooxygenases in inflammation, cancer, and development. *Oncogene*, *18*(55), 7908–7916. https://doi.org/10.1038/sj.onc.1203286

Wishart, D. S., Feunang, Y. D., Guo, A. C., Lo, E. J., Marcu, A., Grant, J. R., Sajed, T., Johnson, D., Li, C., Sayeeda, Z., Assempour, N., Iynkkaran, I., Liu, Y., Maciejewski, A., Gale, N., Wilson, A., Chin, L., Cummings, R., Le, D., … Wilson, M. (2018). DrugBank 5.0: A major update to the DrugBank database for 2018. *Nucleic Acids Research*, *46*(D1), D1074–D1082. https://doi.org/10.1093/nar/gkx1037

Wolfe, K. L., & Liu, R. H. (2007). Cellular Antioxidant Activity (CAA) Assay for Assessing Antioxidants, Foods, and Dietary Supplements. *Journal of Agricultural and Food Chemistry*, *55*(22), 8896–8907. https://doi.org/10.1021/jf0715166

Wong, S. K., Chin, K.-Y., Suhaimi, F. H., Ahmad, F., & Ima-Nirwana, S. (2018). Effects of metabolic syndrome on bone mineral density, histomorphometry and remodelling markers in male rats. *PLOS ONE*, *13*(2), e0192416. https://doi.org/10.1371/journal.pone.0192416

Worch, E. (2012). *Adsorption Technology in Water Treatment: Fundamentals, Processes, and Modeling*. DE GRUYTER. https://doi.org/10.1515/9783110240238

Wu, J., Wang, Z.-R., Hsieh, T.-C., Bruder, J., Zou, J.-G., & Huang, Y.-Z. (2001). Mechanism of cardioprotection by resveratrol, a phenolic antioxidant present in red wine (Review). *International Journal of Molecular Medicine*. https://doi.org/10.3892/ijmm.8.1.3

Wu, S., Wang, Y., Gong, G., Li, F., Ren, H., & Liu, Y. (2015a). Adsorption and desorption properties of macroporous resins for flavonoids from the extract of Chinese wolfberry (Lycium barbarum L.). *Food and Bioproducts Processing*, *93*, 148–155. https://doi.org/10.1016/j.fbp.2013.12.006

Wu, S., Wang, Y., Gong, G., Li, F., Ren, H., & Liu, Y. (2015b). Adsorption and desorption properties of macroporous resins for flavonoids from the extract of Chinese wolfberry (Lycium barbarum L.). *Food and Bioproducts Processing*, *93*, 148–155. https://doi.org/10.1016/j.fbp.2013.12.006

Xagorari, A., Roussos, C., & Papapetropoulos, A. (2002). Inhibition of LPS-stimulated pathways in macrophages by the flavonoid luteolin. *British Journal of Pharmacology*, *136*(7), 1058–1064. https://doi.org/10.1038/sj.bjp.0704803

Xi, L., Mu, T., & Sun, H. (2015). Preparative purification of polyphenols from sweet potato (Ipomoea batatas L.) leaves by AB-8 macroporous resins. *Food Chemistry*, *172*, 166–174. https://doi.org/10.1016/j.foodchem.2014.09.039

Xia, B., Phillips, J., Chen, C.-K., Radovic, L. R., Silva, I. F., & Menéndez, J. A. (1999). Impact of Pretreatments on the Selectivity of Carbon for NO_x Adsorption/Reduction. *Energy & Fuels*, *13*(4), 903–906. https://doi.org/10.1021/ef9802680

Xia, N., Chen, G., Liu, M., Ye, X., Pan, Y., Ge, J., Mao, Y., Wang, H., Wang, J., & Xie, S. (2016). Anti-inflammatory effects of luteolin on experimental autoimmune thyroiditis in mice. *Experimental and Therapeutic Medicine*, *12*(6), 4049–4054. https://doi.org/10.3892/etm.2016.3854

Xianquan, S., Shi, J., Kakuda, Y., & Yueming, J. (2005). Stability of Lycopene During Food Processing and Storage. *Journal of Medicinal Food*, *8*(4), 413–422. https://doi.org/10.1089/jmf.2005.8.413

Xie, Q.-F., Cheng, J.-J., Chen, J.-F., Feng, Y.-C., Lin, G.-S., & Xu, Y. (2020, December 22). *Comparation of Anti-Inflammatory and Antioxidantactivities of Curcumin, Tetrahydrocurcuminand Octahydrocurcuminin LPS-Stimulated RAW264.7 Macrophages* [Research Article]. Evidence-Based Complementary and Alternative Medicine; Hindawi. https://doi.org/10.1155/2020/8856135

Xiong, J., Wang, K., Yuan, C., Xing, R., Ni, J., Hu, G., Chen, F., & Wang, X. (2017). Luteolin protects mice from severe acute pancreatitis by exerting HO-1-mediated anti-inflammatory and antioxidant effects. *International Journal of Molecular Medicine*, *39*(1), 113–125. https://doi.org/10.3892/ijmm.2016.2809

Xiong, W., Ma, H., Zhang, Z., Jin, M., Wang, J., Xu, Y., & Wang, Z. (2019). The protective effect of icariin and phosphorylated icariin against LPS-induced intestinal epithelial cells injury. *Biomedicine & Pharmacotherapy*, *118*, 109246. https://doi.org/10.1016/j.biopha.2019.109246

Xu, C.-Q., Liu, B.-J., Wu, J.-F., Xu, Y.-C., Duan, X.-H., Cao, Y.-X., & Dong, J.-C. (2010). Icariin attenuates LPS-induced acute inflammatory responses: Involvement of PI3K/Akt and NF-κB signaling pathway. *European Journal of Pharmacology*, *642*(1–3), 146–153.

Xu, L., & Diosady, L. L. (1997). Rapid method for total phenolic acid determination in rapeseed/canola meals. *Food Research International*, *30*(8), 571–574. https://doi.org/10.1016/S0963-9969(98)00022-2

Xu, L., & Diosady, L. L. (2000). Interactions between canola proteins and phenolic compounds in aqueous media. *Food Research International*, *33*(9), 725–731.

Xu, Z., Zhang, Q., Chen, J., Wang, L., & Anderson, G. K. (1999). Adsorption of naphthalene derivatives on hypercrosslinked polymeric adsorbents. *Chemosphere*, *38*(9), 2003–2011. https://doi.org/10.1016/S0045-6535(98)00413-5

Yagi, K. (1987). Lipid peroxides and human diseases. *Chemistry and Physics of Lipids*, *45*(2–4), 337–351. https://doi.org/10.1016/0009-3084(87)90071-5

Yahfoufi, N., Alsadi, N., Jambi, M., & Matar, C. (2018). The Immunomodulatory and Anti-Inflammatory Role of Polyphenols. *Nutrients*, *10*(11), 1618. https://doi.org/10.3390/nu10111618

Yang, Q., Zhao, M., & Lin, L. (2016). Adsorption and desorption characteristics of adlay bran free phenolics on macroporous resins. *Food Chemistry*, *194*, 900–907. https://doi.org/10.1016/j.foodchem.2015.08.070

Yang, S.-C., Arasu, M. V., Chun, J.-H., Jang, Y.-S., Lee, Y.-H., Kim, I. H., Lee, K.-T., Hong, S.-T., & Kim, S.-J. (2015). Identification and Determination of Phenolic Compounds in Rapeseed Meals (Brassica napus L.). *Journal of Agricultural Chemistry and Environment*, *04*(01), 14–23. https://doi.org/10.4236/jacen.2015.41002

Yang, W. S., Jeong, D., Yi, Y.-S., Park, J. G., Seo, H., Moh, S. H., Hong, S., & Cho, J. Y. (2013). IRAK1/4-Targeted Anti-Inflammatory Action of Caffeic Acid. *Mediators of Inflammation*, *2013*, 518183. https://doi.org/10.1155/2013/518183

Yang, W., Xue, X., Zheng, F., & Yang, X. (2011). Importance of Surface Area and Pore Size Distribution of Resin for Organic Toxicants Adsorption. *Separation Science and Technology*, *46*(8), 1321–1328. https://doi.org/10.1080/01496395.2011.556102

Yanishlieva, N. V., & Marinova, E. M. (2001). Stabilisation of edible oils with natural antioxidants. *European Journal of Lipid Science and Technology*, *103*(11), 752–767. https://doi.org/10.1002/1438-9312(200111)103:11<752::AID-EJLT752>3.0.CO;2-0

Yao, L. H., Jiang, Y. M., Shi, J., TomS-Barber,N, F. A., Datta, N., Singanusong, R., & Chen, S. S. (2004). Flavonoids in Food and Their Health Benefits. *Plant Foods for Human Nutrition*, *59*(3), 113–122. https://doi.org/10.1007/s11130-004-0049-7

Yasuko, K., Tomohiro, N., Sei-Itsu, M., Ai-Na, L., Yasuo, F., & Takashi, T. (1984). Caffeic acid is a selective inhibitor for leukotriene biosynthesis. *Biochimica et Biophysica Acta (BBA) - Lipids and Lipid Metabolism*, *792*(1), 92–97. https://doi.org/10.1016/0005-2760(84)90287-X

Yemm, E. W., & Willis, A. J. (1954). The estimation of carbohydrates in plant extracts by anthrone. *Biochemical Journal*, *57*(3), 508–514. https://doi.org/10.1042/bj0570508

Yeon, M. J., Lee, M. H., Kim, D. H., Yang, J. Y., Woo, H. J., Kwon, H. J., Moon, C., Kim, S.-H., & Kim, J.-B. (2019). Anti-inflammatory effects of Kaempferol on Helicobacter pylori-induced inflammation. *Bioscience, Biotechnology, and Biochemistry*, *83*(1), 166–173. https://doi.org/10.1080/09168451.2018.1528140

Yoon, J.-H., & Baek, S. J. (2005). Molecular targets of dietary polyphenols with anti-inflammatory properties. *Yonsei Medical Journal*, *46*(5), 585–596.

Youdim, K. A., McDonald, J., Kalt, W., & Joseph, J. A. (2002). Potential role of dietary flavonoids in reducing microvascular endothelium vulnerability to oxidative and inflammatory. *The Journal of Nutritional Biochemistry*, *13*(5), 282–288. https://doi.org/10.1016/S0955-2863(01)00221-2

Yu, W., Xu, Z., Gao, Q., Xu, Y., Wang, B., & Dai, Y. (2020). Protective role of wogonin against cadmium induced testicular toxicity: Involvement of antioxidant, anti-inflammatory and anti-apoptotic pathways. *Life Sciences*, *258*, 118192. https://doi.org/10.1016/j.lfs.2020.118192

Yun, K.-J., Koh, D.-J., Kim, S.-H., Park, S. J., Ryu, J. H., Kim, D.-G., Lee, J.-Y., & Lee, K.-T. (2008). Anti-Inflammatory Effects of Sinapic Acid through the Suppression of Inducible Nitric Oxide Synthase, Cyclooxygase-2, and Proinflammatory Cytokines Expressions via Nuclear Factor-κB Inactivation. *Journal of Agricultural and Food Chemistry*, *56*(21), 10265–10272. https://doi.org/10.1021/jf802095g

Zabkova, M., Otero, M., Minceva, M., Zabka, M., & Rodrigues, A. E. (2006). Separation of synthetic vanillin at different pH onto polymeric adsorbent Sephabeads SP206. *Chemical Engineering and Processing: Process Intensification*, *45*(7), 598–607. https://doi.org/10.1016/j.cep.2006.01.005

Zagklis, D. P., Vavouraki, A. I., Kornaros, M. E., & Paraskeva, C. A. (2015). Purification of olive mill wastewater phenols through membrane filtration and resin adsorption/desorption. *Journal of Hazardous Materials*, *285*, 69–76. https://doi.org/10.1016/j.jhazmat.2014.11.038

Zago, E., Lecomte, J., Barouh, N., Aouf, C., Carré, P., Fine, F., & Villeneuve, P. (2015). Influence of rapeseed meal treatments on its total phenolic content and composition in sinapine, sinapic acid and canolol. *Industrial Crops and Products*, *76*, 1061–1070. https://doi.org/10.1016/j.indcrop.2015.08.022

Zhang, B., Yang, R., Zhao, Y., & Liu, C.-Z. (2008). Separation of chlorogenic acid from honeysuckle crude extracts by macroporous resins. *Journal of Chromatography B*, *867*(2), 253–258. https://doi.org/10.1016/j.jchromb.2008.04.016

Zhang, H., & Tsao, R. (2016). Dietary polyphenols, oxidative stress and antioxidant and anti-inflammatory effects. *Current Opinion in Food Science*, *8*, 33–42. https://doi.org/10.1016/j.cofs.2016.02.002

Zhao, W., Yang, R., Lu, R., Wang, M., Qian, P., & Yang, W. (2008). Effect of PEF on microbial inactivation and physical–chemical properties of green tea extracts. *LWT - Food Science and Technology*, *41*(3), 425–431. https://doi.org/10.1016/j.lwt.2007.03.020

Zhao, Z., Shin, H. S., Satsu, H., Totsuka, M., & Shimizu, M. (2008). 5-Caffeoylquinic Acid and Caffeic Acid Down-Regulate the Oxidative Stress- and TNF-α-Induced Secretion of Interleukin-8 from Caco-2 Cells. *Journal of Agricultural and Food Chemistry*, *56*(10), 3863–3868. https://doi.org/10.1021/jf073168d

Zheng, W., Tao, Z., Cai, L., Chen, C., Zhang, C., Wang, Q., Ying, X., Hu, W., & Chen, H. (2017). Chrysin Attenuates IL-1β-Induced Expression of Inflammatory Mediators by Suppressing NF-κB in Human Osteoarthritis Chondrocytes. *Inflammation*, *40*(4), 1143–1154. https://doi.org/10.1007/s10753-017-0558-9

Zhong, Y., & Shahidi, F. (2012). Lipophilised epigallocatechin gallate (EGCG) derivatives and their antioxidant potential in food and biological systems. *Food Chemistry*, *131*(1), 22–30. https://doi.org/10.1016/j.foodchem.2011.07.089

Zhou, Z., Mou, S., Chen, X., Gong, L., & Ge, W. (2017). Anti-inflammatory activity of resveratrol prevents inflammation by inhibiting NF-κB in animal models of acute pharyngitis. *Molecular Medicine Reports*. https://doi.org/10.3892/mmr.2017.7933

Zhu, F., Du, B., & Xu, B. (2018). Anti-inflammatory effects of phytochemicals from fruits, vegetables, and food legumes: A review. *Critical Reviews in Food Science and Nutrition*, *58*(8), 1260–1270. https://doi.org/10.1080/10408398.2016.1251390

Zhu, J., & Wu, M. (2009). Characterization and Free Radical Scavenging Activity of Rapeseed Meal Polysaccharides WPS-1 and APS-2. *Journal of Agricultural and Food Chemistry*, *57*(3), 812–819. https://doi.org/10.1021/jf802687t

Žilić, S., Dragišić, J. M., Maksimović, V., Maksimović, M., Basić, Z., Crevar, M., & Stanković, G. (2010). The content of antioxidants in sunflower seed and kernel. *Helia*, *33*(52), 75–84. https://doi.org/10.2298/hel1052075z

Zurita, J. L., Jos, Á., del Peso, A., Salguero, M., López-Artíguez, M., & Repetto, G. (2007). Ecotoxicological effects of the antioxidant additive propyl gallate in five aquatic systems. *Water Research*, *41*(12), 2599–2611. https://doi.org/10.1016/j.watres.2007.02.003

Purification et propriétés anti-inflammatoires et anti-oxydantes des fractions phénoliques issues de coproduits de production d'isolats protéiques d'oleoproteagineux

Le colza et le tournesol sont les plantes oléagineuses les plus cultivées en Europe en général, et en France en particulier. Certains industriels se concentrent actuellement sur le développement de procédés industriels d'extraction/purification des protéines des tourteaux de ces deux végétaux. Ces procédés génèrent des coproduits qui sont des effluents aqueux salins riches en composés phénoliques tels que l'acide cholorgénique (CGA, pour le tournesol) et la sinapine (SP, pour le colza). La capture de ces composés phénoliques qui peuvent agir comme anti-oxydants naturels et/ou anti-inflammatoires en nutrition – santé constitue donc une voie de valorisation prometteuse. Les principaux objectifs de ce travail étaient les suivants 1) caractériser et identifier les composés phénoliques des sous-produits d'isolat de protéines à partir de la SFM et de la RSM ; 2) choisir les meilleures résines macroporeuses et étudier le mécanisme d'adsorption des composés phénoliques; 3) optimiser les conditions dans la colonne d'adsorption des composés phénoliques; et 4) évaluer les activités biologiques des fractions phénoliques obtenues, notamment les propriétés antioxydantes et anti-inflammatoires.

Par différentes méthodes analytiques, nous avons déterminé que les effluents liquides étaient constitués de composés phénoliques, d'acides aminés, d'hydrates de carbone et de sel, qui ont un poids moléculaire faible et qui peuvent facilement passer à travers une membrane UF/DF. Tous les composés phénoliques ont été identifiés par analyse HPLC et HPLC-ESI-MS, en comparaison avec des standards. Le CGA est le principal composé phénolique des effluents tournesol. Le principal composé phénolique des effluents colza est la SP. Contrairement au tournesol, ils contiennent aussi de nombreux autres composés mineurs. L'adsorption/désorption des composés phénoliques de tournesol et de colza a été évaluée à l'aide de différentes résines macroporeuses, notamment XAD4, XAD7, XAD16, XAD1180 et HP20. Nous avons constaté que tous les composés phénoliques s'adsorbaient facilement sur les résines. Les résines XAD7 et XAD16 ont montré les meilleures propriétés d'adsorption/désorption dans les effluents liquides de tournesol et de colza, respectivement. Les résultats ont montré que l'adsorption de tous les composés phénoliques suit un modèle. Les isothermes d'adsorption suivent un modèle de Langmuir. Selon les paramètres thermodynamiques déterminés, le processus d'adsorption, est dans tous les cas physique et est exothermique.

La condition optimale pour l'adsorption sur colonne a été déterminée sur les résines sélectionnées par planification expérimentale et optimisation multicritère. Une méthodologie d'optimisation multicritères basée sur des plans d'expériences a montré que les conditions optimales étaient un débit d'adsorption de 15 BV/h à un pH de 2,7 pour le CGA de la SFM. De l'autre côté, un débit d'adsorption de 13,3 BV/h et un pH compris entre 2 et 5 étaient les conditions optimales pour la sinapine du RSM. Des solutions d'éthanol (50% (v/v) pour l'acide chlorogénique, 30% (v/v) pour la sinapine ont été utilisées pour la desorption.

Ces approches ont permis de produire avec succès les fractions phénoliques pour des activités biologiques telles que l'antioxydation et l'anti-inflammation. La fraction phénolique a montré une capacité antioxydante plus élevée que la vitamine C dans le test ABTS (IC50/fractions phénoliques < IC50 vitamine C, $p < 0,05$).

Il a en outre été discuté si les fractions phénoliques obtenues dans le cadre de ce projet présentaient également un effet inflammatoire. La fraction tournesol (CGA) a efficacement inhibé la production de TNF-α, qui est un marqueur pro-inflammatoire lorsqu'un échantillon est traité avec du LPS. Cependant, les fractions colza n'étaient pas efficaces contre les médiateurs pro-inflammatoires. Aucune des fraction n'a montré de cytotoxicité.

Mots-clés : Tourteau de tournesol, tourteau de colza, composés phénoliques, résine macroporeuse, adsorption, désorption, purification, optimisation multicritères, antioxydant, anti-inflammation.

Purification and anti-inflammatory and antioxidant properties of phenolic fractions from co-products of production of oleoproteaginous protein isolates

Rapeseed and sunflower are the most cultivated oilseed plants in Europe in general, and in France in particular. Some industrialists are currently focusing on the development of industrial processes for the extraction/purification of proteins from the oil cakes of these two plants. These processes generate co-products which are saline aqueous effluents rich in phenolic compounds such as cholorgenic acid (CGA, for sunflower) and sinapine (SP, for rapeseed). The capture of these phenolic compounds, which can act as natural antioxidants and/or anti-inflammatory agents in nutrition and health, is therefore a promising way of valorization. The main objectives of this work were: 1) to characterize and identify the phenolic compounds of protein isolate by-products from SFM and RSM; 2) to select the best macroporous resins and to study the adsorption mechanism of phenolic compounds; 3) to optimize the conditions in the phenolic compounds adsorption column; and 4) to evaluate the biological activities of the obtained phenolic fractions, especially the antioxidant and anti-inflammatory properties.

By different analytical methods, we determined that the liquid effluents consisted of phenolic compounds, amino acids, carbohydrates, and salt, which have a low molecular weight and can easily pass through a UF/DF membrane. All phenolic compounds were identified by HPLC and HPLC-ESI-MS analysis in comparison with standards. CGA is the main phenolic compound in the sunflower effluent. The main phenolic compound of rapeseed effluents is MS. Unlike sunflower, they also contain many other minor compounds. The adsorption/desorption of sunflower and rapeseed phenolic compounds was evaluated using different macroporous resins including XAD4, XAD7, XAD16, XAD1180 and HP20. We found that all phenolic compounds adsorbed readily onto the resins. XAD7 and XAD16 resins showed the best adsorption/desorption properties in sunflower and rapeseed liquid effluents, respectively. The results showed that the adsorption of all phenolic compounds follows a Langmuir model. According to the determined thermodynamic parameters, the adsorption process, is in all cases physical and is exothermic.

The optimal condition for column adsorption was determined on the selected resins by experimental planning and multicriteria optimization. A multicriteria optimization methodology based on design of experiments showed the optimal conditions were adsorption flow rate of 15 BV/h at pH 2.7 for CGA from SFM. Meanwhile, adsorption flow rate of 13.3 BV/h and at pH ranging from 2 to 5 were the optimal conditions for sinapine from RSM. Ethanol solutions 50% (v/v) for chlorogenic acid, 30% (v/v) for sinapine were used for desorption.

These approaches successfully produced the phenolic fractions for biological activities such as antioxidation and anti-inflammation. Phenolic fraction showed a higher antioxidant capacity than vitamin C in DPPH and ABTS assays (IC50/phenolic fractions < IC50 vitamin C, $p < 0.05$. In addition, it was discussed whether the phenolic fractions obtained in this project also showed an inflammatory effect. The sunflower fraction (CGA) effectively inhibited the production of TNF-α, which is a pro-inflammatory marker when a sample is treated with LPS. However, the rapeseed fractions were not effective against proinflammatory mediators. None of the fractions showed cytotoxicity.

Keywords: Sunflower meal, rapseed meal, phenolic compounds, macroporous resin, adsorption, desorption, purification, multicriteria optimization, antioxidant, anti-inflammation.